

Dissertation zur Erlangung des Doktorgrades
der Fakultät für Chemie und Pharmazie
der Ludwig-Maximilians-Universität München

**Investigation of New More Environmentally
Benign, Smoke-reduced, Red- and Green-light
Emitting Pyrotechnic Compositions Based on
Nitrogen-rich Coloring Agents**

vorgelegt von
Karina Rosa Tarantik
aus
Dachau

München 2010

Erklärung

Diese Dissertation wurde im Sinne von § 13 Abs. 3 der Promotionsordnung vom 29. Januar 1998 von Herrn Prof. Dr. Thomas M. KLAPÖTKE betreut.

Ehrenwörtliche Versicherung

Diese Dissertation wurde selbstständig, ohne unerlaubte Hilfe erarbeitet.

München, den 08.Juni 2010

Karina R. TARANTIK

Dissertation eingereicht am 10.06.2010

1. Berichtserstatter: Prof. Dr. Thomas M. KLAPÖTKE

2. Berichtserstatter: Prof. Dr. Konstantin KARAGHIOSOFF

Mündliche Prüfung 16. Juli 2010

Die vorliegende Arbeit wurde in der Zeit von Oktober 2007 bis Juni 2010 am
Department Chemie und Biochemie der Ludwig-Maximilians-Universität München
unter der Anleitung von

Prof. Dr. Thomas M. KLAPÖTKE

angefertigt.

Für Mönch Schwarz

Danksagung

Herrn Prof. Dr. Thomas M. KLAPÖTKE danke ich ganz besonders für die freundliche Aufnahme in seinen Arbeitskreis und für die interessante und herausfordernde Themenstellung dieser Dissertation. Des Weiteren bin ich ihm für die gute Betreuung und Unterstützung, stetige Diskussionsbereitschaft, sowie für wertvolle Anregungen, Vorschläge, und hilfreichen Korrekturen zu dieser Arbeit.

Herrn Gary CHEN und seiner Arbeitsgruppe von U.S. Army RDECOM-ARDEC bin ich zu sehr großem Dank für ihre Kooperation verpflichtet. Dazu gehört die Bereitstellung von ausreichend Binder, die Durchführung der *smoke tests* und *static burn tests*, sowie die Möglichkeit an der Teilnahme am *36th International Pyrotechnics Seminar* in Rotterdam.

Herrn Prof. Dr. Konstantin KARAGHIOSOFF danke ich für das Messen von NMR-Spektren (u.a. 2D), anregende Diskussionen (auch am Wochenende), zahlreiche Verbesserungsvorschläge bei dieser Arbeit, sowie die Übernahme des Zweitgutachters.

Herrn Akad. ORat Dr. Burkhard KRUMM danke ich für zahlreiche hilfreiche Tipps, das stete Informieren über jegliches Fußballgeschehen, die Einblicke in das teilweise frustrierende Korrigieren im ACI-Praktikum, sowie für das Korrekturlesen bei dieser Arbeit.

Frau Irene S. SCHECKENBACH danke ich für ihre Freundlichkeit, ihre organisatorische Betreuung, das stete Versorgen von Dr. F. Xaver STEEMANN mit Süßigkeiten und ihre Liebe zu Tieren.

Meinen Laborkollegen Dr. F. Xaver STEEMANN, Norbert T. MAYR, Richard MOLL, Sebastian Rest und Dr. Matthias F. SCHERR danke ich für die stets gute Laune und gute Unterhaltung, wenn auch teilweise mit fraglichem Musikgeschmack. Dr. Matthias F. SCHERR bin ich vor allem dankbar, dass er meine zwei „Anschläge“ ohne Blessuren überstanden hat.

Dr. Jörg STIERSTORFER danke ich für die gute Vorarbeit auf dem Gebiet der 5-Nitriminotetrazole und deren Salze. Dr. Georg STEINHAUSER danke ich für die gute Einführung ins Thema Pyrotechnik, inklusive zahlreicher Literatur.

Dem X-Ray Team danke ich für das Auflegen und Messen meiner vielen Kristalle, insbesondere Franz MARTIN und Karin LUX, die auch bei „zickigen“ Strukturen die Lösung gefunden haben.

Für das Korrekturlesen dieser Arbeit danke ich, neben den schon genannten, Franz MARTIN, Dr. Chrissi ROTTER, Dr. F. Xaver STEEMANN, und Anian NIEDER.

Stefan HUBER danke ich für die unzähligen Bestimmungen der Sensitivitäten und bombenkalorimetrische Messungen.

Dem ganzen Arbeitskreis danke ich für die allzeit bereitwillige Abnahme von sämtlichem Backwerk.

Zu Dank bin ich auch meinen Bachelor- und F-Praktiken verpflichtet, insbesondere Quirin J. AXTHAMMER, Tristan P. HARZER, J. Desiree STICHNOTH und Katharina SCHWINGHAMMER, die einen erheblichen Beitrag zu dieser Arbeit geleistet haben.

Meiner Familie und meinen Freunden danke ich für ihre tatkräftige Unterstützung, Sorgen für Ablenkung und das Ertragen meiner nicht immer extrem guten Laune. Pascal JESCHKE danke ich für die Hilfe diese ganzen Blätter in eine gebundene Form zu bringen.

[Major] Dr. F. Xaver STEEMANN danke ich für alles, vor allem, dass er es so lange nicht nur im Labor mit mir ausgehalten hat.

Abstract

Several hazardous compounds and pollutant effects are known to be released in the course of pyrotechnic applications. This thesis is focused on the development of new green and red light emitting pyrotechnic compositions. They should provide, in addition to a comparable or better color and combustion performance than that of the pyrotechnic formulations used, less smoke production as well as lower toxicity of the components and their combustion products. This was achieved by the employing of nitrogen-rich molecules and their salts to avoid the usage of barium nitrate and potassium perchlorate.

Potassium perchlorate is presumably the most widely used oxidizer in pyrotechnic compositions. In addition to its good oxidizing properties, it serves as chlorine donor, which is essential for the formation of the light emitting species SrCl, BaCl, and CuCl in the gas phase. SrCl emits mainly red light (661–675 nm), BaCl mainly green light (507–532 nm), and the thermally less stable CuCl emits blue light (420–452 nm, 476–488 nm). The toxic effect of perchlorates is based on the fact, that the ClO_4^- ion has a similar ionic radius like the I^- ion, which is essential for the production of thyroidal hormones in human beings. Hence, perchlorate is absorbed in place of iodide by the body and incorporated into the thyroid gland. Alternatives to potassium perchlorate might be other oxidizers, such as ammonium nitrate, potassium nitrate, ammonium dinitramide (ADN) or alkali metals salts of dinitramide anion. However, all these oxidizer do not contain chlorine, which makes an additionally chlorine source necessary. Barium nitrate, $\text{Ba}(\text{NO}_3)_2$, is used as coloring agent in green or white light emitting pyrotechnic compositions. It has coloring properties due to the barium cation and oxidizing properties due to the nitrate anion. However, it is highly water soluble and toxic. Therefore, barium nitrate should be replaced by less soluble barium salts. Furthermore, the use of any barium compound could be avoided, if copper compounds are used instead for generating a green illumination. However, no chlorine should be present to avoid the emission of blue light.

The concept for developing new pyrotechnic formulations is the use of triazoles and tetrazoles, whose high thermal stability along with their energetic character make them ideal precursor molecules for such compositions. In addition, their high nitrogen content guarantees low smoke production during combustion due to the formation of the gaseous products N_2 and CO_2 . Thus, several derivatives of 5-aminotetrazole (**5-At**) and the corresponding 5-nitriminotetrazoles were prepared, including: 1-(2-hydroxyethyl)-5-nitriminotetrazole (**1**), 1-(2-nitratoethyl)-5-nitriminotetrazole monohydrate (**2**), 1-(2-chloroethyl)-5-nitriminotetrazole (**3**), 1-carboxymethyl-5-aminotetrazole (**4**), 1-carboxymethyl-5-nitriminotetrazole monohydrate (**5**), 1- and 2-(2,3-dihydroxypropyl)-5-aminotetrazole (**6a/b**), 1-(2,3-dinitratopropyl)-5-nitriminotetrazolate monohydrate (**7**), 1- and 2-(2,3-dichloropropyl)-5-aminotetrazole (**8a/b**), and 1-(2,3-dichloropropyl)-5-nitriminotetrazole (**9**) (Figure 1).

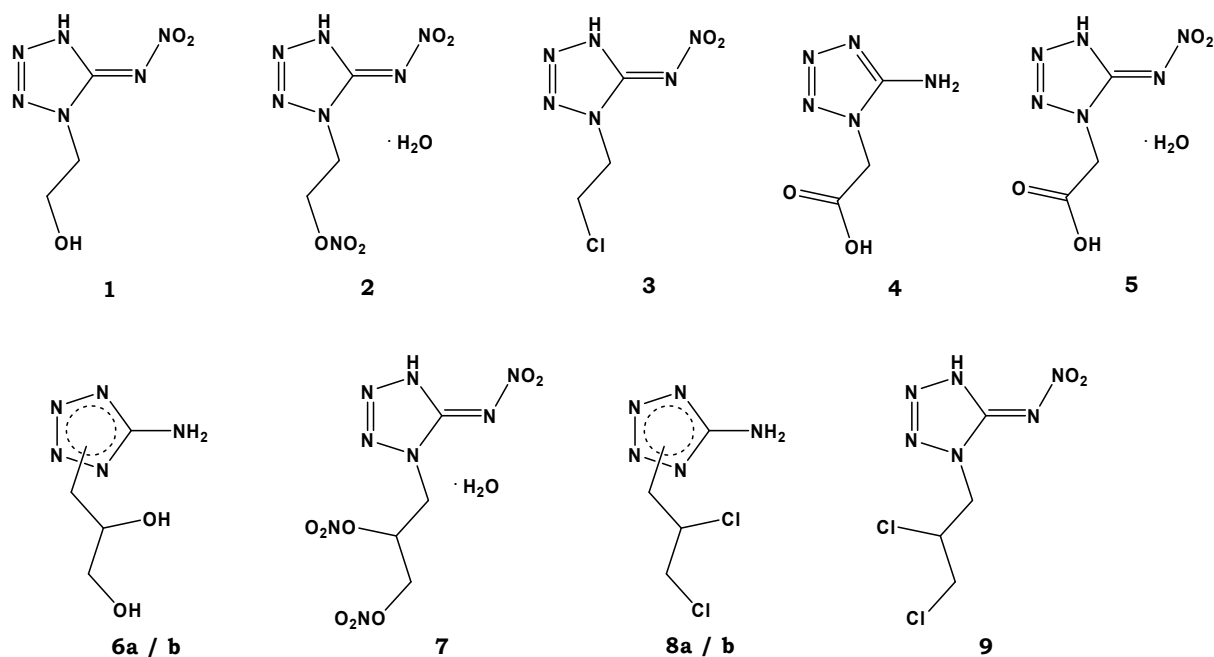


Figure 1 Chemical structures of compounds **1-9**.

In addition to a full characterization of these molecules the corresponding alkali metal and alkaline earth metal salts as well as copper(II) complexes were prepared. They were fully characterized and their sensitivities to mechanical and electric stimuli, thermal stability, and solubility in H₂O at ambient temperature were determined. Special attention was paid to the lithium, calcium, strontium, barium, and copper(II) salts with respect to their color performance and combustion properties. Unfortunately, the salts of **2** and **7** are very sensitive to impact and friction, thermally not very stable (< 200 °C) and combust too vigorously in the flame of a BUNSEN burner, which makes them useless as coloring agents. However, the water-free alkali metal salts **2_Na**, **2_K**, **2_Rb**, and **2-Cs** as well as **7_K** might find application as primary explosives. The best performance as neat compound have strontium 1-(2-chloroethyl)-5-nitriminotetrazolate monohydrate (**3_Sr**) and barium 1-(2-chloroethyl)-5-nitriminotetrazolate monohydrate (**3_Ba**). The pyrotechnically relevant salts of **9** also show good coloring and combustion properties. The barium salts of **1**, **4**, and **5** needed an additionally chlorine source (PVC) to produce a green flame. All tested salts had a good combustion behavior with low smoke production and a small amount of residues. Furthermore, all tested salts have a lower solubility in H₂O at ambient temperature than the corresponding nitrates, which are used in pyrotechnic compositions. The salts of **1**, **3**, **4**, and **5** are thermally very stable with decomposition temperatures above 200 °C and the salts of **4** and **5** are less sensitive to impact and friction.

Another topic dealt with the preparation of 1,2,4-triazole derivatives starting from 3-amino-1,2,4-triazole (**3-ATrz**). Thereby, 3-nitramino-1,2,4-triazole monohydrate (**10**), 3-nitro-1,2,4-triazole (**12**), 2-carboxymethyl-3-amino-1,2,4-triazole (**13**), and 2-carboxymethyl-3-nitrimino-1,2,4-triazole monohydrate (**14**) were prepared as well as some of their

alkali metal, alkaline earth metal salts and copper(II) complexes (Figure 2). All compounds were fully characterized.

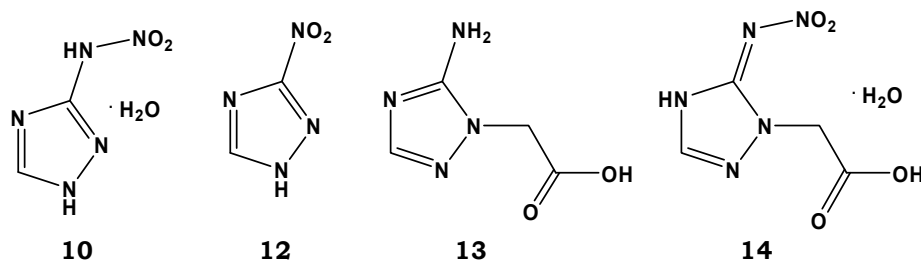


Figure 2 Chemical structures of compounds **10**, **12–14**.

In comparison to the salts of the corresponding tetrazole derivatives, the color performance and combustion behavior of the investigated triazole salts is worse. Nevertheless, they display a higher thermal stability, lower solubility in H₂O and are less sensitive to impact, friction, and electric discharge. Depending of the color performance, combustion behavior, and physico-chemical properties of pyrotechnic relevant salts, pyrotechnic compositions based on these salts could be investigated. Especially, the strontium salts of **10** and **13** are promising candidates as colorant agents.

Furthermore, several barium salts of tetrazole derivatives, barium tetrazolate (**BaTz**), barium 5-aminotetrazolate tetrahydrate (**BaAt**), barium bis(5-nitrimino-1*H*-tetrazolate) tetrahydrate (**Ba1HatNO₂**), barium 5-nitriminotetrazolate dihydrate (**BaAtNO₂**), barium 1-methyl-5-nitriminotetrazolate monohydrate (**Ba1MeAtNO₂**), and barium 2-methyl-5-nitriminotetrazolate dihydrate (**Ba2MeAtNO₂**), were prepared and investigated with respect to their applicability as coloring agent in green or white light emitting pyrotechnic compositions. For comparison the color performance of neat barium chloride dihydrate and barium nitrate, a mixture of both salts, and a mixture of PVC and barium nitrate was determined. The investigated barium salts, especially with anions containing a nitrimino group (**Ba1HAtNO₂**, **BaAtNO₂**, **Ba1MeAtNO₂**, and **Ba2MeAtNO₂**), might be a “greener” alternative in replacing barium nitrate in white or green light emitting pyrotechnic compositions. All offer a comparable or lower solubility than barium nitrate in H₂O at ambient temperature and show without chlorine a very intense white flame. Furthermore, they are insensitive or less sensitive to impact and friction. The barium salts **Ba1HAtNO₂** and **BaAtNO₂** could find further application, if sizzling sound effects are desired.

In the case of salts with convincing properties, their behavior as coloring agents was determined in several pyrotechnic compositions with different oxidizers and fuels. The performance of each composition is compared with formulations used today with respect to color emission, combustion velocity, smoke generation, amount of solid residues, thermal stability, and sensitivity to moisture as well as towards mechanical and electric stimuli.

The following pyrotechnic compositions were used as measures:

US Army red flare composition # M126 A1 (red parachute): 39 wt% $\text{Sr}(\text{NO}_3)_2$, 30 wt% Mg, 13 wt% KClO_4 , 8 wt% VAAR (Figure 3).

US Army composition # M125 A1 (green parachute): 50 wt% $\text{Ba}(\text{NO}_3)_2$, 30 wt% Mg, 15 wt% PVC, 5 wt% VAAR (Figure 3).

SHIMIZU's composition: 15 wt% Cu, 17 wt% PVC, 68 wt% KClO_4 , and 5 wt% Starch (Figure 3).



Figure 3 Controlled burn down of the pyrotechnic compositions M126 A1 (top, left), M125 A1 (top, right), and Shimizu's composition (down).

Pyrotechnic compositions of the salts **3_Sr**, **3_Ba**, **3_Cu_H₂O**, **4_Li**, **4_Sr**, **4_Ba**, **5_Sr1**, **5_Sr2**, **5_Ba1**, **5_Ba2**, **5_Cu_H₂O**, and **5_Cu_NH₃**, were investigated. Thereby, no potassium perchlorate was used, but other oxidizers such as potassium and ammonium nitrate, potassium and ammonium dinitramide (ADN), and potassium permanganate. Different fuels were tested, including magnesium, aluminum, magnalium, boron, and 5-aminotetrazole (**5-At**). The best performing compositions were made of **3_Sr**, **3_Ba**, **4_Sr**, **5_Sr2**, and **5_Ba2**. The use of ADN guaranteed a smoke reduced combustion. However, the compositions were thermally less stable (< 190 °C). Magnesium and aluminum were good fuels in combination with strontium or barium salts, however they increased the amount of smoke produced due to the formation of the solids MgO and Al₂O₃. The combination of copper(II) complexes with boron produced intense green flames, but also a huge amount of sometimes glowing residues.

Furthermore, the in literature described strontium salts: strontium tetrazolate pentahydrate (**SrTz**), strontium 5-aminotetrazolate tetrahydrate (**SrAt**), strontium 1-methyl-5-nitriminotetrazolate monohydrate (**Sr1MeAtNO2**), strontium bis(5-nitrimino-1*H*-tetrazolate) tetrahydrate (**Sr1HAtNO2**), strontium 5-nitriminotetrazolate monohydrate (**SrAtNO2**), and strontium 3,3'-bis(1,2,4-oxadiazol-5-onate) dihydrate (**SrOD**) and copper(II) complexes: diammine bis(tetrazol-5-yl)-aminato- $\kappa^2N1,N6$ copper(II) (**[Cu(bta)(NH₃)₂]**), bis{bis(tetrazol-5-yl)-amine- $\kappa^2N1,N6$ } copper(II) nitrate hemihydrate (**[Cu(H₂bta)₂](NO₃)₂**), diaqua bis(1-methyl-5-aminotetrazole-*N4*) copper(II) nitrate (**[Cu(1MeAt)₂(H₂O)₂](NO₃)₂**), diaqua tetrakis(1-methyl-5-aminotetrazole-*N4*) copper(II) nitrate (**[Cu(1MeAt)₄(H₂O)₂](NO₃)₂**), diammine bis(1-methyl-5-nitriminotetrazolato- $\kappa^2N4,O1$) copper(II) (**[Cu(1MeAtNO₂)₂](NH₃)₂**), bis[(triammine) μ_2 -(5-nitriminotetrazolato) copper(II)] (**[Cu(AtNO₂)(NH₃)₃]₂**), basic copper(II) nitrate (**Cu₂(OH)₃(NO₃)**), and tetrammine copper(II) dinitramide (**[Cu(NH₃)₄][N(NO₂)₂]₂**) were prepared and investigated with respect to their coloring and combustion properties in pyrotechnic compositions.

The salts **SrTz** and **Sr1MeAtNO2** were compared with a standard composition, containing strontium nitrate. Both offer higher spectral purity and average intensity, but a shorter burn time. **Sr1MeAtNO2** possesses the best properties with regard to high decomposition temperature, sensitivity to impact and friction, its behavior in the tested pyrotechnic compositions, and a low solubility in H₂O. The strontium salts **Sr1HAtNO2** and **SrAtNO2** could find application, if sizzling sound effects are desired. All strontium salts produced red light emitting pyrotechnic compositions even without an additional chlorine source. Further investigations of varying the ingredients or using other additives might result in even better formulations. Thus, it could be shown, that the substitution of potassium perchlorate with nitrogen-rich strontium salts is possible.

Static burn tests with **[Cu(bta)(NH₃)₂]**, **[Cu(1MeAt)₂(H₂O)₂](NO₃)₂**, and **[Cu(1MeAt)₄(H₂O)₂](NO₃)₂** were performed. All tested compounds combusted faster than the standard formulation. However, all showed a green flame. The burn time average intensity of all tested copper(II) complexes is lower than of the formulation used as standard. This is also true for the integrated intensity. The peak intensity of the standard is nearly twice that the other formulations. Worst color performance in pyrotechnic compositions showed the copper(II) complexes **[Cu(1MeAtNO₂)₂](NH₃)₂** and **[Cu(AtNO₂)(NH₃)₃]₂**. Also **Cu₂(OH)₃(NO₃)** could not convince as coloring agent. In combination with boron as fuel, **[Cu(NH₃)₄][N(NO₂)₂]₂** displayed the best results with respect to green color and smoke production. The addition of copper(I) iodide can improve the green light emission.

Concluding it can be said, that nitrogen-rich copper(II) complexes can be used as green colorants in pyrotechnic compositions and substitute barium nitrate. However, the combination with oxidizers and fuels is much more challenging compared to barium salts.

Points of concern are the very low decomposition temperatures of some of the investigated compositions as well as their high sensitivity to impact and friction. If these problems can be solved, nitrogen-rich copper(II) compounds are an environmentally more benign alternative to barium salts.

Table of Contents

Abstract		I
1	Introduction	1
1.1	Pyrotechnics	1
1.1.1	Historical	1
1.1.2	Components of a Pyrotechnic Composition	3
1.1.2.1	Fuels and Oxidizer	3
1.1.2.2	Binder	10
1.1.2.3	Colors	11
1.1.3	Flares	15
1.1.4	Safety	16
1.1.5	Environmental Aspects	17
1.1.5.1	Potassium Perchlorate	17
1.1.5.2	Barium Salts	18
1.1.5.3	Smoke	19
1.1.6	Requirements for New Coloring Agents	20
1.2	Nitrogen-rich Molecules	20
1.2.1	Application as High Energetic Materials	21
1.2.2	Tetrazoles	24
1.2.3	Triazoles	26
1.3	Concepts and Aims	27
1.4	Materials and Methods	28
1.4.1	Chemicals	28
1.4.2	Preparation of the Pyrotechnic Compositions	28
1.4.3	General Methods	29
1.5	References	31
2	Salts of 1-(2-Hydroxyethyl)-5-nitriminotetrazole	43
2.1	Results and Discussion	43
2.1.1	Syntheses	43
2.1.2	Molecular Structures	45
2.1.3	Energetic Properties	55
2.1.4	Flame Color and Combustion Behavior	60
2.2	Experimental Part	62
2.2.1	Neutral Precursor Molecules	62
2.2.1.1	1-(2-Hydroxyethyl)-5-aminotetrazole (1-OH)	62
2.2.1.2	2-(2-Hydroxyethyl)-5-aminotetrazole (2-OH)	62
2.2.1.3	1-(2-Hydroxyethyl)-5-nitriminotetrazole (1)	63
2.2.2	Preparation of the Salts	63
2.2.2.1	Lithium 1-(2-Hydroxyethyl)-5-nitriminotetrazolate Monohydrate (1_Li)	63
2.2.2.2	Sodium 1-(2-Hydroxyethyl)-5-nitriminotetrazolate (1_Na)	63
2.2.2.3	Potassium 1-(2-Hydroxyethyl)-5-nitriminotetrazolate (1_K)	64
2.2.2.4	Rubidium 1-(2-Hydroxyethyl)-5-nitriminotetrazolate (1_Rb)	65
2.2.2.5	Cesium 1-(2-Hydroxyethyl)-5-nitriminotetrazolate (1_Cs)	65
2.2.2.6	Magnesium 1-(2-Hydroxyethyl)-5-nitriminotetrazolate Octahydrate (1_Mg)	66

2.2.2.7	Calcium 1-(2-Hydroxyethyl)-5-nitriminotetrazolate Dihydrate (1_Ca)	66
2.2.2.8	Strontium 1-(2-Hydroxyethyl)-5-nitriminotetrazolate Dihydrate (1_Sr)	67
2.2.2.9	Barium 1-(2-Hydroxyethyl)-5-nitriminotetrazolate (1_Ba)	67
2.2.2.10	<i>trans</i> -[Diaqua-bis{1-(2-Hydroxyethyl)-5-nitriminotetrazolato- κ^2N_4,O_5 } Copper(II)] (1_Cu_H₂O)	68
2.2.2.11	Copper(II) 1-(2-Hydroxyethyl)-5-nitriminotetrazolate (1_Cu)	68
2.2.2.12	Tetrammine Copper(II) 1-(2-Hydroxyethyl)-5-nitriminotetrazolate (3_Cu_NH)	69
2.3	Conclusion	69
2.4	References	70
3	Salts of 1-(2-Nitratoethyl)-5-nitriminotetrazole Monohydrate	73
3.1	Results and Discussion	74
3.1.1	Syntheses	74
3.1.2	Comparison of the Constitutional Isomers 2 and 2a	76
3.1.3	Molecular Structures	78
3.1.4	Energetic Properties	86
3.1.5	Flame Color and Combustion Behavior	91
3.2	Experimental Part	92
3.2.1	Products after Nitration	92
3.2.1.1	1-(2-Nitratoethyl)-5-nitriminotetrazole Monohydrate (2)	92
3.2.1.2	1-(2-Nitratoethyl)-5-aminotetrazolium Nitrate (2a)	93
3.2.2	Preparation of the Salts	94
3.2.2.1	Lithium 1-(2-Nitratoethyl)-5-nitriminotetrazolate Monohydrate (2_Li)	94
3.2.2.2	Sodium 1-(2-Nitratoethyl)-5-nitriminotetrazolate (2_Na)	94
3.2.2.3	Potassium 1-(2-Nitratoethyl)-5-nitriminotetrazolate (2_K)	95
3.2.2.4	Rubidium 1-(2-Nitratoethyl)-5-nitriminotetrazolate (2_Rb)	95
3.2.2.5	Cesium 1-(2-Nitratoethyl)-5-nitriminotetrazolate (2_Cs)	96
3.2.2.6	Magnesium 1-(2-Nitratoethyl)-5-nitriminotetrazolate Hexahydrate (2_Mg)	96
3.2.2.7	Calcium 1-(2-Nitratoethyl)-5-nitriminotetrazolate Trihydrate (2_Ca)	97
3.2.2.8	Strontium 1-(2-Nitratoethyl)-5-nitriminotetrazolate Monohydrate (2_Sr)	97
3.2.2.9	Barium 1-(2-Nitratoethyl)-5-nitriminotetrazolate Monohydrate (2_Ba)	98
3.2.2.10	<i>trans</i> -[Diaqua-bis{1-(2-nitratoethyl)-5-nitriminotetrazolato- κ^2N_4,O_1 } Copper(II)] (2_Cu_H₂O)	98
3.2.2.11	<i>trans</i> -[Diammine-bis{1-(2-nitratoethyl)-5-nitriminotetrazolato- κ^2N_4,O_1 } Copper(II)] (2_Cu_NH₃)	99
3.3	Conclusion	99
3.4	References	100
4	Salts of 1-(2-Chloroethyl)-5-nitriminotetrazole	103
4.1	Results and Discussion	103
4.1.1	Syntheses	103
4.1.2	Molecular Structures	106
4.1.3	Energetic Properties	112
4.1.4	Flame Color and Combustion Behavior	115
4.1.5	Pyrotechnic Compositions	116
4.2	Experimental Part	121
4.2.1	Preparation of the Salts	121
4.2.1.1	Lithium 1-(2-Chloroethyl)-5-nitriminotetrazolate (3_Li)	121
4.2.1.2	Sodium 1-(2-Chloroethyl)-5-nitriminotetrazolate (3_Na)	122
4.2.1.3	Potassium 1-(2-Chloroethyl)-5-nitriminotetrazolate (3_K)	122
4.2.1.4	Rubidium 1-(2-Chloroethyl)-5-nitriminotetrazolate (3_Rb)	123

4.2.1.5	Cesium 1-(2-Chloroethyl)-5-nitriminotetrazolate (3_Cs)	124
4.2.1.6	Magnesium 1-(2-Chloroethyl)-5-nitriminotetrazolate Hexahydrate (3_Mg)	124
4.2.1.7	Calcium 1-(2-Chloroethyl)-5-nitriminotetrazolate Monohydrate (3_Ca)	125
4.2.1.8	Strontium 1-(2-Chloroethyl)-5-nitriminotetrazolate Monohydrate (3_Sr)	125
4.2.1.9	Barium 1-(2-Chloroethyl)-5-nitriminotetrazolate Monohydrate (3_Ba)	126
4.2.1.10	<i>trans</i> -[Diaqua-bis{1-(2-chloroethyl)-5-nitriminotetrazolato- $\kappa^2N4,O1$ } Copper(II)] Dihydrate (3_Cu_H₂O)	127
4.2.1.11	Copper(II) 1-(2-Chloroethyl)-5-nitriminotetrazolate (3_Cu)	127
4.2.1.12	<i>trans</i> -[Diammine-bis{1-(2-chloroethyl)-5-nitriminotetrazolato- $\kappa^2N4,O1$ } Copper(II)] (3_Cu_NH₃)	127
4.2.2	Pyrotechnic Compositions	128
4.2.2.1	Pyrotechnic Compositions Based on 3_Sr	128
4.2.2.2	Pyrotechnic Compositions Based on 3_Ba	130
4.2.2.3	Pyrotechnic Compositions Based on 3_Cu_H₂O	132
4.3	Conclusion	134
4.4	References	135
5	Salts of 1-Carboxymethyl-5-aminotetrazole and 1-Carboxymethyl-5-nitriminotetrazole	139
5.1	Results and Discussion	139
5.1.1	Syntheses	139
5.1.2	Molecular Structures	143
5.1.3	Energetic Properties	167
5.1.4	Flame Color and Combustion Behavior	174
5.1.5	Pyrotechnic Compositions	178
5.2	Experimental Part	191
5.2.1	Preparation of the Neutral Precursor Molecules	191
5.2.1.1	1-Carboxymethyl-5-aminotetrazole (4)	191
5.2.1.2	1-Carboxymethyl-5-nitriminotetrazole Monohydrate (5)	192
5.2.2	Salts of 1-Carboxymethyl-5-aminotetrazole (4)	193
5.2.2.1	Lithium 2-(5-Aminotetrazol-1-yl)-acetate Monohydrate (4_Li)	193
5.2.2.2	Sodium 2-(5-Aminotetrazol-1-yl)-acetate Trihydrate (4_Na)	193
5.2.2.3	Potassium 2-(5-Aminotetrazol-1-yl)-acetate (4_K)	194
5.2.2.4	Rubidium 2-(5-Aminotetrazol-1-yl)-acetate Monohydrate (4_Rb)	194
5.2.2.5	Cesium 2-(5-Aminotetrazol-1-yl)-acetate (4_Cs)	195
5.2.2.6	Magnesium 2-(5-Aminotetrazol-1-yl)-acetate Tetrahydrate (4_Mg)	196
5.2.2.7	Calcium 2-(5-Aminotetrazol-1-yl)-acetate Tetrahydrate (4_Ca)	196
5.2.2.8	Strontium 2-(5-Aminotetrazol-1-yl)-acetate Pentahydrate (4_Sr)	197
5.2.2.9	Barium 2-(5-Aminotetrazol-1-yl)-acetate Trihydrate (4_Ba)	197
5.2.2.10	Diaqua Copper(II) 2-(5-Aminotetrazol-1-yl)-acetate (4_Cu)	198
5.2.3	Salts of 1-Carboxymethyl-5-nitriminotetrazole Monohydrate (5)	198
5.2.3.1	Sodium 1-Carboxymethyl-5-nitriminotetrazolate Trihemihydrate (5_Na)	198
5.2.3.2	Potassium 1-Carboxymethyl-5-nitriminotetrazolate Monohydrate (5_K)	199
5.2.3.3	Rubidium 1-Carboxymethyl-5-nitriminotetrazolate Monohydrate (5_Rb)	199
5.2.3.4	Cesium 1-Carboxymethyl-5-nitriminotetrazolate Hemihydrate (5_Cs)	200
5.2.3.5	Magnesium 2-(5-Nitriminotetrazol-1-yl)-acetate Decahydrate (5_Mg1)	200
5.2.3.6	Magnesium 2-(5-Nitriminotetrazolate)-acetate Octahydrate (5_Mg2)	201
5.2.3.7	Calcium 1-Carboxymethyl-5-nitriminotetrazolate Dihydrate (5_Ca1)	201
5.2.3.8	Calcium 2-(5-Nitriminotetrazol-1-yl)-acetate Trihydrate (5_Ca2)	202
5.2.3.9	Strontium 1-Carboxymethyl-5-nitriminotetrazolate Monohydrate (5_Sr1)	202
5.2.3.10	Strontium 2-(5-Nitriminotetrazol-1-yl)-acetate Trihydrate (5_Sr2)	203

5.2.3.11 Barium 1-Carboxymethyl-5-nitriminotetrazolate Monohydrate (5_Ba1)	204
5.2.3.12 Barium 2-(5-Nitriminotetrazol-1-yl)-acetate Heptahemihydrate (5_Ba2)	204
5.2.3.13 <i>trans</i> -[Diaqua-bis(1-carboxymethyl-5-nitriminotetrazolato- <i>N</i> 4, <i>O</i> 1) Copper(II)] Dihydrate (5_Cu_H₂O)	205
5.2.3.14 Bis(diammine [2-(5-nitriminotetrazolato- <i>N</i> 4, <i>O</i> 1)-acetato- <i>O</i> 4] Copper(II); Trihydrate (5_Cu_NH₃)	205
5.2.4 Pyrotechnic Compositions	206
5.2.4.1 Pyrotechnic Compositions Based on 4_Li	206
5.2.4.2 Pyrotechnic Compositions Based on 4_Sr	208
5.2.4.3 Pyrotechnic Compositions Based on 4_Ba	212
5.2.4.4 Pyrotechnic Compositions Based on 5_Sr1	216
5.2.4.5 Pyrotechnic Compositions Based on 5_Sr2	217
5.2.4.6 Pyrotechnic Compositions Based on 5_Ba1	218
5.2.4.7 Pyrotechnic Compositions Based on 5_Ba2	219
5.2.4.8 Pyrotechnic Compositions Based on 5_Cu_H₂O	220
5.2.4.9 Pyrotechnic Compositions Based on 5_Cu_NH₃	223
5.3 Conclusion	226
5.4 References	227
6 Salts of 1-(2,3-Dichloropropyl)-5-nitriminotetrazole and its Precursor Molecules	231
6.1 Results and Discussion	231
6.1.1 Syntheses	231
6.1.2 Analytical Data of the Neutral Molecules	235
6.1.2.1 Spectroscopy	235
6.1.2.2 Molecular Structures	247
6.1.2.3 Energetic Properties	251
6.1.3 Analytical Data of the Salts of 7 and 9	254
6.1.3.1 Molecular Structures	254
6.1.3.2 Energetic Properties	256
6.1.3.3 Flame Color and Combustion Behavior	259
6.2 Experimental Part	261
6.2.1 Preparation of the Neutral Precursor Molecules	262
6.2.1.1 1-(2,3-Dihydroxypropyl)-5-aminotetrazole (6a) and 2-(2,3-Dihydroxypropyl)-5-aminotetrazole (6b)	262
6.2.1.2 1-(2,3-Dinitratopropyl)-5-nitriminotetrazole Monohydrate (7)	263
6.2.1.3 Potassium 1-(2,3-Dinitratopropyl)-5-nitriminotetrazolate (7_K)	264
6.2.1.4 Strontium 1-(2,3-Dinitratopropyl)-5-nitriminotetrazolate Monohydrate (7_Sr)	264
6.2.1.5 Barium 1-(2,3-Dinitratopropyl)-5-nitriminotetrazolate Monohydrate (7_Ba)	265
6.2.1.6 Diaqua 1-(2,3-Dinitratopropyl)-5-nitriminotetrazolato Copper(II) (7_Cu)	266
6.2.1.7 1-(2,3-Dichloropropyl)-5-aminotetrazole (8a)	266
6.2.1.8 2-(2,3-Dichloropropyl)-5-aminotetrazole (8b)	267
6.2.1.9 1-(2,3-Dichloropropyl)-5-nitriminotetrazole (9)	267
6.2.1.10 1-(2,3-Dichloropropyl)-5-nitriminotetrazole Monohydrate (9_H₂O)	268
6.2.2 Salts of 1-(2,3-Dichloropropyl)-5-nitriminotetrazole (9)	268
6.2.2.1 Lithium 1-(2,3-Dichloropropyl)-5-nitriminotetrazolate Dihydrate (9_Li)	268
6.2.2.2 Sodium 1-(2,3-Dichloropropyl)-5-nitriminotetrazolate Trihemihydrate (9_Na)	269
6.2.2.3 Potassium 1-(2,3-Dichloropropyl)-5-nitriminotetrazolate (9_K)	269
6.2.2.4 Rubidium 1-(2,3-Dichloropropyl)-5-nitriminotetrazolate (9_Rb)	270
6.2.2.5 Cesium 1-(2,3-Dichloropropyl)-5-nitriminotetrazolate (9-Cs)	270
6.2.2.6 Strontium 1-(2,3-Dichloropropyl)-5-nitriminotetrazolate Monohydrate (9_Sr)	271
6.2.2.7 Barium 1-(2,3-Dichloropropyl)-5-nitriminotetrazolate Monohydrate (9_Ba)	271

6.2.2.8	Diaqua 1-(2,3-Dichloropropyl)-5-nitriminotetrazolato Copper(II) (9_Cu_H₂O)	272
6.2.2.9	Diammine 1-(2,3-Dichloropropyl)-5-nitriminotetrazolato Copper(II) (9_Cu_NH₃)	272
6.3	Conclusion	273
6.4	References	274
7	Salts of 1,2,4-Triazole Derivatives	277
7.1	Results and Discussion	278
7.1.1	Syntheses	278
7.1.2	Analytical Data of the Precursor Molecules	281
7.1.2.1	Spectroscopy	281
7.1.2.2	Molecular Structures	282
7.1.2.3	Energetic Properties	286
7.1.3	Analytical Data of the Salts	288
7.1.3.1	Molecular Structures	288
7.1.3.2	Energetic Properties	297
7.1.3.3	Flame Color and Combustion Behavior	300
7.2	Experimental Part	303
7.2.1	Preparation of the Neutral Precursor Molecules	303
7.2.1.1	3-Nitramino-1,2,4-triazole Monohydrate (10)	303
7.2.1.2	3-Nitramino-1,2,4-triazole (11)	304
7.2.1.3	3-Nitro-1,2,4-triazole (12)	305
7.2.1.4	2-Carboxymethyl-3-amino-1,2,4-triazole (13)	305
7.2.1.5	2-Carboxymethyl-3-amino-1,2,4-triazolium Chloride (13_HCl)	306
7.2.1.6	2-Carboxymethyl-3-nitrimino-1,2,4-triazole Monohydrate (14)	306
7.2.2	Preparation of the Salts of the Triazole Derivatives	307
7.2.2.1	Salts of 3-Nitramino-1,2,4-triazole Monohydrate (10)	307
7.2.2.2	Salts of 3-Nitro-1,2,4-triazole (12)	310
7.2.2.3	Salts of 2-Carboxymethyl-3-amino-1,2,4-triazole (13) and 2-Carboxymethyl-3-nitrimino-1,2,4-triazole Monohydrate (14)	312
7.3	Conclusion	313
7.4	References	314
8	Barium Salts of Tetrazole Derivatives – Suitable Colorants?	319
8.1	Results and Discussion	319
8.1.1	Syntheses	319
8.1.2	Molecular Structures	321
8.1.3	Energetic Properties	324
8.1.4	Flame Color and Combustion Properties	327
8.2	Experimental Part	329
8.2.1	Barium Tetrazolate (BaTz)	329
8.2.2	Barium 5-Aminotetrazolate Tetrahydrate (BaAt)	330
8.2.3	Barium bis(5-Nitrimino-1 <i>H</i> -tetrazolate) Tetrahydrate (Ba1HAtNO₂)	330
8.2.4	Barium 5-Nitriminotetrazolate Dihydrate (BaAtNO₂)	331
8.2.5	Barium 1-Methyl-5-nitriminotetrazolate Monohydrate (Ba1MeAtNO₂)	331
8.2.6	Barium 2-Methyl-5-nitriminotetrazolate Dihydrate (Ba2MeAtNO₂)	332
8.3	Conclusion	333
8.4	References	333

9	Pyrotechnic Compositions Containing Nitrogen-rich Strontium Salts	337
9.1	Results and Discussion	337
9.1.1	Syntheses	337
9.1.2	Energetic Properties and Solubility in H ₂ O	338
9.1.3	Color Performance and Combustion Behavior	340
9.1.4	Pyrotechnic Compositions	340
9.2	Experimental Part	350
9.2.1	Preparation of the Strontium Salts	350
9.2.2	Pyrotechnic Compositions	353
9.2.2.1	Pyrotechnic Compositions based on Strontium Tetrazolate Pentahydrate (SrTz)	353
9.2.2.2	Pyrotechnic Compositions based on Strontium 5-Aminotetrazolate Tetrahydrate (SrAt)	354
9.2.2.3	Pyrotechnic Compositions based on Strontium 1-Methyl-5-nitriminotetrazolate Monohydrate (Sr1MeAtNO2)	356
9.2.2.4	Pyrotechnic Compositions based on Strontium bis(5-Nitrimino-1 <i>H</i> -tetrazolate) Tetrahydrate (Sr1HAtNO2)	358
9.2.2.5	Pyrotechnic Compositions based on Strontium 5-Nitriminoetrazolate Dihydrate (SrAtNO2)	360
9.2.2.6	Pyrotechnic Compositions based on Strontium 3,3'-Bis(1,2,4-oxadiazol-5-one) Dihydrate (SrOD)	361
9.3	Conclusion	364
9.4	References	364
10	Pyrotechnic Compositions Containing Nitrogen-rich Copper(II) Compounds	367
10.1	Results and Discussion	368
10.1.1	Syntheses	368
10.1.2	Energetic Properties and Solubility in H ₂ O	371
10.1.3	Color Performance and Combustion Behavior	372
10.1.4	Pyrotechnic Compositions	374
10.2	Experimental Part	391
10.2.1	Preparation of the Copper Compounds	391
10.2.2	Pyrotechnic Compositions	395
10.2.2.1	Pyrotechnic Compositions based on Diammine bis(Tetrazol-5-yl)-aminato- $\kappa^2N1,N6$ Copper(II) ([Cu(bta)(NH₃)₂])	395
10.2.2.2	Pyrotechnic Compositions based on Bis{bis(tetrazol-5-yl-ate)-amine- $\kappa^2N1,N6$ } Copper(II) Nitrate Hemihydrate ([Cu(H₂bta)₂](NO₃)₂)	406
10.2.2.3	Pyrotechnic Compositions based on Diaqua bis(1-Methyl-5-aminotetrazole- <i>N4</i>) Copper(II) Nitrate ([Cu(1MeAt)₂(H₂O)₂](NO₃)₂)	408
10.2.2.4	Pyrotechnic Compositions based on Diaqua tetrakis(1-Methyl-5-amino tetrazole- <i>N4</i>) Copper(II) Nitrate ([Cu(1MeAt)₄(H₂O)₂](NO₃)₂)	413
10.2.2.5	Pyrotechnic Compositions based on Diammine bis(1-Methyl-5-nitrimino tetrazolato- $\kappa^2N4,O1$) Copper(II) ([Cu(1MeAtNO₂)₂(NH₃)₂])	415
10.2.2.6	Pyrotechnic Compositions based on Bis(triammine) μ_2 -(5-Nitriminotetrazolato) Dicopper(II) ([Cu(AtNO₂)(NH₃)₃]₂)	418
10.2.2.7	Pyrotechnic Compositions based on Basic Copper(II) Nitrate (Cu₂(OH)₃(NO₃))	419
10.2.2.8	Pyrotechnic Compositions based on Tetrammine Copper(II) Dinitramide ([Cu(NH₃)₄][N(NO₂)₂]₂)	421
10.3	Conclusion	429
10.4	References	430
11	Résumé	435

Appendix	i
I Crystallographic Data of 2-OH and Salts of 1	i
II Crystallographic Data of 2 , 2a , and Salts of 2	iv
III Crystallographic Data of Salts of 3	vi
IV Crystallographic Data of 4 and its Salts	viii
V Crystallographic Data of 5 and its Salts	xi
VI Crystallographic Data of 6a , 6b , 7 , 9 , 9_H₂O and some Salts	xv
VII Crystallographic Data of 13 , 13_HCl , 14 and some Salts	xvii
VIII Crystallographic Data of Nitrogen-rich Barium Salts	xx
IX List of Abbreviations	xxi
X Curriculum Vitae	xxii
XI Full List of Publications	xxiv

1 Introduction

1.1 Pyrotechnics

The expression ‘pyrotechnics’ is derived from the Greek words ‘*pyros*’ (fire, heat) and ‘*techne*’ (art).^[1]

Pyrotechnics is defined as the science of compositions (mixtures of chemicals that include at least one oxidizer and fuel) capable of undergoing self-contained and sustained exothermic chemical reactions for the production of heat, light, gas, smoke, and/or sound. Pyrotechnics do not only include the manufacture of fireworks, but items such as safety matches, fire extinguishers, airbags, propellants, all kinds of flares, military counter-measures (acoustic and optic decoy devices), delusion devices, and igniters.

According to the German *Sprengstoffgesetz (SprengG) Abschnitt 1 Allgemeine Vorschriften* § 3 pyrotechnics are defined as follows:

“Pyrotechnische Sätze sind explosionsgefährliche Stoffe oder Stoffgemische, die zur Verwendung in pyrotechnischen Gegenständen oder zur Erzeugung pyrotechnischer Effekte bestimmt sind.”^[2]

„Pyrotechnische Gegenstände sind Gegenstände, die Vergnügungs- oder technischen Zwecken dienen und in denen explosionsgefährliche Stoffe oder Stoffgemische enthalten sind, die dazu bestimmt sind, unter Ausnutzung der in diesen enthaltenen Energie Licht-, Schall-, Rauch-, Nebel-, Heiz-, Druck- oder Bewegungswirkungen zu erzeugen.“^[2]

1.1.1 Historical

The use of chemicals to produce motion, heat, light, gas, smoke, and sound (pyrotechnics) is known for several thousand years. The birthplace of pyrotechnics is presumably China, several centuries BC. India could be the other possibility due to its natural deposits of saltpeter (potassium nitrate), the oxidizer in black powder.^[3] A description of another pyrotechnic item, bonfires like Solstice and Midsummer fires, can be found first in the literature of the 4th century AD.^[4] However, pyrotechnic compositions usually found military application, especially black powder. Black powder, also known as gun powder is a mixture of saltpeter, sulfur and charcoal in approximate proportions of 75 wt% (percent by weight) saltpeter, 12.5 wt% sulfur and 12.5 wt% charcoal. In the course of time the relative amounts of the components have varied. In particular, after it turned out that the increase of saltpeter increased the velocity of combustion. In the 15th century, it was found that the addition of a small amount of water caused the basic ingredients to cling together insuring a more homogeneous mixture, which offers more continuous burning and is longer storable than only blended black powder.

The use of black powder for military purposes was first recorded in 919.^[5] The knowledge of black powder and its military use disseminated gradually from China to Japan

and India then to the Orient and reached Europe in the 13th century. The today known names of firework articles 'Bengal Fire', 'Greek Fire' and 'Roman Candle' remember of this way of propagation.^[6] During the conquest of Mongolia by the Chinese in the 12th century rockets, containing as payload either fire compositions or sharp objects, and black powder as propellant, were widely-used.^[7] However, in the same period of time also the civil use of pyrotechnic compositions took place.^[8] The Arabs improved black powder for military use and the description of rockets appeared in Arab literature in 1258 for the first time. They adopted the rocket from Mongol invaders during the seventh Crusade and used it against the French army of King Louis IX in 1268.^[5] By the year 1300, rockets had found their way into European arsenals, reaching first France, then Italy and Germany about the year 1500, and later, England.

Two Europeans are intimately related to black powder: the English philosopher Roger BACON (1246–1294) and the German monk Berthold SCHWARZ (civil name: Konstantin ANCKLITZEN, † 1388, Figure 1.1). Both are often referred to be the inventor of black powder, whereas reinventor is more correct. By the way, black powder (in German: *Schwarzpulver*) was named after its black color caused by the charcoal and not as often wrongly assumed from the monk Berthold SCHWARZ.^[7]



Figure 1.1 Left: Copper engraving of the year 1640 with the title: "Des ehrwürdigen und sinnreichen Vatters Berthold SCHWARZ genannt, Franziskaner Ordens, Doctor, Alchemist und Erfinder der freien Kunst des Büchschenschiessens". Right: Monument of Bertold SCHWARZ in Freiburg im Breisgau.

Since the year 1350, black powder had become an effective weapon on the battlefield and had been the only explosive in wide use until the discovery of nitroglycerine in 1846 by SOBRERO in Italy, and NOBEL's work with dynamite, led to the development of a new generation of true high explosives. Furthermore, the development of modern smokeless powder, based on nitrocellulose and nitroglycerine, led a substitution of black powder as the

main propellant for guns. Although black powder has been replaced widely, it is important to recognize the important role it has played in modern civilization.^[9]

Apart from the military application, pyrotechnics were used only for entertainment (fireworks). Progress in both areas followed advances in modern chemistry and also industrialization, as new compounds were isolated and synthesized and became available. For example, the discovery of potassium chlorate by BERTHOLLET in the 1780's offered the ability to produce brilliant colored flames and color was added to the effects of sparks, noise, and motion.^[9] White light and bright sparks could be produced after the manufacturing of the metals magnesium and aluminum by electrolysis was possible in the late 19th century. During the 19th century also strontium, barium and copper compounds became commercially available and offered the ability of producing intense red, green, and blue flames; the beginning of modern pyrotechnic technology.^[9]



Figure 1.2 Picture of the fireworks on the occasion of the “Kaiserfest” in Cologne in 1897 (left), fireworks on the occasion of the opening of the Expo 2010 in Shanghai, China (right).

Besides the popular fireworks, which are part of the cultural heritage of many countries (Sylvester, Independence Day in USA, New Year’s celebration in Chinese culture) civilian applications of pyrotechnics are ranging from the common match to highway warning flares.^[9]

Today, pyrotechnics are also widely used by the military for signaling and training.

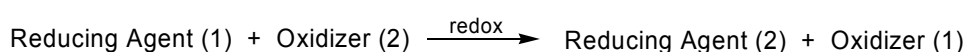
1.1.2 Components of a Pyrotechnic Composition

1.1.2.1 Fuels and Oxidizers

A pyrotechnic composition consists at least of an oxidizer and a fuel, because the exothermic reactions used in pyrotechnics are based on redox reactions. Of course, molecules which are both readily-oxidizable and readily-reducible exist, such as ammonium nitrate, ammonium perchlorate, lead azide, trinitrotoluene (TNT), nitroglycerine, and mercury fulminate ($\text{Hg}(\text{ONC})_2$). However, they are uncommon and usually have explosive properties, which is undesirable in pyrotechnic compositions.^[9] Furthermore, by mixing an oxidizer

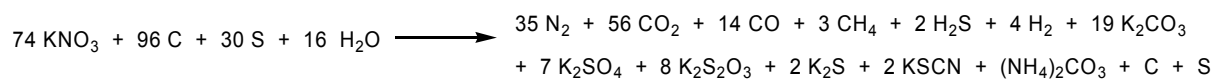
with a fuel it is possible to produce the desired, well-defined effects, such as reaction rate, heat of reaction, reaction temperature, gas production, reaction products, and colored light, needed for a particular application by varying the amounts of the components.^[10] Pyrotechnic compositions are only supposed to burn and not to explode. Therefore, the burning behavior, which is dependent upon several factors, must be controlled by the pyrotechnist. The oxygen, which is needed for the combustion of a pyrotechnic composition, is supplied by an oxygen-rich component (oxidizer) and not required from the presence of oxygen in the ambient air.^[11]

The pyrotechnic redox reaction is usually a solid-solid, solid-liquid or solid-gas state reaction, meanwhile the oxidizer is reduced and the reducing agent (fuel) is oxidized (Scheme 1.1). They take place in a temperature range of 1500–4000 °C.^[10]



Scheme 1.1 Principle of a redox reaction.

Unfortunately, the reaction products of a pyrotechnic redox reaction are usually not the expected according the classical chemistry theory. For example, the combustion reaction of the simple mixture black powder (75.7 wt% KNO₃, 11.7 wt% charcoal (C), 9.7 wt% sulfur (S), 2.9 wt% moisture (H₂O)) are approximated in Scheme 1.2.^[12]



Scheme 1.2 Combustion equation of black powder.

Different important parameters for chemicals used in pyrotechnic compositions must be available, such as purity, particle size, crystal structure (density), and water content.^[10]

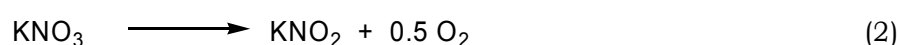
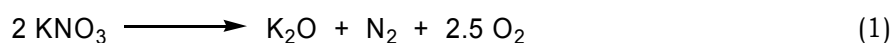
As oxidizers are usually oxygen-rich ionic solids used, which decompose at moderate-to-high temperatures and release gaseous dioxygen (O₂). Common are nitrates, perchlorates, and sometimes chlorates of alkali or alkaline earth metal salts as well as ammonium. An overview of some oxidizers and their physico-chemical properties is given in Table 1.1.

Table 1.1 Overview of the physico-chemical properties of some oxidizers.^[9, 10]

Formula	<i>M</i> [g/mol]	<i>ρ</i> [g/cm ³]	<i>M.p.</i> [°C] ^a	<i>T</i> _{dec} [°C] ^b	H ₂ O-sol. [wt%] ^c	grams of oxygen released per gram of oxidizer
NH ₄ NO ₃	80.0	1.73	170	> 170	65 (20 °C)	0.60 (total 0)
NaNO ₃	85.0	2.26	307	> 380	74 (20 °C)	0.47
KNO ₃	101.1	2.11	334	> 400	24 (20 °C)	0.40
Sr(NO ₃) ₂	211.6	2.99	370	> 370	40 (20 °C)	0.38
Ba(NO ₃) ₂	261.4	3.24	592	> 550	8.3 (20 °C)	0.31
NH ₄ ClO ₄	117.5	1.95	–	210	19 (20 °C)	≈ 0.28
KClO ₄	138.6	2.52	–	> 400	1.8 (20 °C)	0.46
KClO ₃	122.6	3.32	356	> 400	6.8 (20 °C)	0.39
BaO ₂	169.4	4.96	450	795	–	0.09
PbO ₂	239.2	9.38	–	290	insoluble	0.13 (total 0)
Pb ₃ O ₄	685.6	9.53	–	> 500	insoluble	0.093 (total 0)
BaCrO ₄	253.4	4.50	–	–	0.3 (16 °C)	0.095
PbCrO ₄	323.2	6.12	–	844	insoluble	0.074

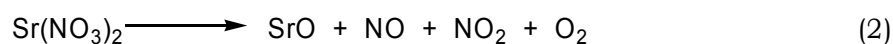
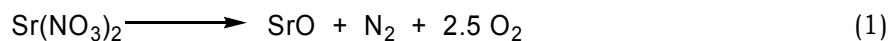
a) Melting point, b) Decomposition temperature c) Solubility in H₂O (H₂O temperature).

Nitrates decompose at higher temperatures than perchlorates and are therefore usually combined with a metal fuel. Potassium nitrate is the most used oxidizer with the nitrate anion. It offers several advantages: it has a very weak flame color, is not hygroscopic, can be ignited easily, is available at very low costs, and is very stable to outer stimuli.^[9] Furthermore, it has an high active oxygen content (39.6 %) and decomposes at high temperature according to Scheme 1.3 (1). This reaction is strongly endothermic with $\Delta_c H^\circ = 316 \text{ kJ/mol}$ and therefore potassium nitrate must be combined with a high energy-output fuel (metals) to achieve rapid burning rates. Combined with other fuels the decomposition might stop at the formation of potassium nitrite (Scheme 1.3 (2)).



Scheme 1.3 Decomposition equations of potassium nitrate.

Strontium nitrate is usually combined with another oxidizer in red flame pyrotechnic compositions. It is slightly hygroscopic and commercially available. It decomposes near its melting point according to Scheme 1.4 (2). Thereby, strontium nitrite is formed as an intermediate and can be found in the ash of mixtures with a low flame temperature.^[9]



Scheme 1.4 Decomposition equations of strontium nitrate.

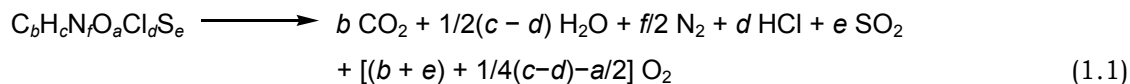
If the reaction temperature is higher, strontium nitrate decomposes according to equation 1, because this reaction is very endothermic ($\Delta_c H = 385 \text{ kJ/mol}$) and corresponds to an active oxygen content of 37.7 %. However, little ash-like residues are produced by this reaction, especially with magnesium as fuel.

Barium nitrate is non-hygroscopic and used as main oxidizer in white flame pyrotechnic compositions. Potassium perchlorate is added, if a green flame should be achieved. Barium nitrate decomposes analog to strontium nitrate at low as well as high temperatures (with 30.6 % available oxygen). The high melting point of barium nitrate (592 °C) is responsible for higher ignition temperatures than to potassium nitrate or potassium perchlorate based compositions.

Details about potassium perchlorate can be found in chapter 1.1.5.1.

The efficiency of an oxidizer in a mixture (or the oxidizing performance of a molecule) can be determined with the oxygen balance (Ω). It is determined according to combustion equation of the molecule or composition (equation 1.1) and calculated according to equation 1.2.^[13] It reflects the (theoretical) ability of a system to be oxidized completely: A negative oxygen balance ($\Omega < 0 \%$) indicates a system in which unburned fuel is left behind or that requires atmospheric oxygen for complete combustion. If $\Omega = 0$, a stoichiometric mixture of reducing atoms and oxidizing atoms exists and the fuel is oxidized completely. A positive

oxygen balance ($\Omega > 0$ %) indicates a system in which there is an excess of oxygen for the combustion of the fuel. The exact oxygen balance can only be obtained, if the exact reaction equation is used, which requires a fundamental, experimentally based understanding of all of the chemical reactions taking place.



$$\Omega = [(aO - 2bC - 1/2(c - d)H - 2eS) \cdot 1600] / M \quad (1.2)$$

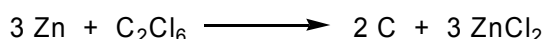
(a : number of oxygen atoms, b : number of carbon atoms, c : number of hydrogen atoms, d : number of chlorine atoms, e : number of sulfur atoms, M : molecular weight)

Besides the above mentioned redox systems using oxygen as oxidizing species, different redox pairs can be used in pyrotechnics. They are based on metals and halogenated organic compounds or polymers. One famous mixture are MTV (magnesium/Teflon®/Viton®) compositions that decompose according to Scheme 1.5.^[14] They usually find application in aerial countermeasures, tracking flares, propellants, signaling applications, and incendiary devices.^[15] Besides Teflon®, other poly(carbon monofluorides) ((CF)_n, also known as graphite fluoride) and magnesium^[16] or other fuels (such as, boron, titanium, silicon or Si alloys) can be combined.^[17]



Scheme 1.5 Redox equation of a MTV composition.

Another widely used redox pair is the so-called BERGER mixture. It is used for the generation of dense, gray smoke with the fuels zinc, aluminum or zinc oxide, in combination with hexachloroethane.^[9] The produced smoke consists of zinc chloride aerosols (Scheme 1.6).



Scheme 1.6 Redox equation of a BERGER mixture.

Several compounds can be used as fuels (reducing agent, electron donor). The variety ranges from metal fuels, such as magnesium, aluminum, magnalium (alloy of Mg and Al, 50:50, MgAl), iron, copper, zinc, and zirconium to non-metallic fuels, including charcoal, sulfur, red and white phosphorus, boron, silicon as well as organic materials, such as starch.^[9, 18] In Table 1.2 an overview of the most common metallic and non-metallic fuels and their properties is given. During the reaction of the released oxygen of the oxidizer heat is produced, which offers the opportunity of producing and varying effects, such as color, motion, light, or noise. Depending on pyrotechnic application different properties are required. In the following only the requirements for colored flame compositions are mentioned.

A high reaction temperature is necessary for a maximum light intensity, but the color quality depends upon proper emitters in the gas phase. That is only guaranteed, if the amount of solid and liquid particle is low, because they emit a broad spectrum of 'white' light.^[9]

Table 1.2 Properties of some metallic and non-metallic fuels.^[9]

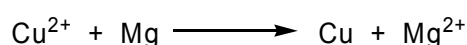
Formula	<i>M</i> [g/mol]	ρ [g/cm ³]	<i>M.p.</i> [°C] ^a	<i>T_b</i> [°C] ^b	combustion product	grams of fuel consumed per gram of O
Al	27.0	2.7	660	2467	Al ₂ O ₃	1.12
Cu	63.5	8.92	1085	2927	CuO	3.97
Fe	55.8	7.87	1535	2750	Fe ₂ O ₃	2.32
Mg	24.3	1.74	649	1107	MgO	1.52
MgAl	–	–	460	–	MgO/Al ₂ O ₃	1.32
Ti	47.9	4.50	1660	3287	TiO ₂	1.50
W	183.8	19.32	3410	5660	WO ₃	3.83
Zn	65.4	7.14	420	970	ZnO	4.09
Zr	91.2	6.52	1852	4377	ZrO ₂	2.85
B	10.8	2.46	2300	2550	B ₂ O ₃	0.45
C	12.0	2.26	dec.	–	CO ₂	0.38
P _{red}	31.0	2.2	590	sublimes	P ₄ O ₁₀	0.78
P ₄	124.0	1.83	44	–	P ₄ O ₁₀	0.78
Si	28.1	2.33	1410	2355	SiO ₂	0.88
S	32.1	2.07	119	445	SO ₂	1.00

a) Melting point, b) Boiling temperature.

A good metallic fuel is insensitive to moisture and oxidation by air, offers a high heat output per gram, and is available at moderate costs in defined fine particle sizes. The appropriateness of a metallic fuel can be examined by its standard potential. A large, negative value implies a readily oxidizable material.

An excellent and widely used fuel is the very reactive metal magnesium. It has a heat of combustion of 5.9 kcal/g and a low boiling point of 1107 °C, which enables excess magnesium in a mixture to vaporize and react with oxygen in the air, providing additional heat. However, neat magnesium is so reactive that it can be oxidized by moist air, forming magnesium hydroxide (Mg(OH)₂), and it reacts easily with all acids, also boric acid and even the ammonium ion. Therefore, the combination of magnesium with ammonium perchlorate or other ammonium salts should be avoided except the metal surface is coated with an oil, like paraffin or a similar material.^[9] Furthermore, in the presence of moisture, chlorate as well as perchlorate salts are able to oxidize magnesium without previous initiation, which is a storage problem. This problem does not occur with nitrate salts.^[19]

Unfortunately, magnesium is also able to react with other metal ion, especially in a moist environment. For example, it reduces Cu²⁺ ions according to Scheme 1.7. The standard potential of the Cu²⁺/Mg pair is +2.72 V indicating a spontaneous effect.



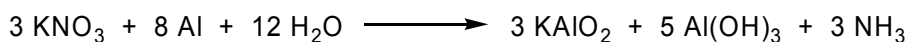
Scheme 1.7 Redox reaction between Mg and Cu²⁺, if H₂O is present.

Therefore, reducible metal ions, such as Cu²⁺ and Pb²⁺, as well as water must be avoided in magnesium containing compositions.

An alternative might be magnalium (MgAl), a 50:50 alloy of magnesium and aluminum. According to SHIMIZU it is a material of a solid solution of Al_3Mg_2 in Al_2Mg_3 , with a melting point of $460\text{ }^\circ\text{C}$.^[19] It offers the stability advantage that it reacts much more slowly than magnesium metal with weak acids. Furthermore, magnalium is more stable than aluminum metal in combination with nitrate salts. Besides that it can be used in fireworks items to produce attractive white sparks, ‘crackling’ effects as well as a branching spark effect with a black powder-type composition.^[19]

Aluminum is probably the most widely used metallic fuel, because of its lightweight, low costs and it is available in a variety of particle sizes and shapes. Depending on the shape (spheres yield the minimum surface area and hence minimum reactivity) and size of the aluminum particles, the kind of application is different. For example, atomized aluminum, rather than the more reactive flake material, is used by the military for heat and light-producing compositions and so called ‘flitter’ aluminum (large flakes) are widely used by in fireworks to produce bright white sparks.^[9] Aluminum has a higher heat of combustion with 7.4 kcal/g than magnesium. Furthermore, its boiling point of almost $2500\text{ }^\circ\text{C}$ is much higher. Aluminum has a more reactive surface than magnesium and is readily oxidized by oxygen in air, forming a protective coating of aluminum oxide (Al_2O_3). Thereby, the particle core of aluminum metal is protected from further oxidation and aluminum powder can be stored for extended periods with little loss of reactivity due to air oxidation.^[9]

Pyrotechnic compositions containing aluminum as fuel are usually quite stable. However, if the mixture contains a nitrate oxidizer, moisture must be excluded. Otherwise, a reaction of the nitrate salt and aluminum metal takes place (Scheme 1.8), as mentioned above.



Scheme 1.8 Reaction of aluminum metal and potassium nitrate in a wet medium.

During this reaction evolving heat and ammonia gas is produced. Autoignition of such compositions is possible, because the reaction is accelerated by the alkaline medium. This can be inhibited by a small quantity of a weak acid such as boric acid by neutralizing the alkaline products and maintaining a weakly acidic environment. Moisture and the hygroscopicity of the oxidizer play a key role in this decomposition process. For example, sodium nitrate can not be combined with aluminum, unless the aluminum powder is coated with a protective organic layer, due to its hygroscopicity. Compositions containing potassium nitrate and aluminum must be kept quite dry in storage, but mixtures of aluminum and non-hygroscopic barium nitrate can be stored, as long as the composition does not actually get wet. Mixtures of magnesium metal with nitrate salts do not have this decomposition problem, because the formation of a magnesium hydroxide coating on the metal surface protects it from further reaction. Aluminum hydroxide (Al(OH)_3) does not offer this protection, because it is soluble in alkaline medium.^[9]

Besides metallic fuels, several readily-oxidized nonmetallic elements have found application in the field of pyrotechnics. Their requirements are the same of metallic fuels, such as stability to air and moisture, good heat-per-gram output, and availability for low costs.

Sulfur is one fuel in black powder and has been used as fuel for several hundred of years. In pyrotechnic compositions usually 'flour of sulfur', a material that has been crystallized from molten sulfur is preferred. If sulfur is purified by sublimation, it is named 'flowers of sulfur'. However, it often significant amounts of oxidized, acidic impurities are present, which can be quite hazardous, especially in mixtures containing a chlorate salt.^[20] Although sulfur has a comparable low heat output (2.2 kcal/g), it can function as a 'tinder' or fire starter, because of its low melting point of 119 °C. Therefore, it can react exothermically with several oxidizers at low temperatures and this heat output can be used to trigger other reactions with better fuels and the presence of sulfur, even in small percentage, has a drastically affect of the ignitibility and ignition temperature. Sulfur combusts to sulfur dioxide and to sulfate salts (compare Scheme 1.2). Sulfur can also be reduced to the sulfide ion (S^{2-}) and therefore act as oxidizer. However, when sulfur is added in large excess, it can volatilize out of the burning mixture as yellowish-white smoke.

Another elemental fuel is boron. It offers a high heat output (14.0 kcal/g) due to its low atomic weight (10.81 u). When it is combined with a high-melting oxidizer, ignition can be hard, because of the high melting point (2300 °C) of boron. This can be avoided by the use of low-melting oxidizers, such as potassium nitrate, yielding good heat production. However, the low melting point of the combustion product (boron oxide, B_2O_3) can prohibit high reaction temperatures.^[21] Furthermore, boron is a quite expensive fuel, but usually only a small amount is required. It finds particularly application as fuel in igniter and delay compositions for military and aerospace applications.^[9]

Silicon is in many ways similar to boron. It is a safe, has a high melting point (1410 °C), but relatively inexpensive fuel used in igniter and delay compositions. Remarkable is the oxidation product, silicon dioxide (SiO_2), because it is high melting and environmentally acceptable.^[9]

A variety of organic (carbon-containing) compounds are common fuels. Through the production of carbon dioxide (CO_2) and water vapor during their combustion, these fuels are able to produce a significant gas pressure, besides their generation of heat. Depending on the amount of present oxygen, the carbon atoms are oxidized to CO_2 with an oxygen-sufficient atmosphere or otherwise to carbon monoxide (CO) or elemental carbon. If the amount of carbon is large (can be observed as carbon black), it can influence the flame color negatively (see black body radiation, chapter 1.1.2.3). The hydrogen atoms in organic compounds are reacted to gaseous water molecules using oxygen. Therefore, if the fuel contains oxygen atoms, the amount of oxygen that must be provided by the oxidizer can be reduced. Hence, hydrocarbons – contains only carbon and hydrogen –will require more

moles of oxygen for complete combustion than will an equal weight carbohydrate or other oxygen-containing compound.

Carbohydrates, a large number of its organic compounds occur naturally, can also serve as fuel. The simplest carbohydrates are 'sugars' and have molecular formulas fitting the pattern $(\text{CH}_2\text{O})_n$. Small deviations can be found of the more complex members. The simpler sugars are preferred as fuels, because they can be obtained in high purity at moderate cost, and toxicity problems carry no weight. They usually combust with a colorless flame and give off less heat per gram than less-oxidized organic fuels.

Common sugars are glucose ($\text{C}_6\text{H}_{12}\text{O}_6$), lactose ($\text{C}_{12}\text{H}_{22}\text{O}_{11}$), and sucrose ($\text{C}_{12}\text{H}_{22}\text{O}_{11}$). Starch is a polysaccharide, consisting of glucose units linked together by α -1,4 and α -1,6 glycosidic bonds. Its molecular formula of starch can be described as $(\text{C}_6\text{H}_{10}\text{O}_5)_n$, and its molecular weight is greater than one million. It can be divided into smaller units by the reaction with acids. Dextrin is partially-hydrolyzed starch and widely-used as fuel and binder. However, its molecular weight, solubility, and chemical behavior can vary substantially from supplier to supplier and from batch to batch. In combination with potassium chlorate lactose is used in some colored smoke mixtures.

Other organic fuels are for example nitrocellulose, polyvinyl alcohol, stearic acid, hexamethylenetetramine, kerosene, epoxy resins, and unsaturated polyester resins such as Laminae.

1.1.2.2 Binder

Besides the oxygen balance, type of chemical or active surface, one important parameter that influence the performance of a redox reaction in pyrotechnic is the homogeneity. The more homogeneous a mixture is the higher is its reaction rate. Homogeneity can be achieved by mixing the different components of a pyrotechnic composition, which should have similar grain sizes. In addition an increase of the degree closeness of the reactive particles enhances the reactivity, because pyrotechnic reactions are usually solid-solid reaction.^[10] This can be provided by the usage of a binder. It prevents the segregation of the different components, provides mechanical stability and can decrease the sensitivity to moisture to some extent.^[18] Both, the type of the binder and the content, influence the reaction rate and less the heat of reaction.^[10] Several binders are common, the choice is depending on the other components. Furthermore, the selected binder should provide good homogeneity with the use of a minimum of polymer. Organic materials react as fuels and reduce the flame temperatures of compositions containing metallic fuels and decrease reaction rates.^[9, 10] Furthermore, they can influence the color purity negatively, if incomplete combustion of the binder occurs. A binder need to be neutral and non-hygroscopic to avoid the problems that water and an acidic or basic environment can introduce. Two different kinds of binder can be distinguished: non-energetic binders, which can be dissolved in water (such as dextrin, polyvinyl alcohol, or Arabic rubber) or are organic-solvents-based (such as vinyl alcohol acetate resin (VAAR), polymethyl

methacrylate,^[22] or other organic polymers). Also binders, such as epoxy binders or Laminac® ^[23] (an unsaturated polyester with styrene crosslinks), which binds upon addition of a catalyst whose application does not provide a solvent exist. Energetic binders (e.g. glycidyl azide polymer (GAP), polynitropolyphenylene, or nitrocellulose) contribute energy to the reaction. However, their reactive functional groups (azido, nitrate, nitro, and hydroxy residues) can lead to undesired reactions with the components.^[24]

1.1.2.3 Colors

The visible spectrum is depicted in Figure 1.3. The human eye is able to see colors in a range of 400 nm to 700 nm. If light is emitted in a particular wavelength, it is called monochromatic.

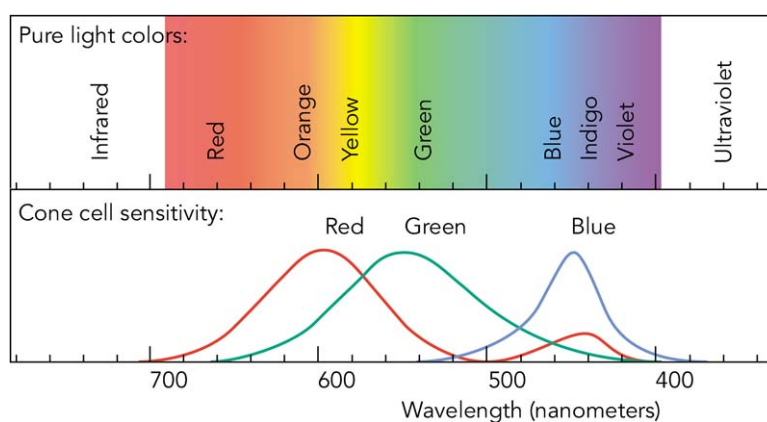


Figure 1.3 Visible spectrum.^[25]

In general, the colored light generated pyrotechnically is not monochromatic, because it usually contains light emitters which emit outside the desired spectral range. Light emitters, which are responsible for the pyrotechnic light emission, can be divided in two main categories: solid state emitters (black body radiation) and gas phase emitters (atoms and molecules). Due to the fact, that black- or better grey-body emitters are not able to produce anything but shades of orange and yellow, gas phase emitters are responsible for the colors observed in pyrotechnics.

To produce color, a color-emitting species and heat, which is usually gained from the reaction between an oxidizer and a fuel, are required. The released light energy depends on the difference of the energy levels (ΔE). The difference is unique for each element. The color is determined by the energy of the emitted photons, which determines their characteristic wavelength (λ) (see equation 1.3). This results in the specific flame color.

$$\Delta E = h \cdot c / \lambda = h \cdot \nu \quad (1.3)$$

c = speed of light (299 792 458 m/s)

h = PLANCK constant ($6.62606896 \cdot 10^{-34}$ Js)

λ = wavelength

ν = frequency

Some elements are even named after the color of their observed spectral lines, such as cesium (*caesius*, lat.: sky blue), rubidium (*rubidus*, lat.: dark red) and indium (indigo).

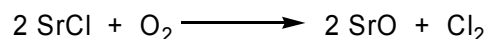
Several elements and their compounds are able to emit visible light. However, only a few are used in pyrotechnical applications (Table 1.3).

Table 1.3 Emitted wavelengths of atomic and molecular emitters of the usually used compounds in pyrotechnics.^[4, 9, 25, 26]

Element	Emitting species	λ [nm]	Color
lithium	atomic Li	670.8	red
		460	blue
		413, 427	violet
		497	bluish-green
sodium	atomic Na	589.0, 589.6	yellow
calcium	CaCl	591–599	yellow
	CaCl	603–608	orange
strontium	SrCl	661.4, 662.0, 674.5, 675.6	red
	SrCl	623.9, 636.2, 648.5	orange
	SrCl	393.7, 396.1, 400.9	violet
	SrOH	605.0, 646.0	orange
	SrOH	659.0, 667.5, 682.0	red
	atomic Sr	460.7	blue
barium	BaCl	507, 513.8, 516.2, 524.1, 532.1	green
	BaCl	649	red
	BaOH	487	greenish-blue
	BaOH	512	green
	BaO	604, 610, 617, 622, 629	orange
	atomic Ba	553.5	green
	atomic Ba	660	red
copper	CuCl	420–452	violet-blue
	CuCl	476–488	blue
	CuOH	525–555	green
	CuO	610–660	red

In general, sodium salts are used to achieve a yellow luminescence, strontium salts a red, barium salts a green, and copper compounds a blue one. Strontium nitrate is the most common used coloring agent in red-light emitting pyrotechnic compositions. Besides its coloring properties, it is a good oxidizer. However, it is not able to produce the molecular emitter strontium monochloride (SrCl), which is besides strontium monohydroxides (SrOH) responsible for an intense red flame.^[9] Therefore, some chlorine donors, like polyvinyl chloride (PVC) and other chlorine-rich organic compounds or the oxidizer potassium perchlorate are added. This is true for green light emitting compositions containing barium as well as blue light emitting compositions based on copper compounds. Furthermore, the monochlorides of calcium, strontium, barium, and copper (CaCl, SrCl, BaCl, and CuCl) are volatile, which ensures a sufficient concentration of emitters in the gas phase even at lower temperatures.^[9] According to SHIMIZU, chlorine donors react in magnesium-containing composition with the formed MgO, which is a powerful grey body emitter, whose

incandescent glow reduce the color purity significantly.^[19] Another widely used strontium salt is strontium carbonate, especially in slow burning compositions. However, only small amounts can be used, because of its inert anion CO_3^{2-} . Strontium chloride, which is available commercially, is too hygroscopic for pyrotechnic applications. Furthermore, it must be avoided that the molecular emitter SrCl is oxidized in the flame according to the following reaction scheme:



Scheme 1.9 Oxidation of SrCl in an oxygen-rich flame.

This reaction can be minimized, if the mixture offers a negative oxygen balance (Ω).

The same problem is of concern with the green-light emitter BaCl. The in an oxygen-rich flame formed molecular emitter barium oxide (BaO) emits in the orange and yellowish-green region and therefore, reduces the color purity. Furthermore, BaCl decomposes, if the flame temperature rises too high. Therefore, the amount of metal fuels, especially magnesium and aluminum must be held to a minimum. Otherwise a brilliant white light emission, from a combination of MgO and BaO is achieved. The addition of chlorine-containing organic fuels is essential, if a green-light emission with barium salts is desired. They not only serve as chlorine donors, but also lower the combustion temperature.^[9]

The most challenging flame color to obtain is blue. The best emitter in the blue region of the visible spectra is the molecular species copper monochloride (CuCl). However, it is only able to be formed under very specific conditions. CuCl is unstable in an oxygen-rich flame and at temperatures above 1200 °C, it decomposes to the molecular emitters copper monohydroxides (CuOH) and copper oxide (CuO). CuO emits in the red region and a reddish seam, where sufficient oxygen from the atmosphere is present, is often observed at flames of copper containing compositions.^[19] CuOH is a green-light emitter, which can overpower the blue-light emission.^[9] Furthermore, chlorine donors are even more essential for the emission of blue light, because only CuCl is able to emit in this region. Usually, potassium perchlorate, ammonium perchlorate or potassium chlorate is used as oxidizer. They offer the ability of releasing oxygen at low temperature and contain chlorine. Copper(II) perchlorate and chlorate are too sensitive to outer stimuli for an application. However, chlorine-free compositions are able to produce green flames and are therefore an alternative for the usage of barium salts. The copper compounds copper(II) oxide, basic copper(II) carbonate and copper(II) sulfate pentahydrate are usually used in blue flame compositions. Until several years ago the very toxic compound copper(II) acetoarsenite ($\text{Cu}(\text{C}_2\text{H}_3\text{O}_2)_2 \cdot 3\text{Cu}(\text{AsO}_2)_2$) – also known as Paris green – was widely used, because it produces an intense blue flame.^[9]

The D-line emission of atomic Na at 589 nm is so strong and excited so easily that impurities of sodium compounds should be strictly prevented. On the other hand, many sodium compounds are quite hygroscopic, such as the also oxidizing salts sodium nitrate, sodium chlorate or perchlorate, which makes them useless as coloring agents in pyrotechnic

compositions. In general, sodium oxalate and cryolite (Na_3AlF_6) are used. Although the emission intensity of atomic Na increases, if the temperature is raised, there is an upper limit of temperature, which should be avoided, because of the ionization of sodium atoms to sodium ions.^[9]

Potassium compounds, which emit with weak atomic lines in the violet region and do not interfere with most colors, can be used as oxidizers and should serve as educt in metathesis reactions for the preparation of calcium, strontium or barium salts.

Rarely used are compounds of boron (green), lithium (red), and calcium (orange-red). Especially boric esters are able to emit light in the green region, but it is also reported that boron combusts in the presence of oxygen under the formation of the boron oxides B_2O_3 , BO_2 in the gas phase.^[27] Therefore, a possible application of boron compounds as barium substitutes is thinkable and some investigations of pyrotechnic compositions with boric acid as coloring agent were performed. They offer a good color purity, with the main molecular gas phase emitter BO_2 , and can be used as indoor green flame fireworks.^[28] Another study investigated the products of boron/alkali-metal nitrate mixtures with an infrared emission alkali-metal metaborates, B_2O_3 (g), BO (g), and B_2O_2 (g).^[29] Also the use of trimethyl borate in green flame military signaling flares was investigated.^[30]

Besides strontium, lithium compounds can be used as coloring agent in red flame pyrotechnic compositions.^[31] Remarkable is the low molecular weight of lithium (6.941 g/mol), but many of its salts are hygroscopic and typically more soluble in H_2O than the corresponding strontium salts (an exception are fluorides and hydroxides). Furthermore, the concentration of the atomic emitter Li in the gas phase is much more temperature dependent than the one of atomic Na or K. According to calculation of DOUDA, the concentration of atomic Li in flames decreases with lowering the temperature from 3000 K to 1200 K.^[32] However, its application as oxidizer (as nitrate, dinitramide, nitroformate, chlorate, perchlorate, iodate, and peroxide salt) or as fuel (elemental, as hydrides or lithium boride).^[31b] A promising application of elemental lithium is as coloring agent in MTV (magnesium/Teflon®/Viton®)-like pyrotechnics as infrared (aerial) decoys and lithium hydride as a gas generator in acoustic (naval) decoys.^[31b]

The elements rubidium and cesium as well as their compounds offer a bluish-violet flame in the BUNSEN burner flame. They emit mainly in the far red (rubidium) and near infrared (cesium: 852.1 nm and 894.3 nm) region. Especially their nitrates are used in technical or military application, where infrared radiation is requested.^[33]

Other light emitting elements in the visible region are gallium (violet), lead, arsenic, antimony, selenium (pale blue), indium (bluish-violet), europium, radium (red), molybdenum (pale green), and thallium as well as tellurium (green). However, they are either too toxic or their compounds are too expensive to find a commercial application as coloring agents in pyrotechnic compositions.

1.1.3 Flares

A flare, also known as fusee, is a kind of pyrotechnic device that produces a brilliant color and/or intense heat during combustion of a pyrotechnic composition.^[34] They can be used in civilian and military applications for signaling, illumination, or defense counter-measures. Flares can be projectile pyrotechnics, ground pyrotechnics, or parachute-suspended to provide a low combustion velocity with a maximum illumination over a large area. They are developed by handheld percussive tubes or flare guns, except decoy flares. The primary needed colors are green, red, yellow, and white. Some formulations are listed in Table 1.4.

Table 1.4 Typical Compositions of Pyrotechnic Flares (the amount of the component is given in percent by weight [wt%]).^[18, 35, 36, 37]

Component	Mk 124: Red Navy Flare	Mk 117: Green Navy Flare	Mk 118: Yellow Navy Flare	Red Highway Flare	White Flame Formulation
Magnesium	24.4	21.0	30.3	–	–
Potassium perchlorate	20.5	32.5	21.0	6.0	–
Strontium nitrate	34.7	–	–	74.0	–
Barium nitrate	–	22.5	20.0	–	55.0
Potassium nitrate	–	–	–	–	25.0
Sodium oxalate	–	–	19.8	–	–
PVC	11.4	12.0	–	–	–
Copper powder	–	7.0	–	–	–
Asphalt	9.0	–	3.9	–	–
Sulfur	–	–	–	10.0	20.0
Binder	–	5.0	5.0	10.0	–

The visible spectra of standard U.S. Navy red, green and yellow signal flares were investigated by WEBSTER.^[37] Among others, they are based on potassium perchlorate as oxidizer, magnesium as fuel as well as the coloring agents strontium nitrate and barium nitrate and sodium oxalate, respectively.^[37] Besides the typically used components, the naval flares contain usually calcium phosphide (Ca_3P_2), which liberates in contact with water phosphine that self-ignites in contact with air.

In civil field of application, flares are usually used as signal, fired as an aerial signal or ignited on the ground (Figure 1.4). They are commonly found in marine survival kits as well as roadside emergency kits. In forestry and firefighting they find application as igniter of controlled burns in fire suppression.^[34] Also misuse of flares occurs, especially during soccer games of hardcore supporter groups (Figure 1.4).



Figure 1.4 Signal flares: maritime distress signal (left), misuse during a soccer game (right).

Another kind of flares, which is used in military aircraft as a defense counter-measure against heat-seeking missiles are decoy flares. They emit mainly in the infrared and are usually based on MTV compositions.

1.1.4 Safety

In the course of manufacturing or handling pyrotechnics, several fires and grave injuries occur annually, affecting victims' extremities, thorax, face, eyes, and hearing.^[35, 38] Therefore, the preparation of pyrotechnic components or compositions should be performed only by well-trained specialists, with proper safety measures and on a reasonably small scale. Nevertheless, the usual 'trial and error' strategy can be extremely hazardous in pyrotechnic experiments. One reason is the incompatibility of several chemicals in a formulation. Some are listed in Table 1.5.

Table 1.5 Incompatible, potentially hazardous combinations of several compounds used pyrotechnic compositions.^[35, 39]

Compound	Chlorates	Perchlorates	Aluminum	Magnesium	Zinc
ClO ₃ ⁻	NA ^a	- ^b	X ^c	X	X
ClO ₄ ⁻	-	NA	? ^d	?	-
Al	X	?	NA	-	-
Mg	X	?	-	NA	-
Zn	X	-	-	-	NA
Acids	X	-	-	X	-
Water	-	-	?	X	?
NH ₄ ⁺	X	-	-	X	-
Cu ²⁺	?	-	? ^e	X ^e	X ^e
S	X	X	-	X	X
S ²⁻	X	X	-	-	-

a) NA: not applicable, b) -: little if any hazard, c) X: significantly hazardous combination, d) ?: potentially hazardous combination, depending on the circumstances, e) requires the presence of traces of H₂O.

Furthermore, technical-grade chemicals usually contain impurities in the percent range, which possibly increase the sensitivity of a mixture and make its behavior extremely unpredictable. For example, the 'infamous' mixture of sodium chlorate and sugar causes severe injuries every year, because sodium chlorate is used in the form of an impure total

herbicide.^[35] Pyrotechnic compositions that are manufactured on an industrial scale also need to be regarded as potentially hazardous and must be handled with utmost care.

Most pyrotechnic compositions show a very high sensitivity to friction and electric discharge. In several cases the electrostatic charge of a human being suffices to ignite a pyrotechnic composition.^[10] For example, black powder is more sensitive to friction and impact than most other conventional secondary explosives (such as TNT or nitropenta), and above all, black powder is extremely sensitive to electric discharge. Therefore, grinding and homogenization of black powder need to be performed in a moistened state.^[35]

1.1.5 Environmental Aspects

Health aspects in pyrotechnics are not restricted to injuries by accidental ignition or incorrect handling. Fireworks and pyrotechnics are also environmental polluters (beyond noise).^[18, 35] Several hazardous substances are released upon explosion, deflagration or burning of the pyrotechnics, including both reaction products and unburned constituents of a pyrotechnic mixture. In addition, during the manufacturing process the dispersion of hazardous chemicals is possible. For example, several years after closing, perchlorate contamination beneath a former flare manufacturing plant in California was first discovered in 2000.^[34] An aerial firework disperses the pollutants over a large area. In other cases, such as handheld military flares, inhalation of toxic combustion products, which exhibits a severe health threat, is of more concern. However, the development and investigation of environmentally more benign products are of importance. The growing number of scientific articles in recent years in this topic (focusing on environmental analyses as well as on syntheses of new energetic compounds) demonstrates this.^[18, 35, 40, 41, 42] However, the preparation and investigation of potentially more environmentally benign pyrotechnic substances and compositions is very challenging. Furthermore, new products have to compete with the low cost of traditional formulations.

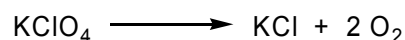
Several hazardous compounds and pollutant effects are known to be released in the course of a pyrotechnic application. Only the most important hazards regarding this thesis are summarized and discussed below.

1.1.5.1 Potassium Perchlorate

As mentioned above, potassium perchlorate is presumably the most widely used oxidizer in pyrotechnic compositions. It is labeled as oxidizing (O) and harmful (Xn) in Germany (and according to NFPA 704: health: 1, flammability: 0, reactivity: 1, Ox).

Potassium perchlorate has replaced potassium chlorate, which is more sensitive and reactive, as oxidizer and chlorine donor in pyrotechnic compositions over the last years. Potassium chlorate is less stable, because of its lower melting point (356 °C) and more exothermic decomposition. Although compositions containing potassium perchlorate are less sensitive to heat, friction and impact than those made with potassium chlorate, special

precautions must be taken, especially static protection. For example, mixtures of perchlorate and a metal fuel such as aluminum can have explosive properties, especially when present in bulk quantities and when confined.^[9] However, potassium perchlorate offers many advantages, it is non-hygroscopic, commercially available and offers an active oxygen content of 46.2 %, one of the highest available to the pyrotechnician.^[9] It decomposes at high temperatures to potassium chloride and gaseous oxygen according to Scheme 1.10 with a heat output of -0.68 kcal/g.



Scheme 1.10 Decomposition of potassium perchlorate.

Therefore, potassium perchlorate is widely used to produce colored flames (especially in combination with barium and strontium nitrate), noise (with aluminum, in 'flash and sound' mixtures), and light (in photoflash mixtures with magnesium).^[9]

Usually, perchlorates are emitted in the form of not or not fully combusted pyrotechnic devices or during the manufacturing process. Although potassium perchlorate is less soluble in H₂O at 20 °C (1.8 wt%) and hence should be not such an economic problem. However, perchlorates are regarded to be persistent in nature and to accumulate in waters and groundwater, what several studies demonstrate.^[34, 43, 44] The toxic effect of perchlorates is that the ClO₄⁻ ion (1.85 Å^[45]) has a similar ionic radius like the I⁻ ion (2.06 Å^[46]), which is essential for the production of thyroidal hormones in human beings. Hence, perchlorate is mistaken for iodide by the body and taken up into the thyroid gland. The long-term consumption of perchlorate-contaminated water may thus fill the thyroid gland with useless perchlorate and consequently competitively block any iodine uptake by the thyroid gland can lead to hypothyroidism.^[47] This is harmful to adults, but it gravely effects the development of fetuses. Therefore, perchlorate is generally regarded as teratogenic. The biodegradation of perchlorate by microorganisms has been object of intense research.^[48]

Alternatives to potassium perchlorate might be the use of other oxidizer, such as ammonium nitrate, potassium nitrate, ammonium dinitramide (ADN) or alkali metals salts of dinitramide. However, all these oxidizer do not contain chlorine, which makes an additionally chlorine donor necessary (in red (with strontium salts), green (with barium salts), and blue (with copper compounds) light emitting compositions). Furthermore, all of them have several different less positive properties, like sensitivity to humidity or much higher or lower decomposition temperatures and a less oxygen release.^[9, 18] However, all of them are less toxic compared to potassium perchlorate.

1.1.5.2 Barium Salts

Pyrotechnic devices are also closely associated to the emission of heavy metal aerosols.^[49, 50] Besides lead aerosols, the emission of soluble barium salts and aerosols is a

cause of concern.^[18, 35, 50] Their inhalation has cardiotoxic and bronchoconstrictor effects, which emerge as an asthmatic symptom.^[51] Several decades ago the coincidence of fireworks events and the suddenly increasing number of patients with chronic respiratory diseases was observed.^[52] Sulfur dioxide has been suspected as the chemical mainly responsible for this, but the possible interrelationship between respiratory effects and barium-rich aerosols could be detected in a recently published study.^[50]

In pyrotechnic compositions the most common barium salt is barium nitrate, used as both oxidizer and coloring agent. It is declared as oxidizing (O) and harmful (Xn) in Germany (NFPA 704: health: 3, flammability: 0, reactivity: 3) and its median lethal dose (LD₅₀) is 355 mg/kg for rats (oral). Symptoms of poisoning include tightness of muscles, muscular tremors, vomiting, diarrhea, abdominal pain, labored breathing, cardiac irregularity, and convulsions.^[53] Death may result from cardiac or respiratory failure, and usually occurs a few hours to a few days following exposure to the compound. Barium nitrate may also cause kidney damage. Its solubility increases by increasing the H₂O temperature (4.7 wt% at 0 °C, 8.3 wt% at 20 °C, 9.5 wt% at 25 °C, 25.7 wt% at 100 °C).^[53]

Especially the H₂O solubility plays a key role in the toxicity of barium compounds. As mentioned above barium nitrate as well as barium chloride (BaCl₂, H₂O-sol.: 26.4 wt% at 20 °C) and barium carbonate (used as rodenticide) are pretty good soluble and very toxic, whereas barium sulfate (BaSO₄) with a H₂O solubility of 2.4·10⁻⁴ wt% is used clinically as a radiocontrast agent for X-ray imaging and other diagnostic procedures. Therefore, barium nitrate could be replaced by lower soluble barium salts. Furthermore, the use of any barium compound can be avoided, if copper compounds for generating a green illumination are used instead. However, no chlorine needs to be present to avoid the emission of blue light.

1.1.5.3 Smoke

Smoke is strictly defined as a mixture of solid particles and gas. Smoke is a multifaceted problem in pyrotechnics, except in cases, where the generation of smoke is a desired effect (several, also colored, smoke compositions are known). It is caused primarily by the combustion products of the fuels, which are traditionally carbon or metal-based. The produced smoke clouds the air and reduces the color illumination due to its particles, which are usually black body emitter. However, besides its negative influence of the color performance, it also causes health problems, beyond the irritation of the performers' and technicians' as well as the spectators' eyes and noses. Several studies have investigated the release of inhalable particulate matter (PM) from fireworks and possible resulting health threats.^[54] Two studies performed in Germany (Mainz and Leipzig in 2000 and 2006) verified a dramatic increase of the PM concentration compared to average ambient conditions following firework displays.^[54b-c] During the Diwali festival in India in 2009 a significant increase in PM 2.5 (< 2.5 μm in diameter) was remarked – probably an effect of the fireworks.

Pyrotechnics are also productive sources of gaseous pollutants.^[49, 54c] Although these are less persistent than heavy metals, they inconvenience the spectators and aerial

fireworks additionally the general population under unfavorable wind conditions. The main gaseous pollutants are carbon oxides (CO and CO₂), nitrogen oxides (NO_x), and sulfoxides (SO_x). The sulfur content of black powder is the main source of SO_x. Less significant in contribution to this pollution are sulfides, which are occasionally used as fuels. NO_x are formed by the decomposition of nitrates and result from the oxidation of ambient nitrogen (N₂) at the high temperatures reached during the combustion of metallic fuels. A statistically significant number of adults was observed to suffer chronic respiratory diseases (asthma) under the influence of firework pollution in an earlier study.^[52] This is in good agreement with another study that reported an increase in the number of asthma patients by about 12 % in the course of the Diwali festival.^[41]

Therefore, it is essential to reduce the smoke as well as the amount of gaseous pollutants. The Walt Disney Company pioneered new technology for reducing the smoke production of their daily fireworks in the U.S. and Europe. They are using environmentally benign compressed air instead of black powder to launch fireworks.^[55] Another alternative might be the use of nitrogen-rich molecules (see chapter 1.2).^[18]

1.1.6 Requirements for New Coloring Agents

Novel developments in pyrotechnics focus on the application of environmentally more benign components in pyrotechnic compositions to primarily avoid perchlorates and heavy metals and reduce the smoke production. Therefore, new coloring agents should possess, besides a comparable or even better color performance and combustion behavior than used compounds, a lower toxicity as well as less or nontoxic combustion products. Their further properties should be high decomposition temperatures (> 200 °C), long-term stability, good performance per gram, and a smoke and residue free combustion. Furthermore, they should be not or less sensitive to impact, friction, and electric discharge as well as moisture, low soluble in H₂O, and compatible to other used compounds, such as oxidizers and fuels. In addition, to compete with known compounds, the new coloring agents need to be cheap, easy to synthesize from low cost starting materials in large amounts, and obtained in high yields.

1.2 Nitrogen-rich Heterocycles

High-nitrogen contents are desirable for reduction of smoke and particulate matter. In contrast to conventional energetic materials, nitrogen-rich compounds do not derive their energy from oxidation of a carbon backbone or a fuel, but rather from high heats of formation due to their large number of inherently energetic N–N and C–N bonds.^[56] They combine several advantages, such as the formation of mostly gaseous products (important for a smoke-less combustion), high flame temperatures, high propulsive power, and high specific impulse.^[57] Heterocyclic-based compounds have beside higher heats of formation, a

higher density, and better oxygen balance than their carbocyclic analogs and therefore have most often been used as energetic materials. When these energetic heterocycles can be deprotonated, the formation of highly energetic salts, such as nitrate, dinitramides or picrates, is possible. The combination of high-nitrogen cations and anions is another expanding area of interest. The salts have the advantage of higher densities and lower vapor pressures than non-ionic molecules.

For pyrotechnics, these nitrogen-rich materials could be used as propellants, coloring agents, and fuels.

1.2.1 Application as High Energetic Materials

Pyrotechnics are only one subgroup of the scientific field of energetic materials, besides propellants and high explosives. High explosives can be further distinguished in primary and secondary explosives. Further classifications can be found in Figure 1.5.^[58]

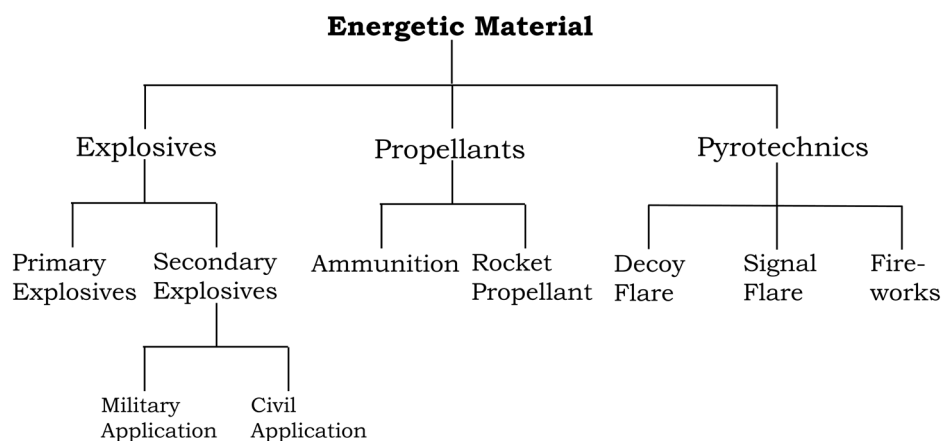


Figure 1.5 Classification of energetic materials.^[58]

Primary explosives are very sensitive explosives and their ignition by friction, impact, electric discharge or heat is very easy. The primary explosive offer quite fast deflagration to detonation process with a shock wave formed, which is able to initiate secondary explosives. The common detonation velocities between 3500 m/s and 5500 m/s are much slower than the detonation velocities of secondary explosives.

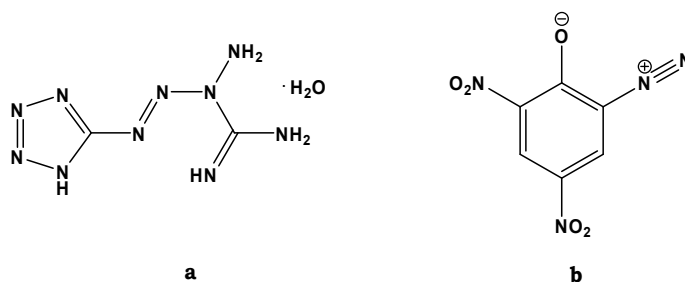


Figure 1.6 Molecular structures of tetracene (a) and 2-diazo-4,6-dinitrophenole (b).

Common primary explosives are lead(II)azide and lead(II)stypnate, cadmium(II)azide or mercury fulminate, which were partly replaced by new less toxic primary explosives based on organic, metal free compounds such as tetracene and 2-diazo-4,6-dinitrophenole (Figure 1.6). The replacement of the toxic cations with less toxic metals like silver^[59], iron^[60] or copper^[61] is another topic of current interest.

The main differences between the secondary explosives and the primary explosives are the high thermal and physical stability of the secondary explosives as well as their higher detonation velocities (5500–10000 m/s). In contrast to primary explosives, the ignition of secondary explosives by friction, impact, electric discharge or heat is more difficult, due to their high stability towards physical and thermal stimuli. Instead they are initiated by the shockwave of primary explosives as mentioned above. Some common secondary explosives are depicted in Figure 1.7.^[58]

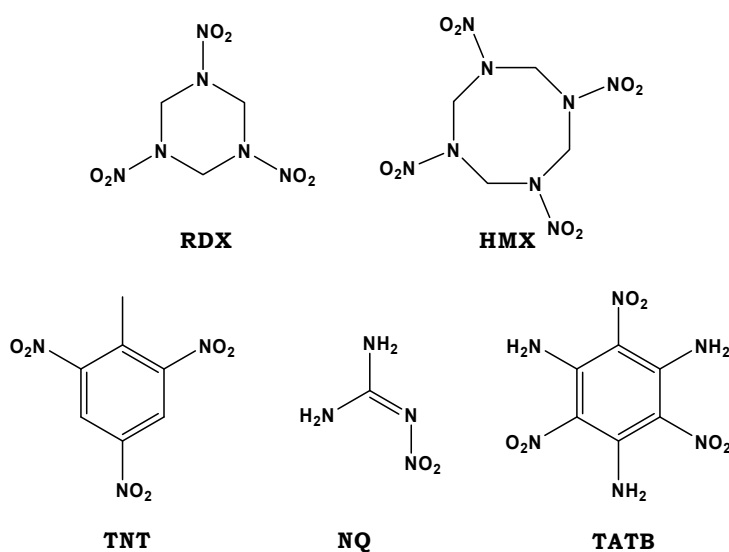


Figure 1.7 Secondary explosives: RDX (1,3,5-trinitro-1,3,5-triazacyclohexane), HMX (octahydro-1,3,5,7-tetranitro-1,3,5,7-tetrazocine), TNT (2,4,6-trinitrotoluene), NQ (2-nitroguanidine), and TATB (1,3,5-triamino-2,4,6-trinitrobenzene).

Important values for the characterization of a secondary explosive are the detonation pressure (p_{C-J} , [kbar]) and velocity (D , [mm/ μ s]). Both values depend on the density (ρ_0) as well as the heat of explosion (Q), and are calculated according equation 1.4 and 1.5, respectively.^[62]

$$p_{C-J} = K \rho_0^2 \Phi \quad (1.4)$$

$$D = A \Phi^2 (1 + B \rho_0) \quad (1.5)$$

$$\Phi = N (M_g Q)^{1/2} \quad (1.6)$$

constants: $K = 15.88$; $A = 1.01$; $B = 1.30$

N = molar quantity of released gases per gram explosive

M_g = mass of gases per mol gas [g]

The detonation pressure and the heat of explosion are both dependent of the density, thus compounds with a high density are of interest. The density can also be influenced by pressing the explosive material (limited by the physical stability of the compound) or by the functional groups of the explosive compound. For example, it is known that nitro groups and large planar aromatic structures increase the density.

The burning rate of the chemical compound determines whether it burns, deflagrates or detonates.^[63] Thereby, the confinement of the material, besides its properties, can be determining, how the compounds decompose. For example, unconfined TNT just burns, whereas confined TNT detonates.^[64] This behavior can be explained by the burning velocity v_b (equation 1.7).

$$v_b = \beta p^a \quad (1.7)$$

β = coefficient (temperature dependent)

a = index, determines the pressure dependency of the burning velocity

p = pressure

Index a is < 1 for the deflagrating energetic materials and > 1 for the detonation of explosives.^[58] If the pressure rises due to the confinement of the energetic material and the formed gases, v_b rises and could reach supersonic velocities resulting in a detonation (never the opposite way).^[58] This transition is termed as Deflagration-to-Detonation-Transition (DDT). A DDT or a direct ignition can cause an explosion.^[65] The DDT takes place, when a weak ignition source is applied. Thereby, the deflagration of the energetic material accelerates the burning rate itself to supersonic velocities by the release of a huge amount of energy and a high rate of gas generation.^[64] The detonation can also be initiated immediately.^[65] Thereby, the direct initiation or shock to detonation transition takes place, if a sufficiently strong shockwave is applied causing the reaction to couple with the shockwave. The shockwave hitting the explosive material leads to a compression of the material that is heated by the resulting adiabatic heat evolution and the temperature rises above the decomposition point. Due to the decomposition of the explosive material, the shockwave is accelerated by the decomposition of the explosive material up to a certain velocity resulting in a detonation.^[58]

In contrast to primary and secondary explosives, propellants should deflagrate and are not meant to detonate. Propellants can be distinguished in their field of application, either as propelling charge for ammunition or as rocket propellant. Propellants used in propelling charges for ammunition need low burning temperatures and the decomposition products should not contain corrosive gases. The specific impulse (I_{sp}) of the compound depends on the burning temperature according equation 1.8. Therefore, the development of propelling charges for ammunition is a challenging field of research.

$$I_{sp} = \sqrt{\frac{2\gamma RT_c}{(\gamma - 1)M}} \quad (1.8)$$

γ = ratio of the specific heat capacity of the gas mixture

R = ideal gas constant (8.3145 J/mol K)

T_c = temperature in the burning chamber [K]

M = average molecular weight [mol/kg]

The first propellant used for ammunition was black powder, but it is no longer used in ammunition charges, due to its corroding combustion products. Nowadays, propellants used in ammunition are usually based on nitrocellulose, because the advantageous ratio of oxygen to carbon leads to a residue-free burning of the compound. It is prepared by the nitration of cellulose with nitrosulfuric acid. If nitrocellulose is used as chief explosive ingredient, it is called single based. In order to improve the specific impulse, double based and triple based propellants were developed, combining nitrocellulose with other explosives. Double based propellants such as nitrocellulose and nitroglycerin compositions possess an enhanced performance, but unfortunately accompanied by a higher erosion of the gun barrel. This can be avoided by triple based propellants, consisting of nitrocellulose, nitroglycerin and nitro guanidine. Whereas the single based propellant nitrocellulose is sufficient for ammunition of guns and pistols, the double and triple based propellants are used in tank and naval artillery ammunition.^[58]

In contrast to guns or cannons, rockets are fired usually only once (fire- and forget weapon systems). Therefore, the erosion of the rocket engine is of less importance, but compounds with a high specific impulse are desired. When the specific impulse is raised by 20 s, the cargo carried by the rocket can be doubled.^[58] Rocket propellants can be divided into solid and liquid propellants. Solid propellants can be ammonium perchlorate/aluminum mixtures, stabilized by a binder (composite propellants), or double based propellants (nitrocellulose and nitroglycerin). Liquid propellants consist of mixtures of an oxidizer and a fuel (bipropellant, e.g. nitric acid / monomethylhydrazine) or hydrazine (monopropellant), which is decomposed catalytically. The propelling charges burn much faster than rocket propellants. As a result, the pressure formed during the decomposition of the rocket propellant (70 bar) is much lower than the pressure formed by the propelling charges (up to 4000 bar).^[58]

1.2.2 Tetrazoles

Tetrazoles are unsaturated five-membered heterocycles containing four nitrogen atoms in the ring. Compared to heterocycles with less nitrogen atoms in the ring system, like imidazole or triazole, tetrazole has the highest heat of formation with 237.2 kJ/mol.^[66] The unsubstituted molecule 1*H*-tetrazole (**1H-Tz**, CH₂N₄) has a nitrogen content of almost 80 wt%. Its deprotonated ring system is aromatic and thus relatively stable. The tetrazole

ring can be varied by different substituent and thus influence its properties. Some tetrazole derivatives are depicted in Figure 1.8.

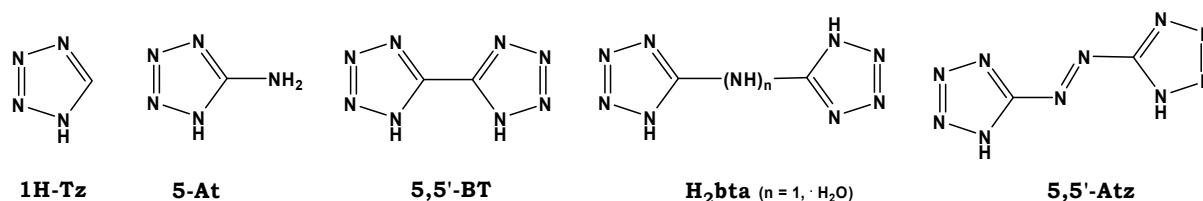
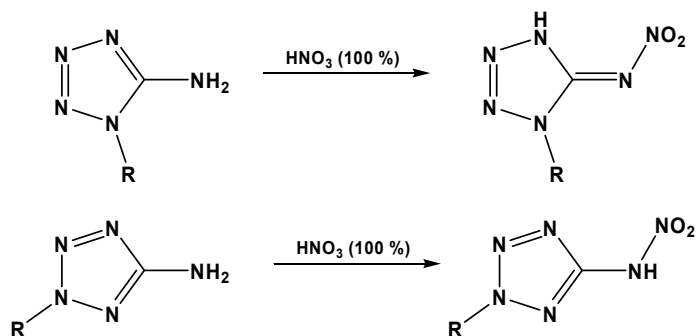


Figure 1.8 Different tetrazole derivatives: 1*H*-tetrazole (**1H-Tz**), 5-aminotetrazole (**5-At**), 5,5'-bistetrazole (**5,5'-BT**), *N,N*-bis(1*H*-tetrazol-5-yl)-amine monohydrate (**H₂bta**), and 5,5'-azotetrazolate (**5,5'-Atz**).

For example, 5-aminotetrazoles have a high nitrogen content and thermally stable, despite their high enthalpies of formation.^[67] 5-Aminotetrazole (**5-At**) is synthesized either from aminoguanidinium nitrate with nitrous acid and basic work-up or in a reaction of cyanamide with hydrazoic acid, but it also commercially available (119.70 €/500 g, Sigma-Aldrich).^[68] **5-At** can be both protonated and deprotonated as well as several alkylation products, yielding the *N*1- and *N*2-isomers, are known.^[69] In a recently published paper, the properties and crystal structures of the alkali metal salts of **5-At** have been presented and discussed.^[70]

Alkylated derivatives of **5-At** usually can not be deprotonated (except the side chain offers this property). However, by nitration of the **5-At** derivatives with nitric acid (100 %), the corresponding 5-nitrimino- and 5-nitraminotetrazoles are obtained (Scheme 1.11), which have the necessary acidic properties for deprotonation.^[71]



Scheme 1.11 Nitration products of the *N*1- and *N*2-isomers of alkylated 5-aminotetrazole derivatives.

Several salts, including metal as well as nitrogen-rich cations, of 5-nitrimino- and nitraminotetrazoles are known and have already been investigated.^[41c,d, 59 71, 72]

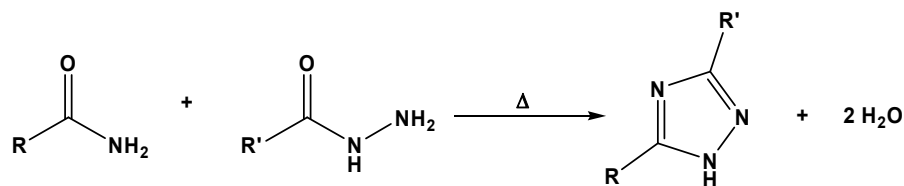
The diprotic acid *N,N*-bis(1*H*-tetrazol-5-yl)-amine monohydrate (**H₂bta**) can be obtained from three different syntheses.^[73] One reaction is based on the use of inexpensive sodium dicyanamide, sodium azide, and a catalyst such as zinc chloride, bromide or perchlorate, followed by acidic work-up.^[73a, b] Another simple synthesis also uses sodium dicyanamide and sodium azide and the slow addition of hydrochloric acid^[73d] or a weak acid such as trimethylammonium chloride, boric acid, ammonium chloride.^[73c] **5-At** can also be used as starting material, thereby it is treated with cyanogen bromide under base-catalyzed

conditions.^[73e] Some salts of **H₂bta** have been prepared and investigated with respect to their possible application as a pyrotechnic fuel, such as its ammonium and diammonium, hydrazinium and dihydrazinium salts as well as strontium *N,N*-bis(1*H*-tetrazol-5yl)-aminatetetrahydrate, barium *N,N*-bis(1*H*-tetrazol-5yl)-aminatetetrahydrate, and copper(II) *N,N*-bis(1*H*-tetrazol-5yl)-aminatetetrahydrate.^[28]

1.2.3 Triazoles

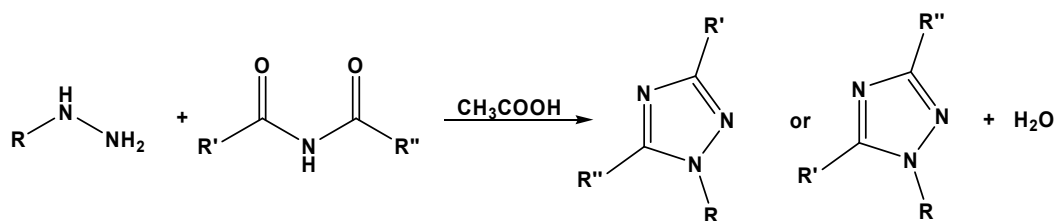
The name triazole was first given to the aromatic heterocyclic ring system consisting of two carbon and three nitrogen atoms by BLADIN, who described derivatives of it in 1885.^[74] Depending on the position of the nitrogen atoms in the ring system, a distinction between 1,2,3-triazole and 1,2,4-triazole is possible. Both, 1,2,3-triazole and 1,2,4-triazole have positive heats of formation of 272 kJ/mol and 109 kJ/mol, respectively.^[75]

Several 1,2,4-triazole derivatives and their salts are described and characterized in literature.^[76, 77, 78] Most of them have potential to find application as pharmaceuticals, because of their antibacterial, antitumor, or antiviral effects.^[79] 1,2,4-Triazoles can be prepared via the EINHORN-BRUNNER reaction or the PELLIZZARI reaction.^[76, 80, 81]



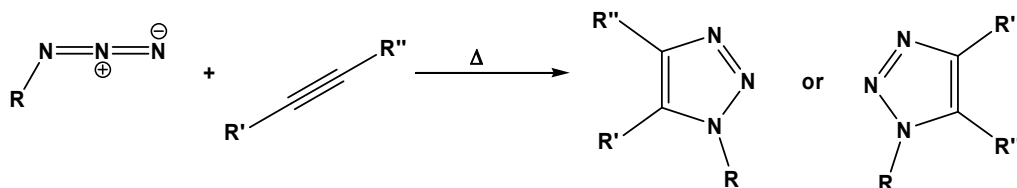
Scheme 1.12 PELLIZZARI reaction.

During the PELLIZZARI reaction a condensation of amides and hydrazine derivatives takes place (Scheme 1.12). Using an imide and alkyl hydrazine in acetic acid leads to a mixture of isomeric 1,2,4-triazoles (EINHORN-BRUNNER reaction).



Scheme 1.13 EINHORN-BRUNNER reaction.

Synthesis of its isomer 1,2,3-triazole is usually carried out via a 1,3-dipolar (HUISGEN) cycloaddition of alkyl azides and acetylene derivatives (Scheme 1.14).^[82]



Scheme 1.14 HUISGEN cycloaddition.

3-Amino-1,2,4-triazole (**3-ATrz**) offers analog to **5-At**, basic and acidic properties and is commercially available (350 €/1000 g, ABCR). Its amino group can be converted into a nitramino or nitro group, which enhances the oxygen balance and acidity, and also alkylation is possible.

1.3 Concepts and Aims

It is highly desirable to avoid toxic components like potassium perchlorate and barium nitrate in pyrotechnic compositions. In addition, the smoke production of the compositions should be strongly reduced. This urgent need for improvement of pyrotechnic compositions together with the challenge to develop new environmentally benign and better coloring agents represent the main motivation of the present work.

The concept for developing new pyrotechnic formulations is the use of triazoles and tetrazoles, whose high thermal stability along with their energetic character make them ideal precursor molecules for such compositions. In addition, their high nitrogen content guarantees a low smoke production during combustion due to the formation of the gaseous products N_2 and CO_2 .

Therefore, the synthesis of several alkylated derivatives of 5-aminotetrazole and full characterization, having different functionalities in the side chain, such as hydroxy and carboxy groups as well as nitrate esters or chlorine is planned. The corresponding 5-nitriminotetrazoles, which should also be prepared, offer the opportunity of the formation of stable anions. The synthesis of the corresponding alkali metal and alkaline earth metal salts as well as of different copper(II) complexes should be attempted. Of course, beryllium (also an alkaline earth metal) was not considered due to its well known high toxicity. All new salts should be investigated with respect to their applicability as coloring agents and in particular, the salts with lithium, calcium, strontium, barium and copper as cations. An important topic of this work is the investigation of the decomposition temperature, sensitivities to mechanical and electric stimuli, solubilities in H_2O , as well as coloring and combustion properties of the new salts. Analogous investigations are planned for 3-amino-1,2,4-triazole in place of the tetrazole moiety, which might allow a fine tuning of the properties of the resulting new pyrotechnic formulations.

The new coloring agents with convincing properties could find application in flares for military use. For this reason, mainly the flame colors red and green are considered and investigations concentrate on compounds producing these colors.

In the case of salts with convincing properties, their behavior as coloring agents should be determined in several pyrotechnic compositions with different oxidizer and fuels. The performance of each composition is compared with formulations used today with respect to color emission, combustion velocity, smoke generation, amount of solid residues, thermal stability, and sensitivity to moisture and towards outer stimuli.

1.4 Materials and Methods

1.4.1 Chemicals

All chemical reagents and solvents of analytical grade were obtained from Sigma-Aldrich, Acros Organics, Alfa Aesar, ABCR or were taken from inventory of the laboratories (e.g. ammonium dinitramide, 1*H*-tetrazole) and used without further purification.

The used boron powder was delivered from Alfa Aesar as boron powder, amorphous -325 mesh, 90 %, Mg nominal. Magnalium was approximately 100 μm and consisted of 48–52 % Mg and 48–52 % Al. Copper(I) oxide was delivered from Alfa Aesar with a purity of 97 %.

The used binder vinyl alcohol acetate resin (VAAR) consists of methyl acetate (58.0–62.0 %), vinyl alcohol acetate resin (25.0–29.0 %), methanol (6.0–8.0 %), propylene oxide (3.0–5.0 %), 1-chloro-2-hydroxypropane (0.1–3.0 %), (*S*)-2-chloro-1-propanol (0.1–3.0 %), and vinyl acetate (0.1–1.0 %). It was supplied by G. CHEN. Therefore, he is gratefully acknowledged.

Carrying out the reactions reported in this dissertation, inert gas like dry nitrogen or argon is not mandatory for a successful performance of the synthesis.

1.4.2 Preparation of the Pyrotechnic Compositions

For preparation of the pyrotechnic compositions all compounds, except the binder, were carefully mixed in a mortar. Then the binder, a solution of 25 % vinyl alcohol acetate resin (VAAR), dissolved in a few milliliters of ethyl acetate was added. The mixture was formed by hand and dried under high vacuum for several hours. For ignition a lighter was used.

The controlled burn down was filmed with a digital video camera recorder (SONY, DCR-HC37E).

The performance of each composition has been evaluated with respect to the following categories:

- color emission (subjective impression)
- smoke generation
- morphology and amount of solid residues
- thermal stability
- moisture sensitivity

The US Army red flare composition # M126 A1 (red parachute) – 39 wt% $\text{Sr}(\text{NO}_3)_2$, 30 wt% Mg, 13 wt% KClO_4 , 8 wt% VAAR – was used as a measure of the red light compositions' performance.

The performance of the compositions for green light were compared to the barium nitrate-based US Army composition # M125 A1 (green parachute): 50 wt% $\text{Ba}(\text{NO}_3)_2$, 30 wt% Mg, 15 wt% PVC, 5 wt% VAAR.

The blue light emitting compositions were compared to SHIMIZU's composition [83]: 15 wt% Cu, 17 wt% PVC, 68 wt% KClO₄, and 5 wt% starch.

1.4.3 General Methods

NMR spectroscopy: The NMR spectra were recorded using a *JEOL Eclipse 270*, *JEOL EX 400* or *JEOL Eclipse 400* instrument. ¹H, ¹³C, ¹⁴N, and ¹⁵N NMR spectra were measured in DMSO-*d*₆ at ambient temperature. The chemical shifts (δ) are given relative to the external standards tetramethylsilane (¹H, ¹³C) or nitromethane (^{14/15}N). Coupling constants (J) are given in hertz (Hz).

IR spectroscopy: IR spectra were recorded using a *Perkin-Elmer Spektrum BX FT-IR* instrument with *Smiths DuraSampl* IR-ATR unit at ambient temperature. The intensities are reported in parentheses, distinguishing between very weak (vw), weak (w), medium (m), strong (s) and very strong (vs).

Raman spectroscopy: Raman spectra were recorded using *Perkin-Elmer Spectrum 2000R NIR FT-Raman* instrument equipped with a Nd:YAG laser (1064 nm) at ambient temperature. The intensities are reported in percentages relative to the most intense peak and are given in parentheses.

Mass spectrometry: Mass spectrometry was performed on a *JEOL MS station JMS-700*. The different ionization methods (EI, DEI, DCI and FAB^{+/-}) are indicated in the experimental section.

Elemental analysis: Elemental analyses were performed with a *Netsch Simultaneous Thermal Analyzer STA 429*. The determined values are given in percent (%).

DSC measurements: DSC measurements were performed by a *Linseis DSC PT-10* instrument at a heating rate β of 5 K/min in closed aluminum containers with a hole (1 μ m) on the top for gas release with a nitrogen flow of 5 mL/min. The reference sample was a closed aluminum container. The measured data was settled with a zero line. However, the resulted base line often has a positive or negative slope.

Melting point: Melting points as well as the releases of crystal water were determined using the DSC data and distinguished by using a *Büchi Melting point B-540*.

Density: The density of the compounds was either obtained from the crystal structure or was measured by Quantachrome instruments *Ultrapyc 1200e* using the amorphous compound (at ambient temperature).

Bomb calorimetric measurements: Bomb Calorimetry was undertaken using a *Parr 1356 Bomb calorimeter* [static jacket] with a *Parr 1108CL* oxygen bomb. For the analysis of solid compounds, approximately 200 mg of the compound was mixed with approximately 800 mg of benzoic acid. The mixture was converted into a pellet which was used for the measurement. The enthalpies of combustion ($\Delta_c H^\circ$) and enthalpies of formation ($\Delta_f H^\circ$) were calculated according to the equations mentioned in the corresponding chapters.

Crystal structures: The crystallographic data were collected using an *Oxford Xcalibur3 diffractometer* with a Spellman generator (voltage 50 kV, current 40 mA) and a Kappa CCD area detector with graphite-monochromated MoK α radiation ($\lambda = 0.71073 \text{ \AA}$). The crystal structures were solved using direct methods (SHELXS-97)^[84] and refined using SHELXL-97.^[85] All non-hydrogen atoms were refined anisotropically. Ortep plots showing thermal ellipsoids with 50% probability for the non-hydrogen atoms.

Impact and friction sensitivity: The impact and friction sensitivity was determined using a BAM drop hammer and a BAM friction tester.^[86] Amending, for the purpose of its adaptation to technical progress, Regulation (EC) No 440/2008 laying down test methods pursuant to Regulation (EC) No 1907/2006 of the European Parliament and of the Council on the Registration, Evaluation, Authorisation and Restriction of Chemicals (REACH). The sensitivities of the compounds are indicated according to the UN Recommendations on the Transport of Dangerous Goods (+): impact: insensitive > 40 J, less sensitive > 35 J, sensitive > 4 J, very sensitive < 4 J; friction: insensitive > 360 N, less sensitive = 360 N, sensitive < 360 N > 80 N, very sensitive < 80 N, extreme sensitive < 10 N. The corresponding grain size of the compounds is given.

Sensitivity to electric discharge: The sensitivity to electric discharge were carried out using an electric spark tester *ESD 2010EN* (OZM Research) operating with the “Winspark 1.15 software package”.^[87] Amending, for the purpose of its adaptation to technical progress, Regulation (EC) No 440/2008 laying down test methods pursuant to Regulation (EC) No 1907/2006 of the European Parliament and of the Council on the Registration, Evaluation, Authorization and Restriction of Chemicals (REACH). The corresponding grain size of the compounds is given.

Grain size: The grain size was determined by sieving the neat compounds.

Combustion behavior: A simple smoke test method for determining the combustion behavior was performed in cooperation with G. CHEN in his research group. Therefore, approx. 1 g sample was placed and heated in a crucible with a gas torch for observation of color, smoke, burn ability (propagation), and level of residue. For doing so he is again gratefully acknowledged.

Color performance: Static burn tests for determining the color performance were performed in cooperation with G. CHEN in his research group. Therefore, the coloring agent was formulated with magnesium powder, polyvinyl chloride, and polyester/styrene binder, leaving the weight ratio equal to M126 A1^[88]. The dry ingredients were sieved through 10-mesh screen and dried prior to mixing in a ceramic bowl. The final dry mixes were pressed to 1.27 cm pellets, each with approx. 6 g. The pellets were consolidated in a die with two increments at a loading pressure of 6000 psi (41.3 MPa). The current M126 A1 igniter slurry (aluminum, silicon, charcoal, potassium nitrate, iron oxide, and nitrocellulose) was applied on top of pellets as first fire. Static burn test on the experimental pellets was conducted in a blackened light tunnel. The samples were placed 50 ft (15.24 m) from the measurement equipment and initiated with an electric match. Color was measured with an *Ocean Optics*

HR2000 spectrometer after calibration. Color measurements were based on the 1931 CIE (*Commission Internationale d'Eclairage*) international standard and calculated using the *Ocean Optics* Spectra-suite software. The CIE chart displays all the chromaticities average human eyes can observe. The three values calculated based on the CIE color matching functions are referred to X, Y and Z. The dominant wavelength (DW) and excitation purity (%) for a test sample were numerically determined with respect to the coordinates of Illuminant C, an established light source. The luminous intensity was measured using an *International Light SEL033* silicon detector coupled to a photopic filter and lens hood. For doing so he is again gratefully acknowledged.

1.5 References

- [1] H. Ellern: *Military and Civilian Pyrotechnics*, Chemical Publishing Company Inc., New York, USA, **1968**.
- [2] Bundesministerium der Justiz, Bürgerliches Gesetzbuch BGB: Sprengstoffgesetz Abschnitt 1 Allgemeine Vorschriften §3.
- [3] U.S. Army Material Command, Engineering Design Handbook, Military Pyrotechnics Series, Part One: *Theory and Application*, Washington D.C. **1967** (AMC Pamphlet 706–185).
- [4] M. Websky: *Lustfeuerwerkkunst*, Verlag F. Hirt und Sohn, Leipzig, **1873**.
- [5] J. Wisniak: The History of Saltpeter Production with a Bit of Pyrotechnics and Lavoisier, *Chem. Educator* **2000**, 5, 205–209.
- [6] H. Ineichen: *Kleine Feuerwerkdokumentation*, H. Hamberger AG, Oberried, CH, **1980**.
- [7] H. Ineichen, B. Berger: Pyrotechnics in Fireworks, *Chimia* **2004**, 56, 369–373.
- [8] D. Jing: Pyrotechnics in China, *7th Int. Pyrotechnics Seminar*, Vail, CO, USA, 14.–18. July, **1980**.
- [9] J. A. Conkling: *Chemistry of Pyrotechnics: Basic Principles and Theory*. M. Dekker, Inc., New York, **1985**.
- [10] B. Berger: Military Pyrotechnics, *Chimia* **2004**, 58, 363–368.
- [11] H. B. Faber: *Military Pyrotechnics*, Vol. 1, Government Printing Office, Washington, USA, **1919**.
- [12] M. S. Russell: *The chemistry of fireworks*, RSC, Cambridge, **2002**.
- [13] a) R. Meyer, J. Köhler, A. Homburg: *Explosives*, 6. ed., Wiley-VCH, Weinheim, **2007**, 240–241. b) N. Kubota: Propellant Chemistry, *J. Pyrotech.* **2000**, 11, 25–45.
- [14] Viton® and Teflon® are DuPont trademarks.

- [15] E.-C. Koch: Metal-fluorocarbon-pyrolants: III. Development and application of magnesium/teflon/viton (MTV), *Propellants Explos. Pyrotech.* **2002**, 27, 262–266.
- [16] E.-C- Koch: Defluorination of graphite fluoride with magnesium, *Z. Naturforsch. B* **2001**, 56, 512–516.
- [17] S. Cudzilo, M. Szala, A. Huczko, M. Bystrzejewski: Combustion reactions of poly(carbon monofluoride), (CF)_n, with different reductants and characterization of the products, *Propellants Explos. Pyrotech.* **2007**, 32, 149–154.
- [18] a) T. M. Klapötke, G. Steinhauser: 'Green' Pyrotechnics: A Chemists' Challenge, *Angew. Chem. Int. Ed.* **2008**, 47, 3330–3347. b) T. M. Klapötke, G. Steinhauser: Pyrotechnik mit dem "Ökosiegel": eine chemische Herausforderung, *Angew. Chem.* **2008**, 120, 3376–3394.
- [19] T. Shimizu, *Fireworks – The Art, Science and Technique*, **1981**, Maruzen Co., Ltd., Tokyo.
- [20] R. Lancaster: *Fireworks – Principles and Practice*, Chemical Publ. Co., Inc., New York, **1972**.
- [21] A. A. Shidlovskiy: *Principles of Pyrotechnics*, 3. Ed., Moscow, **1964** (translated by Foreign Technology Division, Wright-Patterson Air Force Base, Ohio, **1974**).
- [22] S. P. Sontakke, S. D. Kakade, R. M. Wagh, A. G. Dugam, P. P. Sane: Polymethyl methacrylate as a binder for pyrotechnic compositions, *Def. Sci. J.* **1995**, 45, 349–352.
- [23] Laminac® is a trademark of Ashland Speciality Chemical Comp.
- [24] A. Hammerl, K. Harris, T. M. Klapötke, M. A. Bohn: Decomposition of Nitramines with GAPS, 11a Reunión Científica Plenaria de Química Inorgánica, 5a Reunión Científica Plenaria de Química del Estado Sólido, Santiago de Compostela, Spain, 12.–16.Sept. **2004**.
- [25] a) <http://www.physics.umd.edu/grt/taj/104a/visible.jpg>, b) L. A. Bloomfield: *How Everything Works, Making Physics out of the Ordinary*, Wiley, New York, **2007**, 454.
- [26] R. F. Barrow, E. F. Caldin: Some spectroscopic observations on pyrotechnic flames, *Proceedings of the Physical Society*, London **1949**, 62B, 32–39.
- [27] S. Yuasa, H. Isoda: Ignition and combustion of small boron lumps in an oxygen stream, *Combust. Flame* **1991**, 86, 216–222.
- [28] D. E. Chavez, M. A. Hiskey, D. L. Naud: High-nitrogen fuels for low-smoke pyrotechnics, *J. Pyrotech.* **1999**, 10, 17–36.
- [29] K. J. Smit, R. J. Hancox, D. J. Hatt, S. P. Murphy, L. V. de Yong: Infrared-emitting species identified in the combustion of boron-based pyrotechnic compositions, *Appl. Spectrosc.* **1997**, 51, 1400–1404.

- [30] R. M. Blunt, P. J. Keitel: Producing a green flame by aspirating trimethyl borate, *US Pat.* US 3453157, **1969**.
- [31] a) E.-C. Koch: Evaluation of lithium compounds as color agents for pyrotechnic flames, *J. Pyrotech.* **2001**, *13*, 1–8. b) E.-C. Koch: Special materials in pyrotechnics: III. Application of lithium and its compounds in energetic systems, *Propellants Explos. Pyrotech.* **2004**, *29*, 67–80.
- [32] B. E. Douda: Prediction of Line Shapes in Pyrotechnic Flares containing Lithium, *5th Int. Pyrotechnics Seminar*, Vail, CO, USA, 12.–16. July, **1976**, 212.
- [33] E.-C. Koch: Special materials in pyrotechnics part 2 – application of cesium and rubidium compounds in pyrotechnics, *J. Pyrotech.* **2002**, *15*, 9–23.
- [34] [http://en.wikipedia.org/wiki/Flare_\(pyrotechnic\)](http://en.wikipedia.org/wiki/Flare_(pyrotechnic))
- [35] T. M. Klapötke, G. Steinhauser: Using Fireworks To Engage Students in Learning Basic Chemical Principles: A Lesson in Eco-Friendly Pyrotechnics, *J. Chem. Educ.* **2010**, *87*, 150–156.
- [36] C. Jennings-White: Nitrate Colors, *Pyrotechnica* **1993**, *15*, 23–28.
- [37] H. A. Webster III: Visible Spectra of Standard Navy Colored Flares, *Propellants, Explosiv., Pyrotech.* **1985**, *10*, 1–4.
- [38] a) R. S. Moore Jr., V. Tan, J. P. Dormans, D. J. Bozentka: Major Pediatric Hand Trauma Associated With Fireworks, *Orthop. Trauma* **2000**, *14*, 426–428. b) Z. Zohar, I. Waksman, J. Stoloro, G. Volpin, E. Sacagiu, A. Eytan: Injury from fireworks and firecrackers during holidays, *Harefuah* **2004**, *143*, 698–701, 768. c) R. L. Karamanoukian, M. Kilani, D. Lozano, M. Sundine, H. L. Karamanoukian, J. Delarosa, S. Behnam, R. G. D. Evans: Pediatric burns with snap-cap fireworks, *J. Burn Care Res.* **2006**, *27*, 218–220; discussion on page 220. d) D. W. Oliver, M. Ragbir, P. J. Saxby: *Unusual Pattern of Injury Caused by a Pyrotechnic Hand Held Signal Flare*; Department of Plastic and Reconstructive Surgery, Royal Devon and Exeter Hospital: Wonford, UK, **1997**, 258–259. e) F. Romano, L. Catalfamo, E. N. Siniscalchi, A. Conti, F. F. Angileri, F. S. De Ponte, F. Tomasello, *Complex Craniofacial Trauma Resulting from Fireworks Blast*, Department of Maxillo-Facial Surgery, University of Messina: Messina, Italy, **2008**, 322–327. f) D. V. Singh, Y. R. Sharma, R. V. Azad: Visual outcome after fireworks injuries, *J. Trauma* **2005**, *59*, 109–111. g) K. Sundelin, K. Norrsell: Eye injuries from fireworks in Western Sweden, *Acta Ophthalmol. Scand.* **2000**, *78*, 61–64. h) C.-C. Lee, S.-C. Chen: *Images in Emergency Medicine. Eye Globe Rupture from Firework Injury*, Department of Emergency Medicine, National Taiwan University Hospital: Taipei, Taiwan, **2005**, page 94 and 102. i) S. Plontke, C. Herrmann, H. P. Zenner: Hearing loss caused by New Year's fireworks. Survey of incidence of blast and explosion trauma in Germany during the 1998/99 New Year's celebration, *HNO* **1999**, *47*, 1017–1019. j) S. Plontke, H. Schneiderbauer, R. Vonthein, P. K. Plinkert, H. Lowenheim, H. P. Zenner:

Recovery of normal auditory threshold after hearing damage from fireworks and signalling pistols, *HNO* **2003**, *51*, 245–250.

[39] C. Jennings-White, K. Kosanke: Hazardous chemical combinations: A discussion, *J. Pyrotech.* **1995**, *2*, 22–25.

[40] R. P. Singh, R. D. Verma, D. T. Meshri, J. M. Shreeve: Energetic nitrogen-rich salts and ionic liquids, *Angew. Chem.* **2006**, *118*, 3664–3682; Energetic nitrogen-rich salts and ionic liquids, *Angew. Chem. Int. Ed.* **2006**, *45*, 3584–3601.

[41] O. P. Murty: Diwali toxicity, *J. Forensic Med. Toxicol.* **2000**, *17*, 23–26.

[42] a) G. Steinhauser, K. Tarantik, T. M. Klapötke: Copper in pyrotechnics, *J. Pyrotech.* **2008**, *27*, 3–13. b) T. M. Klapötke, K. R. Tarantik: Green pyrotechnic compositions, *New Trends in Research of Energetic Materials, 11th*, Pardubice, Czech Republic, Apr. 9–11, **2008**, Pt. 2, 586–597. c) T. M. Klapötke, J. Stierstorfer, K. R. Tarantik: Salts of 1-(2-chloroethyl)-5-nitriminotetrazole - new candidates for coloring agents in pyrotechnic compositions, *New Trends in Research of Energetic Materials, 12th*, Pardubice, Czech Republic, Apr. 1–3, **2009**, Pt. 2, 647–665. d) T. M. Klapötke, J. Stierstorfer, K. R. Tarantik: Pyrotechnically Relevant Salts of 1-(2-Chloroethyl)-5-nitriminotetrazole – Synthesis and Coloring Properties, *J. Pyrotech.*, **2009**, *28*, 61–77. e) T. M. Klapötke, H. Radies, J. Stierstorfer, K. R. Tarantik, G. Chen, and A. Nagori: Coloring Properties of Various High-Nitrogen Compounds in Pyrotechnic Compositions, *36th International Pyrotechnics Seminar and Symposium*, Proceedings, Rotterdam, The Netherlands, Aug. 23–28. **2009**, 65–72; *Propellants, Explos. Pyrotech.* **2010**, *in press*.

[43] R. T. Wilkin, D. D. Fine, N. G. Burnett: Perchlorate behavior in a municipal lake following fireworks displays, *Environ. Sci. Technol.* **2007**, *41*, 3966–3971.

[44] J. Munster, G. N. Hanson, W. A. Jackson, S. Rajagopalan: The fallout from fireworks: perchlorate in total deposition, *Water, Air, Soil Pollut.* **2009**, *198*, 149–153.

[45] M. Salomon: Solvation of alkali metal perchlorates in water, *J. Electrochem. Soc.* **1971**, *118*, 1614–16.

[46] N. Wiberg, E. Wiberg, A. F. Holleman: *Lehrbuch der Anorganischen Chemie*, deGruyter, Berlin, 102. Ed., **2007**.

[47] a) E. K. Mantus: Health implications of perchlorate ingestion, Prepr. Ext. Abstr. ACS Natl. Meet., ACS Div. *Environ. Chem.* **2005**, *45*, 873. b) J. Sass: U.S. Department of Defense and White House working together to avoid cleanup and liability for perchlorate pollution, *Int. J. Occup. Environ. Health* **2004**, *10*, 330–334. c) O. P. Soldin, L. E. Braverman, S. H. Lamm: Perchlorate clinical pharmacology and human health: a review, *Ther. Drug Monit.* **2001**, *23*, 316–331. d) J. Wolff: Perchlorate and the thyroid gland, *Pharmacol. Rev.* **1998**, *50*, 89–105. e) J. J. J. Clark: *Perchlorate in the Environment* (Ed.: E. T. Urbansky), Kluwer Academic/Plenum, New York, **2000**.

- [48] a) J. D. Coates, L. A. Achenbach: Microbial perchlorate reduction: rocket-fueled metabolism, *Nat. Rev. Microbiol.* **2004**, *2*, 569–580; b) J. D. Coates, U. Michaelidou, R. A. Bruce, S. M. O'Connor, J. N. Crespi, L. A. Achenbach: Ubiquity and diversity of dissimilatory (per)chlorate-reducing bacteria, *Appl. Environ. Microbiol.* **1999**, *65*, 5234–5241; c) S. W. Kengen, G. B. Rikken, W. R. Hagen, C. G. Van Ginkel, A. J. Stams: Purification and characterization of (per)chlorate reductase from the chlorate-respiring strain GR-1, *J. Bacteriol.* **1999**, *181*, 6706–6711.
- [49] a) R. Mandal, B. K. Sen, S. Sen: Impact of fireworks on our environment, *Chem. Environ. Res.* **1996**, *5*, 307–312. b) A. Dutschke, C. Lohrer, S. Seeger, L. Kurth: Gaseous and solid reaction products from burning of indoor fireworks, *Chem. Ing. Tech.* **2009**, *81*, 167–176. c) G. Croteau, R. Dills, M. Beaudreau: Emmission factors and Exposures From Ground Level Pyrotechnics, *Atmos. Environ.* **2010**, *40*, 4316–4327.
- [50] G. Steinhauser, J. H. Sterba, M. Foster, F. Grass, M. Bichler: Heavy metals from pyrotechnics in New Years Eve snow, *Atmos. Environ.* **2008**, *42*, 8616–8622.
- [51] a) R. Hicks, L. Q. Caldas, P. R. Dare, P. J. Hewitt: Cardiotoxic and bronchoconstrictor effects of industrial metal fumes containing barium, *Archives of Toxicology Supplement* **1986**, *9*, 416–420. b) A. L. Reeves: Barium toxicity. *Handbook Toxicological Methods*, **1979**, 321–328.
- [52] W. Bach, L. Dickinson, B. Weiner, G. Costello: Some adverse health effects due to air pollution from fireworks, *Hawaii Med. J.* **1972**, *31*, 459–465.
- [53] [http://en.wikipedia.org/wiki/Ba\(NO3\)2](http://en.wikipedia.org/wiki/Ba(NO3)2)
- [54] a) S. C. Barman, R. Singh, M. P. S. Negi, S. K. Bhargava: Fine particles (PM_{2.5}) in ambient air of Lucknow city due to fireworks on Diwali festival, *J. Environ. Biol.* **2009**, *30*, 625–632. b) F. Drewnick, S. S. Hings, J. Curtius, G. Eerdekens, J. Williams: Measurement of fine particulate and gas-phase species during the New Year's fireworks 2005 in Mainz, Germany, *Atmos. Environ.* **2006**, *40*, 4316–4327. c) B. Wehner, A. Wiedensohler, J. Heintzenberg: Submicrometer aerosol size distributions and mass concentration of the Millennium Fireworks 2000 in Leipzig, Germany, *J. Aerosol Sci.* **2000**, *31*, 1489–1493.
- [55] <http://environment.about.com/od/healthenvironment/a/toxicfireworks.htm>; From Earth Talk: Declare Your Independence from Toxic Fireworks Pollution – Fireworks Litter the Ground, Pollute Water Supplies, and Damage Human Health.
- [56] M. A. Hiskey, D. E. Chavez, D. L. Naud, S. F. Son, H. L. Berghout, C. A. Bolme, *27th Proc. Int. Pyrotech. Sem., Co, USA*, 16.–21. July **2000**, 3–14.
- [57] T. M. Klapötke: *New Nitrogen-Rich High Explosives*: Struct. Bonding, Berlin, **2007**.
- [58] T. M. Klapötke: *Chemie der hochenergetischen Materialien*, 1. Ed., Walter de Gruyter GmbH & Co. KG, Berlin, **2009**.

- [59] T. M. Klapötke, J. Stierstorfer, A. U. Wallek: Nitrogen-Rich Salts of 1-Methyl-5-nitriminotetrazolate: An Auspicious Class of Thermally Stable Energetic Materials, *Chem. Mater.* **2008**, *20*, 4519-4530.
- [60] a) M. H. V. Huynh, M. D. Coburn, T. J. Meyer, M. Wetzler: Green primary explosives: 5-Nitrotetrazolato-*N*²-ferrate hierarchies, *Proceedings of the National Academy of Sciences of the United States of America* **2006**, *103*, 10322-10327; b) M. H. V. Huynh: Transition metal energetic complexes as lead-free detonators for explosives, *Int. Pat.* WO2008143724, **2008**.
- [61] a) J. W. Fronabarger, M. D. Williams, W. B. Sanborn: Copper(II) 5-nitrotetrazolate synthesis as lead-free primary explosive, *Int. Pat.* WO2008048351, **2008**. b) G. Geisberger, T. M. Klapötke, J. Stierstorfer: Manufacture of Copper bis(1-methyl-5-nitriminotetrazolate) as a promising new primary explosive, *Eur. J. Org. Chem.* **2007**, *30*, 4743-4750.
- [62] a) M. J. Kamlet, S. J. Jacobs: Chemistry of detonations. I. Simple method for calculating detonation properties of carbon-hydrogen-nitrogen-oxygen explosives, *J. Chem. Phys.* **1968**, *48*, 23-35. b) M. J. Kamlet, J. E. Ablard: Chemistry of detonations. II. Buffered equilibrium, *J. Chem. Phys.* **1968**, *48*, 36-42. c) M. J. Kamlet, C. Dickinson: Chemistry of detonations. III. Evaluation of the simplified calculational method for Chapman-Jouguet detonation pressures on the basis of available experimental information, *J. Chem. Phys.* **1968**, *48*, 43-50.
- [63] P. R. Lee: *Explosive Effects and Applications*, Springer-Verlag New York, Inc., **1998**.
- [64] E. Anderson: Explosives, *Prog. Astronaut. Aeronaut.* **1993**, *155*, 81-163.
- [65] F. Zhang, P. A. Thibault, S. B. Murray: Transition from deflagration to detonation in an end multiphase slug, *Combust. Flame* **1998**, *114*, 13-25.
- [66] V. A. Ostrrovskii, M. S. Pevzner, T. P. Kofman, I. V. Tselinskii: Energetic 1,2,4-triazoles and tetrazoles synthesis, structure and properties, *Targets Heterocycl. Syst.* **1999**, *3*, 467-526.
- [67] a) A. Gao, Y. Oyumi, T. B. Brill: Thermal decomposition of energetic materials. 49. Thermolysis routes of mono- and diaminotetrazoles, *Combust. Flame* **1991**, *83*, 345-352. b) A. A. Kozyro, V. V. Simirsky, A. P. Krasulin, V. M. Sevruck, G. J. Kabo, M. L. Gopanik, Y. V. Grigotiev: , *Zh. Fiz. Khim.* **1990**, *64*, 656-661.
- [68] a) J. Thiele: Ueber Nitro- und Amidoguanidin, *Justus Liebigs Ann. Chem.* **1892**, *270*, 1-63. b) R. Stoll, W. E. Schick, F. Henke-Stark, L. Krauss, *Ber. Dtsch. Chem. Ges. B* **1929**, *62*, 1118-1126.
- [69] a) R. M. Herbst, C. W. Roberts, E. J. Harvill: The synthesis of 5-aminotetrazole derivatives, *J. Org. Chem.* **1951**, *16*, 139-149. b) R. A. Henry, W. G. Finnegan: Mono-alkylation of sodium 5-aminotetrazole in aqueous medium, *J. Am. Chem. Soc.* **1954**, *76*, 923-926. c) D. F. Percival, R. M. Herbst: Alkylated 5-aminotetrazoles, their preparation and properties, *J. Org. Chem.* **1957**, *22*, 925-933. d) D. W. Renn, R. M. Herbst: Cyanoethylation

of the 5-aminotetrazoles, *J. Org. Chem.* **1959**, *24*, 473–477. e) W. G. Finnegan, R. A. Henry: N-Vinyltetrazoles, *J. Org. Chem.* **1959**, *24*, 1565–1567. f) A. O. Koren, P. N. Gaponik: Selective N-2 alkylation of tetrazole and 5-substituted tetrazoles by alcohols, *Kh. Geterotsiklicheskikh Soedinenii* **1990**, *12*, 1643–1647. g) S. A. Gromova, M. I. Barmin, I. B. Karaulova, A. N. Grebenkin, V. V. Mel'nikov: Alkylation of 5-aminotetrazole potassium salt with α,ω -dibromoalkanes and bis(ω -chloroalkyl) ethers, *Russ. J. Org. Chem. (Translation of Zhurnal Organicheskoi Khimii)* **1998**, *34*, 1043–1046. h) M. I. Barmin, S. A. Gromova, V. V. Mel'nikov: Alkylation of 5-aminotetrazole with dihalo-substituted compounds in dimethylformamide, *Russ. J. App. Chem. (Translation of Zhurnal Prikladnoi Khimii)* **2001**, *74*, 1156–1163. j) F. Einberg: Alkylation of 5-Substituted Tetrazoles with α -Chlorocarbonyl Compounds, *J. Org. Chem.* **1970**, *35*, 3978–3980.

[70] V. Ernst, T. M. Klapötke, J. Stierstorfer: Alkali Salts of 5-aminotetrazole – structures and properties, *Z. Allg. Anorg. Chem.* **2007**, *633*, 879–887.

[71] a) T. M. Klapötke, J. Stierstorfer, K. R. Tarantik: New Energetic Materials: Functionalized 1-Ethyl-5-aminotetrazoles and 1-Ethyl-5-nitriminotetrazoles, *Chem. Eur. J.* **2009**, *15*, 5775–5792. b) J. Stierstorfer: Advanced Energetic Materials based on 5-Aminotetrazole, *PhD Thesis*, **2009**, Ludwig-Maximilian University, Munich.

[72] a) M. Tremblay: Synthesis of some tetrazole salts, *Can. J. Chem.* **1965**, *43*, 1230–1232. b) T. M. Klapötke, H. Radies, J. Stierstorfer: Alkali salts of 1-methyl-5-nitriminotetrazole - structures and properties, *Z. Naturforsch. B* **2007**, *62*, 1343–1352. c) T. M. Klapötke, J. Stierstorfer, A. U. Wallek: N-rich salts of 1-methyl-5-nitriminotetrazolate - an auspicious class of thermal stable high explosives, *New Trends in Research of Energetic Materials*, Proceedings of the Seminar, *11th*, Pardubice, Czech Republic, 9.–11. Apr., **2008**, Pt. 2, 832–854. d) V. Ernst, T. M. Klapötke, J. Stierstorfer: Nitriminotetrazolates as energetic ingredients in innovative pyrotechnical compositions - a comprehensive characterization, *New Trends in Research of Energetic Materials*, Proceedings of the Seminar, *10th*, Pardubice, Czech Republic, 25.–27. Apr., **2007**, Pt. 2, 575–593. e) T. M. Klapötke, J. Stierstorfer, K. R. Tarantik, I. D. Thoma: Strontium Nitriminotetrazolates - Suitable Colorants in Smokeless Pyrotechnic Compositions, *Z. Anorg. Allg. Chem.* **2008**, *634*, 2777–2784. f) R. Damavarapu, T. M. Klapötke, J. Stierstorfer, K. R. Tarantik: Barium Salts of Tetrazole Derivatives – Synthesis and Characterization, *Propellants, Explos. Pyrotech.* **2010**, *in press*.

[73] a) Z. P. Demko, K. B. Sharpless: Preparation of 5-Substituted 1H-Tetrazoles from Nitriles in Water, *J. Org. Chem.* **2001**, *66*, 7945–7950; b) P. Marecek, K. Dudek, F. Liska: Synthesis of di(1H-tetrazole-5-yl)amine (BTA), *New Trends in Research of Energetic Materials*, Proceeding of the Seminar, *7th*, Pardubice, Czech Republic, **2004**, Pt. 2, 566–569. c) T. K. Highsmith, R. M. Hajik, R. B. Wardle, G. K. Lund, R. J. Blau: Methods for synthesizing and processing bis[1(2)H-tetrazol-5-yl]amine, US 5468866, **1995**. d) D. L. Naud, M. A. Hiskey: Process for preparing bis[1(2)H-tetrazol-5-yl]amine monohydrate, US 2003060634, **2003**. e) T. M. Klapötke, C. Kuffer, P. Mayer, K. Polborn, A. Schulz, J. J.

Weigand: The Dianion of 5-Cyanoiminotetrazoline: $C_2N_6^{2-}$, *Inorg. Chem.* **2005**, *44*, 5949–5958.

[74] a) J. A. Bladin, *Ber.* **1885**, *18*, 1544. b) J. A. Bladin, *Ber.* **1886**, *19*, 2598.

[75] J. B. Pedley: *Thermochemical Data and Structure of Organic Compounds*, vol.1, Thermodynamic Research Center, College Station, TX (USA), **1994**. b) P. Jiminez, M. V. Roux, C. J. Turron: , *Chem. Thermodyn.* **1998**, *21*, 759–764.

[76] K. T. Potts: The Chemistry of 1,2,4-Triazoles. *Chem. Rev.* **1961** *61*, 87–127.

[77] a) L. I. Bagal, M. S. Pevzer, A. N. Fralov, N. I. Sheludyakova, *Khim. Geterosiki. Soed.* **1970**, 259. b) G. Evrard, F. Durant, A. Michel, J. G. Fripiat, J. L. Closset, A. Copin: Crystal structure of 3-nitro-1,2,4-triazole, *Bull. Soc. Chim. Belg.* **1984**, *93*, 233–234. c) S.-S. Yun, J.-K. Kim, C.-H. Kim: Lanthanide complexes of some high energetic compounds, crystal structures and thermal properties of 3-nitro-1,2,4-triazole-5-one (NTO) complexes, *J. Alloys Compd.* **2006**, *408*, 945–951. d) J. G. Vos, W. L. Driessen, J. Van der Waal, W. L. Groeneveld: Pyrazolato and related anions. Part VII. Salts of 3-nitro-1,2,4-triazole, *Inorg. Nucl. Chem. Letters* **1978**, *14*, 479–483.

[78] T. P. Kofman, G. Kartseva, M. B. Shcherbinin: 5-Amino-3-nitro-1,2,4-triazole and Its Derivatives, *Russ. J. Org. Chem.* **2002**, *38*, 1343–1350.

[79] a) C. Ainsworth, N. R. Easton, M. Livezey, D. E. Morrison, W. R. Gibson: The anticonvulsant activity of 1,2,4-triazoles, *J. Med. Chem.* **1962**, *5*, 383–389. b) B. Blank, D. M. Nichols, P. D. Vaidya: Synthesis of 1,2,4-triazoles as potential hypoglycemic agents, *J. Med. Chem.* **1972**, *15*, 694–696. c) S. Jantova, G. Greif, R. Pavlovicova, L. Cipak: Antibacterial effects of some 1-substituted 1,2,4-triazoles, *Folia microbiologica* **1998**, *43*, 75–78.

[80] a) A. Einhorn, E. Bischkopff, B. Szelinski, G. Schupp, E. Spröngerts, C. Ladisch, T. Mauermayer: Ueber die N-Methylolverbindungen der Säureamide, *Justus Liebig's Annalen der Chemie* **1905**, *343*, 207–305. b) K. Brunner: Eine neue Darstellungsweise von sekundären Säureamiden, *Chem. Ber.* **1914**, *47*, 2671–2680. c) K. Brunner: Eine neue Darstellungsweise von Triazolen, *Monatsheft für Chemie* **1915**, *36*, 509–534. d) M. R. Atkinson, J. B. Polya: Triazoles. Part II. N-substitution of some 1,2,4-triazoles, *J. Chem. Soc.*, **1954**, *29*, 141–145.

[81] G. Pellizzari, *Gazz. Chim. Ital.* **1911**, *41*, 20.

[82] a) R. H. Wiley, K. F. Hussung, J. Moffat: The preparation of 1,2,3-triazole, *J. Org. Chem.* **1956**, *21*, 190–192; b) R. Huisgen, G. Szeimies, L. Moebius: 1,3-Dipolar cycloadditions. XXIV. Triazolines from organic azides and α,β -unsaturated carbonyl compounds or nitriles., *Chem. Ber.* **1966**, *99*, 475–490; c) K. Banert: Reactions of unsaturated azides. 5. Cycloaddition reactions of 2,3-diazido-1,3-butadienes, *Chem. Ber.* **1989**, *122*, 123–128.

- [83] T. Shimizu: Studies on Blue and Purple Flame Compositions Made With Potassium Perchlorate, *Pyrotechnica* **1980**, 6, 5.
- [84] G. G. M. Sheldrick, Shelxs-97, Program for the Solution of Crystal Structures, University of Göttingen, Göttingen (Germany) **1997**.
- [85] G. M. Sheldrick, Shelxs-97, Program for the Refinement of Crystal Structures, University of Göttingen, Göttingen (Germany) **1997**.
- [86] a) M. Suceska, *Test Methods for Explosives*, Springer, New York, **1995**, p. 21 (impact), p. 27 (friction). b) <http://www.bam.de/>. c) Amending, for the purpose of its adaptation to technical progress, Regulation (EC) No 440/2008 laying down test methods pursuant to Regulation (EC) No 1907/2006 of the European Parliament and of the Council on the Registration, Evaluation, Authorisation and Restriction of Chemicals (REACH).
- [87] a) S. Zeman, V. Pelikán, J. Majzlík: Electric spark sensitivity of nitramines. Part I. Aspects of molecular structure, *Centr. Eur. J. Energ. Mater.* **2006**, 3, 27–44. b) S. Zeman, V. Pelikán, J. Majzlík: Electric spark sensitivity of nitramines. Part II. A problem of "hot spots". *Centr. Eur. J. Energ. Mater.* **2006**, 3, 45–51. c) D. Skinner, D. Olson, A. Block-Bolten: Electrostatic discharge ignition of energetic materials. *Propellants, Explos., Pyrotechn.* **1998**, 23, 34–42. d) OZM research, Czech Republic, e) <http://www.ozm.cz/testing-instruments/pdf/TI-SmallSpark.pdf>.
- [88] G. R. Lakshminarayanan, G. Chen, R. Ames, W. T. Lee, J. Wejsa, K. Meiser, *Laminac Binder Replacement Program*, Aug. **2006**.

2 Salts of 1-(2-Hydroxyethyl)-5-nitriminotetrazole

1-(2-Hydroxyethyl)-5-nitriminotetrazole (**1**) is the nitration product of 1-(2-hydroxyethyl)-5-aminotetrazole (**1-OH**) and has been described in the literature.^[1, 2] In this chapter the preparation of its alkali metal and alkaline earth metal salts are presented and their characterization using multinuclear magnetic resonance as well as vibrational spectroscopy (IR and Raman) and elemental analysis are given. Moreover, their energetic properties, like decomposition temperature and sensitivities to outer stimuli were determined. Furthermore, three different copper(II) compounds with **1** as ligand were prepared and investigated.

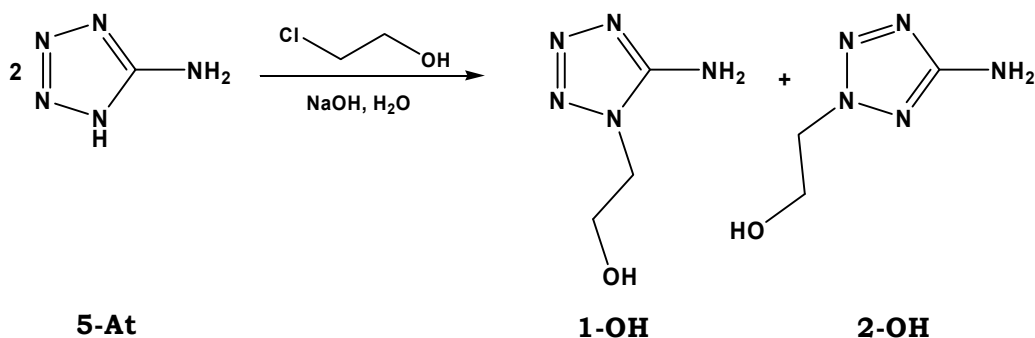
1 was selected, because it combines several properties, which are advantageous for the application as starting material for coloring agents. First of all, it can be deprotonated easily, yielding thermally more stable salts or copper(II) complexes. It consists of a tetrazole ring, which is responsible for the formation of gaseous nitrogen as decomposition product, and includes an energetic nitrimino group, which also improves the oxygen balance. Moreover, its hydroxy group may help forming the light emitting species SrOH, BaOH, and CuOH in the gas phase.^[3] SrOH emits light with the wavelengths 605 nm, 646 nm (orange) and 659 nm, 668 nm, 682 nm (red). BaOH emits at 487 nm and 512 nm (blue-green, green) and CuOH is also able to emit green light (525–555 nm).^[3, 4]

Therefore, the color performances and combustion behavior in the flame of a BUNSEN burner of all prepared compounds of **1** were investigated with regard to their possible application as colorants in pyrotechnic compositions. Besides that, their solubilities in H₂O at ambient temperature were determined.

2.1 Results and Discussion

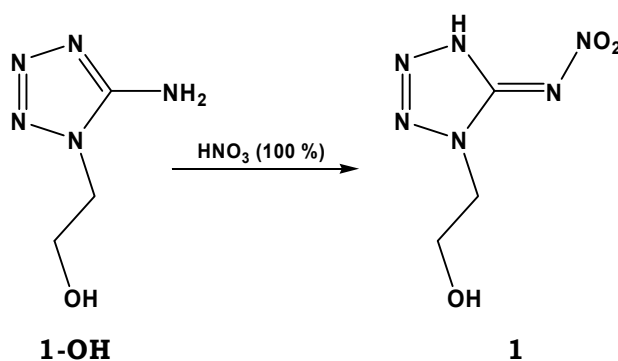
2.1.1 Syntheses

The first preparative step is an alkylation of the commercially available nitrogen-rich five-membered ring 5-aminotetrazole (**5-At**) with 2-chloroethanol according to a procedure known in literature (Scheme 2.1).^[1, 2, 5] Both isomers – 1-(2-hydroxyethyl)- (**1-OH**) and 2-(2-hydroxyethyl)-5-aminotetrazole (**2-OH**) – could be isolated. The work up of **1-OH** was performed analog to literature. For the propose of separating **2-OH**, the yellow solution after filtering **1-OH** off, was concentrated and then dissolved in ethyl acetate. After several days storing at ambient temperature a colorless solid was formed. After several recrystallization steps from ethyl acetate it was possible to obtain colorless crystals of **2-OH**. Due to the fact that the purification of **2-OH** is more time consuming and it can be obtained only in very low yields, the following synthesis steps were performed using **1-OH** exclusively.



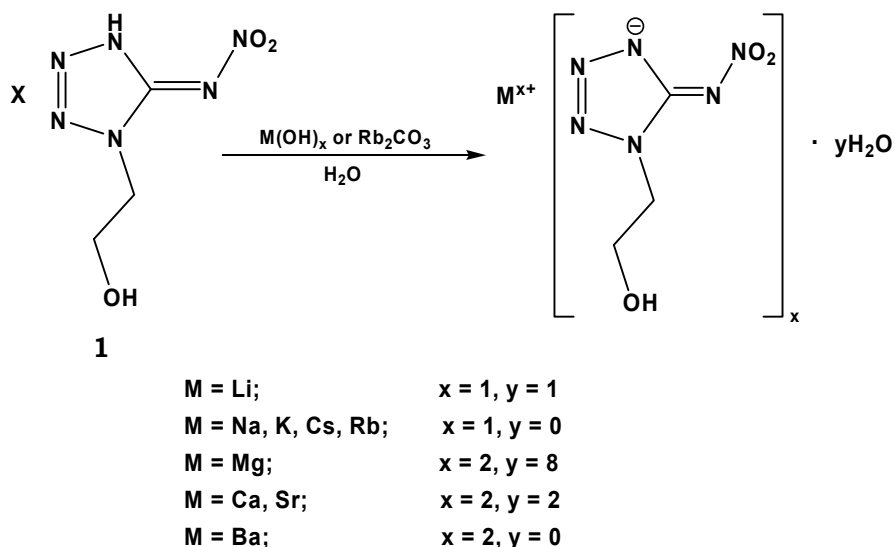
Scheme 2.1 Preparation of 1- and 2-(2-hydroxyethyl)-5-aminotetrazole (**1-/2-OH**).

The nitration of **1-OH** was performed in HNO₃ (100 %), which procedure is well known in the literature (Scheme 2.2).^[1, 2] Therefore, **1-OH** is slowly added to an ice-cooled solution of HNO₃ (100 %) and stirred for at least 17 hours in an open beaker. The colorless solution is poured onto ice and then stored at ambient temperature until colorless crystals of 1-(2-hydroxyethyl)-5-nitriminotetrazole (**1**) are formed. If the excess of nitric acid is too large, 1-(2-nitratoethyl)-5-nitriminotetrazole monohydrate (**2**) can be obtained (see chapter 3).



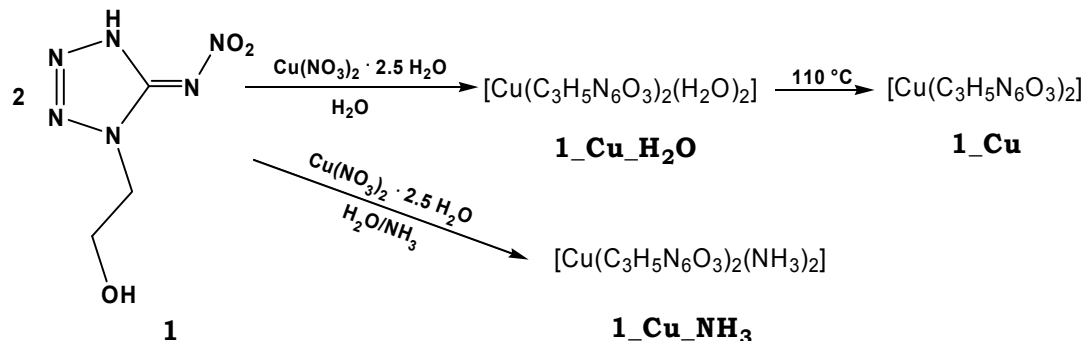
Scheme 2.2 Nitration of **1-OH** to 1-(2-hydroxyethyl)-5-nitriminotetrazole (**1**).

For preparation of the alkali and alkaline earth metal salts, **1** was dissolved in H₂O and the corresponding hydroxides were added. In the case of preparing rubidium 1-(2-hydroxyethyl)-5-nitriminotetrazolate (**1_Rb**) rubidium carbonate was used as a base. The suspension was heated until it became clear. By recrystallization from H₂O, lithium 1-(2-hydroxyethyl)-5-nitriminotetrazolate monohydrate (**1_Li**), sodium 1-(2-hydroxyethyl)-5-nitriminotetrazolate (**1_Na**), potassium 1-(2-hydroxyethyl)-5-nitriminotetrazolate (**1_K**), **1_Rb**, cesium 1-(2-hydroxyethyl)-5-nitriminotetrazolate (**1-Cs**), magnesium 1-(2-hydroxyethyl)-5-nitriminotetrazolate octahydrate (**1_Mg**), calcium 1-(2-hydroxyethyl)-5-nitriminotetrazolate dihydrate (**1_Ca**), strontium 1-(2-hydroxyethyl)-5-nitriminotetrazolate dihydrate (**1_Sr**), and barium 1-(2-hydroxyethyl)-5-nitriminotetrazolate (**1_Ba**) were obtained (Scheme 2.3) and could be isolated in good yields.



Scheme 2.3 Preparation of the alkali and alkaline earth metal salts of **1**.

The copper(II) compound *trans*-[diaqua-bis{1-(2-hydroxyethyl)-5-nitriminotetrazolato- $\kappa^2N4,O5$ } copper(II)] (**1_Cu_H₂O**) was prepared with copper(II) nitrate pentahemihydrate in H₂O according to a procedure known in the literature.^[1, 2] If the blue crystals of **1_Cu_H₂O** are dried under high vacuum or stored in a dry oven at 105 °C for 24 hours, the chemically bound water molecules can be removed and a green powder of copper(II) 1-(2-hydroxyethyl)-5-nitriminotetrazolate (**1_Cu**) is obtained in quantitative yields (Scheme 2.4).



Scheme 2.4 Syntheses of the copper(II) compounds **1_Cu_H₂O**, **1_Cu**, and **1_Cu_NH₃**.

For the preparation of tetrammine copper(II) 1-(2-hydroxyethyl)-5-nitriminotetrazolate (**1_Cu_NH₃**), a diluted aqueous ammonia solution (12 %) is added to a solution of **1** and copper(II) nitrate pentahemihydrate (Scheme 2.4). The dark violet crystals of **1_Cu_NH₃** were formed after storing the dark blue solution at ambient temperature for a few days.

2.1.2 Molecular Structures

The molecular structure of **2-OH** in the solid state could be determined after recrystallization from ethyl acetate. After recrystallization from H₂O, single crystals of the salts **1_Li**, **1_Na**, **1_K**, **1_Rb**, **1-Cs**, **1_Mg**, **1_Ca**, and **1_Sr** suitable for X-ray diffraction

could be obtained. Single crystals of **1-Cu-NH₃** were yielded from the reaction solution. All relevant data and parameters of the X-ray measurements and refinements are given in Appendix I. The structure of **1-Cu-H₂O** is discussed in the literature.^[1, 2]

The 2-isomer 2-(2-hydroxyethyl)-5-aminotetrazole (**2-OH**) crystallizes in the monoclinic space group $P2_1/c$ with four molecules per unit cell (Figure 2.1). Its density of 1.443 g/cm³ is lower than the one of **1-OH** (1.497 g/cm³ [1, 2]).

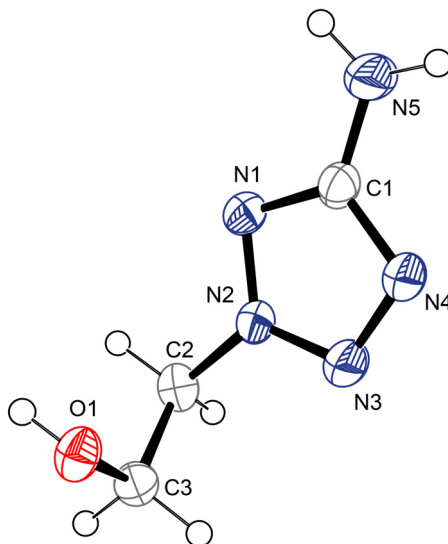


Figure 2.1 Molecular unit of **2-OH**. Hydrogen atoms shown as spheres of arbitrary radius and thermal displacements set at 50 % probability. Geometries: distances (Å) N1–N2 1.338(2), N2–N3 1.300(2), N3–N4 1.334(2), N1–C1 1.337(2), N4–C1 1.348(2), C1–N5 1.345(2), N2–C2 1.465(2), C2–C3 1.507(2), O1–C3 1.419(2); angles (°) N1–C1–N4 112.1(1), N1–C1–N5 124.4(1), N5–C1–N4 123.48(1), N1–N2–N3 114.1(1), N2–N3–N4 106.52(1), N1–N2–C2 123.4(1), N3–N2–C2 122.5(1), C1–N1–N2 101.50(1), N3–N4–C1 105.8(1), N2–C2–C3 111.2(1), O1–C3–C2 112.2(1); torsion angles (°) N3–N2–N1–C1 0.6(2), C2–N2–N1–C1 -178.76(1), N1–N2–N3–N4 -0.2(2), C2–N2–N3–N4 179.1(1), C1–N4–N3–N2 -0.2(2), N3–N2–C2–C3 55.0(2), N1–N2–C2–C3 -125.7(1), O1–C3–C2–N2 58.6(2), N2–N1–C1–N5 177.5(1), N2–N1–C1–N4 -0.7(2), N3–N4–C1–N1 0.6(2), N3–N4–C1–N5 -177.7(1).

The measured bond lengths and angles are comparable to the ones of **1-OH**.^[1, 2] Four different hydrogen bonds can be found. The oxygen atom O1 is twice the donor atom (O1–H1 \cdots N4 i 0.84 Å, 2.04 Å, 2.81 Å, 151.9°; O1–H1 \cdots N3 i 0.84 Å, 2.68 Å, 3.39 Å, 142.3°; i : x , $-y+1/2$, $z+1/2$). The other donor atom is N5 forming hydrogen bonds to N1 and O1 (N5–H5a \cdots N1 ii 0.87 Å, 2.28 Å, 3.14 Å, 168.0°; N5–H5b \cdots O1 iii 0.88 Å, 2.04 Å, 2.91 Å, 175.5°; ii) $-x+1$, $-y$, $-z+1$, iii) $-x+1$, $y-1/2$, $-z+1/2$).

The packing of **2-OH** is characterized by zig-zag layers along the c axis. Thereby, the adverse lying aminotetrazole rings of two molecules are in a line, and the kink is a result of the alkyl rests.

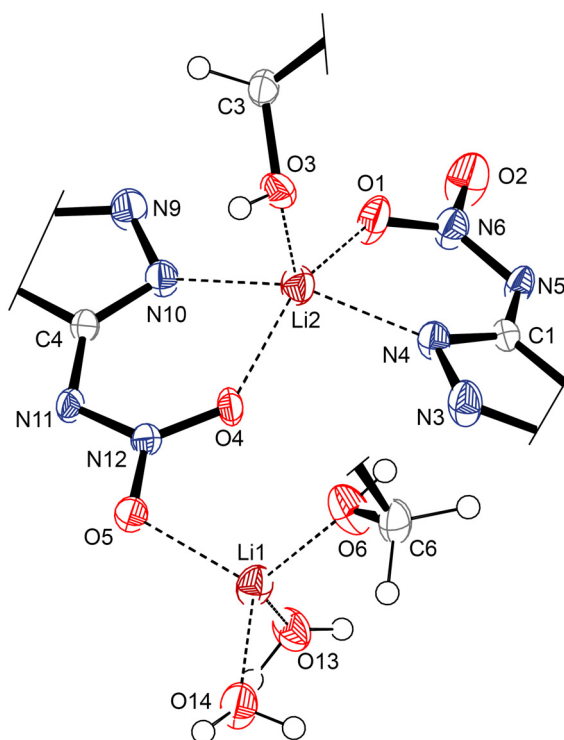


Figure 2.2 Coordination spheres of the lithium atoms in **1_Li**. Hydrogen atoms shown as spheres of arbitrary radius and thermal displacements set at 50 % probability. Selected geometries: distances (Å) N1–N2 1.345(2), N2–N3 1.290(2), N3–N4 1.363(2), N1–C1 1.353(2), N4–C1 1.331(2), C1–N5 1.366(2), N5–N6 1.315(2), O1–N6 1.268(2), O2–N6 1.245(2), N1–C2 1.463(2), Li1–O5 1.991(4), Li1–O6 1.909(4), Li1–O13 1.905(4), Li1–O14 1.924(4), Li2–O3 1.952(4), Li2–N4 2.059(4), Li2–O4 2.085(4), Li2–O1 2.097(3), Li2–N10 2.102(4); angles (°) N1–C1–N4 108.2(2), N1–C1–N5 118.0(2), O1–N6–N5 123.9(2), O1–N6–O2 119.7(2), O13–Li1–O6 117.3(2), O13–Li1–O14 104.7(2), O6–Li1–O14 104.2(2), O13–Li1–O5 101.7(2), O6–Li1–O5 114.0(2), O14–Li1–O5 115.0(2), O3–Li2–N4 106.1(2), O3–Li2–O4 99.9(2), N4–Li2–O4 93.4(2), O3–Li2–O1 109.4(2), N4–Li2–O1 77.8(1), O4–Li2–O1 150.8(2), O3–Li2–N10 98.9(2), N4–Li2–N10 154.6(2), O4–Li2–N10 78.4(1), O1–Li2–N10 97.6(2); torsion angles (°) N6–N5–C1–N1 –177.5(2), C1–N5–N6–O1 –4.3(3).

Lithium 1-(2-hydroxyethyl)-5-nitriminotetrazolate monohydrate (**1_Li**) crystallizes in the triclinic space group $P\bar{1}$ with eight molecular units per unit cell. Thereby two lithium atoms are coordinated differently forming dimers (Figure 2.2). Lithium atom Li1 is coordinated fourfold by two oxygen atoms (O13, O14) of crystal water molecules and O5 of the nitrimino group as well as the oxygen atom of the alkyl rest (O6). Lithium atom Li2 is coordinated fivefold by the oxygen atoms (O4, O1) of the nitrimino group of two different anions, the hydroxyl group (O3), as well as the nitrogen atoms N4 and N10 of the tetrazole ring of two different anions. The distance of the lithium atoms Li1 and Li2 is 4.651 Å. The ionic radius of fourfold coordinated Li^+ is 0.73 Å and of sixfold coordinated Li^+ 0.90 Å.^[6] The sum of both ionic radii is less than the measured distance of Li1–Li2. Its density of 1.628 g/cm³ is as expected the lowest of the alkali metals. The residual density of 0.719 e/Å³ is quite high. However, further analytical data, such as elemental analysis, ¹H and ¹³C NMR, IR, and Raman spectroscopy verified the formation of the salt **1_Li**.

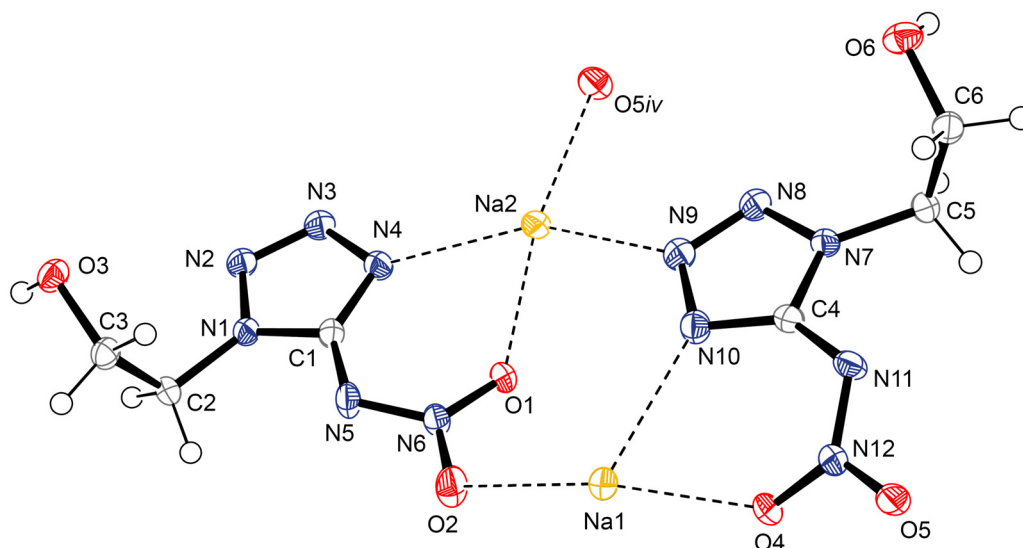


Figure 2.3 Dimer of two molecular units in **1_Na**. Hydrogen atoms shown as spheres of arbitrary radius and thermal displacements set at 50 % probability. Selected geometries: distances (Å) N1–N2 1.345(2), N2–N3 1.300(2), N3–N4 1.367(2), N1–C1 1.355(2), N4–C1 1.331(2), C1–N5 1.373(2), N5–N6 1.321(2), O1–N6 1.256(1), O2–N6 1.245(2), N1–C2 1.466(2), Na1–O4 2.317(1), Na1–O2 2.344(1), Na1–N10 2.536(2), Na1–O4 $_{ii}$ 2.508(1), Na1–O6 $_{iii}$ 2.361(1), Na1–N3 $_{iv}$ 2.562(2), Na2–O1 2.326(2), Na2–O5 2.329(1), Na2–N4 2.491(2), Na2–N9 2.660(2), Na2–O1 $_{i}$ 2.4396(2), Na2–O3 $_{v}$ 2.351(1); angles (°) N1–C1–N4 108.17(13), N1–C1–N5 116.14(12), O1–N6–N5 123.71(12), O1–N6–O2 120.34(11), O4–Na1–O2 165.17(5), O4–Na1–N10 70.60(5), O2–Na1–N10 115.17(6), O1–Na2–O5 169.72(4), O1–Na2–N4 69.04(5), O5–Na2–N4 120.61(5), O1–Na2–N9 81.36(6), O5–Na2–N9 90.24(5), N4–Na2–N9 146.42(4); torsion angles (°) N6–N5–C1–N1 163.4(1), C1–N5–N6–O1 3.0(2); i $-x, -y+1, -z+1$, ii $-x+1, -y+1, -z+1$, iii $-x+1, -y, -z+1$, iv $x+1, y, z$, v $-x, -y+1, -z$.

Analog to **1_Li**, in the crystal structure of sodium 1-(2-hydroxyethyl)-5-nitrinotetrazole (**1_Na**) dimers are formed (Figure 2.3). **1_Na** also crystallizes in the triclinic space group $P\bar{1}$ with four molecular units per unit cell. Its density of 1.814 g/cm³ is higher than the one of **1_Li**. Besides the higher ionic diameter of the sodium atoms, the absence of crystal water molecules might be a reason. The sodium atom Na1 is coordinated sixfold by the atoms O2, O4, N10, O4 $_{ii}$, O6 $_{iii}$, and N3 $_{iv}$. The distance between two Na1 atoms is quite short with 3.769 Å. However, it is larger than the sum the radii of two sixfold coordinated Na⁺, which is 1.16 Å [6]. Na2 is also coordinated sixfold by the atoms, O1, O5, N4, N9, O1 $_{i}$, and O3 $_{v}$. The distance of two Na2 atoms is shorter with 3.492 Å, whereas the distance between Na1 and Na2 is 4.756 Å. A framework is built due to the coordinating of each nitrinotetrazole anion with both sodium atoms Na1 and Na2.

Two different hydrogen bonds are found. In each case the oxygen atom of the hydroxyl group is the donor atom (O6–H6 \cdots N5 $_{vi}$ 0.81(2) Å, 2.21(2) Å, 3.014(2) Å, 171(2)°; O3–H3 \cdots N11 $_{vii}$ 0.77(2) Å, 2.13(2) Å, 2.896(2) Å, 172(2)°; vi) $x, y-1, z+1$, vii) $x-1, y+1, z-1$).

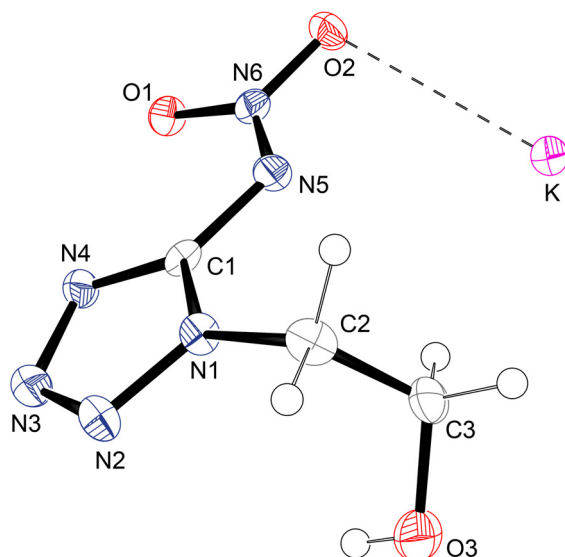


Figure 2.4 Molecular unit of **1_K**. Hydrogen atoms shown as spheres of arbitrary radius and thermal displacements set at 50 % probability. Selected geometries: distances (Å) N1–N2 1.357(2), N2–N3 1.292(2), N3–N4 1.370(3), N1–C1 1.348(3), N4–C1 1.331(3), C1–N5 1.379(3), N5–N6 1.319(3), O1–N6 1.258(2), O2–N6 1.260(2), N1–C2 1.465(3), O2–K1 2.925(2), K1–O1*i* 2.861(2), K1–O1*ii* 2.863(2), K1–O1*iii* 2.865(2), K1–N4*iii* 2.898(2), K1–N4*ii* 2.980(2), K1–O3*v* 3.006(2), K1–O2*i* 3.010(2), K1–N3*iv* 3.082(2); angles (°) N1–C1–N4 108.9(2), N1–C1–N5 116.4(2), O1–N6–N5 124.8(2), O1–N6–O2 119.5(2), N6–O2–K1 103.9(1); torsion angles (°) N6–N5–C1–N1 –178.0(2), C1–N5–N6–O1 –2.5(3); *i*) $-x+1, y-1/2, -z+3/2$, *ii*) $-x+1, y+1/2, -z+3/2$, *iii*) $x, -y+1/2, z-1/2$, *iv*) $x, -y-1/2, z-1/2$, *v*) $x, y+1, z$.

Potassium 1-(2-hydroxyethyl)-5-nitriminotetrazolate (**1_K**) crystallizes in the monoclinic space group $P2_1/c$ with four molecules per unit cell (Figure 2.4). Its density of 1.878 g/cm³ is slightly higher than the one of **1_Na**. The potassium cation is coordinated ninefold, if distances up to 3.1 Å are chosen. Atoms with shorter bond lengths are O2, O1*i*, O1*ii*, O1*iii*, O2*i*, O3*v*, N4*ii*, N4*iii*, and N3*iv*. Each nitriminotetrazole anion is connected with three different potassium cations.

Analog to **1_Na**, two hydrogen bonds are formed. The donor atom is O3 and the acceptor atoms N5*vi* and O2*vi* (O3–H3⋯N5*vi* 0.78(3) Å, 2.12(3) Å, 2.862(3) Å, 160(3)°; O3–H3⋯O2*vi* 0.78(3) Å, 2.61(3) Å, 3.207(3) Å, 135(3)°; *vi*) $x, y-1, z+1$).

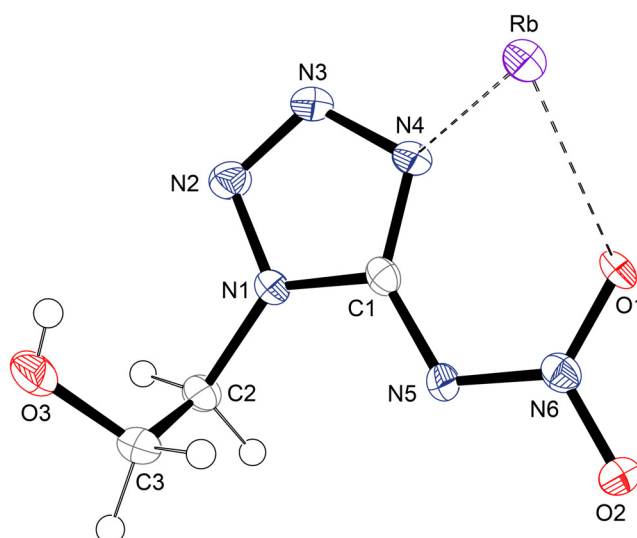


Figure 2.5 Molecular unit of **1_Rb**. Hydrogen atoms shown as spheres of arbitrary radius and thermal displacements set at 50 % probability. Selected geometries: distances (Å) N1–N2 1.349(3), N2–N3 1.304(4), N3–N4 1.375(3), N1–C1 1.347(4), N4–C1 1.341(4), C1–N5 1.373(3), N5–N6 1.322(3), O1–N6 1.254(3), O2–N6 1.258(3), N1–C2 1.470(4), Rb1–O1 2.975(2), Rb1–O1*i* 2.976(2), Rb1–O1*ii* 2.985(2), Rb1–O2*v* 3.017(2), Rb1–N4*ii* 3.036(2), Rb1–O3*iv* 3.071(3), Rb1–N4 3.111(3), Rb1–O2*i* 3.113(2), Rb1–N3*iii* 3.187(3); angles (°) N1–C1–N4 108.3(2), N1–C1–N5 117.2(3), O1–N6–N5 124.3(2), O1–N6–O2 120.3(3), O1–Rb1–N4 51.77(6); torsion angles (°) N6–N5–C1–N1 179.1(2), C1–N5–N6–O1 2.9(4); *i*) $x, y+1, z$, *ii*) $-x+1, -y, -z+1$, *iii*) $-x+1, -y+1, -z+1$, *iv*) $-x+1, y-1/2, -z+1/2$, *v*) $-x+1, y+1/2, -z+1/2$.

Rubidium 1-(2-hydroxyethyl)-5-nitriminotetrazolate (**1_Rb**) crystallizes analog to **1_K** in the monoclinic space group $P2_1/c$ with four molecules per unit cell (Figure 2.5). Its density of 2.174 g/cm³ is significantly higher than the one of **1_K**. If a maximum coordination distance of 3.2 Å is considered, the rubidium ions are also coordinated ninefold. The coordinating atoms are O1, N4, O1*i*, O1*ii*, O2*v*, N4*ii*, O3*iv*, O2*i*, and N3*iii*. Only one hydrogen bond is observed with O3 as donor and N5*i* as acceptor atom (O3–H3⋯N5*i* 0.66(4) Å, 2.26(4) Å, 2.890(4) Å, 161(5)°; *i*) $x, y+1, z$).

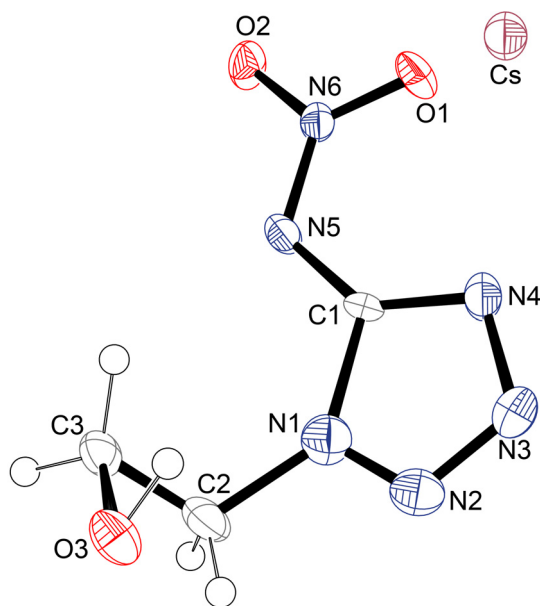


Figure 2.6 Molecular unit of **1-Cs**. Hydrogen atoms shown as spheres of arbitrary radius and thermal displacements set at 50 % probability. Selected geometries: distances (Å) N1–N2 1.137(17), N2–N3 1.316(11), N3–N4 1.358(10), N1–C1 1.566(16), N4–C1 1.333(10), C1–N5 1.359(11), N5–N6 1.336(11), O1–N6 1.251(7), O2–N6 1.253(12), N1–C2 1.520(11), Cs1–O1 3.126(13), Cs1–O1*i* 3.122(5), Cs1–O1*ii* 3.135(13), Cs1–O3*iii* 3.136(6), Cs1–N4*i* 3.228(7), Cs1–O2*ii* 3.246(6), Cs1–O2*iv* 3.249(6) Cs1–N4 3.287(8), Cs1–N3*v* 3.476(8); angles (°) N1–C1–N4 101.5(8), N1–C1–N5 122.3(8), O1–N6–N5 124.3(10), O1–N6–O2 119.6(10), O1–Cs1–N4 49.9(2); torsion angles (°) N6–N5–C1–N1 168.9(10), C1–N5–N6–O1 -2.1(14); *i*) $-x+1, y+1/2, -z$, *ii*) $x, y+1, z$, *iii*) $-x, y-1/2, -z$, *iv*) $-x, y+1/2, -z$, *v*) $-x+1, y-1/2, -z$.

Cesium 1-(2-hydroxyethyl)-5-nitriminotetrazolate (**1-Cs**) crystallizes in the monoclinic space group $P2_1$ with two molecular units per unit cell. Its density of 2.431 g/cm³ is the highest one of the prepared compounds. All cesium cations are coordinated ninefold with a maximum distance of 3.5 Å. Coordinating atoms are O1, O2 of the nitrimino group, the oxygen atom O3 of the hydroxyl residue, as well as the nitrogen atoms N3 and N4 of the tetrazole ring. The ratio of data to parameter is quite low (953:122), due to the refinement of the FLACK parameter.^[7] This led to an inconclusive value.^[8] Therefore, the FRIEDEL equivalents were merged before the final refinement with a MERG 4 command.

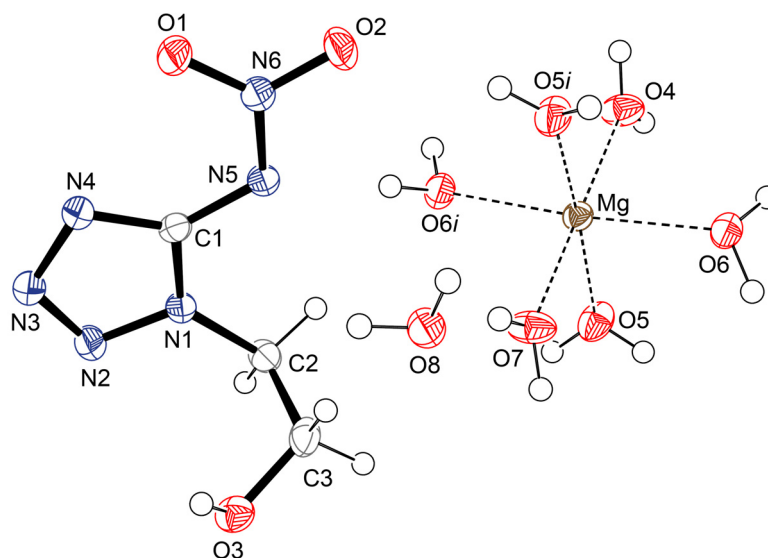


Figure 2.7 Molecular unit of **1_Mg**. For a better overview only one 1-(2-hydroxyethyl)-5-nitriminotetrazole anion and one non-coordinating crystal water molecule are shown. Hydrogen atoms shown as spheres of arbitrary radius and thermal displacements set at 50 % probability. Selected geometries: distances (Å) N1–N2 1.347(1), N2–N3 1.288(1), N3–N4 1.372(1), N1–C1 1.352(2), N4–C1 1.337(1), C1–N5 1.370(2), N5–N6 1.329(1), O1–N6 1.249(1), O2–N6 1.244(1), N1–C2 1.469(2), Mg1–O5 2.034(1), Mg1–O7 2.036(2), Mg1–O6 2.059(1), Mg1–O4 2.070(2); angles (°) N1–C1–N4 108.1(1), N1–C1–N5 117.3(1), O1–N6–N5 123.3(1), O1–N6–O2 120.2(1), O5–Mg1–O7 86.59(3), O5–Mg1–O6 89.41(5), O7–Mg1–O6 93.05(3), O5–Mg1–O4 93.41(3), O7–Mg1–O4 180.0, O6–Mg1–O4 86.95(3); torsion angles (°) N6–N5–C1–N1 176.5(1), C1–N5–N6–O1 $-0.5(2)$.

The alkaline earth metal salt magnesium 1-(2-hydroxyethyl)-5-nitriminotetrazolate octahydrate (**1_Mg**) crystallizes in the monoclinic space group $C2/c$ with four molecular units per unit cell. It offers the lowest density (1.587 g/cm³) of all prepared compounds. This value is even much lower than the density of neutral compound **1** (1.733 g/cm³ [1, 2]). Reason for this might be that the magnesium cations are only coordinated by six crystal water molecules (Figure 2.7). The further two crystal water molecules are non-coordinating, as well as the nitriminotetrazole anions.

Table 2.1 Hydrogen bonds between the Mg coordinating water molecules and 1-(2-hydroxyethyl)-5-nitriminotetrazolate in **1_Mg** (i) $-x, y, -z-1/2$, (ii) $x-1/2, -y-1/2, z-1/2$, (iii) $-x+1/2, y-1/2, -z-1/2$).

D–H··A	D–H [Å]	H··A [Å]	D··A [Å]	<(DHA) [°]
O6–H6a··N5 ⁱ	0.88(2)	1.93(2)	2.808(1)	170(2)
O6–H6a··O2 ⁱ	0.88(2)	2.63(2)	3.289(2)	132(2)
O6–H6a··N6 ⁱ	0.88(2)	2.67(2)	3.504(2)	157(2)
O5–H5b··O2 ⁱ	0.80(2)	2.13(2)	2.903(2)	164(2)
O6–H6b··N4 ⁱⁱ	0.82(2)	2.28(2)	3.024(2)	152(2)
O5–H5a··O3 ⁱⁱⁱ	0.86(2)	1.92(2)	2.770(2)	170(2)

The sixfold coordinated magnesium ions, as well as the 1-(2-hydroxyethyl)-5-nitriminotetrazole anions form separate layers along the *a* axis. They are connected *via* hydrogen bonds (Table 2.1). Furthermore, two intermolecular hydrogen bonds can be found between

the anions ($\text{O3-H3}\cdots\text{N4}$ *iv* 0.80(2) Å, 2.19(2) Å, 2.955(2) Å, 160.7(16)°; $\text{O3-H3}\cdots\text{O1}$ *iv* 0.80(2) Å, 2.32(2) Å, 2.876(2) Å, 128(2)°, *iv* $-x+1/2, -y+1/2, -z$).

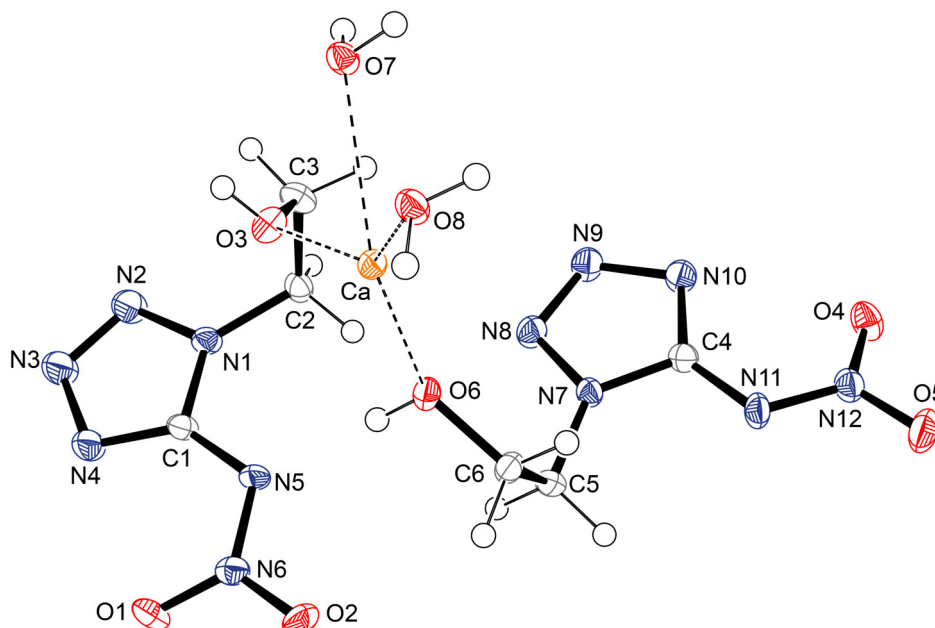


Figure 2.8 Molecular unit of **1_Ca**. Hydrogen atoms shown as spheres of arbitrary radius and thermal displacements set at 50 % probability. Selected geometries: distances (Å) N1–N2 1.343(2), N2–N3 1.297(2), N3–N4 1.363(2), N1–C1 1.352(2), N4–C1 1.329(2), C1–N5 1.368(2), N5–N6 1.319(2), O1–N6 1.251(2), O2–N6 1.258(2), N1–C2 1.465(2), Ca1–O3 2.416(2), Ca1–O6 2.427(1), Ca1–O4*i* 2.444(1), Ca1–O8 2.475(1), Ca1–O1*ii* 2.551(2), Ca1–O7 2.551(2), Ca1–O7*iii* 2.580(1), Ca1–O2*ii* 2.628(1), Ca1–O5*i* 2.675(1); angles (°) N1–C1–N4 107.9(1), N1–C1–N5 118.2(1), O1–N6–N5 123.9(1), O1–N6–O2 119.5(1), O3–Ca1–O6 76.77(6), O3–Ca1–O4*i* 130.21(5), O6–Ca1–O4*i* 75.71(5), O3–Ca1–O8 143.92(4), O6–Ca1–O8 139.31(5), O3–Ca1–O7 76.64(6), O6–Ca1–O7 140.12(4), O8–Ca1–O7 72.32(5); torsion angles (°) N6–N5–C1–N1 $-171.9(1)$, C1–N5–N6–O1 $2.7(2)$; *i* $-x+1, -y, -z+1$, *ii* $-x+1, -y+1, -z+2$, *iii* $-x, -y+1, -z+1$.

In Figure 2.8 the molecular unit of calcium 1-(2-hydroxyethyl)-5-nitriminotetrazolate dihydrate (**1_Ca**) is shown. **1_Ca** crystallizes in the triclinic space group $P\bar{1}$ with two molecular units per unit cell. Its density of 1.804 g/cm³ is significantly higher than the one of **1_Mg**. The calcium cations are ninefold coordinated with respect to distances up to 2.7 Å. The coordinating atoms are O3, O6, O4*i*, O1*ii*, O2*ii*, and O5*i* of the nitriminotetrazole anions as well as the oxygen atoms O7, O7*iii*, and O8 of the crystal water molecules. Eight hydrogen bonds between the crystal water molecules and the nitriminotetrazole anions are observed.

The packing of **1_Ca** is characterized by layers. One layer formed by the crystal water molecules, which is surrounded above and below by layers of calcium ions and the nitriminotetrazolate rings. Their hydroxyethyl residues are forming another layer with the hydroxyl residues of the following nitriminotetrazolate ring and calcium ion layer.

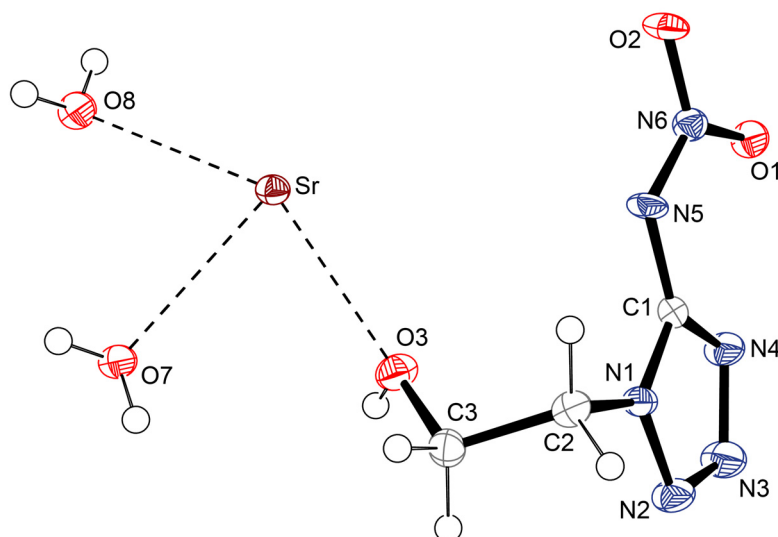


Figure 2.9 Molecular unit of **1_Sr**. For a better overview only one 1-(2-hydroxyethyl)-5-nitriminotetrazole anion is shown. Hydrogen atoms are shown as spheres of arbitrary radius and thermal displacements are set at 50 % probability. Selected geometries: distances (Å) N1–N2 1.355(2), N2–N3 1.296(3), N3–N4 1.362(3), N1–C1 1.346(3), N4–C1 1.332(3), C1–N5 1.374(3), N5–N6 1.315(3), O1–N6 1.252(2), O2–N6 1.260(2), N1–C2 1.464(3), Sr1–O6*i* 2.547(2), Sr1–O3 2.571(2), Sr1–O4*ii* 2.609(2), Sr1–O8 2.614(2), Sr1–O7 2.677(2), Sr1–O1*iii* 2.686(2), Sr1–O7*iv* 2.700(2), Sr1–O2*iii* 2.714(2), Sr1–O5*ii* 2.716(2); angles (°) N1–C1–N4 108.1(1), N1–C1–N5 117.3(1), O1–N6–N5 123.3(1), O1–N6–O2 120.2(1), O3–Sr1–O6*i* 78.53(6), O3–Sr1–O4*ii* 130.96(6), O6*i*–Sr1–O4*ii* 74.15(5), O3–Sr1–O8 142.03(6), O6*i*–Sr1–O8 139.44(6), O3–Sr1–O7 75.45(6), O6*i*–Sr1–O7 141.22(6), O8–Sr1–O7 71.43(6); torsion angles (°) N6–N5–C1–N1 173.1(2), C1–N5–N6–O1 –1.0(3); *i*) $-x+1, -y+1, -z+1$, *ii*) $x, y, z+1$, *iii*) $-x+1, -y, -z+1$, *iv*) $-x+2, -y, -z+2$.

Strontium 1-(2-hydroxyethyl)-5-nitriminotetrazolate dihydrate (**1_Sr**) crystallizes like **1_Ca** in the triclinic space group $P\bar{1}$ with two molecular units per unit cell. The strontium cations are coordinated ninefold by the oxygen atoms O3, O7, O8, O6*i*, O4*ii*, O1*iii*, O7*iv*, O2*iii*, and O5*ii*. The density of **1_Sr** is with 1.924 g/cm³ only slightly higher than the one of **1_Ca**. The packing of layers in **1_Sr** is analog to **1_Ca**.

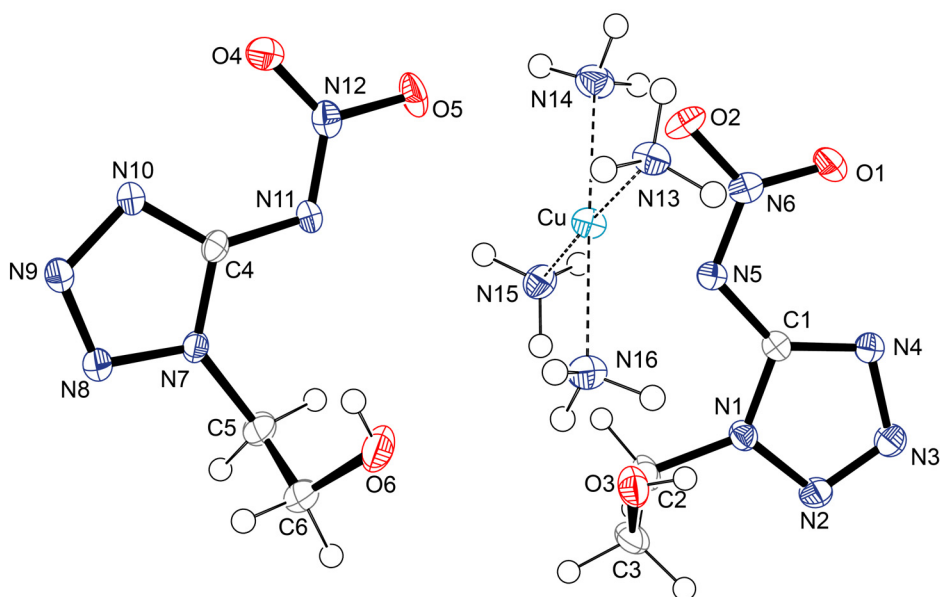


Figure 2.10 Molecular unit of **1-Cu-NH₃**. Hydrogen atoms shown as spheres of arbitrary radius and thermal displacements set at 50 % probability. Selected geometries: distances (Å) N1–N2 1.345(2), N2–N3 1.293(2), N3–N4 1.371(2), N1–C1 1.353(2), C1–N5 1.377(3), N5–N6 1.315(2), O1–N6 1.240(2), O2–N6 1.274(2), N1–C2 1.467(3), Cu–N13 2.008(2), Cu–N15 2.009(2), Cu–N14 2.016(2), Cu–N16 2.035(2), Cu–N9*i* 2.440(2), Cu–N3*ii* 2.741(2); angles (°) N1–C1–N4 108.1(2), N1–C1–N5 117.2(2), O1–N6–N5 125.4(2), O1–N6–O2 119.2(2), N13–Cu1–N15 176.9(1), N13–Cu1–N14 90.06(9), N15–Cu1–N14 89.35(10), N13–Cu1–N16 89.12(10), N15–Cu1–N16 91.41(10), N14–Cu1–N16 178.4(1); torsion angles (°) N6–N5–C1–N1 179.9(2), C1–N5–N6–O1 2.8(3); *i* $-x+1, -y, -z+2$, *ii* $x-1, -y, -z+1$.

The copper(II) complex tetrammine copper(II) 1-(2-hydroxyethyl)-5-nitriminotetrazolate (**1-Cu-NH₃**) crystallizes in the monoclinic space group $P2_1/n$ with four molecular units per unit cell. The copper(II) cation is coordinated fourfold by the nitrogen atoms of the four ammine ligands. The coordination distances are N13–Cu 2.008(2) Å, N14–Cu 2.016(2) Å, N15–Cu 2.009(2) Å, and N16–Cu 2.035(2) Å. This is in accordance with Cu–N bond lengths, such as in tetrammine copper(II) nitrate.^[9] If one is considering an octahedral coordination of the copper(II) atoms, the next neighbour atoms are N9*i* with a distance of 2.440(2) Å, as well as N3*ii* with a distance of 2.741(2) Å. However, the distance Cu–N3*ii* is too long and even 0.3 Å longer than Cu–N9*i* to form an octahedral coordination. Especially, the difference between the distance Cu–N9*i* and Cu–N3*ii* can not be explained by the JAHN-TELLER effect. Therefore, a quadratically planar coordination of the copper(II) atoms must be assumed. This could also explain the low density of 1.724 g/cm³. For comparison, the density of **1-Cu-H₂O** is 1.821 g/cm³.^[1, 2]

The density of copper(II) 1-(2-hydroxyethyl)-5-nitriminotetrazolate (**1-Cu**), determined with a pycnometer at 22 °C, is significantly higher with 2.02 g/cm³.

2.1.3 Energetic Properties

The energetic properties, such as decomposition temperature (T_{dec}), sensitivity to impact (E_{dr}), friction (F_{f}) and electric discharge (E_{el}), were determined. Furthermore, the

solubility in H₂O at ambient temperature of each compound was investigated. An overview of the energetic properties of the alkali metal salts is given in Table 2.2. The properties of the alkaline earth metal salts are shown in Table 2.3 and the properties of the copper(II) compounds can be found in Table 2.4.

Table 2.2 Overview of the physico-chemical properties of **1_Li**, **1_Na**, **1_K**, **1_Rb**, and **1-Cs**.

	1_Li	1_Na	1_K	1_Rb	1-Cs
Formula	C ₃ H ₅ LiN ₆ O ₃ · H ₂ O	C ₃ H ₅ N ₆ NaO ₃	C ₃ H ₅ KN ₆ O ₃	C ₃ H ₅ N ₆ O ₃ Rb	C ₃ H ₅ CsN ₆ O ₃
M [g/mol]	198.07	196.10	212.21	258.58	306.02
E_{dr} [J]^a	20	20	20	10	20
F_r [N]^b	> 360	> 360	> 360	> 360	160
E_{el} [J]^c	1.0	1.2	1.1	0.70	0.50
grain size [μm]	500–1000	> 1000	250–500	500–1000	500–1000
N [%]^d	42.43	42.86	39.60	32.55	27.43
Ω [%]^e	-49	-53	-57	-46	-39
T_{dec} [°C]^f	278	273	271	281	281
ρ [g/cm³]^g	1.63	1.81	1.87	2.17	2.43
H₂O sol. [wt%]^h	12 (22 °C)	28 (22 °C)	45 (22 °C)	24 (22 °C)	19 (22 °C)

a) BAM drop hammer ^[10], b) BAM methods ^[10], c) Electric spark tester, d) Nitrogen content, e) Oxygen balance, f) Decomposition temperature from DSC ($\beta = 5$ K/min), g) determined by X-ray crystallography or pycnometer (*), h) Solubility in H₂O (H₂O temperature).

Table 2.3 Overview of the physico-chemical properties of **1_Mg**, **1_Ca**, **1_Sr**, and **1_Ba**.

	1_Mg	1_Ca	1_Sr	1_Ba
Formula	Mg(C ₃ H ₅ N ₆ O ₃) ₂ · 8H ₂ O	Ca(C ₃ H ₅ N ₆ O ₃) ₂ · 2H ₂ O	Sr(C ₃ H ₅ N ₆ O ₃) ₂ · 2H ₂ O	Ba(C ₃ H ₅ N ₆ O ₃) ₂
M [g/mol]	514.65	422.33	469.87	483.55
E_{dr} [J]^a	35	20	12	10
F_r [N]^b	> 360	> 360	240	> 360
E_{el} [J]^c	1.0	1.0	1.3	1.2
grain size [μm]	500–1000	500–1000	160–250	250–500
N [%]^d	32.66	39.80	35.77	34.76
Ω [%]^e	-37	-46	-41	-40
T_{dec} [°C]^f	301	293	295	301
ρ [g/cm³]^g	1.59	1.80	1.92	2.40* (24 °C)
H₂O sol. [wt%]^h	72 (22 °C)	23 (25 °C)	15 (22 °C)	6.5 (25 °C)

a) BAM drop hammer ^[10], b) BAM methods ^[10], c) Electric spark tester, d) Nitrogen content, e) Oxygen balance, f) Decomposition temperature from DSC ($\beta = 5$ K/min), g) determined by X-ray crystallography or pycnometer (*), h) Solubility in H₂O (H₂O temperature).

For investigating the thermal behavior, ~1.5 mg of each compound was measured *via* differential scanning calorimetry (DSC) in the temperature range from 20–400 °C. The endothermic signals were checked using a *Büchi* melting point apparatus to distinguish melting from loss of crystal water.

Table 2.4 Overview of the physico-chemical properties of **1_Cu_H₂O**, **1_Cu**, and **1_Cu_NH₃**.

	1_Cu_H₂O	1_Cu	1_Cu_NH₃
Formula	[Cu(C ₃ H ₅ N ₆ O ₃) ₂ (H ₂ O) ₂]	[Cu(C ₃ H ₅ N ₆ O ₃) ₂]	[Cu(C ₃ H ₅ N ₆ O ₃) ₂ (NH ₃) ₄]
M [g/mol]	445.80	409.77	443.83
E_{dr} [J]^a	10	1.0	9.0
F_r [N]^b	324	240	> 360
E_{el} [J]^c	0.15	0.20	0.50
grain size [μm]	100–500	500–1000	250–500
N [%]^d	37.70	41.02	44.18
Ω [%]^e	-43	-43	-54
T_{dec} [°C]^f	221	239	225
ρ [g/cm³]^g	1.82	2.02* (22 °C)	1.72
H₂O sol. [wt%]^h	1.0 (25 °C)	1.7 (22 °C)	0.3 (25 °C)

a) BAM drop hammer ^[10], b) BAM methods ^[10], c) Electric spark tester, d) Nitrogen content, e) Oxygen balance, f) Decomposition temperature from DSC ($\beta = 5$ K/min), g) determined by X-ray crystallography or pycnometer (*), h) Solubility in H₂O (H₂O temperature).

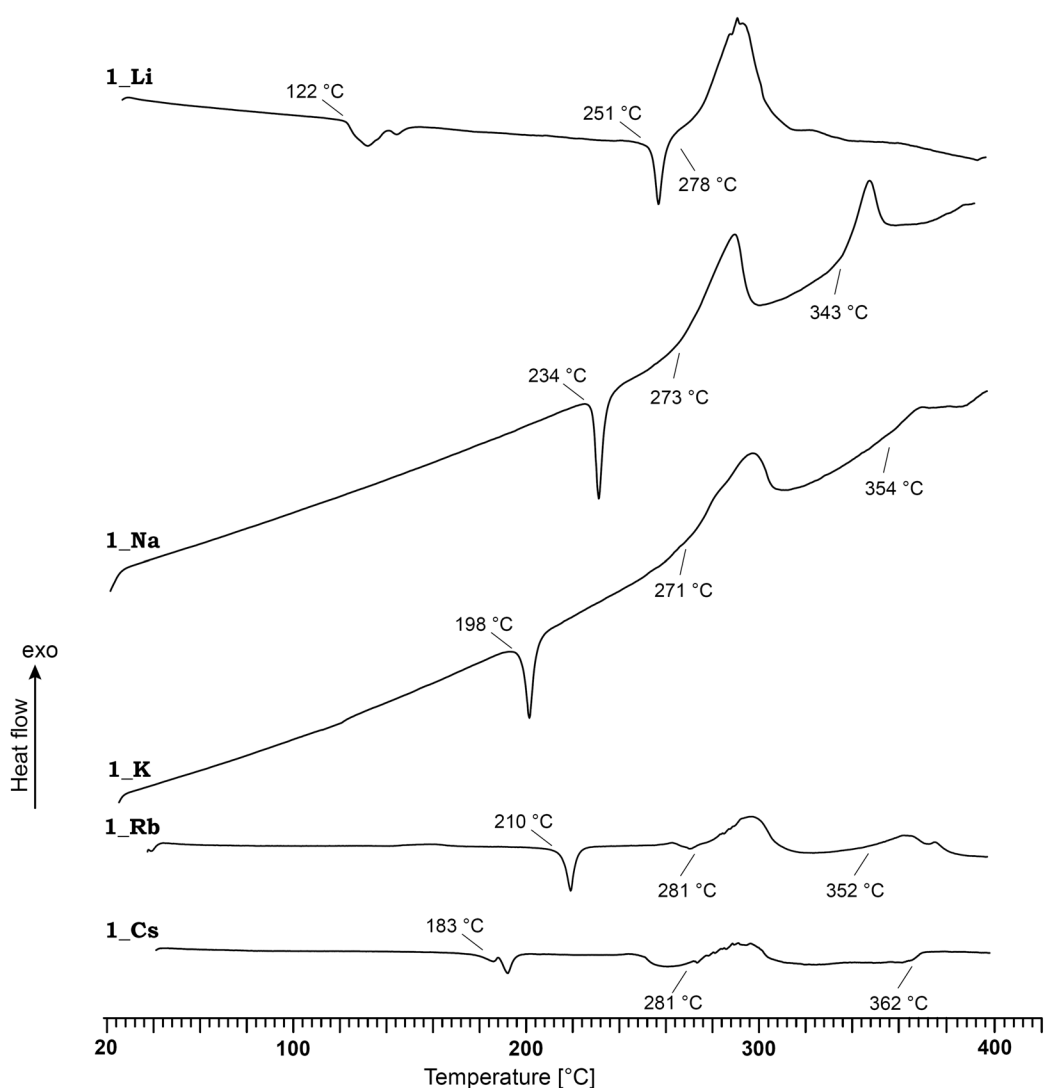


Figure 2.11 DSC thermograms of the alkali metal salts of **1** in a temperature range of 25–400 °C. Decomposition points are given as onset temperatures.

All alkali metal salts of **1** decompose at temperatures above 270 °C (Figure 2.11). All alkali metal salts melt before they decompose (**1_Li**: 251 °C, **1_Na**: 234 °C, **1_K**: 198 °C, **1_Rb**: 210 °C, **1-Cs**: 183 °C). Lithium 1-(2-hydroxyethyl)-5-nitriminotetrazolate monohydrate (**1_Li**) loses its crystal water at temperatures above 122 °C. Furthermore, its melting point is followed by its decomposition. Except **1_Li**, all alkali metal salts decompose in two steps, whereas the first decomposition occurs at about 270–280 °C and the second one in a temperature range of 343–380 °C.

Also the alkaline earth metal salts of **1** are thermally very stable up to temperatures of almost 300 °C (Figure 2.12). The salts, which contain crystal water molecules, lose them before decomposition occurs. In the case of the octahydrate, **1_Mg**, three separate endothermic signals, caused by loss of crystal water, can be observed at 55 °C, 97 °C, and 123 °C. **1_Ca**, **1_Sr**, and **1_Ba** also decompose in two steps (**1_Ca**: 293 °C, 321 °C, **1_Sr**: 295 °C, 325 °C, **1_Ba**: 301 °C, 322 °C). The second exothermic signal is much smaller than the first one.

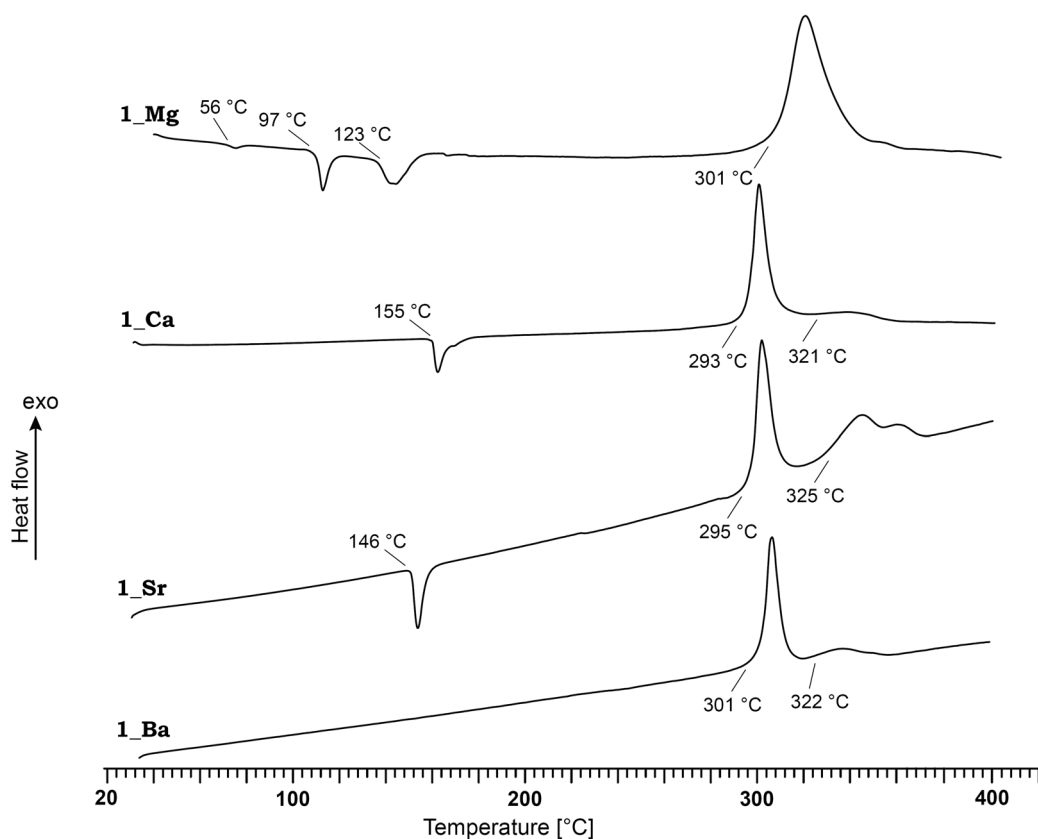


Figure 2.12 DSC thermograms of the alkaline earth metal salts of **1** in a temperature range of 25–400 °C. Decomposition points are given as onset temperatures.

The prepared copper(II) compounds, **1_Cu_H₂O** and **1_Cu_NH₃**, decompose at temperatures above 220 °C (Figure 2.13). **1_Cu** is thermally more stable with a decomposition temperature of 239 °C. In the DSC thermogram of **1_Cu_H₂O** two endothermic signals at 81 °C and 95 °C can be observed. It is caused by the loss of chemically bound water.

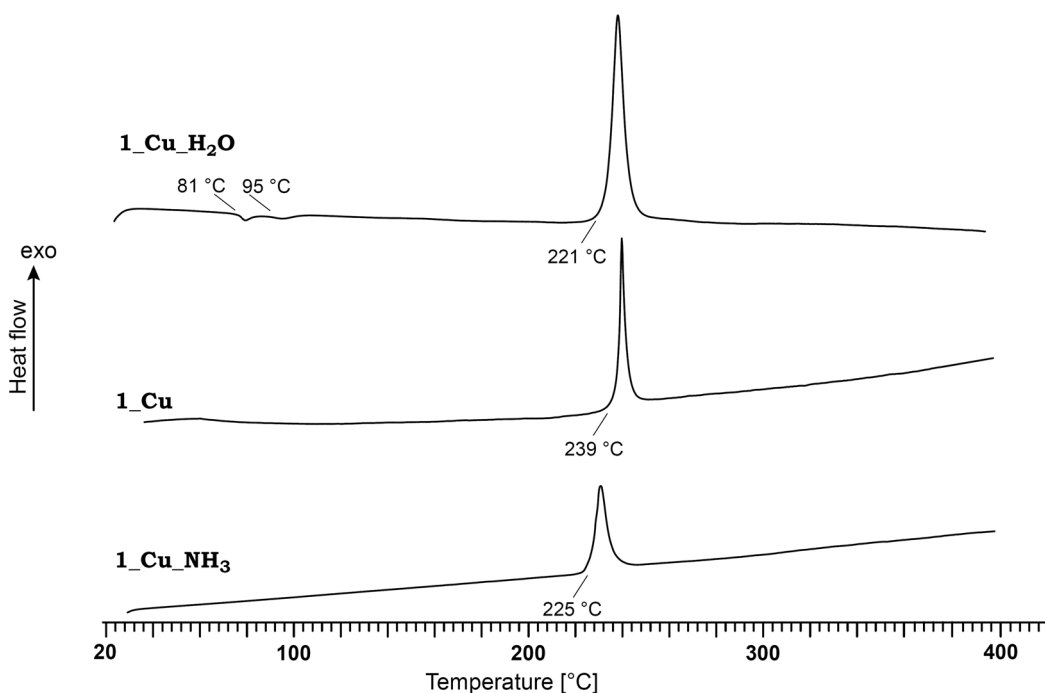


Figure 2.13 DSC thermograms of the copper(II) compounds **1_Cu_H₂O**, **1_Cu**, and **1_Cu_NH₃** in a temperature range of 20–400 °C. Decomposition points are given as onset temperatures.

All prepared compounds of **1** are sensitive to impact according to the literature.^[10] Salt **1_Mg** shows the lowest sensitivity ($E_{dr} = 35$ J), followed by **1_Li**, **1_Na**, **1_K**, **1_Cs**, and **1_Ca** with 20 J. More sensitive are **1_Sr** ($E_{dr} = 12$ J), **1_Rb**, **1_Ba**, and **1_Cu_H₂O** with 10 J, and **1_Cu_NH₃** ($E_{dr} = 9.0$ J). **1_Cu** is the most sensitive compound with 1.0 J. Except **1_Cs** ($F_r = 160$ N), all alkali metal salts are insensitive to friction. This is true for **1_Mg**, **1_Ca**, **1_Ba**, and **1_Cu_NH₃**. **1_Sr** and **1_Cu** are sensitive to friction with 240 N and **1_Cu_H₂O** with 324 N. By comparison of the copper(II) compounds one gets the impression that the inclusion of crystal water decreases the sensitivity to impact and friction.

All determined values for sensitivity to electric discharge are in the range of 0.5–1.3 J, except **1_Ba** ($E_{el} = 0.15$).

For the determination of the solubility, each compound was added to 1 mL H₂O with before noted temperature until the solution was saturated. The solubilities are given in percent by weight (wt%) and were calculated according to equation 2.1.

$$\text{H}_2\text{O-sol.} = \frac{m_{\text{dissolved Compound}}}{m_{\text{dissolved Compound}} + m_{\text{Solvent}}} \cdot 100 \quad (2.1)$$

The magnesium salt **1_Mg** offers the highest solubility with 72 wt%. **1_K** is also very soluble in H₂O with 45 wt%. Surprisingly, **1_Li** is the least soluble salt of the prepared alkali metal salts in this chapter with a solubility of only 12 wt%. The solubilities of **1_Na**, **1_Rb**, **1_Cs**, and **1_Ca** are between 19–28 wt%. As expected, **1_Ba** offers the lowest solubility of the alkaline earth metal salts with 6.5 wt%. The copper(II) compounds, **1_Cu_H₂O**, **1_Cu**, and

1_Cu_NH₃, are almost insoluble in H₂O under these conditions with solubilities less than 2.0 wt%. **1_Cu** is the best soluble copper(II) compound with 1.7 wt% at 22 °C.

2.1.4 Flame Color and Combustion Behavior

Only the salts which might find application as colorants in pyrotechnics – **1_Li**, **1_Ca**, **1_Sr**, **1_Ba**, **1_Cu_H₂O**, **1_Cu**, **1_Cu_NH₃** – were tested with regard to their flame color during combustion in the flame of a BUNSEN burner. Therefore, few milligrams of each compound on a spatula were put into the flame of a BUNSEN burner. The red-colored flames of the salts **1_Li**, **1_Ca**, and **1_Sr** are depicted in Figure 2.14. **1_Li** and **1_Sr** offer a very intense red flame, whereas the flame of **1_Ca** is more orange. Especially **1_Sr** is able to illuminate the surrounding area with its red light.

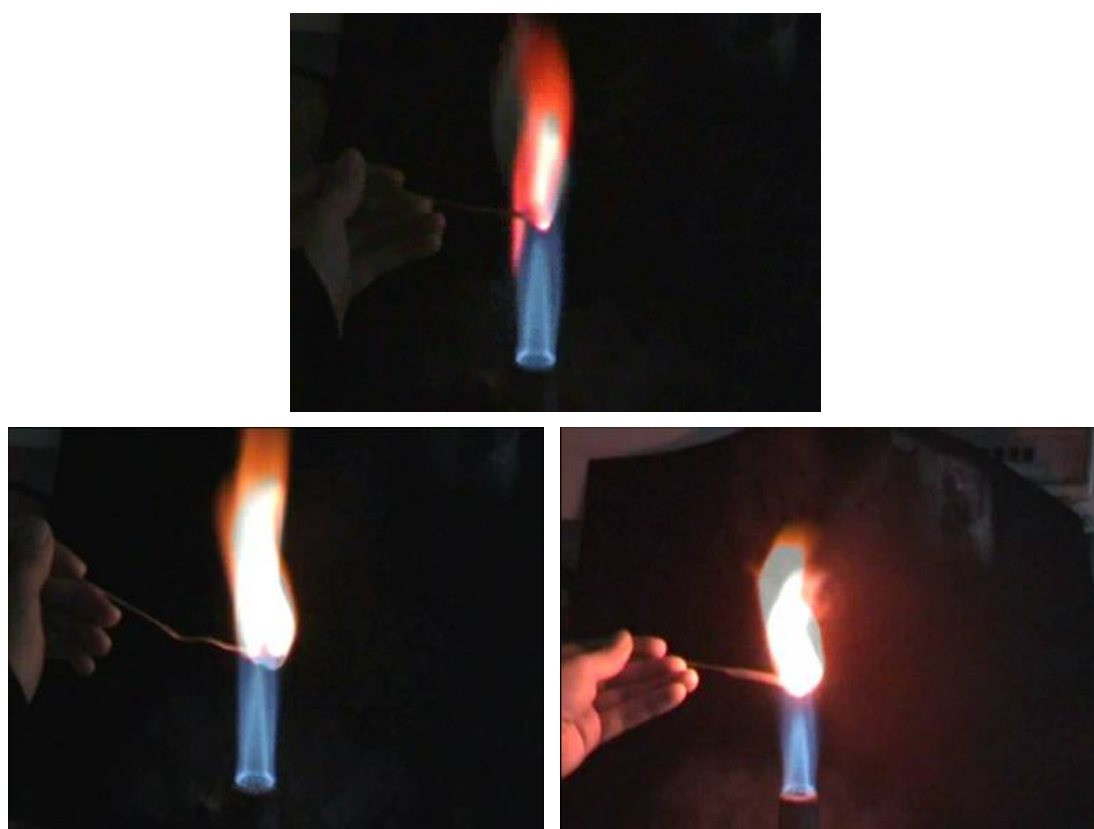


Figure 2.14 Flame color of **1_Li** (up), **1_Ca** (down, left), and **1_Sr** (down, right).

Analog to other chlorine-free barium salts (see chapters 3, 6–8), **1_Ba** combusts with a white flame (Figure 2.15). Therefore, it was mixed with the chlorine donor poly vinyl chloride (PVC) in a ratio of 50 wt%:50 wt% to enhance the green light emission. The resulting flame is pale green. Compared to the flames generated by the copper(II) compounds (Figure 2.15) the **1_Ba** is less intense and rather yellow-green.



Figure 2.15 Flame color of **1_Ba** (left) and a mixture of **1_Ba** and PVC (right).

As mentioned above, the copper(II) complexes **1_Cu_H₂O** and **1_Cu_NH₃** show an intense green flame in the Bunsen burner, whereas the water-free copper(II) compound **1_Cu** deflagrates with a yellow-green flame (Figure 2.16) and therefore is the least suitable colorant of the copper(II) compounds.



Figure 2.16 Flame color of **1_Cu** (up), **1_Cu_H₂O** (down, left), and **1_Cu_NH₃** (down, right).

All tested compounds combust without any visible smoke production or any solid residues.

2.2 Experimental Part

CAUTION! The prepared compounds are sensitive to impact, friction, and electric discharge. Therefore, proper protective measures (safety glasses, face shield, leather coat, earthed equipment and shoes, Kevlar® gloves, and ear plugs) should be used, also during work on the precursor molecule 1-(2-hydroxyethyl)-5-nitriminotetrazole (1).

2.2.1 Neutral Precursor Molecules

2.2.1.1 1-(2-Hydroxyethyl)-5-aminotetrazole (1-OH)

Preparation according to literature.^[1, 2, 5] Yield: 24 %. The analytical data (IR-spectroscopy and ¹H and ¹³C NMR spectroscopy) is in accordance with the data found in literature.^[1, 2]

2.2.1.2 2-(2-Hydroxyethyl)-5-aminotetrazole (2-OH)

After filtering 1-(2-hydroxyethyl)-5aminotetrazole off, the filtrate was concentrated by evaporation. The yellow viscous solution was dissolved in ethyl acetate and stored at ambient temperature until a colorless solid formed. Several recrystallization steps from ethyl acetate yielded colorless crystals suitable for X-ray diffraction. Yield: 14 %.

M.p. 78 °C (DSC-measurement, 5 K/min).

Raman (200 mW, 25 °C, cm⁻¹): 3331 (27), 3232 (32), 3014 (45), 2889 (31), 1648 (23), 1552 (52), 1513 (19), 1468 (39), 1448 (39), 1389 (34), 1365 (72), 1313 (31), 1270 (52), 1206 (43), 1172 (30), 1127 (28), 1088 (100), 1076 (62), 1062 (79), 1023 (84), 961 (36), 869 (59), 787 (31), 683 (18), 644 (65), 523 (37), 465 (51), 351 (48), 329 (37), 270 (26), 245 (39).

IR (Diamond-ATR, cm⁻¹): 3391 (s), 3329 (s), 3241 (s), 3198 (s), 2968 (w), 2950 (w), 2881 (w), 2850 (w), 2755 (vw), 2607 (vw), 1644 (s), 1557 (s), 1463 (w), 1443 (m), 1427 (m), 1385 (m), 1362 (w), 1309 (vw), 1270 (vw), 1202 (m), 1169 (m), 1120 (w), 1076 (m), 1059 (m), 1020 (m), 956 (m), 867 (m), 792 (vw), 757 (m), 687 (w), 676 (w), 639 (m).

¹H NMR (DMSO-*d*₆): 5.96 (s, 2H, NH₂), 4.98 (t, ³J = 5.5 Hz, 1H, OH), 4.39 (t, ³J = 5.5 Hz, 2H, NCH₂), 3.81 (q, ³J = 5.5 Hz, 2H, CH₂OH).

¹³C NMR (DMSO-*d*₆): 167.6 (CN₄), 59.5 (CH₂OH), 55.3 (NCH₂).

Elemental analysis C₃H₇N₅O₃ (129.12 g/mol): calc.: C, 27.91; H, 5.46; N, 54.24; found: C, 27.88; H, 5.55; N, 53.88.

E_{dr} = 40 J (100–500 μm).

F_r = 216 N (100–500 μm).

E_{el} = 0.50 J (100–500 μm).

2.2.1.3 1-(2-Hydroxyethyl)-5-nitriminotetrazole (1)

Preparation according to literature.^[1, 2] Yield: 89 %. The analytical data (IR-spectroscopy and ¹H and ¹³C NMR spectroscopy) is in accordance with the data found in literature.^[1, 2].

2.2.2 Preparation of the Salts

General procedure for preparing the salts of **1**: To a solution of 0.87 g (5.0 mmol) 1-(2-hydroxyethyl)-5-nitriminotetrazole (**1**) in 25 mL H₂O the corresponding hydroxide or carbonate was added. In case of the alkali metal 5.0 mmol of the corresponding hydroxides or 2.5 mmol of the carbonates, in case of the alkaline earth metal salts 2.5 mmol of the corresponding hydroxides or carbonates.

2.2.2.1 Lithium 1-(2-Hydroxyethyl)-5-nitriminotetrazolate Monohydrate (1_Li)

After recrystallization from H₂O, colorless crystals suitable for X-ray diffraction were obtained. Yield: 85 %.

M.p. 122 °C (loss of H₂O), 254 °C, 278 °C (dec., DSC-measurement, 5 K/min).

Raman (200 mW, 25 °C, cm⁻¹): 3008 (4), 2966 (13), 2952 (7), 2897 (1), 1511 (100), 1461 (8), 1419 (5), 1386 (7), 1364 (4), 1334 (14), 1282 (10), 1234 (2), 1152 (1), 1119 (10), 1072 (3), 1043 (21), 1005 (5), 968 (2), 889 (3), 865 (4), 764 (4), 747 (2), 661 (5), 521 (3), 445 (1), 393 (2), 336 (4), 280 (6).

IR (Diamond-ATR, cm⁻¹): 3473 (s), 3418 (s), 3379 (s), 2977 (vw), 2951 (vw), 2837 (vw), 1633 (w), 1509 (s), 1471 (m), 1420 (w), 1400 (m), 1344 (s), 1319 (s), 1282 (m), 1254 (w), 1234 (w), 1152 (w), 1119 (w), 1072 (m), 1040 (m), 1002 (w), 968 (w), 892 (vw), 863 (w), 772 (w), 760 (vw), 743 (w), 662 (w).

¹H NMR (DMSO-*d*₆): 4.92 (*t*, ³*J* = 5.7 Hz, 1H, OH), 4.06 (*t*, ³*J* = 6.0 Hz, 2H, NCH₂), 3.68 (*q*, ³*J* = 5.7 Hz, ³*J* = 6.0 Hz, 2H, CH₂OH), 3.30 (*s*, 2H, H₂O).

¹³C NMR (DMSO-*d*₆): 157.6 (CN₄), 59.1 (CH₂OH), 48.8 (NCH₂).

Elemental analysis C₃H₇LiN₆O₄ (198.07 g/mol): calc.: C, 18.19; H, 3.56; N, 42.43; found: C, 17.93; H, 3.50; N, 41.50.

E_{dr} = 20 J (500–1000 μm).

F_r > 360 N (500–1000 μm).

E_{el} = 1.0 J (500–1000 μm).

H₂O-sol. 12 wt% (22 °C).

2.2.2.2 Sodium 1-(2-Hydroxyethyl)-5-nitriminotetrazolate (1_Na)

After recrystallization from H₂O colorless crystals, suitable for X-ray diffraction, were obtained. Yield: 95 %.

M.p. 236 °C, 273 °C (dec.), 343 °C (dec., DSC-measurement, 5 K/min).

Raman (300 mW, 25 °C, cm⁻¹): 2993 (5), 2963 (25), 1555 (3), 1505 (100), 1452 (5), 1422 (4), 1380 (5), 1352 (14), 1324 (14), 1264 (14), 1230 (3), 1136 (2), 1110 (6), 1072 (6), 1042 (48), 992 (4), 964 (2), 894 (3), 868 (7), 762 (10), 665 (3), 494 (2), 446 (2), 344 (3), 272 (2), 256 (2), 227 (3).

IR (Diamond-ATR, cm⁻¹): 3416 (s), 3340 (s), 2956 (vw), 1638 (vw), 1505 (m), 1463 (w), 1450 (m), 1419 (w), 1385 (m), 1354 (m), 1331 (s), 1315 (s), 1261 (m), 1228 (w), 1135 (vw), 1108 (w), 1072 (w), 1037 (w), 1021 (w), 987 (vw), 962 (vw), 887 (vw), 863 (w), 776 (w), 758 (vw), 734 (vw), 726 (vw), 701 (vw), 688 (vw), 652 (w), 626 (vw), 610 (vw).

¹H NMR (DMSO-*d*₆): 4.92 (*t*, ³*J* = 5.6 Hz, 1H, OH), 4.08 (*t*, ³*J* = 5.9 Hz, 2H, NCH₂), 3.69 (*q*, ³*J* = 5.8 Hz, 2H, CH₂OH).

¹³C NMR (DMSO-*d*₆): 157.1 (CN₄), 58.6 (CH₂OH), 48.3 (NCH₂).

Elemental analysis C₃H₅N₆NaO₃ (196.10 g/mol): calc.: C, 18.37; H, 2.57; N, 42.86; found: C, 18.40; H, 2.65; N, 43.26.

E_{dr} = 20 J (> 1000 μm).

F_r > 360 N (> 1000 μm).

E_{e1} = 1.2 J (> 1000 μm).

H₂O-sol. 28 wt% (22 °C).

2.2.2.3 Potassium 1-(2-Hydroxyethyl)-5-nitriminotetrazolate (1_K)

After recrystallization from H₂O, colorless crystals suitable for X-ray diffraction were obtained Yield: 97 %.

M.p. 198 °C, 271 °C (dec.), 354 °C (dec., DSC-measurement, 5 K/min).

Raman (200 mW, 25 °C, cm⁻¹): 3001 (8), 2989 (14), 2956 (9), 2932 (6), 1565 (2), 1507 (100), 1450 (3), 1432 (4), 1412 (3), 1388 (8), 1362 (8), 1341 (11), 1264 (7), 1225 (1), 1162 (4), 1108 (9), 1053 (9), 1035 (41), 981 (4), 889 (3), 863 (3), 755 (6), 657 (3), 517 (3), 477 (2), 440 (3), 385 (2), 333 (5), 269 (6), 209 (1).

IR (Diamond-ATR, cm⁻¹): 3341 (m), 2992 (vw), 2931 (vw), 2879 (vw), 1504 (m), 1462 (m), 1448 (m), 1427 (m), 1403 (m), 1382 (m), 1365 (w), 1331 (s), 1312 (s), 1262 (m), 1233 (m), 1223 (m), 1160 (w), 1106 (w), 1064 (m), 1053 (m), 1033 (w), 980 (vw), 954 (vw), 887 (w), 862 (w), 782 (w), 746 (w), 653 (w).

¹H NMR (DMSO-*d*₆): 4.89 (s, 1H, OH), 4.01 (*t*, 2H, NCH₂), 3.66 (s, 2H, CH₂OH).

¹³C NMR (DMSO-*d*₆): 157.0 (CN₄), 58.5 (CH₂OH), 48.2 (NCH₂).

Elemental analysis C₃H₅KN₆O₃ (198.18 g/mol): calc.: C, 16.98; H, 2.37; N, 39.60; found: C, 17.03; H, 2.37; N, 39.96.

E_{dr} = 20 J (250–500 μm).

F_r > 360 N (250–500 μm).

E_{e1} = 0.90 J (250–500 μm).

H₂O-sol. 45 wt% (22 °C).

2.2.2.4 Rubidium 1-(2-Hydroxyethyl)-5-nitriminotetrazolate (1_Rb)

After recrystallization from H₂O, colorless crystals suitable for X-ray diffraction were obtained. Yield: 90 %.

M.p. 210 °C, 281 °C (dec.), 352 °C (dec., DSC-measurement, 5 K/min).

IR (Diamond-ATR, cm⁻¹): 3356 (m), 2998 (vw), 2934 (w), 2884 (vw), 1782 (vw), 1583 (vw), 1501 (s), 1459 (m), 1446 (m), 1426 (w), 1397 (m), 1383 (m), 1364 (w), 1333 (s), 1306 (s), 1259 (s), 1233 (m), 1159 (w), 1104 (w), 1052 (m), 1032 (m), 974 (vw), 952 (vw), 886 (vw), 862 (w), 780 (m), 745 (m).

¹H NMR (DMSO-*d*₆): 4.91 (s, 1H, OH), 4.05 (t, ³J = 6.1 Hz, 2H, NCH₂), 3.66 (t, ³J = 6.1 Hz, 2H, CH₂OH).

¹³C NMR (DMSO-*d*₆): 157.0 (CN₄), 59.0 (CH₂OH), 48.9 (NCH₂).

Elemental analysis C₃H₅N₆O₃Rb (258.58 g/mol): calc.: C, 13.93; H, 1.95; N, 32.55; found: C, 13.63; H, 2.17; N, 32.55.

E_{dr} = 10 J (500–1000 μm).

F_r > 360 N (500–1000 μm).

E_{el} = 0.70 J (500–1000 μm).

H₂O-sol. 24 wt% (22 °C).

2.2.2.5 Cesium 1-(2-Hydroxyethyl)-5-nitriminotetrazolate (1_Cs)

After recrystallization from H₂O, colorless crystals suitable for X-ray diffraction were obtained. Yield: 88 %.

M.p. 183 °C, 281 °C, (dec.), 362 °C (dec., DSC-measurement, 5 K/min).

IR (Diamond-ATR, cm⁻¹): 3340 (m), 2970 (vw), 2919 (vw), 2881 (vw), 1635 (w), 1498 (m), 1444 (m), 1421 (m), 1394 (s), 1379 (s), 1333 (s), 1311 (s), 1249 (m), 1233 (m), 1215 (m), 1153 (w), 1104 (w), 1093 (w), 1065 (m), 1051 (m), 1032 (m), 980 (w), 954 (w), 886 (w), 864 (w), 778 (w), 750 (vw), 742 (w), 694 (vw), 659 (vw).

¹H NMR (DMSO-*d*₆): 4.90 (s, 1H, OH), 4.03 (t, ³J = 6.0 Hz, 2H, NCH₂), 3.66 (t, ³J = 6.0 Hz, 2H, CH₂OH).

¹³C NMR (DMSO-*d*₆): 157.6 (CN₄), 59.1 (CH₂OH), 48.8 (NCH₂).

Elemental analysis C₃H₅CsN₆O₃ (306.02 g/mol): calc.: C, 11.77; H, 1.65; N, 27.46; found: C, 11.63; H, 1.94; N, 27.46.

E_{dr} = 20 J (500–1000 μm).

F_r = 160 N (500–1000 μm).

E_{el} = 0.50 J (500–1000 μm).

H₂O-sol. 19 wt% (22 °C).

2.2.2.6 Magnesium 1-(2-Hydroxyethyl)-5-nitriminotetrazolate Octahydrate (1_Mg)

After recrystallization from H₂O, colorless crystals suitable for X-ray diffraction were obtained. Yield: 85 %.

M.p. 56 °C (loss of H₂O), 97 °C (loss of H₂O), 123 °C (loss of H₂O), 301 °C (dec., DSC-measurement, 5 K/min).

Raman (300 mW, 25 °C, cm⁻¹): 3226 (1), 3003 (4), 2963 (4), 2880 (1), 1547 (2), 1506 (100), 1459 (6), 1428 (4), 1379 (5), 1334 (22), 1281 (5), 1235 (2), 1121 (7), 1037 (41), 990 (4), 890 (3), 866 (4), 757 (7), 666 (5), 488 (4), 438 (3), 375 (2), 336 (5), 278 (8).

IR (Diamond-ATR, cm⁻¹): 3257 (br, s), 2362 (s), 2334 (m), 1663 (m), 1623 (w), 1508 (s), 1459 (m), 1436 (m), 1381 (m), 1371 (m), 1343 (s), 1302 (s), 1279 (s), 1229 (m), 1113 (w), 1072 (w), 1054 (m), 1044 (m), 984 (vw), 888 (vw), 862 (w), 744 (m), 675 (m).

¹H NMR (DMSO-*d*₆): 4.90 (*t*, ³*J* = 5.5 Hz, 2H, OH), 4.03 (*t*, ³*J* = 6.1 Hz, 4H, CH₂), 3.65 (*q*, ³*J* = 6.1 Hz, ³*J* = 5.5 Hz, 4H, CH₂OH), 3.44 (*s*, 8H, H₂O).

¹³C NMR (DMSO-*d*₆): 157.0 (CN₄), 58.5 (CH₂OH), 48.3 (NCH₂).

Elemental analysis C₆H₂₆MgN₁₂O₁₄ (514.65 g/mol): calc.: C, 14.00; H, 5.06; N, 32.66; found: C, 13.85; H, 4.90; N, 32.70.

E_{dr} = 35 J (500–1000 μm).

F_r > 360 N (500–1000 μm).

E_{ei} = 1.0 J (500–1000 μm).

H₂O-sol. 72 wt% (22 °C).

2.2.2.7 Calcium 1-(2-Hydroxyethyl)-5-nitriminotetrazolate Dihydrate (1_Ca)

After recrystallization from H₂O, colorless crystals suitable for X-ray diffraction were obtained. Yield: 87 %.

M.p. 155 °C (loss of H₂O), 293 °C (dec.), 321 °C (dec., DSC-measurement, 5 K/min).

Raman (300 mW, 25 °C, cm⁻¹): 3226 (2), 3039 (6), 3022 (6), 2972 (21), 2960 (29), 2888 (3), 1516 (84), 1504 (100), 1456 (14), 1397 (10), 1347 (32), 1335 (31), 1321 (32), 1277 (16), 1263 (5), 1241 (8), 1156 (7), 1122 (36), 1074 (8), 1042 (57), 1037 (59), 1000 (8), 961 (6), 893 (8), 873 (8), 768 (19), 673 (11), 492 (10), 448 (7), 380 (6), 305 (9).

IR (Diamond-ATR, cm⁻¹): 3472 (m), 3416 (m), 3373 (s), 3208 (s), 2972 (w), 2951 (w), 2889 (w), 1633 (vw), 1509 (m), 1467 (m), 1452 (m), 1432 (m), 1387 (m), 1367 (m), 1339 (s), 1326 (s), 1280 (m), 1259 (m), 1233 (w), 1153 (w), 1120 (w), 1067 (m), 1038 (m), 998 (vw), 962 (vw), 887 (vw), 862 (w), 772 (m), 739 (w), 719 (w), 701 (w), 674 (w).

¹H NMR (DMSO-*d*₆): 4.89 (*t*, ³*J* = 5.8 Hz, 2H, OH), 4.03 (*t*, ³*J* = 6.1 Hz, 4H, CH₂), 3.65 (*q*, ³*J* = 6.1 Hz, ³*J* = 5.8 Hz, 4H, CH₂OH).

¹³C NMR (DMSO-*d*₆): 157.0 (CN₄), 58.5 (CH₂OH), 48.2 (NCH₂).

Elemental analysis $C_6H_{14}CaN_{12}O_8$ (422.33 g/mol): calc.: C, 17.06; H, 3.34; N, 39.80; found: C, 17.03; H, 3.47; N, 40.05.

$E_{dr} = 20$ J (500–1000 μm).

$F_r > 360$ N (500–1000 μm).

$E_{el} = 1.0$ J (500–1000 μm).

H₂O-sol. 23 wt% (25 °C).

2.2.2.8 Strontium 1-(2-Hydroxyethyl)-5-nitriminotetrazolate Dihydrate (1_Sr)

After recrystallization from H₂O, colorless crystals suitable for X-ray diffraction were obtained. Yield: 96 %.

M.p. 146 °C (loss of H₂O), 295 °C (dec.), 325 °C (dec., DSC-measurement, 5 K/min).

Raman (300 mW, 25 °C, cm^{-1}): 3237 (2), 3030 (7), 3021 (8), 2974 (27), 2961 (22), 2898 (3), 1515 (99), 1504 (100), 1456 (15), 1438 (8), 1415 (6), 1380 (10), 1368 (9), 1346 (35), 1319 (25), 1274 (14), 1239 (7), 1155 (4), 1122 (36), 1073 (6), 1041 (60), 1000 (7), 960 (3), 892 (6), 873 (6), 765 (19), 672 (9), 490 (6), 445 (5), 395 (4), 380 (4), 316 (11), 261 (5), 220 (4).

IR (Diamond-ATR, cm^{-1}): 3236 (s), 3327 (s), 2952 (vw), 2879 (vw), 2810 (vw), 1508 (m), 1464 (m), 1433 (m), 1383 (m), 1367 (s), 1326 (s), 1271 (m), 1256 (m), 1243 (m), 1152 (w), 1121 (m), 1065 (m), 1050 (m), 1036 (m), 998 (vw), 961 (vw), 872 (w), 862 (w), 772 (m), 762 (m), 740 (m), 690 (m), 667 (m).

¹H NMR (DMSO-*d*₆): 4.89 (s, 2H, OH), 4.04 (t, ³J = 6.0 Hz, 4H, CH₂), 3.66 (t, ³J = 6.0 Hz, 4H, CH₂OH).

¹³C NMR (DMSO-*d*₆): 156.9 (CN₄), 58.5 (CH₂OH), 48.2 (NCH₂).

Elemental analysis $C_6H_{14}N_{12}O_8\text{Sr}$ (469.87 g/mol): calc.: C, 15.34; H, 3.00; N, 35.77; found: C, 15.34; H, 3.07; N, 36.23.

$E_{dr} = 12$ J (160–250 μm).

$F_r = 140$ N (160–250 μm).

$E_{el} = 1.3$ J (160–250 μm).

H₂O-sol. 15 wt% (22 °C).

2.2.2.9 Barium 1-(2-Hydroxyethyl)-5-nitriminotetrazolate (1_Ba)

A colorless powder was obtained after recrystallization from H₂O. Yield: 95 %.

M.p. 301 °C (dec.), 322 °C (dec., DSC-measurement, 5 K/min).

Raman (300 mW, 25 °C, cm^{-1}): 3014 (4), 2991 (3), 2969 (10), 2895 (2), 1537 (3), 1505 (100), 1459 (13), 1417 (3), 1391 (5), 1357 (31), 1340 (11), 1311 (7), 1277 (4), 1256 (3), 1233 (2), 1169 (1), 1113 (6), 1082 (2), 1025 (32), 997 (4), 868 (3), 759 (8), 662 (2), 522 (2), 495 (4), 388 (2), 341 (5), 278 (3), 216 (3).

IR (Diamond-ATR, cm^{-1}): 3408 (m), 3327 (s), 3263 (m), 3225 (w), 3189 (w), 3036 (w), 2948 (vw), 2894 (vw), 1622 (vw), 1514 (m), 1458 (m), 1421 (w), 1403 (m), 1362 (w), 1339 (m), 1301 (s), 1267 (s), 1239 (s), 1220 (m), 1158 (w), 1109 (m), 1054 (m), 1034 (w), 1003 (vw), 951 (vw), 883 (vw), 863 (vw), 772 (w), 758 (vw), 740 (w), 719 (vw), 685 (w), 662 (w).

^1H NMR (DMSO- d_6): 4.92 (t, $^3J = 5.7$ Hz, 2H, OH), 4.07 (t, $^3J = 6.0$ Hz, 4H, CH_2), 3.69 (q, $^3J = 5.9$ Hz, 4H, CH_2OH).

^{13}C NMR (DMSO- d_6): 156.9 (CN_4), 58.5 (CH_2OH), 48.2 (NCH_2).

Elemental analysis $\text{C}_6\text{H}_{10}\text{BaN}_{12}\text{O}_6$ (483.55 g/mol): calc.: C, 14.90; H, 2.08; N, 34.76; found: C, 14.97; H, 2.28; N, 35.27.

E_{dr} = 10 J (250–500 μm).

F_{r} > 360 N (250–500 μm).

E_{el} = 1.2 J (250–500 μm).

$\text{H}_2\text{O-sol.}$ 6.5 wt% (25 $^\circ\text{C}$).

2.2.2.10 ***trans*-[Diaqua-bis{1-(2-Hydroxyethyl)-5-nitriminotetrazolato- $\kappa^2\text{N}4,\text{O}5$ } Copper(II)] (1_Cu_H₂O)**

Preparation according to the literature.^[1, 2] Yield: 81 %.

M.p. 81 $^\circ\text{C}$ (loss of H_2O), 95 $^\circ\text{C}$ (loss of H_2O), 221 $^\circ\text{C}$ (dec., DSC-measurement, 5 K/min).

IR (Diamond-ATR, cm^{-1}): 3388 (m), 3356 (m), 3076 (m), 2958 (m), 2901 (w), 1516 (m), 1461 (m), 1429 (m), 1390 (m), 1346 (s), 1324 (s), 1292 (m), 1259 (m), 1242 (m), 1153 (w), 1110 (w), 1056 (m), 1032 (m), 1018 (w), 956 (w), 875 (w), 865 (m), 762 (w), 736 (m), 684 (w).

Elemental analysis $\text{C}_6\text{H}_{14}\text{CuN}_{12}\text{O}_8$ (445.80 g/mol): calc.: C, 16.17; H, 3.17; N, 37.70; found: C, 16.15; H, 3.13; N, 37.76.

E_{dr} = 10 J (100–500 μm).

F_{r} = 324 N (100–500 μm).

E_{el} = 0.15 J (100–500 μm).

$\text{H}_2\text{O-sol.}$ 1.0 wt% (25 $^\circ\text{C}$).

2.2.2.11 **Copper(II) 1-(2-Hydroxyethyl)-5-nitriminotetrazolate (1_Cu)**

1.5 g (3.4 mmol) *trans*-[Diaqua-bis{1-(2-hydroxyethyl)-5-nitriminotetrazolato- $\kappa^2\text{N}4,\text{O}5$ } copper(II)] (1_Cu_H₂O) was dried under high vacuum for 24 hours. 1_Cu was obtained as green powder. Yield: 100 %.

M.p. 239 $^\circ\text{C}$ (dec., DSC-measurement, 5 K/min).

IR (Diamond-ATR, cm^{-1}): 3357 (m), 2963 (w), 2362 (w), 2337 (w), 1533 (s), 1507 (w), 1490 (m), 1482 (m), 1431 (s), 1396 (m), 1370 (w), 1323 (m), 1291 (m), 1272 (m), 1232 (m), 1219 (m), 1168 (w), 1118 (w), 1075 (w), 1054 (m), 1018 (m), 946 (w), 882 (w), 780 (vw), 753 (w), 731 (m), 657 (w).

Elemental analysis $C_6H_{10}CuN_{12}O_6$ (409.77 g/mol): calc.: C, 17.59; H, 2.46; N, 41.02; found: C, 17.44; H, 2.63; N, 40.68.

E_{dr} = 1.0 J (500–1000 μm).

F_r = 240 N (500–1000 μm).

E_{el} = 0.20 J (500–1000 μm).

H₂O-sol. 1.7 wt% (22 °C).

2.2.2.12 Tetrammine Copper(II) 1-(2-Hydroxyethyl)-5-nitriminotetrazolate (3_Cu_NH₃)

0.88 g (5.0 mmol) 1-(2-hydroxyethyl)-5-nitriminotetrazole (**1**) were dissolved in 25 mL H₂O and 5 mL aqueous ammonia solution (25 %). A solution of 0.66 g (2.5 mmol) copper(II) nitrate pentahemihydrate in 5 mL H₂O was added. The dark blue solution was stored at ambient temperature until blue crystals suitable for X-ray diffraction formed. Yield: 61 %.

M.p. 225 °C (dec., DSC-measurement, 5 K/min).

IR (Diamond-ATR, cm^{-1}): 3408 (m), 3327 (s), 3263 (m), 3225 (w), 3189 (w), 3036 (w), 2948 (vw), 2894 (vw), 1622 (vw), 1514 (m), 1458 (m), 1421 (w), 1403 (m), 1362 (w), 1339 (m), 1301 (s), 1267 (s), 1239 (s), 1220 (m), 1158 (w), 1109 (m), 1054 (m), 1034 (w), 1003 (vw), 951 (vw), 883 (vw), 863 (vw), 772 (w), 758 (vw), 740 (w), 719 (vw), 685 (w), 662 (w).

Elemental analysis $C_6H_{16}CuN_{14}O_6$ (443.83 g/mol): calc.: C, 16.24; H, 3.63; N, 44.18; found: C, 16.12; H, 3.61; N, 44.48.

E_{dr} = 9 J (250–500 μm).

F_r > 360 N (250–500 μm).

E_{el} = 0.50 J (250–500 μm).

H₂O-sol. 0.3 wt% (25 °C).

2.3 Conclusion

The alkali and alkaline earth metal salts of 1-(2-hydroxyethyl)-5-nitriminotetrazole (**1**), lithium 1-(2-hydroxyethyl)-5-nitriminotetrazolate monohydrate (**1_Li**), sodium 1-(2-hydroxyethyl)-5-nitriminotetrazolate (**1_Na**), potassium 1-(2-hydroxyethyl)-5-nitriminotetrazolate (**1_K**), rubidium 1-(2-hydroxyethyl)-5-nitriminotetrazolate (**1_Rb**), cesium 1-(2-hydroxyethyl)-5-nitriminotetrazolate (**1-Cs**), magnesium 1-(2-hydroxyethyl)-5-nitriminotetrazolate octahydrate (**1_Mg**), calcium 1-(2-hydroxyethyl)-5-nitriminotetrazolate dihydrate (**1_Ca**), strontium 1-(2-hydroxyethyl)-5-nitriminotetrazolate dihydrate (**1_Sr**), and barium 1-(2-hydroxyethyl)-5-nitriminotetrazolate (**1_Ba**) were prepared and characterized using vibrational and NMR spectroscopy, elemental analysis, and differential scanning calorimetry (DSC). This is true for the three copper(II) compounds *trans*-[diaqua-bis{1-(2-hydroxyethyl)-5-nitriminotetrazolato- κ^2N_4,O_5 } copper(II)] (**1_Cu_H₂O**), copper(II) 1-(2-hydroxyethyl)-5-nitriminotetrazolate (**1_Cu**), and tetrammine copper(II) 1-(2-hydroxyethyl)-5-nitriminotetrazolate

(**1_Cu_NH₃**). The crystal structures of **1_Li**, **1_Na**, **1_K**, **1_Rb**, **1-Cs**, **1_Mg**, **1_Ca**, **1_Sr**, and **1_Cu_NH₃** were determined and extensively discussed. Furthermore, the sensitivities to impact, friction and electric discharge were determined, as well as the solubility in H₂O at ambient temperature, color performance and combustion properties in the flame of a BUNSEN burner. **1_Ba** combusted with a white flame, but with the addition of PVC a green flame was obtained. All other tested compounds offered the expected flame color. Every combustion occurred without any visible smoke production and any residues. Further investigation of the prepared salts in pyrotechnic composition was not performed, due to comparably high solubilities in H₂O, especially of **1_Sr** and **1_Ba**. Furthermore, both would need a chlorine donor to offer a good color performance. However, the salts **1_Sr**, **1_Ba**, **1_Cu_H₂O**, and **1_Cu_NH₃** are thermally very stable, show a good combustion behavior, and are not very sensitive to impact, friction and electric discharge and easy to prepare from low cost materials. Therefore, their usage in pyrotechnic compositions is possible.

Moreover, the literature described 2-isomer 2-(2-hydroxyethyl)-5-aminotetrazole (**2-OH**) was yielded after several recrystallizations and fully characterized. Its molecular structure was discussed and compared to **1-OH**.

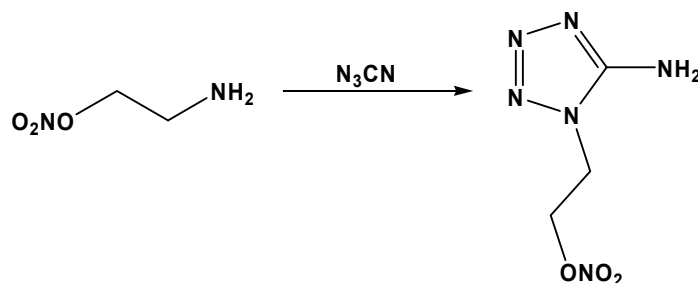
2.4 References

- [1] T. M. Klapötke, J. Stierstorfer, K. R. Tarantik: New Energetic Materials: Functionalized 1-Ethyl-5-aminotetrazoles and 1-Ethyl-5-nitriminotetrazoles, *Chem. Eur. J.* **2009**, *15*, 5775–5792.
- [2] J. Stierstorfer: Advanced Energetic Materials based on 5-Aminotetrazole, *PhD Thesis*, **2009**, Ludwig-Maximilian University, Munich.
- [3] J. A. Conkling: *Chemistry of Pyrotechnics: Basic Principles and Theory*. M. Dekker, Inc., New York, **1985**.
- [4] a) T. M. Klapötke, G. Steinhauser: 'Green' Pyrotechnics: A Chemists' Challenge, *Angew. Chem. Int. Ed.* **2008**, *47*, 3330–3347. b) T. M. Klapötke, G. Steinhauser: Pyrotechnik mit dem "Ökosiegel": eine chemische Herausforderung, *Angew. Chem.* **2008**, *120*, 3376–3394.
- [5] R. A. Henry, W. G. Finnegan: Mono-alkylation of Sodium 5-Aminotetrazole in Aqueous Medium, *J. Am. Chem. Soc.*, **1954**, 923–926.
- [6] N. Wiberg, E. Wiberg, A. F. Holleman: *Lehrbuch der Anorganischen Chemie*, deGruyter, Berlin, 102.Ed., **2007**.
- [7] H. D. Flack: On enantiomorph-polarity estimation, *Acta Crystallogr.* **1983**, *A39*, 876–881.

- [8] H. D. Flack, G. Bernardinelli: Reporting and evaluating absolute-structure and absolute-configuration diffractions, *J. Appl. Crystallogr.* **2000**, 33, 1143–1148.
- [9] B. Morosin: The Crystal Structure of Copper(II) Tetraammine Nitrate, *Acta Crystallogr.* **1976**, B32, 1237–1240.
- [10] a) <http://www.bam.de> b) E_{dr} : insensitive > 40 J, less sensitive ≥ 35 J, sensitive ≥ 4 , very sensitive ≤ 3 J; F_r : insensitive > 360 N, less sensitive = 360 N, sensitive < 360 N > 80 N, very sensitive ≤ 80 N, extreme sensitive ≤ 10 N. According to the UN Recommendations on the Transport of Dangerous Goods.

3 Salts of 1-(2-Nitratoethyl)-5-nitriminotetrazole Monohydrate

During the synthesis of 1-(2-hydroxyethyl)-5-nitriminotetrazole (**1**), the more energetic compound 1-(2-nitratoethyl)-5-nitriminotetrazole monohydrate (**2**) was obtained. **2** is described and characterized in the literature.^[1, 2, 3] It can be prepared via two different synthesis routes. On the one hand by the nitration of 1-(2-hydroxyethyl)-5-aminotetrazole (**1-OH**) with a large excess of 100 % nitric acid in a closed vessel.^[1, 2] On the other hand by the nitration of 1-(2-nitratoethyl)-5-aminotetrazole with 100 % nitric acid according to SHREEVE *et al.*^[3]. In this case, 1-(2-nitratoethyl)-5-aminotetrazole was prepared via the reaction of cyanogen azide with 2-nitratoethylamine (Scheme 3.1).^[4]



Scheme 3.1 Preparation of 1-(2-nitratoethyl)-5-aminotetrazole.

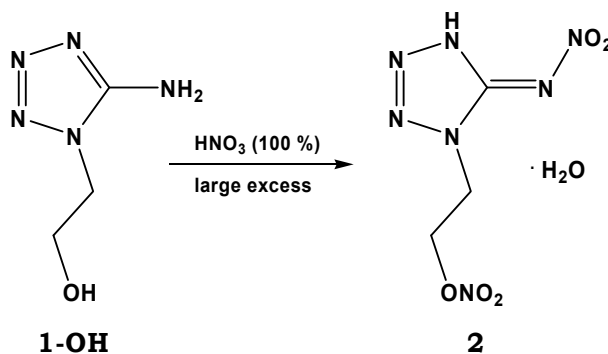
2 was selected, because it combines several properties, which are advantageous for the application as starting material for coloring agents. First of all, it can be deprotonated easily, yielding thermally more stable salts or copper(II) complexes. It consists of a tetrazole ring, which is responsible for the formation of gaseous nitrogen as decomposition product, and includes an energetic nitrimino group and nitrate ester group, which also improve the oxygen balance. However, it must be mentioned, that **2** is much more sensitive towards outer stimuli than **1**. In the literature some nitrogen-rich salts of **2**, like ammonium, guanidinium, aminoguanidinium, or triaminoguanidinium 1-(2-nitratoethyl)-5-nitriminotetrazolate, are described and characterized.^[5, 6]

In this chapter the preparation of its alkali metal and alkaline earth metal salts is presented. In addition the characterization using multinuclear magnetic resonance, as well as vibrational spectroscopy (IR and Raman) and elemental analysis is given. Moreover, their energetic properties, like decomposition temperature and sensitivities to outer stimuli were determined. Furthermore, two different copper(II) compounds with **2** as ligand were prepared and investigated. The color performances and combustion behavior in the flame of a BUNSEN burner of relevant compounds of **2** were investigated with regard to their possible application as colorants in pyrotechnic compositions. Besides that, the solubilities of all prepared compounds of **2** in H₂O at ambient temperature were determined.

3.1 Results and Discussion

3.1.1 Syntheses

When 1-(2-hydroxyethyl)-5-aminotetrazole (**1-OH**) – synthesis see chapter 2 – was nitrated with a large excess of nitric acid (100 %), 1-(2-nitratoethyl)-5-nitriminotetrazole monohydrate (**2**) was obtained (Scheme 3.2). Therefore, **1-OH** is slowly added to an ice-cooled solution of concentrated nitric acid (100 %). The yellow solution was stirred in a beaker, closed with a watch glass, for at least 24 hours.



Scheme 3.2 Preparation of 1-(2-nitratoethyl)-5-nitriminotetrazole monohydrate (**2**).

In few cases, the byproduct 1-(2-nitratoethyl)-5-aminotetrazolium nitrate (**2a**) could be obtained (Figure 3.1). The yields were quite low, however, a full characterization is given. Interestingly, **2a** has the same molecular composition as **2**.

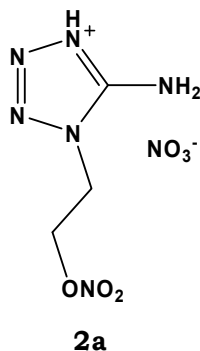
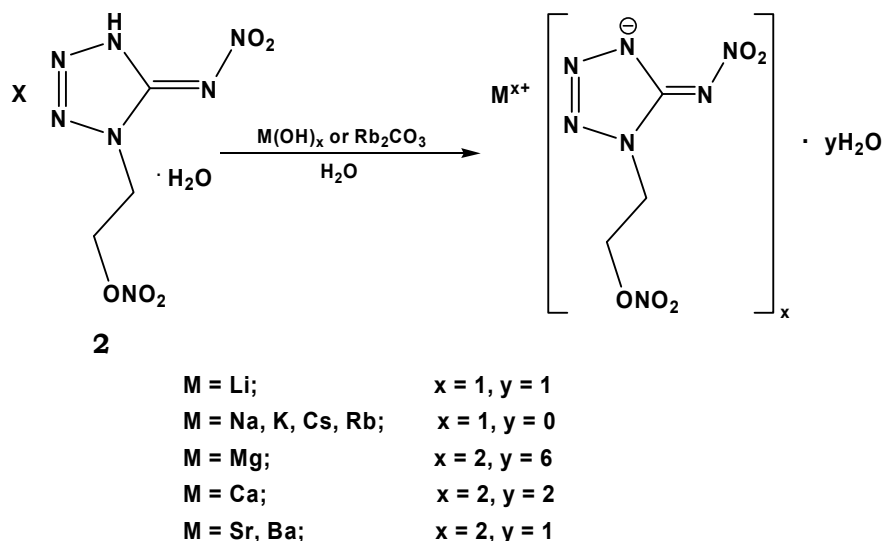


Figure 3.1 1-(2-Nitratoethyl)-5-aminotetrazolium nitrate (**2a**).

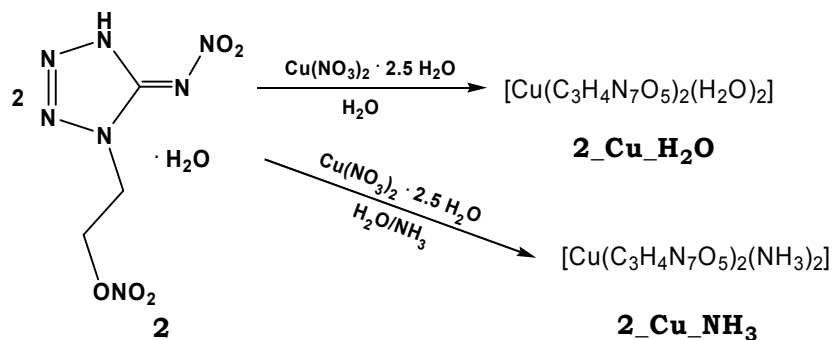
For preparation of the alkali and alkaline earth metal salts, **2** was dissolved in H₂O and the corresponding hydroxides were added. In the case of preparing rubidium 1-(2-nitratoethyl)-5-nitriminotetrazolate (**2_Rb**), rubidium carbonate was used as base. The suspension was heated until it became clear. After recrystallization from H₂O, the salts lithium 1-(2-nitratoethyl)-5-nitriminotetrazolate monohydrate (**2_Li**), sodium 1-(2-nitratoethyl)-5-nitriminotetrazolate (**2_Na**), potassium 1-(2-nitratoethyl)-5-nitriminotetrazolate (**2_K**), **2_Rb**, cesium 1-(2-nitratoethyl)-5-nitriminotetrazolate (**2_Cs**), magnesium 1-(2-nitratoethyl)-5-nitriminotetrazolate hexahydrate (**2_Mg**), calcium 1-(2-nitratoethyl)-5-nitriminotetrazolate trihydrate (**2_Ca**), strontium 1-(2-nitratoethyl)-5-nitriminotetrazolate

monohydrate (**2_Sr**), and barium 1-(2-nitratoethyl)-5-nitriminotetrazolate monohydrate (**2_Ba**) could be obtained (Scheme 3.3). All salts could be isolated in good yields.



Scheme 3.3 Preparation of the alkali metal and alkaline earth metal salts of **2**.

The copper(II) compound *trans*-[diaqua-bis{1-(2-nitratoethyl)-5-nitriminotetrazolato- $\kappa^2N4,O1$ } copper(II)] (**2_Cu_H2O**) was prepared from copper(II) nitrate pentahemihydrate dissolved in H₂O and **2** (Scheme 3.4). The green solution was stored in an open vessel until green crystals formed. In contrast to the aqua copper(II) complexes of 1-(2-hydroxyethyl)-5-nitriminotetrazole (**1**) and 1-(2-chloroethyl)-5-nitriminotetrazole (**3**), the chemically bound water of **2_Cu_H2O** it was not tried to be removed by storing in an drying oven or under high vacuum.



Scheme 3.4 Syntheses of the copper(II) compounds **2_Cu_H2O** and **2_Cu_NH3**.

If diluted aqueous ammonia solution (12 %) is added to a solution of **2** and copper(II) nitrate pentahemihydrate, *trans*-(diammine-bis{1-(2-nitratoethyl)-5-nitriminotetrazolato- $\kappa^2N4,O1$ } copper(II)) (**2_Cu_NH3**) can be obtained (Scheme 3.4). The dark violet crystals of **2_Cu_NH3** formed after storing the dark blue solution at ambient temperature for a few days.

3.1.2 Comparison of the Constitutional Isomers **2** and **2a**

2 and **2a** can be distinguished easily, besides Raman and IR spectroscopy, with ^1H and ^{13}C NMR spectroscopy. In the ^1H NMR spectrum of **2a** a signal at 8.76 ppm due to its amino group can be observed. Furthermore, its quaternary carbon signal is observed at 155.9 ppm in the ^{13}C NMR spectrum, which is typical for *N*1 alkylated aminotetrazole derivatives.^[7] The tetrazole ring carbon of **2** appears at 151.2 ppm, which is typical for nitriminotetrazoles.^[1, 2] In the case of ^{14}N and ^{15}N NMR spectroscopy the difference is even more obvious. In both cases, in the ^{14}N NMR spectra the signal of the nitrate ester group is observed at -44 ppm. The nitrimino group of **2** appears at -18 ppm, whereas the nitrate anion of **2a** appears at -15 ppm. In the ^{15}N NMR spectrum of **2a** the resonance of the amino group can be observed at -332.7 ppm. Discussion of the molecular structure of **2a** can be found in chapter 3.1.3.

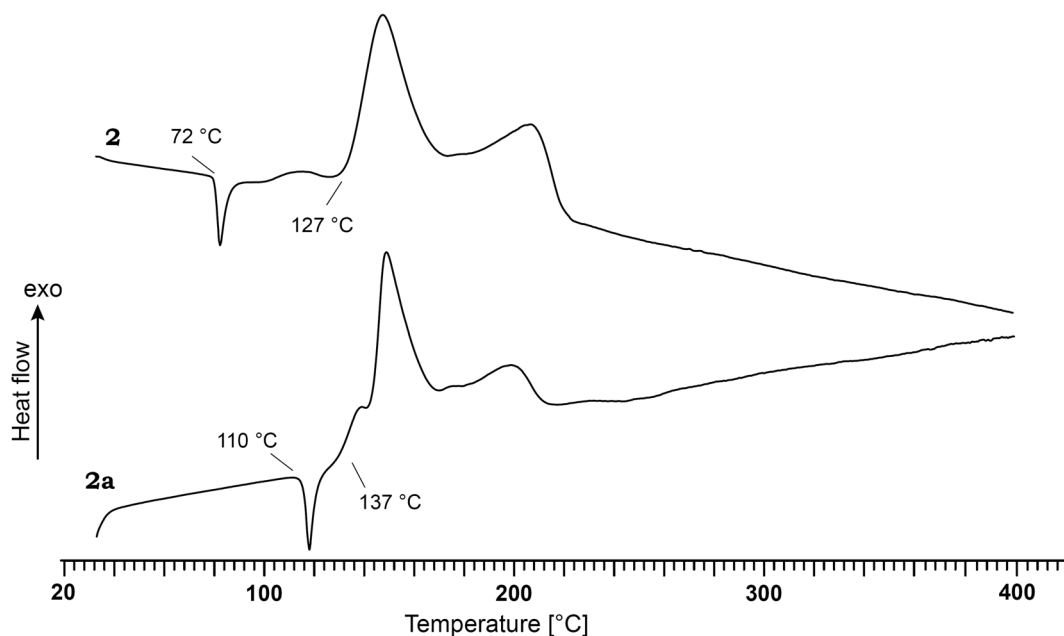


Figure 3.2 DSC thermograms of **2** and **2a** in a temperature range of 25–400 °C. Decomposition points are given as onset temperatures.

An overview of the energetic properties of **2** and **2a** is given in Table 3.1. The data of **2** were adopted from the literature.^[1, 2, 5] As expected, **2** is much more sensitive to impact, friction, and electric discharge compared to **2a**. Furthermore, its decomposition point of 127 °C is about 10 °C lower than the one of **2a** (Figure 3.2). Both, **2** and **2a**, show an endothermic signal in the DSC thermogram (**2**: 72 °C, **2a**: 110 °C) and two exothermic signals, which is a sign of a partial decomposition.

Table 3.1 Overview of the physico-chemical properties of **2** and **2a**.

	2	2a
Formula	C ₃ H ₇ N ₇ O ₆	C ₃ H ₇ N ₇ O ₆
M [g/mol]	237.16	237.16
E_{dr} [J]^a	1.5	10
F_r [N]^b	128	160
E_{el} [J]^c	0.25	0.40
grain size[μm]	250–500	250–1000
N [%]^d	41.3	41.3
Ω [%]^e	-32.6 (CO ₂), -3.4 (CO)	-32.6 (CO ₂), -3.4 (CO)
T_{dec} [°C]^f	127	137
ρ [g/cm³]^g	1.781	1.725
Δ_cU [kJ/kg]^h	-9310	-8845
Δ_cH^o [kJ/mol]ⁱ	-2197	-2088
Δ_fH^o [kJ/mol]^j	16	-94
Δ_fH_m^o [kJ/mol]^k	-24	78
Δ_fU^o [kJ/mol]^l	4	432
EXPLO5 values:		
-Δ_{Ex}U^o [kJ/kg]^m	5415	5783
T_{det} [K]ⁿ	4000	4208
P_{CJ} / [kbar]^o	321	307
V_{Det} [m/s]^p	8712	8637

a) BAM drop hammer ^[8], b) BAM methods ^[8], c) Electric spark tester, d) Nitrogen content, e) Oxygen balance, f) Decomposition temperature from DSC ($\beta = 5$ K/min), g) determined by X-ray crystallography or pycnometer (*), h) Combustion energy, i) Enthalpy of combustion, j) Molar enthalpy of formation, k) Molar enthalpy of formation (calculated), l) Energy of formation (calculated), m) Total energy of detonation, n) Explosion temperature, o) Detonation pressure, p) Detonation velocity.

The detonation parameters were calculated using the program EXPLO5 V5.02.^[9] The program is based on the steady-state model of equilibrium detonation and uses BECKER-KISTIAKOWSKY-WILSON'S equation of state (BKW E.O.S) for gaseous detonation products and COWAN-FICKETT E.O.S. for solid carbon.^[10] The calculation of the equilibrium composition of the detonation products is done by applying modified WHITE, JOHNSON and DANTZIG'S free energy minimization technique. The program is designed to enable the calculation of detonation parameters at the CJ point. The BKW equation in the following form was used with the BKWN set of parameters (a , β , κ , θ) as stated below the equations and X_i being the mol fraction of i -th gaseous product, k_i is the molar co-volume of the i -th gaseous product:^[11]

$$\frac{pV}{RT} = 1 + xe^{\beta x} \quad (3.1)$$

$$x = \frac{\kappa \sum X_i k_i}{[V(T + \theta)]^\alpha} \quad (3.2)$$

$$a = 0.5, \beta = 0.176, \kappa = 14.71, \theta = 6620.$$

The calculations were performed using the theoretical maximum densities (TMD) according to the crystal structures.

The detonation velocities and pressures of the isomers **2** and **2a** are comparable; the ones of **2** are slightly higher due to its higher calculated density. The molar energy of formation is higher for the nitrate salt **2a** (78 kJ/mol), than for **2** (-24 kJ/mol) due to the

strongly negative term for the formation of one equivalent of water. Therefore, also the explosion energy and the detonation temperature of **2a** are higher. Detonation velocities of **2** and **2a** are in the same range of about 8700 ms⁻¹.

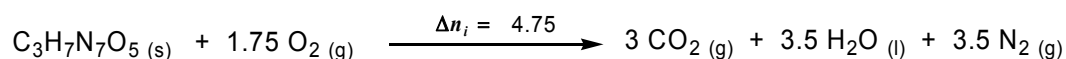
The reported values of the combustion energy ($\Delta_c U$) are the average of three single bomb calorimetry measurements. The standard molar enthalpy of combustion ($\Delta_c H^\circ$) was derived from equation 3.3.

$$\Delta_c H^\circ = \Delta_c U + \Delta n RT \quad (3.3)$$

$$\Delta n = \sum n_i (\text{gaseous products}) - \sum n_i (\text{gaseous educts})$$

$$n_i = \text{molar amount of gas } i.$$

The enthalpy of formation ($\Delta_f H^\circ$) for **2** and **2a** was calculated at 298.15 K using the HESS thermochemical cycle and the following combustion reaction (Scheme 3.5).



Scheme 3.5 Combustion equation for **2** and **2a**.

Surprisingly, the experimentally determined enthalpies of formation of **2** and **2a** differ significantly from the calculated values. Furthermore, the value for $\Delta_f H^\circ$ of **2** (16 kJ/mol) is higher than the one for **2a** (-94 kJ/mol), presumably due to the crystal water of **2**.

3.1.3 Molecular Structures

Single crystals of 1-(2-nitratoethyl)-5-aminotetrazolium nitrate (**2a**) were obtained from the mother liquor of **2**.

The molecular unit of **2a** is depicted in Figure 3.3. **2a** crystallizes in the monoclinic space group $P2_1/c$ with eight molecular units per unit cell, whereas **2** crystallizes in the triclinic space group $P-1$ with two molecules per unit cell.^[1, 2] Compared to **2** (442.2(2) Å³ [1, 2]) the cell volume of **2a** is much larger (1826.3(3) Å³). The calculated density of 1.725 g/cm³ of **2a** is slightly lower than the one of **2** (1.781 g/cm³).^[1, 2]

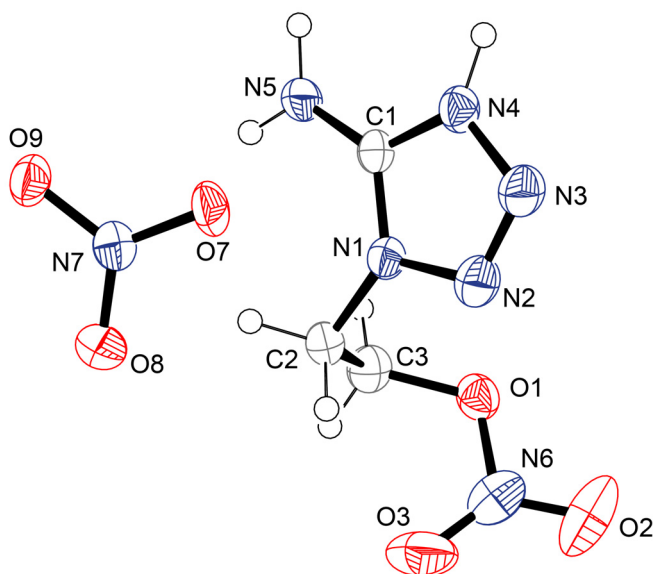


Figure 3.3 Molecular unit of **2a**. Hydrogen atoms shown as spheres of arbitrary radius and thermal displacements set at 50 % probability. Geometries: distances (Å) N1–N2 1.370(2), N2–N3 1.273(2), N3–N4 1.361(2), N1–C1 1.343(2), N4–C1 1.332(2), C1–N5 1.314(2), N1–C2 1.473(2), C2–C3 1.506(2), O1–C3 1.451(2), O1–N6 1.398(2), O2–N6 1.203(2), O3–N6 1.202(2), O7–N7 1.253(2), O8–N7 1.259(2), O9–N7 1.249(2); angles (°) N1–C1–N4 104.8(2), N1–C1–N5 127.9(2), N5–C1–N4 127.3(2), N1–N2–N3 107.8(1), N2–N3–N4 108.3(2), C1–N1–C2 128.6(1), N2–N1–C2 122.0(1), C1–N1–N2 109.3(1), N3–N4–C1 109.8(2), N1–C2–C3 112.5(1), O1–C3–C2 107.0(1), N6–O1–C3 113.5(1), O2–N6–O1 117.6(2), O3–N6–O2 130.1(2), O3–N6–O1 112.3(2), O7–N7–O8 119.3(2), O9–N7–O7 120.8(2), O9–N7–O8 119.9(1); torsion angles (°) N3–N2–N1–C1 -0.3(2), C2–N1–N2–N3 176.3(2), N1–N2–N3–N4 0.0(2), C2–N1–C1–N5 5.3(3), C1–N4–N3–N2 0.3(2), N2–N1–C2–C3 -28.7(2), C1–N1–C2–C3 147.1(2), O1–C3–C2–N1 75.5(2), N2–N1–C1–N5 -178.4(2), N2–N1–C1–N4 0.4(2), N3–N4–C1–N1 -0.4(2), N3–N4–C1–N5 178.5(2), C2–N1–C1–N4 -175.84(2), N6–O1–C3–C2 -165.0(1), C3–O1–N6–O3 -179.7(2), C3–O1–N6–O2 -0.2(2).

The bond lengths and angles in **2** and **2a** are very similar. However, the packing differ. In **2**, alternating layers, formed by hydrogen bonds and alkyl chain interactions, whereas in **2a** layers containing the amine and nitrate moieties connected by hydrogen bonds, can be distinguished.

A comparison of the crystal structures of **2a** and 1-(2-hydroxyethyl)-5-aminotetrazolium nitrate, which is extensively characterized in the literature,^[1, 2] reveals several analogies. Both nitrate salts crystallize in the same space group. The cell volume of **2a** is twice the one of 1-(2-hydroxyethyl)-5-aminotetrazolium nitrate, whereas the last one has four molecular units per unit cell. However, the density of 1-(2-hydroxyethyl)-5-aminotetrazolium nitrate is with 1.602 g/cm³ significantly smaller.^[1, 2] Comparing the bond lengths in **2a** and 1-(2-hydroxyethyl)-5-aminotetrazolium nitrate no large differences stand out. Except the bond length of N1–C1 is in **2a** significantly longer. Also the bond angles are very similar.

Table 3.2 Hydrogen bonds in **2a** (*i* x, y+1, z, *ii* -x+2, -y+2, -z+1, *iii* x, -y+3/2, z+1/2).

D-H...A	D-H [Å]	H...A [Å]	D...A [Å]	<(DHA) [°]
N4-H4...O8 <i>i</i>	0.87(2)	1.81(2)	2.670(2)	171(2)
N4-H4...O7 <i>i</i>	0.87(2)	2.48(2)	3.108(2)	130(2)
N4-H4...N7 <i>i</i>	0.87(2)	2.49(2)	3.306(2)	158(2)
N5-H1a...O7 <i>ii</i>	0.94(2)	2.22(2)	3.064(2)	149(2)
N5-H1a...O7 <i>i</i>	0.94(2)	2.41(2)	3.195(2)	140(2)
N5-H1b...O9 <i>iii</i>	0.85(2)	2.17(2)	2.997(2)	164(2)
N5-H1b...O8 <i>iii</i>	0.85(2)	2.61(2)	3.334(2)	143(2)

Another similarity is the packing in both nitrate salts. Layers containing the amine and nitrate moieties connected by hydrogen bonds are formed. An overview of the hydrogen bonds in **2a** is given in Table 3.2.

After recrystallization from H₂O, single crystals of the salts **2_Na**, **2_K**, **2_Rb**, and **2_Mg** suitable for X-ray diffraction could be obtained. Crystals of **2_Cu_H₂O** and **2_Cu_NH₃** were yielded from the reaction solution. All relevant data and parameters of the X-ray measurements and refinements are given in Appendix II.

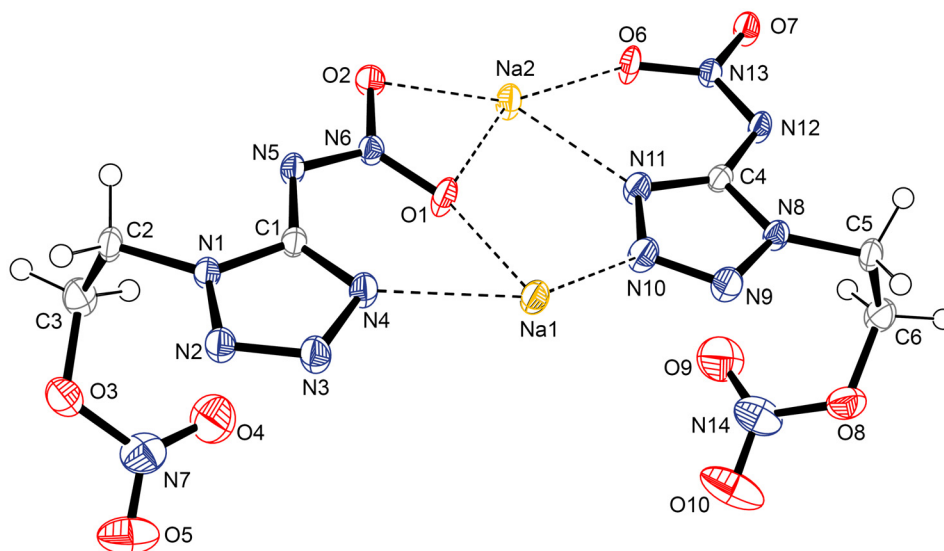


Figure 3.4 Dimer of two molecular units in **2_Na**. Hydrogen atoms shown as spheres of arbitrary radius and thermal displacements set at 50 % probability. Selected geometries: distances (Å) N1-N2 1.346(2), N2-N3 1.289(2), N3-N4 1.369(2), N1-C1 1.350(2), N4-C1 1.335(2), C1-N5 1.368(2), N5-N6 1.310(2), O1-N6 1.2544(1), O2-N6 1.263(1), N1-C2 1.463(2), O3-C3 1.454(2), O3-N7 1.395(2), O4-N7 1.198(2), O5-N7 1.209(2), Na1-O6 2.321(1), Na1-O2 2.414(1), Na1-N11 2.420(1), Na1-O5*i* 2.463(1), Na1-N3*ii* 2.507(1), Na1-O1 2.659(1), Na2-O7*v* 2.378(1), Na2-O1 2.399(1), Na2-O2*iii* 2.445(1), Na2-N4 2.462(1), Na2-O10*iv* 2.495(1), Na2-N10 2.503(1), Na2-O6*v* 2.642(1); angles (°) N1-C1-N4 107.91(11), N1-C1-N5 116.88(11), O1-N6-N5 124.80(11), O1-N6-O2 118.95(10), O1-Na1-O2 50.33(3), O6-Na1-O1 145.97(4), O6-Na1-N6 168.24(4), O2-Na1-N6 25.12(3), O6-Na1-N11 69.59(4), O2-Na1-N11 125.31(4), N11-Na1-O1 76.65(4) O1-Na2-O6 158.33(4), O1-Na2-N4 68.02(4), O1-Na2-N10 76.48(4), N4-Na2-N10 143.88(4), O4-N7-O5 128.52(16), O4-N7-O3 119.48(14), O5-N7-O3 111.99(14); torsion angles (°) N6-N5-C1-N1 -170.47(11), C1-N5-N6-O1 8.36(19), C3-O3-N7-O4 -4.8(2), C3-O3-N7-O5 175.15(12); *i* -x, -y, -z+1, *ii* x-1, y, z, *iii* -x, -y+1, -z+1, *iv* -x, -y, -z, *v* x+1, y, z.

Sodium 1-(2-nitratoethyl)-5-nitriminotetrazolate (**2_Na**) crystallizes analog to sodium 1-(2-hydroxyethyl)-5-nitriminotetrazolate (**1_Na**, chapter 2) in the triclinic space group $P\bar{1}$ with four molecular units per unit cell (Figure 3.4). The density of **2_Na** is with 1.856 g/cm^3 slightly higher than the one of **1_Na**. This might be a reason of the larger nitrate ester residues. In a distance of 2.7 \AA the sodium atom Na1 is coordinated sixfold. Coordinating atoms of Na1 are O6, O2, N11, O5*i*, N3*ii*, and O1. In contrast, sodium atom Na2 is coordinated sevenfold by the atoms O7*v*, O1, O2*iii*, N4, O10*w*, N10, and O6*v*.

The shortest observed distance between Na1 and Na2 is 3.692 \AA , which is quite short regarding an ionic diameter of a sixfold coordinated sodium ion (1.16 \AA ^[12]).

No hydrogen bonds can be observed. In **2_Na** the dimers are forming alternating layers.

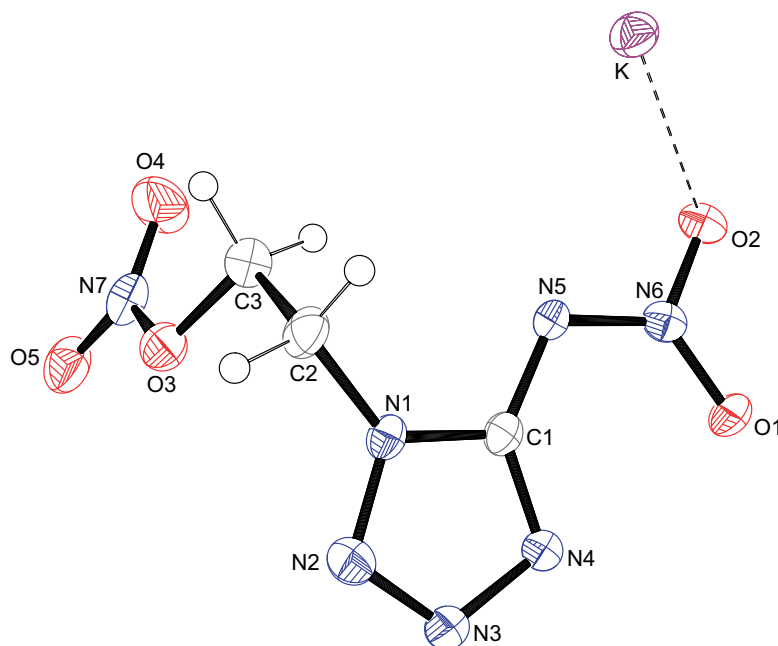


Figure 3.5 Molecular unit of **2_K**. Hydrogen atoms shown as spheres of arbitrary radius and thermal displacements set at 50 % probability. Selected geometries: distances (\AA) C1–N5 1.371(4), N5–N6 1.326(3), O1–N6 1.251(3), O2–N6 1.254(3), N1–C2 1.452(4), O3–C3 1.460(4), O3–N7 1.393(3), O4–N7 1.197(4), O5–N7 1.207(3), O2–K1 2.723(2), K1–N4*i* 2.802(3), K1–O1*i* 2.808(2), K1–O1*ii* 2.913(2), K1–O5*ii* 3.016(2), K1–N4*iii* 3.080(3), K1–O1*iii* 3.083(2), K1–N3*iv* 3.120(3), K1–O2*ii* 3.179(2); angles ($^\circ$) N1–C1–N4 108.2(3), N1–C1–N5 117.5(3), N6–N5–C1 115.6(3), O1–N6–N5 124.1(3), O1–N6–O2 120.0(3), C3–O3–N7 111.2(2), O4–N7–O5 128.8(3), O4–N7–O3 118.8(3), O5–N7–O3 112.4(3), N6–O2–K1 106.6(2); torsion angles ($^\circ$) N6–N5–C1–N1 174.7(2), C1–N5–N6–O1 $-4.8(4)$, C3–O3–N7–O4 $-2.3(4)$, C3–O3–N7–O5 $177.0(3)$; *i*) $x, y-1, z$, *ii*) $x-1/2, -y-1/2, -z$, *iii*) $x+1/2, -y-1/2, -z$, *iv*) $x+1, y-1, z$.

Potassium 1-(2-nitratoethyl)-5-nitriminotetrazole (**2_K**) as well as rubidium 1-(2-nitratoethyl)-5-nitriminotetrazolate (**2_Rb**) crystallize in the orthorhombic space group $P2_12_12_1$. The molecular unit of **2_K** is depicted in Figure 3.5. Both crystallize with four molecular units per unit cell, whereas the density of **2_Rb** (2.164 g/cm^3) is significantly higher than the one of **2_K** (1.918 g/cm^3). These densities are higher than those of the potassium and rubidium salt of 1-(2-hydroxyethyl)-5-nitriminotetrazole (**1**, chapter 2). In **2_K** the cations are coordinated ninefold by the atoms O2, N4*i*, O1*i*, O1*ii*, O5*ii*, N4*iii*, O1*iii*,

N3 iv , and O2 ii , if coordination distances up to 3.2 Å are considered. This is true for the rubidium atoms in **2_Rb**, whereas in this case the coordination atoms are O2, N4 i , O1 i , O1 ii , O5 iii , O1 iv , N4 iv , O2 ii , and N3 v , considering a maximum distance of 3.3 Å. Two cations are connected via the oxygen atoms O1 and O2 of the nitrimino group forming a network of dimers.

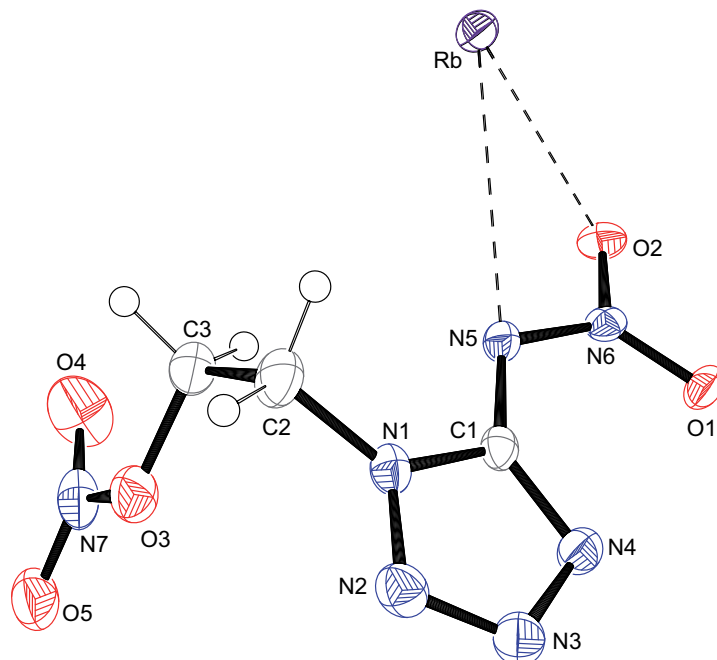


Figure 3.6 Molecular unit of **2_Rb**. Hydrogen atoms shown as spheres of arbitrary radius and thermal displacements set at 50 % probability. Selected geometries: distances (Å) C1–N5 1.366(3), N5–N6 1.324(2), O1–N6 1.257(2), O2–N6 1.252(2), N1–C2 1.453(3), O3–C3 1.453(3), O3–N7 1.389(2), O4–N7 1.193(3), O5–N7 1.211(3), Rb1–O2 2.867(1), Rb1–N4 i 2.948(2), Rb1–O1 i 2.962(2), Rb1–O1 ii 3.009(2), Rb1–O5 iii 3.058(2), Rb1–O1 iv 3.065(2), Rb1–N4 iv 3.199(2), Rb1–O2 ii 3.200(1), Rb1–N3 v 3.231(2); angles (°) N1–C1–N4 107.3(2), N1–C1–N5 118.1(2), O1–N6–N5 123.8(2), O1–N6–O2 119.8(2), C3–O3–N7 112.0(2), O4–N7–O5 128.9(2), O4–N7–O3 119.1(2), O5–N7–O3 112.0(2), O2–Rb1–N5 40.58(4); torsion angles (°) N6–N5–C1–N1 175.2(2), C1–N5–N6–O1 –6.3(3), C3–O3–N7–O4 –1.6(3), C3–O3–N7–O5 178.2(2); i) $x, y+1, z$, ii) $x-1/2, -y+5/2, -z+2$, iii) $x, y-1, z$, iv) $x+1/2, -y+5/2, -z+2$, v) $x+1, y+1, z$.

The shortest distance of two potassium cations in **2_K** is 4.222 Å. The packing of **2_K** is formed by alternating layers with the nitrateethyl residues on the outside.

The shortest distance between rubidium ions is slightly higher with 4.378 Å. The packing is analog to **2_K**. The molecular unit of **2_Rb** is depicted in Figure 3.6.

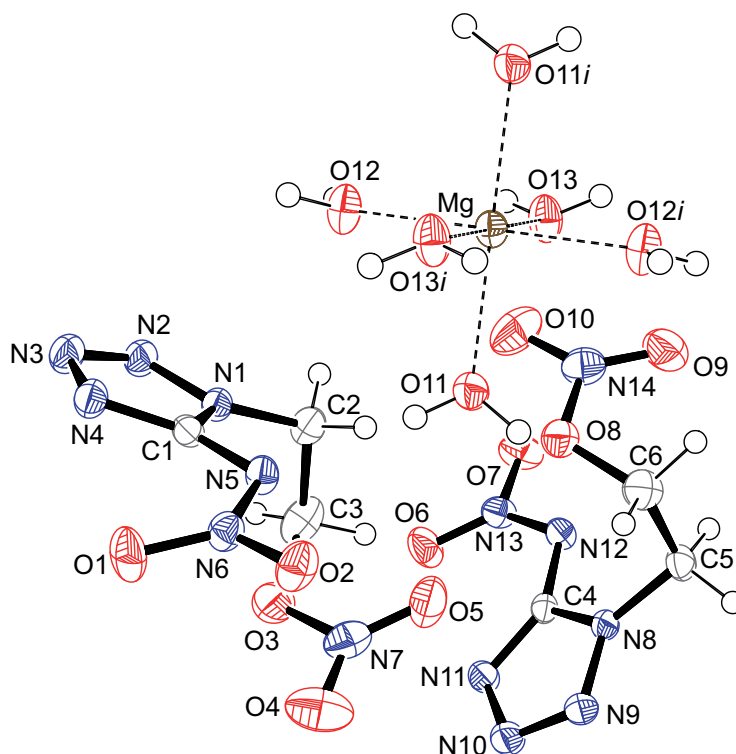


Figure 3.7 Molecular unit of **2_Mg**. Hydrogen atoms shown as spheres of arbitrary radius and thermal displacements set at 50 % probability. Selected geometries: distances (Å) N1–N2 1.347(2), N2–N3 1.287(2), N3–N4 1.366(2), N1–C1 1.348(2), C1–N4 1.334(2), C1–N5 1.374(2), N5–N6 1.325(2), O1–N6 1.247(2), O2–N6 1.250(2), N1–C2 1.465(2), O3–C3 1.451(2), O3–N7 1.391(2), O4–N7 1.200(2), O5–N7 1.198(2), Mg1–O11 2.096(2), Mg1–O12 2.033(1), Mg1–O13 2.091(2); angles (°) N1–C1–N4 108.5(2), N1–C1–N5 117.8(2), O1–N6–N5 123.2(1), O1–N6–O2 121.3(2), C3–O3–N7 114.7(2), O4–N7–O5 128.9(2), O4–N7–O3 112.6(2), O5–N7–O3 118.5(2), O12–Mg1–O11 88.90(6), O13–Mg1–O11 92.04(6), O12–Mg1–O13 90.74(7); torsion angles (°) N6–N5–C1–N1 –160.7(2), C1–N5–N6–O1 9.0(2), C3–O3–N7–O4 176.9(2), C3–O3–N7–O5 –2.5(2); *i*) $-x-1, -y+1, -z$.

The magnesium salt **2_Mg** crystallizes in the triclinic space group $P\bar{1}$ with two molecular units per unit cell. Its density of 1.719 g/cm³ is significantly higher than the one of magnesium 1-(2-hydroxyethyl)-5-nitriminotetrazolate octahydrate (**1_Mg**) with 1.587 g/cm³ (chapter 2). Analog to **1_Mg**, the magnesium ions in **2_Mg** are only coordinated by H₂O molecules forming regular octahedrons with the coordinating distances Mg1–O11 2.096(2) Å, Mg1–O12 2.033(1) Å and Mg1–O13 2.091(2) Å.

Table 3.3 Hydrogen bonds between the Mg coordinating water molecules and 1-(2-nitratoethyl)-5-nitriminotetrazolate in **2_Mg** (*ii*) $-x-1, -y, -z$, *iii*) $-x-1, -y+1, -z+1$, *iv*) $-x, -y+1, -z$, *v*) $x-1, y, z$).

D–H···A	D–H [Å]	H···A [Å]	D···A [Å]	<(DHA) [°]
O11–H11a···N5	0.80(3)	2.10(3)	2.887(3)	170(2)
O11–H11b···N9 ⁱⁱ	0.87(2)	2.10(2)	2.953(2)	170(2)
O12–H12a···O7 ⁱⁱⁱ	0.86(3)	1.84(3)	2.689(2)	166(2)
O12–H12b···O1 ^{iv}	0.87(3)	1.86(3)	2.715(2)	166(2)
O13–H13a···N4 ^v	0.81(3)	2.07(3)	3.074(2)	162(2)
O13–H13b···O6 ⁱⁱⁱ	0.82(3)	2.29(3)	3.074(2)	160(3)
O13–H13b···O7 ⁱⁱⁱ	0.82(3)	2.54(3)	3.243(2)	144(2)

The alternating layers, which are formed by the water coordinated magnesium atoms on the one hand and the nitriminotetrazole anions on the other hand, are connected *via* several hydrogen bonds (Table 3.3). In each case, the donor atoms are oxygen atoms of the crystal water molecules and the acceptor atoms part of the nitriminotetrazolate anions.

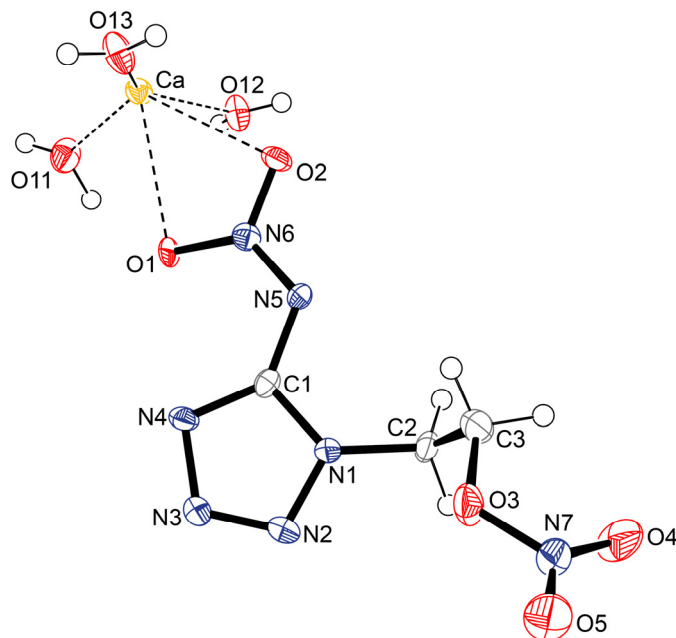


Figure 3.8 Molecular unit of **2_Ca**. For a better overview only one 1-(2-nitratoethyl)-5-nitriminotetrazole anion is shown. Hydrogen atoms shown as spheres of arbitrary radius and thermal displacements set at 50 % probability. Selected geometries: distances (Å) N1–N2 1.345(2), N2–N3 1.298(2), N3–N4 1.374(3), N1–C1 1.343(3), C1–N4 1.337(3), C1–N5 1.379(3), N5–N6 1.310(2), O1–N6 1.274(2), O2–N6 1.262(2), N1–C2 1.469(3), O3–C3 1.451(3), O3–N7 1.404(2), O4–N7 1.197(2), O5–N7 1.210(3), Ca–O13 2.325(2), Ca–O11 2.357(2), Ca–O12 2.424(2), Ca–O2 2.539(2), Ca–O6*i* 2.546(2), Ca–N4*ii* 2.564(2), Ca–O1 2.588(2), Ca–O1*ii* 2.678(2), Ca–O7*i* 2.698(2); angles (°) N1–C1–N4 108.5(2), N1–C1–N5 117.5(2), O1–N6–N5 125.4(2), O1–N6–O2 118.0(2), C3–O3–N7 114.70(19), O4–N7–O5 129.1(3), O4–N7–O3 119.3(2), O5–N7–O3 111.6(2), O13–Ca–O11 139.75(8), O13–Ca–O12 146.67(9), O11–Ca–O12 72.56(8), O13–Ca–O1 87.83(7), O11–Ca–O1 84.02(7), O12–Ca–O1 88.51(6), O2–Ca–O1 50.15(5), O13–Ca–O2 77.86(7), O11–Ca–O2 123.17(7), O12–Ca–O2 74.47(7); torsion angles (°) N6–N5–C1–N1 160.8(2), C1–N5–N6–O1 -0.8(3), C3–O3–N7–O4 -9.0(3), C3–O3–N7–O5 170.5(2); *i* -x+2, -y-3, -z, *ii* -x+1, -y-2, -z.

Calcium 1-(2-nitratoethyl)-5-nitriminotetrazolate (**2_Ca**) crystallizes analog to **2_Mg** in the triclinic space group *P*-1 with two molecular units per unit cell. The calcium atoms are coordinated ninefold by the oxygen atoms O13, O11, O12 of the crystal water molecules and O2, O6*i*, N4*ii*, O1, O1*ii*, and O7*i*, regarding distances up to 2.7 Å. Its density of 1.824 g/cm³ is significantly higher than the one of **2_Mg**, but comparable to the one of **1_Ca** (1.804 g/cm³). Six different hydrogen bonds can be observed. In each case the oxygen atoms of the crystal water molecules are the donor atoms (O13–H13a···N10*iii*: 0.85(3) Å, 2.18(3) Å, 2.935(3) Å, 147(3)°, O12–H12a···N12: 0.73(2) Å, 2.26(2) Å, 2.976(3) Å, 168(3)°, O13–H13b···N5*iii*: 0.75(3) Å, 2.13(3) Å, 2.858(3) Å, 163(4)°, O11–H11a···N11*iv*: 0.93(3) Å, 1.88(3) Å, 2.818(3) Å, 176(3)°, O11–H11b···O7*v*: 0.78(3) Å, 2.08(3) Å, 2.844(3) Å, 168(3)°, O12–H12b···O6*iv*: 0.85(3) Å, 2.20(4) Å, 3.051(3) Å, 177(4)°; *iii*) -x+2, -y-2, -z, *iv*) x-1, y, z, *v*) -x+1,

$-y-3, -z$). The packing of **2_Ca** is characterized by layers parallel to the a axis formed by two calcium atoms surrounded by the water molecules and anions.

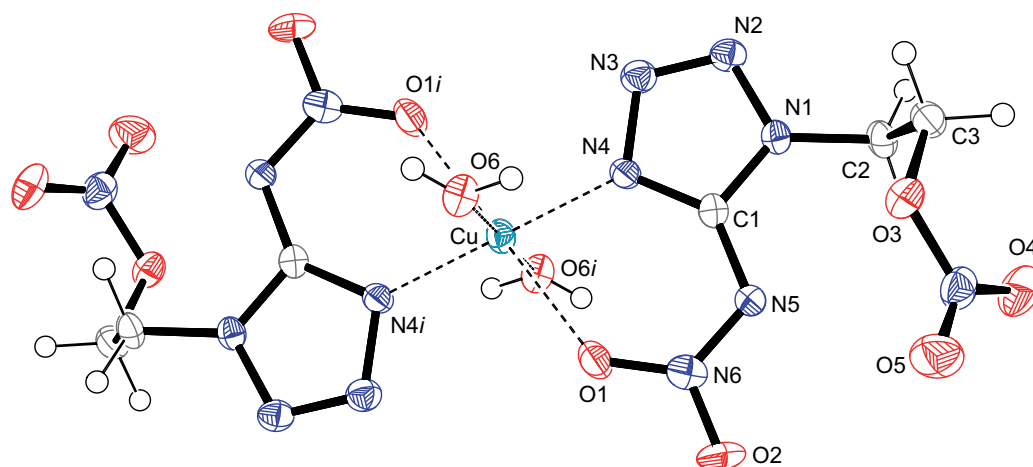


Figure 3.9 Molecular unit of **2_Cu_H₂O**. Hydrogen atoms shown as spheres of arbitrary radius and thermal displacements set at 50 % probability. Selected geometries: distances (Å) N1–N2 1.344(3), N2–N3 1.279(3), N3–N4 1.378(3), N1–C1 1.343(3), C1–N5 1.359(3), N5–N6 1.322(3), O1–N6 1.263(3), O2–N6 1.236(3), N1–C2 1.452(3), O3–C3 1.449(3), O3–N7 1.386(3), O4–N7 1.204(3), O5–N7 1.200(3), Cu1–N4 1.957(2), Cu1–O6 2.021(2), Cu1–O1 2.304(2); angles (°) N1–C1–N4 106.6(2), N1–C1–N5 117.6(2), O1–N6–N5 123.8(2), O1–N6–O2 119.6(2), C3–O3–N7 114.6(2), O4–N7–O5 128.2(3), O4–N7–O3 118.9(3), O5–N7–O3 112.9(2), O6–Cu1–O1 89.68(9), N4–Cu1–O1 77.20(8), N4–Cu1–O6 89.4(1); torsion angles (°) N6–N5–C1–N1 176.2(2), C1–N5–N6–O1 –3.2(4), C3–O3–N7–O4 2.3(3), C3–O3–N7–O5 –178.8(2); i) $-x+1, -y, -z+2$.

The copper(II) complex *trans*-[diaqua-bis{1-(2-nitratoethyl)-5-nitriminotetrazolato- $\kappa^2N4,O1$ } copper(II)] (**2_Cu_H₂O**) crystallizes in the monoclinic space group $P2_1/c$ (Figure 3.9). The unit cell contains two molecular units. The calculated density of 1.971 g/cm³ is significantly higher than the one of *trans*-[diaqua-bis{1-(2-hydroxyethyl)-5-nitriminotetrazolato- $\kappa^2N4,O5$ } copper(II)] (**1_Cu_H₂O**) with 1.821 g/cm³. [1, 2]

The copper(II) ions are sixfold coordinated by the atoms O1, N4, O6, O1 i , N4 i , and O6 i forming an elongated octahedron. This is a result of the JAHN-TELLER effect. The distance between Cu and O1 is the longest with 2.304(2) Å, whereas the distances between Cu–N4 and Cu–O6 are comparable with 1.957(2) Å and 2.021(2) Å, respectively.

Three hydrogen bonds between the H₂O molecules and nitriminotetrazole anions can be observed (O6–H6a···N3 ii : 0.73(3) Å, 2.19(3) Å, 2.894(3) Å, 162(4)°; O6–H6b···O1 iii : 0.82(4) Å, 2.44(4) Å, 2.975(3) Å, 124(3)°; O6–H6b···O2 iii : 0.82(4) Å, 2.57(4) Å, 3.376(3) Å, 171(4)°; ii) $-x+1, -y+1, -z+2$, iii) $x, y+1, z$).

In the packing of **2_Cu_H₂O** stacks consisting of the molecular units along the b axis are formed.

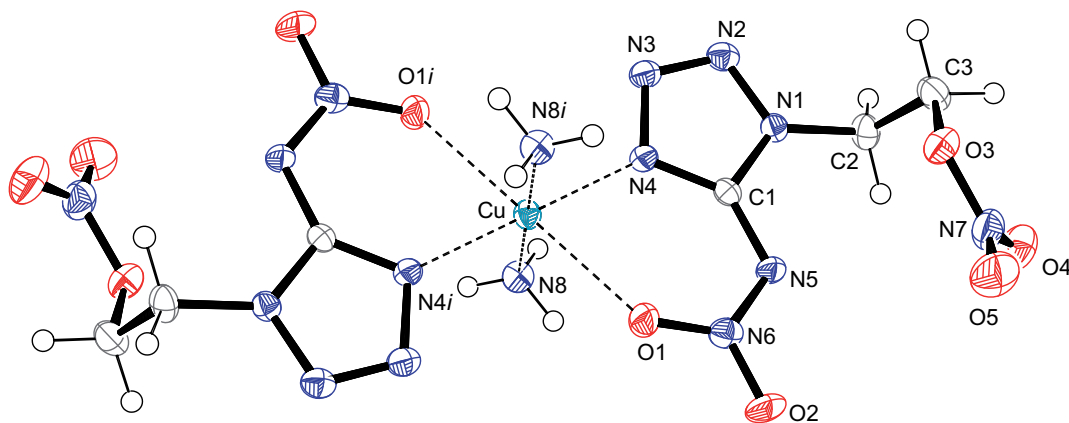


Figure 3.10 Molecular unit of **2_Cu_NH₃**. Hydrogen atoms shown as spheres of arbitrary radius and thermal displacements set at 50 % probability. Selected geometries: distances (Å) N1–N2 1.344(3), N2–N3 1.287(2), N3–N4 1.372(3), N1–C1 1.354(3), C1–N5 1.350(3), N5–N6 1.327(3), O1–N6 1.273(2), O2–N6 1.236(2), N1–C2 1.463(3), O3–C3 1.450(3), O3–N7 1.389(3), O4–N7 1.206(3), O5–N7 1.202(3), Cu1–N4 1.994(2), Cu1–N8 2.010(2), Cu1–O1 2.381(2); angles (°) N1–C1–N4 105.6(2), N1–C1–N5 117.8(2), O1–N6–N5 123.0(2), O1–N6–O2 120.0(2), C3–O3–N7 114.5(2), O4–N7–O5 128.5(3), O4–N7–O3 119.0(2), O5–N7–O3 112.5(2), N8–Cu1–O1 91.35(9), N4–Cu1–O1 75.12(7), N4–Cu1–N8 90.76(9); torsion angles (°) N6–N5–C1–N1 174.7(2), C1–N5–N6–O1 -2.2(3), C3–O3–N7–O4 1.0(3), C3–O3–N7–O5 -180.0(2); *i* -*x*+2, -*y*, -*z*+2.

trans-[Diammine-bis{1-(2-nitratoethyl)-5-nitriminotetrazolato- κ^2 N4,O1}] copper(II) (**2_Cu_NH₃**) crystallizes analog to **2_Cu_H₂O** in the monoclinic space group $P2_1/c$ with two molecular units per unit cell (Figure 3.10). The density of 1.884 g/cm³ is smaller than the calculated one of **2_Cu_H₂O**. Again, a distorted octahedral coordination of the copper(II) atoms can be observed. Coordinating atoms are O1, N4, N8, O1*i*, N4*i*, and N8*i*. The longest distance is between Cu and O1 with 2.381(2) Å.

3.1.4 Energetic Properties

The energetic properties, such as decomposition temperature (T_{dec}), sensitivity to impact (E_{dr}), friction (F_r) and electric discharge (E_{el}), as well as the combustion energy ($\Delta_c U$) were determined. Furthermore, the solubility in H₂O at ambient temperature of each compound was defined. An overview of the energetic properties of the alkali metal salts is given in Table 3.4. In Table 3.5 the properties of the alkaline earth metal salts and copper(II) compounds can be found.

Table 3.4 Overview of the physico-chemical properties of **2_Li**, **2_Na**, **2_K**, **2_Rb**, and **2-Cs**.

	2_Li	2_Na	2_K	2_Rb	2-Cs
Formula	$C_3H_4LiN_7O_5 \cdot H_2O$	$C_3H_4N_7NaO_5$	$C_3H_4KN_7O_5$	$C_3H_4N_7O_5Rb$	$C_3H_4CsN_7O_5$
M [g/mol]	243.06	241.10	257.21	303.58	351.01
E_{dr} [J]^a	40	2.0	2.5	2.0	< 1.0
F_r [N]^b	252	80	60	168	40
E_{el} [J]^c	0.25	0.15	0.02	0.05	0.08
grain size [μm]	250–500	500–1000	> 1000	500–1000	100–500
N [%]^d	40.3	40.7	38.1	32.3	27.9
Ω [%]^e	-26	-27	-31	-26	-23
T_{dec} [°C]^f	171	163	169	157	149
ρ [g/cm³]^g	1.59* (23 °C)	1.86	1.92	2.16	2.62* (22 °C)
Δ_cU [kJ/kg]^k	n.d.**	n.d.**	-8302	n.d.**	n.d.**
Δ_cH° [kJ/mol]ⁱ	-	-	-2077	-	-
Δ_fH° [kJ/mol]^j	-	-	-245	-	-
H₂O sol. [wt%]^k	21 (22 °C)	20 (22 °C)	18 (22 °C)	25 (22 °C)	29 (22 °C)

a) BAM drop hammer [8], b) BAM methods [8], c) Electric spark tester, d) Nitrogen content, e) Oxygen balance, f) Decomposition temperature from DSC ($\beta = 5$ K/min), g) determined by X-ray crystallography or pycnometer (*), h) Combustion energy, i) Enthalpy of combustion, j) Molar enthalpy of formation, k) Solubility in H₂O (H₂O temperature), **) not determined.

Table 3.5 Overview of the physico-chemical properties of **2_Mg**, **2_Ca**, **2_Sr**, **2_Ba**, **2_Cu_H₂O**, and **2_Cu_NH₃**.

	2_Mg	2_Ca	2_Sr	2_Ba	2_Cu_H₂O	2_Cu_NH₃
Formula	$Mg(C_3H_4N_7O_5)_2 \cdot 6H_2O$	$Ca(C_3H_4N_7O_5)_2 \cdot 3H_2O$	$Sr(C_3H_4N_7O_5)_2 \cdot H_2O$	$Ba(C_3H_4N_7O_5)_2 \cdot H_2O$	$[Cu(C_3H_4N_7O_5)_2 (H_2O)_2]$	$[Cu(C_3H_4N_7O_5)_2 (NH_3)_2]$
M [g/mol]	568.61	530.34	541.85	591.56	535.79	533.82
E_{dr} [J]^a	3.5	3.0	1.0	< 1.0	2.5	2.0
F_r [N]^b	324	288	144	120	192	160
E_{el} [J]^c	0.20	0.10	0.10	0.08	0.40	0.75
grain size [μm]	> 1000	100–500	> 1000	> 1000	> 1000	> 1000
N [%]^d	34.5	38.3	36.2	33.2	36.6	42.0
Ω [%]^e	-20	-13	-12	-19	-21	-30
T_{dec} [°C]^f	191	224	222	209	196	194
ρ [g/cm³]^g	1.72	1.82	2.11* (24 °C)	2.25* (24 °C)	1.97	1.88
Δ_cU [kJ/kg]^k	n.d.**	n.d.**	-7967	-6879	-8202	-8729
Δ_cH° [kJ/mol]ⁱ	-	-	-4307	-4046	-4371	-4638
Δ_fH° [kJ/mol]^j	-	-	-668	-814	-20	-404
H₂O sol. [wt%]^k	29 (21 °C)	38 (22 °C)	20 (23 °C)	1.8 (23 °C)	0.8 (25 °C)	0.4 (25 °C)

a) BAM drop hammer [8], b) BAM methods [8], c) Electric spark tester, d) Nitrogen content, e) Oxygen balance, f) Decomposition temperature from DSC ($\beta = 5$ K/min), g) determined by X-ray crystallography or pycnometer (*), h) Combustion energy, i) Enthalpy of combustion, j) Molar enthalpy of formation, k) Solubility in H₂O (H₂O temperature), **) not determined.

For investigating the thermal behavior, ~1.5 mg of each compound was measured by differential scanning calorimetry (DSC) in the temperature range from 20–400 °C. The endothermic signals have been checked using a *Büchi* melting point apparatus to distinguish melting points from loss of crystal water.

All alkali metal salts of **2** decompose at temperatures below 175 °C (Figure 3.11). **2_Cs** decomposes even at 149 °C, after melting at 137 °C. In the case of **2_Li** loss of crystal water can be observed at 103 °C. All alkali metal salts of **2** show a second exothermic signal at temperatures between 290 °C and 380 °C. This could be also observed in the case of the alkali metal salts of **1** (see chapter 2). **2_Na** and **2_K** offer an endothermic signal at 291 °C and 324 °C, respectively.

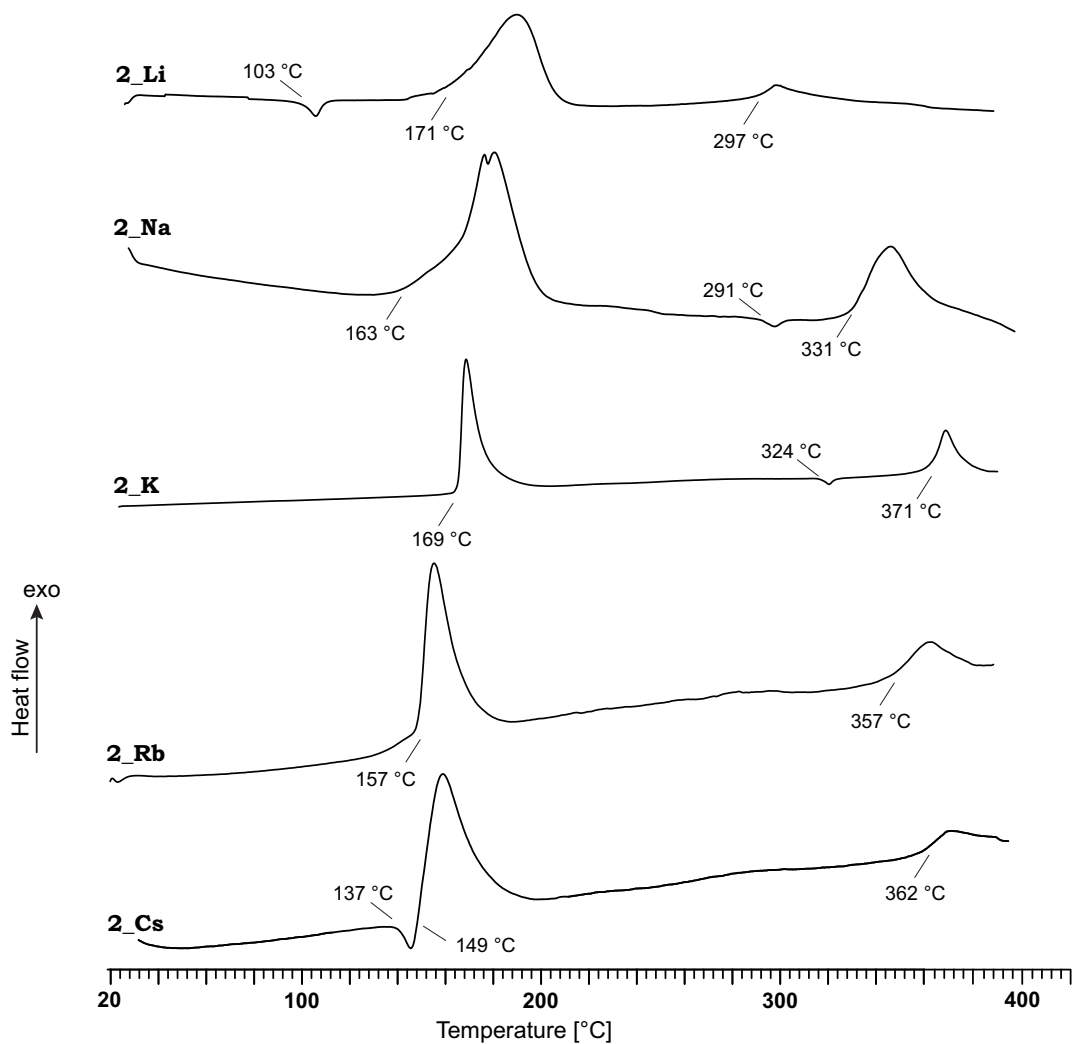


Figure 3.11 DSC thermograms of the alkali metal salts of **2** in a temperature range of 25–400 °C. Decomposition points are given as onset temperatures.

The alkaline earth metal salts of **2** show higher decomposition temperatures compared to its alkali salts (Figure 3.12). Comparing the alkaline earth metal salts of **2**, **2_Ca** has the highest decomposition point of 224 °C and **2_Mg** the lowest (191 °C). Loss of H₂O can be observed in the case of **2_Mg**, **2_Ca**, and **2_Sr** at 114 °C, 125 °C, and 168 °C, respectively.

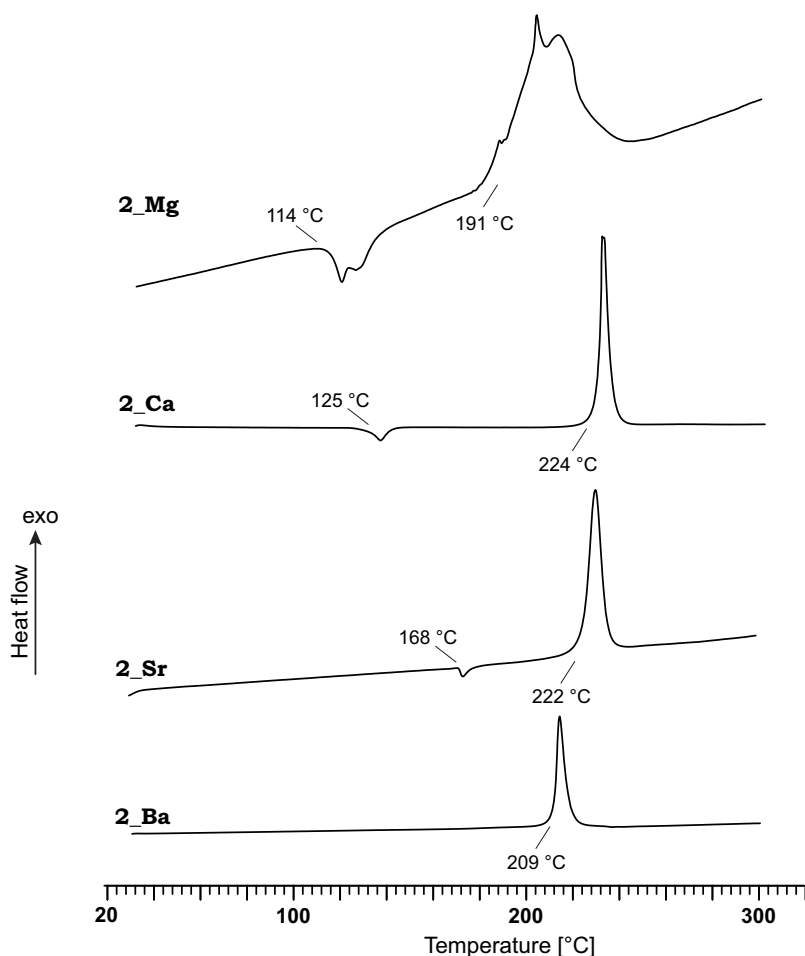


Figure 3.12 DSC thermograms of the alkaline earth metal salts of **2** in a temperature range of 25–300 °C. Decomposition points are given as onset temperatures.

The copper(II) compounds, **2_Cu_H₂O** and **2_Cu_NH₃**, decompose at temperatures below 200 °C (Figure 3.13). In the DSC thermogram of **2_Cu_H₂O** an endothermic signal at 100 °C can be observed. This is caused by the loss of crystal water molecules.

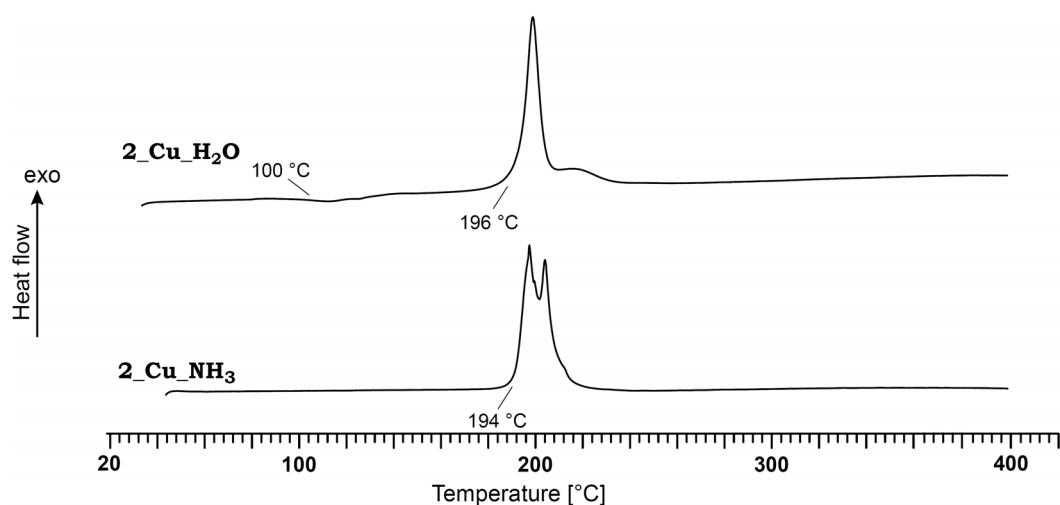
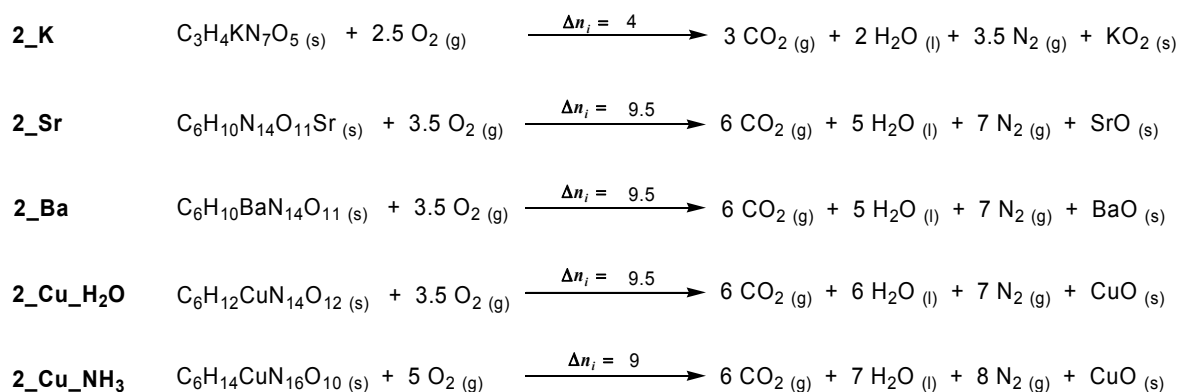


Figure 3.13 DSC thermograms of the copper(II) compounds **2_Cu_H₂O** and **2_Cu_NH₃** in a temperature range of 35–400 °C. Decomposition points are given as onset temperatures.

Compared to the salts of **1** (see chapter 2), the prepared compounds of **2** are much more sensitive towards outer stimuli. Except **2_Li** ($E_{\text{dr}} = 40$ J), all compounds of **2a** are very sensitive to impact ($E_{\text{dr}} \leq 3.0$ J).^[8] Furthermore, all show a sensitivity to friction with values between 40 N and 324 N. The determined values of their sensitivities toward electric discharge are quite low ($E_{\text{el}} < 0.75$ J), whereas the copper(II) compounds, **2_Cu_H₂O** and **2_Cu_NH₃**, are the less sensitive ones. Due to the high sensitivities of the compounds of **2**, they can be excluded for an application as colorants in pyrotechnic compositions. But they could find application as primaries, especially the water-free alkali metal salts **2_Na**, **2_K**, **2_Rb**, and **2_Cs**.

The reported values of the combustion energy ($\Delta_c U$) are the average of three single bomb calorimetry measurements. The standard molar enthalpy of combustion ($\Delta_c H^\circ$) was derived from equation 3.3.

The enthalpy of formation ($\Delta_f H^\circ$) for the compounds **2_K**, **2_Sr**, **2_Ba**, **2_Cu_H₂O**, and **2_Cu_NH₃** was calculated at 298.15 K using the HESS thermochemical cycle and the following combustion reactions (Scheme 3.6).



Scheme 3.6 Combustion equations of **2_K**, **2_Sr**, **2_Ba**, **2_Cu_H₂O**, and **2_Cu_NH₃**.

The heats of formation of the combustion products H₂O (l) (−286 kJ/mol), CO₂ (g) (−393 kJ/mol), KO₂ (s) (−284.5 kJ/mol), SrO (s) (−592 kJ/mol), BaO (s) (−548 kJ/mol), and CuO (s) (−157 kJ/mol) were adopted from literature.^[13] The enthalpies of formation of **2_K**, **2_Sr**, and **2_Cu_NH₃** were determined to −245 kJ/mol, −668 kJ/mol, and −404 kJ/mol, respectively. The copper(II) compound **2_Cu_H₂O** has the smallest negative heat of formation (−20 kJ/mol), whereas **2_Ba** offers the largest negative value (−804 kJ/mol).

For the determination of the solubility, each compound was added to 1 mL H₂O with before noted temperature until the solution was saturated. The solubilities are given in percent by weight (wt%) and were calculated according to equation 3.4.

$$\text{H}_2\text{O-sol.} = \frac{m_{\text{dissolved Compound}}}{m_{\text{dissolved Compound}} + m_{\text{Solvent}}} \cdot 100 \quad (3.4)$$

The calcium salt **2_Ca** offers the highest solubility with 38 wt%. **2_Ba** has a very low solubility in H₂O with 1.8 wt%. **2_Cu_H₂O** and **2_Cu_NH₃**, are almost insoluble in H₂O at ambient temperature with solubilities less than 1.0 wt%. All other compounds show H₂O-solubilities between 18 wt% and 29 wt%. Compared to the salts of **1**, the solubilities of the salts of **2** in H₂O at ambient temperature are smaller.

3.1.5 Flame Color and Combustion Behavior

Only the salts, which might find application as colorants in red or green light emitting pyrotechnics – **2_Li**, **2_Ca**, **2_Sr**, **2_Ba**, **2_Cu_H₂O**, **2_Cu_NH₃** – were tested with regard to their flame color during combustion in the flame of a BUNSEN burner. **2_Li**, **2_Ca**, and **2_Sr** offer, as expected, a red flame (Figure 3.14). In comparison to the corresponding salts of 1-(2-hydroxyethyl)-5-nitriminotetrazole (**1**), the reaction of **2_Li**, **2_Ca**, and **2_Sr** in the flame is more vigorous. They deflagrate subsonic.



Figure 3.14 Flame color of **2_Li** (up), **2_Ca** (down, left), and **2_Sr** (down, right).

Analog to **1_Ba** and other chlorine-free barium salts, **2_Ba** offers a white flame during deflagration (Figure 3.15, chapters 2, 6–8). A mixture of **2_Ba** and a chlorine donor, like PVC, was not further investigated.

The copper(II) compounds **2_Cu_H₂O** and **2_Cu_NH₃** offer a more intense green flame. However, a red seam on top of the flames can be observed. This is a result of the formation of the red light emitting gas species CuO.

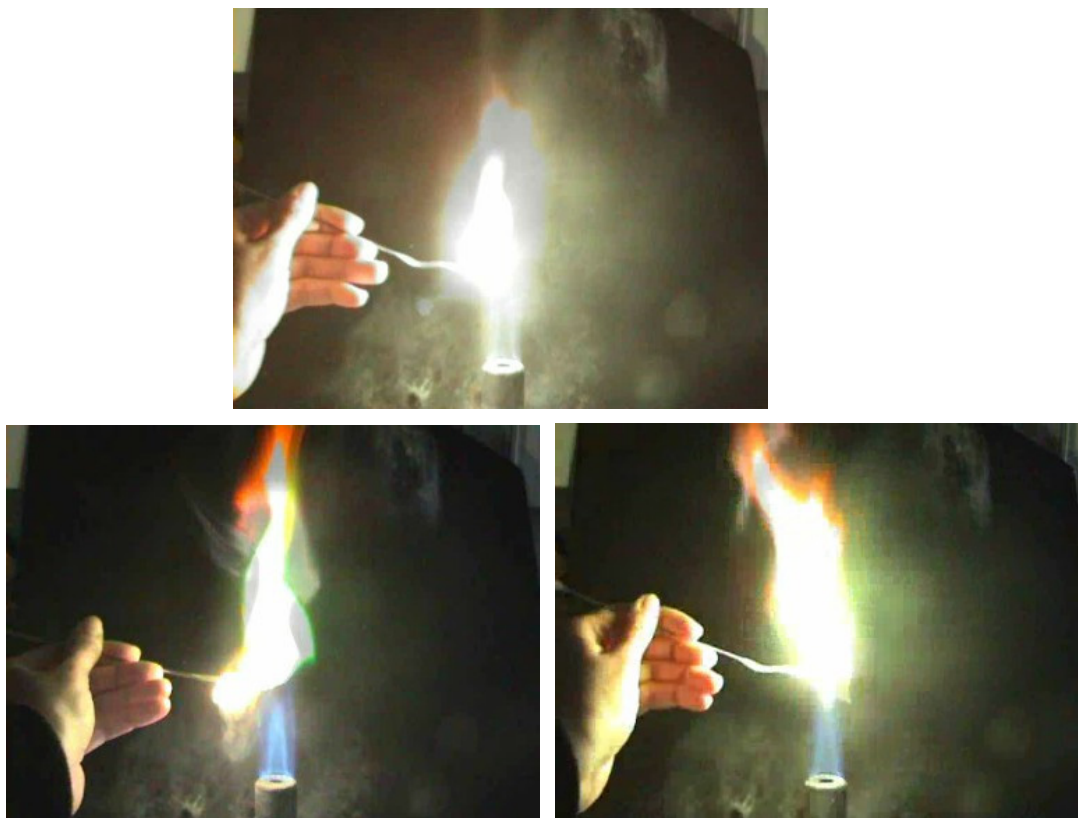


Figure 3.15 Flame color of **2_Ba** (up), **2_Cu_H₂O** (down, left), and **2_Cu_NH₃** (down, right).

All tested compounds combust without any visible smoke production and any solid residues. However, they deflagrate making a sizzling noise. Due to their vigorous behavior in the flame, the tested salts are less suitable as colorants in pyrotechnic compositions.

3.2 Experimental Part

*CAUTION! The prepared compounds are sensitive to impact, friction, and electric discharge. Therefore, proper protective measures (safety glasses, face shield, leather coat, earthed equipment and shoes, Kevlar® gloves and ear plugs) should be used, also during work on the precursor molecule 1-(2-nitratoethyl)-5-nitriminotetrazole monohydrate (**2**).*

3.2.1 Products after Nitration

3.2.1.1 1-(2-Nitratoethyl)-5-nitriminotetrazole Monohydrate (**2**)

5.0 g 1-(2-hydroxyethyl)-5-aminotetrazole (**1-OH**) was slowly added to 50 mL nitric acid (100 %) at 0 °C. After stirring the reaction solution for more than 24 hours at ambient temperature, the colorless solution was poured onto ice. The formed crystals were filtered off and analyzed by ¹H and ¹³C NMR, or Raman spectroscopy for determining the purity. Yield: 88 %. The analytical data (Raman, ¹H and ¹³C NMR spectroscopy) are in accordance with the data found in literature.^[1, 2]

IR (Diamond-ATR, cm^{-1}): 3546 (m), 3445 (m), 3018 (w), 2977 (w), 2729 (w), 2642 (w), 1697 (vw), 1640 (s), 1579 (s), 1490 (s), 1450 (m), 1413 (m), 1391 (w), 1374 (w), 1350 (m), 1314 (m), 1289 (s), 1257 (s), 1246 (s), 1224 (s), 1158 (w), 1080 (w), 1057 (m), 1032 (w), 1021 (m), 991 (vw), 975 (m), 896 (m), 883 (m), 852 (m), 778 (w), 755 (w), 724 (w), 706 (w), 680 (vw), 658 (vw).

^{14}N NMR (DMSO- d_6): -18 (NNO₂), -44 (ONO₂).

^{15}N NMR (DMSO- d_6): -18.8 (NNO₂), -27.7 (N3), -28.7 (t, N2, $^3J(^1\text{H}, ^{15}\text{N}) = 1.9$ Hz), -43.6 (t, ONO₂, $^3J(^1\text{H}, ^{15}\text{N}) = 3.2$ Hz), -157.5 (N5), -158.6 (N4), -174.9 (t, N1, $^3J(^1\text{H}, ^{15}\text{N}) = 2.7$ Hz).

$E_{\text{dr}} = 1.5$ J (250–500 μm).

$F_{\text{r}} = 128$ N (250–500 μm).

$E_{\text{el}} = 0.25$ J (250–500 μm).

$\Delta_c U = -2224$ cal/g.

3.2.1.2 1-(2-Nitratoethyl)-5-aminotetrazolium Nitrate (2a)

Compound **2a** was obtained during the reaction of 1-(2-hydroxyethyl)-5-amino-tetrazole with nitric acid (100 %). It is a byproduct during the synthesis of 1-(2-nitratoethyl)-5-nitriminotetrazole monohydrate (**2**). Yield: 8 %

M.p. 110 °C, 137 °C (dec., DSC-measurement, 5 K/min).

Raman (200 mW, 25 °C, cm^{-1}): 3243 (4), 3031 (17), 2982 (41), 2966 (19), 1684 (6), 1638 (9), 1598 (7), 1562 (3), 1503 (10), 1455 (13), 1433 (12), 1380 (14), 1290 (18), 1228 (5), 1144 (5), 1048 (100), 950 (5), 860 (7), 845 (17), 768 (38), 717 (12), 673 (9), 639 (10), 571 (19), 535 (4), 493 (4), 444 (7), 414 (8), 333 (6), 306 (5), 284 (5), 248 (8), 208 (5).

IR (Diamond-ATR, cm^{-1}): 3347 (m), 3158 (w), 2920 (m), 2853 (w), 2363 (m), 2337 (w), 1690 (m), 1636 (s), 1581 (m), 1548 (w), 1532 (w), 1493 (m), 1447 (m), 1407 (m), 1372 (m), 1341 (m), 1310 (m), 1283 (s), 1241 (m), 1145 (vw), 1060 (w), 1042 (w), 1018 (w), 976 (w), 946 (vw), 894 (w), 871 (w), 852 (w), 843 (w), 778 (vw), 756 (w), 724 (w), 672 (vw), 625 (w).

^1H NMR (DMSO- d_6): 8.76 (s, 2H, NH₂), 4.86 (t, $^3J = 4.9$ Hz, 2H, CH₂), 4.51 (t, $^3J = 4.9$ Hz, 2H, CH₂).

^{13}C NMR (DMSO- d_6): 155.9 (CN₄), 70.9 (CH₂ONO₂), 43.0 (NCH₂).

^{14}N NMR (DMSO- d_6): -15 (NNO₂), -44 (ONO₂).

^{15}N NMR (DMSO- d_6): -5.7 (N3), -14.8 (NO₃), -25.5 (N2, $^3J(^1\text{H}, ^{15}\text{N}) = 1.6$ Hz), -43.6 (t, ONO₂, $^3J(^1\text{H}, ^{15}\text{N}) = 3.3$ Hz), -116.5 (N4), -180.7 (N1), -332.7 (N5).

Elemental analysis C₃H₇N₇O₆ (237.13 g/mol): calc.: C, 15.20; H, 2.98; N, 41.35; found: C, 15.08; H, 3.24; N, 41.32.

m/z (FAB⁺): 175 [100, C₃H₇N₆O₃], (FAB⁻): 62 [100, NO₃⁻].

$E_{\text{dr}} = 10$ J (250–1000 μm).

$F_{\text{r}} = 160$ N (250–1000 μm).

$E_{\text{el}} = 0.40$ J (250–1000 μm).

$\Delta_c U = -2113$ cal/g.

3.2.2 Preparation of the Salts

General procedure for preparing the salts of **2**: To a solution of 0.87 g (5.0 mmol) 1-(2-nitratoethyl)-5-nitriminotetrazole monohydrate (**2**) in 25 mL H₂O the corresponding hydroxide or carbonate was added. In case of the alkali metal 5.0 mmol, in case of the alkaline earth metal salts 2.5 mmol.

3.2.2.1 Lithium 1-(2-Nitratoethyl)-5-nitriminotetrazolate Monohydrate (**2_Li**)

After recrystallization from H₂O, a colorless powder was obtained. Yield: 84 %.

M.p. 103 °C (loss of H₂O), 171 °C (dec., DSC-measurement, 5 K/min).

IR (Diamond-ATR, cm⁻¹): 3410 (s), 2910 (vw), 1643 (s), 1628 (s), 1512 (m), 1459 (m), 1421 (w), 1339 (s), 1313 (s), 1281 (s), 1163 (w), 1111 (w), 1068 (vw), 1036 (m), 995 (w), 969 (vw), 946 (vw), 889 (m), 874 (m), 846 (m), 770 (vw), 745 (w), 698 (w), 670 (w), 628 (vw).

¹H NMR (DMSO-*d*₆): 4.83 (*t*, ³*J* = 5.0 Hz, 2H, CH₂), 4.40 (*t*, ³*J* = 5.0 Hz, 2H, CH₂), 3.31 (*s*, 2H, H₂O).

¹³C NMR (DMSO-*d*₆): 157.2 (CN₄), 70.2 (CH₂ONO₂), 43.0 (NCH₂).

Elemental analysis C₃H₆LiN₇O₆ (243.06 g/mol): calc.: C, 14.82; H, 2.49; N, 40.34; found: C, 14.58; H, 2.55; N, 39.79.

E_{dr} = 40 J (250–500 μm).

F_r = 252 N (250–500 μm).

E_{el} = 0.25 J (250–500 μm).

H₂O-sol. 21 wt% (22 °C).

3.2.2.2 Sodium 1-(2-Nitratoethyl)-5-nitriminotetrazolate (**2_Na**)

After recrystallization from H₂O, colorless crystals suitable for X-ray diffraction were obtained. Yield: 87 %.

M.p. 163 °C (dec., DSC-measurement, 5 K/min).

Raman (200 mW, 25 °C, cm⁻¹): 3016 (4), 2972 (11), 1629 (1), 1553 (2), 1503 (100), 1465 (2), 1435 (4), 1378 (7), 1349 (11), 1331 (5), 1278 (13), 1239 (1), 1176 (2), 1112 (6), 1064 (3), 1037 (29), 994 (1), 847 (2), 759 (7), 677 (1), 585 (3), 506 (2), 449 (1), 371 (1), 308 (2), 255 (3).

IR (Diamond-ATR, cm⁻¹): 3544 (w), 3432 (w), 3015 (vw), 2961 (vw), 1742 (vw), 1627 (s), 1580 (w), 1504 (m), 1448 (m), 1434 (m), 1411 (w), 1375 (m), 1346 (s), 1316 (s), 1288 (s), 1263 (s), 1233 (m), 1158 (w), 1111 (w), 1075 (vw), 1060 (w), 1035 (m), 987 (w), 971 (w), 946 (w), 896 (m), 877 (m), 844 (m), 778 (w), 755 (w), 724 (vw), 707 (vw), 675 (vw).

¹H NMR (DMSO-*d*₆): 4.84 (*t*, ³*J* = 5.1 Hz, 2H, CH₂), 4.42 (*t*, ³*J* = 5.1 Hz, 2H, CH₂).

¹³C NMR (DMSO-*d*₆): 157.2 (CN₄), 70.2 (CH₂ONO₂), 43.0 (NCH₂).

Elemental analysis C₃H₄N₇NaO₅ (241.10 g/mol): calc.: C, 14.94; H, 1.67; N, 40.67; found: C, 15.15; H, 1.67; N, 40.43.

$E_{dr} = 2.0 \text{ J}$ (500–1000 μm).

$F_r = 80 \text{ N}$ (500–1000 μm).

$E_{el} = 0.15 \text{ J}$ (500–1000 μm).

H₂O-sol. 20 wt% (22 °C).

3.2.2.3 Potassium 1-(2-Nitratoethyl)-5-nitriminotetrazolate (2_K)

After recrystallization from H₂O, colorless crystals suitable for X-ray diffraction were obtained. Yield: 96 %.

M.p. 169 °C (dec., DSC-measurement, 5 K/min).

Raman (300 mW, 25 °C, cm^{-1}): 3012 (7), 2965 (20), 2903 (2), 1651 (2), 1564 (3), 1502 (100), 1463 (8), 1418 (6), 1388 (11), 1333 (14), 1299 (5), 1282 (12), 1271 (12), 1248 (2), 1233 (2), 1170 (4), 1109 (10), 1076 (3), 1035 (52), 998 (3), 985 (6), 879 (6), 855 (6), 758 (7), 711 (2), 679 (6), 571 (6), 514 (4), 475 (6), 450 (3), 374 (3), 311 (5), 271 (7), 213 (4).

IR (Diamond-ATR, cm^{-1}): 1632 (s), 1558 (vw), 1499 (s), 1453 (m), 1416 (w), 1387 (m), 1362 (vw), 1333 (s), 1306 (s), 1284 (s), 1268 (s), 1246 (m), 1168 (w), 1107 (w), 1075 (vw), 1034 (w), 1014 (vw), 987 (vw), 984 (vw), 898 (m), 878 (w), 860 (w), 848 (w), 781 (w), 759 (w), 741 (w), 709 (w), 690 (vw), 677 (vw), 636 (vw).

¹H NMR (DMSO-*d*₆): 4.86 (t, $^3J = 5.0 \text{ Hz}$, 2H, CH₂), 4.44 (t, $^3J = 5.0 \text{ Hz}$, 2H, CH₂).

¹³C NMR (DMSO-*d*₆): 157.1 (CN₄), 70.2 (CH₂ONO₂), 43.1 (NCH₂).

Elemental analysis C₃H₄KN₇O₅ (257.51 g/mol): calc.: C, 14.01; H, 1.57; N, 38.12; found: C, 13.85; H, 1.71; N, 38.05.

$E_{dr} = 2.5 \text{ J}$ (> 1000 μm).

$F_r = 60 \text{ N}$ (> 1000 μm).

$E_{el} = 0.02 \text{ J}$ (> 1000 μm).

$\Delta_c U = -1938 \text{ cal/g}$.

H₂O-sol. 18 wt% (22 °C).

3.2.2.4 Rubidium 1-(2-Nitratoethyl)-5-nitriminotetrazolate (2_Rb)

After recrystallization from H₂O, colorless crystals suitable for X-ray diffraction were obtained. Yield: 89 %.

M.p. 157 °C (dec., DSC-measurement, 5 K/min).

IR (Diamond-ATR, cm^{-1}): 3457 (w), 1644 (s), 1631 (s), 1581 (w), 1497 (s), 1451 (s), 1417 (m), 1384 (s), 1330 (s), 1302 (s), 1283 (vs), 1266 (s), 1243 (s), 1168 (m), 1106 (m), 1071 (w), 1032 (m), 995 (vw), 982 (vw), 899 (m), 876 (m), 858 (m), 845 (w), 780 (m), 758 (w), 740 (w), 710 (w), 677 (w).

¹H NMR (DMSO-*d*₆): 4.87 (t, $^3J = 5.0 \text{ Hz}$, 2H, CH₂), 4.44 (t, $^3J = 5.0 \text{ Hz}$, 2H, CH₂).

¹³C NMR (DMSO-*d*₆): 157.4 (CN₄), 70.8 (CH₂ONO₂), 43.7 (NCH₂).

Elemental analysis C₃H₄N₆O₅Rb (303.58 g/mol): calc.: C, 11.87; H, 1.33; N 32.30; found: C, 12.14; H, 1.65; N, 32.54.

E_{dr} = 2.0 J (500–1000 μm).

F_r = 186 N (500–1000 μm).

E_{el} = 0.05 J (500–1000 μm).

H₂O-sol. 25 wt% (22 °C).

3.2.2.5 Cesium 1-(2-Nitratoethyl)-5-nitriminotetrazolate (2_Cs)

After recrystallization from H₂O, colorless crystals were obtained. Yield: 92 %.

M.p. 137 °C, 149 °C (dec., DSC-measurement, 5 K/min).

IR (Diamond-ATR, cm⁻¹): 3262 (br, w), 3020 (w), 2970 (w), 2914 (vw), 1637 (s), 1503 (s), 1444 (m), 1426 (m), 1372 (m), 1309 (s), 1282 (s), 1263 (s), 1242 (m), 1166 (w), 1104 (m), 1071 (vw), 1029 (m), 1000 (w), 978 (vw), 901 (m), 884 (w), 863 (m), 780 (w), 754 (w), 726 (w), 716 (vw), 700 (vw), 681 (w).

¹H NMR (DMSO-*d*₆): 4.87 (*t*, ³*J* = 5.1 Hz, 2H, CH₂), 4.44 (*t*, ³*J* = 5.1 Hz, 2H, CH₂).

¹³C NMR (DMSO-*d*₆): 157.8 (CN₄), 70.8 (CH₂ONO₂), 43.7 (NCH₂).

Elemental analysis C₃H₄CsN₇O₅ (351.01 g/mol): calc.: C, 10.27; H, 1.15; N, 27.93; found: C, 10.10; H, 1.15; N, 27.49.

E_{dr} < 1.0 J (100–500 μm).

F_r = 40 N (100–500 μm).

E_{el} = 0.08 J (100–500 μm).

H₂O-sol. 29 wt% (22 °C).

3.2.2.6 Magnesium 1-(2-Nitratoethyl)-5-nitriminotetrazolate Hexahydrate (2_Mg)

After recrystallization from H₂O, colorless crystals suitable for X-ray diffraction were obtained. Yield: 88 %.

M.p. 119 °C (loss of H₂O), 191 °C (dec., DSC-measurement, 5 K/min).

Raman (300 mW, 25 °C, cm⁻¹): 3234 (1), 3032 (6), 3012 (13), 2991 (22), 2971 (21), 1510 (100), 1425 (7), 1394 (7), 1362 (7), 1332 (60), 1282 (21), 1235 (3), 1169 (1), 1124 (20), 1082 (6), 1049 (60), 1012 (9), 959 (2), 897 (6), 842 (11), 763 (13), 686 (9), 644 (3), 578 (10), 496 (8), 448 (4), 379 (5), 359 (6), 298 (12), 259 (5).

IR (Diamond-ATR, cm⁻¹): 3479 (s), 3351 (s), 3245 (s), 3035 (w), 2991 (w), 2904 (vw), 2361 (vw), 1662 (w), 1626 (s), 1583 (vw), 1526 (m), 1512 (m), 1456 (m), 1433 (m), 1392 (m), 1334 (s), 1316 (s), 1262 (m), 1165 (vw), 1120 (w), 1080 (vw), 1049 (vw), 1011 (w), 988 (vw), 958 (vw), 877 (w), 842 (w), 778 (vw), 741 (vw), 707 (w), 682 (w), 637 (w).

¹H NMR (DMSO-*d*₆): 4.86 (*t*, ³*J* = 5.1 Hz, 4H, CH₂), 4.43 (*t*, ³*J* = 5.1 Hz, 4H, CH₂), 3.38 (s, 12H, H₂O).

¹³C NMR (DMSO-*d*₆): 157.1 (CN₄), 70.2 (CH₂ONO₂), 43.1 (NCH₂).

Elemental analysis $C_6H_{20}MgN_{14}O_{16}$ (568.61 g mol⁻¹): calc.: C, 12.67; H, 3.55; N, 34.49; found: C, 12.68; H, 3.62; N, 34.68.

E_{dr} = 3.5 J (> 1000 μ m).

F_r = 324 N (> 1000 μ m).

E_{el} = 0.20 J (> 1000 μ m).

H₂O-sol. 29 wt% (21 °C).

3.2.2.7 Calcium 1-(2-Nitratoethyl)-5-nitriminotetrazolate Trihydrate (2_Ca)

After recrystallization from H₂O, a colorless powder was obtained. Yield: 81 %.

M.p. 125 °C (loss of H₂O), 224 °C (dec., DSC-measurement, 5 K/min).

IR (Diamond-ATR, cm⁻¹): 3428 (br, m), 3026 (vw), 2971 (vw), 2909 (vw), 2360 (vw), 1738 (vw), 1631 (s), 1511 (m), 1462 (m), 1373 (m), 1342 (s), 1316 (s), 1274 (s), 1169 (w), 1109 (w), 1068 (vw), 1032 (m), 1011 (w), 985 (w), 878 (m), 842 (m), 771 (w), 755 (w), 742 (w), 705 (vw), 674 (w), 631 (w).

¹H NMR (DMSO-*d*₆): 4.87 (*t*, ³*J* = 5.1 Hz, 4H, CH₂), 4.43 (*t*, ³*J* = 5.1 Hz, 4H, CH₂).

¹³C NMR (DMSO-*d*₆): 157.4 (CN₄), 70.8 (CH₂ONO₂), 43.7 (NCH₂).

Elemental analysis $C_6H_{14}CaN_{14}O_{13}$ (530.34 g/mol): calc.: C, 14.07; H, 2.36; N, 38.28; found: C, 13.76; H, 2.46; N, 36.87.

E_{dr} = 3.0 J (100–500 μ m).

F_r = 288 N (100–500 μ m).

E_{el} = 0.10 J (100–500 μ m).

H₂O-sol. 38 wt% (22 °C).

3.2.2.8 Strontium 1-(2-Nitratoethyl)-5-nitriminotetrazolate Monohydrate (2_Sr)

After recrystallization from H₂O, a colorless powder was obtained. Yield: 89 %.

M.p. 168 °C (loss of H₂O), 222 °C (dec., DSC-measurement, 5 K/min).

Raman (300 mW, 25 °C, cm⁻¹): 3015 (5), 2979 (16), 1543 (4), 1508 (100), 1463 (5), 1424 (6), 1374 (6), 1341 (28), 1282 (12), 1240 (2), 1176 (4), 1112 (9), 1068 (2), 1030 (42), 994 (4), 876 (4), 842 (3), 766 (10), 742 (2), 679 (2), 634 (2), 584 (5), 507 (4), 451 (4), 383 (6), 313 (5), 273 (4), 217 (4).

IR (Diamond-ATR, cm⁻¹): 3642 (w), 3485 (w), 1632 (s), 1513 (m), 1457 (m), 1434 (w), 1419 (w), 1382 (s), 1365 (s), 1354 (s), 1337 (s), 1314 (s), 1280 (s), 1236 (m), 1176 (vw), 1110 (w), 1062 (vw), 1028 (m), 1016 (w), 994 (w), 950 (w), 892 (w), 874 (m), 848 (w), 836 (m), 765 (w), 750 (w), 740 (w), 700 (vw), 680 (w), 641 (vw), 632 (vw).

¹H NMR (DMSO-*d*₆): 4.87 (*t*, ³*J* = 5.1 Hz, 4H, CH₂), 4.45 (*t*, ³*J* = 5.1 Hz, 4H, CH₂).

¹³C NMR (DMSO-*d*₆): 157.7 (CN₄), 70.8 (CH₂ONO₂), 434.7 (NCH₂).

Elemental analysis C₆H₁₀N₁₄O₁₁Sr (541.85 g/mol): calc.: C, 13.30; H, 1.86; N, 36.19; found: C, 13.27; H, 1.88; N, 35.74.

$$E_{\text{dr}} = 1.0 \text{ J} \quad (> 1000 \text{ } \mu\text{m}).$$

$$F_{\text{r}} = 144 \text{ N} \quad (> 1000 \text{ } \mu\text{m}).$$

$$E_{\text{el}} = 0.10 \text{ J} \quad (> 1000 \text{ } \mu\text{m}).$$

$$\Delta_c U = -1904 \text{ cal/g.}$$

H₂O-sol. 20 wt% (23 °C).

3.2.2.9 Barium 1-(2-Nitratoethyl)-5-nitriminotetrazolate Monohydrate (2_Ba)

After recrystallization from H₂O, a colorless powder was obtained. Yield: 93 %.

M.p. 209 °C (dec., DSC-measurement, 5 K/min).

Raman (300 mW, 25 °C, cm⁻¹): 3012 (4), 2980 (13), 1537 (3), 1504 (100), 1458 (6), 1430 (7), 1372 (7), 1341 (30), 1305 (5), 1282 (9), 1260 (3), 1234 (4), 1173 (5), 1112 (9), 1030 (40), 993 (5), 875 (5), 851 (4), 762 (10), 583 (6), 380 (7), 312 (5).

IR (Diamond-ATR, cm⁻¹): 3642 (w), 3456 (w), 3034 (vw), 2982 (vw), 2910 (vw), 1650 (m), 1630 (s), 1508 (m), 1453 (m), 1433 (m), 1418 (w), 1377 (m), 1351 (m), 1335 (s), 1312 (s), 1278 (s), 1232 (m), 1176 (w), 1110 (m), 1027 (m), 1012 (m), 993 (w), 967 (vw), 950 (w), 896 (w), 872 (m), 849 (m), 837 (m), 770 (w), 760 (w), 738 (w), 704 (vw), 695 (vw), 678 (w).

¹H NMR (DMSO-*d*₆): 4.86 (*t*, ³*J* = 5.1 Hz, 4H, CH₂), 4.44 (*t*, ³*J* = 5.1 Hz, 4H, CH₂), 3.29 (*s*, 2H, H₂O).

¹³C NMR (DMSO-*d*₆): 157.1 (CN₄), 70.2 (CH₂ONO₂), 43.1 (NCH₂).

Elemental analysis C₆H₁₀BaN₁₄O₁₁ (591.56 g/mol): calc.: C, 12.18; H, 1.70; N, 33.15; found: C, 12.08; H, 1.81; N, 32.49.

$$E_{\text{dr}} < 1.0 \text{ J} \quad (1000 \text{ } \mu\text{m}).$$

$$F_{\text{r}} = 120 \text{ N} \quad (1000 \text{ } \mu\text{m}).$$

$$E_{\text{el}} = 0.80 \text{ J} \quad (1000 \text{ } \mu\text{m}).$$

$$\Delta_c U = -1643 \text{ cal/g.}$$

H₂O-sol. 1.8 wt% (23 °C).

3.2.2.10 *trans*-[Diaqua-bis{1-(2-nitratoethyl)-5-nitriminotetrazolato-κ²N4,O1} Copper(II)] (2_Cu_H₂O)

A solution of 0.233 g (1.0 mmol) copper(II) nitrate pentahemihydrate in 2 mL H₂O was combined with a solution of 0.474 g (2.0 mmol) 1-(2-nitratoethyl)-5-nitriminotetrazole monohydrate (**2**) in 15 mL H₂O. The bright green solution was stored at ambient temperature until green single crystals, suitable for X-ray diffraction, were formed. Yield: 66 %.

M.p. 100 °C (loss of H₂O), 196 °C (dec., DSC-measurement, 5 K/min).

IR (Diamond-ATR, cm^{-1}): 3350 (w), 3225 (w), 3036 (w), 1639 (s), 1525 (m), 1473 (m), 1426 (w), 1408 (s), 1382 (w), 1356 (w), 1299 (m), 1279 (s), 1245 (m), 1163 (vw), 1122 (vw), 1087 (vw), 1029 (vw), 988 (w), 971 (vw), 893 (w), 871 (w), 852 (m), 773 (vw), 756 (vw), 740 (vw), 703 (vw), 689 (vw), 655 (w).

Elemental analysis $\text{C}_6\text{H}_{12}\text{CuN}_{14}\text{O}_{12}$ (535.79 g/mol): calc.: C, 13.45; H, 2.26; N, 36.60; found: C, 13.32; H, 2.22; N, 35.95.

$$E_{\text{dr}} = 2.5 \text{ J} \quad (> 1000 \mu\text{m}).$$

$$F_{\text{r}} = 192 \text{ N} \quad (> 1000 \mu\text{m}).$$

$$E_{\text{el}} = 0.40 \text{ J} \quad (> 1000 \mu\text{m}).$$

$$\Delta_c U = -1959 \text{ cal/g.}$$

H₂O-sol. 0.8 wt% (25 °C).

3.2.2.11 *trans*-[Diammine-bis{1-(2-nitratoethyl)-5-nitriminotetrazolato- $\kappa^2\text{N4},\text{O1}$ } Copper(II)] (2_Cu_NH₃)

After a solution of 0.474 g (2.0 mmol) 1-(2-nitratoethyl)-5-nitriminotetrazole monohydrate (**2**) in 15 mL H₂O was combined with a solution of 0.233 g (1.0 mmol) copper(II) nitrate pentahemihydrate 2 mL of aqueous ammonia solution (25 %) was added. After storing the dark blue solution at ambient temperature for several hours deep blue single crystals, suitable for X-ray diffraction, could be obtained. Yield: 55 %.

M.p. 194 °C (dec., DSC-measurement, 5 K/min).

IR (Diamond-ATR, cm^{-1}): 3337 (w), 3263 (w), 3178 (vw), 3034 (vw), 2997 (vw), 2884 (vw), 1636 (s), 1518 (m), 1466 (s), 1446 (vw), 1428 (w), 1404 (s), 1380 (m), 1348 (m), 1294 (m), 1279 (s), 1270 (s), 1237 (s), 1163 (w), 1116 (w), 1083 (vw), 1022 (w), 984 (m), 972 (w), 892 (w), 868 (m), 850 (m), 772 (w), 756 (w), 739 (w), 703 (vw), 687 (w), 653 (w).

Elemental analysis $\text{C}_6\text{H}_{14}\text{CuN}_{16}\text{O}_{10}$ (533.82 g/mol): calc.: C, 13.50; H, 2.64; N, 41.98; found: C, 13.42; H, 2.52; N, 42.06.

$$E_{\text{dr}} = 2.0 \text{ J} \quad (> 1000 \mu\text{m}).$$

$$F_{\text{r}} = 160 \text{ N} \quad (> 1000 \mu\text{m}).$$

$$E_{\text{el}} = 0.75 \text{ J} \quad (> 1000 \mu\text{m}).$$

$$\Delta_c U = -2085 \text{ cal/g.}$$

H₂O-sol. 0.4 wt% (25 °C).

3.3 Conclusion

The alkali metal and alkaline earth metal salts of 1-(2-nitratoethyl)-5-nitriminotetrazole monohydrate (**2**), lithium 1-(2-nitratoethyl)-5-nitriminotetrazolate monohydrate (**2_Li**), sodium 1-(2-nitratoethyl)-5-nitriminotetrazolate (**2_Na**), potassium 1-(2-nitratoethyl)-5-nitriminotetrazolate (**2_K**), rubidium 1-(2-nitratoethyl)-5-nitriminotetrazolate (**2_Rb**), cesium 1-(2-nitratoethyl)-5-nitriminotetrazolate (**2-Cs**) were prepared and characterized

using vibrational and NMR spectroscopy, elemental analysis, and differential scanning calorimetry (DSC). This applies to the alkaline earth metal salts magnesium 1-(2-nitratoethyl)-5-nitriminotetrazolate hexahydrate (**2_Mg**), calcium 1-(2-nitratoethyl)-5-nitriminotetrazolate trihydrate (**2_Ca**), strontium 1-(2-nitratoethyl)-5-nitriminotetrazolate monohydrate (**2_Sr**), and barium 1-(2-nitratoethyl)-5-nitriminotetrazolate monohydrate (**2_Ba**). Furthermore, two copper(II) compounds *trans*-[diaqua-bis{1-(2-nitratoethyl)-5-nitriminotetrazolato- $\kappa^2N4,O1$ } copper(II)] (**2_Cu_H2O**) and *trans*-[diammine-bis{1-(2-nitratoethyl)-5-nitriminotetrazolato- $\kappa^2N4,O1$ } copper(II)] (**2_Cu_NH3**) were prepared and fully characterized. The crystal structures of **2_Na**, **2_K**, **2_Rb**, **2_Mg**, **2_Ca**, **2_Cu_H2O**, **2_Cu_NH3** as well as **2a** were determined and extensively discussed. The sensitivities to impact, friction, and electric discharge, as well as the solubility in H₂O at ambient temperature of all mentioned compounds of **2** were determined. Additionally, the color performance and combustion properties in the flame of a BUNSEN burner of **2_Li**, **2_Ca**, **2_Sr**, **2_Ba**, **2_Cu_H2O**, and **2_Cu_NH3** were investigated. **2_Ba** combusted with a white flame, analog to **1_Ba**. Due to its vigorous combustion behavior, a mixture of PVC and **2_Ba** to achieve a green flame was not investigated. All other investigated compounds offered the expected flame color. Every compound combusted without any visible smoke production and any residues. However, they deflagrate making a sizzling noise. Further investigations of the prepared salts in pyrotechnic composition have not been performed, due to their vigorous behavior in the flame. Furthermore, the salts **2_Sr**, **2_Ba**, **2_Cu_H2O**, and **2_Cu_NH3** decompose at low temperatures (< 225 °C), are very sensitive to impact, friction and electric discharge and offer quite high solubilities in H₂O. However, they are easy to prepare from low cost materials. Therefore, their usage as primary explosives might be possible. Especially the water-free salts alkali metal salts **2_Na**, **2_K**, **2_Rb**, and **2-Cs**.

Moreover, the constitutional isomer of **2**, 1-(2-nitratoethyl)-5-aminotetrazolium nitrate (**2a**) was obtained and fully characterized. Its energetic properties, among others the total energy of detonation, explosion temperature, detonation pressure, and detonation velocity, were determined and compared to **2**. Its molecular structure was discussed and compared to **2a**.

3.4 References

- [1] T. M. Klapötke, J. Stierstorfer, K. R. Tarantik: New Energetic Materials: Functionalized 1-Ethyl-5-aminotetrazoles and 1-Ethyl-5-nitriminotetrazoles, *Chem. Eur. J.* **2009**, *15*, 5775–5792.
- [2] J. Stierstorfer: Advanced Energetic Materials based on 5-Aminotetrazole, *PhD Thesis*, **2009**, Ludwig-Maximilian University, Munich.

- [3] Y.-H. Joo, J. M. Shreeve: Energetic Mono-, Di-, and Trisubstituted Nitroiminotetrazoles, *Angew. Chem., Int. Ed.* **2009**, *48*, 564–567.
- [4] Y.-H. Joo, J. M. Shreeve: 1-Substituted 5-Aminotetrazoles: Syntheses from CNN_3 with Primary Amines *Org. Lett.* **2008**, *10*, 4665–4667.
- [5] N. Fischer, T. M. Klapötke, J. Stierstorfer, K. R. Tarantik: 1-Nitratoethyl-5-nitriminotetrazole Derivatives –Shaping Future High Explosives, *New Trends in Research of Energetic Materials*, Proceedings of the Seminar, 13th, Pardubice, Czech Republic, 21.–23. Apr. **2010**, Pt. 2, 455–467.
- [6] Y.-H. Joo, J. M. Shreeve: 1,3-Diazido-2-(azidomethyl)-2-propylammonium Salts, *Inorg. Chem.* **2009**, *48*, 8431–8438.
- [7] W. Bocian, J. Jazwinski, W. Kozminski, L. Stefaniak, G. A. Webb: A Multinuclear NMR Study of Some Mesoionic 1,3-Dimethyltetrazoles, 1- and 2-Methyltetrazoles and Related Compounds, *J. Chem. Soc. Perkin Trans. 2* **1994**, *6*, 1327–1332.
- [8] a) <http://www.bam.de> b) E_{dr} : insensitive > 40 J, less sensitive \geq 35 J, sensitive \geq 4, very sensitive \leq 3 J; F_r : insensitive > 360 N, less sensitive = 360 N, sensitive < 360 N > 80 N, very sensitive \leq 80 N, extreme sensitive \leq 10 N. According to the UN Recommendations on the Transport of Dangerous Goods.
- [9] a) M. Suceška: EXPLO5.V2, Computer program for calculation of detonation parameters. *Proceedings of the 32nd Int. Annual Conference of ICT*, 3.–6. Jul., **2001**, Karlsruhe, Germany, 110–111. b) M. Suceška: Calculation of detonation heat by EXPLO5 computer code, *Proceedings of 30th Int. Annual Conference of ICT*, 29. Jun.–2. Jul., **1999**, Karlsruhe, Germany, 50/1–50/14.
- [10] M. Suceška: Calculation of the detonation properties of C-H-N-O explosives, *Propellants, Explos., Pyrotech.* **1991**, *16*, 197–202.
- [11] a) M. Suceška: Calculation of detonation parameters by EXPLO5 computer program, *Mater. Sci. Forum* **2004**, *465-466*, 325–330. b) M. Suceška: Evaluation of detonation energy from EXPLO5 computer code results, *Propellants, Explos., Pyrotech.* **1999**, *24*, 280–285. c) M. L. Hobbs, M. R. Baer: Calibration of the BKW-EOS With a Large Product Species Data Base and Measured C-J Properties, *Proceedings of the 10th Symp. (International) on Detonation*, ONR 33395-12, Boston, MA, 12.–16. Jul., **1993**, 409.
- [12] N. Wiberg, E. Wiberg, A. F. Holleman: *Lehrbuch der Anorganischen Chemie*, deGruyter, Berlin, 102. Ed., **2007**.
- [13] <http://webbook.nist.gov/>

4 Salts of 1-(2-Chloroethyl)-5-nitriminotetrazole

Colors in pyrotechnics are obtained by the addition of substances with the desired flame color. Emission of red light is achieved by the addition of strontium nitrate, which acts as both coloring agent and oxidizer. This is also true for barium nitrate, the agent for intensive green colors. The corresponding light emitting species in the gas phase are the monohydroxides, SrOH and BaOH, and the monochlorides, SrCl and BaCl, respectively. If a blue flame is desired, usually copper or copper compounds are combined with a chlorine donor like polyvinyl chloride (PVC). This is necessary, because the formation of CuCl is responsible for the emission of blue light.^[1] If no chlorine is present or if the temperature rises above 1200 °C in an oxygen-rich flame, CuOH and CuO – light emitting species of green and red, respectively – are formed.^[2] On this account, in common fireworks for red, green or blue flame color, potassium perchlorate is widely added, besides its property as oxidizer.

Furthermore, chlorine in pyrotechnic composition is responsible for the formation of volatile chlorine-containing molecular species, which guarantees that the concentration of emitters in the vapour phase is high enough.^[2] So the addition of chlorine donors achieves usually more intense flame colors, especially if strontium, barium or copper compounds are used.

1-(2-Chloroethyl)-5-nitriminotetrazole (**3**) combines three important properties. It contains chlorine, offers a tetrazole ring, which is responsible for the formation of gaseous nitrogen as decomposition product, and includes an energetic nitrimino group, which also improves the oxygen balance. Furthermore, **3** can be deprotonated easily, yielding thermally more stable salts or copper(II) complexes. Therefore, the alkali and alkaline earth metal salts of 1-(2-chloroethyl)-5-nitriminotetrazole (**3**), and three different copper(II) compounds were prepared. Besides their chemical and energetic characterization, the pyrotechnically relevant salts, containing strontium, barium, and copper(II), were investigated relating to their coloring properties as neat compounds and as additives in pyrotechnic compositions.

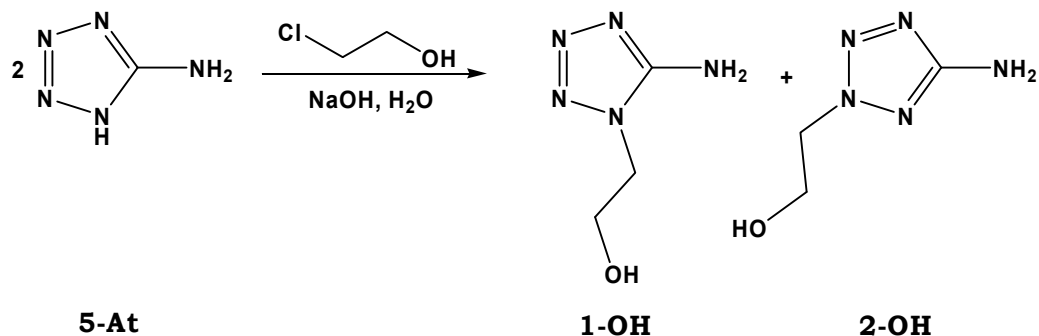
Smoke reduced pyrotechnic formulations with convincing color performances were further investigated.

4.1 Results and Discussion

4.1.1 Syntheses

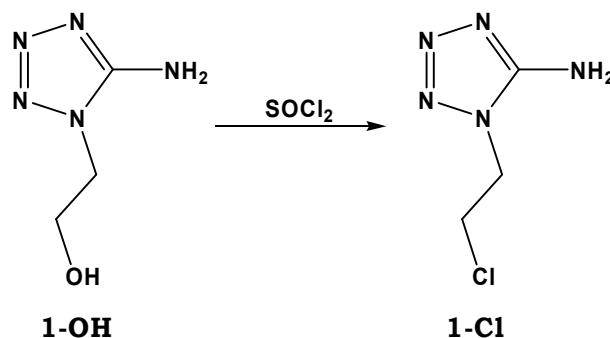
The first preparative step is an alkylation of the commercially available chemical 5-aminotetrazole (**5-At**) with 2-chloroethanol according to a procedure known in literature (Scheme 4.1).^[3, 4, 5] Both isomers – 1-(2-hydroxyethyl)- (**1-OH**) and 2-(2-hydroxyethyl)-5-

aminotetrazole (**2-OH**) – could be isolated. Due to the fact that the purification of **2-OH** is more time consuming, the following synthesis steps were performed using exclusively **1-OH**.



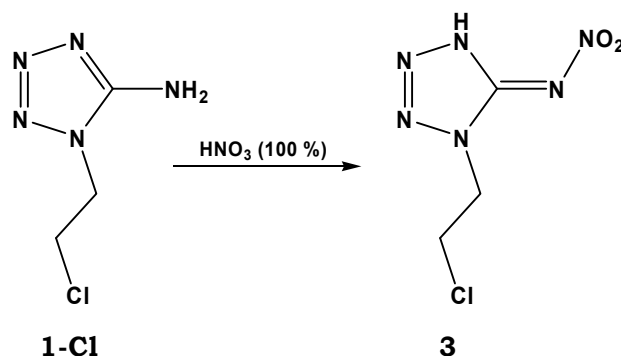
Scheme 4.1 Preparation of 1-and 2-(2-hydroxyethyl)-5-aminotetrazole (**1-/2-OH**).

The hydroxy group was chlorinated by using thionyl chloride as both reactant and solvent according to FINNEGAN *et. al.* (Scheme 4.2).^[6] Decolorization of the yellow powder could be achieved by washing with acetonitrile.^[4, 5]



Scheme 4.2 Chlorination of **1-OH**.

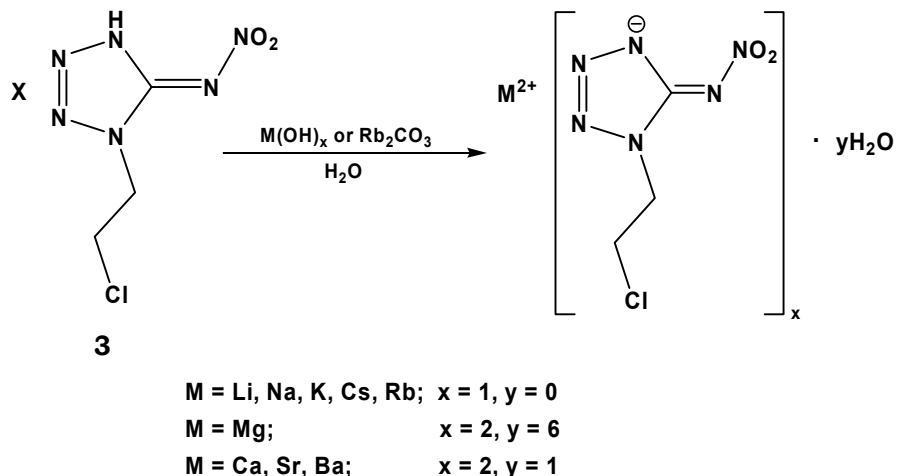
The nitration of **1-Cl** was performed in HNO₃ (100 %), a procedure well known in the literature (Scheme 4.3).^[4, 5] Therefore, **1-Cl** was slowly added to an ice-cooled solution of HNO₃ (100 %) and stirred for at least 17 hours. Afterwards the colorless solution was poured onto ice. The slowly growing colorless crystals were by and by filtered off and dried on air.



Scheme 4.3 Preparation of 1-(2-chloroethyl)-5-nitriminotetrazole (**3**).

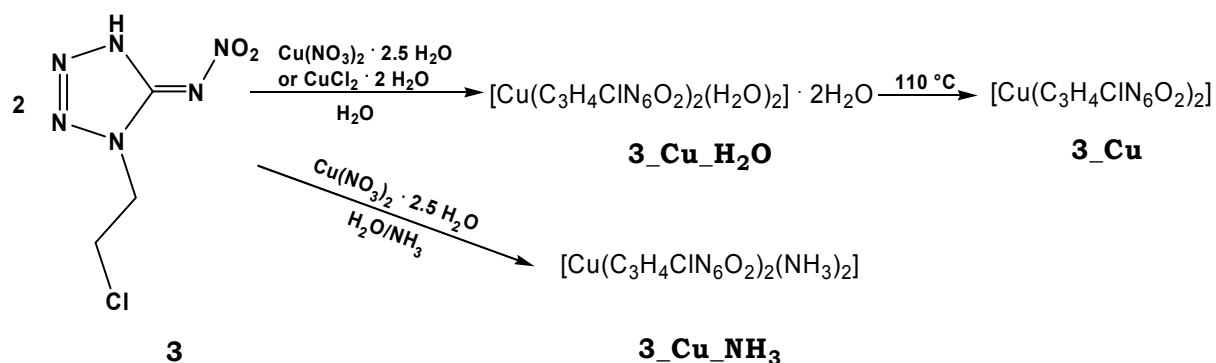
For preparation of the alkali and alkaline earth metal salts, compound **3** was dissolved in H₂O and the corresponding hydroxides – in the case of **3_Rb** Rb₂CO₃ – were added. The suspension was heated until it became clear. By recrystallization from H₂O, the

salts lithium 1-(2-chloroethyl)-5-nitriminotetrazolate (**3_Li**), sodium 1-(2-chloroethyl)-5-nitriminotetrazolate (**3_Na**), potassium 1-(2-chloroethyl)-5-nitriminotetrazolate (**3_K**), rubidium 1-(2-chloroethyl)-5-nitriminotetrazolate (**3_Rb**), cesium 1-(2-chloroethyl)-5-nitriminotetrazolate (**3_Cs**), magnesium 1-(2-chloroethyl)-5-nitriminotetrazolate hexahydrate (**3_Mg**), calcium 1-(2-chloroethyl)-5-nitriminotetrazolate monohydrate (**3_Ca**), strontium 1-(2-chloroethyl)-5-nitriminotetrazolate monohydrate (**3_Sr**), and barium 1-(2-chloroethyl)-5-nitriminotetrazolate monohydrate (**3_Ba**) could be obtained (Scheme 4.4). All salts could be isolated in very high yields.



Scheme 4.4 Preparation of the alkali and alkaline earth metal salts of **3**.

The copper(II) complex *trans*-[diaqua-bis{1-(2-chloroethyl)-5-nitriminotetrazolato- $\kappa^2N4,O5$ } copper(II)] dihydrate (**3_Cu_H₂O**) could be obtained during the reaction of **3** with either copper(II) chloride dihydrate or copper(II) nitrate pentahydrate, in H₂O (Scheme 4.5). The water free copper salt copper(II) 1-(2-chloroethyl)-5-nitriminotetrazolate (**3_Cu**) was prepared by removing the coordinated water of powdered **3_Cu_H₂O** at 110 °C in quantitative yields.



Scheme 4.5 Preparation of the copper compounds **3_Cu_H₂O**, **3_Cu** and **3_Cu_NH₃**.

In the presence of diluted ammonia solution *trans*-[diammine-bis{1-(2-chloroethyl)-5-nitriminotetrazolato- $\kappa^2N4,O1$ }] copper(II) (**3_Cu_NH₃**) was yielded from **3** in an ammoniacal copper(II) nitrate solution. Deep violet crystals formed after storing the solution for a few days at ambient temperature.

3_Na and **3_Cu_H₂O** as well as ammonium 1-(2-chloroethyl)-5-nitriminotetrazolate have already been described and characterized in literature.^[4, 5]

4.1.2 Molecular Structures

After recrystallization from H₂O, single crystals of salts **3_K**, **3_Rb**, **3-Cs**, **3_Mg**, **3_Sr** and **3_Ba** suitable for X-ray diffraction could be obtained. Single crystals of **3_Cu** grew in half-concentrated HNO₃ (35 %). Suitable single crystals of **3_Cu_NH₃** were formed in the mother liquor. All relevant data and parameters of the X-ray measurements and refinements are given in Appendix III. The structures of **3_Na** and **3_Cu_H₂O** have been discussed in STIERSTORFER^[5] and KLAPÖTKE *et al.*^[4].

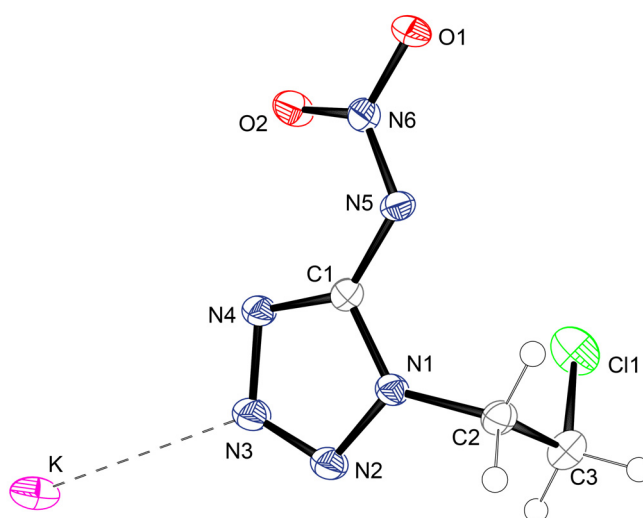


Figure 4.1 Molecular unit of **3_K**. Hydrogen atoms shown as spheres of arbitrary radius and thermal displacements set at 50 % probability. Selected geometries: distances (Å) N1–N2 1.352(2), N2–N3 1.297(2), N3–N4 1.371(2), N1–C1 1.353(2), N4–C1 1.333(2), C1–N5 1.378(2), N5–N6 1.320(2), O1–N6 1.258(2), O2–N6 1.249(2), N1–C2 1.459(2), K–N3 3.029(2); angles (°) N1–C1–N4 107.9(2), N1–C1–N5 116.9(2), O1–N6–N5 116.0(2), O1–N6–O2 120.1(2); torsion angles (°) N6–N5–C1–N1 168.7(2), C1–N5–N6–O1 –179.9(1).

Potassium 1-(2-chloroethyl)-5-nitriminotetrazolate (**3_K**) crystallizes in the monoclinic space group $P2_1/c$ with four formula units per unit cell (Figure 4.1). Its density of 1.868 g/cm³ is consistent with the one observed for the sodium salt **3_Na** (1.862 g/cm³^[4, 5]). The potassium atoms are coordinated eightfold by the atoms O1, O2, N3, N5, and N6 building no regular coordination polyhedron. Analog to the sodium salt, the coordination of O1 to two different potassium atoms leads to the formation of dimers.^[4, 5]

Since the C1–N1 distance of 1.378(2) Å resembles more to a N–C double bond (1.30 Å) than to a N–C single bond (1.47 Å^[7]), the nomenclature “nitriminotetrazole” is legitimated. The nitrimino group follows the planarity of the tetrazole ring (C1–N5–N6–O2 –1.0(2)°).

The packing of **3_K** is characterized by the anions forming stacks along the *c* axis. They are formed by bridging the potassium atoms.

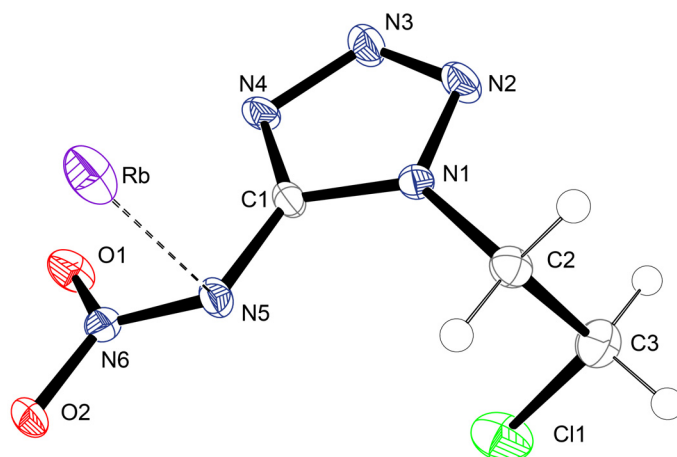


Figure 4.2 Molecular unit of **3_Rb**. Hydrogen atoms shown as spheres of arbitrary radius and thermal displacements set at 50 % probability. Selected geometries: distances (Å) N1–N2 1.351(3), N2–N3 1.298(4), N3–N4 1.375(4), N1–C1 1.349(4), N4–C1 1.332(4), C1–N5 1.382(4), N5–N6 1.320(4), O1–N6 1.256(3), O2–N6 1.255(3), N1–C2 1.458(4), Rb–N5 3.160(3), Rb–O1*i* 2.794(2), Rb–O1*ii* 2.893(2), Rb–O2*iii* 2.827(2); angles (°) N1–C1–N4 108.8(3), N1–C1–N5 116.5(3), O1–N6–N5 123.8(3), O1–N6–O2 120.7(3); torsion angles (°) N6–N5–C1–N1 –170.4(3), C1–N5–N6–O1 2.6(5); *i*) $-x+1, -y, -z+2$, *ii*) $-x+1, y-1/2, -z+5/2$; *iii*) $x, -y-1/2, z-1/2$.

Both, **3_Rb** and **3_Cs**, crystallize like **3_K** in the monoclinic space group $P2_1/c$ with four formula units per unit cell (Figure 4.2 and Figure 4.3). Their densities show higher values with 2.184 g/cm³ and 2.462 g/cm³, respectively.

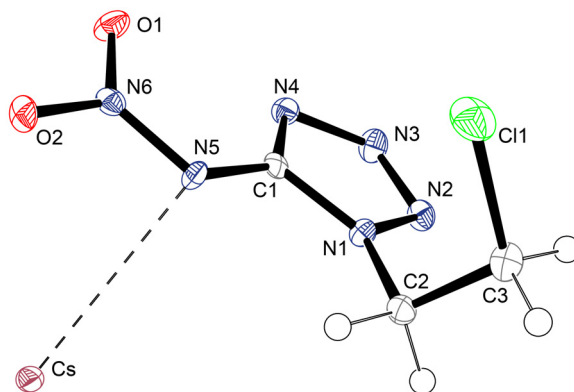


Figure 4.3 Molecular unit of **3_Cs**. Hydrogen atoms shown as spheres of arbitrary radius and thermal displacements set at 50 % probability. Selected geometries: distances (Å) N1–N2 1.354(3), N2–N3 1.301(3), N3–N4 1.370(3), N1–C1 1.354(3), N4–C1 1.335(4), C1–N5 1.371(3), N5–N6 1.320(3), O1–N6 1.253(3), O2–N6 1.259(3), N1–C2 1.455(4), Cs–N5 3.217(2), Cs–O1*i* 2.953(2), Cs–O1*ii* 3.0443(19), Cs–O2 3.417(2); angles (°) N1–C1–N4 108.5(2), N1–C1–N5 116.4(2), O1–N6–N5 123.6(2), O1–N6–O2 120.4(2); torsion angles (°) N6–N5–C1–N1 174.9(2), C1–N5–N6–O1 –4.4(4); *i*) $-x+1, -y, -z$, *ii*) $-x+1, y+1/2, -z-1/2$.

As expected, the bond lengths in the anion of **3_Na**, **3_K**, **3_Rb**, and **3_Cs** are comparable.^[4, 5]

The packing of **3_Rb** and **3_Cs** is analog to **3_K** with stacks along the *c* axis by bridging the cations. No hydrogen bonds could be observed in the structures of **3_K**, **3_Rb**, and **3_Cs**.

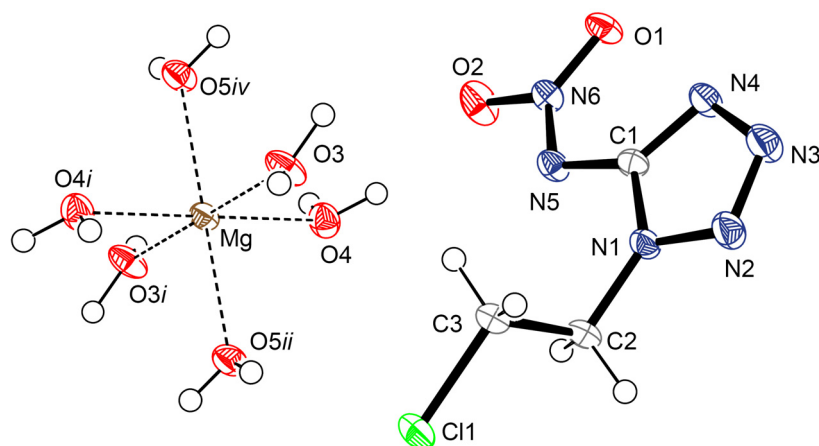


Figure 4.4 Molecular unit of **3_Mg**. For a better overview, only one 1-(2-chloroethyl)-5-nitriminotetrazole anion is shown. Hydrogen atoms shown as spheres of arbitrary radius and thermal displacements set at 50 % probability. Selected geometries: distances (Å) N1–N2 1.347(2), N2–N3 1.290(2), N3–N4 1.365(2), N5–N6 1.308(2), N4–C1 1.323(2), N1–C1 1.353(2), N5–C1 1.373(2), O1–N6 1.247(1), O2–N6 1.269(2), Mg–O3 2.056(1), Mg–O4 2.075(1), Mg–O5 ii 2.087(1), N1–C2 1.458(2), C2–C3 1.506(2), C1–C3 1.789(1); angles (°) N6–N5–C1 116.2(1), O1–N6–N5 125.4(1), O2–N6–O1 119.7(1), O3–Mg–O4 91.41(5), O3–Mg–O5 ii 91.04(5), O4–Mg–O5 ii 89.91(4); torsion angles (°) N6–N5–C1–N4 7.1(2), C1–N5–N6–O1 –2.1(2); i) $-x+3, -y+2, -z+1$, ii) $x, y, z-1$, iv) $-x+3, -y+2, -z+2$.

3_Mg crystallizes in the monoclinic space group $P-1$ with one molecular unit per unit cell (Figure 4.4). The calculated density is with 1.697 g/cm³ lower than the values of the water free alkali metal salts. In contrast to **3_Sr** and **3_Ba**, only the six water molecules coordinate the magnesium cation. This could also be observed in the molecular structures of magnesium 1-(2-hydroxyethyl)-5-nitriminotetrazolate octahydrate (**1_Mg**, chapter 2) and magnesium 1-(2-nitratoethyl)-5-nitriminotetrazolate hexahydrate (**2_Mg**, chapter 3).

The 1-(2-chloroethyl)-5-nitriminotetrazole anions are located without any significant interaction with the magnesium cation in the unit cell. However, several hydrogen bonds can be observed. In each case, the oxygen atoms of the water molecules serve as donor atoms. Acceptors are atoms of the tetrazolate derivative as the oxygen atoms O1 and O2, the nitrogen atoms N3 and N4, as well as the chlorine atom.

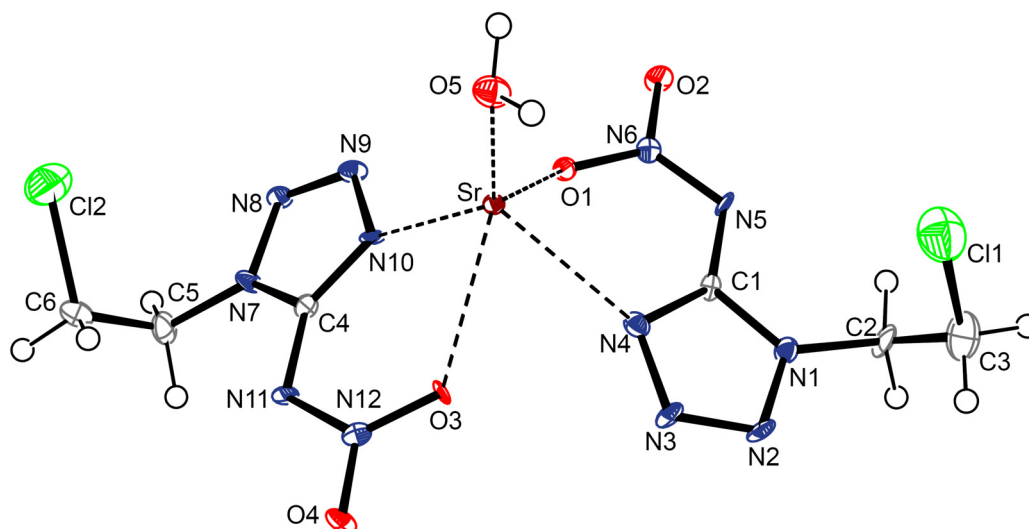


Figure 4.5 Molecular unit of **3_Sr**. Hydrogen atoms shown as spheres of arbitrary radius and thermal displacements set at 50 % probability. Selected geometries: distances (Å) N1–N2 1.346(7), N7–N8 1.357(6), N2–N3 1.295(7), N8–N9 1.304(7), N3–N4 1.367(7), N9–N10 1.358(7), N5–N6 1.311(7), N11–N12 1.314(7), N4–C1 1.323(8), N10–C4 1.321(8), N1–C1 1.344(8), N7–C4 1.355(7), N5–C1 1.381(7), N11–C4 1.376(7), O1–N6 1.279(6), O3–N12 1.281(6), O2–N6 1.251(6), O4–N12 1.253(6), Sr–N4 2.788(5), Sr–N10 2.728(5), Sr–O1 2.699(4), Sr–O3 2.684(4), Sr–O5 2.597(5), N1–C2 1.462(7), N7–C5 1.470(8), C2–C3 1.485(10), C5–C6 1.497(9), C11–C3 1.767(8), C12–C6 1.826(7); angles (°) N6–N5–C1 116.0(5), N12–N11–C4 115.7(5), O1–N6–N5 123.7(4), O3–N12–N11 124.2(5), O2–N6–O1 118.9(5), O4–N12–O3 118.7(5), N4–Sr–O1 67.5(1), N10–Sr–O3 67.0(1); torsion angles (°) N6–N5–C1–N4 –7.1(1), C1–N5–N6–O1 –0.2(8).

The strontium salt **3_Sr** crystallizes as monohydrate in the orthorhombic space group *Pbca*. The unit cell contains eight formula units (Figure 4.5). The calculated density is 2.033 g/cm³. The strontium cation is coordinated by the atoms O1, O2, O3, O4, N3, N4, N9, N10, and the oxygen atom of the crystal water (O5). The oxygen atoms O1 and O3 are each coordinated to two different strontium atoms. Three different hydrogen bonds can be observed. In each case, O5 is the donor atom (H⋯A (Å): H1a⋯N2 i 2.40(6), H1a⋯O2 ii 2.51(7), H1b⋯N5 ii 2.49(4); D⋯A (Å): O5⋯N2 i 3.233(7), O5⋯O2 ii 2.936(6), O5⋯N5 ii 3.250(7); angle DHA (°): O5H1aN2 i 173(8), O5H1aO2 ii 113(6), O5H1bN5 ii 151(8); i) $x+1/2$, $-y+1/2$, $-z+1$, ii) $x+1/2$, $-y+3/2$, $-z+1$). The nitrimino groups of both anions follow the planarity of the tetrazole ring with a twist angle of $\sim 0^\circ$ (C1–N5–N6–O1) and $\sim 1^\circ$ (C4–N11–N12–O3), respectively.

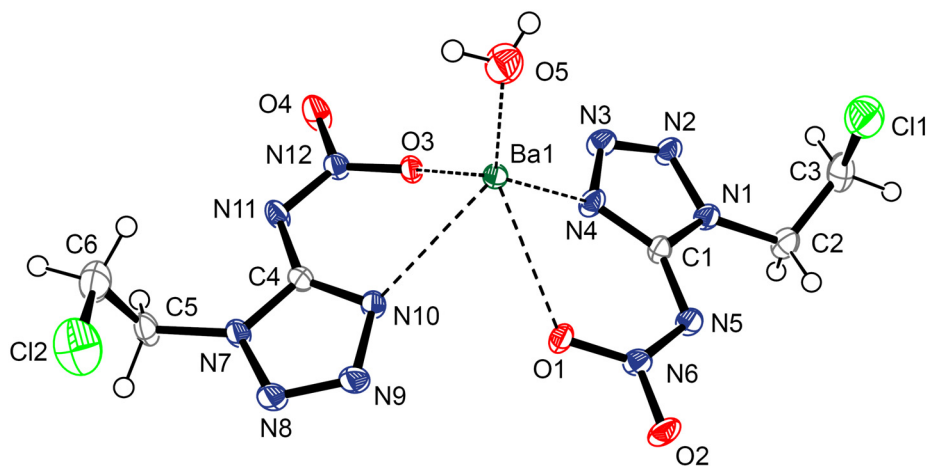


Figure 4.6 Molecular unit of **3_Ba**. Hydrogen atoms shown as spheres of arbitrary radius and thermal displacements set at 50 % probability. Selected geometries: distances (Å) N1–N2 1.353(5), N7–N8 1.348(5), N2–N3 1.287(5), N8–N9 1.292(5), N3–N4 1.369(5), N9–N10 1.373(5), N5–N6 1.296(5), N11–N12 1.306(5), N4–C1 1.331(5), N10–C4 1.320(5), N1–C1 1.350(5), N7–C4 1.349(5), N5–C1 1.381(5), N11–C4 1.382(5), O1–N6 1.273(4), O3–N12 1.266(4), O2–N6 1.268(4), O4–N12 1.258(4), Ba–N4 2.908(4), Ba–N10 2.944(3), Ba–O1 2.864(3), Ba–O3 2.841(3), Ba–O5 2.767(4), N1–C2 1.463(5), N7–C5 1.463(5), C2–C3 1.514(6), C5–C6 1.510(7), Cl1–C3 1.783(5), Cl2–C6 1.794(6); angles (°) N6–N5–C1 116.7(3), N12–N11–C4 116.2(3), O1–N6–N5 125.0(3), O3–N12–N11 124.8(3), O2–N6–O1 117.9(3), O4–N12–O3 118.5(3), N4–Ba–O1 129.68(9), N10–Ba–O3 128.13(8); torsion angles (°) N6–N5–C1–N4 8.9(7), C1–N5–N6–O1 –0.2(6).

As observed for strontium 1-methyl-5-nitriminotetrazolate monohydrate (**Sr1MeAtNO2**)^[5, 8], the packing of **3_Sr** is strongly influenced by the formation of stacks. The crystal water molecules affect no bridging and are coordinated alternatively up and down.

The barium salt **3_Ba** crystallizes in the monoclinic space group *P*-1, analog to **3_Mg**, with only two formula units per unit cell (Figure 4.6). The calculated density (2.180 g/cm³) of **3_Ba** is comparable to the one of **3_Sr**. The coordinating atoms of the barium atoms are analog to the one of the strontium atoms in **3_Sr**. Furthermore, the nitrimino group is not twisted out of the tetrazole ring plane. One hydrogen bond between O5 and O2_{*i*} (H⋯A (Å): H1b⋯O2_{*i*} 2.047; DHA (°): 166.98; D⋯A (Å): O5⋯O2_{*i*} 2.858; *i* x, y-1, z.) can be found. **3_Mg**, **3_Sr** and **3_Ba** show similar bond lengths and angles of their anions.

Also the packing of **3_Ba** is dominated by stacks, formed along the *a* axis with the crystal water molecules coordinated alternatively up and down.

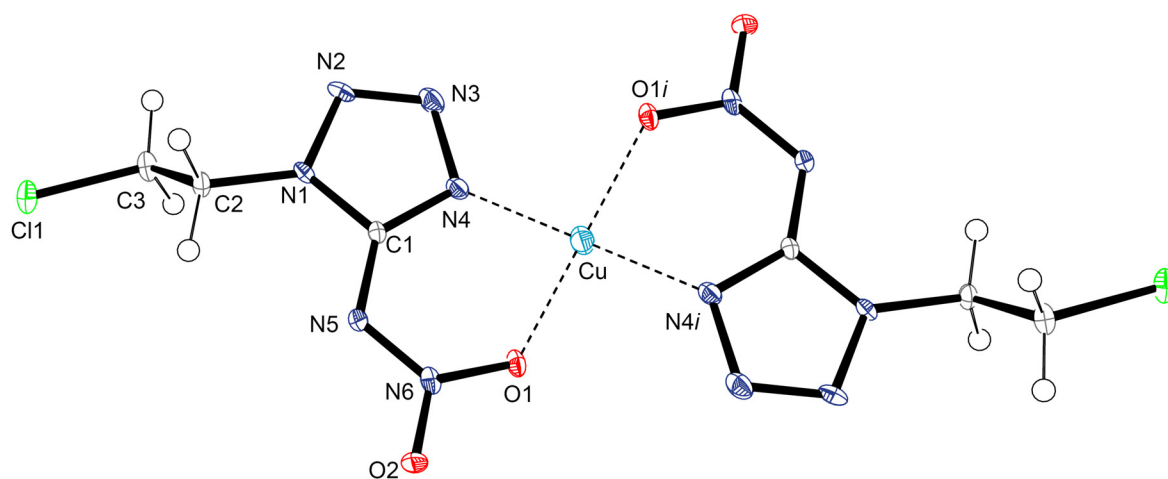


Figure 4.7 Molecular unit of **3_Cu**. Hydrogen atoms shown as spheres of arbitrary radius and thermal displacements set at 50 % probability. Selected geometries: distances (Å) N1–N2 1.362(4), N2–N3 1.280(5), N3–N4 1.381(5), N5–N6 1.308(5), N4–C1 1.329(5), N1–C1 1.347(5), N5–C1 1.362(5), O1–N6 1.293(4), O2–N6 1.245(4), Cu–N4 1.954(3), Cu–O1 1.954(3), N1–C2 1.463(5), C2–C3 1.515(5), Cl1–C3 1.785(4); angles (°) N6–N5–C1 117.1(3), O1–N6–N5 124.8(3), O2–N6–O1 117.9(3), N4–Cu–O1 84.81(13); torsion angles (°) N6–N5–C1–N4 –10.6(6), C1–N5–N6–O1 –3.4(5); i $-x, -y+1, -z$.

The copper salt **3_Cu** crystallizes analog to *trans*-[diaqua-bis{1-(2-chloroethyl)-5-nitriminotetrazolato- κ^2 N4,O5}copper(II)] dihydrate (**3_Cu_H₂O**) in the monoclinic space group $P2_1/c$ with two molecular units per unit cell.^[4, 5] As expected, the calculated density of **3_Cu** (2.107 g/cm) is higher than the one of **3_Cu_H₂O** (1.871 g/cm^[4, 5]). The copper(II) atoms are located on the center of inversion and the 1-(2-chloroethyl)-5-nitriminotetrazole anions act as bidentate ligands (Figure 4.7).

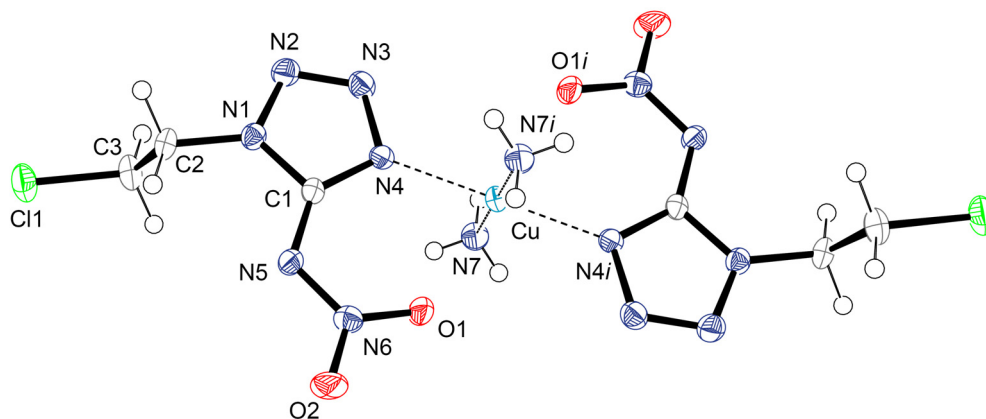


Figure 4.8 Molecular unit of **3_Cu_NH₃**. Hydrogen atoms shown as spheres of arbitrary radius and thermal displacements set at 50 % probability. Selected geometries: distances (Å) N1–N2 1.343(2), N2–N3 1.286(2), N3–N4 1.362(2), N5–N6 1.318(2), N4–C1 1.332(3), N1–C1 1.356(2), N5–C1 1.359(3), O1–N6 1.262(2), O2–N6 1.241(2), Cu–N4 2.011(2), Cu–O1 2.352(2), Cu–N7 2.005(2), N1–C2 1.456(2), C2–C3 1.509(3), Cl1–C3 1.788(2); angles (°) N6–N5–C1 117.3(2), O1–N6–N5 123.6(2), O2–N6–O1 118.8(2), N4–Cu–O1 76.04(6), N4–Cu–N7 88.81(9), N7–Cu–O1 90.05(8); torsion angles (°) N6–N5–C1–N4 –8.4(4), C1–N5–N6–O1 –2.4(3); i $-x+2, -y, -z+2$.

A JAHN-TELLER-distorted octahedral coordination of the copper cations is observed. Interestingly, the Cu–N4 and Cu–O1 distances are equal with 1.954 Å and the distance

between the copper cation and O2 of 2.602 Å is significantly longer. No hydrogen bonds could be observed.

Copper(II) complex **3_Cu_NH₃** also crystallizes in the space group $P2_1/c$ with two molecular units per unit cell (Figure 4.8). The calculated density of 1.878 g/cm³ is comparable with the one of **3_Cu_H₂O**. Analog to **3_Cu**, the copper(II) cations are located on the center of inversion and are coordinated by the 5-nitriminotetrazole anions and neutral ammonia ligands forming a JAHN-TELLER-distorted octahedron. The copper nitrogen distances are comparable in length (Cu–N4 2.011(2) Å and Cu–N7 2.005(2) Å), but the Cu–O1 distance is clearly longer with 2.352 (2) Å, which is in agreement of the coordination sphere in **3_Cu_H₂O**.

4.1.3 Energetic Properties

The energetic properties, such as decomposition temperature (T_{dec}), sensitivity to impact (E_{dir}), friction (F_r) and electric discharge (E_{el}), and combustion energy ($\Delta_c U$) were determined. Furthermore, the solubilities in H₂O at ambient temperature of the pyrotechnic relevant compounds were defined. The data of **3_Na** and **3_Cu_H₂O** were adopted from literature^[4, 5] to present a complete summary. An overview of the energetic properties of the alkali metal salts is given in Table 4.1. Table 4.2 and Table 4.3 contain the properties of the alkaline earth metal salts and copper compounds, respectively.

Table 4.1 Overview of the physico-chemical properties of **3_Li**, **3_Na**, **3_K**, **3_Rb**, and **3-Cs**.

	3_Li	3_Na	3_K	3_Rb	3-Cs
Formula	C ₃ H ₄ ClLiN ₆ O ₂	C ₃ H ₄ ClN ₆ NaO ₂	C ₃ H ₄ ClKN ₆ O ₂	C ₃ H ₄ ClN ₆ O ₂ Rb	C ₃ H ₄ ClCsN ₆ O ₂
M [g/mol]	198.50	214.55	230.65	277.02	324.46
E_{dir} [J]^a	17	2.0	5.0	5.0	10
F_r [N]^b	240	> 360	> 360	160	160
E_{el} [J]^c	0.50	0.50	1.0	0.50	0.50
grain size [µm]	100–250	< 100	100–250	250–500	100–500
N [%]^d	42.34	39.17	36.44	30.34	25.90
Ω [%]^e	-24	-56	-52	-43	-37
T_{dec} [°C]^f	185	187	196	184	161
ρ [g/cm³]^g	1.50* (22 °C)	1.86	1.87	2.18	2.46
Δ_cU [kJ/kg]^h	-10404	-9855	-7863	-7758	-6176
Δ_cH^o [kJ/mol]ⁱ	-2055	-2106	-1806	-2140	-1994
Δ_fH^o [kJ/mol]^j	-246	-109	-466	11	-111

a) BAM drop hammer ^[9], b) BAM methods ^[9], c) Electric discharge tester, d) Nitrogen content, e) Oxygen balance, f) Decomposition temperature from DSC ($\beta = 5$ K/min), g) determined by X-ray crystallography or pycnometer (*), h) Combustion energy, i) Enthalpy of combustion, j) Molar enthalpy of formation, k) Solubility in H₂O (H₂O temperature).

Table 4.2 Overview of the physico-chemical properties of **3_Mg**, **3_Ca**, **3_Sr**, and **3_Ba**.

	3_Mg	3_Ca	3_Sr	3_Ba
Formula	Mg(C ₃ H ₄ ClN ₆ O ₂) ₂ · 6H ₂ O	Ca(C ₃ H ₄ ClN ₆ O ₂) ₂ · H ₂ O	Sr(C ₃ H ₄ ClN ₆ O ₂) ₂ · H ₂ O	Ba(C ₃ H ₄ ClN ₆ O ₂) ₂ · H ₂ O
M [g/mol]	515.51	441.21	488.78	538.50
E_{dr} [J]^a	25	8.0	10	3.0
F_r [N]^b	240	> 360	> 360	144
E_{el} [J]^c	0.15	0.80	0.75	1.0
grain size [μm]	100–500	160–250	160–250	250–500
N [%]^d	32.60	38.10	34.4	31.2
Ω [%]^e	-37	-44	-39	-36
T_{dec} [°C]^f	226	188	208	207
ρ [g/cm³]^g	1.70	1.68* (22°C)	2.03	2.18
Δ_cU [kJ/kg]^h	-8421	-9345	-7030	-6330
Δ_cH^o [kJ/mol]ⁱ	-4321	-4163	-3416	-3389
Δ_fH^o [kJ/mol]^j	-2287	-857	-743	-846
H₂O sol. [wt%]^k	n.d.**	n.d.**	14 (21 °C)	0.8 (21 °C)

a) BAM drop hammer ^[9], b) BAM methods ^[9], c) Electric discharge tester, d) Nitrogen content, e) Oxygen balance, f) Decomposition temperature from DSC ($\beta = 5$ K/min), g) determined by X-ray crystallography or pycnometer (*), h) Combustion energy, i) Enthalpy of combustion, j) Molar enthalpy of formation, k) Solubility in H₂O (H₂O temperature), **) n.d. = not determined.

Table 4.3 Overview of the physico-chemical properties of the copper compounds of **3**.

	3_Cu_H₂O	3_Cu	3_Cu_NH₃
Formula	C ₆ H ₁₆ Cl ₂ CuN ₁₂ O ₈	C ₆ H ₈ Cl ₂ CuN ₁₂ O ₄	C ₆ H ₁₄ Cl ₂ CuN ₁₄ O ₄
M [g/mol]	518.72	446.68	480.75
E_{dr} [J]^a	> 50	6.0	6.0
F_r [N]^b	> 360	192	> 360
E_{el} [J]^c	0.60	0.50	0.50
grain size [μm]	< 100	< 100	250–500
N [%]^d	32.4	37.6	40.8
Ω [%]^e	-37	-43	-53
T_{dec} [°C]^f	242	238	205
ρ [g/cm³]^g	1.87	2.11	1.89
Δ_cU [kJ/kg]^h	-7042	-8797	-10238
Δ_cH^o [kJ/mol]ⁱ	-3633	-3908	-4893
Δ_fH^o [kJ/mol]^j	-1068	346	474
H₂O sol. [wt%]^k	0.9 (23 °C)	0.7 (23 °C)	0.4 (23 °C)

a) BAM drop hammer ^[9], b) BAM methods ^[9], c) Electric discharge tester, d) Nitrogen content, e) Oxygen balance, f) Decomposition temperature from DSC ($\beta = 5$ K/min), g) determined by X-ray crystallography or pycnometer (*), h) Combustion energy, i) Enthalpy of combustion, j) Molar enthalpy of formation, k) Solubility in H₂O (H₂O temperature).

The thermal behavior of ca. 2 mg of the compounds **3_Li**, **3_Na**, **3_K**, **3_Rb**, **3-Cs**, **3_Mg**, **3_Ca**, **3_Sr**, **3_Ba**, **3_Cu_H₂O**, **3_Cu**, and **3_Cu_NH₃** was determined *via* differential scanning calorimetry (DSC) in the temperature range from 50 °C to 400 °C. All compounds offer high decomposition temperatures above 180 °C, besides **3-Cs** ($T_{dec} = 161$ °C). The other alkali metal salts decompose at between 184–196 °C. The copper(II) compounds **3_Cu_H₂O** and **3_Cu** offer the highest decomposition temperatures of 242 °C and 238 °C, respectively. Due to the high decomposition temperature of **3_Cu_H₂O** and its loss of H₂O at 103 °C, it was possible to obtain **3_Cu** by removing the chemically bound water of **3_Cu_H₂O**. In the case of copper(II) complex **3_Cu_NH₃** no loss of ammonia could be observed in its DSC thermogram. Loss of crystal water could also be observed in the case of **3_Mg** in a temperature range of 110–160 °C, but its decomposition point ($T_{dec} = 226$ °C) is the highest

one of the alkaline earth metal salts of **3** (**3_Ca**: $T_{\text{dec}} = 188\text{ }^{\circ}\text{C}$, **3_Sr**: $T_{\text{dec}} = 208\text{ }^{\circ}\text{C}$ and **3_Ba**: $T_{\text{dec}} = 207\text{ }^{\circ}\text{C}$).

All investigated compounds of **3** are sensitive to impact according to literature,^[9] except **3_Cu_H2O**. Salt **3_Mg** shows the lowest sensitivity (25 J), but is the most sensitive compound to electric discharge (0.15 J). The sodium salt **3_Na** and barium salt **3_Ba** are very sensitive to impact with 2.0 J and 3.0 J, respectively. The copper(II) complexes **3_Cu_H2O** and **3_Cu_NH3** are insensitive to friction. **3_Cu_H2O** is also insensitive towards shock, whereas **3_Cu_NH3** offers an impact sensitivity of 6.0 J and the water free compound **3_Cu** is sensitive to both stimuli (E_{dr} : 6 J, F_{r} : 192 N). This is a hint that the inclusion of crystal water decreases the sensitivity to impact and friction (see chapter 2).

All determined values for sensitivity to electric discharge, except the one of **3_Mg**, are in the range of 0.5–1.0 J.

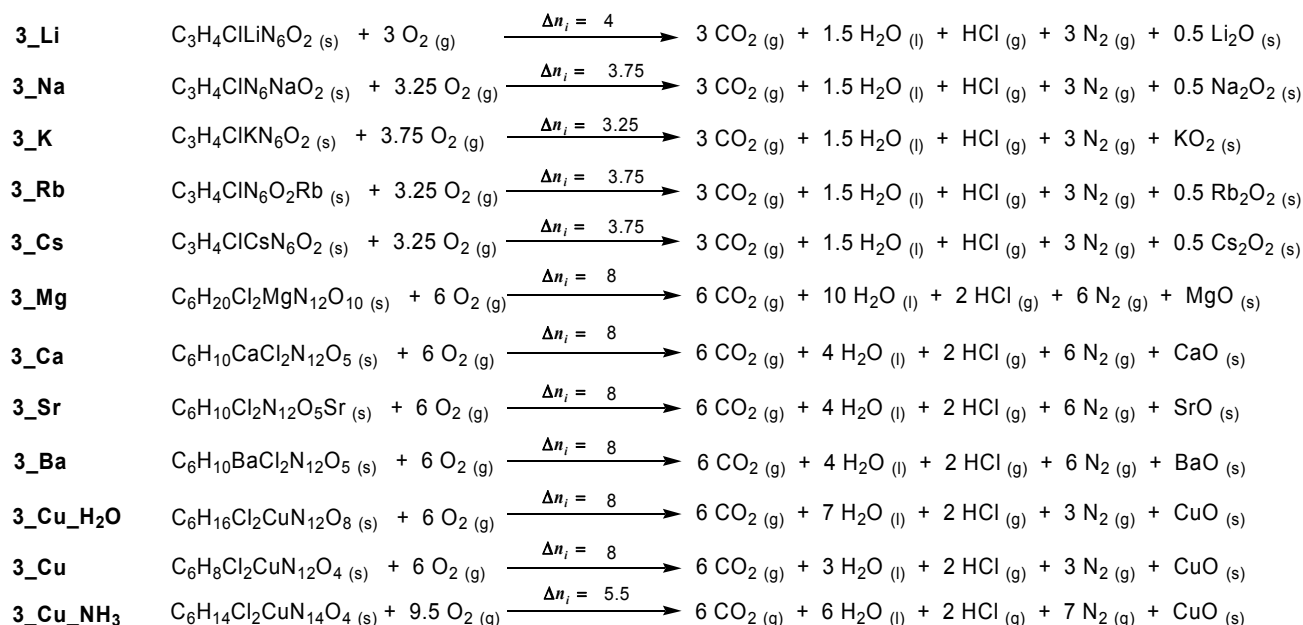
The reported values of the combustion energy ($\Delta_c U$) are the average of three single bomb calorimetry measurements. The standard molar enthalpy of combustion ($\Delta_c H^\circ$) was derived from equation 4.1.

$$\Delta_c H^\circ = \Delta_c U + \Delta nRT \quad (4.1)$$

$$\Delta n = \sum n_i (\text{gaseous products}) - \sum n_i (\text{gaseous educts})$$

n_i = molar amount of gas i .

The enthalpy of formation ($\Delta_f H^\circ$) for each compound prepared of **3** was calculated at 298.15 K using the HESS thermochemical cycle and the following combustion reactions (Scheme 4.6).



Scheme 4.6 Combustion equations.

The heats of formation of the combustion products $\text{H}_2\text{O}_{(l)}$ (-286 kJ/mol), $\text{CO}_2_{(g)}$ (-393 kJ/mol), $\text{HCl}_{(g)}$ (-92.3 kJ/mol), $\text{Li}_2\text{O}_{(s)}$ (-599 kJ/mol), $\text{Na}_2\text{O}_2_{(s)}$ (-513 kJ/mol), $\text{KO}_2_{(s)}$ (-284.5 kJ/mol), $\text{Rb}_2\text{O}_2_{(s)}$ (-426 kJ/mol), $\text{Cs}_2\text{O}_2_{(s)}$ (-403 kJ/mol), $\text{MgO}_{(s)}$ (-601.2 kJ/mol), $\text{CaO}_{(s)}$ (-635 kJ/mol), $\text{SrO}_{(s)}$ (-592 kJ/mol), $\text{BaO}_{(s)}$ (-548 kJ/mol), and $\text{CuO}_{(s)}$ (-157 kJ/mol) were adopted from literature.^[7, 10]

Except for **3_Rb**, **3_Cu** and **3_Cu_NH₃**, all compounds were calculated to be formed exothermically. Salt **3_Mg** shows the highest negative value for the heat of formation (-22878 kJ/mol¹). This might be due to the six crystal water molecules. In contrast to that, the copper compounds **3_Cu** and **3_Cu_NH₃** offer the highest positive heats of formation.

For determining the solubility, each compound was added to 1 mL H_2O with before noted temperature until the solution was saturated. The solubilities are given in percent by weight (wt%) and were calculated according to equation 4.2.

$$\text{H}_2\text{O-sol.} = \frac{m_{\text{dissolved Compound}}}{m_{\text{dissolved Compound}} + m_{\text{Solvent}}} \cdot 100 \quad (4.2)$$

The strontium salt **3_Sr** offers the highest solubility with 14 wt%. All other compounds, **3_Ba**, **3_Cu_H₂O**, **3_Cu**, **3_Cu_NH₃**, are almost insoluble in H_2O at ambient temperature with solubilities less than 1.0 wt%.

4.1.4 Flame Color and Combustion Behavior

Only the pyrotechnic relevant salts – **3_Sr**, **3_Ba**, **3_Cu_H₂O**, **3_Cu**, **3_Cu_NH₃** – were tested regarding to their flame color. All show the expected flame color – with regard to their corresponding cations – in the flame of a BUNSEN burner (Figure 4.9). Furthermore, their combustion occurs without smoke production. The strontium salt **3_Sr** combusts with a very intense red flame, significantly more intense than the other nitrogen-rich salts strontium 5-nitriminotetrazolate dihydrate, strontium (5-nitrimino-1*H*-tetrazolate) tetrahydrate, strontium (1-methyl-5-nitriminotetrazolate) monohydrate and strontium (2-methyl-5-nitriminotetrazolate) (see chapter 9).^[5, 8] A very intense green flame is shown by **3_Ba**, also significantly more intense than other barium salts like barium tetrazolate, barium 5-aminotetrazolate tetrahydrate, barium 5-nitriminotetrazolate dihydrate, barium bis(5-nitrimino-1*H*-tetrazolate) tetrahydrate, barium 1-methyl-5-nitriminotetrazolate monohydrate, or barium 2-methyl-5-nitriminotetrazolate dihydrate (chapter 8).^[11]

Since the copper salts contain chlorine, **3_Cu_H₂O** combusts with a bright blue flame and the water free **3_Cu** deflagrates fast (but subsonic) with the formation of a bright blue flame. The ammine complex **3_Cu_NH₃** shows an analog combustion behavior to **3_Cu_H₂O**. All salts feature no solid residues after their combustion.



Figure 4.9 Color performances of **3_Sr** (top, left), **3_Ba** (top, right), **3_Cu_H₂O** (down, left), **3_Cu** (down, middle), **3_Cu_NH₃** (down, right) in the flame of a BUNSEN burner.

Furthermore, the combustion behavior of the strontium salt **3_Sr** – analog to strontium tetrazolate pentahydrate (**SrTz**), strontium 1-methyl-5-nitriminotetrazolate monohydrate (**Sr1MeAtNO₂**), and strontium 3,3'-bis(1,2,4-oxadiazol-5-onate) dihydrate (**SrOD**) (see chapter 8) – was qualitatively characterized with a simple smoke test method. Therefore, approx. 1 g sample of **3_Sr** was placed and heated in a crucible with a gas torch for observation of color, smoke, burn ability (propagation), and level of residue. It verified the in BUNSEN burner observed red flame color and did not need a constant torch. Only smoke, but no residues were observed.

4.1.5 Pyrotechnic Compositions

The compounds **3_Sr**, **3_Ba** and **3_Cu_H₂O** were chosen as coloring agents for pyrotechnic compositions. They offer the possibility of the formation of SrCl, BaCl, and CuCl, respectively – their corresponding light emitting species in the gas phase – without additional chlorine donors. All other cations used do not need any chlorine for a more intense flame color. No composition was prepared with **3_Cu** and **3_Cu_NH₃**, because of their higher sensitivity and the fast deflagration of **3_Cu**. Furthermore, **3_Cu_NH₃** shows the lowest decomposition temperature. In Table 4.4 the results of the two best formulations of each salt are listed. All mentioned compositions were prepared by hand. The performance of each composition has been evaluated with respect to the following categories:

- color emission (subjective impression)
- smoke generation
- morphology and amount of solid residues
- thermal stability
- moisture sensitivity

The US Army red flare composition # M126 A1 (red parachute) – 39 wt% Sr(NO₃)₂, 30 wt% Mg, 13 wt% KClO₄, 8 wt% VAAR – was used as a measure of the red light compositions' performance (Figure 4.10). Its decomposition point was determined at 360 °C by DSC-measurement ($\beta = 5$ K/ min). Composition M126 A1 is sensitive to impact with 10 J, to friction with 144 N, and to electric discharge with 0.75 J.

The performance of the compositions for green light were compared to the barium nitrate-based US Army composition # M125 A1 (green parachute): 50 wt% Ba(NO₃)₂, 30 wt% Mg, 15 wt% PVC, 5 wt% VAAR (Figure 4.12). Its decomposition point is 244 °C. It is sensitive to impact (9.0 J), friction (288 N), and electric discharge (1.2 J).

The blue light emitting compositions were compared to SHIMIZU's composition [12]: 15 wt% Cu, 17 wt% PVC, 68 wt% KClO₄, and 5 wt% Starch (Figure 4.13). Its sensitivities are 8.5 J (impact), 324 N (friction), and 1.0 J (electric discharge). SHIMIZU's composition decomposes at temperatures above 307 °C.

All mentioned compositions were prepared by hand. Details can be found in chapter 4.2.2.

Table 4.4 General summary of the pyrotechnic compositions' performances.

Pyrotechnic composition	Color emission	Smokeless combustion	Amount of solid residues	Thermal stability	Moisture stability	Environmental compatibility
3_Sr_8.3	+++	++	++	--	-	+++
3_Sr_2.1	+	+	+	--	-	+++
M126 A1	++	---	++	+++	+++	--
3_Ba_4.2	++	++	++	-	-	-
3_Ba_3.2	+++	+	++	--	-	-
M125 A1	++	---	++	+++	+++	---
3_Cu_H₂O_5.4	++	+	+	--	+	++
3_Cu_H₂O_6.3	+	++	-	-	++	++
SHIMIZU	+++	-	++	+++	+++	---

The strontium salt **3_Sr** was combined with the oxidizers potassium permanganate, potassium nitrate, ammonium nitrate, ammonium dinitramide (ADN) and the fuels magnesium, magalium, and **5-At** (Table 4.6–Table 4.13). Compositions containing potassium permanganate or nitrate could not be ignited or showed a yellow or violet flame. Mixtures with ammonium nitrate and ADN offered good coloring and burning properties. The composition **3_Sr_8.3** consists of 11 wt% **3_Sr**, 44 wt% ADN 34 wt% **5-At** and 11 wt% VAAR (Table 4.13). The observed red flame color is significantly more intense than the one of M126 A1. Furthermore, the combustion occurs very fast and smokeless. The composition shows high sensitivities to impact (4.5 J), friction (54 N), and electric discharge (0.75 J). It has a lack of thermal stability ($T_{dec} = 167$ °C) and is slightly sensitive towards moisture, but its coloring properties are very good. The mixture **3_Sr_2.1** contains 14% **3_Sr**, 68 wt% NH₄NO₃, 7 wt% Mg and 11 wt% VAAR (Table 4.7). The observed flame is intense red, but

smaller compared to M126 A1. The combustion velocity is significantly slower than the one of **3_Sr_8.3**. Almost no smoke is produced, but some magnesium sparks could be observed. A very small amount of solid residues was obtained. The decomposition temperature is comparable to **3_Sr_8.3** ($T_{dec} = 165\text{ °C}$), but **3_Sr_2.1** is less sensitive to impact (6 J), friction (240 N) and electric discharge (1.2 J). Furthermore, it is more stable towards moisture. Figure 4.10 shows the burn downs of all red burning compositions.



Figure 4.10 Burn downs of the US Army composition # M126 A1 (top), the compositions **3_Sr_8.3** (left) and **3_Sr_2.1** (right).

Besides the mentioned compositions, **3_Sr** was formulated with magnesium powder, polyvinyl chloride, and polyester/styrene binder, leaving the weight ratio equal to M126 A1 [13]. The dry ingredients were sieved through 10-mesh screen and dried prior to mixing in a ceramic bowl. The final dry mixes were pressed to 1.27 cm pellets, each with approx. 6 g. The pellets were consolidated in a die with two increments at a loading pressure of 6000 psi (41.3 MPa). The current M126 A1 igniter slurry (aluminum, silicon, charcoal, potassium nitrate, iron oxide, and nitrocellulose) was applied on top of pellets as first fire.

Static burn tests on the experimental pellets were conducted in a blackened light tunnel. The samples were placed 50 ft (15.24 m) from the measurement equipment and initiated with an electric match. Color was measured with an *Ocean Optics* HR2000 spectrometer after calibration. Color measurements were based on the 1931 CIE (*Commission Internationale d'Eclairage*) international standard and calculated using the *Ocean Optics* Spectra-suite software. The CIE chart displays all the chromaticities average human eyes can observe. The three values calculated based on the CIE color matching functions are referred to X, Y and Z. The dominant wavelength (DW) and excitation purity (%) for a test sample were numerically determined with respect to the coordinates of Illuminant C, an

established light source. The luminous intensity was measured using an *International Light SELO33* silicon detector coupled to a photopic filter and lens hood. The representative still images captured from the static burn test are illustrated below (Figure 4.11). Result suggests there is no significant difference among the sample groups in flame size based on visual observation.

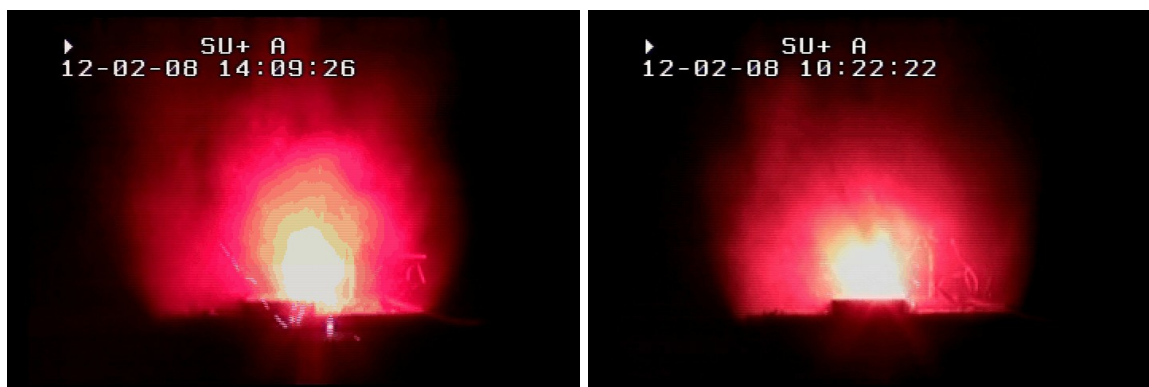


Figure 4.11 Static burn test of **3_Sr** (left) and control (right).

Static burn test results for **3_Sr** formulated pellets as well as the perchlorate-based control pellets ^[14] are shown in Table 4.5.

Table 4.5 Experimental pellets performance data.

Compound	3_Sr	Control
burn time [s]	11.7	11.8
average intensity [cd]	1562	1570
integrated intensity [cd·s]	17 523	19 749
dominant wavelength [nm]	615	610
spectral purity [%]	96	11.8

Samples containing **3_Sr** burned with a bright, intense red flame and their respective color purity exceeded the control value. Some broken pellets were obtained, suggesting a higher consolidation force is required. The pellets of **3_Sr** burned most comparable to the control, followed by compound **SrTz** and then compound **Sr1MeAtNO2**.

The barium salt **3_Ba** was mixed with the fuels magnesium, magnalium, **5-At** or aluminum and the oxidizers potassium nitrate, ammonium nitrate or ADN (Table 4.14–Table 4.19). In the case of using potassium nitrate as oxidizer, the compositions could not be ignited or burned with a white flame. This is true, if ammonium nitrate and **5-At** were added. The pyrotechnic composition **3_Ba_4.2** consists of 25 wt% **3_Ba**, 45 wt% ADN, 10 wt% **5-At** and 20 wt% VAAR (Table 4.16). It combusts with a very intense green flame (more intense than M125 A1) and without smoke production. The reaction velocity is comparable to M125 A1. The sensitivities to impact (2.0 J), friction (160 N), and electric discharge

(0.65 J) are very high, but similar to **3_Ba_4.2**. Moreover, the decomposition occurs below 180 °C ($T_{\text{dec}} = 175^{\circ}\text{C}$) and the mixture is slightly sensitive to moisture. Composition **3_Ba_3.2** is made of 20 wt% **3_Ba**, 60 wt% NH_4NO_3 , 4 wt% **5-At**, 7 wt% magnalium, and 9 wt% VAAR (Table 4.17). Its flame color is comparably intense to **3_Ba_4.2**, but the combustion occurs more slowly. As in the case of **3_Sr_2.1**, some magnalium sparks and no smoke production could be observed. The combustion occurred completely without solid residues. **3_Ba_3.2** shows the lowest decomposition temperature with 154 °C. It is very sensitive to impact (4.5 J) and electric discharge (1.0 J), but insensitive towards friction (> 360 N). A comparison of the combustion behavior of the green burning mixtures can be found in Figure 4.12.



Figure 4.12 Burn down of the US Army composition # M125 A1 (top), the compositions **3_Ba_4.2** (left) and **3_Ba_3.2** (right).

3_CuH2O was only combined with the oxidizers ammonium nitrate or dinitramide (ADN). As fuels were chosen copper(I) oxide, boron, and starch due to their lower combustion temperature. This guarantees temperatures below 1200 °C at which the blue light emitting species CuCl is stable.^[2] For the preparation of composition **3_CuH2O_5.4**, the copper compound **3_CuH2O** was used (43 wt% **3_CuH2O**, 43 wt% ADN, 4 wt% starch and 10 wt% VAAR, Table 4.24). The observed flame color is comparably intense to SHIMIZU's composition (Figure 4.13). This is true for the combustion velocity. Smoke could be detected during combustion but less than during the burn down of SHIMIZU's composition and a small amount of solid residues was obtained. The composition **3_CuH2O_5.4** decomposes at temperatures above 150 °C and is very sensitive to impact (< 1.0 J) and friction (108 N). A marginal sensitivity to moisture exists. The pyrotechnic composition **3_CuH2O_6.3** (24 wt% **3_CuH2O**, 12 wt% ADN, 43 wt% NH_4NO_3 , 4 wt% boron and 17 wt% VAAR, Table 4.25) shows a less brilliant blue flame color compared to SHIMIZU's composition. However, its combustion

occurs smokeless and with a marginal amount of solid residues. The combustion velocity is lower than the one of **3_CuH2O_5.4**. Composition **3_CuH2O_6.3** is not sensitive to moisture. Its decomposition point is at 159 °C. The sensitivities to impact and friction were determined to be 2.5 J and 192 N.



Figure 4.13 Burn down of the SHIMIZU's composition (top), the compositions **3_CuH2O_5.4** (left) and **3_CuH2O_6.3** (right).

4.2 Experimental Part

*CAUTION! The prepared compounds or their pyrotechnic compositions are sensitive to impact, friction, and electric discharge. Therefore, proper protective measures (safety glasses, face shield, leather coat, earthed equipment and shoes, Kevlar® gloves, and ear plugs) should be used, also during work on the precursor molecule 1-(2-chloroethyl)-5-nitriminotetrazole (**3**).*

4.2.1 Preparation of the Salts

4.2.1.1 Lithium 1-(2-Chloroethyl)-5-nitriminotetrazolate (**3_Li**)

A solution of 1.31 g (6.8 mmol) 1-(2-chloroethyl)-5-nitriminotetrazole (**3**) and 0.50 g (6.8 mmol) lithium carbonate in 15 mL H₂O was refluxed for 10 minutes. The solvent was removed under high vacuum to obtain 1.26 g of a colorless powder. Yield: 91 %.

M.p. 185 °C (dec., DSC-measurement, 5 K/min).

Raman (200 mW, 25 °C, cm⁻¹): 3018 (5), 2972 (30), 1506 (100), 1431 (7), 1387 (7), 1349 (23), 1295 (8), 1246 (3), 1124 (14), 1113 (10), 1090 (3), 1038 (36), 1012 (5), 878 (4), 756 (7), 679 (6), 657 (12), 480 (3), 367 (6), 302 (6), 213 (5).

IR (Diamond-ATR, cm^{-1}): 3575 (vw), 3320 (w, br), 3020 (vw), 2970 (vw), 2360 (w), 2336 (w), 1636 (vw), 1582 (w), 1509 (m), 1459 (w), 1377 (m), 1343 (s), 1314 (s), 1242 (s), 1121 (w), 1034 (m), 984 (vw), 956 (vw), 910 (vw), 878 (w), 832 (w), 770 (m), 740 (m), 708 (s), 680 (m).

^1H NMR (DMSO- d_6): 4.35 (t, 2H, $^3J=5.9$ Hz, CH_2Cl), 3.94 (t, 2H, $^3J=5.9$ Hz, NCH_2).

^{13}C NMR (DMSO- d_6): 157.1 (CN_4), 47.3 (NCH_2), 41.6 (CH_2Cl).

Elemental analysis $\text{C}_3\text{H}_4\text{ClLiN}_6\text{O}_2$ (198.50 g/mol): calc.: C, 18.15; H, 2.03; N, 42.34; found: C, 18.43; H, 2.06; N, 42.16.

$$E_{\text{dr}} = 17 \text{ J} \quad (100\text{--}250 \mu\text{m}).$$

$$F_{\text{r}} = 240 \text{ N} \quad (100\text{--}250 \mu\text{m}).$$

$$E_{\text{el}} = 0.50 \text{ J} \quad (100\text{--}250 \mu\text{m}).$$

$$\Delta_c U = -2485 \text{ cal/g}.$$

4.2.1.2 Sodium 1-(2-Chloroethyl)-5-nitriminotetrazolate (**3_Na**)

A solution of 1.31 g (6.8 mmol) 1-(2-chloroethyl)-5-nitriminotetrazole (**3**) and 0.27 g (6.8 mmol) sodium hydroxide in 10 mL H_2O was refluxed for 10 minutes. The solvent was removed under high vacuum to obtain a colorless powder. Yield: 97 %.

M.p. 187 °C (dec., DSC-measurement, 5 K/min).

Raman (200 mW, 25 °C, cm^{-1}): 3015 (5), 2977 (7), 2984 (5), 1550 (3), 1498 (100), 1462 (5), 1433 (7), 1377 (8), 1347 (15), 1323 (8), 1298 (8), 1264 (3), 1134 (2), 1108 (10), 1037 (38), 992 (2), 875 (4), 759 (9), 678 (4), 653 (9), 510 (3), 443 (2), 370 (4), 307 (6), 246 (8), 208 (6).

IR (Diamond-ATR, cm^{-1}): 3518 (m, br), 3019 (m), 2972 (m), 2375 (w), 1646 (w), 1578 (m), 1500 (s), 1463 (m), 1457 (m), 1443 (m), 1390 (s), 1336 (s, br), 1287 (s), 1255 (s), 1237 (s), 1180 (m), 1130 (w), 1105 (m), 1033 (m), 953 (w), 910 (w), 873 (w), 774 (w), 758 (w), 739 (w), 718 (vw), 676 (w), 655 (w).

^1H NMR (DMSO- d_6): 4.37 (t, 2H, $^3J=5.8$ Hz, CH_2Cl), 3.95 (t, 2H, $^3J=5.8$ Hz, NCH_2).

^{13}C NMR (DMSO- d_6): 157.2 (CN_4), 47.3 (NCH_2), 41.7 (CH_2Cl).

Elemental analysis $\text{C}_3\text{H}_4\text{ClNaN}_6\text{O}_2$ (214.55 g/mol): calc.: C, 16.79; H, 1.88; N, 39.17; found: C, 16.81; H, 1.77; N, 38.99.

$$E_{\text{dr}} = 2.0 \text{ J} \quad (< 100 \mu\text{m}).$$

$$F_{\text{r}} > 360 \text{ N} \quad (< 100 \mu\text{m}).$$

$$E_{\text{el}} = 0.50 \text{ J} \quad (< 100 \mu\text{m}).$$

$$\Delta_c U = -2354 \text{ cal/g}.$$

4.2.1.3 Potassium 1-(2-Chloroethyl)-5-nitriminotetrazolate (**3_K**)

A solution of 1.31 g (6.8 mmol) 1-(2-chloroethyl)-5-nitriminotetrazole (**3**) and 0.38 g (6.8 mmol) potassium hydroxide in 10 mL H_2O was refluxed for 10 minutes. The solvent was

removed under high vacuum. Recrystallization from H₂O yielded colorless blocks suitable for X-ray diffraction. Yield: 98 %.

M.p. 196 °C (dec., DSC-measurement, 5 K/min).

Raman (200 mW, 25 °C, cm⁻¹): 3030 (4), 3017 (12), 2973 (30), 1549 (2), 1498 (100), 1456 (6), 1431 (4), 1409 (2), 1383 (9), 1329 (23), 1316 (17), 1294 (3), 1253 (3), 1206 (2), 1134 (2), 1105 (9), 1040 (42), 992 (3), 954 (2), 911 (2), 875 (2), 758 (11), 673 (4), 653 (16), 518 (3), 479 (3), 428 (5), 369 (4), 302 (7), 245 (5), 205 (3).

IR (Diamond-ATR, cm⁻¹): 3029 (w), 3017 (w), 2971 (w), 1647 (vw), 1498 (m), 1460 (w), 1448 (m), 1440 (m), 1388 (m), 1337 (s), 1290 (m), 1237 (m), 1252 (w), 1206 (w), 1130 (vw), 1103 (m), 1042 (w), 991(vw), 953 (vw), 909 (vw), 875 (vw), 774 (w), 756 (vw), 736 (vw), 704 (vw), 672 (vw), 652 (m).

¹H NMR (DMSO-*d*₆): 4.39 (*t*, 2H, ³*J* = 5.9 Hz, CH₂Cl), 3.97 (*t*, 2H, ³*J* = 5.9 Hz, NCH₂).

¹³C NMR (DMSO-*d*₆): 157.7 (CN₄), 47.8 (NCH₂), 42.2 (CH₂Cl).

Elemental analysis C₃H₄ClKN₆O₂ (230.65 g/mol): calc.: C, 15.62; H, 1.75; N, 36.44; found: C, 15.64; H, 1.84; N, 36.56.

$$E_{\text{dr}} = 5.0 \text{ J} \quad (100\text{--}250 \text{ }\mu\text{m}).$$

$$F_{\text{r}} > 360 \text{ N} \quad (100\text{--}250 \text{ }\mu\text{m}).$$

$$E_{\text{el}} = 1.0 \text{ J} \quad (100\text{--}250 \text{ }\mu\text{m}).$$

$$\Delta_{\text{c}}U = -1878 \text{ cal/g.}$$

4.2.1.4 Rubidium 1-(2-Chloroethyl)-5-nitriminotetrazolate (3_Rb)

A solution of 1.00 g (5.2 mmol) 1-(2-chloroethyl)-5-nitriminotetrazole (**3**) and 0.60 g (2.6 mmol) rubidium carbonate in 10 mL H₂O was refluxed for 10 minutes. After storing the reaction solution at ambient temperature for several days colorless blocks suitable for X-ray diffraction were obtained and filtered off. Yield: 92 %.

M.p. 184 °C (dec., DSC-measurement, 5 K/min).

IR (Diamond-ATR, cm⁻¹): 3429 (w), 3018 (vw), 2966 (vw), 1640 (vw), 1498 (m), 1455 (w), 1446 (m), 1440 (w), 1388 (m), 1359 (m), 1333 (s), 1290 (m), 1248 (m), 1236 (m), 1204 (w), 1124 (vw), 1100 (m), 1040 (w), 987 (vw), 954 (vw), 908 (vw), 874 (vw), 774 (w), 753 (w), 735 (w), 672 (vw), 651 (m).

¹H NMR (DMSO-*d*₆): 4.35 (*t*, 2H, ³*J* = 5.8 Hz, CH₂Cl), 3.93 (*t*, 2H, ³*J* = 5.8 Hz, NCH₂).

¹³C NMR (DMSO-*d*₆): 157.7 (CN₄), 47.8 (NCH₂), 42.1 (CH₂Cl).

Elemental analysis C₃H₄ClN₆O₂Rb (277.02 g/mol): calc.: C, 13.01; H, 1.46; N, 30.34; Cl, 12.80; found: C, 12.94; H, 1.62; N, 30.28; Cl, 12.91.

$$E_{\text{dr}} = 5.0 \text{ J} \quad (250\text{--}500 \text{ }\mu\text{m}).$$

$$F_{\text{r}} = 160 \text{ N} \quad (250\text{--}500 \text{ }\mu\text{m}).$$

$$E_{\text{el}} = 0.5 \text{ J} \quad (250\text{--}500 \text{ }\mu\text{m}).$$

$$\Delta_{\text{c}}U = -1853 \text{ cal/g.}$$

4.2.1.5 Cesium 1-(2-Chloroethyl)-5-nitriminotetrazolate (3_Cs)

A solution of 1.00 g (5.2 mmol) 1-(2-chloroethyl)-5-nitriminotetrazole (**3**) and 0.37 g (5.2 mmol) cesium hydroxide monohydrate in 15 mL H₂O was refluxed for 10 minutes. After storing the solution at ambient temperature for several days colorless blocks suitable for X-ray diffraction were obtained and filtered off. Yield: 91 %.

M.p. 161 °C (dec., DSC-measurement, 5 K/min).

IR (Diamond-ATR, cm⁻¹): 3313 (w), 3022 (w), 1641 (vw), 1545 (vw), 1496 (m), 1450 (w), 1444 (m), 1434 (m), 1385 (m), 1324 (s), 1248 (m), 1233 (m), 1202 (w), 1127 (vw), 1099 (w), 1037 (w), 987 (vw), 949 (vw), 909 (vw), 874 (vw), 830 (vw), 774 (w), 745 (w), 735 (w), 689 (vw), 670 (vw), 650 (w).

¹H NMR (DMSO-*d*₆): 4.35 (*t*, 2H, ³*J* = 5.8 Hz, CH₂Cl), 3.94 (*t*, 2H, ³*J* = 5.8 Hz, NCH₂).

¹³C NMR (DMSO-*d*₆): 157.7 (CN₄), 47.8 (NCH₂), 42.1 (CH₂Cl).

Elemental analysis C₃H₄ClN₆O₂Cs (324.46 g/mol): calc.: C, 11.11; H, 1.24; N, 25.90; found: C, 11.20; H, 1.18; N, 25.87.

$$E_{\text{dr}} = 10 \text{ J} \quad (100\text{--}500 \text{ }\mu\text{m}).$$

$$F_{\text{r}} = 160 \text{ N} \quad (100\text{--}500 \text{ }\mu\text{m}).$$

$$E_{\text{el}} = 0.5 \text{ J} \quad (100\text{--}500 \text{ }\mu\text{m}).$$

$$\Delta_c U = -1475 \text{ cal/g}.$$

4.2.1.6 Magnesium 1-(2-Chloroethyl)-5-nitriminotetrazolate Hexahydrate (3_Mg)

A solution of 1.31 g (6.8 mmol) 1-(2-chloroethyl)-5-nitriminotetrazole (**3**) and 0.20 g (3.4 mmol) magnesium hydroxide in 50 mL H₂O was refluxed for 30 minutes. The solvent was evaporated to obtain a colorless powder. Recrystallization from H₂O yielded colorless crystals suitable for X-ray diffraction after storing the solution at ambient temperature for several days. Yield: 90 %.

M.p. 111 °C (loss of H₂O), 123 °C (loss of H₂O), 157 °C (loss of H₂O), 226 °C (dec., DSC-measurement, 5 K/min).

IR (Diamond-ATR, cm⁻¹): 3576 (m, br), 3381 (s), 3201 (m), 3085 (m), 2363 (vw), 1669 (w), 1649 (w), 1510 (m), 1456 (m), 1442 (w), 1423 (w), 1379 (m), 1344 (s), 1330 (s), 1284 (m), 1264 (w), 1240 (w), 1129 (w), 1118 (w), 1039 (m), 989 (vw), 889 (w), 790 (vw), 771 (w), 737 (w), 705 (m).

¹H NMR (DMSO-*d*₆): 4.35 (*t*, 2H, ³*J* = 5.9 Hz, CH₂Cl), 3.94 (*t*, 2H, ³*J* = 5.9 Hz, NCH₂).

¹³C NMR (DMSO-*d*₆): 157.7 (CN₄), 47.8 (NCH₂), 42.1 (CH₂Cl).

Elemental analysis C₆H₂₀Cl₂N₁₂MgO₁₀ (515.51 g/mol): calc.: C, 13.98; H, 3.91; N, 32.60; found: C, 14.02; H, 3.87; N, 32.10.

$$E_{\text{dr}} = 25 \text{ J} \quad (100\text{--}500 \text{ }\mu\text{m}).$$

$$F_{\text{r}} = 240 \text{ N} \quad (100\text{--}500 \text{ }\mu\text{m}).$$

$$E_{\text{el}} = 0.15 \text{ J} \quad (100\text{--}500 \text{ }\mu\text{m}).$$

$$\Delta_c U = -2011 \text{ cal/g.}$$

4.2.1.7 Calcium 1-(2-Chloroethyl)-5-nitriminotetrazolate Monohydrate (3_Ca)

A solution of 1.31 g (6.8 mmol) **3** and 0.25 g (3.4 mmol) calcium hydroxide in 60 mL H₂O was refluxed for 30 minutes. The solvent was evaporated to obtain colorless powder. Recrystallization from H₂O yielded 1.35 g of a colorless powder. Yield: 89 %.

M.p. 175 °C (loss of H₂O), 188 °C (dec., DSC-measurement, 5 K/min).

IR (Diamond-ATR, cm⁻¹): 3408 (s, br), 1644 (w), 1608 (w), 1506 (m), 1459 (m), 1436 (w), 1391 (s), 1355 (s), 1295 (m), 1254 (m), 1239 (m), 1183 (w), 1103 (m), 1032 (m), 1001 (w), 943 (w), 910 (w), 872 (w), 759 (w), 738 (w), 675 (w), 655 (w).

¹H NMR (DMSO-*d*₆): 4.39 (*t*, 2H, ³*J* = 5.8 Hz, CH₂Cl), 3.98 (*t*, 2H, ³*J* = 5.8 Hz, NCH₂).

¹³C NMR (DMSO-*d*₆): 157.7 (CN₄), 47.9 (NCH₂), 42.2 (CH₂Cl).

Elemental analysis C₆H₁₀CaCl₂N₁₂O₅ (441.21 g/mol): calc.: C, 16.33; H, 2.28; N, 38.10; found: C, 16.14; H, 2.46; N, 37.92.

$$E_{dr} = 8.0 \text{ J} \quad (160\text{--}250 \mu\text{m}).$$

$$F_r > 360 \text{ N} \quad (160\text{--}250 \mu\text{m}).$$

$$E_{el} = 0.80 \text{ J} \quad (160\text{--}250 \mu\text{m}).$$

$$\Delta_c U = -2232 \text{ cal/g.}$$

4.2.1.8 Strontium 1-(2-Chloroethyl)-5-nitriminotetrazolate Monohydrate (3_Sr)

A solution of 1.31 g (6.8 mmol) **3** and 0.90 g (3.4 mmol) strontium hydroxide octahydrate in 25 mL H₂O was refluxed for 15 minutes. The solvent was removed under high vacuum to obtain a colorless powder. Recrystallization from H₂O yielded 1.51 g of colorless needles suitable for X-ray diffraction after storing the solution at ambient temperature for few hours. Yield: 91 %.

M.p. 208 °C (dec., DSC-measurement, 5 K/min).

Raman (200 mW, 25 °C, cm⁻¹): 3016 (6), 2967 (15), 1647 (5), 1542 (3), 1507 (100), 1462 (6), 1438 (6), 1380 (6), 1344 (24), 1291 (7), 1261 (3), 1245 (2), 1205 (3), 1111 (10), 1031 (37), 995 (3), 875 (4), 766 (10), 743 (3), 653 (6), 507 (2), 473 (2), 371 (3), 306 (5), 196 (5).

IR (Diamond-ATR, cm⁻¹): 3501 (w), 3015 (vw), 2966 (vw), 2852 (vw), 2363 (vw), 2340 (vw), 1640 (w), 1508 (m), 1462 (m), 1421 (w), 1380 (s), 1340 (s), 1310 (s), 1257 (m), 1236 (s), 1130 (w), 1109 (m), 1027 (m), 996 (w), 954 (w), 904 (w), 871 (w), 771 (w), 764 (w), 740 (w), 708 (vw), 677 (w), 653 (w).

¹H NMR (DMSO-*d*₆): 4.39 (*t*, 2H, ³*J* = 5.9 Hz, CH₂Cl), 3.98 (*t*, 2H, ³*J* = 5.9 Hz, NCH₂), 3.32 (*s*, 2H, H₂O).

¹³C NMR (DMSO-*d*₆): 157.7 (CN₄), 47.8 (NCH₂), 42.1 (CH₂Cl).

Elemental analysis C₆H₁₀Cl₂N₁₂O₅Sr (488.75 g/mol): calc.: C, 14.74; H, 2.06; N, 34.39; found: C, 14.85; H, 2.20; N, 34.62.

E_{dr} = 10 J (160–250 μm).

F_r > 360 N (160–250 μm).

E_{el} = 0.75 J (160–250 μm).

Δ_cU = -1679 cal/g.

H₂O-sol. 14 wt% (21 °C).

4.2.1.9 Barium 1-(2-Chloroethyl)-5-nitriminotetrazolate Monohydrate (3_Ba)

A solution of 1.31 g (6.8 mmol) 1-(2-chloroethyl)-5-nitriminotetrazole (**3**) and 1.07 g (3.4 mmol) barium hydroxide octahydrate in 25 mL H₂O was refluxed for 15 minutes. The solvent was evaporated to obtain a colorless powder. Recrystallization from H₂O/ethanol (1:1) yielded 1.75 g of colorless needles suitable for X-ray diffraction after cooling the reaction solution to ambient temperature. Yield: 95 %.

M.p. 207 °C (dec., DSC-measurement, 5 K/min).

Raman (200 mW, 25 °C, cm⁻¹): 3022 (5), 2974 (12), 1538 (2), 1496 (100), 1460 (4), 1383 (7), 1351 (26), 1315 (6), 1293 (6), 1258 (2), 1199 (1), 1108 (11), 1028 (35), 999 (3), 872 (3), 758 (5), 677 (5), 646 (4).

IR (Diamond-ATR, cm⁻¹): 3607 (w), 3406 (w), 3025 (w), 3002 (vw), 2363 (vw), 2341 (vw), 1783 (vw), 1629 (w), 1496 (m), 1458 (w), 1444 (m), 1429 (m), 1340 (s), 1315 (s), 1258 (m), 1242 (m), 1229 (m), 1136 (w), 1106 (m), 1025 (m), 1000 (w), 961 (vw), 942 (w), 909 (w), 870 (w), 768 (w), 755 (w), 746 (w), 738 (w), 710 (vw), 672 (w), 655 (w), 646 (w).

¹H NMR (DMSO-*d*₆): 4.39 (*t*, 2H, ³*J* = 5.9 Hz, CH₂Cl), 3.98 (*t*, 2H, ³*J* = 5.9 Hz, NCH₂), 3.32 (*s*, 2H, H₂O).

¹³C NMR (DMSO-*d*₆): 157.7 (CN₄), 47.8 (NCH₂), 42.1 (CH₂Cl).

Elemental analysis C₆H₁₀Cl₂N₁₂O₅Ba (538.45 g/mol): calc.: C, 13.38; H, 1.87; N, 31.22; found: C, 13.35; H, 1.85; N, 31.46.

E_{dr} = 3.0 J (250–500 μm).

F_r = 144 N (250–500 μm).

E_{el} = 1.0 J (250–500 μm).

Δ_cU = -1512 cal/g.

H₂O-sol. 0.8 wt% (21 °C).

4.2.1.10 *trans*-[Diaqua-bis{1-(2-chloroethyl)-5-nitriminotetrazolato-κ²N4,O1}] Copper(II) Dihydrate (3_Cu_H₂O)

A solution of 2.00 g (10.4 mmol) **3** in 20 mL H₂O and a solution of 1.21 g (5.2 mmol) copper(II) nitrate pentahydrate in 10 mL H₂O were combined at 50 °C. Blue crystals formed after one day storing the blue solution at ambient temperature. Yield: 85 %.

M.p. 103 °C (loss of H₂O), 242 °C (dec., DSC-measurement, 5 K/min).

IR (Diamond-ATR, cm⁻¹): 3649 (w), 3588 (m), 3497 (w), 3168 (s, br), 3031 (s), 2392 (vw), 2286 (vw), 1515 (s), 1463 (s), 1435 (w), 1425 (w), 1383 (s), 1349 (s), 1297 (s), 1268 (s), 1253 (s), 1211 (m), 1138 (w), 1111 (m), 1036 (w), 1010 (w), 959 (w), 904 (w), 872 (w), 810 (w), 772 (w), 764 (w), 740 (m), 684 (w), 662 (w).

Elemental analysis C₆H₁₆Cl₂CuN₁₂O₈ (518.72 g/mol): calc.: C, 13.89; H, 3.11; N, 32.40; Cl, 13.67; found: C, 13.79; H, 2.90; N, 32.55; Cl, 13.68.

E_{dr} = 50 J (< 100 μm).

F_r > 360 N (< 100 μm).

E_{el} = 0.60 J (< 100 μm).

Δ_cU = -1682 cal/g.

H₂O-sol. 0.9 wt% (23 °C).

4.2.1.11 Copper(II) 1-(2-Chloroethyl)-5-nitriminotetrazolate (3_Cu)

1.00 g (1.9 mmol) *trans*-[Diaqua-bis{1-(2-chloroethyl)-5-nitriminotetrazolato-κ²N4,O1} copper(II)] dihydrate (3_Cu_H₂O) was stored for 48 hours at 110 °C to remove the crystal water. 0.84 g of a green powder 3_Cu could be obtained. Yield: 100 %.

M.p. 238 °C (dec., DSC-measurement, 5 K/min).

IR (Diamond-ATR, cm⁻¹): 3033 (w), 3002 (vw), 2964 (vw), 2360 (w), 2331 (vw), 1739 (w), 1533 (m), 1488 (s), 1452 (m), 1436 (s), 1429 (m), 1388 (w), 1341 (m), 1304 (s), 1235 (s), 1133 (w), 1107 (w), 1047 (vw), 1001 (m), 873 (w), 793 (vw), 775 (vw), 740 (w), 730 (w), 708 (m), 687 (w).

Elemental analysis C₆H₈Cl₂CuN₁₂O₄ (446.66 g/mol): calc.: C, 16.13; H, 1.81; N, 37.63; found: C, 16.04; H, 1.85; N, 37.60.

E_{dr} = 6.0 J (< 100 μm).

F_r = 192 N (< 100 μm).

E_{el} = 0.50 J (< 100 μm).

Δ_cU = -2245 cal/g.

H₂O-sol. 0.7 wt% (23 °C).

4.2.1.12 *trans*-[Diammine-bis{1-(2-chloroethyl)-5-nitriminotetrazolato-κ²N4,O1}] Copper(II) (3_Cu_NH₃)

At 50 °C 5.0 mL aqueous ammonia solution (25 %) were added to a solution of 2.0 g (10.4 mmol) 1-(2-chloroethyl)-5-nitriminotetrazole (3) in 25 mL H₂O. The mixture was combined with a solution of 1.2 g (5.2 mmol) copper(II) nitrate pentahemihydrate in 10 mL H₂O. The deep blue solution was stored at ambient temperature for two days until deep blue single crystals, suitable for X-ray diffraction, were formed. Yield: 81 %.

M.p. 205 °C (dec., DSC-measurement, 5 K/min).

IR (Diamond-ATR, cm^{-1}): 3332 (w), 3264 (w), 3177 (vw), 1611 (vw), 1512 (m), 1459 (m), 1438 (w), 1396 (s), 1363 (w), 1342 (m), 1301 (w), 1283 (s), 1268 (m), 1234 (s), 1128 (w), 1106 (w), 1026 (w), 991 (vw), 873 (vw), 790 (vw), 766 (vw), 750 (vw), 732 (vw), 708 (w).

Elemental analysis $\text{C}_6\text{H}_{14}\text{Cl}_2\text{CuN}_{16}\text{O}_4$ (480.72 g/mol): calc.: C, 14.99; H, 2.94; N, 40.79; found: C, 15.01; H, 3.13; N, 40.63.

$E_{\text{dr}} = 6.0 \text{ J}$ (250–500 μm).

$F_{\text{r}} > 360 \text{ N}$ (250–500 μm).

$E_{\text{el}} = 0.50 \text{ J}$ (250–500 μm).

$\Delta_c U = -2245 \text{ cal/g}$.

H₂O-sol. 0.4 wt% (23 °C).

4.2.2 Pyrotechnic Compositions

For preparation of the pyrotechnic compositions all compounds, except the binder, were carefully mixed in a mortar. Then the binder, a solution of 25 % vinyl alcohol acetate resin (VAAR), dissolved in a few milliliters of ethyl acetate was added. The mixture was formed by hand and dried under high vacuum for several hours.

The controlled burn down was filmed with a digital video camera recorder (SONY, DCR-HC37E).

4.2.2.1 Pyrotechnic Compositions Based on 3_Sr

In Table 4.6–Table 4.13, all tested pyrotechnic compositions containing **3_Sr** as colorant are listed. Potassium permanganate, potassium nitrate, ammonium nitrate, and ammonium dinitramide were used as oxidizers. The fuels magnesium, magnalium or **5-At** were added.

Table 4.6 Pyrotechnic formulations containing **3_Sr** and potassium permanganate.

	3_Sr [wt%]	KMnO₄ [wt%]	Mg [wt%]	VAAR [wt%]	observed behavior
3_Sr_1.1	14	68	7	11	yellow-violet flame, easy to ignite, moderate velocity, much smoke, solid glowing residues
3_Sr_1.2	17	66	4	13	yellow-violet flame, easy to ignite, high velocity, much smoke, solid long glowing residues
3_Sr_1.3	15	58	15	12	violet flame, easy to ignite, reacts too violently
3_Sr_1.4	18	52	18	12	violet-red flame, easy to ignite, high velocity, much smoke, small amount of solid glowing residues

Table 4.7 Pyrotechnic formulations containing **3_Sr** and ammonium nitrate.

	3_Sr [wt%]	NH₄NO₃ [wt%]	Mg [wt%]	VAAR [wt%]	observed behavior
3_Sr_2.1	14	68	7	11	intense red flame, easy to ignite, moderate velocity, less smoke, Mg sparks, blinking, small amount of solid residues
3_Sr_2.2	11	67	11	11	red flame, easy to ignite, low velocity, no proper burning, blinking, Mg sparks, small amount of solid residues
3_Sr_2.3	11	75	3	11	yellow-red flame, easy to ignite, low velocity, Mg sparks, solid residues

Table 4.8 Pyrotechnic formulations containing **3_Sr** and potassium nitrate.

	3_Sr [wt%]	KNO₃ [wt%]	Mg [wt%]	VAAR [wt%]	observed behavior
3_Sr_3.1	11	75	5	9	violet flame, hard to ignite, moderate velocity, much smoke, solid glowing residues
3_Sr_3.2	10	72	10	8	violet-red flame, moderate to ignite, high velocity, much smoke, solid glowing residues
3_Sr_3.3	13	76	13	8	white-violet flame, hard to ignite, low velocity, much smoke, solid glowing residues

Table 4.9 Pyrotechnic formulations containing **3_Sr** and strontium nitrate.

	3_Sr [wt%]	Sr(NO₃)₂ [wt%]	Mg [wt%]	VAAR [wt%]	observed behavior
3_Sr_4	18	53	18	11	intense red flame, easy to ignite, high velocity, much smoke, few Mg sparks, small amount of solid residues

Table 4.10 Pyrotechnic formulations containing **3_Sr** and **5-At**.

	3_Sr [wt%]	KMnO₄ [wt%]	5-At [wt%]	VAAR [wt%]	observed behavior
3_Sr_5	18	53	18	11	violet-white flame, easy to ignite, moderate velocity, much smoke, solid glowing residues

Table 4.11 Pyrotechnic formulations containing **3_Sr** and magnalium.

	3_Sr [wt%]	KNO₃ [wt%]	MgAl [wt%]	VAAR [wt%]	observed behavior
3_Sr_6	12	68	11	9	cannot be ignited

Table 4.12 Pyrotechnic formulations containing **3_Sr**, **5-At**, and potassium nitrate.

	3_Sr	ADN	KNO₃	5-At	VAAR	observed behavior
	[wt%]	[wt%]	[wt%]	[wt%]	[wt%]	
3_Sr_7.1	15	28	19	28	10	intense red flame, easy to ignite, high velocity, less smoke, no solid residues
3_Sr_7.2	14	28	20	28	10	violet-red flame, easy to ignite, high velocity, smoke, no solid residues
3_Sr_7.3	14	28	22	26	10	violet-red flame, easy to ignite, high velocity, smoke, small amount of solid residues

Table 4.13 Pyrotechnic formulations containing **3_Sr** and ammonium dinitramide.

	3_Sr	ADN	5-At	VAAR	observed behavior
	[wt%]	[wt%]	[wt%]	[wt%]	
3_Sr_8.1	19	36	36	11	very intense red flame, easy to ignite, high velocity, no smoke, small amount of solid glowing residues
3_Sr_8.2	15	40	35	10	very intense red flame, easy to ignite, high velocity, no smoke, small amount of solid residues
3_Sr_8.3	11	44	34	11	very intense red flame, easy to ignite, high velocity, no smoke, almost no solid residues

4.2.2.2 Pyrotechnic Compositions Based on **3_Ba**

In Table 4.14–Table 4.19 all prepared pyrotechnic compositions containing **3_Ba** as colorant are listed. Potassium nitrate, ammonium nitrate, and ADN were used as oxidizers. The fuels magnesium, magnalium, **5-At** or aluminum were added.

Table 4.14 Pyrotechnic formulations containing **3_Ba** and potassium nitrate.

	3_Ba	KNO₃	Mg	VAAR	observed behavior
	[wt%]	[wt%]	[wt%]	[wt%]	
3_Ba_1.1	21	60	10	9	white flame, easy to ignite, moderate velocity, much smoke, solid glowing residues
3_Ba_1.2	17	70	4	9	cannot be ignited
3_Ba_1.3	21	65	4	10	white flame, easy to ignite, uncontinuous burning, much smoke, solid glowing residues
3_Ba_1.4	22	66	4	8	cannot be ignited

Table 4.15 Pyrotechnic formulations containing **3_Ba** and **5-At**.

	3_Ba	KNO₃	5-At	VAAR	observed behavior
	[wt%]	[wt%]	[wt%]	[wt%]	
3_Ba_2.1	21	61	10	8	cannot be ignited
3_Ba_2.2	13	66	13	8	cannot be ignited

Table 4.16 Pyrotechnic formulations containing **3_Ba** and ammonium nitrate.

	3_Ba	NH₄NO₃	MgAl	5-At	VAAR	observed behavior
	[wt%]	[wt%]	[wt%]	[wt%]	[wt%]	
3_Ba_3.1	23	58	9	0	10	white-green flame, easy to ignite, low velocity, blinking, less smoke, Mg sparks, small amount of solid residues
3_Ba_3.2	20	60	7	4	9	green flame, easy to ignite, moderate velocity, blinking, less smoke, few Mg sparks, almost no solid residues
3_Ba_3.3	19	60	7	0	14	white-green small flame, easy to ignite, low velocity, blinking, smoke, Mg sparks, small amount of solid residues
3_Ba_3.4	19	64	6	2	9	white-greenish flame, moderate to ignite, low velocity, less smoke, Mg sparks, solid glowing residues
3_Ba_3.5	18	64	6	3	9	white-green flame, easy to ignite, low velocity, blinking, less smoke, Mg sparks, small amount of solid residues
3_Ba_3.6	15	68	6	3	8	white-green flame, easy to ignite, low velocity, blinking, less smoke, Mg sparks, solid residues

Table 4.17 Pyrotechnic formulations containing **3_Ba** and ADN.

	3_Ba	ADN	5-At	VAAR	observed behavior
	[wt%]	[wt%]	[wt%]	[wt%]	
3_Ba_4.1	23	46	11	20	green flame, easy to ignite, high velocity, no smoke, small amount of solid glowing residues
3_Ba_4.2	25	45	10	20	intense green flame, easy to ignite, high velocity, no smoke, almost no solid residues
3_Ba_4.3	26	46	8	20	green-yellow flame, easy to ignite, high velocity, no smoke, small amount of solid glowing residues
3_Ba_4.4	27	43	10	20	green flame, easy to ignite, high velocity, no smoke, small amount of solid glowing residues

Table 4.18 Pyrotechnic formulations containing **3_Ba**, **5-At**, and ammonium nitrate.

	3_Ba [wt%]	NH₄NO₃ [wt%]	5-At [wt%]	VAAR [wt%]	observed behavior
3_Ba_5.1	12	72	6	10	white-yellow flame, easy to ignite, low velocity, no smoke, almost no solid residues
3_Ba_5.2	13	70	7	10	white flame, easy to ignite, low velocity, no smoke, small amount of solid residues
3_Ba_5.3	9	78	5	8	small white flame, hard to ignite, no proper burning

Table 4.19 Pyrotechnic formulation containing **3_Ba** and aluminum.

	3_Ba [wt%]	NH₄NO₃ [wt%]	Al [wt%]	VAAR [wt%]	observed behavior
3_Ba_6	9	77	5	9	small yellow flame, easy to ignite, low velocity, solid residues

4.2.2.3 Pyrotechnic Compositions Based on **3_Cu_H₂O**

No composition was prepared with **3_Cu** and **3_Cu_NH₃**, because of their higher sensitivities compared to **3_Cu_H₂O** and the fast deflagration of **3_Cu**. Furthermore, **3_Cu_NH₃** shows the lowest decomposition temperature and **3_Cu_H₂O** is the most insensitive one of these copper compounds. **3_Cu_H₂O** was combined with the oxidizer ammonium nitrate or ammonium dinitramide and the fuels copper(I) oxide, boron and starch.

Table 4.20 Pyrotechnic formulation containing **3_Cu_H₂O** and ammonium nitrate.

	3_Cu_H₂O [wt%]	NH₄NO₃ [wt%]	VAAR [wt%]	observed behavior
3_Cu_H₂O_1	15	76	9	cannot be ignited

Table 4.21 Pyrotechnic formulation containing **3_Cu_H₂O** and copper(I) oxide.

	3_Cu_H₂O [wt%]	NH₄NO₃ [wt%]	Cu₂O [wt%]	VAAR [wt%]	observed behavior
3_Cu_H₂O_2	11	75	5	9	small white-blue flame, moderate to ignite, no proper burning, smoke

Table 4.22 Pyrotechnic formulation containing **3_Cu_H2O** and boron.

	3_Cu_H2O [wt%]	NH₄NO₃ [wt%]	B [wt%]	VAAR [wt%]	observed behavior
3_Cu_H2O_3	13	77	1	9	small white-blue flame, hard to ignite, less smoke, no proper burning

Table 4.23 Pyrotechnic formulations containing **3_Cu_H2O** and ADN.

	3_Cu_H2O [wt%]	ADN wt%	B [wt%]	VAAR [wt%]	observed behavior
3_Cu_H2O_4.1	36	44	9	11	intense blue flame, easy to ignite, reacts too violently, solid glowing residues
3_Cu_H2O_4.2	37	37	15	11	white-blue flame, easy to ignite, high velocity, huge amount of solid glowing residues
3_Cu_H2O_4.3	40	39	10	11	intense blue flame, easy to ignite, reacts too violently, solid glowing residues
3_Cu_H2O_4.4	42	38	9	11	purple-blue flame, easy to ignite, high velocity, less smoke, solid glowing residues

Table 4.24 Pyrotechnic formulations containing **3_Cu_H2O** and starch.

	3_Cu_H2O [wt%]	ADN [wt%]	Starch [wt%]	VAAR [wt%]	observed behavior
3_Cu_H2O_5.1	36	44	9	11	intense blue flame, easy to ignite, reacts too violently
3_Cu_H2O_5.2	37	37	15	11	purple-blue flame, easy to ignite, moderate velocity, less smoke, small amount of solid glowing residues
3_Cu_H2O_5.3	42	38	9	11	purple-blue flame, easy to ignite, moderate velocity, less smoke, almost no solid residues
3_Cu_H2O_5.4	43	43	4	10	intense blue flame, easy to ignite, high velocity, smoke, almost no solid glowing residues

Table 4.25 Pyrotechnic formulations containing **3_Cu_H2O**, ADN, and ammonium nitrate.

	3_Cu_H2O	ADN	NH₄NO₃	B	VAAR	observed behavior
	[wt%]	[wt%]	[wt%]	[wt%]	[wt%]	
3_Cu_H2O_6.1	21	19	38	10	12	blue-yellow-red flame, easy to ignite, moderate velocity, less smoke, huge amount of solid glowing residues
3_Cu_H2O_6.2	22	18	42	5	13	blue-yellow flame, easy to ignite, moderate velocity, less smoke, solid glowing residues
3_Cu_H2O_6.3	24	12	43	4	17	intense blue flame, easy to ignite, high velocity, less smoke, small amount of solid glowing residues

4.3 Conclusion

The alkali and alkaline earth metal salts of 1-(2-chloroethyl)-5-nitriminotetrazole (**3**), lithium 1-(2-chloroethyl)-5-nitriminotetrazolate (**3_Li**), sodium 1-(2-chloroethyl)-5-nitriminotetrazolate (**3_Na**), potassium 1-(2-chloroethyl)-5-nitriminotetrazolate (**3_K**), rubidium 1-(2-chloroethyl)-5-nitriminotetrazolate (**3_Rb**), cesium 1-(2-chloroethyl)-5-nitriminotetrazolate (**3_Cs**), magnesium 1-(2-chloroethyl)-5-nitriminotetrazolate hexahydrate (**3_Mg**), calcium 1-(2-chloroethyl)-5-nitriminotetrazolate monohydrate (**3_Ca**), strontium 1-(2-chloroethyl)-5-nitriminotetrazolate monohydrate (**3_Sr**), and barium 1-(2-chloroethyl)-5-nitriminotetrazolate monohydrate (**3_Ba**), as well as the copper(II) compounds *trans*-[diaqua-bis{1-(2-chloroethyl)-5-nitriminotetrazolato- $\kappa^2N4,O5$ } copper(II)] dihydrate (**3_Cu_H2O**), copper(II) 1-(2-chloroethyl)-5-nitriminotetrazolate (**3_Cu**), and *trans*-[diammine-bis{1-(2-chloroethyl)-5-nitriminotetrazolato- $\kappa^2N4,O1$ }] copper(II) (**3_Cu_NH₃**) were prepared and characterized using vibrational and multinuclear magnetic resonance spectroscopy, elemental analysis, and differential scanning calorimetry (DSC). The crystal structures of **3_K**, **3_Rb**, **3_Cs**, **3_Mg**, **3_Sr**, **3_Ba**, **3_Cu**, and **3_Cu_NH₃** were determined, discussed and compared to in the literature described salts of **3**.

Furthermore, their sensitivities to impact, friction and electric discharge were determined. The heats of formation were calculated from bomb calorimetric measurements.

The solubility in H₂O at ambient temperature, color performance and combustion properties of the pyrotechnically relevant salts **3_Sr**, **3_Ba**, **3_Cu_H2O**, **3_Cu**, and **3_Cu_NH₃** were analyzed with regard to their use as potential coloring agents in pyrotechnic compositions. Additionally, the combustion behavior of **3_Sr** was qualitatively characterized with a simple smoke test method. A pyrotechnic composition containing **3_Sr** was tested with a static burn test and offered the best performance compared to other nitrogen-rich strontium salts (see chapter 9).^[15]

Furthermore, several pyrotechnic compositions, containing **3_Sr**, **3_Ba** or **3_Cu_H₂O**, were prepared and compared to known formulations. Most promising are the formulations **3_Sr_8.3** and **3_Ba_4.2**, containing ADN as oxidizer, with respect to color performance, reduced smoke production and high combustion velocity. The best formulation containing **3_Cu_H₂O** shows heavy smoke production due to the use of starch as fuel. The decomposition temperatures and sensitivities to impact, friction and electric discharge of pyrotechnic compositions with the best performance were determined. Unfortunately, all further investigated mixtures show decomposition temperatures below 180 °C. This probably can be improved, if a different oxidizer offering an equal performance or a stabilizing additive is used.

Nevertheless, the prepared salts **3_Sr**, **3_Ba**, and **3_Cu_H₂O** are a step forward in the preparation of more environmentally benign pyrotechnic compositions without potassium perchlorate.

4.4 References

- [1] B. T. Sturman: On the emitter of blue light in copper-containing pyrotechnic flames, *Propellants Explos. Pyrotech.* **2006**, *31*, 70–74.
- [2] J. A. Conkling: *Chemistry of Pyrotechnics: Basic Principles and Theory*. M. Dekker, Inc., New York, **1985**.
- [3] R. A. Henry, W. G. Finnegan: Mono-alkylation of Sodium 5-Aminotetrazole in Aqueous Medium, *J. Am. Chem. Soc.*, **1954**, 923–926.
- [4] T. M. Klapötke, J. Stierstorfer, K. R. Tarantik: New Energetic Materials: Functionalized 1-Ethyl-5-aminotetrazoles and 1-Ethyl-5-nitriminotetrazoles, *Chem. Eur. J.* **2009**, *15*, 5775–5792.
- [5] J. Stierstorfer: Advanced Energetic Materials based on 5-Aminotetrazole, *PhD Thesis*, **2009**, Ludwig-Maximilian University, Munich.
- [6] R. A. Henry, W. G. Finnegan: N-Vinylnitrazoles, *J. Org. Chem.*, **1959**, 923–926.
- [7] N. Wiberg, E. Wiberg, A. F. Holleman: *Lehrbuch der Anorganischen Chemie*, deGruyter, Berlin, 102.Ed., **2007**.
- [8] T. M. Klapötke, J. Stierstorfer, K. R. Tarantik, I. D. Thoma: Strontium Nitriminotetrazolates - Suitable Colorants in Smokeless Pyrotechnic Compositions, *Z. Anorg. Allg. Chem.* **2008**, *634(15)*, 2777–2784.
- [9] a) <http://www.bam.de> b) E_{dr} : insensitive > 40 J, less sensitive \geq 35 J, sensitive \geq 4, very sensitive \leq 3 J; F_r : insensitive > 360 N, less sensitive = 360 N, sensitive < 360 N > 80 N,

very sensitive ≤ 80 N, extreme sensitive ≤ 10 N. According to the UN Recommendations on the Transport of Dangerous Goods.

[10] <http://webbook.nist.gov/>

[11] R. Damavarapu, T. M. Klapötke, J. Stierstorfer, K. R. Tarantik: Barium Salts of Tetrazole Derivatives – Synthesis and Characterization, *Propellants, Explos. Pyrotech.* **2010**, *in press*.

[12] T. Shimizu: Studies on Blue and Purple Flame Compositions Made With Potassium Perchlorate, *Pyrotechnica* **1980**, 6, 5.

[13] G. R. Lakshminarayanan, G. Chen, R. Ames, W. T. Lee, J. Wejsa, K. Meiser, *Laminac Binder Replacement Program*, Aug. **2006**.

[14] G. Chen, *Application of High Nitrogen Energetics in Pyrotechnic*, Program Review Presentation to US Army RDECOM, 20. Jan. **2009**.

[15] a) T. M. Klapötke, H. Radies, J. Stierstorfer, K. R. Tarantik, G. Chen, and A. Nagori: Coloring Properties of Various High-Nitrogen Compounds in Pyrotechnic Compositions, *36th International Pyrotechnics Seminar and Symposium*, Proceedings, Rotterdam, The Netherlands, 23–28. Aug. **2009**, 65–72. b) T. M. Klapötke, H. Radies, J. Stierstorfer, K. R. Tarantik, G. Chen, and A. Nagori: Coloring Properties of Various High-Nitrogen Compounds in Pyrotechnic Compositions, *Propellants, Explos. Pyrotech.* **2010**, *in press*.

5 Salts of 1-Carboxymethyl-5-aminotetrazole and 1-Carboxymethyl-5-nitriminotetrazole

1-Carboxymethyl-5-aminotetrazole (**4**) is another alkylated 5-aminotetrazole derivative, which is characterized in the literature.^[1, 2] In this chapter the preparation of its alkali metal and alkaline earth metal salts is presented and their characterization using multinuclear magnetic resonance as well as vibrational spectroscopy (IR and Raman) and elemental analysis is given. Moreover, their energetic properties, like decomposition temperature and sensitivities to outer stimuli, were determined. Furthermore, one copper(II) compound with **4** as ligand was prepared and investigated. 1-Carboxymethyl-5-nitriminotetrazole monohydrate (**5**) is the nitration product of **4**. Its synthesis and full characterization is given in this chapter. The alkali metal salts of **5** were also investigated. Furthermore, a full characterization of its alkaline earth metal salts and two copper(II) complexes – with **5** as mono- and bisanion – is given.

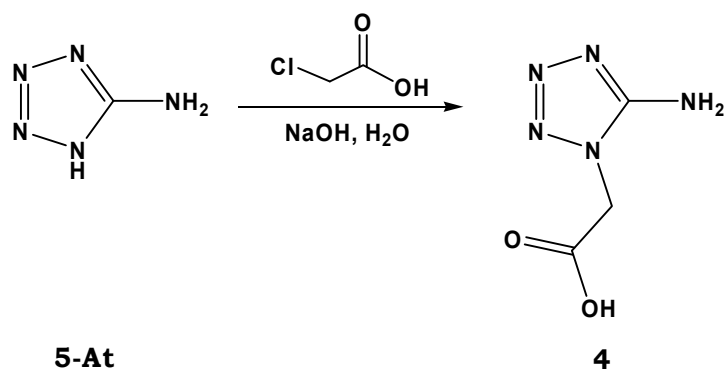
4 was selected, because it combines several properties, which are advantageous for the application as starting material for the synthesis of coloring agents. First of all, it is a thermally quite stable and insensitive 5-aminotetrazole derivative, which can be deprotonated easily due to its carboxyl group.^[1, 2] It consists of a tetrazole ring, which is responsible for the formation of gaseous nitrogen as decomposition product and includes a carboxyl group, which improves the oxygen balance. Moreover, its carboxyl group may help by forming the light emitting species SrOH, BaOH, and CuOH in the gas phase.^[3] SrOH emits light with the wavelengths 605 nm, 646 nm (orange) and 659 nm, 668 nm, 682 nm (red). BaOH emits at 487 nm and 512 nm (blue-green, green) and CuOH is also able to emit green light (525–555 nm).^[3, 4] This is true also for **5**, which contains in addition an energetic nitrimino group and can therefore be deprotonated twice.

The color performances and combustion behavior in the flame of a BUNSEN burner of all pyrotechnically interesting compounds of **4** and **5** were investigated with regard to their possible application as colorants in pyrotechnic compositions. Besides that, the solubilities in H₂O of all mentioned salts were determined at ambient temperature.

5.1 Results and Discussion

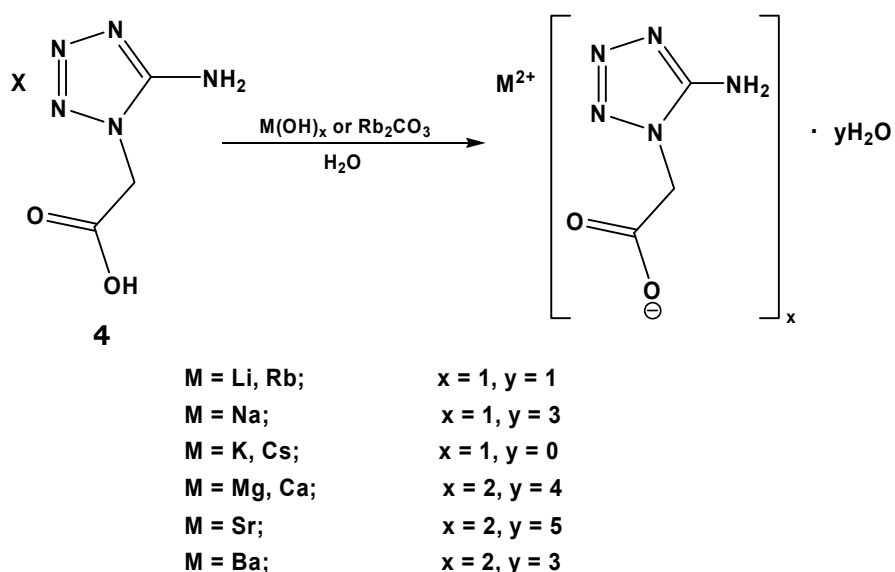
5.1.1 Syntheses

The first synthetic step is the alkylation of 5-aminotetrazole (**5-At**) with chloroacetic acid (Scheme 5.1). This procedure is known in literature.^[1] In contrast to the alkylation of **5-At** with 1-chloroethanol, 1-carboxymethyl-5-aminotetrazole (**4**) can be obtained as main product in yields above 50 %.



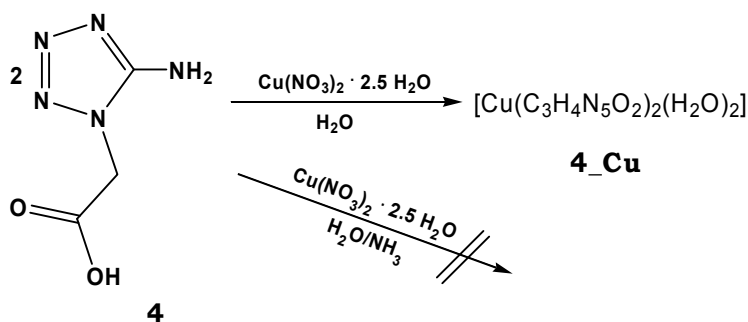
Scheme 5.1 Alkylation of **5-At** with chloroacetic acid.

The salts lithium 2-(5-aminotetrazol-1-yl)-acetate monohydrate (**4_Li**), sodium 2-(5-aminotetrazol-1-yl)-acetate trihydrate (**4_Na**), potassium 2-(5-aminotetrazol-1-yl)-acetate (**4_K**), rubidium 2-(5-aminotetrazol-1-yl)-acetate monohydrate (**4_Rb**), cesium 2-(5-aminotetrazol-1-yl)-acetate (**4-Cs**), magnesium 2-(5-aminotetrazol-1-yl)-acetate tetrahydrate (**4_Mg**), calcium 2-(5-aminotetrazol-1-yl)-acetate tetrahydrate (**4_Ca**), strontium 2-(5-aminotetrazol-1-yl)-acetate pentahydrate (**4_Sr**), and barium 2-(5-aminotetrazol-1-yl)-acetate trihydrate (**4_Ba**) were prepared by deprotonation of **4** with the corresponding hydroxides or carbonates (Scheme 5.2). H₂O was used as solvent. After crystallization from H₂O, all salts of **4** could be obtained in high yields.



Scheme 5.2 Preparation of the salts of **4**.

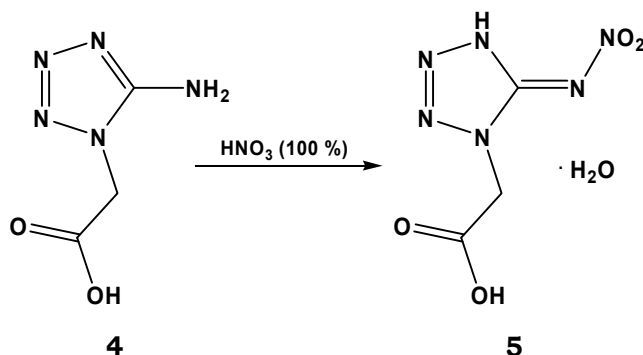
4 was also reacted with copper(II) nitrate pentahemihydrate in H₂O and aqueous ammonia solution. If aqueous ammonia solution was used, only a violet precipitate was obtained. Its characterization *via* elemental analysis offered no convincing result for the determining of a reasonable composition. It is assumed, that several copper(II) complexes were formed.



Scheme 5.3 Preparation of **4_Cu**.

In the case of using H₂O as solvent, a green precipitate was formed immediately after combining the dissolved copper(II) nitrate with a solution of **4** in H₂O (Scheme 5.3). The results of elemental analysis lead to the conclusion, that the copper(II) complex diaqua copper(II) 2-(5-aminotetrazol-1-yl)-acetate (**4_Cu**) was exclusively formed.

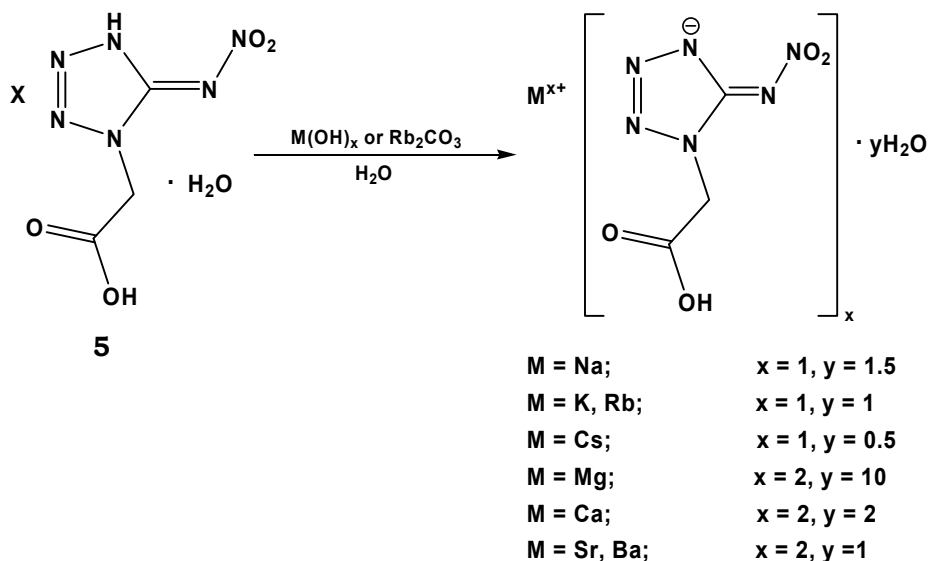
To obtain 1-carboxymethyl-5-nitriminetrazole monohydrate (**5**), **4** was nitrated using 100 % nitric acid (Scheme 5.4), the procedure of which is well known in the literature.^[5, 6] Compound **4** is slowly added to an ice-cooled solution of HNO₃ (100 %) and stirred for 17 hours in an open beaker glass. The colorless solution is poured onto ice and then stored at ambient temperature until colorless crystals of 1-carboxymethyl-5-nitriminetrazole monohydrate (**5**) are formed.



Scheme 5.4 Nitration of **4**.

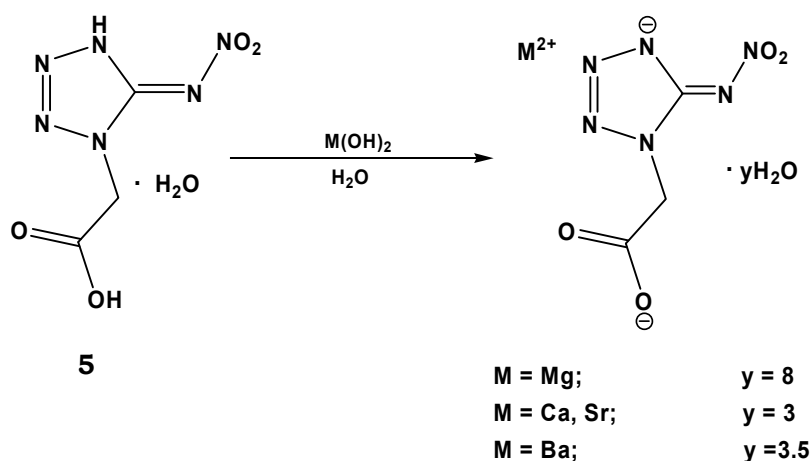
For preparation of the alkali metal salts of **5**, the compound was dissolved in H₂O and the corresponding hydroxides were added. In the case of preparing rubidium 1-carboxymethyl-5-nitriminetrazolate monohydrate (**5_Rb**), rubidium carbonate was used as base. The suspension was heated until it became a clear solution. Recrystallization from H₂O yielded sodium 1-carboxymethyl-5-nitriminetrazolate trihemihydrate (**5_Na**), potassium 1-carboxymethyl-5-nitriminetrazolate monohydrate (**5_K**), **5_Rb**, and cesium 1-carboxymethyl-5-nitriminetrazolate hemihydrate (**5-Cs**) (Scheme 5.5). The lithium salt of **5** could not be obtained as pure compound, via deprotonation of **5** neither using lithium hydroxide nor carbonate in H₂O or methanol. Besides that, it was tried to precipitate the lithium salt of **5** from the reaction solution of by fresh prepared **5** by adding lithium hydroxide until the solution became alkaline. In this case only lithium nitrate and carbonate were obtained. No

further attempts were undertaken, because these results lead to the assumption, that the lithium salt of **5** is highly soluble in water and therefore useless for the application as colorant in pyrotechnic compositions.



Scheme 5.5 Preparation of the alkali metal salts of **5** and **5_Mg1**, **5_Ca1**, **5_Sr1**, and **5_Ba1**.

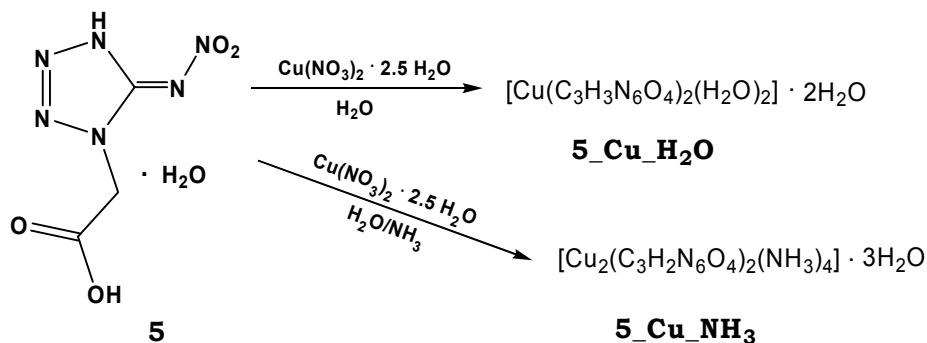
If **5** is reacted with hydroxides of the alkaline earth metals magnesium, calcium, strontium and barium in a molar ratio of 2:1 in H₂O, magnesium 1-carboxymethyl-5-nitriminotetrazolate decahydrate (**5_Mg1**), calcium 1-carboxymethyl-5-nitriminotetrazolate dihydrate (**5_Ca1**), strontium 1-carboxymethyl-5-nitriminotetrazolate monohydrate (**5_Sr1**), and barium 1-carboxymethyl-5-nitriminotetrazolate monohydrate (**5_Ba1**) were obtained (Scheme 5.5). The monoanion of **5** is present in these compounds. Analog to the alkali metal salts of **5**, the tetrazole ring is deprotonated and not the carboxy residue. For further information see chapter 5.1.2.



Scheme 5.6 Preparation of the salts **5_Mg2**, **5_Ca2**, **5_Sr2**, and **5_Ba2**.

To obtain salts with dianion 2-(5-nitriminotetrazolate)-acetate, **5** is reacted with the corresponding alkaline earth metal hydroxides in a molar ratio of 1:1 using H₂O as solvent (Scheme 5.6). Magnesium 2-(5-nitriminotetrazolate)-acetate octahydrate (**5_Mg2**), calcium

2-(5-nitriminetrazolate)-acetate trihydrate (**5_Ca2**), strontium 2-(5-nitriminetrazolate)-acetate trihydrate (**5_Sr2**) as well as barium 2-(5-nitriminetrazolate)-acetate heptahemihydrate (**5_Ba2**) were obtained. All salts of **5** mentioned were recrystallized from H₂O.



Scheme 5.7 Preparation of the copper(II) compounds **5_Cu_H₂O** and **5_Cu_NH₃**.

The copper(II) compound *trans*-[diaqua-bis(1-carboxymethyl-5-nitriminetrazolato-*N*₄,*O*₁) copper(II)] dihydrate (**5_Cu_H₂O**) was prepared with copper(II) nitrate pentahemihydrate in H₂O. After a few hours at ambient temperature green crystals of **5_Cu_H₂Oa** were obtained from the reaction solution and filtered off. From the residual solution blue crystals (**5_Cu_H₂Ob**) with analogous composition, according to the result of X-ray diffraction, as compared to that of the green crystals, were grown. Elemental analysis confirmed the same composition of the green and blue crystals. However, some differences in their IR-spectra can be observed.

For the preparation of bis[diammine 2-(5-nitriminetrazolato-*N*₄,*O*₁)-acetato-*O*₄-copper(II)] trihydrate (**5_Cu_NH₃**) a diluted aqueous ammonia solution (12 %) is added to a solution of **5** and copper(II) nitrate pentahemihydrate in H₂O (Scheme 5.7). Dark blue crystals of **5_Cu_NH₃** formed after storing the dark blue solution at ambient temperature for a few days.

5.1.2 Molecular Structures

After recrystallization from H₂O, single crystals of **4**, **4_Li**, **4_Na**, **4_K**, **4_Rb**, **4_Cs**, **4_Mg**, **4_Ca**, **4_Sr**, **4_Ba**, **5_K**, **5_Rb**, **5_Mg1**, **5_Mg2**, **5_Ca1**, **5_Ca2**, **5_Sr1**, **5_Sr2**, and **5_Ba1** suitable for X-ray diffraction could be obtained. Single crystals of **5**, **5_Cu_H₂Oa**, **5_Cu_H₂Ob**, as well as **5_Cu_NH₃** formed directly from the reaction solution. All relevant data and parameters of the X-ray measurements and refinements are given in Appendixes IV and V.

1-Carboxymethyl-5-aminotetrazole (**4**) crystallizes in the orthorhombic space group *Pbca* with eight molecules per unit cell. Its density of 1.660 g/cm³ is comparably high to other *N*₁-alkylated 5-aminotetrazole derivatives, like 1-(2-hydroxyethyl)-5-aminotetrazole (**1-OH**) with a density of 1.497 g/cm³ or 1-(2-chloroethyl)-5-aminotetrazole (**1-Cl**) with a density of 1.547 g/cm³.^[5a, 6]

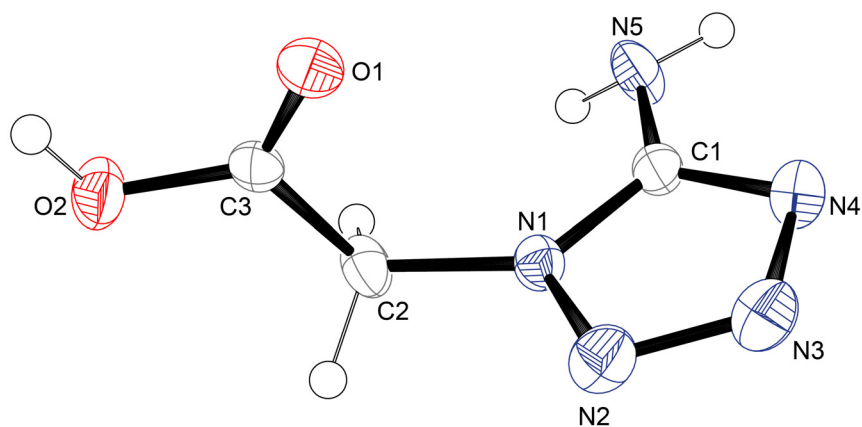


Figure 5.1 Molecular unit of **4**. Hydrogen atoms are shown as spheres of arbitrary radius and thermal displacements are set at 50 % probability. Geometries: distances (Å) N1–N2 1.366(2), N2–N3 1.291(2), N3–N4 1.366(2), N1–C1 1.341(2), N4–C1 1.324(2), C1–N5 1.350(2), N1–C2 1.462(2), C2–C3 1.505(2), O1–C3 1.213(2), O2–C3 1.306(2); angles (°) N1–C1–N4 108.0(2), N1–C1–N5 125.2(2), N5–C1–N4 126.1(2), C1–N4–N3 106.3(1), N1–N2–N3 106.0(1), N2–N3–N4 110.9(1), N1–C2–C3 111.6(1), N2–N1–C2 120.2(1), C1–N1–N2 108.7(1), C1–N1–C2 130.7(1), O1–C3–C2 123.4(1), O2–C3–C2 110.9(1), O1–C3–O2 125.7(2); torsion angles (°) N3–N4–C1–N1 0.5(2), N2–N1–C1–N4 -0.6(2), C2–N1–C1–N4 171.5(2), N2–N1–C1–N5 -179.1(2), C2–N1–C1–N5 -7.1(3), N4–N3–N2–N1 -0.1(2), C1–N1–N2–N3 0.4(2), C2–N1–N2–N3 -172.6(1), C1–N4–N3–N2 -0.2(2), C1–N1–C2–C3 -96.9(2), N2–N1–C2–C3 74.4(2), O1–C3–C2–N1 10.0(2), O2–C3–C2–N1 -169.9(1).

Bond lengths and angles of the aminotetrazole ring are comparable to those of other N1-alkylated 5-aminotetrazole derivatives.^[5a, 6]

The packing of **4** is characterized by zig-zag layers along the *c* axis. These are connected through two types of hydrogen bonds. In each case the nitrogen atom N5 is the donor atom, while the acceptor atoms are N3 and O1 (N5–H5b···N3ⁱⁱ: 0.83 Å, 2.42 Å, 3.25 Å, 175.4°; N5–H5a···O1ⁱⁱⁱ: 0.91 Å, 2.07 Å, 2.96 Å, 168.5°; ⁱⁱ) *x*-1/2, -*y*+1/2, -*z*, ⁱⁱⁱ) -*x*+1, *y*-1/2, -*z*+1/2). Within the layers the molecules are connected through hydrogen bonds between O2 and N4 (O2–H2···N4ⁱ: 0.84 Å, 1.81 Å, 2.63 Å, 166.7°; ⁱ) *x*, -*y*+1/2, *z*+1/2). Thus, altogether three different hydrogen bonds are observed.

Lithium 2-(5-aminotetrazol-1-yl)-acetate monohydrate (**4-Li**) crystallizes with four molecular units per unit cell in the monoclinic space group *P*2₁/*c* (Figure 5.2). Its density of 1.608 g/cm³ is slightly lower than the one of **4**. Each lithium atom is coordinated by the atoms O1^{*i*}, O2^{*ii*}, O3 and O3^{*iii*} forming a distorted tetrahedron. Within these tetrahedra the lithium atoms are located closer to the area formed by O1^{*i*}, O2^{*ii*} and O3^{*iii*}.

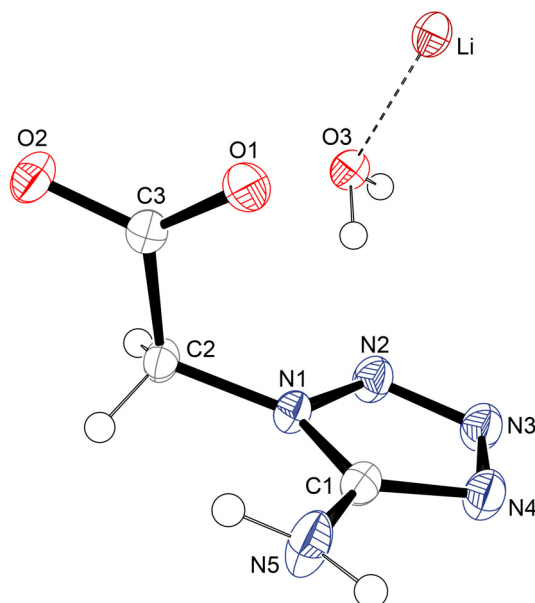


Figure 5.2 Molecular unit of **4_Li**. Hydrogen atoms are shown as spheres of arbitrary radius and thermal displacements are set at 50 % probability. Selected geometries: distances (Å) N1–N2 1.356(2), N2–N3 1.289(1), N3–N4 1.358(2), N1–C1 1.345(2), N4–C1 1.331(2), C1–N5 1.341(2), O1–C3 1.239(2), O2–C3 1.259(1), N1–C2 1.454(2), Li–O1 i 1.920(2), Li–O2 ii 1.925(2), Li–O3 1.971(3), Li–O3 iii 2.003(2); angles (°) N1–C1–N4 108.3(1), N1–C1–N5 125.3(1), N4–C1–N5 126.4(1), O1–C3–C2 118.7(1), O2–C3–C2 115.3(1), O1–C3–O2 126.0(1), O1 i –Li–O3 105.5(1), O2 ii –Li–O3 110.6(1), O3–Li–O3 iii 107.0(1), Li–O3–Li i 117.79(7); torsion angles (°) N1–C2–C3–O1 -4.2(2), N1–C2–C3–O2 176.4(1), Li iii –O1–C3–O2 -40.6(2), Li iii –O1–C3–C2 140.0(1); i) $x, -y+1/2, z-1/2$, ii) $-x+1, y-1/2, -z+1/2$, iii) $-x+1, y+1/2, -z+1/2$.

The shortest distance between two lithium atoms is 3.402(2) Å. This is much shorter than the distance found in lithium 1-(2-hydroxyethyl)-5-nitriminetetrazolate monohydrate (**1_Li**, chapter 2). The oxygen atom of the water molecule is connected to two different lithium atoms. This is also true for the oxygen atoms O1 and O2, whereby stacks of two opposed anions along the b axis are formed. These stacks are connected *via* the water molecules. Four different hydrogen bonds are observed. O3 acts twice as the donor atom (O3–H3a \cdots N2: 0.87 Å, 1.97 Å, 2.83 Å, 172.3°; O3–H3b \cdots O2 vi : 0.89 Å, 1.77 Å, 2.65 Å, 168.5°; vi) $x, -y-1/2, z-1/2$). The two other hydrogen bonds connect the aminotetrazole anions with each other. In each case N5 is the donor atom (N5–H5a \cdots N3 iv : 0.89 Å, 2.22 Å, 3.07 Å, 163.0°; N5–H5b \cdots N4 v : 0.88 Å, 2.11 Å, 2.97 Å, 165.7°; v) $x, -y+1/2, z+1/2$, iv) $-x+2, -y+1, -z+1$).

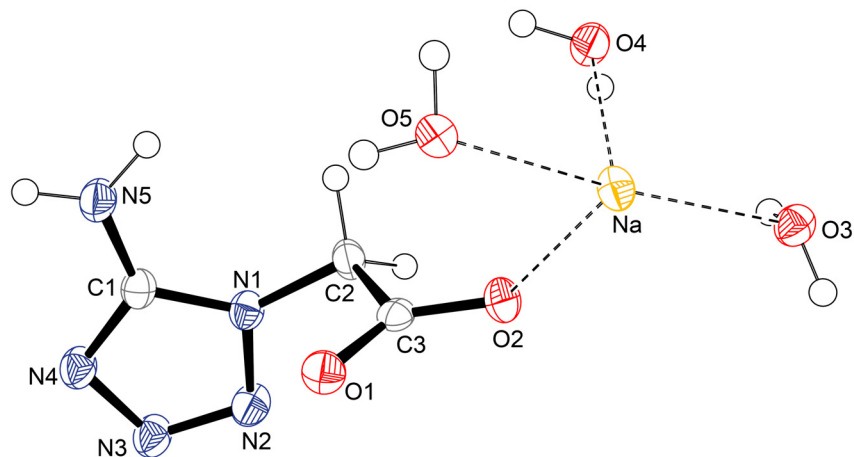


Figure 5.3 Molecular unit of **4_Na**. Hydrogen atoms are shown as spheres of arbitrary radius and thermal displacements are set at 50 % probability. Selected geometries: distances (Å) N1–N2 1.363(2), N2–N3 1.284(1), N3–N4 1.361(1), N1–C1 1.344(2), N4–C1 1.331(2), C1–N5 1.338(2), O1–C3 1.259(1), O2–C3 1.241(1), N1–C2 1.451(2), Na–O2 2.329(1), Na–O3 i 2.385(1), Na–O3 2.392(1), Na–O5 2.394(1), Na–O5 ii 2.434(1), Na–O4 2.468(1); angles (°) N1–C1–N4 108.4(1), N1–C1–N5 125.6(1), N4–C1–N5 126.0(1), O1–C3–C2 117.1(1), O2–C3–C2 115.8(1), O1–C3–O2 127.1(1), O2–Na–O3 92.05(3), O2–Na–O4 80.55(3), O2–Na–O5 94.20(4), O3–Na–O4 80.41(4), O3–Na–O5 173.74(4), O5–Na–O4 100.84(4), C3–O2–Na 132.20(8); torsion angles (°) N1–C2–C3–O1 –21.1(1), N1–C2–C3–O2 159.1(1), O3–Na–O2–C3 –172.1(1), O4–Na–O2–C3 –92.2(1), O5–Na–O2–C3 8.1(1); i $-x+1, -y, -z+1$, ii $-x+2, -y, -z+1$.

The molecular unit of sodium 2-(5-aminotetrazol-1-yl)-acetate trihydrate (**4_Na**) is depicted in Figure 5.3. **4_Na** crystallizes in the triclinic space group $P\bar{1}$ with two molecular units per unit cell and a density of 1.611 g/cm³. This value is higher than for **4_Li**, whereas smaller than the one of **4**. The sodium atoms are sixfold coordinated by the atoms O2, O3, O4, O5, O3 i , and O5 ii (i $-x+1, -y, -z+1$, ii $-x+2, -y, -z+1$). The shortest distance between two sodium atoms is 3.358 Å. The packing of **4_Na** is characterized by stacks consisting of two molecular units, which are located opposite to each other. These ‘dimers’ are connected along the a axis by hydrogen bonds involving the oxygen atoms O3 and O5 of the water molecules, coordinating to two different sodium atoms. Seven different hydrogen bonds can be observed.

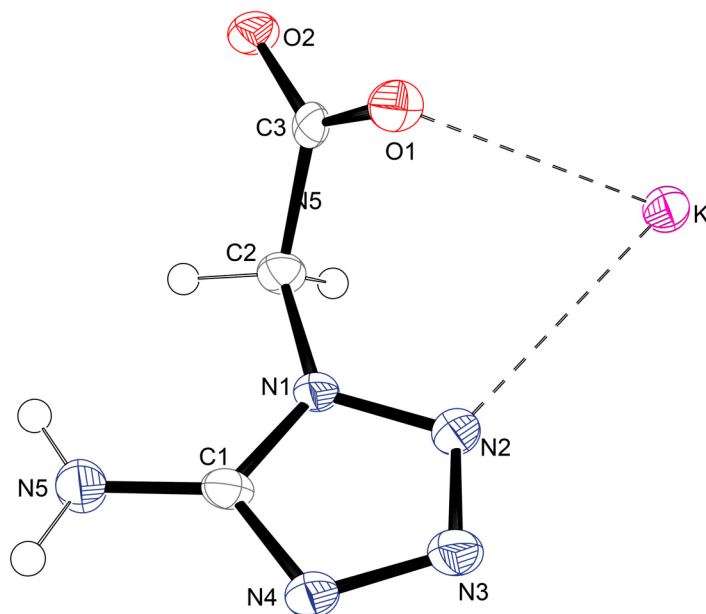


Figure 5.4 Molecular unit of **4_K**. Hydrogen atoms are shown as spheres of arbitrary radius and thermal displacements are set at 50 % probability. Selected geometries: distances (Å) N1–N2 1.359(2), N2–N3 1.292(2), N3–N4 1.359(2), N1–C1 1.349(3), N4–C1 1.333(2), C1–N5 1.330(3), O1–C3 1.241(2), O2–C3 1.251(2), N1–C2 1.450(2), K–O2*i* 2.695(2), K–O1*ii* 2.709(2), K–O2*iii* 2.742(2), K–O1 2.814(2), K–O2*iv* 2.821(2), K–N2 2.877(2), K–O1*iv* 2.918(2); angles (°) N1–C1–N4 107.9(2), N1–C1–N5 125.9(2), N4–C1–N5 126.2(2), O1–C3–C2 119.3(2), O2–C3–C2 114.2(2), O1–C3–O2 126.5(2), O1–K–N2 65.19(5); torsion angles (°) N1–C2–C3–O1 17.3(3), N1–C2–C3–O2 –165.0(2), N2–K–O1–C3 –71.6(1); *i*) $x, -y+1/2, z-1/2$, *ii*) $x, y+1, z$, *iii*) $x, -y-1/2, z-1/2$, *iv*) $-x+2, y+1/2, -z+1/2$.

Potassium 2-(5-aminotetrazol-1-yl)-acetate (**4_K**) crystallizes in analogy to **4_Li** in the monoclinic space group $P2_1/c$ with four molecular units per unit cell (Figure 5.4). Its density of 1.824 g/cm³ is significantly higher than the one of **4_Na** or **4_Li**. This might be, because **4_K** does not contain any crystal water. The potassium atoms are sevenfold coordinated by the atoms O2*i*, O1*ii*, O2*iii*, O1, O2*iv*, O1*iv* and N2 with maximum distances of 3.0 Å. Two hydrogen bonds are observed. In each case, N5 is the donor atom (N5–H5a···O2*v*: 0.91 Å, 1.96 Å, 2.86 Å, 176°; N5–H5b···N2*vi*: 0.67 Å, 2.40 Å, 3.07 Å, 170°; *v*) $x+1, -y+1, -z+1$ *vi*) $-x, -y, -z+1$).

The packing of **4_K** is characterized by layers along the *b* axis. These layers are connected *via* the above mentioned hydrogen bonds.

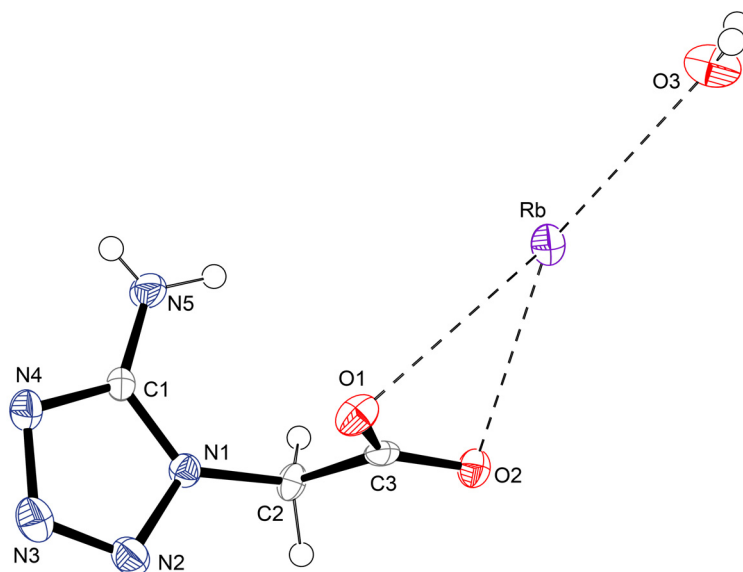


Figure 5.5 Molecular unit of **4_Rb**. Hydrogen atoms are shown as spheres of arbitrary radius and thermal displacements are set at 50 % probability. Selected geometries: distances (Å) N1–N2 1.374(4), N2–N3 1.290(4), N3–N4 1.370(4), N1–C1 1.349(4), N4–C1 1.326(4), C1–N5 1.343(4), O1–C3 1.262(4), O2–C3 1.247(4), N1–C2 1.443(4), Rb–O1*i* 2.982(3), Rb–O2 2.983(3), Rb–O3 2.984(3), Rb–O1*ii* 3.027(4), Rb–O3*iii* 3.048(3), Rb–N4*iv* 3.050(3), Rb–O2*i* 3.124(2), Rb–N2*ii* 3.237(3), Rb–O1 3.260(3); angles (°) N1–C1–N4 109.3(3), N1–C1–N5 123.8(3), N4–C1–N5 126.9(3), O1–C3–C2 118.3(3), O2–C3–C2 115.4(3), O1–C3–O2 126.3(3), O2–Rb–O1 41.7(1), O3–Rb–O1 141.1(1), O2–Rb–O3 154.7(1); torsion angles (°) N1–C2–C3–O1 –3.8(4), N1–C2–C3–O2 176.5(3), O1–Rb–O2–C3 21.2(2), O2–Rb–O1–C3 –21.2(2), O3–Rb–O1–C3 –162.0(2), O3–Rb–O2–C3 132.4(2), Rb–O1–C3–O2 45.6(3), Rb–O1–C3–C2 –134.0(3), Rb–O2–C3–O1 –50.4(3), Rb–O2–C3–C2 129.2(2); *i* $-x+1, -y+1, -z+2$, *ii* $x+1, y, z$, *iii* $-x+2, -y+1, -z+2$, *iv* $-x+1, -y+1, -z+1$.

Like **4_Na**, rubidium 2-(5-aminotetrazol-1-yl)-acetate monohydrate (**4_Rb**) crystallizes in the triclinic space group $P\bar{1}$ with two molecular units per unit cell (Figure 5.5). Its density of 2.137 g/cm³ is quite high. In **4_Rb** the rubidium atoms are ninefold coordinated by the atoms O1*i*, O2, O3, O1*ii*, O3*iii*, N4*iv*, O2*i*, N2*ii*, and O1 with a maximum distance of 3.3 Å (*i*) $-x+1, -y+1, -z+2$, *ii*) $x+1, y, z$, *iii*) $-x+2, -y+1, -z+2$). Four different hydrogen bonds can be observed. Two of them connect the crystal water molecule with the aminotetrazole anion with O3 as donor and O2 as acceptor (O3–H3a··O2*v*: 0.87 Å, 1.96 Å, 2.82 Å, 169°, O3–H3b··O2*iii*: 0.69 Å, 2.66 Å, 3.22 Å, 140°; *iii*) $-x+2, -y+1, -z+2$, *v*) $x, y+1, z$). The others are between different aminotetrazole anions with N5 as donor atom (N5–H5a··N3*ii*: 0.91 Å, 2.14 Å, 3.04 Å, 168°, N5–H5b··O1*iv*: 0.73 Å, 2.17 Å, 2.87 Å, 171°; *ii*) $x+1, y, z$, *iv*) $-x+1, -y+1, -z+1$). The shortest distance between two rubidium atoms observed is 3.809(2) Å. This is quite short, because the ionic radius of ninefold coordinated rubidium cations is 1.77 Å.^[7]

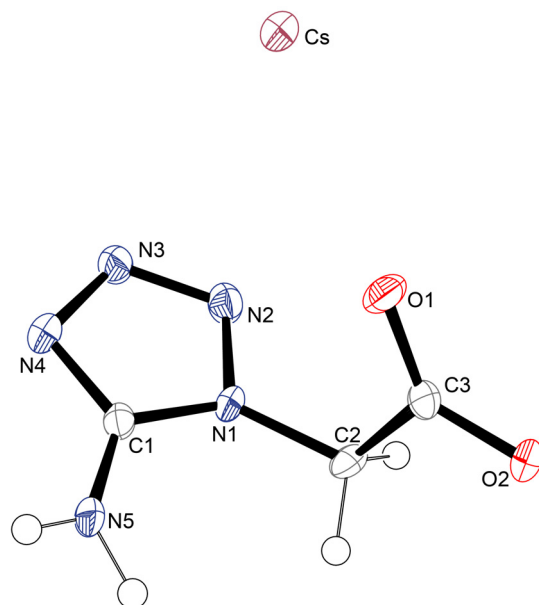


Figure 5.6 Molecular unit of **4-Cs**. Hydrogen atoms are shown as spheres of arbitrary radius and thermal displacements are set at 50 % probability. Selected geometries: distances (Å) N1–N2 1.365(6), N2–N3 1.314(6), N3–N4 1.356(6), N1–C1 1.332(7), N4–C1 1.323(6), C1–N5 1.353(7), O1–C3 1.244(6), O2–C3 1.254(6), N1–C2 1.461(6), Cs–O1 2.969(3), Cs–O2*i* 3.091(4), Cs–O1*ii* 3.113(4), Cs–O2*ii* 3.199(4), Cs–N3*iii* 3.250(4), Cs–N2*iv* 3.346(5), Cs–N4*iii* 3.458(4), Cs–N3*v* 3.467(5); angles (°) N1–C1–N4 109.5(4), N1–C1–N5 123.9(5), N4–C1–N5 126.5(5), O1–C3–C2 118.4(4), O2–C3–C2 114.7(4), O1–C3–O2 126.9(5), O1–Cs–N2 55.8(1), O1–Cs–N3 70.7(1), N2–Cs–N3 21.0(1); torsion angles (°) N1–C2–C3–O1 –11.0(7), N1–C2–C3–O2 170.4(5), N2–Cs–O1–C3 32.3(8), N3–Cs–O1–C3 48.8(8), Cs–O1–C3–O2 133.5(6); *i*) $-x+1, -y+1, -z$, *ii*) $-x, -y+1, -z$, *iii*) $-x, -y, -z$, *iv*) $x-1, y, z$, *v*) $-x+1, -y, -z$.

The molecular unit of cesium 2-(5-aminotetrazol-1-yl)-acetate (**4-Cs**) is depicted in Figure 5.6. It crystallizes analogously to **4-Na** and **4-Rb** in the triclinic space group $P\bar{1}$ with two molecular units per unit cell. The calculated density of 2.555 g/cm³ is the highest one of the salts of **4** here described. The reason for this are the absence of crystal water in **4-Cs** and the comparably huge dimension of the cesium cations, which require much space. Therefore, the packing is very dense and such a high density can be achieved. The cesium cations are eightfold coordinated by the atoms O1, O2*i*, O1*ii*, O2*ii*, N3*iii*, N2*iv*, N4*iii*, and N3*v* (*i*) $-x+1, -y+1, -z$, *ii*) $-x, -y+1, -z$, *iii*) $-x, -y, -z$, *iv*) $x-1, y, z$, *v*) $-x+1, -y, -z$), considering distances up to 3.5 Å. Analogous to **4-K** two hydrogen bonds with N5 as donor atom can be observed, connecting the aminotetrazole anions.

Magnesium 2-(5-aminotetrazol-1-yl)-acetate tetrahydrate (**4-Mg**) crystallizes in the triclinic space group $P\bar{1}$ with one molecular unit per unit cell. Its density of 1.744 g/cm³ is higher than the one of **4-Na**. The magnesium cations are sixfold coordinated by the four water molecules as well as the oxygen atom O2 of each aminotetrazole anion forming a regular octahedron (Figure 5.7).

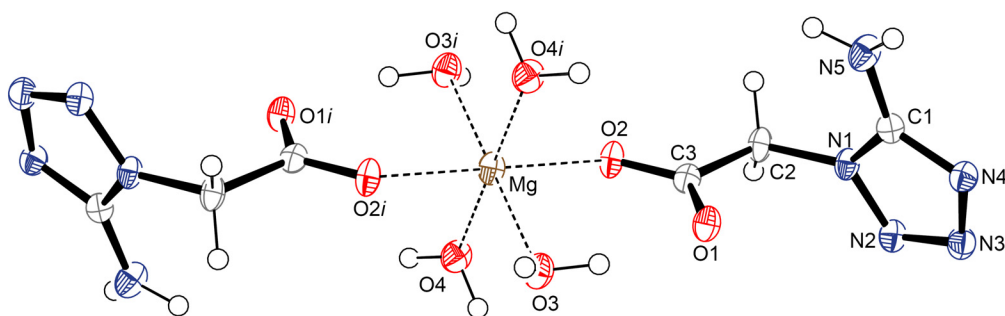


Figure 5.7 Molecular unit of **4_Mg**. Hydrogen atoms are shown as spheres of arbitrary radius and thermal displacements are set at 50 % probability. Selected geometries: distances (Å) N1–N2 1.368(2), N2–N3 1.293(2), N3–N4 1.371(2), N1–C1 1.347(2), N4–C1 1.329(2), C1–N5 1.336(2), O1–C3 1.264(2), O2–C3 1.248(2), N1–C2 1.450(2), Mg–O2*i* 2.064(1), Mg–O4 2.075(1), Mg–O3 2.103(2); angles (°) N1–C1–N4 108.5(2), N1–C1–N5 124.4(2), N4–C1–N5 127.1(2), O1–C3–C2 118.9(2), O2–C3–C2 115.6(2), O1–C3–O2 125.4(2), O2*i*–Mg–O4 91.81(5), O4–Mg–O3 92.33(6); torsion angles (°) N1–C2–C3–O1 –3.6(2), N1–C2–C3–O2 176.6(2), Mg–O2–C3–O1 13.5(3); *i* $-x, -y+1, -z+1$.

Two hydrogen bonds connect the aminotetrazole anions with each other. The nitrogen atom of the amino group is the donor atom, the nitrogen atom N3 of the tetrazole ring and the oxygen atom O1 of the carboxy group act as acceptors (N5–H1a···N3*ii*: 0.88 Å, 2.19 Å, 3.06 Å, 167°; N5–H1b···O1*iii*: 0.90 Å, 1.93 Å, 2.84 Å, 176°; *ii*) $x-1, y, z$, *iii*) $-x, -y+1, -z$). The oxygen atoms O3 and O4 of the crystal water molecules act as donors for the other four hydrogen bonds observed. Acceptors are again the nitrogen atom N3 and the oxygen atom O1 (O4–H4b···N4*iv*: 0.89 Å, 2.03 Å, 2.91 Å, 167°; O4–H4a···O1*v*: 0.87 Å, 1.87 Å, 2.73 Å, 168°; O3–H3a···O1*vi*: 0.90 Å, 1.87 Å, 2.72 Å, 157°; O3–H3b···N2*vii*: 0.85 Å, 2.29 Å, 3.10 Å, 160°; *iv*) $x, y, z+1$, *v*) $-x+1, -y+1, -z+1$, *vii*) $x+1, y, z$, *vii*) $x, y+1, z$).

Calcium 2-(5-aminotetrazol-1-yl)-acetate tetrahydrate (**4_Ca**) crystallizes in the monoclinic space group $C2/c$. Its unit cell contains eight molecular units. Interestingly, its density of 1.742 g/cm³ is slightly lower than the one of **4_Mg**. The calcium atoms are sevenfold coordinated by the atoms O1, O2, O3, O5, O6, O7, and O8 (Figure 5.8).

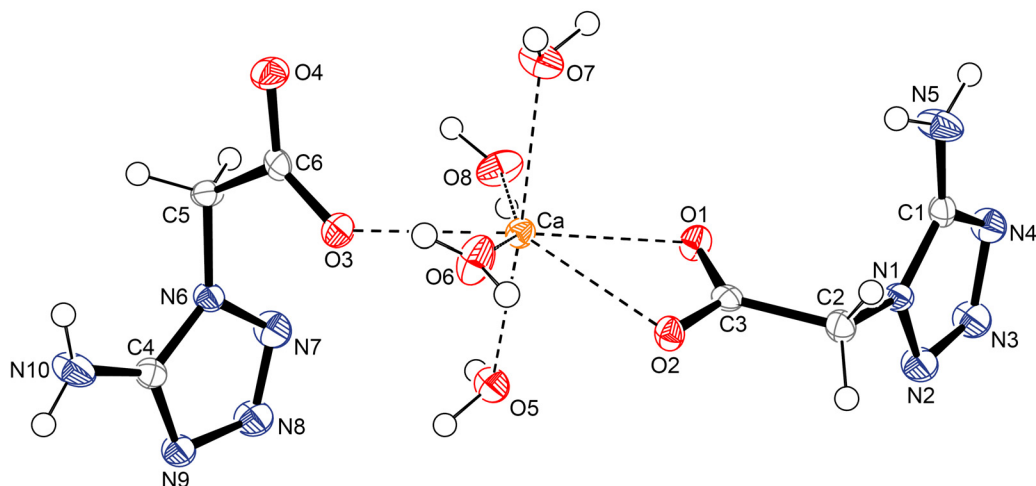


Figure 5.8 Molecular unit of **4_Ca**. Hydrogen atoms are shown as spheres of arbitrary radius and thermal displacements are set at 50 % probability. Selected geometries: distances (Å) N1–N2 1.360(2), N2–N3 1.283(2), N3–N4 1.361(2), N1–C1 1.345(2), N4–C1 1.326(2), C1–N5 1.331(2), O1–C3 1.253(2), O2–C3 1.259(2), N1–C2 1.448(2), Ca–O7 2.327(2), Ca–O6 2.372(2), Ca–O3 2.374(1), Ca–O8 2.376(2), Ca–O2 2.437(1), Ca–O5 2.445(2), Ca–O1 2.558(2); angles (°) N1–C1–N4 108.3(2), N1–C1–N5 125.1(2), N4–C1–N5 126.7(2), O1–C3–C2 121.4(2), O2–C3–C2 115.2(2), O1–C3–O2 123.5(2), O7–Ca–O6 84.10(7), O7–Ca–O3 95.32(6), O6–Ca–O3 75.19(6), O7–Ca–O8 84.65(6), O6–Ca–O8 155.47(6), O3–Ca–O8 84.25(6), O7–Ca–O2 108.86(5), O6–Ca–O2 77.73(6), O3–Ca–O2 141.30(4), O8–Ca–O2 126.64(6), O7–Ca–O5 163.91(6), O6–Ca–O5 110.49(6), O3–Ca–O5 82.46(6), O8–Ca–O5 79.27(6), O2–Ca–O5 81.72(5), O7–Ca–O1 93.15(6), O6–Ca–O1 126.28(6), O3–Ca–O1 157.71(4), O8–Ca–O1 76.05(5), O2–Ca–O1 52.52(4), O5–Ca–O1 83.70(6); torsion angles (°) N1–C2–C3–O1 –9.4(2), N1–C2–C3–O2 172.15(1), O1–Ca–O3–C6 –70.5(2), O5–Ca–O3–C6 –122.6(2), O1–Ca–O2–C3 3.88(8), O5–Ca–O2–C3 92.3(1), O3–Ca–O2–C3 159.08(9), Ca–O1–C3–O2 7.2(2).

The packing in **4_Ca** is characterized by layers consisting of the molecular units along the *a* axis. These are connected by hydrogen bonds between the aminotetrazole anions (N3, N4, N5, N8, N9, N10, O1) themselves as well as the crystal water molecules (O5, O7). Further observed hydrogen bonds connect the layers with each other (Table 5.1). In this case, the donor as well as the acceptor atoms are oxygen atoms.

Table 5.1 Hydrogen bonds in **4_Ca** (*i*) $-x, y, -z+1/2$, (*ii*) $x, -y, z-1/2$, (*iii*) $x, y+1, z$, (*iv*) $-x+1/2, -y-1/2, -z+1$, (*v*) $x, y-1, z$, (*vi*) $x, -y+1, z+1/2$).

D–H···A	D–H [Å]	H···A [Å]	D···A [Å]	<(DHA) [°]
O5–H5f···N9 <i>i</i>	0.89(2)	1.88(2)	2.768(2)	176(2)
O8–H8b···O2 <i>ii</i>	0.92(2)	1.86(3)	2.780(2)	176(2)
N10–H10b···O3 <i>i</i>	0.86(2)	2.21(2)	3.028(2)	160(2)
N5–H5c···N3 <i>iii</i>	0.86(2)	2.13(2)	2.978(3)	168(2)
O6–H6b···O5 <i>iii</i>	0.74(2)	2.21(2)	2.944(3)	171(2)
O7–H7a···O1 <i>iii</i>	0.83(2)	2.00(2)	2.821(3)	171(2)
O7–H7b···N4 <i>iv</i>	0.88(2)	1.91(2)	2.790(2)	176(2)
O8–H8a···O4 <i>v</i>	0.83(2)	2.07(2)	2.830(3)	162(2)
N10–H10a···N8 <i>iii</i>	0.88(2)	2.07(2)	2.942(3)	171(2)
O6–H6a···O4 <i>vi</i>	0.93(3)	1.90(3)	2.821(2)	172(2)
N5–H5d···O1 <i>iv</i>	0.85(2)	2.33(2)	3.111(2)	153(2)
O5–H5e···O4 <i>v</i>	0.84(3)	2.33(3)	3.141(2)	161(2)
O5–H5e···O3 <i>v</i>	0.84(3)	2.63(3)	3.218(3)	128(2)

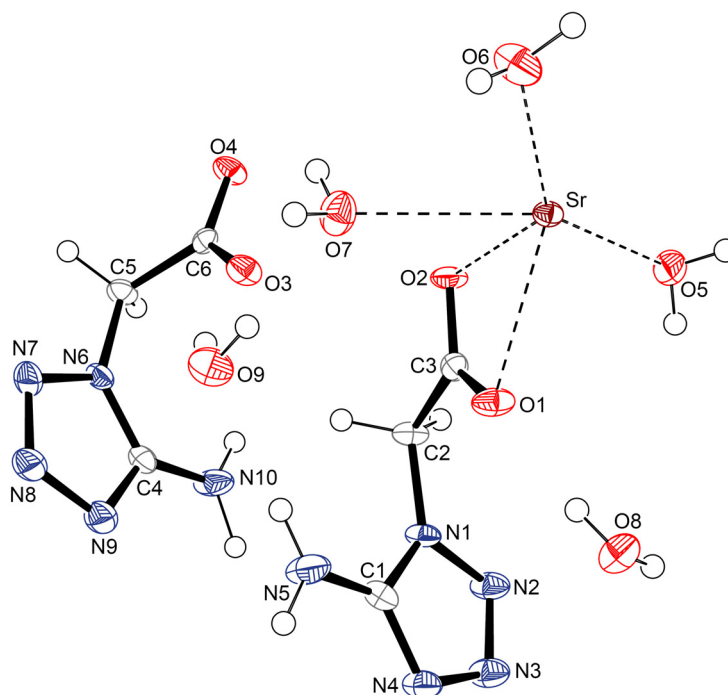


Figure 5.9 Molecular unit of **4_Sr**. Hydrogen atoms are shown as spheres of arbitrary radius and thermal displacements are set at 50 % probability. Selected geometries: distances (Å) N1–N2 1.360(3), N2–N3 1.289(3), N3–N4 1.361(3), N1–C1 1.360(3), N4–C1 1.330(3), C1–N5 1.447(3), O1–C3 1.252(3), O2–C3 1.242(3), N1–C2 1.447(3), Sr–O2*i* 2.489(2), Sr–O4*ii* 2.525(2), Sr–O6 2.574(2), Sr–O2 2.681(2), Sr–O5*i* 2.691(2), Sr–O1 2.701(2), Sr–O7 2.720(2), Sr–O4*i* 2.731(2), Sr–O3*i* 2.760(2); angles (°) N1–C1–N4 108.2(2), N1–C1–N5 125.0(3), N4–C1–N5 126.7(2), O1–C3–C2 120.0(2), O2–C3–C2 116.1(2), O1–C3–O2 123.9(2), O6–Sr–O2 135.35(7), O6–Sr–O5 142.57(7), O2–Sr–O5 67.86(6), O6–Sr–O1 144.53(7), O2–Sr–O1 48.26(5), O5–Sr–O1 72.29(6), O6–Sr–O7 74.12(7), O2–Sr–O7 69.96(6), O5–Sr–O7 137.76(7), O1–Sr–O7 78.35(6); torsion angles (°) N1–C2–C3–O1 -4.1(3), N1–C2–C3–O2 176.9(2), O6–Sr–O2–C3 -131.3(2), O5–Sr–O2–C3 84.8(2), O1–Sr–O2–C3 -0.8(1), O7–Sr–O2–C3 -93.0(2); *i*) -x+1, -y+1, -z+1, *ii*) -x+1, y, z.

Like **4_Mg**, strontium 2-(5-aminotetrazol-1-yl)-acetate pentahydrate (**4_Sr**) crystallizes in the triclinic space group $P\bar{1}$ with two molecular units per unit cell. Its density of 1.721 g/cm³ is extremely low, lower than the one of **4_Mg** or **4_Ca**. This is presumably the consequence of the five crystal water molecules (Figure 5.9). Only three of them are directly coordinated to the strontium ions. The two other crystal water molecules are located freely in the unit cell only connected by hydrogen bonds (Table 5.2). Therefore, closer packing is not possible. The strontium ion is ninefold coordinated by the oxygen atoms O2*i*, O4*ii*, O6, O2, O5*i*, O1, O7, O4*i*, and O3*i* (*i*) -x+1, -y+1, -z+1, *ii*) -x+1, y, z).

Table 5.2 Hydrogen bonds in **4_Sr** (*i*) $-x+1, -y+1, -z+1$, *iii*) $-x, -y, -z$, *iv*) $-x+2, -y+1, -z+1$, *v*) $-x+1, -y, -z+1$, *vi*) $x-1, y, z$, *vii*) $-x+1, -y, -z$, *viii*) $x+1, y+1, z$, *ix*) $-x+1, -y+1, -z$)

D-H...A	D-H [Å]	H...A [Å]	D...A [Å]	<(DHA) [°]
N10-H10b...N9 <i>iii</i>	1.00(3)	2.06(4)	3.057(4)	173(3)
O6-H6b...O8 <i>iv</i>	0.88(3)	1.93(3)	2.811(3)	176(3)
O7-H7a...O9 <i>v</i>	0.83(4)	2.14(4)	2.946(3)	162(3)
O7-H7b...O5 <i>i</i>	0.79(3)	2.16(3)	2.939(3)	167(3)
O9-H9b...O3	0.79(3)	2.04(3)	2.788(3)	158(3)
N10-H10a...O8 <i>vi</i>	0.88(3)	2.00(3)	2.869(3)	171(3)
N5-H1b...N4 <i>vii</i>	0.94(4)	2.03(4)	2.971(3)	172(3)
N5-H1a...O9	0.87(3)	2.12(3)	2.978(4)	172(3)
O5-H3a...N7 <i>viii</i>	0.81(4)	2.27(4)	3.006(3)	151(3)
O8-H8b...N2 <i>ix</i>	0.78(3)	2.14(3)	2.874(3)	156(3)
O5-H3b...N3 <i>ix</i>	0.83(4)	2.06(4)	2.871(3)	166(4)
O8-H8a...O1	0.83(3)	1.85(4)	2.667(3)	172(3)
O9-H9a...O7	0.87(3)	2.06(3)	2.918(3)	171(3)
O6-H6a...N8 <i>v</i>	0.70(4)	2.88(3)	2.876(3)	173(4)

Barium 2-(5-aminotetrazol-1-yl)-acetate trihydrate (**4_Ba**) crystallizes in the monoclinic space group $P2_1/m$ with two molecular units per unit cell. Its density of 2.107 g/cm³ is significantly higher than that of **4_Mg**, **4_Ca** and **4_Sr**.

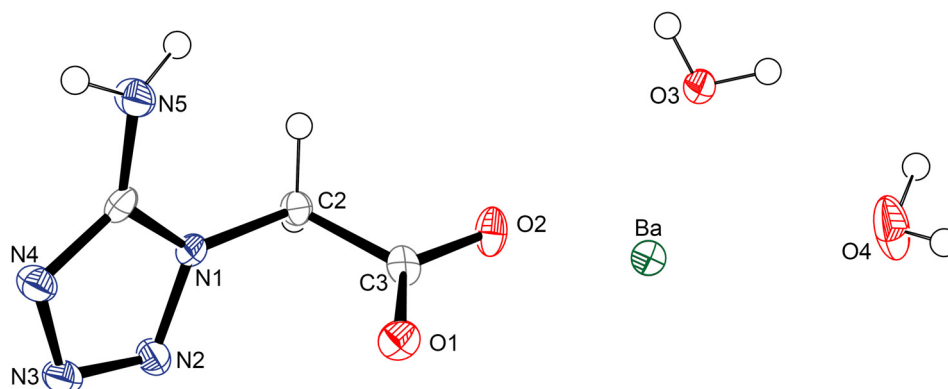


Figure 5.10 Asymmetric unit of **4_Ba**. Hydrogen atoms are shown as spheres of arbitrary radius and thermal displacements are set at 50 % probability. Selected geometries: distances (Å) N1-N2 1.367(3), N2-N3 1.293(3), N3-N4 1.365(4), N1-C1 1.347(4), N4-C1 1.326(4), C1-N5 1.340(4), O1-C3 1.245(4), O2-C3 1.252(3), N1-C2 1.454(4), Ba-O2*i* 2.710(3), Ba-O2*ii* 2.710(3), Ba-O4*iii* 2.769(3), Ba-O4 2.769(3), Ba-O2 2.873(3), Ba-O2*iii* 2.873(3), Ba-O3*i* 2.927(4), Ba-O3 2.936(4), Ba-O1 3.063(2), Ba-O1*iii* 3.063(2); angles (°) N1-C1-N4 108.6(3), N1-C1-N5 125.2(3), N4-C1-N5 126.1(3), O1-C3-C2 120.3(3), O2-C3-C2 114.3(3), O1-C3-O2 125.5(3), O2-Ba-O1 43.77(6), O3-Ba-O1 105.43(8), O4-Ba-O1 158.44(8), O2-Ba-O3 62.53(9), O4-Ba-O2 122.43(8), O4-Ba-O3 68.12(7); torsion angles (°) N1-C2-C3-O1 -3.2(4), N1-C2-C3-O2 178.7(3), O4-Ba-O1-C3 -72.2(3), O2-Ba-O1 C3 -14.4(2), O3-Ba-O1-C3 -2.9(2), O4-Ba-O2-C3 172.8(2); *i*) $x+1, y, z$, *ii*) $x+1, -y+1/2, z$, *iii*) $x, -y+1/2, z$.

The barium cations are tenfold coordinated by the oxygen atoms O2*i*, O2*ii*, O4*iii*, O4, O2, O2*iii*, O3*i*, O3, O1, and O1*iii* (*i*) $x+1, y, z$, *ii*) $x+1, -y+1/2, z$, *iii*) $x, -y+1/2, z$). Two hydrogen bonds between the aminotetrazole anions with N5 as donor can be observed (N5-H5b...N4*iv*: 0.83 Å, 2.15 Å, 2.98 Å, 175°; N5-H5a...N3*v*: 0.89 Å, 2.14 Å, 3.02 Å, 173°; *iv*) $-x+1, -y, -z+1$, *v*) $x, y, z+1$). Three further hydrogen bonds connect the crystal water molecules with the anion (O4-H4a...N2*vi*: 0.70 Å, 2.29 Å, 2.98 Å, 171°; O3-H3...O1*vii*: 0.82 Å,

2.02 Å, 2.84 Å, 171°; O4–H4b···O1*vii*: 0.99 Å, 1.89 Å, 2.84 Å, 160°; *vj*) x+1, -y+1/2, z+1, *vii*) x, -y+1/2, z+1).

The bond lengths and bonds angles of the aminotetrazole anion in the salts of **4** are all in the same range.

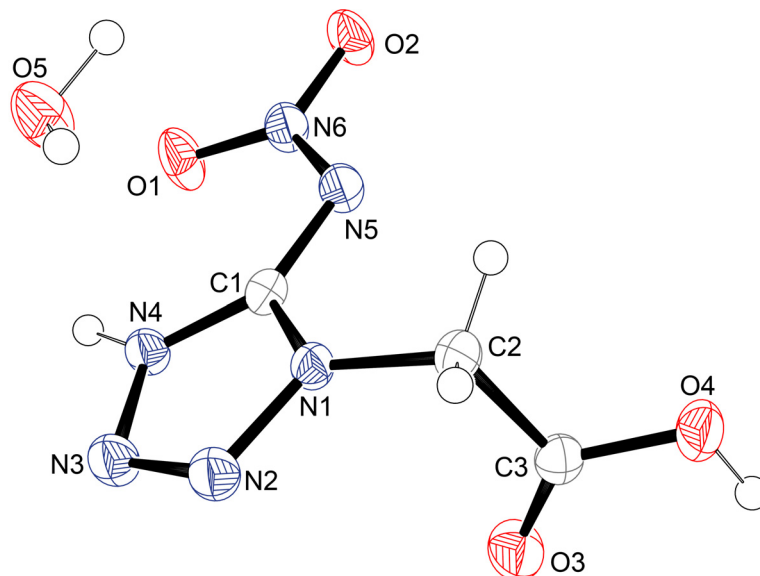


Figure 5.11 Molecular unit of **5**. Hydrogen atoms are shown as spheres of arbitrary radius and thermal displacements are set at 50 % probability. Geometries: distances (Å) N1–N2 1.358(2), N2–N3 1.281(2), N3–N4 1.361(2), N1–C1 1.353(2), N4–C1 1.337(2), C1–N5 1.341(2), N1–C2 1.458(2), N5–N6 1.338(2), O1–N6 1.248(1), N6–O2 1.252(2), C2–C3 1.513(2), O3–C3 1.204(2), O4–C3 1.321(2); angles (°) N1–C1–N4 104.3(1), N1–C1–N5 118.8(1), N5–C1–N4 137.0(1), C1–N4–N3 109.8(1), N1–N2–N3 107.6(1), N2–N3–N4 108.4(1), N1–C2–C3 110.0(1), N2–N1–C2 122.0(1), C1–N1–N2 109.9(1), N6–N5–C1 114.8(1), O1–N6–O2 121.1(1), O1–N6–N5 123.3(1), O2–N6–N5 115.6(1), C1–N1–C2 127.5(1), O3–C3–C2 123.5(1), O2–C3–C2 111.0(1), O3–C3–O4 125.4(1); torsion angles (°) N3–N4–C1–N1 0.8(2), N2–N1–C1–N4 -0.2(2), C2–N1–C1–N4 171.8(1), N2–N1–C1–N5 178.6(1), N3–N4–C1–N5 -177.7(2), C2–N1–C1–N5 -9.4(2), N4–N3–N2–N1 1.0(2), C1–N1–N2–N3 -0.5(2), C2–N1–N2–N3 -173.0(1), C1–N4–N3–N2 -1.2(2), N6–N5–C1–N4 2.0(2), N6–N5–C1–N1 -176.32(1), N6–N5–C1–N1 -177.5(2), C1–N5–N6–O1 -0.6(2), C1–N5–N6–O2 179.0(1), C1–N1–C2–C3 -88.8(2), N2–N1–C2–C3 82.3(2), O3–C3–C2–N1 -15.0(2), O4–C3–C2–N1 165.5 (1).

1-Carboxymethyl-5-nitriminotetrazolate monohydrate (**5**) crystallizes in the orthorhombic space group *Pbcn* with eight molecular units per unit cell. The molecular unit of **5** is depicted in Figure 5.11. The density of **5** of 1.725 g/cm³ is significantly higher than the one of its aminotetrazole analogue **4**, however, it is in the range of other *N1*-alkylated nitriminotetrazoles like 1-(2-hydroxyethyl)-5-nitriminotetrazole (**1**, 1.733 g/cm³), 1-(2-nitrate-ethyl)-5-nitriminotetrazole monohydrate (**2**, 1.781 g/cm³) or 1-(2-chloroethyl)-5-nitriminotetrazole (**3**, 1.724 g/cm³).^[5a, 6]

The nitriminotetrazole unit is almost planar, thus making the formation of an intramolecular hydrogen bond between the donor N4 and the acceptor O1 possible. Further hydrogen bonds are listed in Table 5.3.

Table 5.3 Hydrogen bonds in **5** (i) $-x+1, y, -z+3/2$, (ii) $x, -y, z-1/2$, (iii) $x, -y+1, z-1/2$, (iv) $-x+1/2, y-1/2, z$.

D-H...A	D-H [Å]	H...A [Å]	D...A [Å]	<(DHA) [°]
N4-H4...O5 <i>i</i>	0.94(2)	1.73(2)	2.652(2)	165(2)
O5-H5a...N3 <i>ii</i>	0.78(2)	2.26(2)	3.030(2)	168(2)
O5-H5b...O1 <i>iii</i>	0.92(2)	1.98(2)	2.900(2)	175(2)
O5-H5b...O2 <i>iii</i>	0.92(2)	2.45(2)	3.013(2)	120(1)
O5-H5b...N6 <i>iii</i>	0.92(2)	2.54(2)	3.362(2)	149(2)
O4-H4a...O2 <i>iv</i>	0.87(2)	1.86(2)	2.732(2)	176(2)
O4-H4a...N5 <i>iv</i>	0.87(2)	2.61(2)	3.216(2)	128(1)
O4-H4a...6 <i>iv</i>	0.87(2)	2.62(2)	3.439(2)	158(1)

The packing of **5** is characterized by zig-zag layers along the *a* axis. The molecules are connected by hydrogen bonds (Table 5.3). No hydrogen bonds between the layers can be observed.

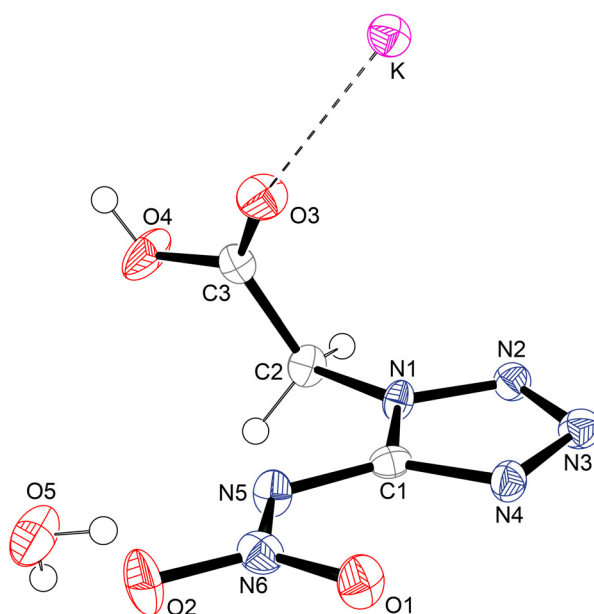


Figure 5.12 Molecular unit of **5_K**. Hydrogen atoms are shown as spheres of arbitrary radius and thermal displacements are set at 50 % probability. Selected geometries: distances (Å) N1-N2 1.348(2), N2-N3 1.305(2), N3-N4 1.373(3), N1-C1 1.353(3), N4-C1 1.342(2), C1-N5 1.365(3), N5-N6 1.332(2), O1-N6 1.261(2), N6-O2 1.249(2), O3-C3 1.193(2), O4-C3 1.317(3), N1-C2 1.454(2), K-O3 2.650(2), K-O1*i* 2.849(3), K-O1*ii* 2.873(2), K-N2*iii* 2.883(2), K-N4*iv* 2.884(2), K-N4*ii* 2.934(2), K-N3*v* 2.938(2), K-O1*iv* 2.960(3); angles (°) N1-C1-N4 107.3(2), N1-C1-N5 117.5(2), O1-N6-N5 123.1(2), O1-N6-O2 120.4(2), O3-C3-C2 125.2(2), O4-C3-C2 109.9(2), O3-C3-O4 124.9(2), C3-O3-K 163.4(2); torsion angles (°) O1-N6-N5-C1 -1.4(3), N1-C2-C3-O3 13.9(3), N1-C2-C3-O4 -166.5(2), K-O3-C3-O4 -132.3(4), K-O3-C3-C2 47.2(7); *i*) $x, -y-3/2, z+1/2$, *ii*) $-x+2, -y-1, -z+1$, *iii*) $x, y-1, z$, *iv*) $x, -y-1/2, z+1/2$, *v*) $-x+2, -y, -z+1$.

Potassium 1-carboxymethyl-5-nitriminetetrazolate monohydrate (**5_K**) crystallizes in the monoclinic space group $P2_1/c$ with a density of 1.863 g/cm³. Its unit cell contains four molecular units. The potassium atoms are eightfold coordinated by the atoms O3, O1*i*, O1*ii*, N2*iii*, N4*iv*, N4*ii*, N3*v*, and O1*iv* (*i*) $x, -y-3/2, z+1/2$, *ii*) $-x+2, -y-1, -z+1$, *iii*) $x, y-1, z$, *iv*) $x, -y-1/2, z+1/2$, *v*) $-x+2, -y, -z+1$), taking into account a maximum distance of 3.0 Å. Remarkably, the crystal water molecule is not involved in the coordination of the potassium

ion. Furthermore, the nitriminotetrazole molecule is deprotonated at the nitrogen atom N4 and not at the carboxy group, which should offer the more acidic hydrogen atom ($pK_a(\text{COOH}) = 2.1$ [1], $pK_a(\text{nitriminotetrazole}) \approx 2.5$ [5c, 8]). This can be explained by the coordination sphere of the potassium atoms. Due to the deprotonation of N4, the formation of a chelate complex with the bidentate ligand 1-carboxymethyl-5-nitriminotetrazolate *via* the coordinating atoms O1 and N4 is possible. Five hydrogen bonds between the crystal water molecule and the anion can be observed. The shortest distance between two potassium atoms is 4.076(2) Å.

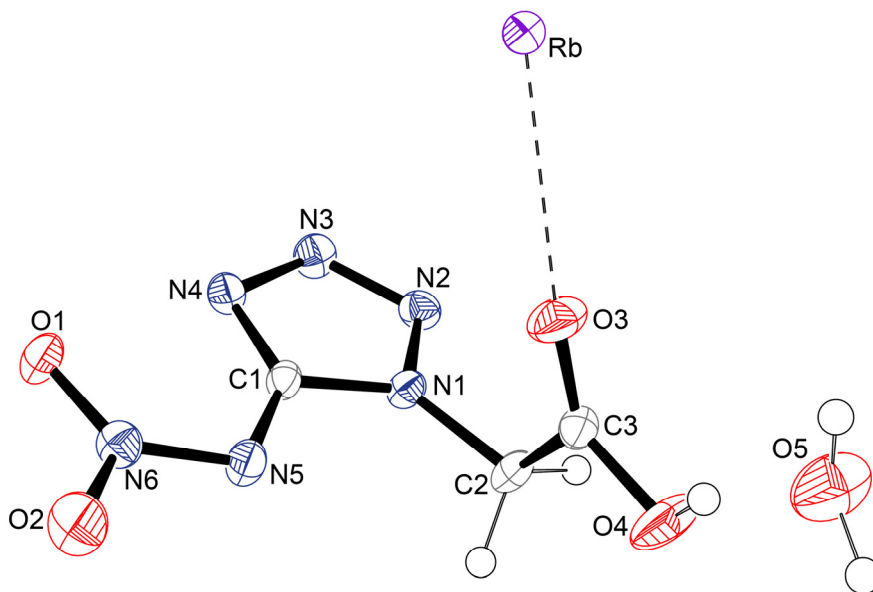


Figure 5.13 Molecular unit of **5-Rb**. Hydrogen atoms are shown as spheres of arbitrary radius and thermal displacements are set at 50 % probability. Selected geometries: distances (Å) N1–N2 1.354(3), N2–N3 1.294(4), N3–N4 1.367(3), N1–C1 1.354(4), N4–C1 1.335(4), C1–N5 1.368(4), N5–N6 1.331(3), O1–N6 1.252(3), N6–O2 1.251(3), O3–C3 1.201(4), O4–C3 1.304(4), N1–C2 1.449(4), Rb–O3 2.783(2), Rb–O1*i* 2.966(3), Rb–N2*ii* 3.014(3), Rb–N4*iii* 3.024(3), Rb–O1*iii* 3.038(3), Rb–O1*iv* 3.049(2), Rb–N4*iv* 3.049(3), Rb–N3*v* 3.090(3); angles (°) N1–C1–N4 107.7(3), N1–C1–N5 117.0(3), O1–N6–N5 123.3(3), O1–N6–O2 120.5(3), O3–C3–C2 124.1(3), O4–C3–C2 110.5(3), O3–C3–O4 125.4(3), O3–Rb–O1*i* 102.98(7), O3–Rb–O1*iii* 70.02(7); torsion angles (°) O1–N6–N5–C1 2.2(4), N1–C2–C3–O3 –11.7(4), N1–C2–C3–O4 168.4(3), Rb–O3–C3–O4 128.5(6); *i*) $x, -y+3/2, z-1/2$, *ii*) $x, y+1, z$, *iii*) $x, -y+1/2, z-1/2$, *iv*) $-x, -y+1, -z$, *v*) $-x, -y, -z$.

Rubidium 1-carboxymethyl-5-nitriminotetrazolate monohydrate (**5-Rb**) crystallizes in analogy to **5-K** in the monoclinic space group $P2_1/c$ with four molecular units per unit cell. Its density of 2.099 g/cm³ is significantly higher than the one of **5-K**. The coordination of the rubidium atoms is in analogy to **5-K** eightfold and the tetrazole ring is deprotonated. Again the crystal water molecule is not involved in the coordination of the cation. The five hydrogen bonds are like in **5-K** (O5–H5b···N5*vi*: 0.87 Å, 2.12 Å, 2.98 Å, 176°; O5–H5b···O2*vi*: 0.87 Å, 2.62 Å, 3.17 Å, 122°; O5–H5a···O2*i*: 0.79 Å, 2.31 Å, 2.97 Å, 141°; O5–H5a···O5*vii*: 0.79 Å, 2.51 Å, 3.13 Å, 136°; O4–H4···O5: 0.76 Å, 1.85 Å, 2.59 Å, 165°; *i*) $x, -y+3/2, z-1/2$, *vi*) $-x+1, -y+1, -z$, *vii*) $-x+1, y+1/2, -z-1/2$). The shortest observed distance between two rubidium ions is approximately 4.240 Å.

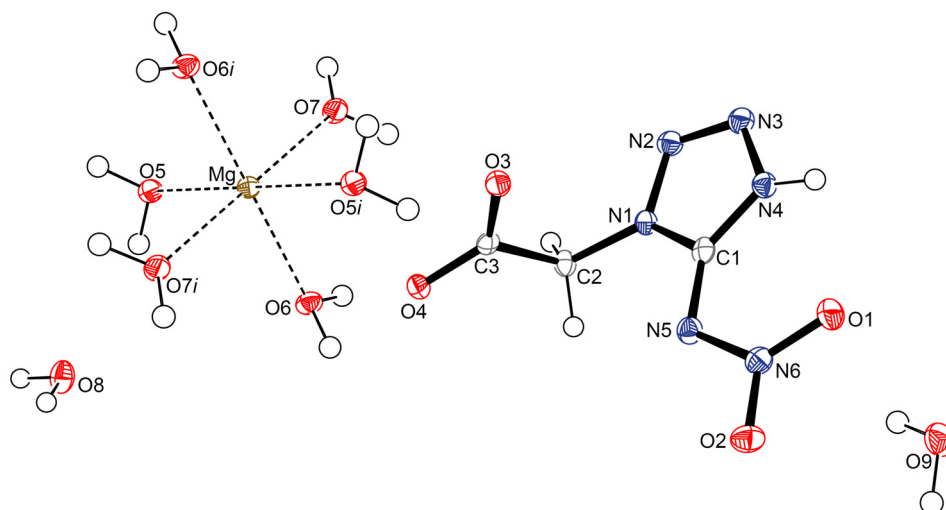


Figure 5.14 Molecular unit of **5_Mg1**. For a better overview only one anion is shown. Hydrogen atoms are shown as spheres of arbitrary radius and thermal displacements are set at 50 % probability. Selected geometries: distances (Å) N1–N2 1.354(1), N2–N3 1.279(2), N3–N4 1.356(1), N1–C1 1.344(2), N4–C1 1.335(2), C1–N5 1.341(2), N5–N6 1.348(1), O1–N6 1.242(1), N6–O2 1.240(1), O3–C3 1.246(2), O4–C3 1.260(1), N1–C2 1.455(2), O5–Mg 2.0960(9), O6–Mg 2.0545(9), O7–Mg 2.0558(9); angles (°) N1–C1–N4 104.4(1), N1–C1–N5 119.5(1), O1–N6–N5 122.2(1), O1–N6–O2 122.2(1), O3–C3–C2 117.9(1), O4–C3–C2 115.8(1), O3–C3–O4 126.3(1), O6–Mg–O5 88.74(4), O6–Mg–O6*i* 180.0, O6–Mg–O7 87.63(4), O7–Mg–O5 90.42(3); torsion angles (°) O1–N6–N5–C1 1.0(2), N1–C2–C3–O3 12.2(2), N1–C2–C3–O4 –169.8(1); *i*) $-x+1, -y+1, -z$.

Magnesium 2-(5-nitriminetrazol-1-yl)-acetate decahydrate (**5_Mg1**) crystallizes in the monoclinic space group $P2_1/c$ with two molecular units per unit cell. Its density of 1.666 g/cm³ is significantly lower than the one of **5**. The magnesium cations are sixfold coordinated without exception by crystal water molecules (Figure 5.14). Due to this fact, the carboxyl group of the 1-carboxymethyl-5-nitriminetrazole molecule is deprotonated and not the tetrazole ring at N4, like in **5_K** or **5_Rb** mentioned above. Four further crystal water molecules are located without coordination to the magnesium atoms in the unit cell. They are connected *via* hydrogen bonds to the anions and magnesium coordinating water molecules (Table 5.4).

Table 5.4 Hydrogen bonds in **5_Mg1** (*ii*) $-x+1, -y+1, -z+1$, (*iii*) $-x+1, y-1/2, -z+3/2$, (*iv*) $x, -y+1/2, z-1/2$, (*v*) $-x+2, y-1/2, -z+1/2$, (*vi*) $x, y, z-1$, (*vii*) $x, y+1, z$.

D–H···A	D–H [Å]	H···A [Å]	D···A [Å]	<(DHA) [°]
O7–H7a···O3	0.87(2)	1.86(2)	2.722(1)	178(2)
O9–H9b···O1	0.83(2)	2.19(2)	2.939(1)	151(2)
O9–H9b···O2	0.83(2)	2.31(2)	3.055(1)	149(2)
O9–H9b···N6	0.83(2)	2.57(2)	3.392(1)	170(2)
O8–H8b···O3 <i>ii</i>	0.82(2)	2.07(2)	2.839(1)	157(2)
O8–H8a···N5 <i>iii</i>	0.83(2)	2.11(2)	2.936(1)	171(2)
O8–H8a···O2 <i>iii</i>	0.83(2)	2.61(2)	3.223(1)	132(2)
O7–H7b···O4 <i>iv</i>	0.79(2)	2.14(2)	2.875(1)	155(2)
O6–H6b···O4	0.84(2)	1.91(2)	2.748(1)	176(2)
N4–H4···O9 <i>v</i>	0.87(2)	1.79(2)	2.645(1)	169(2)
O5–H5a···O8 <i>vi</i>	0.85(2)	1.83(2)	2.663(1)	171(2)
O5–H5b···O4 <i>ii</i>	0.85(2)	1.89(2)	2.733(1)	174(2)
O9–H9a···N3 <i>vii</i>	0.90(2)	2.07(2)	2.951(1)	165(2)

The packing of **5_Mg1** is characterized by layers along the *c* axis. A layer of magnesium atoms and the coordinating water molecules is surrounded on both sides by layers of anions. The free water molecules are located between these two different layers. The layer built by the anions is on the other side connected through hydrogen bonds with another layer of anions.

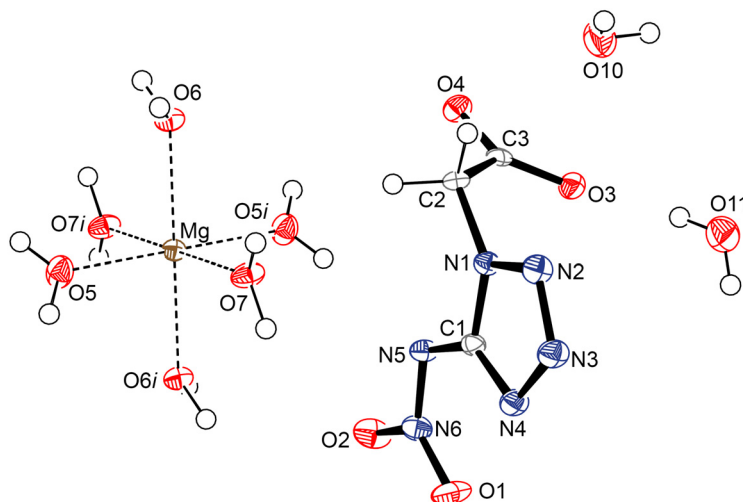


Figure 5.15 Molecular unit of **5_Mg2**. Hydrogen atoms are shown as spheres of arbitrary radius and thermal displacements are set at 50 % probability. Selected geometries: distances (Å) N1–N2 1.345(2), N2–N3 1.287(2), N3–N4 1.361(2), N1–C1 1.355(2), N4–C1 1.331(2), C1–N5 1.368(2), N5–N6 1.324(2), O1–N6 1.238(2), N6–O2 1.266(2), O3–C3 1.254(2), O4–C3 1.262(2), N1–C2 1.448(2), O5–Mg 2.039(1), O6–Mg 2.103(1), O7–Mg 2.065(1); angles (°) N1–C1–N4 107.6(1), N1–C1–N5 117.6(1), O1–N6–N5 124.0(1), O1–N6–O2 119.9(1), O3–C3–C2 119.1(1), O4–C3–C2 115.2(1), O3–C3–O4 125.7(1), O5–Mg–O5*i* 180.0, O6–Mg–O5 89.29(5), O6–Mg–O7 87.36(5), O7–Mg–O5 92.16(5); torsion angles (°) O1–N6–N5–C1 –0.9(2), N1–C2–C3–O3 –25.8(2), N1–C2–C3–O4 155.2(1); *i*) $-x+2, -y, -z$.

Magnesium 2-(5-nitriminotetrazolate)-acetate octahydrate (**5_Mg2**) crystallizes in the triclinic space group *P*-1 with two formula units per unit cell. Interestingly, its density of 1.667 g/cm³ is almost the same as that of **5_Mg1**. Like in **5_Mg1** the magnesium cations are sixfold coordinated exclusively by crystal water molecules (Figure 5.15). The other two water molecules are located in the unit cell without coordination to the cations, but connected *via* hydrogen bonds with the anion (O12–H12b··O4*ii*: 0.85 Å, 1.97 Å, 2.812 Å, 169°; O11–H11b··O2*iii*: 0.78 Å, 2.33 Å, 3.107 Å, 174°; O11–H11b··O1*iii*: 0.78 Å, 2.53 Å, 3.013 Å, 121°; O11–H11a··O3: 0.79 Å, 2.25 Å, 3.026 Å, 167°; *ii*) $-x+1, -y, -z$, *iii*) $-x+1, -y+1, -z$) and the coordinated water molecules (O8–H8a··O11*iv*: 0.88 Å, 1.95 Å, 2.828 Å, 176°; *iv*) $-x+2, -y+1, -z+1$). Further hydrogen bonds can be found between the coordinating water molecules and the twice deprotonated 1-carboxymethyl-5-nitriminotetrazole molecules.

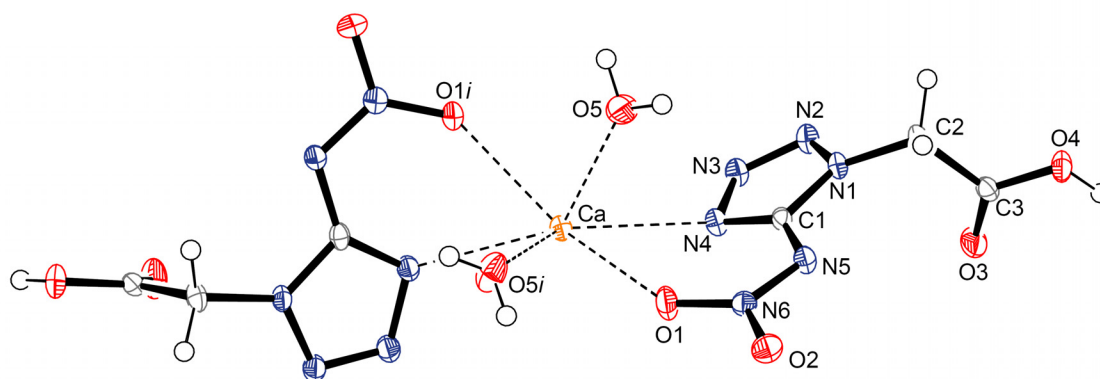


Figure 5.16 Molecular unit of **5_Ca1**. Hydrogen atoms are shown as spheres of arbitrary radius and thermal displacements are set at 50 % probability. Selected geometries: distances (Å) N1–N2 1.346(2), N2–N3 1.287(2), N3–N4 1.362(2), N1–C1 1.353(2), N4–C1 1.334(2), C1–N5 1.364(2), N5–N6 1.317(2), O1–N6 1.256(2), N6–O2 1.252(2), O3–C3 1.299(2), O4–C3 1.212(2), N1–C2 1.443(2), Ca–O1 2.484(1), Ca–O4 2.372(1), Ca–O5 2.369(2), Ca–N4 2.624(2); angles (°) N1–C1–N4 107.7(1), N1–C1–N5 117.2(1), O1–N6–N5 124.4(1), O1–N6–O2 119.5(1), O3–C3–C2 111.6(1), O4–C3–C2 123.1(2), O3–C3–O4 125.3(2), O4–Ca–O1 75.33(5), O5–Ca–O1 80.49(5), O5–Ca–O4 149.08(5), O5–Ca–O5*i* 91.12(8), O1–Ca–N4 63.14(4), O4–Ca–N4 78.32(4), O5–Ca–N4 73.66(5); torsion angles (°) O1–N6–N5–C1 –5.8(2), N1–C2–C3–O3 178.8(1), N1–C2–C3–O4 –1.5(2), O5–Ca–O4–C3 –133.5(3); *i*) –*x*, *y*, –*z*+3/2.

The calcium salt of monodeprotonated **5**, calcium 1-carboxymethyl-5-nitriminotetrazolate dihydrate (**5_Ca1**), crystallizes in the monoclinic space group *C2/c* with four molecules per unit cell. In contrast to **5_Mg1**, in **5_Ca1** the 1-carboxymethyl-5-nitriminotetrazole molecule is deprotonated at the tetrazole ring and not at the carboxy group (Figure 5.16). Thus a bidentate coordination through N4 and O1 of the anions is possible analogous to the one observed in **5_K** or **5_Rb**. The density of 1.898 g/cm³ is significantly higher than the one of **5_Mg1**, but comparable to that of other calcium salts of *N1*-alkylated nitriminotetrazoles (see chapter 2–4). The calcium atoms are eightfold coordinated by the atoms O1, N4, O4, O5, O1*i*, N4*i*, O4*i*, and O5*i* (*i*) –*x*, *y*, –*z*+3/2). Two different hydrogen bonds between the crystal water molecules and the anions (O5–H5a···N2*ii*: 0.84 Å, 2.20 Å, 3.014 Å, 163°; O5–H5b···O2*iii*: 0.78 Å, 2.16 Å, 2.913 Å, 163°; *ii*) –*x*+1/2, –*y*+1/2, –*z*+2, *iii*) –*x*, –*y*+1, –*z*+2), as well as one hydrogen bond connecting the anions (O3–H3···N3*i*: 0.90 Å, 1.82 Å, 2.704 Å, 169°) can be observed.

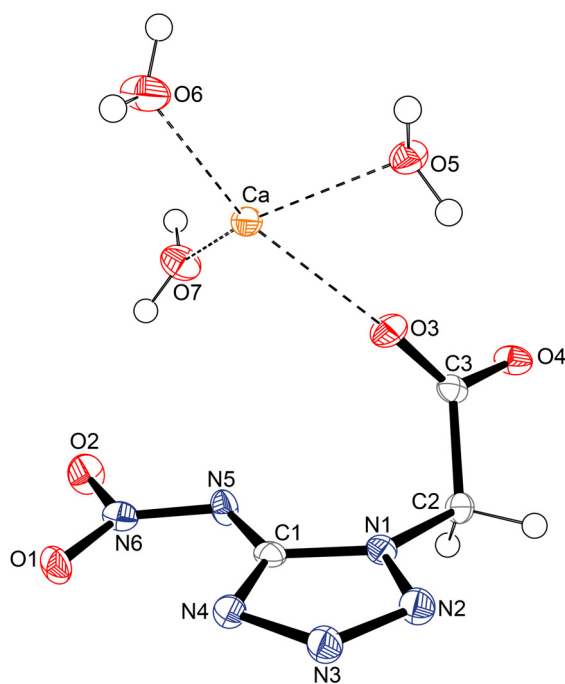


Figure 5.17 Molecular unit of **5_Ca2**. Hydrogen atoms are shown as spheres of arbitrary radius and thermal displacements are set at 50 % probability. Selected geometries: distances (Å) N1–N2 1.352(3), N2–N3 1.288(3), N3–N4 1.364(3), N1–C1 1.349(3), N4–C1 1.331(3), C1–N5 1.371(3), N5–N6 1.319(3), O1–N6 1.254(2), N6–O2 1.257(2), O3–C3 1.237(3), O4–C3 1.262(3), N1–C2 1.458(3), Ca–O3 2.283(2), Ca–O4*i* 2.372(2), Ca–O5 2.416(2), Ca–O6 2.392(3), Ca–O7 2.397(2), Ca–O1*ii* 2.480(2), Ca–N4*ii* 2.526(2); angles (°) N1–C1–N4 108.1(2), N1–C1–N5 117.7(2), O1–N6–N5 124.4(2), O1–N6–O2 119.8(2), O3–C3–C2 120.1(2), O4–C3–C2 113.7(2), O3–C3–O4 126.3(2), O3–Ca–O5 73.93(8), O3–Ca–O6 153.08(7), O3–Ca–O7 85.08(8), O6–Ca–O5 81.21(8), O7–Ca–O5 147.39(7), O6–Ca–O7 121.82(8); torsion angles (°) O1–N6–N5–C1 –1.1(3), N1–C2–C3–O3 3.6(3), N1–C2–C3–O4 –176.8(2), O5–Ca–O3–C3 –154.4(8), O6–Ca–O3–C3 –177.6(7), O7–Ca–O3–C3 0.4(8); *i* –*x*, –*y*, –*z*, *ii* –*x*, –*y*–1, –*z*–1.

Calcium 2-(5-nitriminotetrazolate)-acetate trihydrate (**5_Ca2**) crystallizes like **5_Mg2** in the triclinic space group $P\bar{1}$ with two molecular units per unit cell. The molecular unit of **5_Ca2** is depicted in Figure 5.17. The calculated density of 1.870 g/cm³ is smaller than the one of **5_Ca1**. The calcium atoms are sevenfold coordinated by the atoms O3, O4*i*, O5, O6, O7, O1*ii*, and N4*ii* (*i* –*x*, –*y*, –*z*, *ii* –*x*, –*y*–1, –*z*–1). Only hydrogen bonds between the water molecules and the anions can be found (O6–H6b··N5*iii*: 0.74 Å, 2.26 Å, 2.985 Å, 170°, O7–H7b··O2: 0.78 Å, 2.27 Å, 3.013 Å, 160°, O7–H7a··N3*iv*: 0.84 Å, 2.10 Å, 2.947 Å, 179°, O6–H6a··O5*v*: 0.79 Å, 2.02 Å, 2.784 Å, 162°, O5–H5a··N2*vi*: 0.81 Å, 2.16 Å, 2.963 Å, 171°, O5–H5b··O4*iii*: 0.88 Å, 1.83 Å, 2.694 Å, 164°; *iii*) *x*+1, *y*, *z*, *iv*) *x*, *y*, *z*+1, *v*) –*x*+1, –*y*, –*z*, *vi*) –*x*, –*y*, –*z*–1).

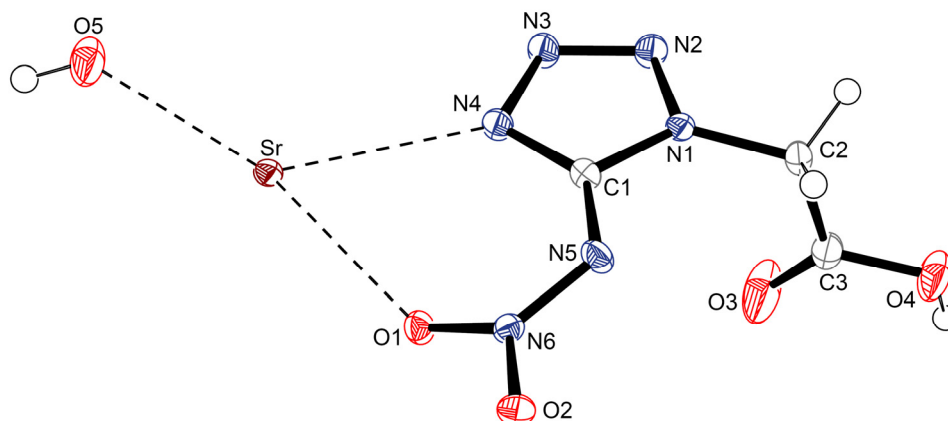


Figure 5.18 Asymmetric unit of **5_Sr1**. Hydrogen atoms are shown as spheres of arbitrary radius and thermal displacements are set at 50 % probability. Selected geometries: distances (Å) N1–N2 1.342(2), N2–N3 1.299(2), N3–N4 1.361(2), N1–C1 1.341(2), N4–C1 1.326(2), C1–N5 1.379(2), N5–N6 1.300(2), O1–N6 1.262(2), N6–O2 1.271(2), O3–C3 1.187(3), O4–C3 1.315(2), N1–C2 1.448(2), Sr–O1 2.712(2), Sr–O5 2.544(2), Sr–N4 2.766(12), Sr–N3*i* 2.875(2); angles (°) N1–C1–N4 108.33(2), N1–C1–N5 117.4(2), O1–N6–N5 125.5(1), O1–N6–O2 118.1(1), O3–C3–C2 123.8(2), O4–C3–C2 110.8(2), O3–C3–O4 125.5(2), O5–Sr–O1 136.38(3), O1–Sr–N4 59.46(5), O1–Sr–N3*i* 61.94(5), O5–Sr–N3*i* 76.48(3), N4–Sr–N3*i* 84.82(5); torsion angles (°) O1–N6–N5–C1 -2.1(2), N1–C2–C3–O3 3.5(3), N1–C2–C3–O4 -176.35(2), O5–Sr–O1–N6 75.5(2), N3*i*–Sr–O1–N6 56.1(1), N4–Sr–O1–N6 -45.20(14); *i* x, -y, z-1/2.

In Figure 5.18 the asymmetric unit of strontium 1-carboxymethyl-5-nitriminotetrazolate monohydrate (**5_Sr1**) is depicted. **5_Sr1** crystallizes in analogy to **5_Ca1** in the monoclinic space group $C2/c$ with four molecular units per unit cell. Its density of 1.938 g/cm³ is slightly higher than the one of **5_Ca1**, but comparable to the one of **1_Sr** (see chapter 2). Again the tetrazole ring is deprotonated. In **5_Sr1** the strontium atoms are elevenfold coordinated by the atoms O5, O1*ii*, O1, O1*iii*, O1*iv*, O2*iii*, O2*iv*, N4*ii*, N4, N3*i*, and N3*v* considering maximum distances of 2.9 Å (*i*) x, -y, z-1/2, *ii*) -x+2, y, -z+1/2, *iii*) -x+2, -y, -z, *iv*) x, -y, z+1/2, *v*) -x+2, -y, -z+1). The shortest distance between two strontium ions is 4.407(2) Å. Like in **5_Ca1** three hydrogen bonds are observed: one connecting the crystal water molecule with the anions (O5–H5···O3*vi*: 0.77 Å, 2.12 Å, 2.880 Å, 172°; *vi*) -x+2, y-1, -z+1/2) and two others connecting the anions with each other (O4–H4···O2*vii*: 0.84 Å, 1.91 Å, 2.752 Å, 174°; O4–H4···N6*viii*: 0.84 Å, 2.66 Å, 3.401 Å, 148°; *viii*) x, -y+1, z+1/2). The packing of **5_Sr1** is characterized by stacks along the *c* axis.

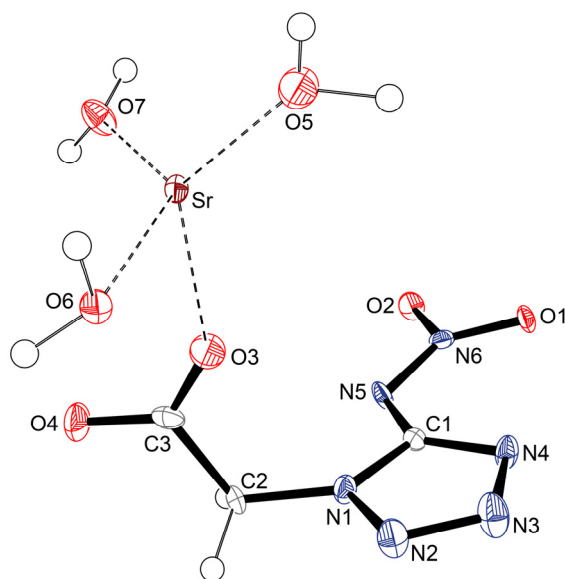


Figure 5.19 Molecular unit of **5_Sr2**. Hydrogen atoms are shown as spheres of arbitrary radius and thermal displacements are set at 50 % probability. Selected geometries: distances (Å) N1–N2 1.356(4), N2–N3 1.304(4), N3–N4 1.370(4), N1–C1 1.340(4), N4–C1 1.335(4), C1–N5 1.370(4), N5–N6 1.312(3), O1–N6 1.268(3), N6–O2 1.258(4), O3–C3 1.247(4), O4–C3 1.249(4), N1–C2 1.463(4), Sr–O3 2.508(3), Sr–O5 2.557(2), Sr–O6 2.664(3), Sr–O7 2.541(3), Sr–O1*i* 2.696(2), Sr–N4*ii* 2.699(3), Sr–O6*iii* 2.711(3), Sr–O2*i* 2.716(2), Sr–O1*ii* 2.768(3); angles (°) N1–C1–N4 108.8(3), N1–C1–N5 117.0(3), O1–N6–N5 124.2(3), O1–N6–O2 119.3(3), O3–C3–C2 118.8(3), O4–C3–C2 114.4(3), O3–C3–O4 126.8(4), O3–Sr–O7 83.69(9), O3–Sr–O5 132.5(1), O7–Sr–O5 131.4(1), O3–Sr–O6 95.11(8), O7–Sr–O6 136.57(9), O5–Sr–O6 79.47(9); torsion angles (°) O1–N6–N5–C1 -1.1(5), N1–C2–C3–O3 -5.8(5), N1–C2–C3–O4 173.9(3), O7–Sr–O3–C3 -59.7(4), O5–Sr–O3–C3 157.1(4), O6–Sr–O3–C3 76.7(4); *i*) $x, -y+5/2, z+1/2$, *ii*) $-x, y+1/2, -z+1/2$, *iii*) $-x, -y+2, -z+1$.

Strontium 2-(5-nitriminotetrazolate)-acetate trihydrate (**5_Sr2**) crystallizes in the monoclinic space group $P2_1/c$ with four molecular units per unit cell (Figure 5.19). Its density of 2.146 g/cm³ is significantly higher than the one of **5_Sr1**. The shortest observed distance between two strontium cations of 4.4052(8) Å is comparable with the one found in **5_Sr1**. In **5_Sr2** each strontium atom is ninefold coordinated by the atoms O3, O5, O6, O7, O1*i*, N4*ii*, O6*iii*, O2*i*, and O1*ii* (*i*) $x, -y+5/2, z+1/2$, *ii*) $-x, y+1/2, -z+1/2$, *iii*) $-x, -y+2, -z+1$). One hydrogen bond can be observed between two crystal water molecules (O5–H5b···O7*iv*: 0.73 Å, 2.45 Å, 2.978 Å, 130°; *iv*) $-x, -y+3, -z+1$). The six other hydrogen bonds connect the crystal water molecules with the anions.

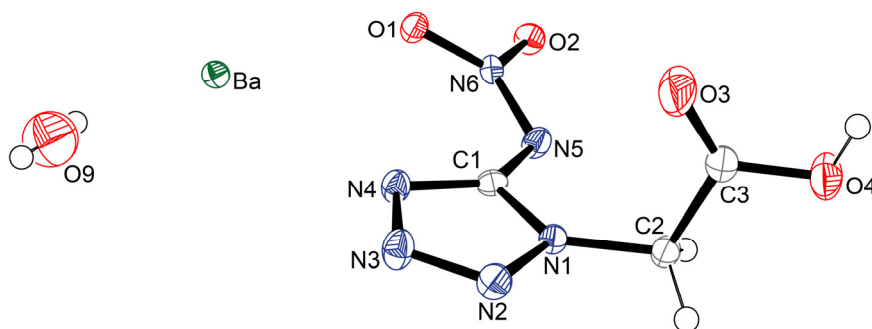


Figure 5.20 Asymmetric unit of **5_Ba1**. Hydrogen atoms are shown as spheres of arbitrary radius and thermal displacements are set at 50 % probability. Selected geometries: distances (Å) N1–N2 1.336(4), N2–N3 1.293(4), N3–N4 1.364(4), N1–C1 1.340(5), N4–C1 1.320(5), C1–N5 1.386(4), N5–N6 1.291(4), O1–N6 1.263(4), N6–O2 1.276(4), O3–C3 1.188(5), O4–C3 1.312(5), N1–C2 1.452(5), Ba–O1 2.816 (3), Ba–O9 2.700(6), Ba–O2*i* 2.858(3), Ba–O1*i* 2.884(3), Ba–N4 2.946(3); angles (°) N1–C1–N4 108.8(3), N1–C1–N5 117.1(3), O1–N6–N5 125.5(3), O1–N6–O2 118.2(3), O3–C3–C2 124.3(4), O4–C3–C2 110.6(3), O3–C3–O4 125.1(4), O1–Ba–O9 80.62(6); \bar{j} $-x, 1-y, 1-z$.

In analogy to **5_Ca1** and **5_Sr1**, barium 1-carboxymethyl-5-nitriminetetrazolate monohydrate (**5_Ba1**) crystallizes in the monoclinic space group $C2/c$ with four molecular units per unit cell. Its asymmetric unit is depicted in Figure 5.20. The calculated density of 2.063 g/cm³ is higher than the one of **5_Sr1**, but smaller than the one of **5_Sr2**. Again, the tetrazole ring is deprotonated and not the carboxy group. The barium cations are ninefold coordinated by the atoms O1, N4, O9, O1*i*, O1*ii*, N4*ii*, O2*ii*, O1*iii* and O2*iii*, considering maximum distances up to 3.0 Å (\bar{j} $-x, -y+1, -z+1$, \bar{i} $-x, y, -z+1/2$, \bar{iii} $x, -y+1, z-1/2$). The oxygen atom O9 of the crystal water molecules is the closest with a distance of 2.700(6) Å. Only one hydrogen bond between the anions was found (O4–H4 \cdots O2*iv*: 0.82 Å, 1.91 Å, 2.711 Å, 167°; \bar{iv} $x, -y, z-1/2$). The shortest distance between two barium cations is 4.551(1) Å. The packing in **5_Ba1** is characterized by layers along the c axis. In these layers, the barium atoms connect two anion pairs and the crystal water molecules are located between the layers of anions.

Single crystals of **5_Ba2** suitable for X-ray diffraction could be obtained, however solution of the structure presents difficulties, most probably due to a disorder of the crystal water molecules, and is still in work.

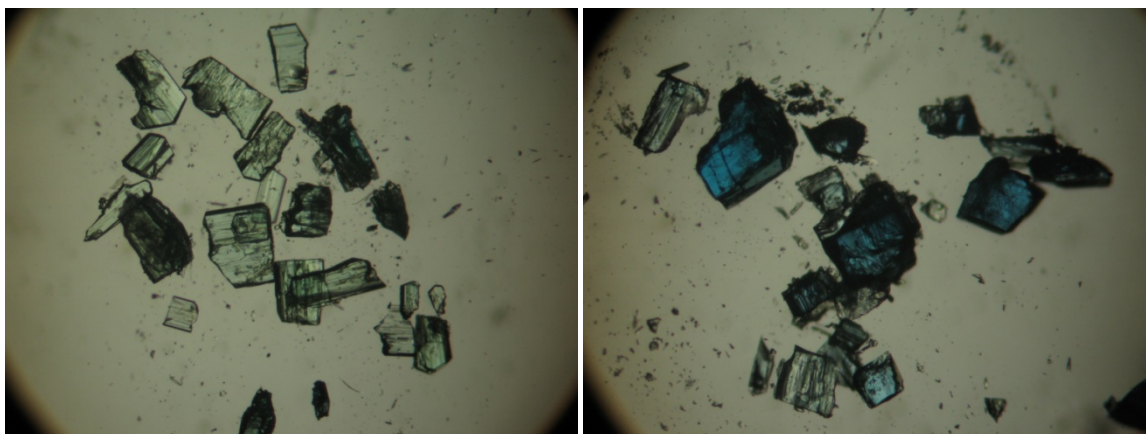


Figure 5.21 Crystals of both isomers of **5_Cu_H₂O** (a: left. b: right).

As mentioned above, two isomers of *trans*-[diaqua-bis(1-carboxymethyl-5-nitrimino-tetrazolato-*N*4,*O*1) copper(II)] dihydrate (**5_Cu_H₂O**) could be obtained. In the following, the green crystal, which were obtained first, are abbreviated as **5_Cu_H₂Oa**. From the mother liquor obtained blue crystals are abbreviated as **5_Cu_H₂Ob**. Both kinds of crystals are depicted in Figure 5.21.

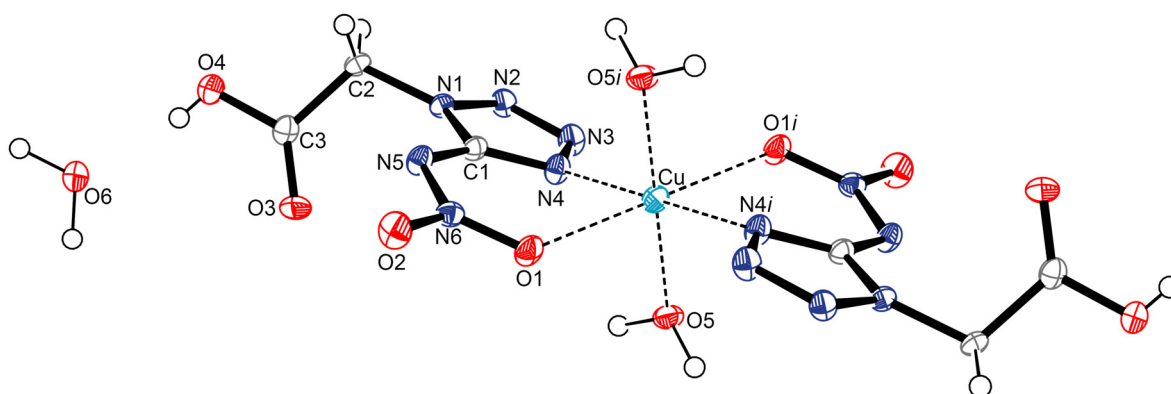


Figure 5.22 Molecular unit of **5_Cu_H₂Oa** (green crystals). Hydrogen atoms are shown as spheres of arbitrary radius and thermal displacements are set at 50 % probability. Selected geometries: distances (Å) N1–N2 1.355(4), N2–N3 1.283(4), N3–N4 1.376(4), N1–C1 1.358(4), N4–C1 1.332(4), C1–N5 1.359(4), N5–N6 1.334(3), O1–N6 1.270(3), N6–O2 1.235(3), O3–C3 1.205(4), O4–C3 1.323(4), N1–C2 1.461(4), Cu–N4 1.958(2), Cu–O5 2.022(2), Cu–O1 2.317(2); angles (°) N1–C1–N4 106.0(3), N1–C1–N5 118.8(3), O1–N6–N5 123.2(2), O1–N6–O2 120.2(2), O3–C3–C2 124.9(3), O4–C3–C2 109.5(3), O3–C3–O4 125.6(3), N4–Cu–O1 77.0(1), N4–Cu–O5 89.9(1), O5–Cu–O1 91.4(1); torsion angles (°) O1–N6–N5–C1 2.5(4), N1–C2–C3–O3 –0.5(4), N1–C2–C3–O4 179.0(3), O1–Cu–N4–C1 30.4(2), O5–Cu–N4–C1 121.9(3), O5–Cu–N4–N3 –80.0(2), O5–Cu–O1–N6 –126.4(2); *i* –x, –y, –z.

5_Cu_H₂Oa crystallizes in the monoclinic space group $P2_1/c$ with two formula units per unit cell. Like to **5_Ca**, the ring of the 1-carboxy-5-nitriminotetrazole molecule is deprotonated and the other acidic proton is bonded to the carboxyl group. The calculated density of 1.938 g/cm³ is quite high, comparable with the one of **5_Sr1** or of the copper(II) complex **2_Cu_H₂O** (see chapter 3). The copper(II) ion is sixfold coordinated by the atoms

O1, N4, O5, O1*i*, N4*i*, and O5*i* forming a distorted octahedron (*i*) $-x, -y, -z$). The longest coordination bond is found between Cu and O1 with a distance of 2.317(2) Å, whereas the others are comparable with 1.958(2) Å and 2.022(2) Å. This is a consequence of the expected JAHN-TELLER effect. Two crystal water molecules are not involved in the coordination of the copper(II) ions (Figure 5.22). Their distance to the copper(II) ion is quite long with 4.475(4) Å. They are connected *via* hydrogen bonds with the anions (O6–H6b··N5*ii*: 0.97 Å, 1.92 Å, 2.884 Å, 169°, O6–H6b··O2*ii*: 0.97 Å, 2.48 Å, 3.224 Å, 133°, O6–H6b··N6*ii*: 0.97 Å, 2.59 Å, 3.523 Å, 161°, O6–H6a··O6*iii*: 0.98 Å, 1.92 Å, 2.883 Å, 167°, O4–H4··O6: 0.66 Å, 2.00 Å, 2.645 Å, 163°; *ii*) $-x+1, -y, -z$, *iii*) $x, -y-1/2, z-1/2$). Four further hydrogen bonds are observed between the aqua ligands and the anions (O5–H5a··N3*iii*: 0.99 Å, 2.07 Å, 3.038 Å, 169°, O5–H5b··O1*iv*: 0.99 Å, 1.91 Å, 2.825 Å, 153°, O5–H5b··O2*iv*: 0.99 Å, 2.49 Å, 3.368 Å, 149°, O5–H5b··N6*iv*: 0.99 Å, 2.54 Å, 3.519 Å, 173°; *iv*) $-x, -y, -z-1$).

The packing in **5_Cu_H2Oa** is characterized by layers along the *c* axis. In these layers the anions are connected *via* the above mentioned hydrogen bonds to the noncoordinating water molecules, which are located between two layers.

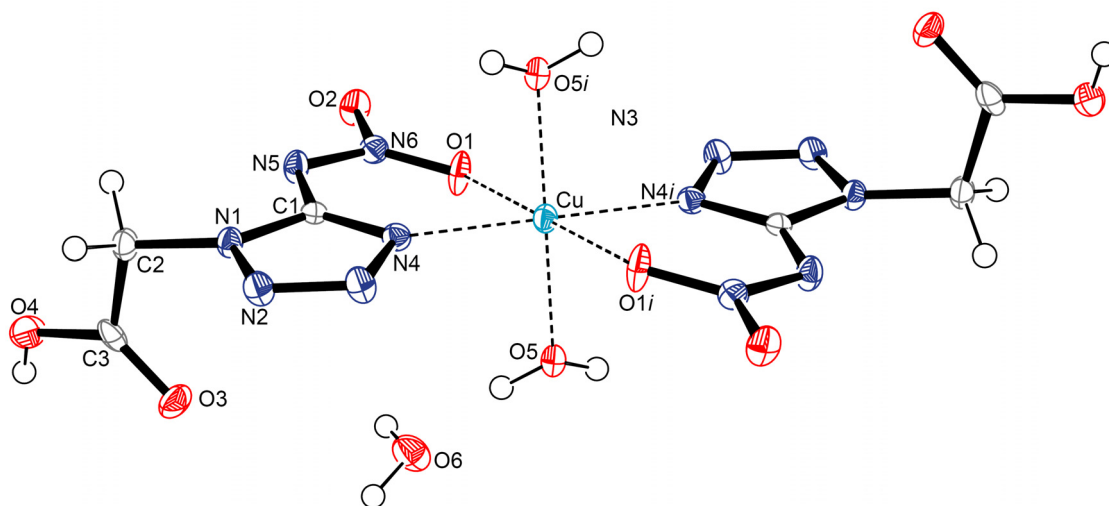


Figure 5.23 Molecular unit of **5_Cu_H2Ob** (blue crystals). Hydrogen atoms are shown as spheres of arbitrary radius and thermal displacements are set at 50 % probability. Selected geometries: distances (Å) N1–N2 1.348(3), N2–N3 1.288(2), N3–N4 1.369(2), N1–C1 1.350(3), N4–C1 1.336(3), C1–N5 1.367(3), N5–N6 1.320(2), O1–N6 1.240(2), N6–O2 1.270(2), O3–C3 1.216(3), O4–C3 1.304(3), N1–C2 1.442(3), Cu–O5 1.941(2), Cu–N4 2.006(2), Cu–O1 2.391(2); angles (°) N1–C1–N4 106.9(2), N1–C1–N5 116.1(2), O1–N6–N5 125.3(2), O1–N6–O2 119.8(2), O3–C3–C2 122.5(2), O4–C3–C2 112.0(2), O3–C3–O4 125.6(2), N4–Cu–O1 75.75(7), N4–Cu–O5 89.61(8), O5–Cu–O1 94.26(7); torsion angles (°) O1–N6–N5–C1 3.1(3), N1–C2–C3–O3 10.4(3), N1–C2–C3–O4 $-170.2(2)$, O1–Cu–N4–C1 $-7.6(2)$, O5–Cu–N4–C1 $-102.1(2)$, O5–Cu–N4–N3 76.7(2), O5–Cu–O1–N6 107.3(2), N4–Cu–O1–N6 18.7(2); *i*) $-x+1, -y, -z+1$.

5_Cu_H2Ob crystallizes in the monoclinic space group $P2_1/n$ with two formula units per unit cell (Figure 5.23). Its density of 1.917 g/cm³ is slightly lower than the one of **5_Cu_H2Oa**. This can be explained by the larger cell volume of **5_Cu_H2Ob**. The coordination sphere of the copper(II) ions is analogous to that of **5_Cu_H2Oa**. A difference can be observed in the angles N4–Cu–O1 (**a**: 77.0°, **b**: 75.8°) and O5–Cu–O1 (**a**: 91.4°, **b**: 94.3°).

Table 5.5 Hydrogen bonds in **5_Cu_H2Ob** (*ii*) $-x, -y, -z+1$, (*iii*) $x+1/2, -y+1/2, z+1/2$, (*iv*) $x-1, y, z, v$) $-x, -y+1, -z+1$).

D-H...A	D-H [Å]	H...A [Å]	D...A [Å]	<(DHA) [°]
O5-H5b...O2 ⁱⁱ	0.75(2)	2.04(2)	2.789(3)	175(3)
O5-H5a...O6	0.84(3)	1.76(3)	2.589(3)	169(3)
O6-H6a...O2 ⁱⁱⁱ	0.89(3)	1.98(3)	2.861(3)	169(3)
O6-H6b...N3 ^{iv}	0.72(3)	2.24(3)	2.953(3)	167(3)
O4-H4...O3 ^v	0.75(3)	1.91(3)	2.661(3)	175(3)

Furthermore, in **5_Cu_H2Ob** the carboxymethyl substituents are twisted to the opposite side as compared to **5_Cu_H2Oa**. Despite the larger cell volume in **5_Cu_H2Ob**, the noncoordinating crystal water molecules are located significantly closer to the copper(II) ions (4.404 Å). Thereby, different and fewer hydrogen bonds are formed (Table 5.5).

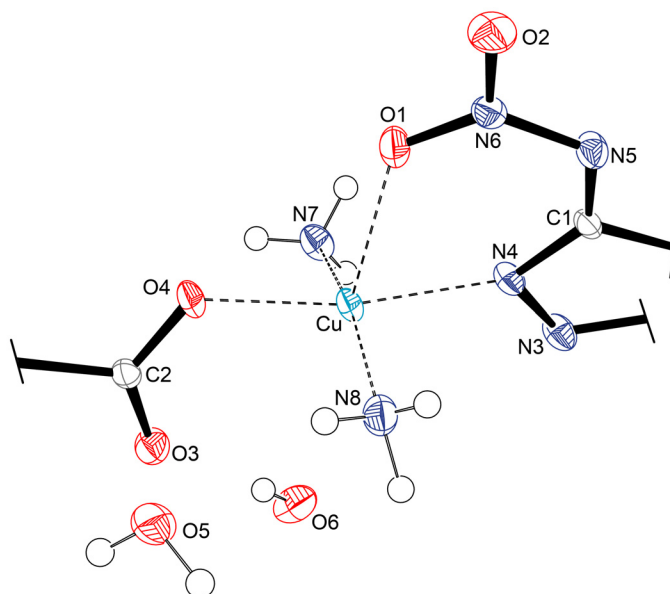


Figure 5.24 Coordination of the copper(II) ions in **5_Cu_NH3**. Hydrogen atoms are shown as spheres of arbitrary radius and thermal displacements are set at 50 % probability. Selected geometries: distances (Å) N1-N2 1.358(2), N2-N3 1.282(2), N3-N4 1.365(2), N1-C1 1.347(2), N4-C1 1.334(2), C1-N5 1.360(2), N5-N6 1.332(2), O1-N6 1.252(2), N6-O2 1.238(2), O3-C3 1.230(2), O4-C3 1.274(2), N1-C2 1.453(2), Cu-O4 1.959(1), Cu-N7 1.983(2), Cu-N8 1.990(2), Cu-N4 2.007(1), Cu-O1 2.336(2); angles (°) N1-C1-N4 106.6(1), N1-C1-N5 118.2(1), O1-N6-N5 123.3(1), O1-N6-O2 120.8(1), O3-C3-C2 121.1(1), O4-C3-C2 112.0(1), O3-C3-O4 126.9(1), O4-Cu-N7 90.81(7), O4-Cu-N8 89.64(8), N7-Cu-N8 164.31(8), O4-Cu-N4 167.12(5), N7-Cu-N4 90.32(7), N8-Cu-N4 92.72(7), O4-Cu-O1 91.90(6), N7-Cu-O1 104.30(7), N8-Cu-O1 91.36(7), N4-Cu-O1 75.39(6); torsion angles (°) O1-N6-N5-C1 1.9(2), N1-C2-C3-O3 -2.9(2), N1-C2-C3-O4 177.2(2), O4-Cu-O1-N6 154.1(1), N7-Cu-O1-N6 -114.6(1), N8-Cu-O1-N6 64.4(2), N4-Cu-O1-N6 -28.1(1), N7-Cu-O4-C3 80.8(1), N8-Cu-O4-C3 -83.5(1), N4-Cu-O4-C3 175.8(2), O1-Cu-O4-C3 -174.9(1).

The packing in **5_Cu_H2Ob** also differs from the one in **5_Cu_H2Oa**. It is characterized by chains along the *b* axis. They are formed by the copper(II) ions and their ligands. The anions are aligned along the *b* axis and connected *via* one hydrogen bond. The different chains are connected *via* the hydrogen bonds of the noncoordinating water molecules.

The copper(II) complex bis{diammine [2-(5-nitriminetetrazolato-*N*4,O1)-acetato-O4] copper(II)} trihydrate (**5_Cu_NH₃**) crystallizes in analogy to **5_Ca1**, **5_Sr1**, and **5_Ba1** in the monoclinic space group *C2/c* with eight formula units per unit cell. In contrast to **5_Cu_H₂O**, 1-carboxymethyl-5-nitriminetetrazole is deprotonated twice (like in the **5_M2** salts). The calculated density of 1.925 g/cm³ is in between the densities of **5_Cu_H₂Oa** and **5_Cu_H₂Ob**. In contrast to the coordination in the above mentioned copper(II) complexes, in **5_Cu_NH₃** the copper(II) ion is fivefold coordinated by the atoms O1, N4, O4, N7, and N8 forming a distorted trigonal bipyramid. The longest coordination distances are 1.959(2) Å and 2.007(1) Å. The crystal water molecules do not take part in coordination, but are connected *via* hydrogen bonds with each other, the anion, and the ammine ligands (N7–H7b···O6*i*: 0.80 Å, 2.29 Å, 3.076 Å, 167°; O5–H5a···O5*ii*: 0.87 Å, 1.88 Å, 2.747 Å, 170°; O5–H5b···N5*iii*: 0.73 Å, 2.17 Å, 2.896 Å, 168°; O6–H6a···O3: 0.77 Å, 2.07 Å, 2.840 Å, 171°; N8–H8a···O5: 0.73 Å, 2.39 Å, 3.078 Å, 158°; *i*) *x*, *y*–1, *z*, *ii*) *–x*+3/2, *y*+1/2, *–z*+3/2, *iii*) *x*, *–y*+1, *z*+1/2). The shortest distances to the copper(II) ion are 3.877(2) Å (O6) and 4.337(2) Å (O5). Further hydrogen bonds are formed by the ammine ligands and the anions (N7–H7a···N3*i*: 0.80 Å, 2.43 Å, 3.132 Å, 147°; N7–H7c···O3*iv*: 0.81 Å, 2.54 Å, 3.143 Å, 132°; N8–H8c···O4*v*: 0.91 Å, 2.24 Å, 3.108 Å, 158°; N8–H8a···O1*v*: 0.66 Å, 2.68 Å, 3.011 Å, 114°; *iv*) *–x*+2, *y*, *–z*+3/2, *v*) *x*, *y*+1, *z*).

The packing in **5_Cu_NH₃** is characterized by chains along the *c* axis. The stacks are formed by the copper(II) ions and their ligands, with the 1-carboxymethyl-nitriminetetrazole anion connecting two copper(II) ions *via* the atoms N4, O1 and O4.

5.1.3 Energetic Properties

The energetic properties, such as decomposition temperature (T_{dec}), sensitivity to impact (E_{dr}), friction (F_r) and electric discharge (E_{el}), as well as the combustion energy ($\Delta_c U$) were determined. The properties of **4** and **5** are given in Table 5.6.

Table 5.6 Overview of the physico-chemical properties of the precursor molecules **4** and **5**.

	4	5
Formula	C ₃ H ₅ N ₅ O ₂	C ₃ H ₆ N ₆ O ₅
<i>M</i> [g/mol]	143.10	206.12
<i>E</i>_{dr} [J]^a	> 100	25
<i>F</i>_r [N]^b	> 360	216
<i>E</i>_{el} [J]^c	0.15	0.25
grain size[μm]	100–250	> 1000
<i>N</i> [%]^d	48.9	40.8
<i>Ω</i> [%]^e	–72 (CO ₂), –39 (CO)	–31 (CO ₂), –7.8 (CO)
<i>T</i>_{dec} [°C]^f	230	165
<i>ρ</i> [g/cm³]^g	1.66	1.73
<i>Δ</i>_c<i>U</i> [kJ/kg]^h	–11664	–7972
<i>Δ</i>_c<i>H</i>^o [kJ/mol]ⁱ	–1661	–1633
<i>Δ</i>_f<i>H</i>^o [kJ/mol]^j	–234	–405

a) BAM drop hammer [9], *b*) BAM methods [9], *c*) Electric discharge tester, *d*) Nitrogen content, *e*) Oxygen balance, *f*) Decomposition temperature from DSC ($\beta = 5$ K/min), *g*) determined by X-ray crystallography or pycnometer (*), *h*) Combustion energy, *i*) Enthalpy of combustion, *j*) Molar enthalpy of formation.

In analogy to other alkylated aminotetrazoles, **4** is neither sensitive to impact nor to friction, but its sensitivity to electric discharge is high with 0.15 J.^[5a, 6] In contrast to **1-OH** and **1-Cl**, **4** shows no definite melting point but decomposes at 230 °C (Figure 5.25).^[5a, 6] Its calculated density of 1.66 g/cm³ is higher than the densities of **1-OH** and **1-Cl**.^[5a, 6] The oxygen balance of **4**, depending on the formation of CO₂ or CO, is negative (Ω (CO₂) = -72 %, Ω (CO) = -39 %), despite its carboxy group.

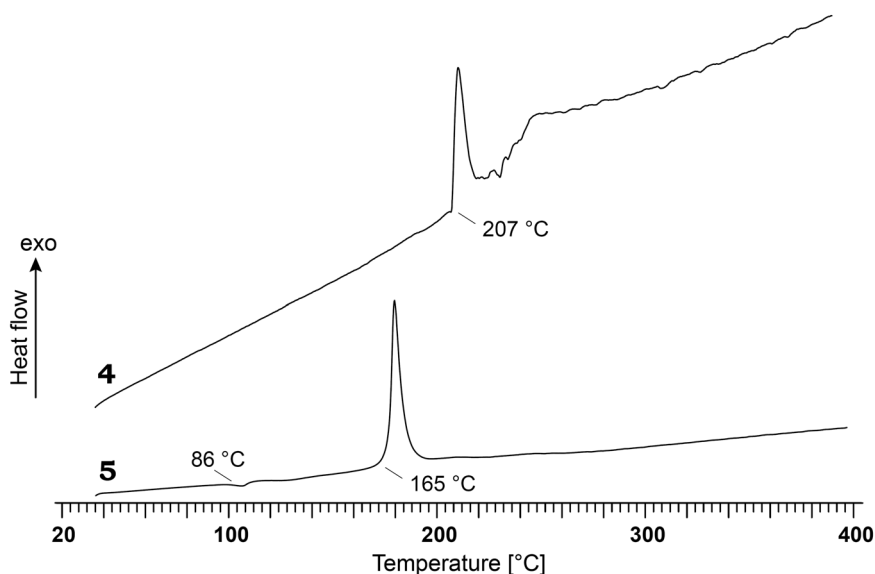


Figure 5.25 DSC thermograms of **4** and **5** in a range of 25–400 °C. Decomposition points are given as onset temperatures.

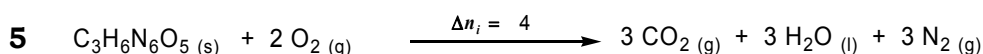
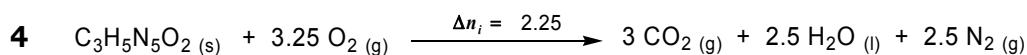
The reported values of the combustion energy ($\Delta_c U$) are the average of three single bomb calorimetry measurements. The standard molar enthalpy of combustion ($\Delta_c H^\circ$) was derived from equation 5.1.

$$\Delta_c H^\circ = \Delta_c U + \Delta n RT \quad (5.1)$$

$$\Delta n = \sum n_i (\text{gaseous products}) - \sum n_i (\text{gaseous educts})$$

$$n_i = \text{molar amount of gas } i.$$

The enthalpies of formation ($\Delta_f H^\circ$) for **4** and **5** were calculated at 298.15 K using the HESS thermochemical cycle and the following combustion reactions (Scheme 5.8).



Scheme 5.8 Combustion equations of **4** and **5**.

Applying these equations to **4**, an enthalpy of combustion of -1661 kJ/mol and an enthalpy of formation of -234 kJ/mol are obtained.

As expected, **5**, the nitrated compound of **4**, is sensitive to impact and friction with 25 J and 216 N, respectively. However, **5** is less sensitive to electric discharge than **4** with 0.25 J. In the DSC thermogram of **5**, at 86 °C an endothermic signal can be observed, due to the loss of crystal water (Figure 5.25). Thus it should be possible to obtain water-free 1-carboxymethyl-5-nitriminotetrazolate by storing **5** at temperatures above 86 °C or under high vacuum. This was not further investigated, because water-free **5** might be more sensitive and the reactions with **5** were performed in H₂O. The oxygen balance Ω of **5** is less negative compared to that of **4**, because of its nitrimino group ($\Omega(\text{CO}_2) = -31\%$, $\Omega(\text{CO}) = -7.8\%$). The enthalpy of combustion of **5** is with -1633 kJ/mol slightly more exothermic than the one of **4** and was calculated according equation 5.1. The enthalpy of formation of **5** is also exothermic with -405 kJ/mol.

An overview of the energetic properties, including the solubility in H₂O at ambient temperature, of the alkali metal salts of **4** is given in Table 5.7 and of the alkaline earth metal salts of **4**, as well as **4_Cu** in Table 5.8.

Table 5.7 Overview of the physico-chemical properties of **4_Li**, **4_Na**, **4_K**, **4_Rb**, and **4_Cs**.

	4_Li	4_Na	4_K	4_Rb	4_Cs
Formula	C ₃ H ₄ LiN ₅ O ₂ · H ₂ O	C ₃ H ₄ NaN ₅ O ₂ · 3H ₂ O	C ₃ H ₄ KN ₅ O ₂	C ₃ H ₄ N ₅ O ₃ Rb · H ₂ O	C ₃ H ₄ CsN ₅ O ₂
M [g/mol]	167.05	219.13	181.20	245.58	275.00
E_{dr} [J]^a	> 100	> 100	> 100	> 100	> 100
F_r [N]^b	> 360	> 360	> 360	> 360	> 360
E_{el} [J]^c	1.2	1.0	1.5	1.0	0.80
grain size [μm]	160–250	100–500	> 1000	500–1000	> 1000
N [%]^d	41.9	32.0	38.7	28.5	25.5
Ω [%]^e	-62.2	-51.1	-70.6	-52.1	-46.5
T_{dec} [°C]^f	317	298	345	365	364
ρ [g/cm³]^g	1.61	1.61	1.82	2.14	2.56
Δ_cU [kJ/kg]^h	-9441	-7959	-8403	-7228	-4413
Δ_cH^o [kJ/mol]ⁱ	-1572	-1739	-1519	-1770	-1209
Δ_tH^o [kJ/mol]^j	-1066	-1902	-803	-409	-936
H₂O sol. [wt%]^k	19 (25 °C)	25 (22 °C)	41 (22 °C)	63 (23 °C)	38 (22 °C)

a) BAM drop hammer [9], b) BAM methods [9], c) Electric discharge tester, d) Nitrogen content, e) Oxygen balance, f) Decomposition temperature from DSC ($\beta = 5$ K/min), g) determined by X-ray crystallography or pycnometer (*), h) Combustion energy, i) Enthalpy of combustion, j) Molar enthalpy of formation, k) Solubility in H₂O (H₂O temperature).

The alkali metal salts as well as the alkaline earth metal salts of **4** decompose at temperatures above 300 °C (**4_Li**: 317 °C, **4_K**: 345 °C, **4_Rb**: 365 °C, **4_Cs**: 364 °C, **4_Mg**: 327 °C, **4_Ca**: 315 °C, **4_Sr**: 304 °C, **4_Ba**: 315 °C), except **4_Na** ($T_{\text{dec}} = 298$ °C). Interestingly, **4_Cu** displays a very low decomposition point of 220 °C, which is even lower

than the one of **4**. All salts of **4**, which contain crystal water, show endothermic signals in their DSC thermograms due to the loss of water (**4_Li**: 107 °C, **4_Na**: 53 °C, 164 °C, **4_Rb**: 63 °C, **4_Mg**: 166 °C, **4_Ca**: 103 °C, 173 °C, **4_Sr**: 121 °C, **4_Ba**: 102 °C). The alkali salts **4_K**, **4_Rb**, and **4_Cs** show an endothermic signal in the temperature range of 243–290 °C. This is caused by melting of the compounds. In the case of **4_Na**, melting starts at 293 °C before decomposition occurs.

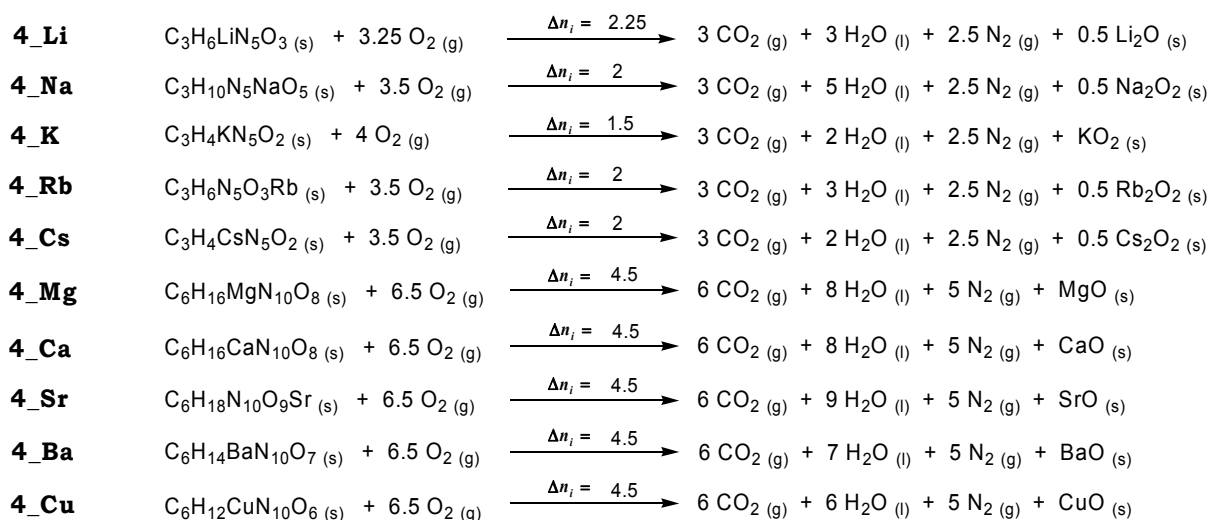
Table 5.8 Overview of the physico-chemical properties of **4_Mg**, **4_Ca**, **4_Sr**, **4_Ba**, and **4_Cu**.

	4_Mg	4_Ca	4_Sr	4_Ba	4_Cu
Formula	Mg(C ₃ H ₄ N ₅ O ₂) ₂ · 4H ₂ O	Ca(C ₃ H ₃ N ₅ O ₂) ₂ · 4H ₂ O	Sr(C ₃ H ₄ N ₆ O ₂) ₂ · 5H ₂ O	Ba(C ₃ H ₄ N ₅ O ₂) ₂ · 3H ₂ O	[Cu(C ₃ H ₄ N ₅ O ₂) ₂ (H ₂ O) ₂]
M [g/mol]	380.56	396.33	461.89	475.57	383.77
E_{dr} [J]^a	> 100	> 100	> 100	> 100	> 100
F_r [N]^b	> 360	> 360	> 360	288	> 360
E_{el} [J]^c	1.2	1.0	1.1	1.1	1.0
grain size [μm]	100–250	> 1000	> 1000	< 250	100–250
N [%]^d	36.8	35.3	30.3	29.5	36.5
Ω [%]^e	-54.7	-52.5	-45.0	-43.7	-45.9
T_{dec} [°C]^f	327	315	304	315	220
ρ [g/cm³]^g	1.74	1.74	1.72	2.11	2.17* (25°C)
Δ_cU [kJ/kg]^h	-7804	-8240	-7159	-6167	-8616
Δ_cH^o [kJ/mol]ⁱ	-2959	-3254	-3296	-2922	-3293
Δ_fH^o [kJ/mol]^j	-2892	-2664	-2823	-2625	-1098
H₂O sol. [wt%]^k	12 (23 °C)	18 (24 °C)	7.2 (24 °C)	5.0 (24 °C)	< 0.2 (23 °C)

a) BAM drop hammer [9], b) BAM methods [9], c) Electric discharge tester, d) Nitrogen content, e) Oxygen balance, f) Decomposition temperature from DSC ($\beta = 5$ K/min), g) determined by X-ray crystallography or pycnometer (*), h) Combustion energy, i) Enthalpy of combustion, j) Molar enthalpy of formation, k) Solubility in H₂O (H₂O temperature), **) n.d. = not determined.

All salts of **4** prepared are insensitive to impact. This is also true for the sensitivity to friction, except **4_Ba**, which is with 288 N less sensitive. Furthermore, all compounds of **4** display very high values for the sensitivity to electric discharge ($E_{el} \geq 1.0$ J). The standard molar enthalpy of combustion ($\Delta_c H^o$) was derived from equation 5.1. The enthalpies of formation ($\Delta_f H^o$) for the salts of **4** were calculated at 298.15 K using the HESS thermochemical cycle and the combustion reactions shown in Scheme 5.9.

All salts are calculated to be formed exothermically. The enthalpies of formation of the alkali metal salts, except of **4_Na**, are higher than the ones of the alkaline earth metal salts. The smallest value is found for **4_Mg**, presumably due to its four crystal water molecules. The highest $\Delta_f H^o$ value is that of **4_Rb**. The $\Delta_f H^o$ value of **4_Cu** is comparable to the one of **4_Li**.

**Scheme 5.9** Combustion equations of the compounds of **4**.

For determining the solubility in H₂O, each compound was added to 1 mL of H₂O under a definite temperature until the solution was saturated. The solubilities are given in percent by weight (wt%) and were calculated according to equation 5.2.

$$\text{H}_2\text{O-sol.} = \frac{m_{\text{dissolved Compound}}}{m_{\text{dissolved Compound}} + m_{\text{Solvent}}} \cdot 100 \quad (5.2)$$

All alkali metal salts of **4** show a higher solubility in H₂O than the alkaline earth metal salts. The highest solubility has **4_Rb** with 63 wt%, followed by **4_K** and **4Cs** with 41 wt% and 38 wt%. Low solubilities were found for **4_Sr** (7.2 wt%), **4_Ba** (5.0 wt%), and **4_Cu** (< 0.2 wt%). Also the solubility of **4_Li** (19 wt%) is quite low, compared to that of other lithium salts.

The data of the alkali metal salts of **5** can be found in Table 5.9. An overview of the properties of the alkaline earth metal salts and copper compounds of **5** is given in Table 5.10 and Table 5.11.

Compared to the salts of **4**, the salts of **5** are significantly more sensitive to impact, friction, and electric discharge. However, there is also a difference between the alkaline earth metal salts with two monoanions and the alkaline earth metal salts with one dianion. The latter are insensitive to impact and friction. Their sensitivities to electric discharge are between 0.15 J and 0.60 J. **5_Mg1**, **5_Ca1**, **5_Sr1**, and **5_Ba1** are sensitive to impact with values of 30 J, 5.0 J, 6.0 J, and less than 5.0 J, respectively. Their sensitivities to electric discharge were determined with values between 0.10 J and 0.30 J. Only **5_Mg1** is sensitive to friction with a value of 324 N. **5_Cs** is the most sensitive of the alkali metal salts of **5** ($E_{\text{dr}} = 3.0 \text{ J}$, $F_{\text{r}} = 252 \text{ N}$, $E_{\text{el}} = 0.15 \text{ J}$). **5_Na** is neither sensitive to impact nor to friction. **5_K** and **5_Rb** are less sensitive to impact with 30 J, but only **5_Rb** is sensitive to friction with 240 N. The sensitivities of the two copper(II) complexes **5_Cu_H2O** and **5_Cu_NH3** are

comparable. Both are insensitive to friction, but sensitive to impact with 10 J and 15 J, respectively. **5_Cu_NH₃** is slightly less sensitive to electric discharge with 0.80 J.

Table 5.9 Overview of the physico-chemical properties of **5_Na**, **5_K**, **5_Rb**, and **5_Cs**.

	5_Na	5_K	5_Rb	5_Cs
Formula	C ₃ H ₆ N ₆ NaO _{5.5}	C ₃ H ₅ KN ₆ O ₅	C ₃ H ₅ N ₆ O ₅ Rb	C ₃ H ₄ CsN ₆ O _{4.5}
M [g/mol]	246.12	244.21	290.58	329.00
E_{dr} [J]^a	40	30	30	3.0
F_r [N]^b	> 360	> 360	240	252
E_{el} [J]^c	0.25	0.20	0.20	0.15
grain size [μm]	250–1000	250–500	> 1000	250–500
N [%]^d	35.4	34.4	28.9	25.5
Ω [%]^e	-29.3	-36.0	-30.3	-26.7
T_{dec} [°C]^f	222	220	184	166
ρ [g/cm³]^g	2.19* (22 °C)	1.86	2.10	2.50* (22 °C)
Δ_cU [kJ/kg]^h	-6712	-6548	-5273	-3587
Δ_cH^o [kJ/mol]ⁱ	-1643	-1591	-1524	-1171
Δ_fH^o [kJ/mol]^j	-909	-873	-1224	-985
H₂O sol. [wt%]^k	83 (22 °C)	9.3 (22 °C)	18 (22 °C)	45 (24 °C)

a) BAM drop hammer ^[9], b) BAM methods ^[9], c) Electric discharge tester, d) Nitrogen content, e) Oxygen balance, f) Decomposition temperature from DSC ($\beta = 5$ K/min), g) determined by X-ray crystallography or pycnometer (*), h) Combustion energy, i) Enthalpy of combustion, j) Molar enthalpy of formation, k) Solubility in H₂O (H₂O temperature).

The decomposition temperatures of the alkali metal salts of **5** are significantly lower than those of the corresponding salts of **4**. Especially **5_Cs** decomposes at a quite low temperature of 184 °C. Except for **5_Cs**, the loss of crystal water can be found in the DSC thermograms (**5_Na**: 103 °C, 142 °C, **5_K**: 140 °C, **5_Rb**: 118 °C). Again a noticeable difference between the decomposition temperatures of the mono- and dianionic salts of **5** can be observed. The salts with the dianions are about 100 °C more stable (**5_Mg1**: 282 °C, **5_Mg2**: 301 °C, **5_Ca1**: 194 °C, **5_Ca2**: 308 °C, **5_Sr1**: 218 °C, **5_Sr2**: 308 °C, **5_Ba1**: 243 °C, **5_Ba2**: 342 °C). Except for **5_Ca1**, **5_Sr1**, and **5_Ba1**, endothermic signals due to the loss of crystal water can be observed. The decomposition points of the copper(II) compounds **5_Cu_H₂O** and **5_Cu_NH₃** are with 237 °C and 216 °C comparable to the ones of the monoanionic salts of **5**. Both show additional endothermic signals at 130 °C, 120 °C and 155 °C, due to the loss of H₂O or NH₃.

The solubilities of the compounds of **5** were determined according to equation 5.2. The solubilities of the alkali metal salts differ much from each other. **5_Na** is the best soluble compound with a solubility of 83 wt%. Surprisingly, **5_K** shows the lowest solubility (9.3 wt%). A comparison of the solubilities of the mono- and dianion salts, reveals, that the monoanion salts (**5_M1**) are better soluble in H₂O than the corresponding dianion salts (**5_M2**). The lowest solubilities are found for **5_Ba2** (3.0 wt%) and for the two copper(II) compounds **5_Cu_H₂O** (3.0 wt%) and **5_Cu_NH₃** (1.0 wt%), whereas both magnesium salts (**5_Mg1** and **5_Mg2**) are the best soluble ones.

Table 5.10 Overview of the physico-chemical properties of **5_Mg1**, **5_Ca1**, **5_Sr1**, **5_Ba1**, and **5_Cu_H₂O**.

	5_Mg1	5_Ca1	5_Sr1	5_Ba1	5_Cu_H₂O
Formula	Mg(C ₃ H ₃ N ₆ O ₄) ₂ · 10H ₂ O	Ca(C ₃ H ₃ N ₆ O ₄) ₂ · 2H ₂ O	Sr(C ₃ H ₃ N ₆ O ₄) ₂ · H ₂ O	Ba(C ₃ H ₃ N ₆ O ₄) ₂ · H ₂ O	[Cu(C ₃ H ₃ N ₆ O ₄) ₂ (H ₂ O)] ₂ · 2H ₂ O
M [g/mol]	578.65	450.30	479.82	529.53	509.80
E_{dr} [J]^a	30	5.0	6.0	< 5.0	10
F_r [N]^b	324	> 360	> 360	> 360	> 360
E_{el} [J]^c	0.30	0.30	0.10	0.25	0.20
grain size [μm]	500–1000	100–500	250–500	100–500	> 1000
N [%]^d	29.1	37.3	35.0	31.7	33.0
Ω [%]^e	-22.1	-28.4	-26.7	-24.3	-25.1
T_{dec} [°C]^f	282	194	218	243	237
ρ [g/cm³]^g	1.67	1.90	1.94	2.06	1.98
Δ_cU [kJ/kg]^h	-6913	-7747	-6433	-5592	-7913
Δ_cH^o [kJ/mol]ⁱ	-3981	-3469	-3066	-2940	-4012
Δ_fH^o [kJ/mol]^j	-3299	-1592	-1624	-1518	-665
H₂O sol. [wt%]^k	37 (22 °C)	28 (23 °C)	19.5 (24 °C)	6.0 (25 °C)	3.0 (23 °C)

a) BAM drop hammer ^[9], b) BAM methods ^[9], c) Electric discharge tester, d) Nitrogen content, e) Oxygen balance, f) Decomposition temperature from DSC ($\beta = 5$ K/min), g) determined by X-ray crystallography or pycnometer (*), h) Combustion energy, i) Enthalpy of combustion, j) Molar enthalpy of formation, k) Solubility in H₂O (H₂O temperature), **) n.d. = not determined.

Table 5.11 Overview of the physico-chemical properties of **5_Mg2**, **5_Ca2**, **5_Sr2**, **5_Ba2**, and **5_Cu_NH₃**.

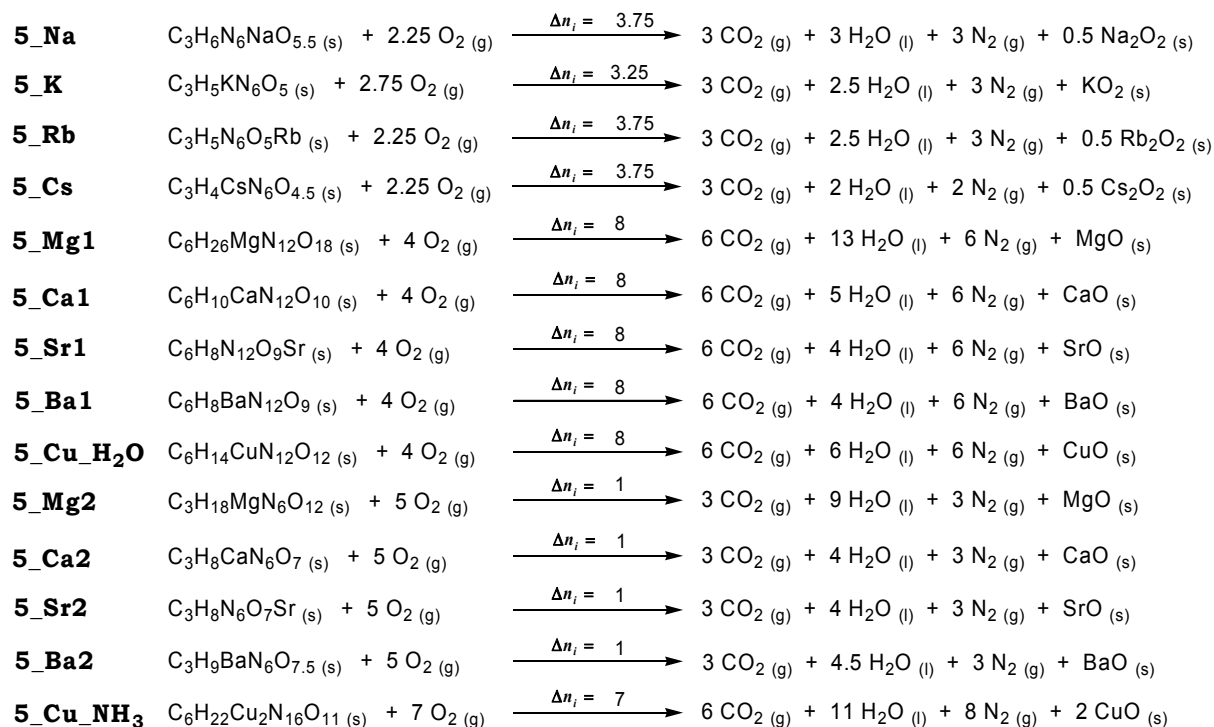
	5_Mg2	5_Ca2	5_Sr2	5_Ba2	5_Cu_NH₃
Formula	Mg(C ₃ H ₂ N ₆ O ₄) · 8H ₂ O	Ca(C ₃ H ₂ N ₆ O ₄) · 3H ₂ O	Sr(C ₃ H ₂ N ₆ O ₄) · 3H ₂ O	Ba(C ₃ H ₂ N ₆ O ₄) · 3.5H ₂ O	[Cu ₂ (C ₃ H ₂ N ₆ O ₄) ₂ (NH ₃) ₄] · 3H ₂ O
M [g/mol]	354.51	280.21	327.75	383.47	567.39
E_{dr} [J]^a	> 50	40	> 100	> 100	15
F_r [N]^b	> 360	360	> 360	> 360	> 360
E_{el} [J]^c	0.60	0.60	0.25	0.15	0.80
grain size [μm]	250–500	> 1000	> 1000	250–500	> 1000
N [%]^d	23.7	30.0	25.6	21.8	39.5
Ω [%]^e	-18.1	-22.8	-19.5	-16.6	-67.7
T_{dec} [°C]^f	301	308	308	342	216
ρ [g/cm³]^g	1.67	1.87	2.15	2.65* (21 °C)	1.93
Δ_cU [kJ/kg]^h	-4833	-5498	-4965	-7917	-7909
Δ_cH^o [kJ/mol]ⁱ	-1711	-1538	-1618	-3121	-4486
Δ_fH^o [kJ/mol]^j	-3245	-2056	-1891	-585	-1648
H₂O sol. [wt%]^k	35 (22 °C)	25 (23 °C)	15.6 (24 °C)	3.0 (25 °C)	1.1 (23 °C)

a) BAM drop hammer ^[9], b) BAM methods ^[9], c) Electric discharge tester, d) Nitrogen content, e) Oxygen balance, f) Decomposition temperature from DSC ($\beta = 5$ K/min), g) determined by X-ray crystallography or pycnometer (*), h) Combustion energy, i) Enthalpy of combustion, j) Molar enthalpy of formation, k) Solubility in H₂O (H₂O temperature), **) n.d. = not determined.

The enthalpy of formation ($\Delta_f H^o$) for each compound of **5** prepared was calculated at 298.15 K using the HESS thermochemical cycle and the combustion reactions shown in Scheme 5.10.

All compounds of **5** are calculated to form exothermically. The alkali metal salts of **5** show smaller enthalpies of formation than the alkaline earth metal salts. Again, a difference

between the salts with mono- or dianions can be observed. Salts with dianions have smaller enthalpies of formations. An exception is **5_Ba2** with $\Delta_f H^\circ = -585$ kJ/mol and **2_Ba1** with $\Delta_f H^\circ = -1518$ kJ/mol.



Scheme 5.10 Combustion equations of the salts of **5**.

The heats of formation of the combustion products $H_2O (l)$ (-286 kJ/mol), $CO_2 (g)$ (-393 kJ/mol), $Li_2O (s)$ (-599 kJ/mol), $Na_2O_2 (s)$ (-513 kJ/mol), $KO_2 (s)$ (-284.5 kJ/mol), $Rb_2O_2 (s)$ (-426 kJ/mol), $Cs_2O_2 (s)$ (-403 kJ/mol), $MgO (s)$ (-601.2 kJ/mol), $CaO (s)$ (-635 kJ/mol), $SrO (s)$ (-592 kJ/mol), $BaO (s)$ (-548 kJ/mol), and $CuO (s)$ (-157 kJ/mol) were taken from literature.^[7, 10]

5.1.4 Flame Color and Combustion Behavior

Only the salts, which could find an application as colorants in pyrotechnics – **4_Li**, **4_Ca**, **4_Sr**, **4_Ba**, **4_Cu**, **5_Ca1**, **5_Ca2**, **5_Sr1**, **5_Sr2**, **5_Ba1**, **5_Ba2**, **5_Cu_H2O**, and **5_Cu_NH3** – were tested with regard to their emitting color during combustion in the flame of a BUNSEN burner. For this, a few milligrams of each compound on a spatula were put into the flame of a BUNSEN burner.

In Figure 5.26 the flames of the red light emitting salts of **4**, **4_Li**, **4_Ca**, and **4_Sr**, are depicted. **4_Li** offers a very intense dark red, but small flame. The flames of **4_Ca** and **4_Sr** are more orange-red.

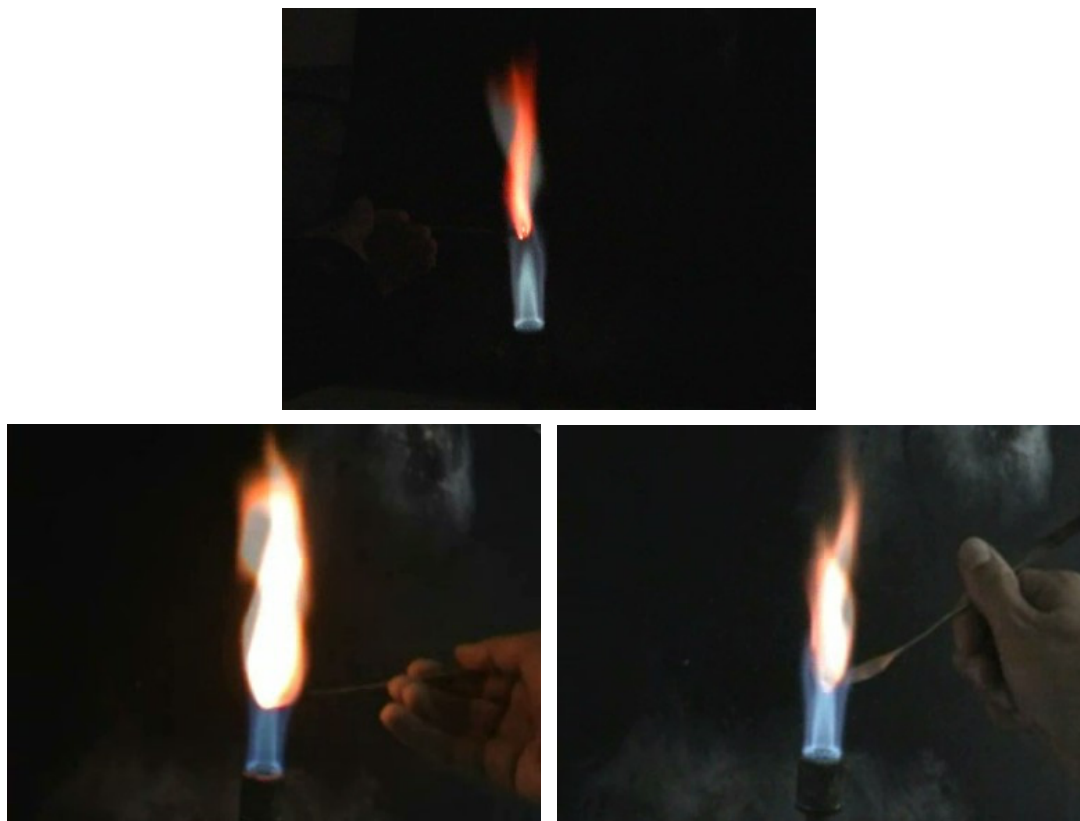


Figure 5.26 Flame color of **4_Li** (top), **4_Ca** (down, left), and **4_Sr** (down, right).

In analogy to other chlorine-free barium salts, **4_Ba** shows an intense tall white flame (Figure 5.27). If a mixture of **4_Ba** and PVC (in a ratio of 50 wt% : 50 wt%) is inserted into the flame of a BUNSEN burner, the light emission turns into yellow-green.

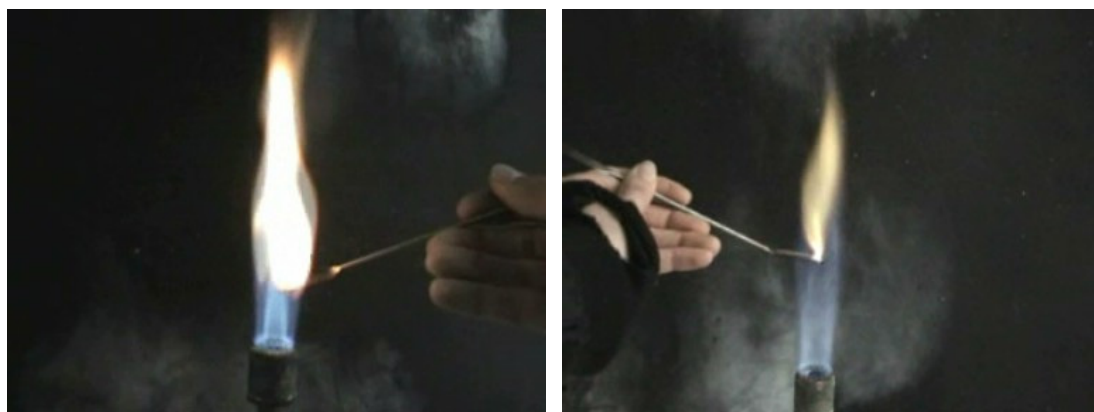


Figure 5.27 Flame color of **4_Ba** (left) and a mixture of **4_Ba** and PVC (right).



Figure 5.28 Flame color of **4_Cu** in the flame of a BUNSEN burner.

4_Cu has, as expected, a very intense dark green and tall flame (Figure 5.28). The compounds of **4** tested combust slowly and without any sound. No smoke, but a very small amount of solid black residues was observed.

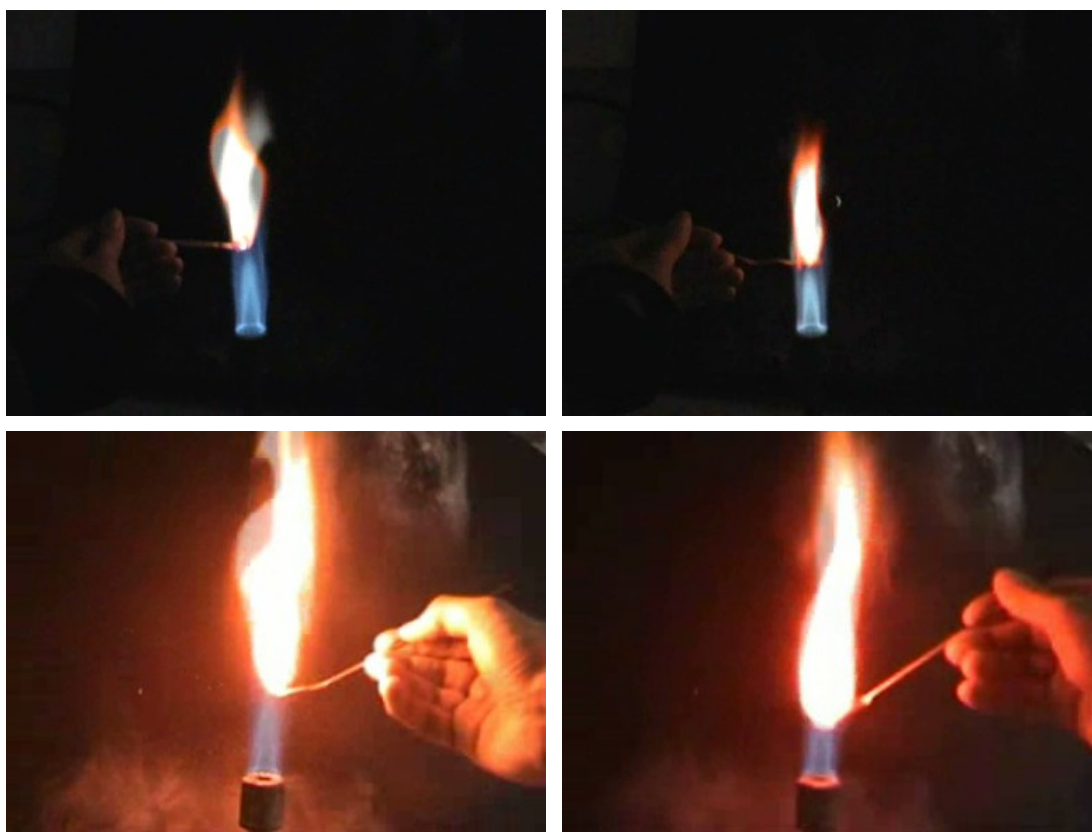


Figure 5.29 Flame color of **5_Ca1** (top, left), **5_Ca2** (top, right), **5_Sr1** (down, left), and **5_Sr2** (down, right).

The calcium and strontium salts of **5** show a red flame (Figure 5.29). **5_Sr2** has the most intense red light emission. The calcium salts **5_Ca1** and **5_Ca2** show a smaller flame and the flames are more orange-red.

The neat barium salts **5_Ba1** and **5_Ba2** combust with a tall white flame (Figure 5.30). However, if they are combined with PVC in a ratio of 50 wt% : 50 wt%, the light

emission changes into green. However, it is less intense compared to the one of the copper(II) compounds (Figure 5.31).



Figure 5.30 Flame color of **5_Ba1** (top, left), **5_Ba2** (top, right), a mixture of **5_Ba1** and PVC (down, left), and a mixture of **5_Ba2** and PVC (down, right)

Both copper(II) compounds of **5**, **5_Cu_H₂O** and **5_Cu_NH₃**, show a very intense dark green color emission in the flame of a BUNSEN burner.

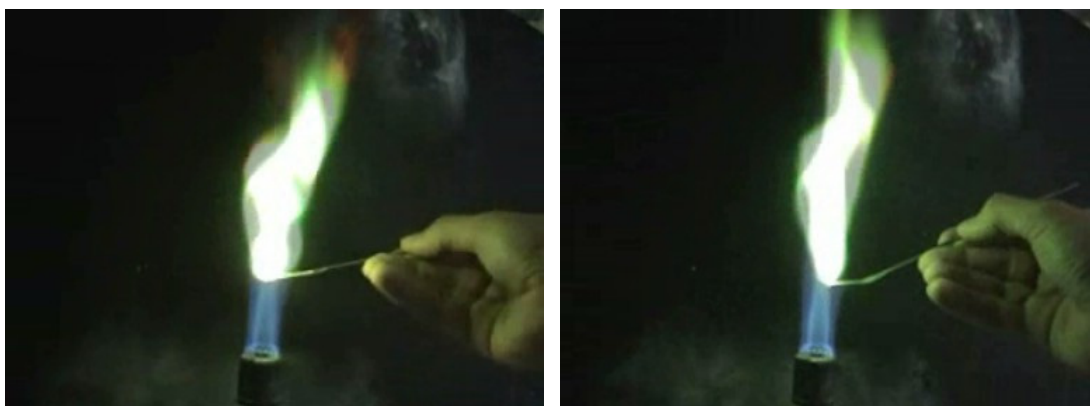


Figure 5.31 Flame color of **5_Cu_H₂O** (left) and **5_Cu_NH₃** (right).

All salts of **5** combust without any visible smoke production and no solid residues were observed. Compared to the salts of **4**, they combust with a higher velocity.

5.1.5 Pyrotechnic Compositions

The compounds **4_Li**, **4_Sr**, and **4_Ba**, as well as **5_Sr1**, **5_Sr2**, **5_Ba1**, **5_Ba2**, **5_Cu_H₂O**, and **5_Cu_NH₃** were chosen to be investigated as coloring agents for pyrotechnic compositions. All mentioned compositions were prepared manually. Details can be found in chapter 5.2.4.

The performance of each composition has been evaluated with respect to the following aspects:

- color emission (subjective impression)
- smoke generation
- morphology and amount of solid residues
- thermal stability
- moisture sensitivity

The US Army red flare composition # M126 A1 (red parachute) – 39 wt% Sr(NO₃)₂, 30 wt% Mg, 13 wt% KClO₄, 8 wt% VAAR – was used as a measure for the performance of the red light compositions. Its decomposition point was determined at 360 °C by DSC-measurement ($\beta = 5$ K/min). Composition # M126 A1 is sensitive to impact with 10 J, to friction with 144 N, and to electric discharge with 0.75 J.

The performance of the compositions for green light were compared to the barium nitrate-based US Army composition # M125 A1 (green parachute): 50 wt% Ba(NO₃)₂, 30 wt% Mg, 15 wt% PVC, 5 wt% VAAR. Its decomposition point is 244 °C. It is sensitive to impact (9.0 J), friction (288 N), and electric discharge (1.2 J).

The lithium salt **4_Li** was combined with the oxidizers ammonium nitrate, potassium permanganate, ammonium dinitramide (ADN), and potassium dinitramide (KDN). Magnesium, silicon, starch, and charcoal were used as fuels. An overview of all compositions containing **4_Li** can be found in chapter 5.2.4.1. The compositions containing KDN either did not burn or had a violet flame. If ammonium nitrate or potassium permanganate were used, the compositions produced in general a yellow or orange flame. The best performing composition containing **4_Li** is **4_Li_7.2**, which consists of 35 wt% **4_Li**, 46 wt% ADN, 7 wt% magnesium, and 12 wt% VAAR (Table 5.18). This mixture could be ignited easily and has an intense deep red flame (Figure 5.32). The combustion occurred fast and almost smokeless. A very small amount of solid residues was observed.

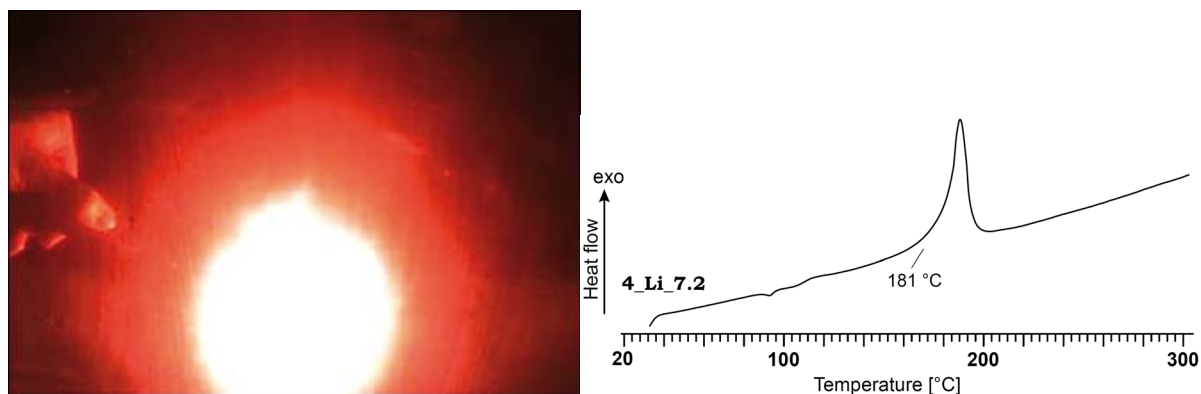


Figure 5.32 Burn down of the composition **4_Li_7.2** (left) and DSC thermogram of **4_Li_7.2** (right) in the temperature range of 30–300 °C.

4_Li_7.2 decomposes at temperatures above 181 °C. This is caused by the decomposition of ADN.^[11] **4_Li_7.2** is very sensitive to impact (3.0 J) and sensitive to friction (120 N), but insensitive to electric discharge (1.5 J).

4_Sr was combined with potassium permanganate, potassium nitrate, manganese dioxide, ammonium nitrate, ADN, and KDN, as well as magnesium, magnalium, aluminum, and **5-At**. Specific information about the exact ratios can be found in chapter 5.2.4.1. Using potassium permanganate, nitrate, or dinitramide as oxidizer caused a violet flame. In the case of potassium permanganate, the combustion occurred too vigorously or without a flame. Compositions with manganese dioxide could not be ignited. If ammonium nitrate and **5-At** or magnalium were added, no ignition was possible. However, two of the best performing compositions with **4_Sr** contain ammonium nitrate. **4_Sr_2.7** consists of 41 wt% ammonium nitrate, 25 wt% **4_Sr**, 20 wt% magnesium, and 14 wt% VAAR (Table 5.22). Its intense red flame is comparable to the one of composition **4_Sr_7.2** (60 wt% ammonium nitrate, 20 wt% **4_Sr**, 7 wt% magnesium, 3 wt% **5-At**, and 10 wt% VAAR; Table 5.27). The burn downs of both compositions are depicted in Figure 5.33.

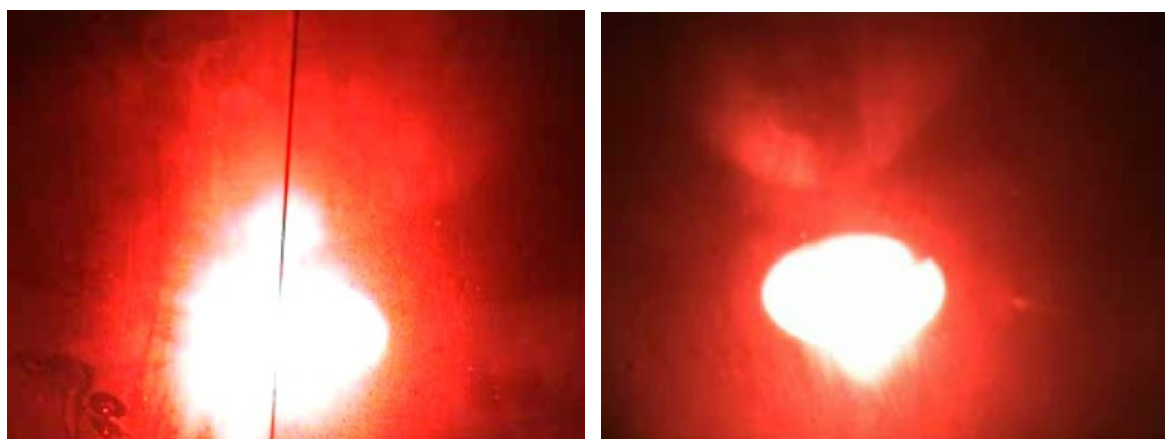


Figure 5.33 Burn down of the pyrotechnic compositions **4_Sr_2.7** (left) and **4_Sr_7.2** (right).

Both combusted with a moderate velocity and were easy to ignite. Almost no smoke could be observed, however some sparks and a very small amount of solid residues were

detected. **4_Sr_2.7** and **4_Sr_7.2** show similar decomposition points of 285 °C and 289 °C (Figure 5.34).

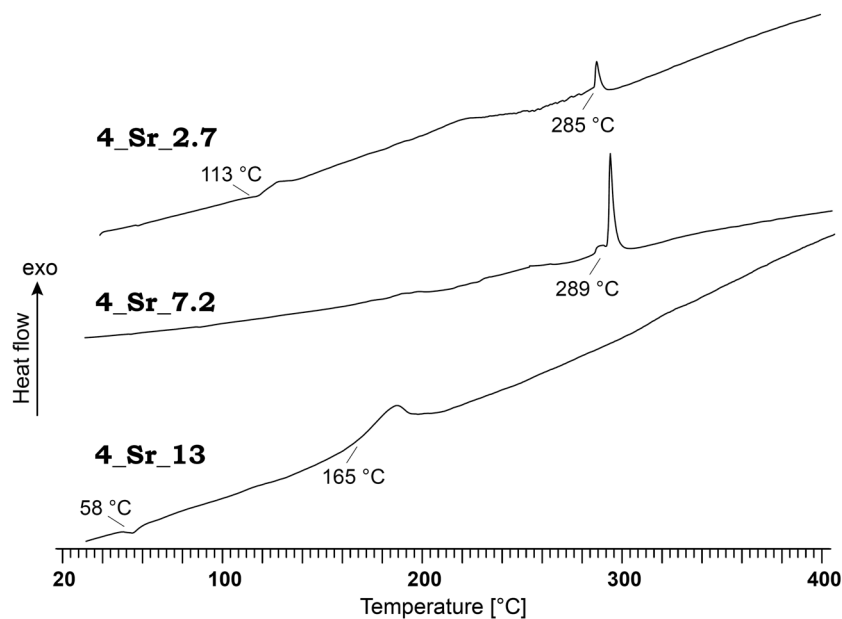


Figure 5.34 DSC thermograms of the pyrotechnic compositions **4_Sr_2.7**, **4_Sr_7.2**, and **4_Sr_13** in a temperature range of 30–400 °C. Decomposition points are given as onset temperatures.

Both, composition **4_Sr_2.7** and **4_Sr_7.2**, are less sensitive to impact with 30 J and 35 J, respectively, and insensitive to electric discharge (1.5 J). **4_Sr_7.2** is insensitive to friction (> 350 N), however **4_Sr_2.7** is sensitive with 240 N.

The third pyrotechnic composition of **4_Sr**, **4_Sr_13**, which combusts with a very intense red flame (Figure 5.35), was made up of 46 wt% ADN, 35 wt% **4_Sr**, 7 wt% magnesium, and 12 wt% VAAR (Table 5.33). The combustion occurred fast and smoke-free. Only a very small amount of solid residues was observed.

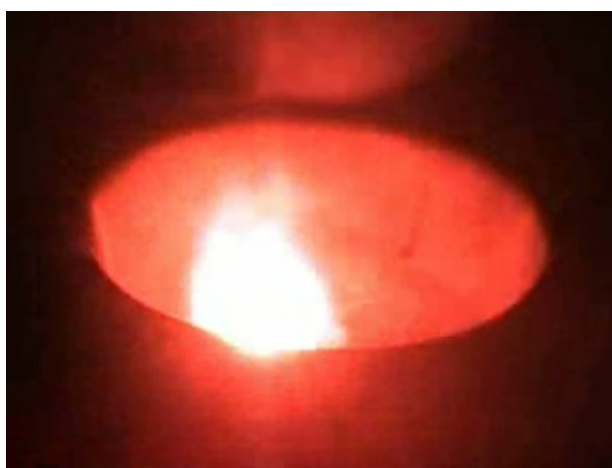


Figure 5.35 Burn down of the pyrotechnic composition **4_Sr_13**.

Compared to **4_Sr_2.7** and **4_Sr_7.2**, **4_Sr_13** is thermally less stable with a decomposition temperature of 165 °C (Figure 5.34). It is also much more sensitive to impact with 3.5 J and friction with 80 N. However, it is insensitive to electric discharge.

The barium salt **4_Ba** was combined with the oxidizers ammonium nitrate, potassium nitrate, ADN, and KDN and the fuels magnesium, magnalium, boron, **5-At**, and aluminum (see chapter 5.2.4.3). Furthermore, PVC was added to some compositions to improve the emission of green light (Table 5.40 and Table 5.44). However, these compositions produced a yellow or yellow-green flame. If magnalium or **5-At** were used, the compositions could not be ignited or just glowed. Again, ammonium nitrate and ADN were the best oxidizers to obtain the desired green flame. This is true also for the fuels magnesium and boron, whereas the addition of magnesium caused some sparks and the usage of boron could also lead to a yellow flame. Two compositions with a convincing color performance could be found: **4_Ba_4.2** and **4_Ba_14.2**. Both combusted with a green flame (Figure 5.36). **4_Ba_4.2** consists of 57 wt% ammonium nitrate, 19 wt% **4_Ba**, 16 wt% boron, and 8 wt% VAAR (Table 5.38) and **4_Ba_14.2** of 41 wt% ADN, 31 wt% **4_Ba**, 8 wt% magnesium, 10 wt% boron, and 10 wt% VAAR (Table 5.48).



Figure 5.36 Burn down of the pyrotechnic compositions **4_Ba_4.2** (left) and **4_Ba_14.2** (right).

Composition **4_Ba_14.2** combusted faster with more sparks than **4_Ba_4.2**, but without glowing residues and no smoke. **4_Ba_4.2** is thermally more stable with a decomposition temperature of 230 °C than **4_Ba_14.2** with a decomposition temperature of 170 °C (Figure 5.38). In the DSC thermogram of **4_Ba_4.2** three endothermic signals at 52 °C, 125 °C, and 164 °C were observed. They are caused by phase transitions of ammonium nitrate.^[12]

Both compositions are very sensitive to impact with 3.0 J (**4_Ba_4.2**) and less than 1.0 J (**4_Ba_14.2**). **4_Ba_14.2** is sensitive to friction (108 N), whereas **4_Ba_4.2** is insensitive (> 360 N). The sensitivities to electric discharge were determined with 1.5 J (**4_Ba_4.2**) and 0.75 J (**4_Ba_14.2**).



Figure 5.37 Burn down of the pyrotechnic composition **4_Ba_11.3**.

If KDN was used, an intense white flame could be observed (Figure 5.37), especially, with aluminum as fuel. Composition **4_Ba_11.3** consists of 44 wt% **4_Ba**, 43 wt% KDN, 2 wt% aluminum, and 11 wt% VAAR (Table 5.45). It combusted quite fast with a very intense white flame and some smoke. No solid residues were observed. Composition **4_Ba_11.3** decomposes at temperatures above 197 °C in several steps (Figure 5.38). At 81 °C an endothermic signal can be observed. **4_Ba_11.3** is sensitive to impact (10 J), but insensitive to friction (> 360 N) and electric discharge (1.5 J).

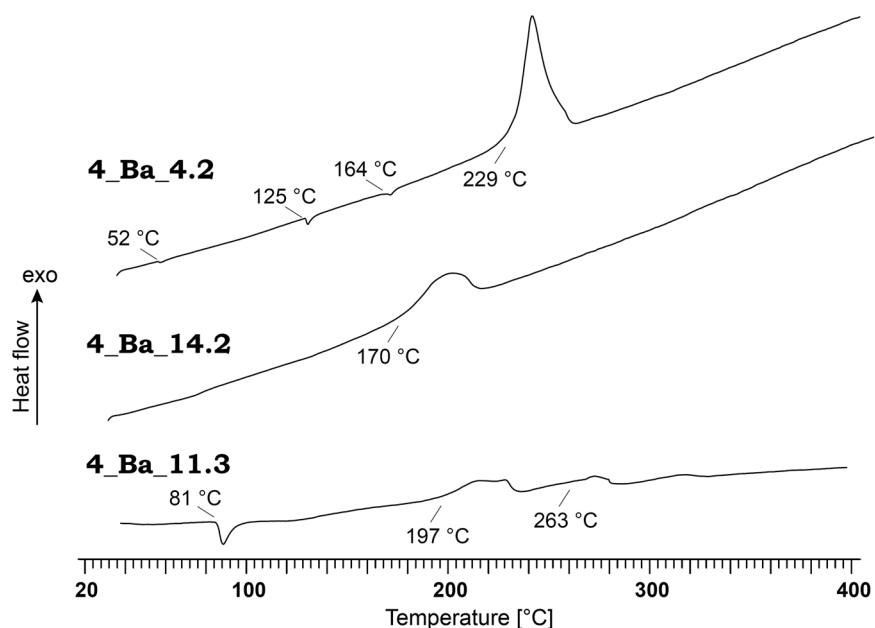


Figure 5.38 DSC thermograms of the pyrotechnic compositions **4_Ba_4.2**, **4_Ba_14.2**, and **4_Ba_11.3** in the temperature range of 30–400 °C. Decomposition points are given as onset temperatures.

Also the strontium salts of **5**, **5_Sr1** and **5_Sr2**, were investigated as colorants in pyrotechnic compositions (see chapter 5.2.4.4 and 5.2.4.5). Each of it was combined with the oxidizers ammonium nitrate or ADN and the fuels magnesium, **5-At** or aluminum. The two best performing compositions containing **5_Sr1** are **5_Sr1_1** and **5_Sr1_4.1**. **5_Sr1_1** consists of 46 wt% ADN, 35 wt% **5_Sr1**, 8 wt% magnesium, and 11 wt% VAAR (Table 5.53). It combusted very fast with a very intense red flame (Figure 5.39). Thereby no smoke or solid

residues, but several sparks were observed. Composition **5_Sr1_4.1** consists of 43 wt% ammonium nitrate, 23 wt% **5_Sr1**, 19 wt% magnesium, and 15 wt% VAAR (Table 5.56). It combusted also with a very intense red flame (Figure 5.39), but with a lower velocity than composition **5_Sr1_1**. Few sparks, less smoke and a small amount of solid residues were observed.



Figure 5.39 Burn down of the pyrotechnic compositions **5_Sr1_1** (left) and **5_Sr1_4.1** (right).

Composition **5_Sr1_1** decomposes at lower temperatures ($T_{\text{dec}} = 180\text{ }^{\circ}\text{C}$) than **5_Sr1_4.1** ($T_{\text{dec}} = 262\text{ }^{\circ}\text{C}$), because it contains ADN (Figure 5.40). This also explains the higher sensitivity of **5_Sr1_1** to impact (5.0 J), friction (80 N), and electric discharge (1.25 J). **5_Sr1_4.1** is sensitive to impact with 10 J, to friction with 324 N and insensitive to electric discharge ($> 1.50\text{ J}$).

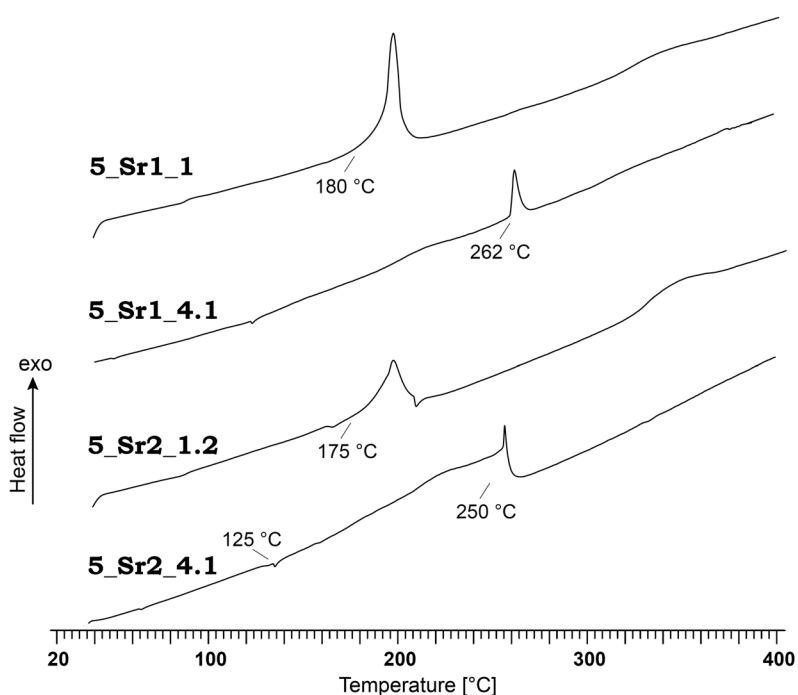


Figure 5.40 DSC thermograms of the pyrotechnic compositions **5_Sr1_1**, **5_Sr1_4.2**, **5_Sr2_1.2**, and **5_Sr2_4.1** in the temperature range of 30–400 °C. Decomposition points are given as onset temperatures.

The two best performing compositions containing **5_Sr2** have similar formulations like those of **5_Sr1**. Pyrotechnic composition **5_Sr2_1.2** consists of 45 wt% ADN, 35 wt% **5_Sr2**, 7 wt% magnesium, and 13 wt% VAAR (Table 5.57). Composition **5_Sr2_4.1** consists of 45 wt% ammonium nitrate, 25 wt% **5_Sr2**, 15 wt% magnesium, and 15 wt% VAAR (Table 5.60). Both compositions produce a very intense red flame (Figure 5.41).

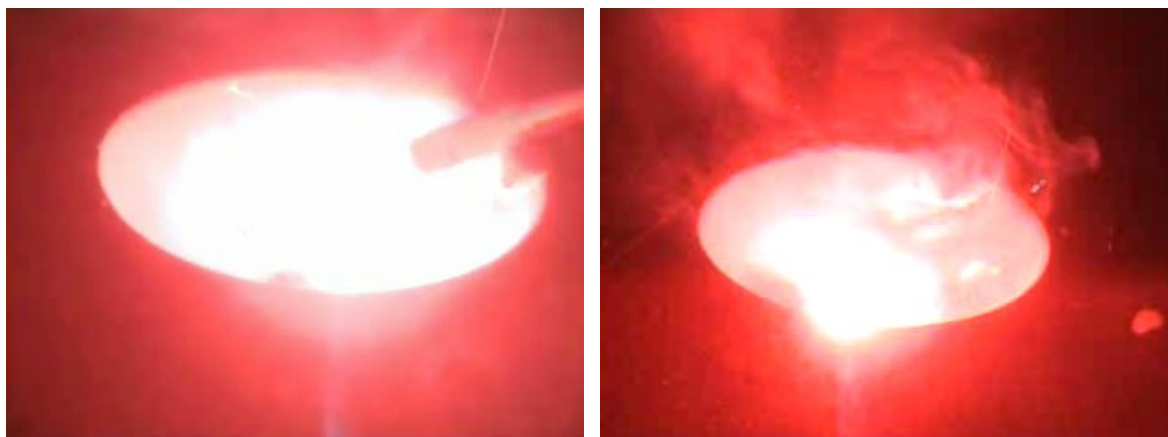


Figure 5.41 Burn down of the pyrotechnic compositions **5_Sr2_1.2** (left) and **5_Sr2_4.1** (right).

In analogy to the above mentioned compositions of **5_Sr1**, composition **5_Sr2_1.2** combusted with much higher velocity than **5_Sr2_4.1**. In both cases smoke and sparks were produced. After the combustion of **5_Sr2_1.2** a smaller amount of solid residues compared to that of **5_Sr2_4.1** was observed. As expected, **5_Sr2_4.1** is thermally more stable than **5_Sr2_1.2**. **5_Sr2_1.2** decomposes at temperatures above 175 °C, **5_Sr2_4.1** at temperatures above 250 °C (Figure 5.40). Its DSC thermogram shows an endothermic signal at 125 °C, due to a phase transition of ammonium nitrate.^[12] **5_Sr2_4.1** is less sensitive to impact (10 J) and friction (324 N) than **5_Sr2_1.2** ($E_{dr} = 5.0$ J, $F_r = 144$ N). However, it is more sensitive to electric discharge (1.25 J) than **5_Sr2_1.2** (1.50 J).

Comparing the strontium salts **5_Sr1** and **5_Sr2** regarding their performance as coloring agents in the investigated compositions, it turns out that – contrary to the results of the coloring behavior in the flame of a BUNSEN burner – **5_Sr1** displays the better performance with respect to red light emission.

The barium salts of **5**, **5_Ba1** and **5_Ba2**, were investigated for their coloring properties as green and white light emitting colorants in pyrotechnic compositions. For the tests, they were combined with ADN, KDN, and ammonium nitrate, as well as boron and magnesium (see chapters 5.2.4.6 and 5.2.4.7). Based on **5_Ba1**, the best performing compositions with a green flame are **5_Ba1_3.1** and **5_Ba1_4.3**. **5_Ba1_3.1** consists of 29 wt% **5_Ba1**, 51 wt% ammonium nitrate, 7 wt% boron, and 13 wt% VAAR (Table 5.63) and **5_Ba1_4.3** consists of 48 wt% **5_Ba1**, 38 wt% ADN, 2 wt% magnesium, and 12 wt% VAAR (Table 5.64). Both compositions produce a green flame, whereas the one of **5_Ba1_3.1** is

much more intense (Figure 5.42). **5_Ba1_4.3** combusted faster without residues, but some smoke and sparks were observed. The combustion of **5_Ba1_3.1** was slower, but smoke-free.



Figure 5.42 Burn down of the pyrotechnic compositions **5_Ba1_3.1** (left) and **5_Ba1_4.3** (right).

The decomposition temperatures of **5_Ba1_3.1** and **5_Ba1_4.3** were determined to be 213 °C and 157 °C, respectively (Figure 5.43). In the DSC thermogram of **5_Ba1_3.1** an endothermic signal at 126 °C is the result of a phase transition of ammonium nitrate.^[12] In the case of **5_Ba1_4.3** a further exothermic signal at 364 °C can be observed. **5_Ba1_4.3** is more sensitive to impact (6.0 J), friction (60 N), and electric discharge (1.50 J) than **5_Ba1_3.1** ($E_{dr} = 10$ J, $F_r = 288$ N, $E_{el} = 1.5$ J).

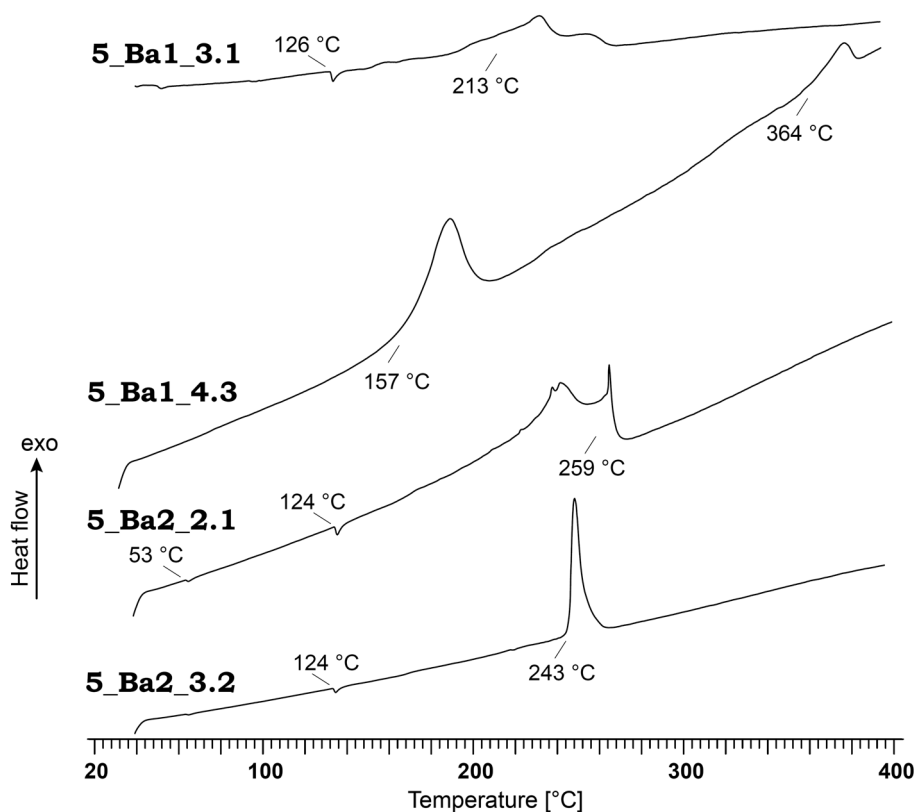


Figure 5.43 DSC thermograms of the pyrotechnic compositions **5_Ba1_3.1**, **5_Ba1_4.3**, **5_Ba2_2.1**, and **5_Ba2_3.2** in the temperature range of 30–400 °C. Decomposition points are given as onset temperatures.

Using **5_Ba2** as coloring agent for green light emitting pyrotechnic compositions, the two best performing formulations are **5_Ba2_2.1** and **5_Ba2_3.2**. **5_Ba2_2.1** consists of 53 wt% ammonium nitrate, 20 wt% **5_Ba2**, 7 wt% magnesium, 7 wt% boron, and 13 wt% VAAR (Table 5.67). **5_Ba2_3.2** consists of 51 wt% ammonium nitrate, 29 wt% **5_Ba2**, 7 wt% boron, and 13 wt% VAAR (Table 5.68). Both compositions produce a similar intense green flame (Figure 5.44). **5_Ba2_2.1** and **5_Ba2_3.2** combusted at a moderate velocity. Thereby, less smoke and some sparks could be observed as well as a small amount of solid residues.

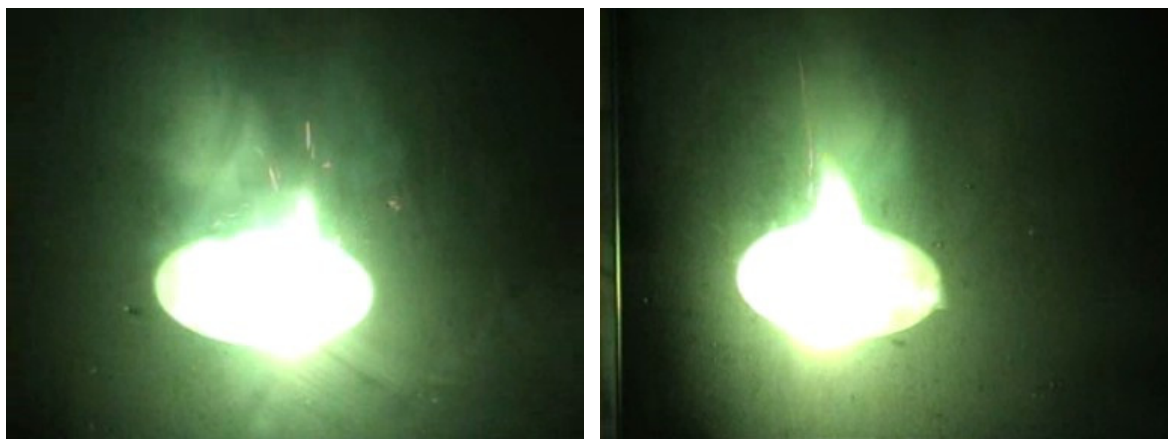


Figure 5.44 Burn down of the pyrotechnic compositions **5_Ba2_2.1** (left) and **5_Ba2_3.2** (right).

As expected, their sensitivities to impact (6.0 J, 10 J), friction (324 N), and electric discharge (1.50 J) are comparable, due to the similar components. Furthermore, similar decomposition temperatures were determined (Figure 5.43). In both DSC thermograms the phase transition of ammonium nitrate at 124 °C can be observed. In the case of **5_Ba2_2.1** another phase transition of ammonium nitrate at 53 °C appears.

For producing a white flame with **5_Ba1** or **5_Ba2** a higher flame temperature must be achieved. This was possible with the oxidizers ADN, KDN, and ammonium nitrate. Depending on the amount of oxidizer, the emitted color can change into light green. Based on **5_Ba1**, the two best performing compositions with a white flame are **5_Ba1_1.2** and **5_Ba1_5**. **5_Ba1_1.2** consists of 21 wt% **5_Ba1**, 57 wt% ammonium nitrate, 11 wt% magnesium, and 11 wt% VAAR (Table 5.61). It combusted slower than composition **5_Ba1_5**, which was made up of 53 wt% **5_Ba1**, 35 wt% KDN, 2 wt% magnesium, and 10 wt% VAAR (Table 5.65). Both compositions produce an intense white flame (Figure 5.1). However, smoke, sparks, and few residues were observed.



Figure 5.45 Burn down of the pyrotechnic compositions **5_Ba1_1.2** (left) and **5_Ba1_5** (right).

Composition **5_Ba1_5** decomposes at temperatures above 158 °C in several steps. This is at much lower temperature than **5_Ba1_1.2** ($T_{\text{dec}} = 219$ °C). In both cases an endothermic signal is observed (Figure 5.46). This is caused by melting of the ingredients ammonium nitrate and KDN, respectively.^[12, 13] Due to the usage of KDN, **5_Ba1_5** is more sensitive to impact (5.0 J), friction (192 N), and electric discharge (1.0 J) than **5_Ba1_1.2** ($E_{\text{dr}} = 10$ J, $F_{\text{r}} = 360$ N, $E_{\text{el}} = 1.5$ J).

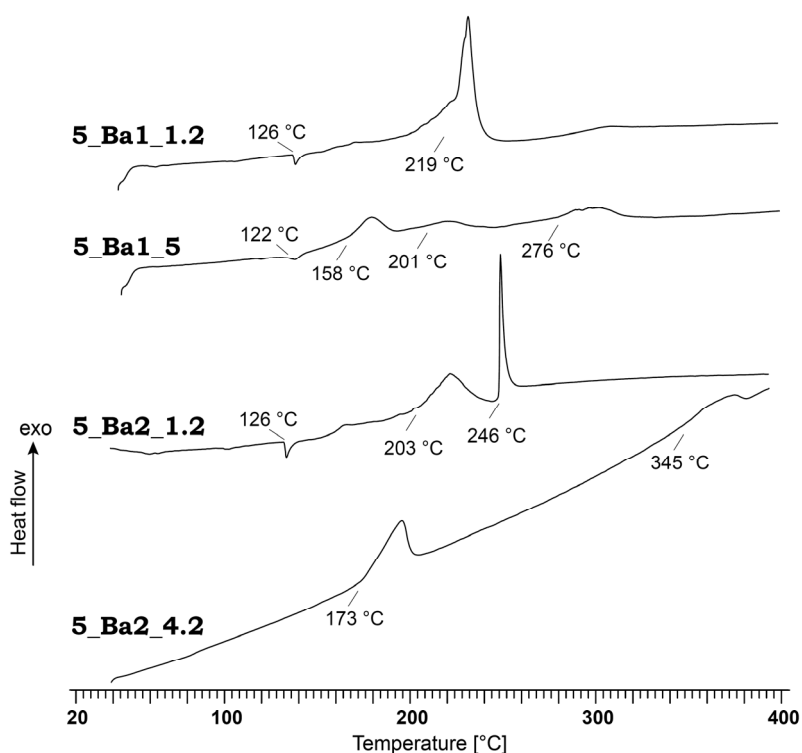


Figure 5.46 DSC thermograms of the pyrotechnic compositions **5_Ba1_1.2**, **5_Ba1_5**, **5_Ba2_1.2**, and **5_Ba2_4.2** in the temperature range of 30–400 °C. Decomposition points are given as onset temperatures.

The compositions **5_Ba2_1.2** and **5_Ba2_4.2** display the best performance regarding white light emission. **5_Ba2_1.2** was made up of 19 wt% **5_Ba2**, 58 wt% ammonium nitrate, 13 wt% magnesium, and 10 wt% VAAR (Table 5.66) and **5_Ba2_4.2** of 49 wt% **5_Ba2**, 37 wt%

ADN, 2 wt% magnesium, and 12 wt% VAAR (Table 5.69). The white flames of both compositions are comparable in intensity (Figure 5.47). Both combusted with low smoke production, a few sparks, and almost no solid residues. **5_Ba2_4.2** showed a higher combustion velocity than **5_Ba2_1.2**.



Figure 5.47 Burn down of the pyrotechnic compositions **5_Ba2_1.2** (left) and **5_Ba2_4.2** (right).

Composition **5_Ba2_4.2** is sensitive to impact (5.0 J) and friction (120 N), but insensitive to electric discharge (1.50 J). The DSC thermogram of **5_Ba2_1.2** is comparable to the one of **5_Ba1_1.2** (Figure 5.46). **5_Ba2_1.2** decomposes at temperatures above 203 °C. At 126 °C an endothermic signal is observed due to a phase transition of ammonium nitrate.^[12] **5_Ba2_4.2** decomposes at temperatures above 173 °C due to its ingredient ADN (Figure 5.46).^[11] Furthermore, **5_Ba2_4.2** is more sensitive to outer stimuli ($E_{dr} = 5.0$ J, $F_r = 120$ N, $E_{el} = 1.5$ J) than **5_Ba2_1.2** ($E_{dr} = 12$ J, $F_r = 360$ N, $E_{el} = 1.5$ J).

The copper(II) compounds **5_Cu_H2O** and **5_Cu_NH3** were combined with the oxidizers ammonium nitrate, ADN, and KDN. The fuels **5_At**, zinc or boron were added as well as the copper compounds, copper, copper(I) oxide or tetrammine copper(II) dinitramide ($[\text{Cu}(\text{NH}_3)_4][\text{N}(\text{NO}_2)_2]_2$). Although **5_Cu_H2O** as well as **5_Cu_NH3** show in the flame of a BUNSEN burner a very intense dark green light emission (Figure 5.31), most of the compositions prepared combusted with a yellow or, in the beginning, green and then yellow flame (see chapters 5.2.4.8 and 5.2.4.9).

Despite that, two pyrotechnic compositions containing **5_Cu_H2O** or **5_Cu_NH3** with a green flame could be identified. Composition **5_Cu_H2O_1.8** consists of 26 wt% **5_Cu_H2O**, 52 wt% ammonium nitrate, 9 wt% boron, and 13 wt% VAAR (Table 5.71). It produces an intense green flame and less smoke during a moderately fast combustion (Figure 5.48). However, some glowing residues were observed afterwards. The flame of composition **5_Cu_H2O_6.2**, which consists of 43 wt% ADN, 43 wt% **5_Cu_H2O**, 3 wt% boron, and 11 wt% VAAR (Table 5.76), is less intense green, but taller (Figure 5.48). Furthermore, no smoke, and only some sparks were observed. In analogy to **5_Cu_H2O_1.8**, some glowing residues remained after combustion.



Figure 5.48 Burn down of the pyrotechnic compositions **5_Cu_H₂O_1.8** (left) and **5_Cu_H₂O_6.2** (right).

Unfortunately, **5_Cu_H₂O_1.8** and **5_Cu_H₂O_6.2** decompose at temperatures below 160 °C (Figure 5.49). Composition **5_Cu_H₂O_1.8** decomposes at 107 °C in three steps. In the DSC thermograms of both compositions at 53 °C and 54 °C, respectively, an endothermic signal can be observed. Composition **5_Cu_H₂O_6.2** is significantly more sensitive to impact (2.0 J), friction (69 N), and electric discharge (1.5 J) than composition **5_Cu_H₂O_1.8** ($E_{dr} = 7.0$ J, $F_r = 240$ N, $E_{el} = 1.5$ J).

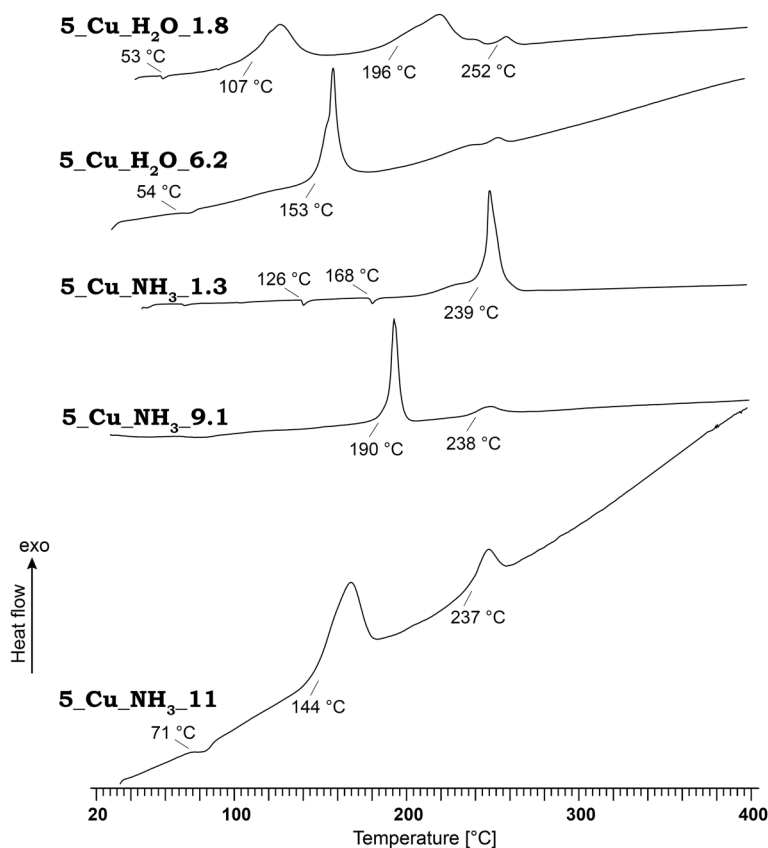


Figure 5.49 DSC thermograms of the pyrotechnic compositions **5_Cu_H₂O_1.8**, **5_Cu_H₂O_6.2**, **5_Cu_NH₃_1.3**, **5_Cu_NH₃_9.1**, and **5_Cu_NH₃_11** in the temperature range of 30–400 °C. Decomposition points are given as onset temperatures.

Composition **5_Cu_NH₃_1.3** consists of 21 wt% **5_Cu_NH₃**, 55 wt% ammonium nitrate, 14 wt% boron, and 10 wt% VAAR (Table 5.80). It combusted with a green flame and without any smoke at a moderate velocity (Figure 5.50). Again a glowing residue remained. Another convincing composition with **5_Cu_NH₃**, **5_Cu_NH₃_9.1**, contains a further copper(II) complex (43 wt% **5_Cu_NH₃**, 43 wt% **[Cu(NH₃)₄][N(NO₂)₂]₂**, 2 wt% boron, 12 wt% VAAR, Table 5.88). It produces an intense green flame (Figure 5.50). Almost no smoke, but some glowing residues were observed. The combustion velocity was moderately fast.



Figure 5.50 Burn down of the pyrotechnic compositions **5_Cu_NH₃_1.3** (left) and **5_Cu_H₃_9.1** (right).

Composition **5_Cu_NH₃_1.3** is more sensitive to outer stimuli ($E_{dr} = 5.0$ J, $F_r = 216$ N, $E_{el} = 1.0$ J) than composition **5_Cu_NH₃_9.1** ($E_{dr} = 7.0$ J, $F_r = 288$ N, $E_{el} = 1.5$ J), although **5_Cu_NH₃_9.1** contains the sensitive copper(II) complex **[Cu(NH₃)₄][N(NO₂)₂]₂**. In contrast, **5_Cu_NH₃_1.3** is thermally more stable with a decomposition temperature of 239 °C than **5_Cu_NH₃_9.1**, which decomposes in two steps at temperatures above 190 °C (Figure 5.49). In the case of **5_Cu_NH₃_1.3** two endothermic signals can be observed, caused by phase transitions of ammonium nitrate.^[12]

Another composition, **5_Cu_NH₃_11**, containing **5_Cu_H₂O** as well as **5_Cu_NH₃**, (43 wt% ADN, 26 wt% **5_Cu_H₂O**, 17 wt% **5_Cu_NH₃**, 3 wt% boron, and 11 wt% VAAR; Table 5.90) also produces a green flame (Figure 5.51). It was easy to ignite and combusted with high velocity. Only a few sparks, less smoke production, and a small amount of glowing residues were observed.



Figure 5.51 Burn down of the pyrotechnic composition **5_Cu_NH₃_11**.

5_Cu_NH₃_11 is very sensitive to impact (1.0 J) and to friction (70 N). Its sensitivity to electric discharge was determined to 1.0 J. In its DSC thermogram two exothermic signals at 144 °C and 237 °C can be observed (Figure 5.49). They are caused by the decomposition of ADN and the copper(II) compounds. The endothermic signal at 71 °C indicates the loss of ammonia or H₂O.

5.2 Experimental Part

*CAUTION! Some of the prepared compounds or of their pyrotechnic compositions are sensitive to impact, friction, and electric discharge. Therefore, proper protective measures (safety glasses, face shield, leather coat, earthed equipment and shoes, Kevlar[®] gloves, and ear plugs) should be used, especially during work on the precursor molecule 1-carboxymethyl-5-nitriminotetrazole monohydrate (**5**).*

5.2.1 Preparation of the Neutral Precursor Molecules

5.2.1.1 1-Carboxymethyl-5-aminotetrazole (**4**)

Preparation according to literature.^[1] 42.5 g (0.5 mol) 5-Aminotetrazole (**5-At**) and 40.0 g (1.0 mol) sodium hydroxide were dissolved in 1 L methanol. 47.3 g (0.5 mol) 1-Chloroacetic acid was added and the solution refluxed for 24 hours. The reaction mixture was cooled to 15 °C and the colorless precipitate was filtered off. It was dissolved completely in 200 mL H₂O and the pH of the solution was reduced to less than 2 with approximately 40 mL concentrated hydrochloric acid. The immediately formed colourless precipitate was filtered off. After recrystallization from H₂O, 34.9 g of purified product were obtained. Yield: 71 %.

M.p. 207 °C, 230 °C (dec., DSC-measurement, 5 K/min).

Raman (300 mW, 25 °C, cm⁻¹): 3014 (8), 2968 (15), 1751 (5), 1560 (4), 1504 (100), 1461 (4), 1409 (7), 1334 (28), 1276 (5), 1250 (2), 1150 (3), 1110 (10), 1036 (60), 1000 (5), 914 (3), 894 (7), 805 (2), 757 (9), 741 (5), 704 (2), 484 (6), 460 (3), 407 (2), 382 (2), 291 (8), 273 (8).

IR (Diamond-ATR, cm^{-1}): 3386 (m), 3313 (m), 3103 (m), 3009 (m), 2976 (m), 1697 (vs), 1636 (s), 1588 (s), 1496 (s), 1451 (m), 1419 (m), 1357 (m), 1342 (m), 1303 (m), 1260 (s), 1162 (m), 1091 (s), 1054 (m), 946 (m), 905 (m), 820 (s), 754 (s), 694 (w), 659 (m), 614 (w).

^1H NMR (DMSO- d_6): 6.78 (s, 2H, NH_2), 4.99 (s, 2H, CH_2).

^{13}C NMR (DMSO- d_6): 168.1 (COOH), 156.2 (CNH $_2$), 46.1 (CH_2).

Elemental analysis $\text{C}_3\text{H}_5\text{N}_5\text{O}_2$ (143.10 g/mol) calc.: C, 48.94; H, 3.52; N, 48.94. found: C, 49.13; H, 3.57; N, 49.13.

m/z (DEI+): 143 (13, M^+).

E_{dr} > 100 J (100–250 μm).

F_{r} > 360 N (100–250 μm).

E_{el} = 0.15 J (100–250 μm).

$\Delta_c U$ = -2796 cal/g.

5.2.1.2 1-Carboxymethyl-5-nitriminotetrazole Monohydrate (5)

At 0 °C 5.0 g (35 mmol) 1-carboxymethyl-5-aminotetrazole (**4**) were slowly added to 15 mL nitric acid (100 %). After stirring for 16 hours the solution was poured onto ice. The colorless crystals, which formed after a few days formed, were filtered off and washed with H_2O . Yield: 80 %.

M.p. 87 °C (loss of H_2O), 165 °C (dec., DSC-measurement, 5 K/min).

Raman (300 mW, 25 °C, cm^{-1}): 3015 (22), 2969 (49), 1732 (17), 1643 (8), 1590 (100), 1555 (13), 1412 (62), 1332 (10), 1304 (16), 1273 (24), 1240 (12), 1074 (31), 1043 (33), 999 (34), 951 (13), 886 (23), 788 (9), 760 (32), 727 (9), 644 (4), 496 (21), 403 (6), 408 (4), 301 (17), 284 (21), 212 (7).

IR (Diamond-ATR, cm^{-1}): 3539 (m), 3313 (m), 3103 (vs), 3462 (vs), 3014 (s), 2968 (s), 2930 (s), 2641 (m), 2357 (m), 1732 (s), 1700 (m), 1634 (m), 1579 (s), 1481 (s), 1398 (s), 1333 (s), 1303 (s), 1261 (s), 1208 (s), 1142 (m), 1070 (m), 1054 (m), 100 (m), 951 (m), 882 (m).

^1H NMR (DMSO- d_6): 7.96 (s, 1H, NH), 5.11 (s, 2H, CH_2).

^{13}C NMR (DMSO- d_6): 167.1 (COOH), 150.6 (CNNO $_2$), 47.7 (CH_2).

Elemental analysis $\text{C}_3\text{H}_6\text{N}_6\text{O}_5$ (206.12 g/mol) calc.: C, 17.48; H, 2.93; N, 40.77. found: C, 17.36; H, 2.92; N, 40.56.

m/z (DEI+): 188 (6, $[\text{M}-\text{H}_2\text{O}]^+$).

E_{dr} = 25 J (> 1000 μm).

F_{r} = 216 N (> 1000 μm).

E_{el} = 0.25 J (> 1000 μm).

$\Delta_c U$ = -1904 cal/g.

5.2.2 Salts of 1-Carboxymethyl-5-aminotetrazole (4)

General procedure:

1.4 g (10 mmol) of 1-carboxymethyl-5-aminotetrazole (**4**) was dissolved in 25 mL H₂O. After adding the corresponding hydroxides (alkali metal: 10 mmol, alkaline earth metal: 5.0 mmol), the solution was heated until a clear solution was obtained.

5.2.2.1 Lithium 2-(5-Aminotetrazol-1-yl)-acetate Monohydrate (**4_Li**)

After recrystallization from H₂O colorless crystals, suitable for X-ray diffraction, were obtained. Yield: 71 %.

M.p. 108 °C (loss of H₂O), 317 °C (dec., DSC-measurement, 5 K/min).

Raman (300 mW, 25 °C, cm⁻¹): 3014 (8), 2968 (15), 1751 (5), 1560 (4), 1504 (100), 1461 (4), 1409 (7), 1334 (28), 1276 (5), 1250 (2), 1150 (3), 1110 (10), 1036 (60), 1000 (5), 914 (3), 894 (7), 805 (2), 757 (9), 741 (5), 704 (2), 484 (6), 460 (3), 407 (2), 382 (2), 291 (8), 273 (8).

IR (Diamond-ATR, cm⁻¹): 3341 (s), 3149 (s), 2739 (w), 1671 (s), 1627 (vs), 1589 (s), 1487 (m), 1438 (m), 1401 (s), 1344 (m), 1318 (m), 1293 (w), 1278 (w), 1144 (w), 1120 (m), 1025 (w), 954 (vw), 925 (vw), 896 (w), 826 (m), 757 (w), 739 (w), 696 (m), 668 (m).

¹H NMR (DMSO-*d*₆): 6.75 (s, 2H, NH₂), 4.94 (s, 2H, CH₂).

¹³C NMR (DMSO-*d*₆): 168.1 (COOH), 156.1 (CNH₂), 46.1 (CH₂).

Elemental analysis C₃H₆N₅O₃Li (167.05 g/mol) calc.: C, 21.57; H, 3.62; N, 41.92. found: C, 21.78; H, 3.72; N, 39.83.

E_{dr} > 100 J (160–250 μm).

F_r > 360 N (160–250 μm).

E_{el} = 1.2 J (160–250 μm).

Δ_cU = -2255 cal/g.

H₂O-sol. 19 wt% (25 °C).

5.2.2.2 Sodium 2-(5-Aminotetrazol-1-yl)-acetate Trihydrate (**4_Na**)

After recrystallization from H₂O colorless crystals, suitable for X-ray diffraction, were obtained. Yield: 76 %.

M.p. 53 °C (loss of H₂O), 165 °C (loss of H₂O), 298 °C (dec., DSC-measurement, 5 K/min).

Raman (300 mW, 25 °C, cm⁻¹): 3147 (22), 3002 (54), 2968 (26), 2950 (63), 1664 (20), 1638 (13), 1580 (32), 1483 (23), 1433 (23), 1393 (50), 1342 (46), 1312 (96), 1287 (29), 1266 (15), 1136 (45), 1123 (26), 1022 (21), 953 (12), 930 (21), 916 (39), 823 (100), 758 (53), 740 (19), 682 (10), 579 (11), 484 (36), 410 (27), 323 (23), 304 (48), 276 (18), 215 (18).

IR (Diamond-ATR, cm⁻¹): 3385 (m), 3166 (m), 2997 (w), 2362 (w), 2331 (w), 2191 (vw), 2145 (vw), 1633 (vs), 1616 (vs), 1584 (vs), 1491 (m), 1434 (m), 1390 (s), 1323 (m), 1271 (m), 1102 (w), 1008 (w), 931 (w), 827 (m), 737 (m), 657 (m).

¹H NMR (DMSO-*d*₆): 6.39 (s, 2H, NH₂), 4.39 (s, 2H, CH₂).

¹³C NMR (DMSO-*d*₆): 167.8 (COOH), 156.0 (CNH₂), 49.6 (CH₂).

Elemental analysis C₃H₁₀N₅O₅Na (219.13 g/mol) calc.: C, 16.44; H, 4.60; N, 31.96. found: C, 17.17; H, 3.83; N, 33.75.

E_{dr} > 100 J (100–500 μm).

F_r > 360 N (100–500 μm).

E_{el} = 1.0 J (100–500 μm).

Δ_cU = -1901 cal/g.

H₂O-sol. 25 wt% (22 °C).

5.2.2.3 Potassium 2-(5-Aminotetrazol-1-yl)-acetate (4_K)

After recrystallization from H₂O colorless crystals, suitable for X-ray diffraction, were obtained. Yield: 86 %.

M.p. 266 °C, 345 °C (dec., DSC-measurement, 5 K/min).

Raman (300 mW, 25 °C, cm⁻¹): 3125 (17), 3000 (64), 2958 (97), 1669 (15), 1625 (18), 1579 (21), 1428 (17), 1399 (42), 1344 (20), 1313 (99), 1283 (17), 1263 (14), 1143 (27), 1131 (18), 1120 (15), 1023 (21), 911 (46), 831 (100), 747 (27), 739 (19), 696 (7), 575 (13), 472 (27), 393 (22), 303 (51), 274 (17).

IR (Diamond-ATR, cm⁻¹): 3346 (s), 3251 (m), 3137 (s), 2997 (m), 2951 (m), 2739 (w), 1674 (m), 1640 (m), 1587 (s), 1483 (m), 1424 (m), 1378 (s), 1342 (m), 1309 (m), 1279 (w), 1262 (m), 1138 (m), 1101 (m), 1018 (w), 946 (w), 910 (w) 829 (m), 742 (w), 729 (w), 695 (m), 649 (w).

¹H NMR (DMSO-*d*₆): 6.38 (s, 2H, NH₂), 4.33 (s, 2H, CH₂).

¹³C NMR (DMSO-*d*₆): 167.3 (COOH), 156.6 (CNH₂), 50.7 (CH₂).

Elemental analysis C₃H₄N₅O₂K (181.19 g/mol) calc.: C, 19.89; H, 2.23; N, 38.65. found: C, 19.66; H, 2.29; N, 38.55.

E_{dr} > 100 J (> 1000 μm).

F_r > 360 N (> 1000 μm).

E_{el} = 1.5 J (> 1000 μm).

Δ_cU = -2007 cal/g.

H₂O-sol. 41 wt% (22 °C).

5.2.2.4 Rubidium 2-(5-Aminotetrazol-1-yl)-acetate Monohydrate (4_Rb)

After recrystallization from H₂O colorless crystals, suitable for X-ray diffraction, were obtained. Yield: 89 %.

M.p. 63 °C (loss of H₂O), 243 °C, 365 °C (dec., DSC-measurement, 5 K/min).

Raman (300 mW, 25 °C, cm⁻¹): 3166 (17), 2995 (62), 2951 (87), 1662 (16), 1619 (19), 1585 (18), 1485 (24), 1428 (12), 1388 (75), 1332 (25), 1311 (100), 1285 (19), 1124 (21),

1102 (24), 1012 (25), 915 (61), 828 (87), 757 (47), 677 (18), 585 (8), 490 (29), 400 (23), 354 (11), 310 (21), 280 (20).

IR (Diamond-ATR, cm^{-1}): 3612 (m), 3339 (s), 3163 (s), 2994 (m), 2749 (w), 1662 (m), 1601 (s), 1583 (s), 1484 (m), 1430 (m), 1383 (s), 1335 (m), 1317 (m), 1271 (m), 1199 (w), 1134 (m), 1103 (m), 1010 (m), 946 (m), 916 (m), 824 (m), 753 (w), 737 (w), 693 (w), 675 (m).

^1H NMR (DMSO- d_6): 6.39 (s, 2H, NH_2), 4.35 (s, 2H, CH_2).

^{13}C NMR (DMSO- d_6): 167.4 (COOH), 156.6 (CNH_2), 50.6 (CH_2).

Elemental analysis $\text{C}_3\text{H}_6\text{N}_5\text{O}_3\text{Rb}$ (245.58 g/mol) calc.: C, 14.67; H, 2.46; N, 28.52. found: C, 14.36; H, 2.48; N, 27.94.

E_{dr} > 100 J (500–1000 μm).

F_{r} > 360 N (500–1000 μm).

E_{el} = 1.0 J (500–1000 μm).

$\Delta_c U$ = -1726 cal/g.

$\text{H}_2\text{O-sol}$. 63 wt% (23 °C).

5.2.2.5 Cesium 2-(5-Aminotetrazol-1-yl)-acetate (4_Cs)

After recrystallization from H_2O colorless crystals, suitable for X-ray diffraction, were obtained. Yield: 77 %.

M.p. 257 °C, 364 °C (dec., DSC-measurement, 5 K/min).

Raman (300 mW, 25 °C, cm^{-1}): 3105 (15), 2992 (49), 2955 (79), 1679 (10), 1610 (14), 1587 (26), 1485 (16), 1435 (12), 1379 (72), 1345 (23), 1311 (100), 1288 (17), 1152 (20), 1093 (16), 1013 (18), 949 (8), 912 (35), 823 (69), 756 (34), 735 (14), 696 (6), 678 (10), 585 (7), 485 (21), 409 (25), 356 (9), 323 (28), 283 (23).

IR (Diamond-ATR, cm^{-1}): 3354 (m), 3294 (s), 3112 (s), 2992 (m), 2956 (m), 2801 (w), 2760 (w), 1679 (m), 1615 (s), 1594 (s), 1535 (m), 1490 (m), 1432 (w), 1381 (s), 1335 (m), 1304 (m), 1269 (m), 1127 (w), 1092 (m), 1060 (w), 1011 (w), 975 (w), 950 (w), 907 (w), 820 (m), 752 (w), 729 (w), 692 (w), 683 (w), 623 (w).

^1H NMR (DMSO- d_6): 6.39 (s, 2H, NH_2), 4.34 (s, 2H, CH_2).

^{13}C NMR (DMSO- d_6): 167.1 (COOH), 156.6 (CNH_2), 50.7 (CH_2).

Elemental analysis $\text{C}_3\text{H}_4\text{N}_5\text{O}_2\text{Cs}$ (275.00 g/mol) calc.: C, 13.10; H, 1.47; N, 25.47. found: C, 13.19; H, 1.59; N, 25.81.

E_{dr} > 100 J (> 1000 μm).

F_{r} > 360 N (> 1000 μm).

E_{el} = 0.80 J (> 1000 μm).

$\Delta_c U$ = -1054 cal/g.

$\text{H}_2\text{O-sol}$. 38 wt% (22 °C).

5.2.2.6 Magnesium 2-(5-Aminotetrazol-1-yl)-acetate Tetrahydrate (4_Mg)

After recrystallization from H₂O colorless crystals, suitable for X-ray diffraction, were obtained. Yield: 88 %.

M.p. 166 °C (loss of H₂O), 327 °C (dec., DSC-measurement, 5 K/min).

Raman (200 mW, 25 °C, cm⁻¹): 3195 (24), 2992 (65), 2953 (67), 1652 (28), 1617 (13), 1588 (17), 1492 (34), 1441 (13), 1395 (64), 1344 (71), 1323 (31), 1296 (55), 1273 (14), 1126 (28), 1099 (25), 1014 (24), 951 (11), 930 (40), 831 (100), 757 (35), 737 (15), 669 (14), 593 (9), 494 (22), 438 (16), 329 (37), 290 (25), 217 (29).

IR (Diamond-ATR, cm⁻¹): 3488 (vs), 3346 (s), 3190 (s), 2994 (s), 2349 (w), 2169 (m), 2017 (w), 1652 (s), 1618 (s), 1582 (s), 1488 (m), 1444 (m), 1398 (s), 1339 (w), 1320 (m), 1290 (w), 1135 (w), 1102 (m), 1012 (w), 827 (m), 760 (w), 737 (w), 672 (s), 635 (m), 608 (m).

¹H NMR (DMSO-*d*₆): 6.42 (s, 2H, NH₂), 4.60 (s, 2H, CH₂).

¹³C NMR (DMSO-*d*₆): 170.2 (COOH), 156.6 (CNH₂), 49.3 (CH₂).

Elemental analysis C₆H₁₆N₁₀O₈Mg (380.56 g/mol) calc.: C, 18.94; H, 4.24; N, 36.81. found: C, 18.69; H, 4.05; N, 36.61.

E_{dr} > 100 J (100–250 μm).

F_r > 360 N (100–250 μm).

E_{el} = 1.2 J (100–250 μm).

Δ_cU = -1864 cal/g.

H₂O-sol. 12 wt% (23 °C).

5.2.2.7 Calcium 2-(5-Aminotetrazol-1-yl)-acetate Tetrahydrate (4_Ca)

After recrystallization from H₂O colorless crystals, suitable for X-ray diffraction, were obtained. Yield: 87 %.

M.p. 104 °C (loss of H₂O), 174 °C (loss of H₂O), 315 °C (dec., DSC-measurement, 5 K/min).

Raman (200 mW, 25 °C, cm⁻¹): 3179 (26), 2993 (78), 2950 (90), 1664 (18), 1612 (21), 1492 (38), 1448 (19), 1395 (76), 1345 (85), 1321 (100), 1142 (28), 1101 (31), 1016 (25), 935 (34), 925 (39), 832 (96), 753 (60), 701 (16), 581 (13), 486 (33), 404 (27), 299 (44), 215 (18).

IR (Diamond-ATR, cm⁻¹): 3732 (m), 3359 (s), 3173 (s), 2997 (w), 2362 (s), 2336 (s), 1649 (m), 1588 (vs), 1445 (w), 1390 (m), 1339 (w), 1099 (w), 825 (w).

¹H NMR (DMSO-*d*₆): 6.45 (s, 2H, NH₂), 4.57 (s, 2H, CH₂).

¹³C NMR (DMSO-*d*₆): 170.2 (COOH), 156.6 (CNH₂), 49.3 (CH₂).

Elemental analysis C₆H₁₆N₁₀O₈Ca (396.33 g/mol) calc.: C, 18.19; H, 4.16; N, 35.71. found: C, 18.18; H, 4.07; N, 35.34.

E_{dr} > 100 J (> 1000 μm).

F_r > 360 N (> 1000 μm).

E_{el} = 1.0 J (> 1000 μm).

$$\Delta_c U = -1968 \text{ cal/g.}$$

H₂O-sol. 18 wt% (24 °C).

5.2.2.8 Strontium 2-(5-Aminotetrazol-1-yl)-acetate Pentahydrate (4_Sr)

After recrystallization from H₂O colorless crystals, suitable for X-ray diffraction, were obtained. Yield: 90 %.

M.p. 121 °C (loss of H₂O), 304 °C (dec., DSC-measurement, 5 K/min).

Raman (200 mW, 25 °C, cm⁻¹): 3146 (24), 2996 (39), 2965 (57), 1612 (18), 1482 (16), 1449 (24), 1402 (100), 1336 (46), 1316 (55), 1287 (17), 1150 (27), 1135 (21), 1021 (18), 943 (31), 932 (39), 822 (71), 761 (24), 693 (16), 483 (29), 420 (22), 303 (23), 282 (22).

IR (Diamond-ATR, cm⁻¹): 3463 (m), 3325 (s), 3155 (m) 2996 (w), 1676 (m), 1598 (s), 1489 (vw), 1446 (m), 1435 (m), 1399 (s), 1312 (w), 1297 (w), 1150 (w), 1125 (w), 1113 (w), 1015 (vw), 940 (vw), 930 (w), 821 (w), 759 (w), 682 (m).

¹H NMR (DMSO-*d*₆): 6.44 (s, 2H, NH₂), 4.54 (s, 2H, CH₂).

¹³C NMR (DMSO-*d*₆): 171.3 (COOH), 156.6 (CNH₂), 49.4 (CH₂).

Elemental analysis C₆H₁₈N₁₀O₉Sr (461.89 g/mol): calc.: C, 15.60; H, 3.93; N, 30.32. found: C, 15.28; H, 3.83; N, 29.76.

$$E_{dr} > 100 \text{ J} \quad (> 1000 \text{ } \mu\text{m}).$$

$$F_r > 360 \text{ N} \quad (> 1000 \text{ } \mu\text{m}).$$

$$E_{el} = 1.1 \text{ J} \quad (> 1000 \text{ } \mu\text{m}).$$

$$\Delta_c U = -1710 \text{ cal/g.}$$

H₂O-sol. 7.2 wt% (24 °C).

5.2.2.9 Barium 2-(5-Aminotetrazol-1-yl)-acetate Trihydrate (4_Ba)

After recrystallization from H₂O colorless crystals, suitable for X-ray diffraction, were obtained. Yield: 92 %.

M.p. 102 °C (loss of H₂O), 315 °C (dec., DSC-measurement, 5 K/min).

Raman (200 mW, 25 °C, cm⁻¹): 3319 (5), 3238 (5), 3137 (21), 3005 (62), 2971 (84), 1667 (11), 1584 (30), 1482 (17), 1442 (17), 1408 (49), 1346 (21), 1314 (100), 1286 (10), 1268 (12), 1144 (32), 1107 (16), 1025 (15), 953 (7), 929 (40), 825 (94), 750 (23), 735 (15), 699 (12), 578 (5), 486 (17), 409 (17), 353 (8), 305 (29), 280 (10), 217 (9).

IR (Diamond-ATR, cm⁻¹): 3463 (m), 3326 (m), 3147 (m) 1644 (m), 1592 (s), 1447 (w), 1398 (s), 1310 (w), 1266 (vw), 1109 (w), 923 (vw), 822 (w), 747 (w), 694 (m).

¹H NMR (DMSO-*d*₆): 6.44 (s, 2H, NH₂), 4.55 (s, 2H, CH₂).

¹³C NMR (DMSO-*d*₆): 171.4 (COOH), 156.6 (CNH₂), 49.7 (CH₂).

Elemental analysis C₆H₁₄N₁₀O₇Ba (475.57 g/mol): calc.: C, 15.15; H, 2.97; N, 29.45. found: C, 14.85; H, 2.97; N, 29.05.

$E_{dr} > 100 \text{ J}$ ($< 250 \text{ }\mu\text{m}$).

$F_r = 288 \text{ N}$ ($< 250 \text{ }\mu\text{m}$).

$E_{el} = 1.1 \text{ J}$ ($< 250 \text{ }\mu\text{m}$).

$\Delta_c U = -1473 \text{ cal/g}$.

H₂O-sol. 5.0 wt% (24 °C).

5.2.2.10 Diaqua Copper(II) 2-(5-Aminotetrazol-1-yl)-acetate (4_Cu)

A solution of 2.86 g (20 mmol) 1-carboxymethyl-5-aminotetrazole (**4**) in 50 mL H₂O was combined with a solution of 2.32 g (10 mmol) copper(II) nitrate pentahemihydrate in 10 mL H₂O. The immediately formed green precipitate was filtered off and washed with H₂O. Yield: 64 %.

M.p. 141 °C (loss of H₂O), 220 °C (dec., DSC-measurement, 5 K/min).

IR (Diamond-ATR, cm⁻¹): 3491 (m), 3442 (w), 3294 (w), 3068 (m) 2966 (w), 2361 (w), 2199 (w), 2012 (w), 1644 (s), 1602 (s), 1497 (s), 1422 (m), 1378 (vs), 1357 (s), 1289 (s), 1278 (m), 1151 (m), 1114 (m), 1079 (m), 825 (vs), 752 (m), 734 (m), 702 (m), 682 (w), 654 (w), 615 (w).

Elemental analysis C₆H₁₂CuN₁₀O₆ (383.77 g/mol): calc.: C, 18.78; H, 3.15; N, 36.50. found: C, 18.75; H, 3.07; N, 36.83.

$E_{dr} > 100 \text{ J}$ (100–250 μm).

$F_r > 360 \text{ N}$ (100–250 μm).

$E_{el} = 1.0 \text{ J}$ (100–250 μm).

$\Delta_c U = -2058 \text{ cal/g}$.

H₂O-sol. $< 0.2 \text{ wt\%}$ (23 °C).

5.2.3 Salts of 1-Carboxymethyl-5-nitriminotetrazole Monohydrate (5)

General procedure:

1.0 g (5.0 mmol) of 1-carboxymethyl-5-nitriminotetrazole monohydrate (**5**) was dissolved in 15 mL H₂O. After adding the corresponding hydroxides (alkali metal: 5.0 mmol, alkaline earth metal: 2.5 mmol or 5.0 mmol), the reaction mixture was heated until a clear solution was obtained.

5.2.3.1 Sodium 1-Carboxymethyl-5-nitriminotetrazolate Trihemihydrate (5_Na)

After recrystallization from H₂O a colorless powder was obtained. Yield: 52 %.

M.p. 102 °C (loss of H₂O), 143 °C (loss of H₂O), 223 °C (dec., DSC-measurement, 5 K/min).

Raman (300 mW, 25 °C, cm⁻¹): 3014 (8), 2968 (15), 1751 (5), 1560 (4), 1505 (100), 1461 (4), 1409 (7), 1334 (28), 1276 (5), 1250 (2), 1150 (3), 1110 (10), 1036 (60), 1000 (5), 914 (3), 894 (7), 805 (2), 757 (9), 741 (5), 704 (2), 484 (6), 460 (3), 407 (2), 382 (2), 291 (8), 273 (8).

IR (Diamond-ATR, cm^{-1}): 3579 (m), 3374 (m), 3014 (w), 2966 (w), 2536 (w), 2350 (w), 2168 (w), 1741 (s), 1636 (w), 1503 (s), 1464 (m), 1439 (w), 1392 (m), 1362 (m), 1332 (s), 1293 (s), 1274 (s), 1244 (s), 1230 (s), 1147 (m), 1107 (m), 1034 (w), 956 (w), 910 (w), 890 (m), 802 (m), 780 (w), 756 (w), 740 (w), 700 (w), 676 (w), 636 (w).

$^1\text{H NMR}$ (DMSO- d_6): 4.83 (s, CH_2).

$^{13}\text{C NMR}$ (DMSO- d_6): 168.0 (COOH), 157.2 (CNNO₂), 46.4 (CH_2).

Elemental analysis $\text{C}_3\text{H}_6\text{N}_6\text{NaO}_{5.5}$ (237.11 g/mol): calc.: C, 15.20; H, 2.55; N, 35.44. found: C, 15.08; H, 2.25; N, 34.73.

E_{dr} = 40 J (250–1000 μm).

F_{r} > 360 N (250–1000 μm).

E_{el} = 0.25 J (250–1000 μm).

$\Delta_c U$ = -1603 cal/g.

$\text{H}_2\text{O-sol.}$ 83 wt% (22 °C).

5.2.3.2 Potassium 1-Carboxymethyl-5-nitriminotetrazolate Monohydrate (5_K)

After recrystallization from H_2O colorless crystals, suitable for X-ray diffraction, were obtained. Yield: 72 %.

M.p. 140 °C (loss of H_2O), 220 °C (dec., DSC-measurement, 5 K/min).

Raman (300 mW, 25 °C, cm^{-1}): 3014 (8), 2968 (15), 1751 (5), 1560 (4), 1504 (100), 1461 (4), 1409 (7), 1334 (28), 1276 (5), 1250 (2), 1150 (3), 1110 (10), 1036 (60), 1000 (5), 914 (3), 894 (7), 805 (2), 757 (9), 741 (5), 704 (2), 484 (6), 460 (3), 407 (2), 382 (2), 291 (8), 273 (8).

IR (Diamond-ATR, cm^{-1}): 3746 (w), 3567 (m), 3374 (m), 3014 (w), 2966 (w), 2536 (w), 2350 (w), 2168 (w), 1741 (s), 1636 (w), 1503 (s), 1464 (m), 1439 (w), 1392 (m), 1362 (m), 1332 (s), 1293 (s), 1274 (s), 1245 (s), 1232 (s), 1147 (m), 1107 (m), 1034 (w), 956 (w), 910 (w), 890 (m), 802 (m), 780 (w), 756 (w), 740 (w), 700 (w), 667 (w), 636 (w).

$^1\text{H NMR}$ (DMSO- d_6): 4.85 (s, CH_2).

$^{13}\text{C NMR}$ (DMSO- d_6): 168.0 (COOH), 157.3 (CNNO₂), 46.5 (CH_2).

Elemental analysis $\text{C}_3\text{H}_5\text{N}_6\text{O}_5\text{K}$ (244.21 g/mol): calc.: C, 14.75; H, 2.06; N, 34.41. found: C, 14.67; H, 2.26; N, 34.56.

E_{dr} = 30 J (> 1000 μm).

F_{r} > 360 N (> 1000 μm).

E_{el} = 0.20 J (> 1000 μm).

$\Delta_c U$ = -1564 cal/g.

$\text{H}_2\text{O-sol.}$ 9.3 wt% (22 °C).

5.2.3.3 Rubidium 1-Carboxymethyl-5-nitriminotetrazolate Monohydrate (5_Rb)

After recrystallization from H_2O colorless crystals, suitable for X-ray diffraction, were obtained. Yield: 58 %.

M.p. 123 °C (loss of H₂O), 184 °C (dec., DSC-measurement, 5 K/min).

Raman (300 mW, 25 °C, cm⁻¹): 3016 (6), 2968 (14), 1751 (5), 1558 (4), 1502 (100), 1457 (3), 1406 (9), 1333 (33), 1274 (5), 1246 (2), 1150 (3), 1108 (11), 1035 (63), 1000 (5), 910 (3), 893 (7), 803 (2), 755 (9), 741 (7), 703 (2), 483 (7), 460 (4), 407 (2), 379 (2), 290 (9), 273 (12).

IR (Diamond-ATR, cm⁻¹): 3564 (m), 3383 (m), 3016 (m), 2966 (m), 2730 (m), 2636 (m), 2556 (m), 1817 (w), 1742 (vs), 1607 (w), 1553 (w), 1500 (s), 1461 (s), 1439 (m), 1392 (s), 1359 (m), 1332 (s), 1295 (vs), 1273 (s), 1246 (s), 1230 (s), 1149 (m), 1106 (m), 1034 (w), 956 (w), 905 (w), 889 (m), 802 (m), 779 (w), 754 (w), 740 (w), 700 (w), 666 (w).

¹H NMR (DMSO-*d*₆): 4.87 (s, CH₂).

¹³C NMR (DMSO-*d*₆): 168.0 (COOH), 157.3 (CNNO₂), 46.5 (CH₂).

Elemental analysis C₃H₅N₆O₅Rb (290.58 g/mol): calc.: C, 12.40; H, 1.73; N, 28.92. found: C, 12.34; H, 1.98; N, 28.93.

E_{dr} = 30 J (> 1000 μm).

F_r = 240 N (> 1000 μm).

E_{el} = 0.20 J (> 1000 μm).

Δ_cU = -1260 cal/g.

H₂O-sol. 18 wt% (22 °C).

5.2.3.4 Cesium 1-Carboxymethyl-5-nitriminotetrazolate Hemihydrate (5_Cs)

After recrystallization from H₂O small colorless crystals were obtained. Yield: 58 %.

M.p. 166 °C (dec., DSC-measurement, 5 K/min).

IR (Diamond-ATR, cm⁻¹): 3444 (m), 2996 (w), 2960 (w), 2404 (w), 1864 (vw), 1814 (vw), 1737 (m), 1606 (w), 1505 (m), 1464 (m), 1427 (w), 1393 (m), 1354 (m), 1334 (s), 1290 (s), 1247 (s), 1230 (s), 1145 (m), 1104 (m), 1032 (w), 978 (w), 955 (vw), 945 (w), 907 (vw), 893 (w), 834 (vw), 799 (m), 779 (w), 743 (m), 704 (vw), 690 (vw), 655 (w).

¹H NMR (DMSO-*d*₆): 4.93 (s, CH₂).

¹³C NMR (DMSO-*d*₆): 168.3 (COOH), 156.4 (CNNO₂), 47.4 (CH₂).

Elemental analysis C₃H₆CsN₆O_{5.5} (329.00 g/mol): calc.: C, 10.95; H, 1.23; N, 25.54. found: C, 10.97; H, 1.24; N, 25.52.

E_{dr} = 3.0 J (250–500 μm).

F_r = 252 N (250–500 μm).

E_{el} = 0.15 J (250–500 μm).

Δ_cU = -857 cal/g.

H₂O-sol. 45 wt% (24 °C).

5.2.3.5 Magnesium 2-(5-Nitriminotetrazol-1-yl)-acetate Decahydrate (5_Mg1)

After recrystallization from H₂O colorless crystals, suitable for X-ray diffraction, were obtained. Yield: 68 %.

M.p. 55 °C (loss of H₂O), 74 °C (loss of H₂O) 113 °C (loss of H₂O), 134 °C (loss of H₂O), 282 °C (dec., DSC-measurement, 5 K/min).

IR (Diamond-ATR, cm⁻¹): 3549 (m), 3492 (s), 3362 (s), 3140 (s), 2957 (m), 2851 (w), 1679 (w), 1581 (s), 1525 (m), 1494 (m), 1454 (m), 1416 (w), 1392 (m), 1350 (m), 1312 (m), 1259 (m), 1166 (w), 1143 (w), 1130 (w), 1086 (w), 1037 (w), 999 (w), 956 (w), 903 (w), 809 (w), 774 (w), 726 (w), 695 (m), 678 (m).

¹H NMR (DMSO-*d*₆): 4.76 (s, 2H, CH₂).

¹³C NMR (DMSO-*d*₆): 168.7 (COO), 157.2 (CNNO₂), 47.5 (CH₂).

Elemental analysis C₆H₂₆N₁₂O₁₈Mg (578.65 g/mol): calc.: C, 12.45; H, 4.53; N, 29.05. found: C, 11.88; H, 4.51; N, 27.81.

E_{dr} = 30 J (500–1000 μm).

F_r = 324 N (500–1000 μm).

E_{el} = 0.20 J (500–1000 μm).

Δ_cU = -1651 cal/g.

H₂O-sol. 37 wt% (22 °C).

5.2.3.6 Magnesium 2-(5-Nitriminotetrazolate)-acetate Octahydrate (5_Mg2)

After recrystallization from H₂O colorless crystals, suitable for X-ray diffraction, were obtained. Yield: 44 %.

M.p. 83 °C (loss of H₂O), 107 °C (loss of H₂O), 301 °C (dec., DSC-measurement, 5 K/min).

IR (Diamond-ATR, cm⁻¹): 3486 (s), 3366 (s), 3188 (s), 3027 (s), 2981 (m), 2289 (w), 1680 (w), 1642 (w), 1588 (m), 1524 (m), 1467 (m), 1434 (vw), 1392 (m), 1354 (m), 1314 (m), 1292 (m), 1168 (w), 1135 (w), 1044 (vw), 903 (vw), 700 (vw).

¹H NMR (DMSO-*d*₆): 4.58 (s, CH₂).

¹³C NMR (DMSO-*d*₆): 170.8 (COO), 157.6 (CNNO₂), 49.6 (CH₂).

Elemental analysis C₃H₁₈N₆O₁₂Mg (354.51 g/mol): calc.: C, 10.16; H, 5.12; N, 23.71. found: C, 10.12; H, 5.00; N, 23.52.

E_{dr} > 50 J (250–500 μm).

F_r > 360 N (250–500 μm).

E_{el} = 0.60 J (250–500 μm).

Δ_cU = -1154 cal/g.

H₂O-sol. 35 wt% (22 °C).

5.2.3.7 Calcium 1-Carboxymethyl-5-nitriminotetrazolate Dihydrate (5_Ca1)

After recrystallization from H₂O colorless crystals, suitable for X-ray diffraction, were obtained. Yield: 51 %.

M.p. 194 °C (dec., DSC-measurement, 5 K/min).

IR (Diamond-ATR, cm^{-1}): 3564 (m), 3433 (m), 2997 (m), 1727 (s), 1712 (m), 1638 (w), 1518 (s), 1467 (s), 1411 (s), 1354 (s), 1313 (s), 1287 (m), 1258 (s), 1239 (s), 1166 (m), 1128 (m), 1047 (w), 1009 (w), 956 (w), 893 (m), 802 (m), 764 (w), 741 (m), 698 (w).

^1H NMR (DMSO- d_6): 13.18 (s, 1H, OH), 4.88 (s, 2H, CH_2).

^{13}C NMR (DMSO- d_6): 167.9 (COOH), 157.2 (CNNO $_2$), 46.6 (CH_2).

Elemental analysis $\text{C}_6\text{H}_{10}\text{N}_{12}\text{O}_{10}\text{Ca}$ (450.30 g/mol): calc.: C, 16.00; H, 2.24; N, 37.33. found: C, 15.93; H, 2.33; N, 37.25.

E_{dr} = 30 J (100–500 μm).

F_{r} = 240 N (100–500 μm).

E_{el} = 0.20 J (100–500 μm).

$\Delta_c U$ = -1850 cal/g.

H_2O -sol. 28 wt% (23 °C).

5.2.3.8 Calcium 2-(5-Nitriminotetrazolate)-acetate Trihydrate (5_Ca2)

After recrystallization from H_2O colorless crystals, suitable for X-ray diffraction, were obtained. Yield: 42 %.

M.p. 175 °C (loss of H_2O), 191 °C (loss of H_2O), 309 °C (dec., DSC-measurement, 5 K/min).

Raman (300 mW, 25 °C, cm^{-1}): 2986 (15), 2952 (14), 1633 (4), 1514 (100), 1467 (10), 1409 (14), 1383 (3), 1341 (60), 1301 (7), 1167 (4), 1123 (18), 1043 (50), 1013 (9), 947 (5), 902 (4), 793 (4), 750 (14), 495 (8), 472 (10), 412 (5), 283 (24), 243 (3), 219 (3).

IR (Diamond-ATR, cm^{-1}): 3530 (m), 3456 (s), 3230 (m), 3127 (m), 2985 (m), 2357 (w), 2331 (w), 1633 (s), 1518 (m), 1469 (m), 1447 (w), 1432 (w), 1402 (m), 1383 (m), 1346 (m), 1317 (s), 1286 (m), 1241 (m), 1156 (w), 1042 (w), 1006 (w), 967 (w), 897 (w), 803 (w), 773 (w), 740 (w), 703 (w), 683 (w).

^1H NMR (DMSO- d_6): 4.54 (s, CH_2).

^{13}C NMR (DMSO- d_6): 170.9 (COO), 157.5 (CNNO $_2$), 49.7 (CH_2).

Elemental analysis $\text{C}_3\text{H}_8\text{N}_6\text{O}_7\text{Ca}$ (280.21 g/mol): calc.: C, 12.86; H, 2.88; N, 29.99. found: C, 12.88; H, 2.82; N, 30.32.

E_{dr} = 40 J (> 1000 μm).

F_{r} = 360 N (> 1000 μm).

E_{el} = 0.60 J (> 1000 μm).

$\Delta_c U$ = -1313 cal/g.

H_2O -sol. 25 wt% (23 °C).

5.2.3.9 Strontium 1-Carboxymethyl-5-nitriminotetrazolate Monohydrate (5_Sr1)

After recrystallization from H_2O colorless crystals, suitable for X-ray diffraction, were obtained. Yield: 88 %.

M.p. 218 °C (dec., DSC-measurement, 5 K/min).

Raman (300 mW, 25 °C, cm^{-1}): 2991 (3), 2955 (6), 1519 (100), 1477 (3), 1385 (20), 1336 (17), 1275 (3), 1155 (1), 1118 (5), 1037 (30), 1007 (3), 891 (6), 764 (2), 701 (2), 497 (3), 416 (4), 380 (2), 294 (4), 213 (3).

IR (Diamond-ATR, cm^{-1}): 3509 (w), 2944 (w), 2366 (w), 1969 (w), 1752 (m), 1650 (w), 1520 (m), 1473 (m), 1458 (w), 1424 (w), 1406 (w), 1345 (s), 1326 (s), 1274 (m), 1259 (m), 1208 (s), 1153 (m), 1107 (m), 1034 (m), 1006 (w), 954 (w), 885 (m), 806 (m), 756 (m), 729 (m), 698 (w), 636 (m).

^1H NMR (DMSO- d_6): 13.16 (s, 1H, OH), 4.85 (s, 2H, CH_2).

^{13}C NMR (DMSO- d_6): 168.0 (COOH), 157.2 (CNNO₂), 46.6 (CH_2).

Elemental analysis $\text{C}_6\text{H}_8\text{N}_{12}\text{O}_9\text{Sr}$ (479.82 g/mol): calc.: C, 15.02; H, 1.68; N, 35.03. found: C, 14.35; H, 1.88; N, 33.81.

$E_{\text{dr}} = 6.0 \text{ J}$ (> 1000 μm).

$F_{\text{r}} > 360 \text{ N}$ (> 1000 μm).

$E_{\text{el}} = 0.10 \text{ J}$ (> 1000 μm).

$\Delta_c U = -1536 \text{ cal/g}$.

H₂O-sol. 20 wt% (24 °C).

5.2.3.10 Strontium 2-(5-Nitriminotetrazolate)-acetate Trihydrate (5_Sr2)

After recrystallization from H₂O colorless crystals, suitable for X-ray diffraction, were obtained. Yield: 58 %.

M.p. 148 °C (loss of H₂O), 308 °C (dec., DSC-measurement, 5 K/min).

Raman (300 mW, 25 °C, cm^{-1}): 3005 (6), 2967 (12), 1519 (100), 1464 (9), 1399 (12), 1379 (18), 1327 (24), 1308 (17), 1262 (8), 1244 (4), 1150 (3), 1115 (11), 1044 (62), 1013 (10), 927 (6), 894 (8), 764 (8), 736 (3), 700 (4), 493 (3), 476 (4), 405 (7), 294 (9), 224 (4).

IR (Diamond-ATR, cm^{-1}): 3566 (w), 3390 (m), 2362 (w), 2331 (w), 1649 (s), 1620 (m), 1600 (m), 1520 (s), 1463 (m), 1408 (m), 1383 (s), 1360 (vs), 1323 (m), 1306 (s), 1256 (m), 1241 (w), 1148 (w), 1111 (m), 1039 (w), 1011 (w), 954 (w), 923 (w), 892 (w), 801 (w), 763 (m), 734 (w), 698 (w), 680 (w).

^1H NMR (DMSO- d_6): 4.56 (s, CH_2).

^{13}C NMR (DMSO- d_6): 172.7 (COO), 157.4 (CNNO₂), 49.8 (CH_2).

Elemental analysis $\text{C}_3\text{H}_8\text{N}_6\text{O}_7\text{Sr}$ (327.75 g/mol): calc.: C, 10.99; H, 2.46; N, 25.64. found: C, 11.06; H, 2.48; N, 26.08.

$E_{\text{dr}} > 100 \text{ J}$ (> 1000 μm).

$F_{\text{r}} > 360 \text{ N}$ (> 1000 μm).

$E_{\text{el}} = 0.25 \text{ J}$ (> 1000 μm).

$\Delta_c U = -1186 \text{ cal/g}$.

H₂O-sol. 16 wt% (24 °C).

5.2.3.11 Barium 1-Carboxymethyl-5-nitriminotetrazolate Monohydrate (5_Ba1)

After recrystallization from H₂O colorless crystals, suitable for X-ray diffraction, were obtained. Yield: 81 %.

M.p. 244 °C (dec., DSC-measurement, 5 K/min).

Raman (200 mW, 25 °C, cm⁻¹): 2995 (3), 2954 (7), 1514 (100), 1472 (3), 1389 (21), 1334 (18), 1268 (4), 1152 (1), 1115 (5), 1035 (26), 1004 (3), 889 (5), 803 (1), 760 (3), 701 (2), 655 (1), 495 (3), 413 (4), 379 (2), 288 (5), 215 (1).

IR (Diamond-ATR, cm⁻¹): 3746 (w), 3566 (w), 3510 (w), 3312 (w), 2535 (w), 2160 (w), 2016 (w), 1752 (m), 1645 (w), 1517 (m), 1469 (m), 1456 (m), 1380 (s), 1338 (s), 1260 (m), 1218 (s), 1151 (w), 1105 (w), 1034 (m), 886 (w), 807 (w), 757 (w), 647 (w).

¹H NMR (DMSO-*d*₆): 4.90 (s, 2H, CH₂).

¹³C NMR (DMSO-*d*₆): 168.5 (COOH), 157.7 (CNNO₂), 47.1 (CH₂).

Elemental analysis C₆H₈N₁₂O₉Ba (529.53 g/mol): calc.: C, 13.61; H, 1.52; N, 31.74. found: C, 13.52; H, 1.52; N, 31.70.

E_{dr} = 5.0 J (> 1000 μm).

F_r > 360 N (> 1000 μm).

E_{el} = 0.25 J (> 1000 μm).

Δ_cU = -1336 cal/g.

H₂O-sol. 6.0 wt% (24 °C).

5.2.3.12 Barium 2-(5-Nitriminotetrazolate)-acetate Heptahemihydrate (5_Ba2)

After recrystallization from H₂O colorless crystals were obtained. Yield: 87 %.

M.p. 63 °C (loss of H₂O), 95 °C (loss of H₂O), 342 °C (dec., DSC-measurement, 5 K/min).

Raman (300 mW, 25 °C, cm⁻¹): 3226 (1), 3002 (4), 2964 (11), 1590 (2), 1512 (100), 1458 (11), 1386 (9), 1356 (16), 1345 (18), 1326 (12), 1311 (24), 1255 (4), 1241 (4), 1151 (2), 1108 (6), 1035 (57), 1011 (6), 922 (6), 894 (5), 798 (2), 758 (10), 709 (2), 681 (2), 487 (4), 410 (4), 386 (4), 304 (4), 213 (3).

IR (Diamond-ATR, cm⁻¹): 3386 (s), 3000 (m), 2964 (m), 2350 (w), 2154 (w), 2018 (w), 1636 (w), 1589 (s), 1506 (m), 1455 (m), 1428 (m), 1358 (s), 1342 (s), 1308 (s), 1252 (m), 1104 (m), 1032 (w), 1008 (w), 962 (w), 920 (w), 892 (w), 855 (w), 822 (w), 792 (w), 775 (w), 733 (w), 706 (w), 677 (w).

¹H NMR (DMSO-*d*₆): 4.56 (s, CH₂).

¹³C NMR (DMSO-*d*₆): 172.2 (COO), 157.1 (CNNO₂), 50.6 (CH₂).

Elemental analysis C₃H₉N₆O_{7.5}Ba (386.47 g/mol): calc.: C, 9.32; H, 2.35; N, 21.75. found: C, 9.21; H, 2.36; N, 21.40.

E_{dr} > 100 J (> 1000 μm).

F_r > 360 N (> 1000 μm).

E_{el} = 0.15 J (> 1000 μm).

$$\Delta_c U = -1891 \text{ cal/g.}$$

H₂O-sol. 3.0 wt% (25 °C).

5.2.3.13 trans-[Diaqua-bis(1-Carboxymethyl-5-nitriminotetrazolato-N4,O1) Copper(II)] Dihydrate (5_Cu_H₂O)

1.02 g (5.0 mmol) 1-Carboxymethyl-5-nitriminotetrazole monohydrate (**5**) was dissolved in 20 ml water before 0.58 g (5.0 mmol) copper(II) nitrate pentahemihydrate in 5 mL water was added. After a few days at ambient temperature green single crystals, suitable for X-ray diffraction, were obtained. Yield: 60 %.

M.p. 130 °C (loss of H₂O), 238 °C (dec., DSC-measurement, 5 K/min).

IR (Diamond-ATR, cm⁻¹): 3402 (m), 2171 (s), 1752 (w), 1640 (s), 1491 (s), 1435 (vs), 1301 (w), 1234 (w), 1193 (w), 1093 (w), 794 (w), 732 (w).

Elemental analysis C₆H₁₄CuN₁₂O₁₂ (509.80 g/mol): calc.: C, 14.14; H, 2.77; N, 32.97. found: C, 14.20; H, 2.90; N, 33.20.

$$E_{dr} = 10 \text{ J} \quad (> 1000 \mu\text{m}).$$

$$F_r > 360 \text{ N} \quad (> 1000 \mu\text{m}).$$

$$E_{el} = 0.20 \text{ J} \quad (> 1000 \mu\text{m}).$$

$$\Delta_c U = -1890 \text{ cal/g.}$$

H₂O-sol. 3.0 wt% (23 °C).

5.2.3.14 Bis(diammine [2-(5-Nitriminotetrazolato-N4,O1)-acetato-O4] Copper(II)) Trihydrate (5_Cu_NH₃)

To a solution of (1.02 g, 5.0 mmol) 1-carboxymethyl-5-nitriminotetrazole monohydrate (**5**) in 20 mL H₂O, first 20 mL aqueous ammonia solution (25 %) and then 0.58 g (5.0 mmol) copper(II) nitrate pentahemihydrate in 5 mL H₂O were added. After a few days storing at ambient temperature dark blue single crystals, suitable for X-ray diffraction, were obtained. Yield: 76 %.

M.p. 120 °C (loss of NH₃ or H₂O), 155 °C (loss of NH₃ or H₂O), 217 °C (dec., DSC-measurement, 5 K/min).

IR (Diamond-ATR, cm⁻¹): 3414 (m), 3348 (vs), 3266 (s), 3224 (m), 3185 (m), 3005 (w), 2964 (w), 2671 (w), 2169 (w), 1626 (s), 1608 (m), 1520 (s), 1479 (m), 1412 (m), 1391 (s), 1344 (m), 1317 (w), 1269 (vs), 1241 (vs), 1149 (w), 1112 (w), 1036 (w), 960 (w), 892 (w), 805 (m), 772 (w), 759 (w), 732 (w), 679 (w).

Elemental analysis C₆H₂₂N₁₆O₁₀Cu₂ (567.39): calc.: C, 11.60; H, 3.57; N, 36.06. found: C, 11.66; H, 3.37; N, 36.41.

$$E_{dr} = 15 \text{ J} \quad (> 1000 \mu\text{m}).$$

$$F_r > 360 \text{ N} \quad (> 1000 \mu\text{m}).$$

$$E_{el} = 0.80 \text{ J} \quad (> 1000 \mu\text{m}).$$

$$\Delta_c U = -1889 \text{ cal/g.}$$

H₂O-sol. 1.1 wt% (23 °C).

5.2.4 Pyrotechnic Compositions

For the preparation of the pyrotechnic compositions all compounds, except the binder, were carefully mixed in a mortar. Then the binder, a solution of 25 % vinyl alcohol acetate resin (VAAR), dissolved in a few milliliters of ethyl acetate was added. The mixture was formed by hand and dried under high vacuum for several hours.

The controlled burn down was filmed with a digital video camera recorder (SONY, DCR-HC37E).

5.2.4.1 Pyrotechnic Compositions Based on 4_Li

In Table 5.12–Table 5.20, all tested pyrotechnic compositions containing **4_Li** as colorant are listed. Potassium permanganate, potassium dinitramide (KDN), ammonium nitrate, and ammonium dinitramide (ADN) were used as oxidizers. The fuels magnesium, silicon, charcoal, or starch were added.

Table 5.12 Pyrotechnic formulations containing **4_Li**, ammonium nitrate, and magnesium.

	4_Li [wt%]	NH₄NO₃ [wt%]	Mg [wt%]	VAAR [wt%]	observed behavior
4_Li_1.1	16	53	16	15	light red flame, easy to ignite, sparks, blinking, low velocity, no smoke, few pale grey residues
4_Li_1.2	26	50	11	13	yellow flame, many sparks, low velocity, less smoke, small amount of colorless residues
4_Li_1.3	8	47	31	14	small orange flame, did not burn completely, low velocity, no smoke, few pale grey residues

Table 5.13 Pyrotechnic formulations containing **4_Li**, ammonium nitrate, and silicon.

	4_Li [wt%]	NH₄NO₃ [wt%]	Si [wt%]	VAAR [wt%]	observed behavior
4_Li_2.1	12	62	12	14	tall yellow flame, moderate to ignite, low velocity, black residue
4_Li_2.2	10	51	25	14	yellow flame, hard to ignite, short-term flame, glows, black residue
4_Li_2.3	29	51	7	13	orange flame, short-term flame, glows, black residue

Table 5.14 Pyrotechnic formulation containing **4_Li**, ammonium nitrate, and charcoal.

	4_Li	NH₄NO₃	C	VAAR	observed behavior
	[wt%]	[wt%]	[wt%]	[wt%]	
4_Li_3	18	62	6	14	no flame, glowing, much smoke

Table 5.15 Pyrotechnic formulation containing **4_Li**, ammonium nitrate, and starch.

	4_Li	NH₄NO₃	Starch	VAAR	observed behavior
	[wt%]	[wt%]	[wt%]	[wt%]	
4_Li_4	19	61	6	14	no flame, glowing, much smoke

Table 5.16 Pyrotechnic formulation containing **4_Li**, ammonium nitrate, magnesium, and silicon.

	4_Li	NH₄NO₃	Mg	Si	VAAR	observed behavior
	[wt%]	[wt%]	[wt%]	[wt%]	[wt%]	
4_Li_5.1	26	53	5	3	13	orange flame, moderate to ignite, sparks, no smoke, low velocity, small amount of grey residues
4_Li_5.2	4	47	3	33	13	light orange flame, hard to ignite, sparks, less smoke, low velocity, small amount of black residues
4_Li_5.3	31	50	3	3	13	orange flame, hard to ignite, many sparks, less smoke, low velocity, black residues

Table 5.17 Pyrotechnic formulations containing **4_Li**, ammonium nitrate, potassium permanganate, and magnesium.

	4_Li	NH₄NO₃	KMnO₄	Mg	VAAR	observed behavior
	[wt%]	[wt%]	[wt%]	[wt%]	[wt%]	
4_Li_6.1	35	36	6	6	17	yellow flame, hard to ignite, sparks, low velocity, unsteady burning, glowing residues
4_Li_6.2	46	18	15	9	12	yellow flame, sparks, slow, glowing, much smoke

Table 5.18 Pyrotechnic formulations containing **4_Li**, ADN, and magnesium.

	4_Li	ADN	Mg	VAAR	observed behavior
	[wt%]	[wt%]	[wt%]	[wt%]	
4_Li_7.1	26	53	8	13	yellow-red flame, easy to ignite, less smoke, almost no residues
4_Li_7.2	35	46	7	12	red flame, easy to ignite, high velocity, less smoke, almost no residues

Table 5.19 Pyrotechnic formulation containing **4_Li**, ADN, and silicon.

	4_Li	ADN	Si	VAAR	observed behavior
	[wt%]	[wt%]	[wt%]	[wt%]	
4_Li_8	35	47	7	11	orange flame, easy to ignite, few sparks, smoke, moderate velocity, glowing residue

Table 5.20 Pyrotechnic formulations containing **4_Li**, KDN, and magnesium.

	4_Li	KDN	Mg	VAAR	observed behavior
	[wt%]	[wt%]	[wt%]	[wt%]	
4_Li_9.1	41	38	8	13	violet flame, hard to ignite, much smoke, sparks, small amount of solid residues
4_Li_9.2	51	26	10	13	cannot be ignited

5.2.4.2 Pyrotechnic Compositions Based on **4_Sr**

In Table 5.21–Table 5.34, all tested pyrotechnic compositions, containing **4_Sr** as colorant, are listed. As oxidizer potassium permanganate, potassium nitrate, manganese dioxide, ammonium nitrate, ammonium dinitramide, and potassium dinitramide were used. The fuels magnesium, magnalium, aluminum or **5-At** were added.

Table 5.21 Pyrotechnic formulations containing **4_Sr**, potassium nitrate, and magnesium.

	4_Sr	KNO₃	Mg	VAAR	observed behavior
	[wt%]	[wt%]	[wt%]	[wt%]	
4_Sr_1.1	20	51	20	7	violet flame, moderate to ignite, much smoke, high velocity, few colorless residues
4_Sr_1.2	24	38	19	19	violet flame, moderate to ignite, much smoke, high velocity, few colorless residues
4_Sr_1.3	31	31	15	23	violet-red flame, moderate to ignite, much smoke, moderate velocity, few colorless residues
4_Sr_1.4	33	27	20	20	violet-red flame, moderate to ignite, much smoke, sparks, moderate velocity, residues
4_Sr_1.5	39	23	23	15	violet-red flame, moderate to ignite, much smoke, sparks, low velocity, residues
4_Sr_1.6	41	17	25	17	violet-red flame, moderate to ignite, smoke, sparks, low velocity, few black residues
4_Sr_1.7	38	16	31	15	yellow-red flame, hard to ignite, smoke, sparks, low velocity, few black residues

Table 5.22 Pyrotechnic formulations containing **4_Sr**, ammonium nitrate, and magnesium

	4_Sr	NH₄NO₃	Mg	VAAR	observed behavior
	[wt%]	[wt%]	[wt%]	[wt%]	
4_Sr_2.1	17	59	17	7	red flame, moderate to ignite, less smoke, few sparks, moderate velocity, small amount of residues
4_Sr_2.2	14	51	22	13	red flame, hard to ignite, less smoke, few sparks, low velocity, small amount of residues
4_Sr_2.3	19	51	19	11	red flame, hard to ignite, no smoke, few sparks, unsteady burning, small amount of residues
4_Sr_2.4	24	49	18	9	red flame, hard to ignite, less smoke, few sparks, unsteady burning, few glowing residues
4_Sr_2.5	24	44	19	13	red flame, hard to ignite, less smoke, low velocity glowing residues
4_Sr_2.6	22	48	18	12	yellow-red flame, hard to ignite, sparks, less smoke, moderate velocity, few glowing residues
4_Sr_2.7	25	41	20	14	intense red flame, hard to ignite, less smoke, few sparks, moderate velocity, almost no residues
4_Sr_2.8	28	46	11	15	red flame, hard to ignite, sparks, low velocity, grey residues
4_Sr_2.9	28	40	23	9	small red flame, hard to ignite, less smoke, sparks, low velocity, grey residues
4_Sr_2.10	24	43	5	28	small yellow flame, hard to ignite, very low velocity, some grey residues

Table 5.23 Pyrotechnic formulation containing **4_Sr**, potassium nitrate, and magnalium.

	4_Sr	KNO₃	MgAl	VAAR	observed behavior
	[wt%]	[wt%]	[wt%]	[wt%]	
4_Sr_3	29	36	22	13	yellow-violet flame, hard to ignite, low velocity, smoke, glowing residues

Table 5.24 Pyrotechnic formulation containing **4_Sr**, ammonium nitrate, and magnalium.

	4_Sr	NH₄NO₃	MgAl	VAAR	observed behavior
	[wt%]	[wt%]	[wt%]	[wt%]	
4_Sr_4	21	43	27	9	no flame, glowing

Table 5.25 Pyrotechnic formulations containing **4_Sr**, ammonium nitrate, potassium nitrate, and magnesium.

	4_Sr	NH₄NO₃	Mg	VAAR	observed behavior
	[wt%]	[wt%]	[wt%]	[wt%]	
4_Sr_5.1	23	35	11	11	violet-yellow flame, hard to ignite, smoke, moderate velocity, large amount of glowing residues
4_Sr_5.2	23	35	12	12	violet-red flame, hard to ignite, smoke, moderate velocity, glowing residues

Table 5.26 Pyrotechnic formulation containing **4_Sr**, ammonium nitrate, and **5-At**.

	4_Sr	NH₄NO₃	5-At	VAAR	observed behavior
	[wt%]	[wt%]	[wt%]	[wt%]	
4_Sr_6	24	56	8	12	cannot be ignited

Table 5.27 Pyrotechnic formulations containing **4_Sr**, ammonium nitrate, magnesium, and **5-At**.

	4_Sr	NH₄NO₃	5-At	Mg	VAAR	observed behavior
	[wt%]	[wt%]	[wt%]	[wt%]	[wt%]	
4_Sr_7.1	22	57	7	3	11	small yellow-red flame, hard to ignite, sparks, low velocity, few residues
4_Sr_7.2	20	60	3	7	10	intense red flame, easy to ignite, some sparks, no smoke, moderate velocity, almost no solid residues
4_Sr_7.3	18	59	8	6	9	yellow-red flame, hard to ignite, sparks, low velocity, few colorless residues
4_Sr_7.4	21	54	11	6	8	yellow-red flame, hard to ignite, few sparks, less smoke, some grey residues
4_Sr_7.5	20	50	15	7	8	red-orange flame, blinking, few sparks, no smoke, low velocity, glowing residues
4_Sr_7.6	22	48	17	6	7	small yellow-orange flame, sparks, low velocity, some grey residues

Table 5.28 Pyrotechnic formulations containing **4_Sr**, ammonium nitrate, magnesium, and aluminum.

	4_Sr	NH₄NO₃	Mg	Al	VAAR	observed behavior
	[wt%]	[wt%]	[wt%]	[wt%]	[wt%]	
4_Sr_8.1	16	42	16	10	16	red flame, sparks, smoke, easy to ignite, low velocity, small amount of solid residues
4_Sr_8.2	18	48	12	8	14	red flame, moderate to ignite, sparks, less smoke, low velocity, small amount of solid residues
4_Sr_8.3	24	48	6	8	14	red flame, blinking, sparks, unsteady burning, grey residues
4_Sr_8.4	23	53	4	7	13	small red flame, few sparks, less smoke, low velocity, grey residues
4_Sr_8.5	22	54	3	7	14	red flame, hard to ignite, few sparks, less smoke, unsteady burning, grey residues
4_Sr_8.6	20	54	1	10	15	small yellow-red flame, no smoke, low velocity

Table 5.29 Pyrotechnic formulations containing **4_Sr**, potassium permanganate, and magnesium.

	4_Sr [wt%]	KMnO₄ [wt%]	Mg [wt%]	VAAR [wt%]	observed behavior
4_Sr_9.1	18	47	23	12	violet flame, hard to ignite, much smoke, high velocity, glowing residue
4_Sr_9.2	29	38	19	14	violet flame, moderate to ignite, much smoke, high velocity, glowing residue
4_Sr_9.3	47	23	12	18	cannot be ignited

Table 5.30 Pyrotechnic formulations containing **4_Sr**, ammonium nitrate, potassium permanganate, and magnesium.

	4_Sr [wt%]	NH₄NO₃ [wt%]	KMnO₄ [wt%]	Mg [wt%]	VAAR [wt%]	observed behavior
4_Sr_10.1	25	37	12	12	14	violet flame, sparks, smoke, glowing residue
4_Sr_10.2	39	31	8	8	14	violet-red flame, hard to ignite, few sparks, less smoke, low velocity, glowing residue
4_Sr_10.3	34	27	13	13	13	red-violet-yellow flame, sparks, less smoke, moderate velocity, glowing residue

Table 5.31 Pyrotechnic formulations containing **4_Sr**, manganese dioxide, and magnesium.

	4_Sr [wt%]	MnO₂ [wt%]	Mg [wt%]	VAAR [wt%]	observed behavior
4_Sr_11.1	25	49	12	14	cannot be ignited
4_Sr_11.2	19	48	19	14	cannot be ignited

Table 5.32 Pyrotechnic formulations containing **4_Sr**, manganese dioxide, and aluminum.

	4_Sr [wt%]	MnO₂ [wt%]	Al [wt%]	VAAR [wt%]	observed behavior
4_Sr_12.1	34	33	20	14	cannot be ignited
4_Sr_12.2	20	40	25	14	cannot be ignited

Table 5.33 Pyrotechnic formulation containing **4_Sr**, ADN, and magnesium.

	4_Sr [wt%]	ADN [wt%]	Mg [wt%]	VAAR [wt%]	observed behavior
4_Sr_13	35	46	7	12	intense red, easy to ignite, no smoke, moderate velocity, very small amount of solid residues

Table 5.34 Pyrotechnic formulations containing **4_Sr**, KDN, and magnesium.

	4_Sr	KDN	Mg	VAAR	observed behavior
	[wt%]	[wt%]	[wt%]	[wt%]	
4_Sr_14.1	39	39	8	14	violet flame, hard to ignite, sparks, smoke, high velocity, glowing residues
4_Sr_14.2	40	40	10	10	violet flame, sparks, smoke, high velocity, glowing residues
4_Sr_14.3	52	31	6	11	no flame, glowing

5.2.4.3 Pyrotechnic Compositions Based on **4_Ba**

In Table 5.35–Table 5.52, all tested pyrotechnic compositions, containing **4_Ba** as colorant, are listed. Potassium nitrate, ammonium nitrate, ammonium dinitramide, potassium dinitramide, and potassium perchlorate were used as oxidizers. The fuels magnesium, magnalium, boron, aluminum, PVC or **5-At** were added.

Table 5.35 Pyrotechnic formulations containing **4_Ba**, ammonium nitrate, and magnesium.

	4_Ba	NH₄NO₃	Mg	VAAR	observed behavior
	[wt%]	[wt%]	[wt%]	[wt%]	
4_Ba_1.1	14	54	8	24	small green flame, less smoke, low velocity, unsteady burning, small amount of solid residues
4_Ba_1.2	10	50	10	30	small green flame, few sparks, no smoke, low velocity, blinking, small amount of solid residues
4_Ba_1.3	14	59	12	15	small green flame, few sparks, less smoke, low velocity, blinking, almost no solid residues
4_Ba_1.4	13	63	11	13	green-white flame, sparks, low velocity, some colorless residues
4_Ba_1.5	11	69	8	12	yellow-white flame, many sparks, low velocity, small amount of solid residues
4_Ba_1.6	11	66	7	16	yellow flame, hard to ignite, sparks, low velocity, some colorless residues

Table 5.36 Pyrotechnic formulations containing **4_Ba**, ammonium nitrate, and magnalium.

	4_Ba	NH₄NO₃	MgAl	VAAR	observed behavior
	[wt%]	[wt%]	[wt%]	[wt%]	
4_Ba_2.1	14	54	8	24	cannot be ignited
4_Ba_2.2	9	71	5	15	cannot be ignited

Table 5.37 Pyrotechnic formulations containing **4_Ba**, ammonium nitrate, magnesium, and boron.

	4_Ba	NH₄NO₃	Mg	B	VAAR	observed behavior
	[wt%]	[wt%]	[wt%]	[wt%]	[wt%]	
4_Ba_3.1	13	60	5	9	13	green flame, few sparks, less smoke, moderate velocity, small amount of glowing residues
4_Ba_3.2	23	52	5	7	13	green-yellow flame, few sparks, no smoke, moderate velocity, glowing residues
4_Ba_3.3	37	52	4	4	13	cannot be ignited
4_Ba_3.4	16	57	5	8	14	tall yellow-green flame, few sparks, less smoke, moderate velocity, almost no residues
4_Ba_3.5	28	49	7	4	12	small yellow flame, few sparks, no smoke, low velocity, glowing residues

Table 5.38 Pyrotechnic formulations containing **4_Ba**, ammonium nitrate, and boron.

	4_Ba	NH₄NO₃	B	VAAR	observed behavior
	[wt%]	[wt%]	[wt%]	[wt%]	
4_Ba_4.1	19	52	19	10	green in the end yellow flame, less smoke, moderate velocity, glowing residue
4_Ba_4.2	19	57	16	8	green flame, easy to ignite, less smoke, moderate velocity, glowing residue
4_Ba_4.3	19	56	14	11	green-yellow flame, less smoke, low velocity, glowing residue
4_Ba_4.4	23	47	18	12	yellow flame, no smoke, moderate velocity, glowing residue
4_Ba_4.5	17	55	17	11	yellow-green flame, no smoke, moderate velocity, glowing residue
4_Ba_4.6	21	47	21	11	yellow flame, hard to ignite, no smoke, low velocity, glowing residue

Table 5.39 Pyrotechnic formulation containing **4_Ba**, potassium nitrate, and boron.

	4_Ba	KNO₃	B	VAAR	observed behavior
	[wt%]	[wt%]	[wt%]	[wt%]	
4_Ba_5	24	40	24	12	red flame, hard to ignite, glowing residue

Table 5.40 Pyrotechnic formulation containing **4_Ba**, ammonium nitrate, magnesium and PVC.

	4_Ba	NH₄NO₃	Mg	PVC	VAAR	observed behavior
	[wt%]	[wt%]	[wt%]	[wt%]	[wt%]	
4_Ba_6	10	62	10	2	16	yellow-green flame, blinking, few sparks, low velocity, glowing residue

Table 5.41 Pyrotechnic formulation containing **4_Ba**, ammonium nitrate, and **5-At**.

	4_Ba	NH₄NO₃	5-At	VAAR	observed behavior
	[wt%]	[wt%]	[wt%]	[wt%]	
4_Ba_7	24	54	8	14	short-term yellow flame, glowing

Table 5.42 Pyrotechnic formulation containing **4_Ba**, ammonium nitrate, **5-At**, and magnesium.

	4_Ba	NH₄NO₃	5-At	Mg	VAAR	observed behavior
	[wt%]	[wt%]	[wt%]	[wt%]	[wt%]	
4_Ba_8	23	54	8	3	12	small pale green flame, hard to ignite, sparks, almost no solid residues

Table 5.43 Pyrotechnic formulations containing **4_Ba**, ADN, and magnesium.

	4_Ba	ADN	Mg	VAAR	observed behavior
	[wt%]	[wt%]	[wt%]	[wt%]	
4_Ba_9.1	34	47	7	12	yellow flame, less smoke, sparks, glowing residue
4_Ba_9.2	47	38	6	9	white-yellow flame, easy to ignite, no smoke, high velocity, glowing residues
4_Ba_9.3	56	27	4	13	no flame, glowing

Table 5.44 Pyrotechnic formulations containing **4_Ba**, ADN, magnesium, and PVC.

	4_Ba	ADN	Mg	PVC	VAAR	observed behavior
	[wt%]	[wt%]	[wt%]	[wt%]	[wt%]	
4_Ba_10.1	48	36	2	2	12	yellow flame, no smoke, few sparks, low velocity, glowing residue
4_Ba_10.2	48	35	4	1	12	short term yellow flame, glowing

Table 5.45 Pyrotechnic formulations containing **4_Ba**, KDN, and aluminum.

	4_Ba	KDN	Al	VAAR	observed behavior
	[wt%]	[wt%]	[wt%]	[wt%]	
4_Ba_11.1	46	35	7	12	no flame, glowing
4_Ba_11.2	42	43	4	11	small white flame, smoke, low velocity, glowing residue
4_Ba_11.3	44	43	2	11	intense white flame, smoke, moderate velocity, very small amount of solid glowing residues
4_Ba_11.4	39	49	2	10	white flame, hard to ignite, smoke, almost no residues

Table 5.46 Pyrotechnic formulations containing **4_Ba**, ADN, and **5-At**.

	4_Ba	ADN	5-At	VAAR	observed behavior
	[wt%]	[wt%]	[wt%]	[wt%]	
4_Ba_12.1	43	32	15	10	no flame, glowing
4_Ba_12.2	48	32	8	12	no flame, glowing

4_Ba_12.3	43	41	6	10	no flame, glowing
------------------	----	----	---	----	-------------------

Table 5.47 Pyrotechnic formulations containing **4_Ba**, ADN, magnesium, and boron.

	4_Ba [wt%]	ADN [wt%]	Mg [wt%]	B [wt%]	VAAR [wt%]	observed behavior
4_Ba_13.1	21	43	8	14	14	green flame, easy to ignite, sparks less smoke, high velocity, glowing residue
4_Ba_13.2	29	39	10	12	10	green flame, easy to ignite, less smoke, sparks, combusts too violently, glowing residues
4_Ba_13.3	31	41	8	10	10	green flame, easy to ignite, less smoke, sparks, high velocity, almost no residues
4_Ba_13.4	33	44	7	5	11	yellow flame, less smoke, glowing residue

Table 5.48 Pyrotechnic formulations containing **4_Ba**, ADN, and magnesium.

	4_Ba [wt%]	ADN [wt%]	Mg [wt%]	VAAR [wt%]	observed behavior
4_Ba_14.1	10	47	28	15	cannot be ignited
4_Ba_14.2	17	49	17	17	intense green flame, easy to ignite, less smoke, high velocity, almost no solid residues

Table 5.49 Pyrotechnic formulations containing **4_Ba**, KDN, and magnesium.

	4_Ba [wt%]	KDN [wt%]	Mg [wt%]	VAAR [wt%]	observed behavior
4_Ba_15.1	42	42	6	10	white flame, sparks, smoke, moderate velocity, glowing residues
4_Ba_15.2	54	33	2	11	short-term white flame, smoke, glowing

Table 5.50 Pyrotechnic formulations containing **4_Ba**, KDN, magnesium, and boron.

	4_Ba [wt%]	KDN [wt%]	Mg [wt%]	B [wt%]	VAAR [wt%]	observed behavior
4_Ba_16.1	28	40	10	12	10	yellow flame, many sparks, glowing residue
4_Ba_16.2	41	41	4	4	10	white flame, sparks, smoke, high velocity, glowing residue

Table 5.51 Pyrotechnic formulations containing **4_Ba**, KDN, magnesium, and aluminum.

	4_Ba	KDN	Mg	B	VAAR	observed behavior
	[wt%]	[wt%]	[wt%]	[wt%]	[wt%]	
4_Ba_17.1	29	55	3	3	10	violet-white flame, much smoke, many sparks, moderate velocity, no residues
4_Ba_17.2	21	52	15	2	10	white flame, hard to ignite, many sparks, much smoke, almost no residues
4_Ba_17.3	32	53	2	2	11	tall white flame, hard to ignite, much smoke, sparks, moderate velocity, almost no residues

Table 5.52 Pyrotechnic formulation containing **4_Ba**, ADN, magnesium, and aluminum.

	4_Ba	ADN	Mg	Al	VAAR	observed behavior
	[wt%]	[wt%]	[wt%]	[wt%]	[wt%]	
4_Ba_18	35	48	3	2	12	yellow flame, few sparks, no smoke, moderate velocity, glowing residue

5.2.4.4 Pyrotechnic Compositions Based on 5_Sr1

In Table 5.53–Table 5.56, all tested pyrotechnic compositions, containing **5_Sr1** as colorant, are listed. As oxidizer ammonium nitrate and ammonium dinitramide were used. The fuels magnesium, aluminum or **5-At** were added.

Table 5.53 Pyrotechnic formulation containing **5_Sr1**, ADN, and magnesium.

	5_Sr1	ADN	Mg	VAAR	observed behavior
	[wt%]	[wt%]	[wt%]	[wt%]	
5_Sr1_1	35	46	8	11	intense red flame, easy to ignite, sparks, no smoke, high velocity, no residues

Table 5.54 Pyrotechnic formulation containing **5_Sr1**, ADN, magnesium, and aluminum.

	5_Sr1	ADN	Mg	Al	VAAR	observed behavior
	[wt%]	[wt%]	[wt%]	[wt%]	[wt%]	
5_Sr1_2	17	43	17	11	12	red flame, easy to ignite, sparks, less smoke, high velocity, small amount of glowing residues

Table 5.55 Pyrotechnic formulation containing **5_Sr1**, ammonium nitrate, magnesium, and **5-At**.

	5_Sr1	NH₄NO₃	Mg	5-At	VAAR	observed behavior
	[wt%]	[wt%]	[wt%]	[wt%]	[wt%]	
5_Sr1_3	19	59	6	3	13	small orange-red flame, sparks, no smoke, blinking, low velocity, grey residues

Table 5.56 Pyrotechnic formulations containing **5_Sr1**, ammonium nitrate, and magnesium.

	5_Sr1	NH₄NO₃	Mg	VAAR	observed behavior
	[wt%]	[wt%]	[wt%]	[wt%]	
5_Sr1_4.1	23	43	19	15	intense red flame, few sparks, less smoke, moderate velocity, small amount of solid residues
5_Sr1_4.2	25	46	15	15	red flame, sparks, less smoke, moderate velocity, small amount of residues
5_Sr1_4.3	28	43	14	15	red flame, sparks, less smoke, moderate velocity, small amount of solid residues

5.2.4.5 Pyrotechnic Compositions Based on 5_Sr2

In Table 5.57–Table 5.60, all tested pyrotechnic compositions, containing **5_Sr2** as colorant, are listed. Ammonium nitrate and ammonium dinitramide were used as oxidizers and the fuels magnesium, aluminum or **5-At** were added.

Table 5.57 Pyrotechnic formulations containing **5_Sr2**, ADN, and magnesium.

	5_Sr2	ADN	Mg	VAAR	observed behavior
	[wt%]	[wt%]	[wt%]	[wt%]	
5_Sr2_1.1	32	43	6	19	short-term red flame, glowing
5_Sr2_1.2	35	45	7	13	intense red flame, few sparks, less smoke, moderate velocity, almost no residues

Table 5.58 Pyrotechnic formulations containing **5_Sr2**, ADN, magnesium, and aluminum.

	5_Sr2	ADN	Mg	Al	VAAR	observed behavior
	[wt%]	[wt%]	[wt%]	[wt%]	[wt%]	
5_Sr2_2.1	16	44	16	11	13	red flame, blinking, sparks, smoke, moderate velocity, almost no residues
5_Sr2_2.2	17	46	12	12	13	red flame, sparks, less smoke, moderate velocity, solid residue

Table 5.59 Pyrotechnic formulations containing **5_Sr2**, ammonium nitrate, magnesium, and **5-At**.

	5_Sr2	NH₄NO₃	Mg	5-At	VAAR	observed behavior
	[wt%]	[wt%]	[wt%]	[wt%]	[wt%]	
5_Sr2_3.1	20	58	6	3	13	red flame, sparks, no smoke, low velocity, almost no residues
5_Sr2_3.2	18	61	4	3	14	red-yellow flame, sparks, no smoke, low velocity, almost no residues
5_Sr2_3.3	18	60	5	4	13	red flame, sparks, no smoke, low velocity, almost no residues

Table 5.60 Pyrotechnic formulations containing **5_Sr2**, ammonium nitrate, and magnesium.

	5_Sr2	NH₄NO₃	Mg	VAAR	observed behavior
	[wt%]	[wt%]	[wt%]	[wt%]	
5_Sr2_4.1	24	43	19	14	red flame, sparks, smoke, low velocity, small amount of solid residues
5_Sr2_4.2	25	45	15	15	red flame, hard to ignite, blinking, almost no solid residues

5.2.4.6 Pyrotechnic Compositions Based on 5_Ba1

In Table 5.61–Table 5.65, all tested pyrotechnic compositions, containing **5_Ba1** as colorant, are listed. Ammonium nitrate, ammonium dinitramide and potassium dinitramide were used as oxidizers, as well as magnesium and boron as fuels.

Table 5.61 Pyrotechnic formulations containing **5_Ba1**, ammonium nitrate, and magnesium.

	5_Ba1	NH₄NO₃	Mg	VAAR	observed behavior
	[wt%]	[wt%]	[wt%]	[wt%]	
5_Ba1_1.1	18	53	18	11	green-white flame, smoke, blinking, low velocity, few residues
5_Ba1_1.2	21	57	11	11	white flame, smoke, few sparks, moderate velocity, few residues
5_Ba1_1.3	34	46	10	10	yellow flame, smoke, low velocity, some residues

Table 5.62 Pyrotechnic formulations containing **5_Ba1**, ammonium nitrate, magnesium, and boron.

	5_Ba1	NH₄NO₃	Mg	B	VAAR	observed behavior
	[wt%]	[wt%]	[wt%]	[wt%]	[wt%]	
5_Ba1_2.1	20	53	5	8	14	tall yellow-green flame, less smoke, few sparks, moderate velocity, black residue
5_Ba1_2.2	27	47	5	7	14	yellow flame, few sparks, less smoke, low velocity, black residue

Table 5.63 Pyrotechnic formulations containing **5_Ba1**, ammonium nitrate, and boron.

	5_Ba1	NH₄NO₃	B	VAAR	observed behavior
	[wt%]	[wt%]	[wt%]	[wt%]	
5_Ba1_3.1	29	51	7	13	green flame, easy to ignite, no smoke, moderate velocity, black residue
5_Ba1_3.2	34	46	7	13	yellow flame, some sparks, low velocity, large residue

Table 5.64 Pyrotechnic formulations containing **5_Ba1**, ADN, and magnesium.

	5_Ba1	ADN	Mg	VAAR	observed behavior
	[wt%]	[wt%]	[wt%]	[wt%]	
5_Ba1_4.1	42	43	4	11	green flame, easy to ignite, lifts off
5_Ba1_4.2	48	36	4	12	green flame, easy to ignite, some sparks, less smoke, combusts too violently, no residues
5_Ba1_4.3	48	38	2	12	intense green flame, easy to ignite, some sparks, less smoke, high velocity, no residues
5_Ba1_4.4	45	41	2	12	yellow flame, sparks, less smoke, few residues

Table 5.65 Pyrotechnic formulation containing **5_Ba1**, KDN, and magnesium.

	5_Ba1	KDN	Mg	VAAR	observed behavior
	[wt%]	[wt%]	[wt%]	[wt%]	
5_Ba1_5	53	35	2	10	white flame, sparks, smoke, high velocity, few residues

5.2.4.7 Pyrotechnic Compositions Based on 5_Ba2

In Table 5.66–Table 5.70, all tested pyrotechnic compositions, containing **5_Ba2** as colorant, are listed. Ammonium nitrate and ammonium dinitramide were used as oxidizers. The fuels magnesium or boron were added.

Table 5.66 Pyrotechnic formulations containing **5_Ba2**, ammonium nitrate, and magnesium.

	5_Ba2	NH₄NO₃	Mg	VAAR	observed behavior
	[wt%]	[wt%]	[wt%]	[wt%]	
5_Ba2_1.1	18	56	13	13	white-green flame, blinking, few sparks, smoke, low velocity, almost no residues
5_Ba2_1.2	19	58	13	10	white flame, few sparks, less smoke, low velocity, almost no residues

Table 5.67 Pyrotechnic formulations containing **5_Ba2**, ammonium nitrate, magnesium, and boron.

	5_Ba2	NH₄NO₃	Mg	B	VAAR	observed behavior
	[wt%]	[wt%]	[wt%]	[wt%]	[wt%]	
5_Ba2_2.1	20	53	7	7	13	intense green flame, few sparks, less smoke, moderate velocity, almost no residues
5_Ba2_2.2	17	59	4	8	12	yellow-green flame, sparks, less smoke, moderate velocity, some residues
5_Ba2_2.3	26	61	2	2	9	green-white flame, no proper burning, low velocity, glowing residue
5_Ba2_2.4	23	54	3	9	11	small green-white flame, no proper burning, low velocity, glowing residue

5_Ba2_2.5	23	55	2	8	12	green-yellow flame, less smoke, few sparks, moderate velocity, small glowing residue
5_Ba2_2.6	31	47	2	8	12	green-yellow flame, no smoke, few sparks, moderate velocity, almost no residues
5_Ba2_2.7	30	52	1	6	11	yellow flame, few sparks, no smoke, low velocity, some residues
5_Ba2_2.8	35	43	2	9	11	green-yellow flame, sparks, less smoke, moderate velocity, small amount of residues

Table 5.68 Pyrotechnic formulations containing **5_Ba2**, ammonium nitrate, and boron.

	5_Ba2	NH₄NO₃	B	VAAR	observed behavior
	[wt%]	[wt%]	[wt%]	[wt%]	
5_Ba2_3.1	31	46	9	14	green flame, sparks, no smoke, high velocity, almost no residues
5_Ba2_3.2	29	51	7	13	intense green flame, few sparks, no smoke, high velocity, almost no residues
5_Ba2_3.3	42	42	6	10	yellow flame, few sparks, no smoke, moderate velocity, small amount of black residues
5_Ba2_3.4	47	38	6	9	yellow flame, no smoke, moderate velocity, small amount of black residues

Table 5.69 Pyrotechnic formulations containing **5_Ba2**, ADN, and magnesium.

	5_Ba2	ADN	Mg	VAAR	observed behavior
	[wt%]	[wt%]	[wt%]	[wt%]	
5_Ba2_4.1	43	42	4	11	green-white flame, easy to ignite, few sparks, smoke, combusts too vigorously, no residues
5_Ba2_4.2	49	37	2	12	white flame, few sparks, smoke, high velocity, very small amount of solid residues

Table 5.70 Pyrotechnic formulation containing **5_Ba2**, ADN, magnesium, and boron.

	5_Ba2	ADN	Mg	B	VAAR	observed behavior
	[wt%]	[wt%]	[wt%]	[wt%]	[wt%]	
5_Ba2_5	42	40	2	6	10	tall yellow flame, sparks, glowing residue

5.2.4.8 Pyrotechnic Compositions Based on **5_Cu_H2O**

In Table 5.71–Table 5.79, all tested pyrotechnic compositions containing **5_Cu_H2O** as colorant are listed. Ammonium nitrate, ammonium dinitramide, and potassium dinitramide were used as oxidizers. The fuels **5-At** or boron were added as well as the following copper compounds, copper, copper(I) oxide and $[\text{Cu}(\text{NH}_3)_4][\text{N}(\text{NO}_2)_2]_2$.

Table 5.71 Pyrotechnic formulations containing **5_Cu_H2O**, ammonium nitrate, and boron.

	5_Cu_H2O	NH₄NO₃	B	VAAR	observed behavior
	[wt%]	[wt%]	[wt%]	[wt%]	
5_Cu_H2O_1.1	17	53	17	13	yellow flame, easy to ignite, less smoke, moderate velocity, glowing residue
5_Cu_H2O_1.2	21	55	14	10	green-yellow flame, easy to ignite, no smoke, moderate velocity, glowing residue
5_Cu_H2O_1.3	19	58	13	10	yellow-green flame, less smoke, moderate velocity, glowing residue
5_Cu_H2O_1.4	20	60	10	10	green-yellow flame, almost no smoke, moderate velocity, glowing residue
5_Cu_H2O_1.5	27	56	7	10	green-yellow flame, no smoke, moderate velocity, glowing residue
5_Cu_H2O_1.6	35	41	14	10	yellow flame, no smoke, moderate velocity, glowing residue
5_Cu_H2O_1.7	33	53	4	10	small yellow flame, less smoke, low velocity, glowing residue
5_Cu_H2O_1.8	26	52	9	13	intense green flame, less smoke, moderate velocity, glowing residue

Table 5.72 Pyrotechnic formulation containing **5_Cu_H2O**, ammonium nitrate, boron, and **5-At**.

	5_Cu_H2O	NH₄NO₃	B	5-At	VAAR	observed behavior
	[wt%]	[wt%]	[wt%]	[wt%]	[wt%]	
5_Cu_H2O_2	33	34	10	7	16	yellow flame, smoke, low velocity, glowing residue

Table 5.73 Pyrotechnic formulations containing **5_Cu_H2O**, ammonium nitrate, and **5-At**.

	5_Cu_H2O	NH₄NO₃	5-At	VAAR	observed behavior
	[wt%]	[wt%]	[wt%]	[wt%]	
5_Cu_H2O_3.1	38	25	25	12	yellow-green flame, hard to ignite, much smoke, low velocity, glowing residue
5_Cu_H2O_3.2	20	27	40	13	yellow-green flame, much smoke, no proper burning, low velocity, glowing residue

Table 5.74 Pyrotechnic formulations containing **5_Cu_H2O**, ammonium nitrate, and copper.

	5_Cu_H2O	NH₄NO₃	Cu	VAAR	observed behavior
	[wt%]	[wt%]	[wt%]	[wt%]	
5_Cu_H2O_4.1	25	49	12	14	yellow flame no smoke, hard to ignite, low velocity, glowing residue

5_Cu_H2O_4.2	17	41	29	13	small yellow flame, hard to ignite, glowing residue
---------------------	----	----	----	----	---

Table 5.75 Pyrotechnic formulation containing **5_Cu_H2O**, ammonium nitrate, boron, and copper(I) oxide.

	5_Cu_H2O [wt%]	NH4NO3 [wt%]	B [wt%]	Cu2O [wt%]	VAAR [wt%]	observed behavior
5_Cu_H2O_5	25	48	5	8	14	yellow flame, no smoke, low velocity, glowing residue

Table 5.76 Pyrotechnic formulations containing **5_Cu_H2O**, ADN, and boron.

	5_Cu_H2O [wt%]	ADN [wt%]	B [wt%]	VAAR [wt%]	observed behavior
5_Cu_H2O_6.1	31	52	6	11	yellow flame, easy to ignite, sparks, high velocity, glowing residue
5_Cu_H2O_6.2	43	43	3	11	green flame, easy to ignite, sparks, no smoke, high velocity, glowing residue

Table 5.77 Pyrotechnic formulations containing **5_Cu_H2O**, **[Cu(NH3)4][N(NO2)2]2**, and boron.

	5_Cu_H2O [wt%]	[Cu(NH3)4][N(NO2)2]2 [wt%]	B [wt%]	VAAR [wt%]	observed behavior
5_Cu_H2O_7.1	43	43	3	11	green-white flame, combusts too violently, glowing residues
5_Cu_H2O_7.2	51	35	2	12	no flame, glowing
5_Cu_H2O_7.3	43	44	2	11	green flame, almost no smoke, high velocity, glowing residue
5_Cu_H2O_7.4	44	44	1	11	green-yellow flame, much smoke, high velocity, glowing residue

Table 5.78 Pyrotechnic formulations containing **5_Cu_H2O**, **[Cu(NH3)4][N(NO2)2]2**, and **5-At**.

	5_Cu_H2O [wt%]	[Cu(NH3)4][N(NO2)2]2 [wt%]	5-At [wt%]	VAAR [wt%]	observed behavior
5_Cu_H2O_8.1	38	29	14	19	no flame, glowing
5_Cu_H2O_8.2	50	32	5	13	green-yellow flame, less smoke, moderate velocity, glowing residue
5_Cu_H2O_8.3	49	33	5	13	green-yellow flame, less smoke, low velocity, glowing residue
5_Cu_H2O_8.4	46	40	2	12	no flame, glowing

Table 5.79 Pyrotechnic formulations containing **5_Cu_H₂O**, KDN, and boron.

	5_Cu_H₂O	KDN	B	VAAR	observed behavior
	[wt%]	[wt%]	[wt%]	[wt%]	
5_Cu_H₂O_7.1	43	43	3	11	lifts off
5_Cu_H₂O_7.2	49	37	2	12	lifts off

5.2.4.9 Pyrotechnic Compositions Based on **5_Cu_NH₃**

In Table 5.80–Table 5.90, all tested pyrotechnic compositions, containing **5_Cu_NH₃** as colorant, are listed. Ammonium nitrate, ammonium dinitramide, and potassium dinitramide were used as oxidizers. The fuels **5-At**, zinc or boron were added as well as the copper compounds, copper, copper(I) oxide and **[Cu(NH₃)₄][N(NO₂)₂]₂**. Furthermore, a composition containing **5_Cu_NH₃** and **5_Cu_H₂O** was prepared.

Table 5.80 Pyrotechnic formulations containing **5_Cu_NH₃**, ammonium nitrate, and boron.

	5_Cu_NH₃	NH₄NO₃	B	VAAR	observed behavior
	[wt%]	[wt%]	[wt%]	[wt%]	
5_Cu_NH₃_1.1	17	53	17	13	green-yellow flame, easy to ignite, no smoke, low velocity, glowing residue
5_Cu_NH₃_1.2	21	57	11	11	green-yellow flame, no smoke, low velocity, glowing residue
5_Cu_NH₃_1.3	21	55	14	10	green flame, no smoke, moderate velocity, glowing residue
5_Cu_NH₃_1.4	19	58	13	10	yellow-green flame, no smoke, moderate velocity, glowing residue
5_Cu_NH₃_1.5	23	46	23	8	yellow flame, no smoke, moderate velocity, glowing residue
5_Cu_NH₃_1.6	27	55	9	9	green-yellow flame, less smoke, moderate velocity, glowing residue
5_Cu_NH₃_1.7	30	54	8	8	yellow-green flame, no smoke, low velocity, glowing residue
5_Cu_NH₃_1.8	29	59	5	7	yellow-green flame, no smoke, low velocity, glowing residue
5_Cu_NH₃_1.9	42	42	6	10	yellow flame, no smoke, low velocity, glowing residue

Table 5.81 Pyrotechnic formulation containing **5_Cu_NH₃**, ammonium nitrate, boron, and **5-At**.

	5_Cu_NH₃ [wt%]	NH₄NO₃ [wt%]	B [wt%]	5-At [wt%]	VAAR [wt%]	observed behavior
5_Cu_NH₃_2	33	33	10	7	17	small yellow flame, low velocity, glowing residue

Table 5.82 Pyrotechnic formulation containing **5_Cu_NH₃** and ammonium nitrate.

	5_Cu_NH₃ [wt%]	NH₄NO₃ [wt%]	VAAR [wt%]	observed behavior
5_Cu_NH₃_3	44	44	12	small yellow flame, hard to ignite, low velocity, black residue

Table 5.83 Pyrotechnic formulation containing **5_Cu_NH₃**, ammonium nitrate, and **5-At**.

	5_Cu_NH₃ [wt%]	NH₄NO₃ [wt%]	5-At [wt%]	VAAR [wt%]	observed behavior
5_Cu_NH₃_4	37	25	25	13	small yellow-green flame, less smoke, small amount of glowing residues

Table 5.84 Pyrotechnic formulations containing **5_Cu_NH₃**, ammonium nitrate, and zinc.

	5_Cu_NH₃ [wt%]	NH₄NO₃ [wt%]	Zn [wt%]	VAAR [wt%]	observed behavior
5_Cu_NH₃_5.1	25	49	12	14	small yellow flame, hard to ignite, few sparks, less smoke, low velocity, glowing residue
5_Cu_NH₃_5.2	17	41	29	13	yellow flame, hard to ignite, few sparks, less smoke, no proper burning, glowing residue

Table 5.85 Pyrotechnic formulation containing **5_Cu_NH₃**, ammonium nitrate, and copper.

	5_Cu_NH₃ [wt%]	NH₄NO₃ [wt%]	Cu₂O [wt%]	VAAR [wt%]	observed behavior
5_Cu_NH₃_6	28	43	15	14	small yellow-green flame, less smoke, small amount of glowing residues

Table 5.86 Pyrotechnic formulations containing **5_Cu_H₂O**, ammonium nitrate, copper(I) oxide, and copper.

	5_Cu_NH₃ [wt%]	NH₄NO₃ [wt%]	Cu₂O [wt%]	Cu [wt%]	VAAR [wt%]	observed behavior
5_Cu_NH₃_7.1	23	40	12	12	13	short-term yellow flame, glowing
5_Cu_NH₃_7.2	29	44	7	7	13	short-term yellow flame, glowing

Table 5.87 Pyrotechnic formulations containing **5_Cu_NH₃**, ADN, and boron.

	5_Cu_NH₃ [wt%]	ADN [wt%]	B [wt%]	VAAR [wt%]	observed behavior
5_Cu_NH₃_8.1	43	43	3	11	green-yellow flame with red frame, lifts off
5_Cu_NH₃_8.2	50	35	2	13	yellow-green flame, easy to ignite, few sparks, high velocity, almost no residues
5_Cu_NH₃_8.3	47	40	1	12	yellow-green flame, easy to ignite, few sparks, high velocity, almost no residues
5_Cu_NH₃_8.4	46	41	1	12	yellow-green flame with red frame, easy to ignite, few sparks, high velocity, almost no residues
5_Cu_NH₃_8.5	47	41	2	10	green-yellow flame with red frame, easy to ignite, few sparks, high velocity, almost no residues
5_Cu_NH₃_8.6	58	28	2	12	green-yellow flame with red frame, easy to ignite, few sparks, high velocity, almost no residues

Table 5.88 Pyrotechnic formulations containing **5_Cu_NH₃**, **[Cu(NH₃)₄][N(NO₂)₂]₂**, and boron.

	5_Cu_NH₃ [wt%]	[Cu(NH₃)₄][N(NO₂)₂]₂ [wt%]	B [wt%]	VAAR [wt%]	observed behavior
5_Cu_NH₃_9.1	43	43	2	12	green flame, easy to ignite, less smoke, moderate velocity, glowing residue
5_Cu_NH₃_9.2	44	44	1	11	green in the end yellow flame with red frame, easy to ignite, less smoke, moderate velocity, glowing residue

Table 5.89 Pyrotechnic formulation containing **5_Cu_NH₃**, ADN, copper(I) oxide, and copper.

	5_Cu_NH₃ [wt%]	ADN [wt%]	Cu₂O [wt%]	Cu [wt%]	VAAR [wt%]	observed behavior
5_Cu_NH₃_10	45	34	5	5	11	cannot be ignited

Table 5.90 Pyrotechnic formulation containing **5_Cu_NH₃**, **5_Cu_H₂O**, ADN, and boron.

	5_Cu_NH₃ [wt%]	5_Cu_H₂O [wt%]	ADN [wt%]	B [wt%]	VAAR [wt%]	observed behavior
5_Cu_NH₃_11	17	26	43	3	11	green flame, easy to ignite, high velocity, few sparks, less smoke, small amount of glowing residues

5.3 Conclusion

The literature known compound 1-carboxymethyl-5-aminotetrazole (**4**) was prepared and fully characterized. Its alkali and alkaline earth metal salts lithium 2-(5-aminotetrazol-1-yl)-acetate monohydrate (**4_Li**), sodium 2-(5-aminotetrazol-1-yl)-acetate trihydrate (**4_Na**), potassium 2-(5-aminotetrazol-1-yl)-acetate (**4_K**), rubidium 2-(5-aminotetrazol-1-yl)-acetate monohydrate (**4_Rb**), cesium 2-(5-aminotetrazol-1-yl)-acetate (**4-Cs**), magnesium 2-(5-aminotetrazol-1-yl)-acetate tetrahydrate (**4_Mg**), calcium 2-(5-aminotetrazol-1-yl)-acetate tetrahydrate (**4_Ca**), strontium 2-(5-aminotetrazol-1-yl)-acetate pentahydrate (**4_Sr**), and barium 2-(5-aminotetrazol-1-yl)-acetate trihydrate (**4_Ba**), as well as the copper(II) complex diaqua copper(II) 2-(5-aminotetrazol-1-yl)-acetate (**4_Cu**) were prepared and characterized using vibrational and multinuclear magnetic resonance spectroscopy, elemental analysis, and differential scanning calorimetry (DSC). Furthermore, their sensitivities to impact, friction and electric discharge and their solubilities in H₂O at ambient temperature were determined. The heats of formation were calculated from bomb calorimetric measurements. The crystal structures of **4**, **4_Li**, **4_Na**, **4_K**, **4_Rb**, **4-Cs**, **4_Mg**, **4_Sr**, and **4_Ba** were determined and extensively discussed. The color performance and combustion properties of the pyrotechnically relevant salts **4_Li**, **4_Ca**, **4_Sr**, **4_Ba**, and **4_Cu** were investigated with regard to their use as potential coloring agents in pyrotechnic compositions. Although the addition of PVC to **4_Ba** did not improve the emission of green light, several pyrotechnic compositions were prepared. The mixtures **4_Ba**_{4.2} and **4_Ba**_{14.2} showed a green flame, whereas composition **4_Ba**_{11.3} produced an intense white flame. Therefore, **4_Ba** might also find application as additive in white flame pyrotechnic compositions. Further compositions containing **4_Li** or **4_Sr** were prepared and compared to known formulations. Although **4_Li** produces as neat compound a very intense deep red flame color, its color performance in the investigated compositions was not very convincing. Good results could be achieved using **4_Sr**. Best performing compositions **4_Sr**_{2.7} and **4_Sr**_{7.2} have, besides a tall very intense red flame, quite high decomposition temperatures of above 280 °C. Furthermore, they are less sensitive towards outer stimuli. Due to the insensitivity to impact, friction, and electric discharge, to its easy preparation from low cost materials and the low solubility in H₂O of **4_Sr**, this compound is a very promising coloring agent, which might find application in environmentally more benign pyrotechnic compositions without potassium perchlorate.

The nitrimino derivative of **4**, 1-carboxymethyl-5-nitriminotetrazole monohydrate (**5**) was prepared and fully characterized. Furthermore, its alkali metal salts sodium 1-carboxymethyl-5-nitriminotetrazolate trihemihydrate (**5_Na**), potassium 1-carboxymethyl-5-nitriminotetrazolate monohydrate (**5_K**), rubidium 1-carboxymethyl-5-nitriminotetrazolate monohydrate (**5_Rb**), and cesium 1-carboxymethyl-5-nitriminotetrazolate hemihydrate (**5-Cs**) were prepared. Due to the presence of two acidic protons the alkaline earth metal salts magnesium 1-carboxymethyl-5-nitriminotetrazolate decahydrate (**5_Mg1**), magnesium 2-(5-nitriminotetrazolate)-acetate octahydrate (**5_Mg2**), calcium 1-carboxymethyl-5-nitri-

minotetrazolate dihydrate (**5_Ca1**), calcium 2-(5-nitriminotetrazolate)-acetate trihydrate (**5_Ca2**), strontium 1-carboxymethyl-5-nitriminotetrazolate monohydrate (**5_Sr1**), strontium 2-(5-nitriminotetrazolate)-acetate trihydrate (**5_Sr2**), barium 1-carboxymethyl-5-nitriminotetrazolate monohydrate (**5_Ba1**), barium 2-(5-nitriminotetrazolate)-acetate heptahydrate (**5_Ba2**) as well as the copper(II) complexes *trans*-[diaqua-bis(1-carboxymethyl-5-nitriminotetrazolato-*N4,O1*) copper(II)] dihydrate (**5_Cu_H2O**) and bis[diammine 2-(5-nitriminotetrazolato-*N4,O1*)-acetato-*O4* copper(II)] trihydrate (**5_Cu_NH3**) could be obtained. All salts of **5** were investigated using vibrational and multinuclear magnetic resonance spectroscopy, elemental analysis, differential scanning calorimetry (DSC), and their sensitivities to impact, friction, and electric discharge as well as their solubilities in H₂O at ambient temperature were determined. The heats of formation were calculated from bomb calorimetric measurements. The crystal structures of **5**, **5_K**, **5_Rb**, **5_Mg**, **5_Mg2**, **5_Ca1**, **5_Ca2**, **5_Sr1**, **5_Sr2**, **5_Ba1**, as well as **5_Cu_H2O** and **5_Cu_NH3** were determined and extensively discussed. In the flame of a BUNSEN burner the color performance of **5_Ca1**, **5_Ca2**, **5_Sr1**, **5_Sr2**, **5_Ba1**, **5_Ba2**, **5_Cu_H2O**, and **5_Cu_NH3** was investigated with regard to their use as potential coloring agents in pyrotechnic compositions. The compounds **5_Sr1**, **5_Sr2**, **5_Ba1**, **5_Ba2**, **5_Cu_H2O**, and **5_Cu_NH3** were investigated as colorants in several pyrotechnic compositions. Two, in color performance and combustion behavior convincing, compositions of the strontium salts **5_Sr1** and **5_Sr2** could be figured out. Both barium salts, **5_Ba1** and **5_Ba2**, are suitable as coloring agents in green as well as white light emitting pyrotechnic compositions. In analogy to **4Li**, the copper(II) compounds **5_Cu_H2O** and **5_Cu_NH3** showed less good coloring properties in pyrotechnic compositions than as neat compounds in the flame of a BUNSEN burner.

Concluding it can be said, that the investigated strontium and barium salts, especially **4_Sr**, **5_Sr2**, and **5_Ba2**, are suitable as coloring agents in more environmentally benign pyrotechnic compositions without potassium perchlorate due to their properties.

5.4 References

- [1] F. Einberg: Alkylation of 5-Substituted Tetrazoles with *α*-Chlorocarbonyl Compounds, *J. Org. Chem.* **1970**, 35, 3978–3980.
- [2] R. Raap, J. Howard: Tetrazolylacetic acid, *J. Can. Chem.* **1969**, 47, 813–819.
- [3] J. A. Conkling: *Chemistry of Pyrotechnics: Basic Principles and Theory*. M. Dekker, Inc., New York, **1985**.
- [4] a) T. M. Klapötke, G. Steinhauser: 'Green' Pyrotechnics: A Chemists' Challenge, *Angew. Chem. Int. Ed.* **2008**, 47, 3330–3347. b) T. M. Klapötke, G. Steinhauser: Pyrotechnik mit dem "Ökosiegel": eine chemische Herausforderung, *Angew. Chem.* **2008**, 120, 3376–3394.

- [5] a) T. M. Klapötke, J. Stierstorfer, K. R. Tarantik: New Energetic Materials: Functionalized 1-Ethyl-5-aminotetrazoles and 1-Ethyl-5-nitriminotetrazoles, *Chem. Eur. J.* **2009**, *15*, 5775–5792. b) T. M. Klapötke, J. Stierstorfer: Investigations of nitrated aminotetrazoles as promising energetic materials -synthesis, structures and properties-. *New Trends in Research of Energetic Materials*, Proceedings of the Seminar, *10th*, Pardubice, Czech Republic, 25.–27. Apr. **2007**, Pt. 2, 674–690. c) T. M. Klapötke, J. Stierstorfer: Nitration products of 5-amino-1H-tetrazole and methyl-5-amino-1H-tetrazoles – structures and properties of promising energetic materials, *Helv. Chim. Acta* **2007**, *90*, 2132–2150.
- [6] J. Stierstorfer: Advanced Energetic Materials based on 5-Aminotetrazole, *PhD Thesis*, **2009**, Ludwig-Maximilian University, Munich.
- [7] N. Wiberg, E. Wiberg, A. F. Holleman: *Lehrbuch der Anorganischen Chemie*, deGruyter, Berlin, 102. Ed., **2007**.
- [8] N. Fischer, T. M. Klapötke, J. Stierstorfer: New nitriminotetrazoles – synthesis, structures and characterization, *Z. Anorg. Allg. Chem.* **2009**, *635*, 271–281.
- [9] a) <http://www.bam.de> b) E_{dr} : insensitive > 40 J, less sensitive \geq 35 J, sensitive \geq 4, very sensitive \leq 3 J; F_r : insensitive > 360 N, less sensitive = 360 N, sensitive < 360 N > 80 N, very sensitive \leq 80 N, extreme sensitive \leq 10 N. According to the UN Recommendations on the Transport of Dangerous Goods.
- [10] <http://webbook.nist.gov/>
- [11] Albert S. Tompa: Thermal analysis of ammonium dinitramide (ADN), *Thermochim. Acta* **2000**, *357–358*, 177–193.
- [12] G. Rasulic, S. Jovanovic and Lj. Milanovic: Ammonium Nitrate Changes During Thermal Analysis, *J. Thermal Anal.* **1985**, *30*, 65–72.
- [13] B. P. Berger, J. Mathieu, P. Folly: Alkali-Dinitramide Salts Part 2: Oxidizers for Special Pyrotechnic Applications, *Propellants, Explos., Pyrotech.* **2006**, *31*, 269–277.

6 Salts of 1-(2,3-Dichloropropyl)-5-nitriminotetrazole and its Precursor Molecules

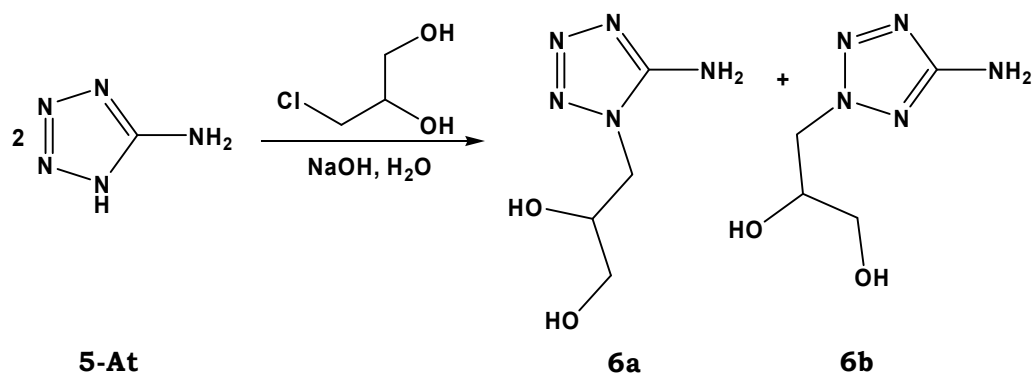
The preparation of the analogous derivatives of 1- and 2-(2-hydroxyethyl)-5-aminotetrazole (**1-OH** and **2-OH**) with a propyl side chain containing two hydroxy groups was investigated with respect to their use as precursor molecules for the synthesis of the isomeric 1- and 2-(2,3-dichloropropyl)-5-aminotetrazole (**8a** and **8b**), the analogous derivatives of 1-(2-chloroethyl)-5-aminotetrazole (**1-Cl**). The corresponding 5-nitriminotetrazoles 1-(2,3-dinitratopropyl)-5-nitriminotetrazole monohydrate (**7**) as well as 1-(2,3-dichloropropyl)-5-nitriminotetrazole (**9**) were obtained in order to prepare several alkali metal, alkaline earth metal and copper(II) salts. Especially the salts of **9** were extensively characterized, also regarding their properties as coloring agents. They were compared to the corresponding salts of 1-(2-chloroethyl)-5-nitriminotetrazole (**3**, chapter 4).

Compound **9** was chosen as precursor molecule, because it can be deprotonated easily, yielding thermally more stable salts or copper(II) complexes and, in analogy to **3**, combines three further important properties: it contains chlorine, offers a tetrazole ring, which is responsible for the formation of gaseous nitrogen as decomposition product, and includes an energetic nitrimino group, which also improves the oxygen balance. Especially the copper(II), strontium and barium salts of **9** are of special interest, because these cations need chlorine donors for a higher color brilliance, which is achieved by the emitting species CuCl, SrCl, and BaCl in the gas phase.^[1, 2] With the anion of **9** as counterion, there is an excess of chlorine present, therefore these salts could be used as additive in perchlorate-free compositions acting both as coloring agents and as chlorine donors. Furthermore, it is expected that the salts of **9** will show lower sensitivity to impact, friction and electric discharge and will be less soluble in H₂O at ambient temperature due to their longer alkyl chain than the corresponding salts of **3** (see chapter 4).

6.1 Results and Discussion

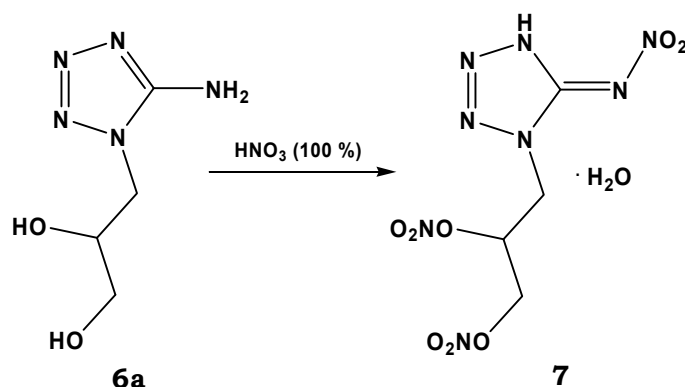
6.1.1 Syntheses

First step of the preparation is the alkylation of 5-aminotetrazole (**5-At**) with 3-chloro-1,2-propanediol to yield the isomers 1-(2,3-dihydroxypropyl)-5-aminotetrazole (**6a**) and 2-(2,3-dihydroxypropyl)-5-aminotetrazole (**6b**) (Scheme 6.1). Both can be isolated as pure compounds due to their different solubility in ethanol. Work up is analogous to the alkylation of **5-At** with 1-chloroethanol (see chapter 2).



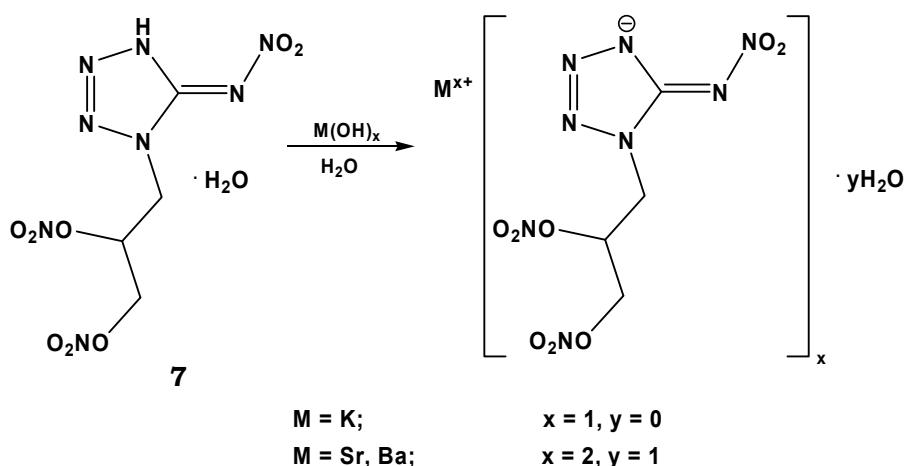
Scheme 6.1 Preparation of 1- (**6a**) and 2-(2,3-dihydroxypropyl)-5-aminotetrazole (**6b**).

6a was nitrated with 100 % nitric acid in analogy to the before mentioned 5-amino-tetrazole derivatives. In contrast to the nitration of the 1-(2-hydroxyethyl)-5-aminotetrazole (**1-OH**), only the nitrate ester 1-(2,3-dinitratopropyl)-5-nitriminotetrazole monohydrate (**7**) was obtained (Scheme 6.2). Like 1-(2-nitratoethyl)-5-nitriminotetrazole monohydrate (**2**), **7** decomposes slowly after several months when storing at ambient temperature.



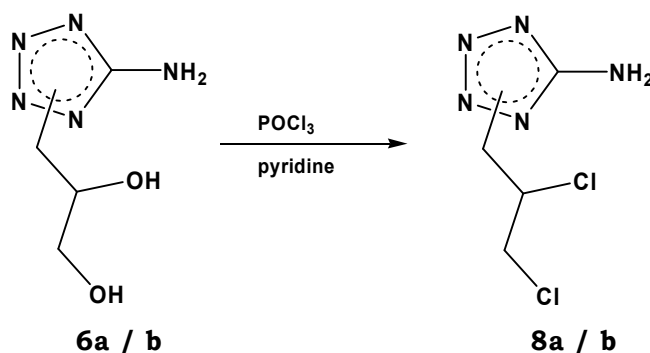
Scheme 6.2 Nitration of **6a**.

Although **7** is very sensitive towards outer stimuli, three different salts and one copper(II) complex of **7** were prepared. By reaction of **7** with the hydroxides of potassium, strontium or barium in H₂O, potassium 1-(2,3-dinitratopropyl)-5-nitriminotetrazolate (**7_K**), strontium 1-(2,3-dinitratopropyl)-5-nitriminotetrazolate monohydrate (**7_Sr**), and barium 1-(2,3-dinitratopropyl)-5-nitriminotetrazolate monohydrate (**7_Ba**) were obtained. Furthermore, the copper(II) complex diaqua 1-(2,3-dinitratopropyl)-5-nitriminotetrazolato copper(II) (**7_Cu**) could be prepared by reaction of **7**, dissolved in H₂O, with copper(II) nitrate pentahemihydrate. After storing the green solution at ambient temperature for a few hours, a green precipitate of **7_Cu** was obtained.



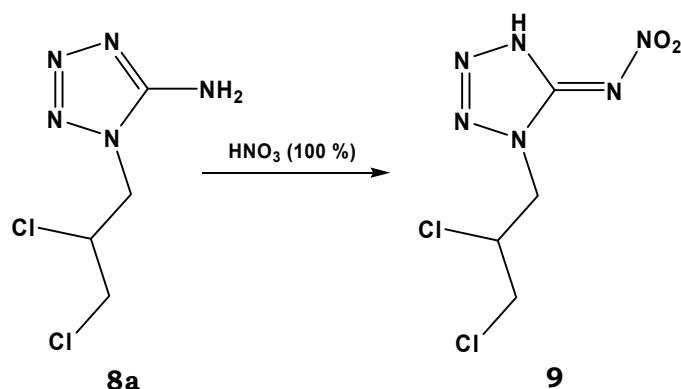
Scheme 6.3 Preparation of the salts of **7**.

In analogy to the chlorination of **1-OH**, also **6a** and **6b** were reacted with thionyl chloride. However, no hydroxy group could be chlorinated. Using phosphorus oxychloride in huge excess and pyridine the chlorination was successful (Scheme 6.4). After stirring for five hours the cooled yellow solution was slowly poured onto ice. Sodium or potassium hydroxide was added until the solution became neutral. The yellow precipitate is filtered off and recrystallized from ethanol. 1-(2,3-Dichloropropyl)-5-aminotetrazole (**8a**) and 2-(2,3-dichloropropyl)-5-aminotetrazole (**8b**) were obtained, however in low yields.



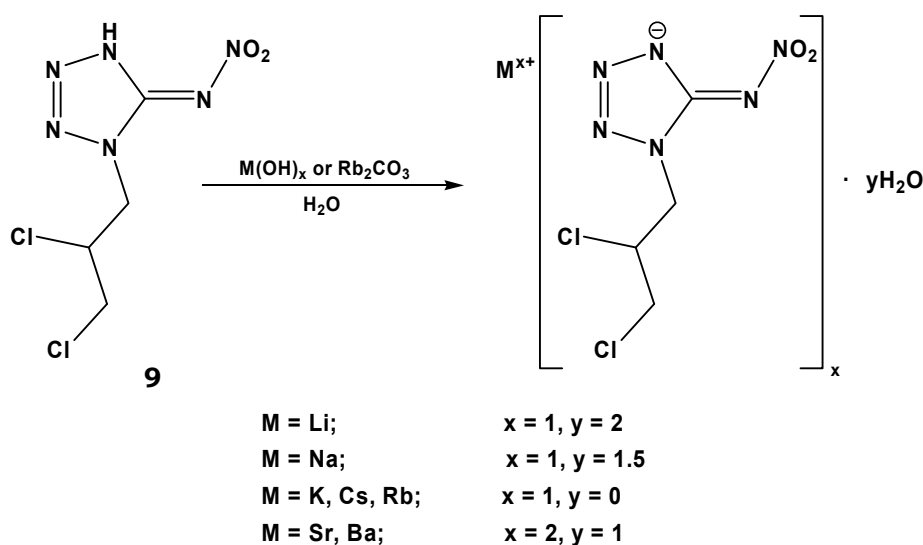
Scheme 6.4 Chlorination of **6a** and **6b**.

1-(2,3-dichloropropyl)-5-aminotetrazole (**8a**) was nitrated in analogy to **6a** (Scheme 6.5) to yield 1-(2,3-dichloropropyl)-5-nitriminotetrazole (**9**). If **9** was recrystallized from H_2O or very diluted nitric acid, the monohydrate 1-(2,3-dichloropropyl)-5-nitriminotetrazole monohydrate (**9_H₂O**) was obtained.



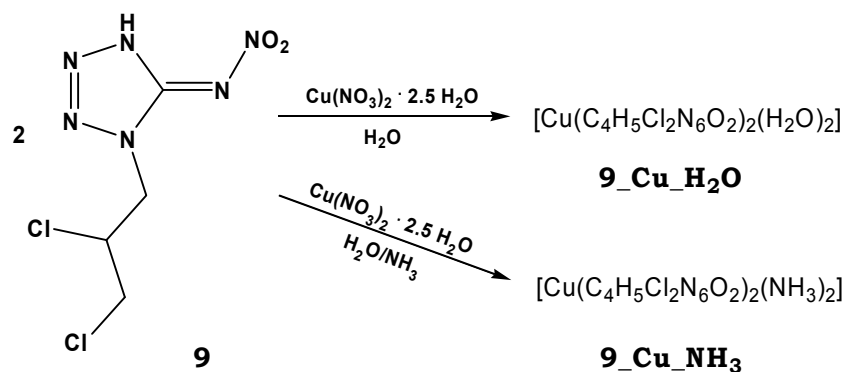
Scheme 6.5 Nitration of **8a**.

Starting from **9**, the salts lithium 1-(2,3-dichloropropyl)-5-nitriminotetrazolate dihydrate (**9_Li**), sodium 1-(2,3-dichloropropyl)-5-nitriminotetrazolate trihemihydrate (**9_Na**), potassium 1-(2,3-dichloropropyl)-5-nitriminotetrazolate (**9_K**), rubidium 1-(2,3-dichloropropyl)-5-nitriminotetrazolate (**9_Rb**), cesium 1-(2,3-dichloropropyl)-5-nitriminotetrazolate (**9-Cs**), strontium 1-(2,3-dichloropropyl)-5-nitriminotetrazolate monohydrate (**9_Sr**), and barium 1-(2,3-dichloropropyl)-5-nitriminotetrazolate monohydrate (**9_Ba**) were prepared. For the synthesis, **9** was dissolved in H₂O and the corresponding hydroxides, or rubidium carbonate, were added (Scheme 6.6). The solution was heated until it became clear and then stored at ambient temperature until a colorless solid was formed.



Scheme 6.6 Preparation of the alkali and alkaline earth metal salts of **9**.

Furthermore, two copper(II) complexes with **9** as anionic ligand were prepared (Scheme 6.7). For the synthesis, **9** was dissolved in H₂O and copper(II) nitrate pentahydrate in a few milliliters of H₂O was added. After several hours a green precipitate of diaqua 1-(2,3-dichloropropyl)-5-nitriminotetrazolato copper(II) (**9_Cu_H2O**) was formed and filtered off. Recrystallization from H₂O was not possible due to its low solubility.



Scheme 6.7 Preparation of the copper(II) compounds **9_Cu_H₂O** and **9_Cu_NH₃**.

If ammonia was additionally added, the copper(II) compound diammine 1-(2,3-dichloropropyl)-5-nitriminotetrazolato copper(II) (**9_Cu_NH₃**) crystallized after a few days at ambient temperature. Unfortunately, the crystals were grown together so that the molecular structure could not be determined by X-ray diffraction.

6.1.2 Analytical Data of the Neutral Molecules

6.1.2.1 Spectroscopy

For determining the conversion and purity of the compounds **6–9** NMR spectroscopy was used, in particular ¹H and ¹³C NMR spectra were measured. DMSO-*d*₆ was used as solvent. Especially ¹³C NMR spectroscopy (a pulse delay > 2.5 s is advantageous) is helpful and a fast method to distinguish between the *N*1- and *N*2-isomers as well as 5-amino- from 5-nitriminotetrazoles.^[3, 4] In the case of **6a**, **6b**, **8a**, and **8b** 2D NMR spectroscopy (¹H, ¹H COSY45; ¹H, ¹³C HMQC; ¹H, ¹³C HMBC) was the method of choice, because of the complex coupling pattern in the one-dimensional ¹H NMR spectra, in order to allow a correct assignment of the signals in the ¹³C NMR spectra. IR and Raman spectroscopy of all prepared compounds were also recorded.

In the ¹H NMR spectrum of **6a** six different signals can be observed at 6.47 ppm (NH₂), 5.14 ppm (OH), 4.83 ppm (OH), 4.13 ppm (CHa/b), 3.96 ppm (CHa/b), 3.81–3.78 ppm (CH), and 3.36–3.29 ppm (CH₂) with a proportion of intensities of 2:1:1:1:1:2. In the ¹H, ¹H COSY45 spectrum of **6a** the coupling between the hydrogen atoms can be observed (Figure 6.1). Both hydrogen atoms of the hydroxyl group show a splitting, due to their interaction with the hydrogen atoms at C4 and C3, respectively. The signal of **H** is a doublet of doublets, which can be identified by the additional coupling between **Ha** and **Hb**. The doublet of doublets for **Ha** and **Hb** with a “*Dacheffekt*” are caused by an ABX spin system, due to the center of chirality at C3. The hydrogen atom **H** couples to the hydrogen atoms at C4 (**H**), **H** as well as **Ha** and **Hb** causing a multiplet. In the multiplet of the chemically equivalent hydrogen atoms at C4 (**H**) the signal of H₂O – which is usually present in DMSO-*d*₆ – is hidden at 3.33 ppm. In the ¹H, ¹³C HMQC spectrum of **6a**, correlation is based

on $^1J_{CH}$ coupling (Figure 6.2). Based on that, an assignment of the signals in the ^{13}C NMR spectrum is easy.

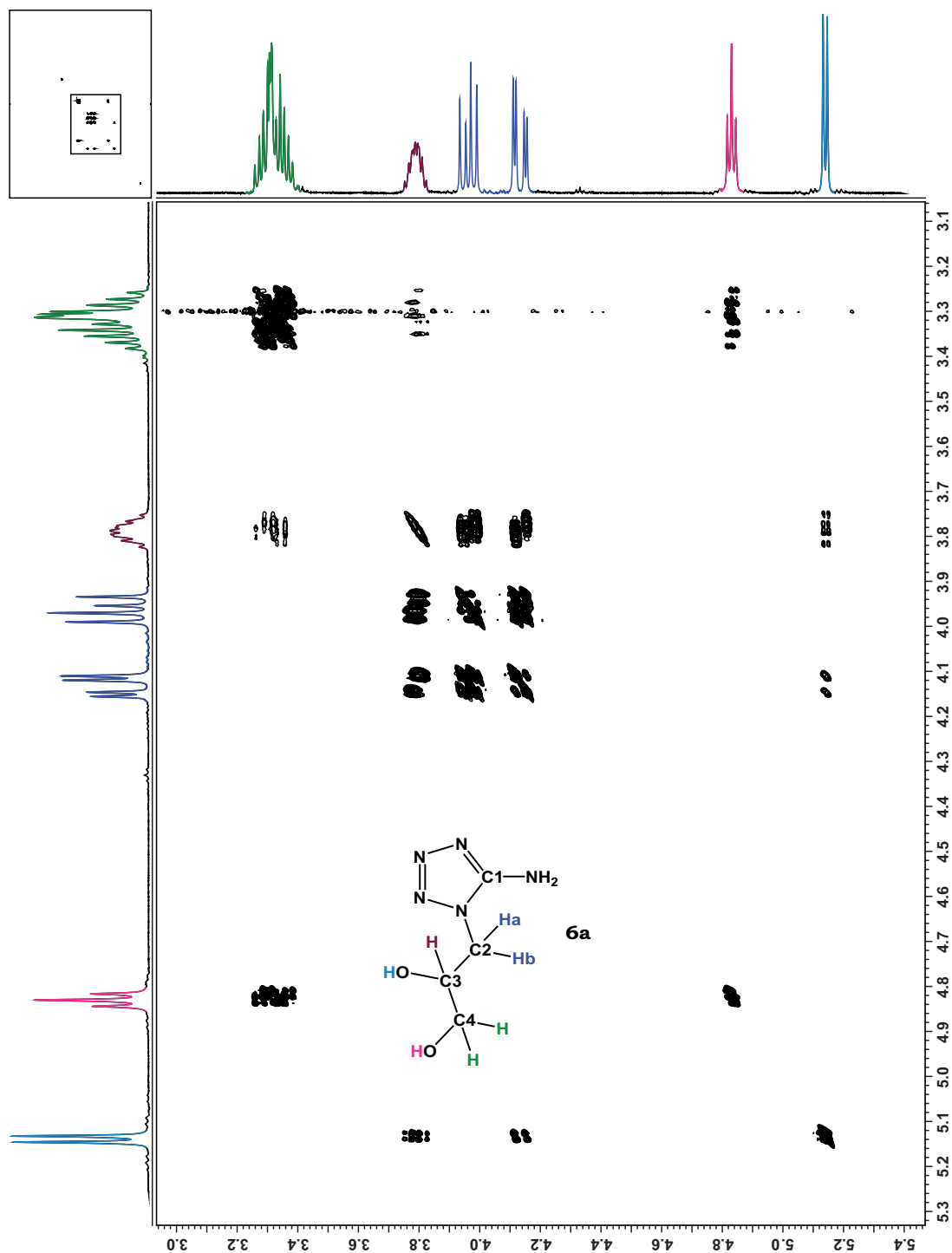


Figure 6.1 $^1H,^1H$ cosy45 spectrum of **6a** in the range of 3.0–5.4 ppm (about 0.1 M in $DMSO-d_6$, recorded with field gradient, matrix 1024×2048, zerofilling :2, sinbell auto, no symmetrization).

The signal of carbon atom C2 is located at 48.0 ppm. Interestingly, the signal of C3 (70.0 ppm) is shifted to lower field than that of carbon atom C4 (63.2 ppm). As expected, the signal of the quaternary carbon atom C1 is observed at 156.2 ppm. In the $^1H,^{13}C$ HMBC spectrum correlation is based on $^2J_{CH}$ and $^3J_{CH}$ couplings present in **6a** (Figure 6.3).

Surprisingly, $^3J_{CH}$ between the hydrogen atoms at C2 and the carbon atom C1 can be observed. This coupling takes place over the nitrogen atom N1. All hydrogen atoms, except the one of the hydroxyl group at C4 (**H**), couple with C2. Both, the $^2J_{CH}$ and $^3J_{CH}$, coupling between the hydrogen atoms of the hydroxyl groups (**H**, **H**) and the carbon atoms C2, C3, and C4 is observable.

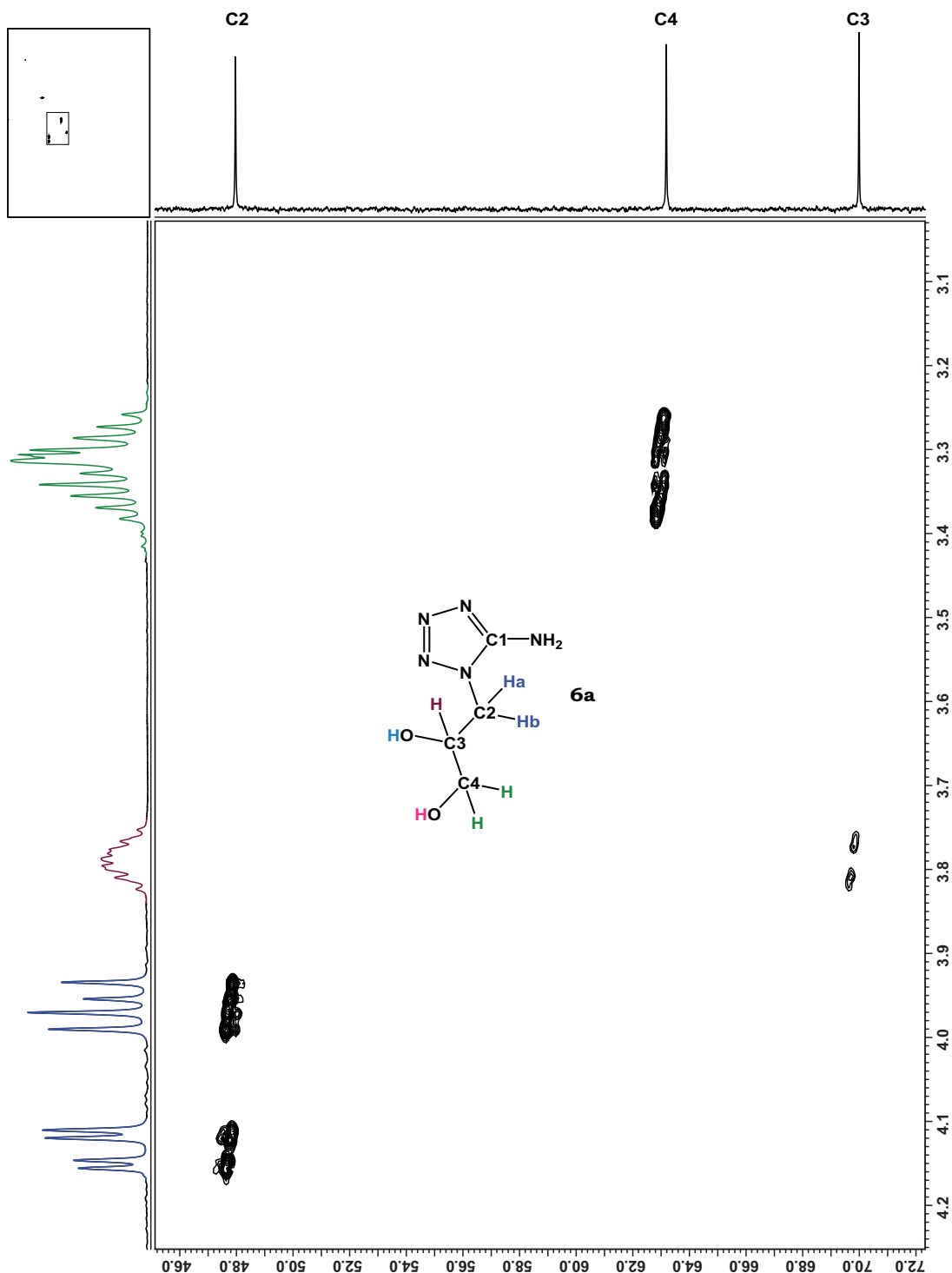


Figure 6.2 $^1H,^{13}C$ HMQC spectrum of **6a** (about 0.1 M in $DMSO-d_6$, recorded with field gradient, matrix 2048×1024 , zerofilling: 2, sinbell auto).

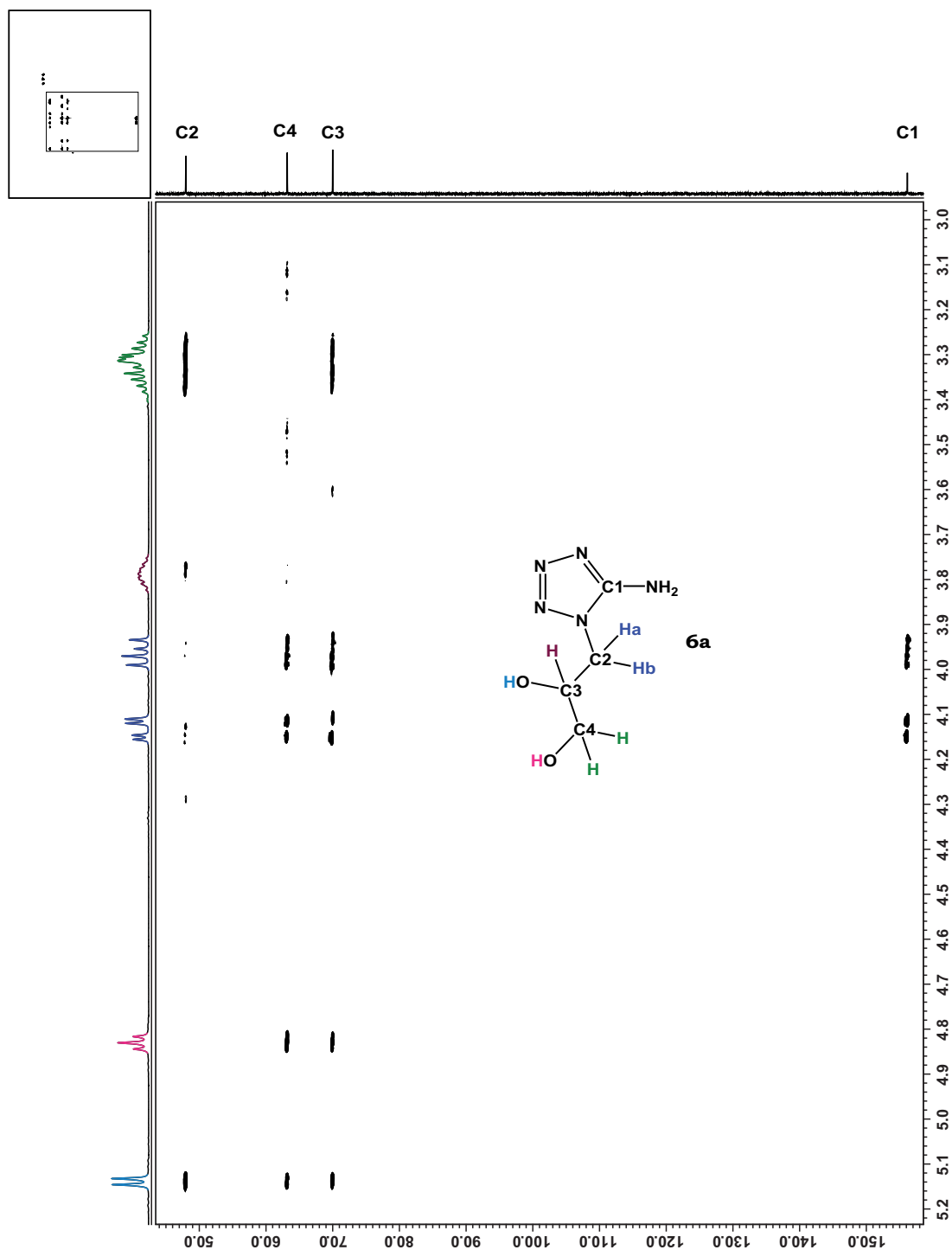


Figure 6.3 $^1\text{H},^{13}\text{C}$ HMBC spectrum of **6a** (about 0.1 M in $\text{DMSO}-d_6$, recorded with field gradient, matrix 2048×1024 , zerofilling: 2, sinbell auto).

The ^1H NMR spectrum of **6b** displays a splitting of the signals analogous to that of the *N1*-isomer **6a** with the identical proportion of intensities, whereas the signal of the hydrogen atoms at the amino group is shifted to higher field (5.93 ppm). This is also true for the signals of the hydrogen atoms of the hydroxy groups (5.05 ppm and 4.79 ppm). All signals of the remaining hydrogen atoms are shifted to lower field. The $^1\text{H},^1\text{H}$ COSY45 spectrum of **6b** is very similar to the one of **6a** (Figure 6.4).

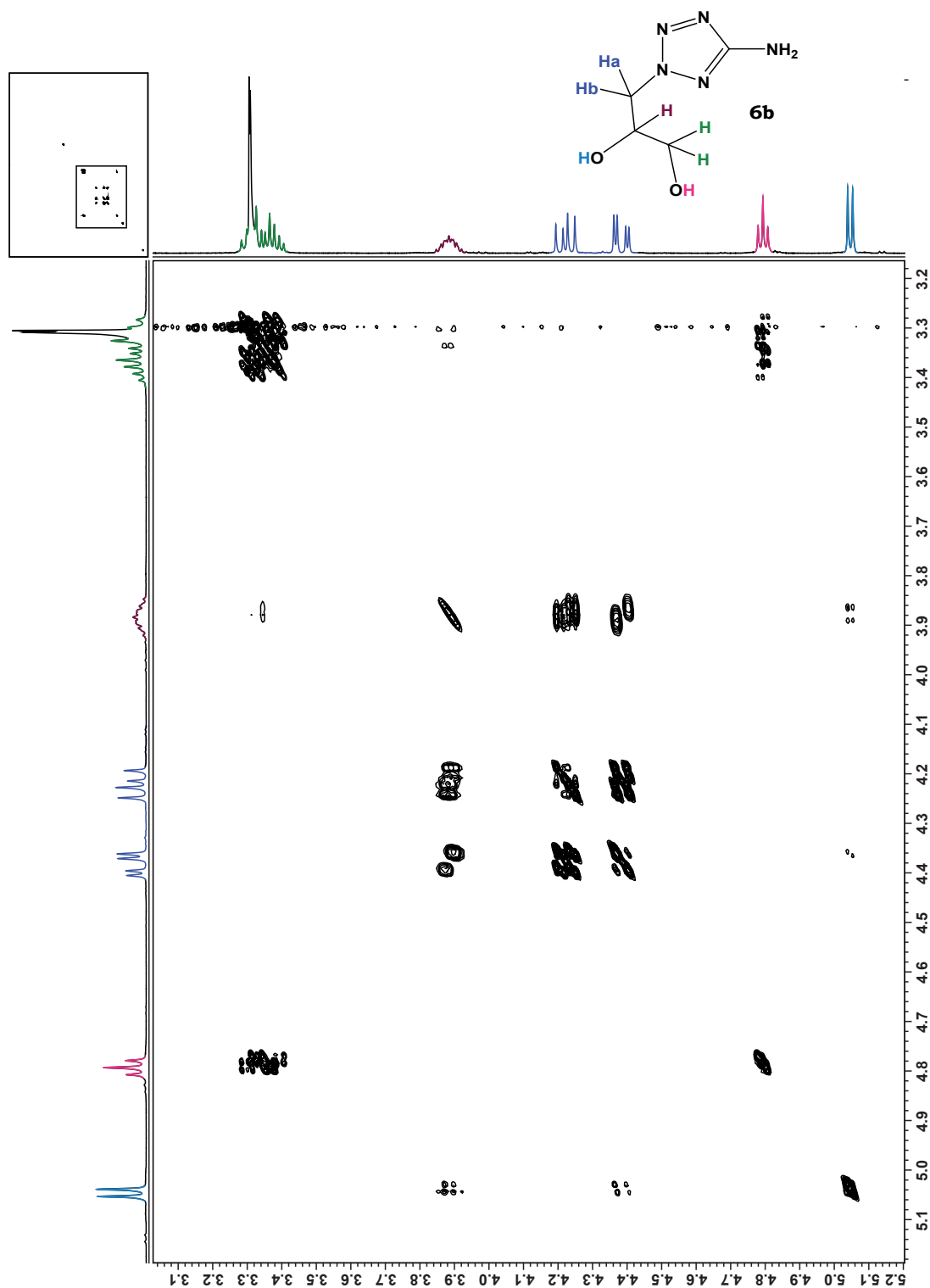


Figure 6.4 $^1\text{H},^1\text{H}$ COSY45 spectrum of **6b** in the range of 3.1–5.2 ppm (about 0.1 M in $\text{DMSO}-d_6$, recorded with field gradient, matrix 1024×2048 , zerofilling :2, sinbell auto, no symmetrization).

The difference of the shifts in the ^{13}C NMR spectra of **6a** and **6b** is more pronounced. Especially the signals of the carbon atoms C1 (166.9 ppm) and C2 (55.5 ppm) are significantly shifted to lower field. The $^1\text{H},^{13}\text{C}$ HMQC spectrum of **6b** is similar to the one of **6a**. In contrast to **6a**, in the $^1\text{H},^{13}\text{C}$ HMBC spectrum of **6b** the $^3J_{\text{CH}}$ coupling between C1 and the hydrogen atoms at the amino group is observable (Figure 6.5).

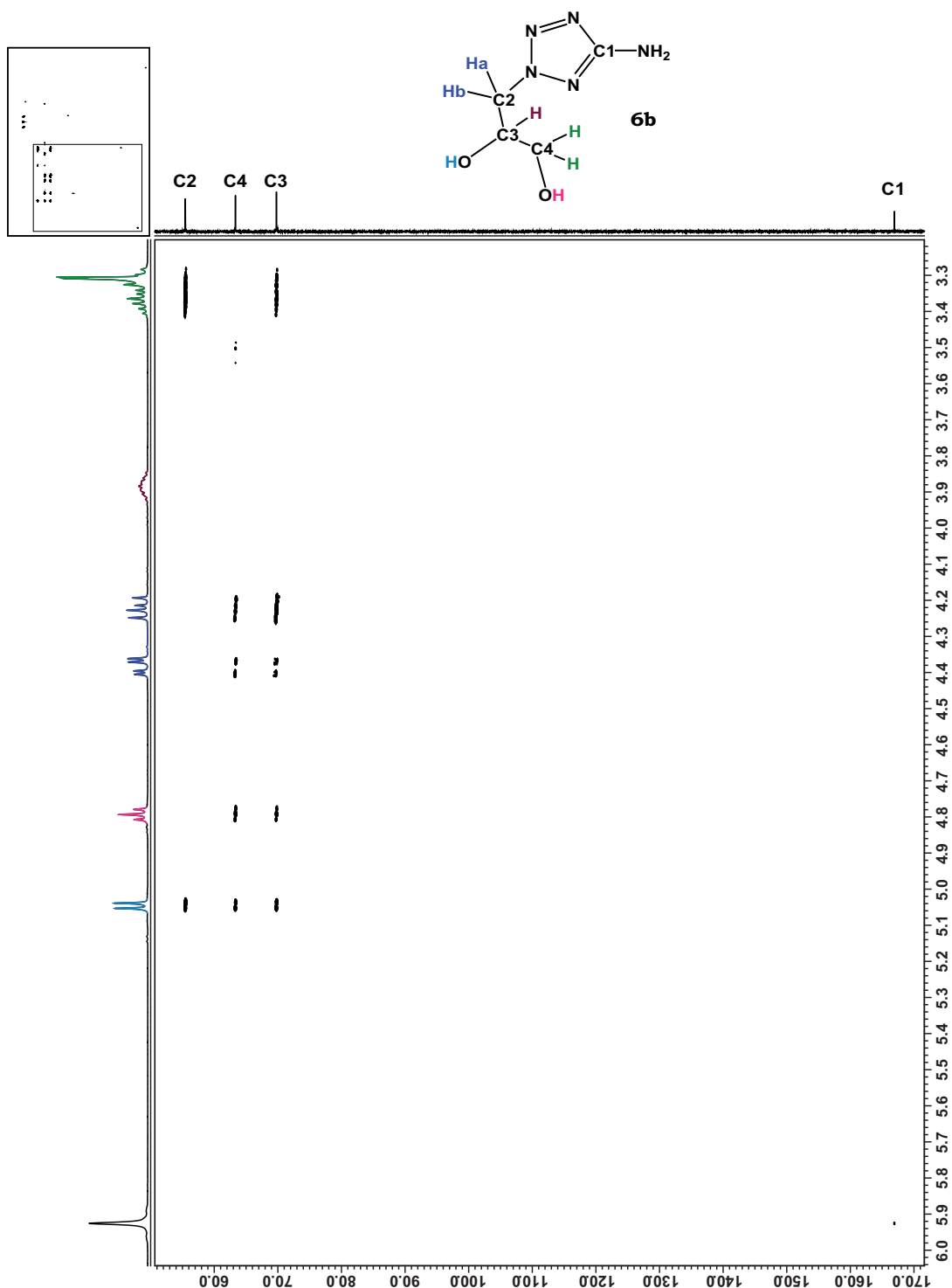


Figure 6.5 $^1\text{H},^{13}\text{C}$ HMBC spectrum of **6b** (about 0.1 M in $\text{DMSO}-d_6$, recorded with field gradient, matrix 2048×1024 , zerofilling: 2, sinbell auto).

The signals of the hydrogen atoms of **7** – the nitration product of **6a** – are significantly shifted to lower field. This is true in particular for the signal of the hydrogen atom at C3 (**H**: 5.78 ppm). The ^{14}N and ^{15}N NMR spectra of **7** were recorded. In the ^{14}N NMR spectrum only two signals can be observed. One belongs to N6 of the nitrimino group (–19 ppm), the other belongs to the nitrogen atoms of nitrate esters (–47 ppm). In contrast all eight signals are observable in the ^{15}N NMR spectrum: –19.4 (N3), –26.9 (N2), –29.5 (N6),

-45.6 (N7/8), -48.3 (N7/8), -156.1 (N5), -156.3 (N4), -178.1 (N1). The assignment was performed in analogy to 5-nitriminotetrazole derivatives described in literature.^[3, 4]

In the IR-spectrum of **7** the vibrations at 1550 cm⁻¹ and 1360 cm⁻¹ are very dominant. The signals originate from the antisymmetric and symmetric vibrations of the nitrate ester and nitro groups.^[5]

In the ¹H NMR spectrum of **8a** six different signals can be observed with a proportion of intensities of 2:1:1:1:1:1, whereas the doublets of doublets of the hydrogen atoms at C2 and C4 are located very closely together (C2**Ha/b**: 4.53 ppm, C2**Ha/b**: 4.45 ppm, C4**Ha/b**: 4.00 ppm, C4**Ha/b**: 3.94 ppm) and are shifted to lower field compared to the precursor molecule **6a**. This is also true for the hydrogen atoms of the amino group as well as C3**H**. The ¹H,¹H cosy45 spectrum of **8a** is depicted in Figure 6.6. The ³J_{HH} coupling between C**H** and C**Ha/b** as well as C4**Ha/b** can be observed.

The ¹³C NMR spectrum shows four different signals, as expected (C1: 156.0 ppm, C2: 47.8 ppm, C3: 58.7 ppm, C4: 46.8 ppm). With the help of the ¹H,¹³C HMQC spectrum, which shows the ¹J_{CH} coupling, and the ¹H,¹³C HMBC spectrum of **8a** (Figure 6.7), the hydrogen atoms could be easily assigned to the corresponding carbon atoms. The hydrogen atom at C3 (**H**) shows a ²J_{CH} coupling to the carbon atoms C2 and C4. As expected, the ²J_{CH} and ²J_{CH} coupling between the hydrogen atoms at C4 (**Ha/b**) and the carbon atoms C3 as well as C2 is observable. Furthermore, the hydrogen atoms at C2 (**Ha/b**) show a coupling to the carbon atoms C1, C3, and C4, like in **6a**.

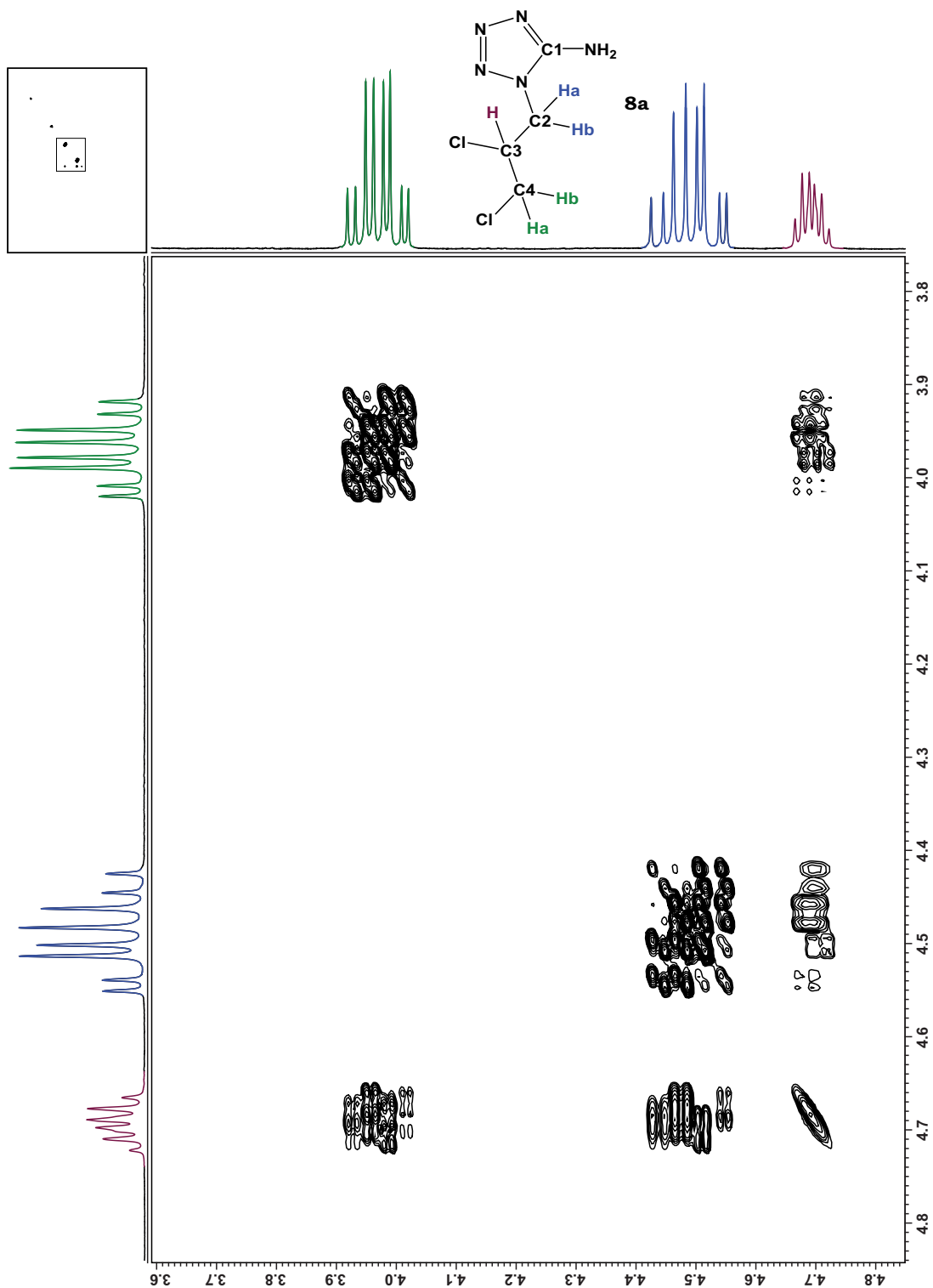


Figure 6.6 $^1\text{H}, ^1\text{H}$ COSY45 spectrum of **8a** in the range of 3.6–4.8 ppm (about 0.1 M in $\text{DMSO}-d_6$, recorded with field gradient, matrix 1024×2048 , zerofilling :2, sinbell auto, no symmetrization).

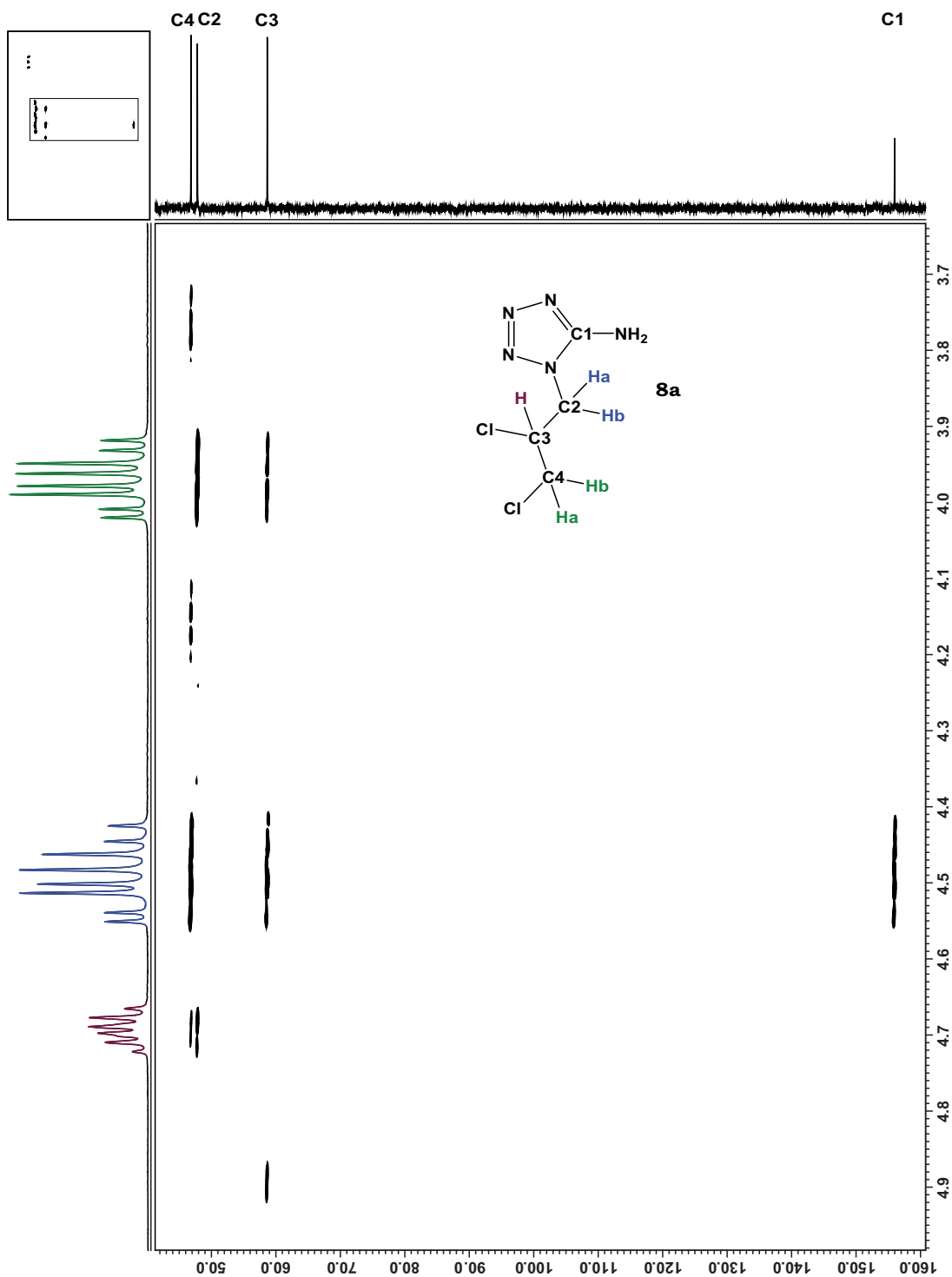


Figure 6.7 ^1H , ^{13}C HMBC spectrum of **8a** (about 0.1 M in DMSO- d_6 , recorded with field gradient, matrix 2048 \times 1024, zerofilling: 2, sinbell auto).

In the ^1H NMR spectrum of **8b** only two signals can be distinguished accurately – a multiplet for the hydrogen atoms at C4 (**H**) at 4.10–4.00 ppm and a singlet for the hydrogen atoms at the amino group at 6.13 ppm with an equal intensity. The two multiplets in the range of 4.94–4.72 ppm are caused by an interaction of the doublet of doublets of the hydrogen atoms **Ha** and **Hb** as well as by the multiplet of the hydrogen atom at C3 (**H**). The ^1H , ^1H COSY45 spectrum of **8b** is depicted in Figure 6.8. Unfortunately, it also cannot make

an accurate assignment of the multiplets possible. This might be possible with a ^1H - J -resolved spectrum.

With the help of the ^1H , ^{13}C HMQC and ^1H , ^{13}C HMBC spectra of **8b** the assignment of the signals in the ^{13}C NMR spectrum is possible (Figure 6.9 and Figure 6.10). Compared to the precursor molecule **6b**, the position of the signal of C1 (167.9 ppm) is almost similar, whereas the other signals are shifted significantly to higher field. Furthermore, their order has changed (C3: 59.0 ppm, C2: 55.4 ppm, C4: 47.0 ppm).

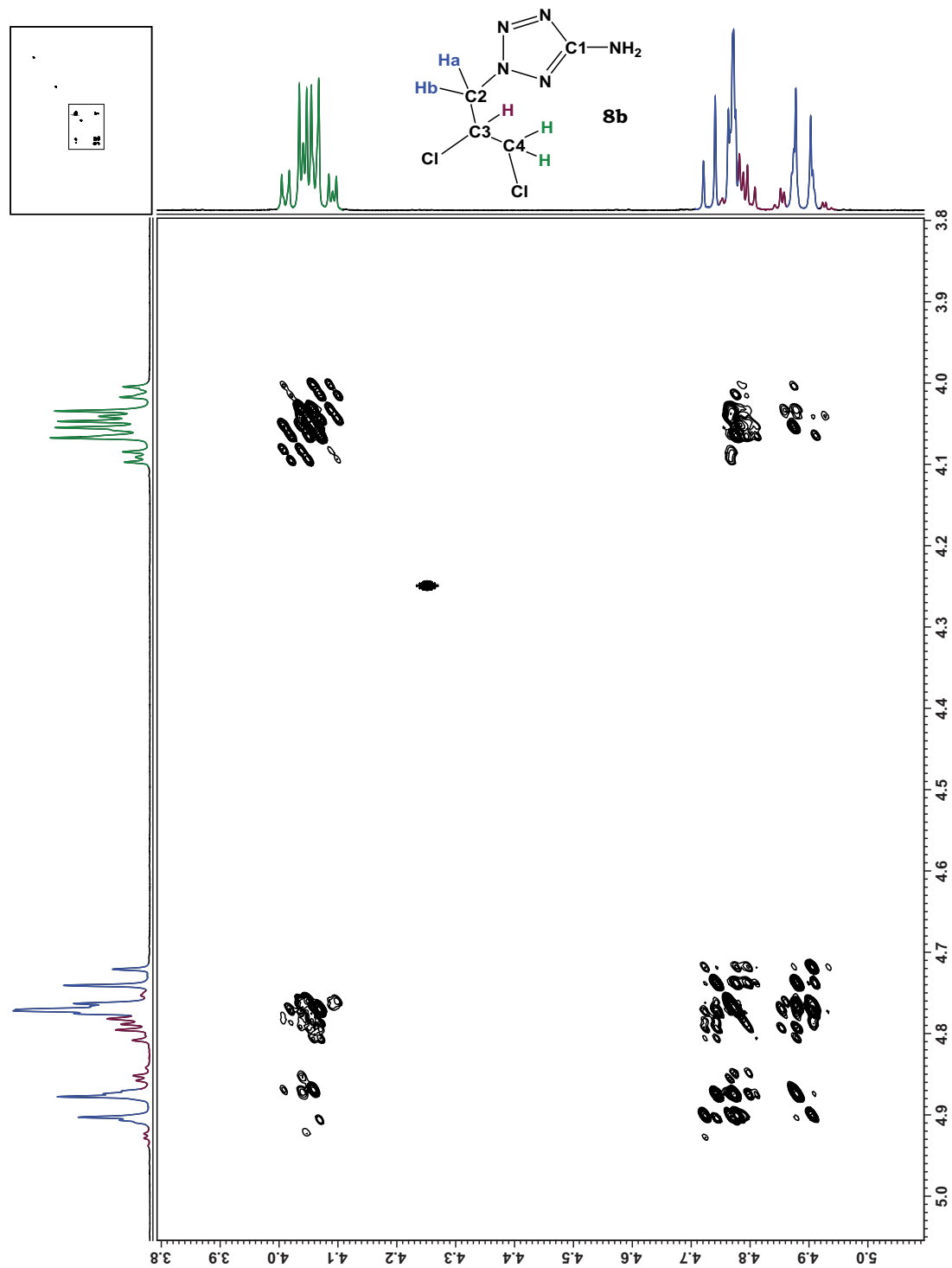


Figure 6.8 ^1H , ^1H COSY45 spectrum of **8b** in the range of 3.8–5.1 ppm (about 0.1 M in $\text{DMSO-}d_6$, recorded with field gradient, matrix 2048×1024 , zerofilling :2, sinbell auto, no symmetrization).

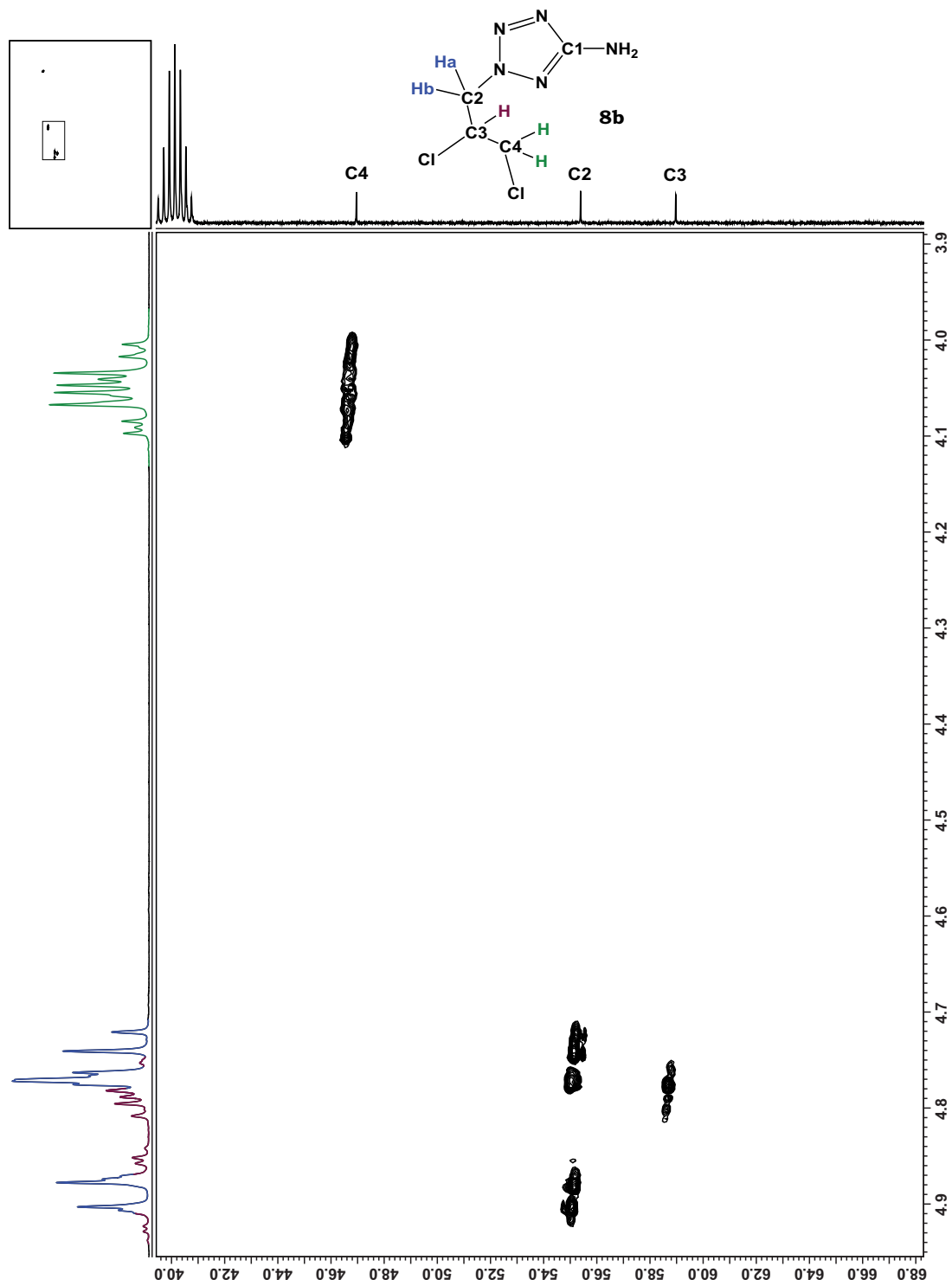


Figure 6.9 ^1H , ^{13}C HMQC spectrum of **8b** (about 0.1 M in $\text{DMSO}-d_6$, recorded with field gradient, matrix 2048×1024 , zerofilling: 2, sinbell auto).

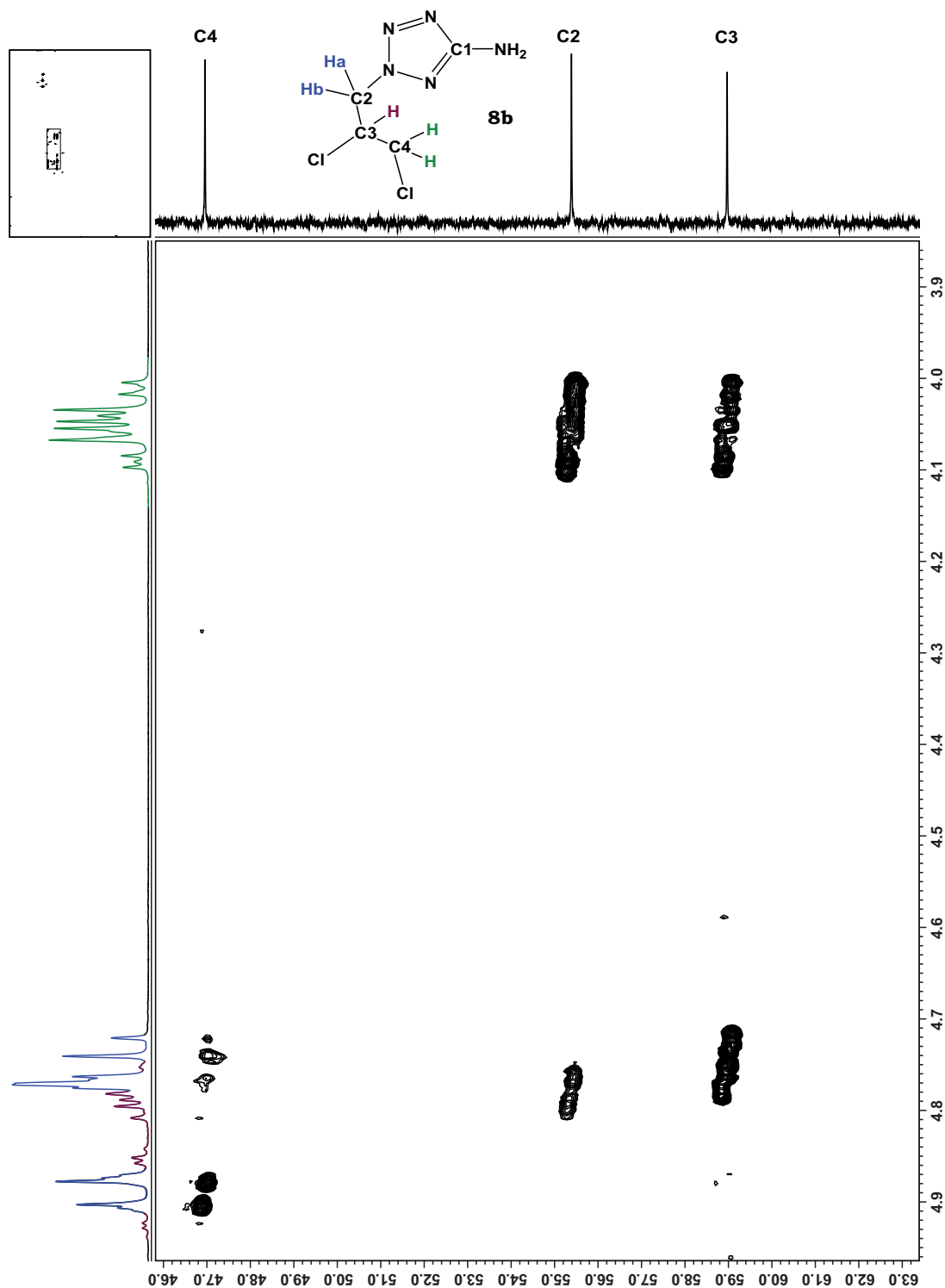


Figure 6.10 ^1H , ^{13}C HMBC spectrum of **8b** (about 0.1 M in $\text{DMSO-}d_6$, recorded with field gradient, matrix 2048×1024 , zerofilling: 2, sinbell auto).

Like in **7**, the signals in the ^1H and ^{13}C NMR spectra of **9** are shifted to lower field compared to its precursor molecule **8a**. Furthermore, the signals of the hydrogen atoms **Ha** and **Hb** at C2 are separated from each other (4.69–4.64 ppm, 4.56–4.50 ppm). In contrast, all signals of the carbon atoms are shifted to higher field, especially that of the quaternary carbon atom C1 (151.5 ppm).

In the IR spectra of **9_H₂O** the corresponding vibration of the crystal water molecule at 3559 cm⁻¹ and 3483 cm⁻¹ can be observed, which is missing of course in the spectrum of **9**. The positions of all other bands are very similar.

6.1.2.2 Molecular Structures

The molecular structures of **6a** and **6b** in the solid state could be determined after recrystallization from ethanol. After recrystallization from H₂O, single crystals of **9_H₂O** suitable for X-ray diffraction could be obtained. Single crystals of **7** and **9** formed directly from the reaction solution. All relevant data and parameters of the X-ray measurements and refinements are given in Appendix VI.

1-(2,3-Dihydroxypropyl)-5-aminotetrazole (**6a**) crystallizes in the triclinic space group *P*-1 with two molecules per unit cell. Its density of 1.534 g/cm³ is higher than the one of 1-(2-hydroxyethyl)-5-aminotetrazole (**1-OH**).^[3, 4] Both hydroxy groups are orientated staggered to each other with a dihedral angle of about 64° (Figure 6.11).

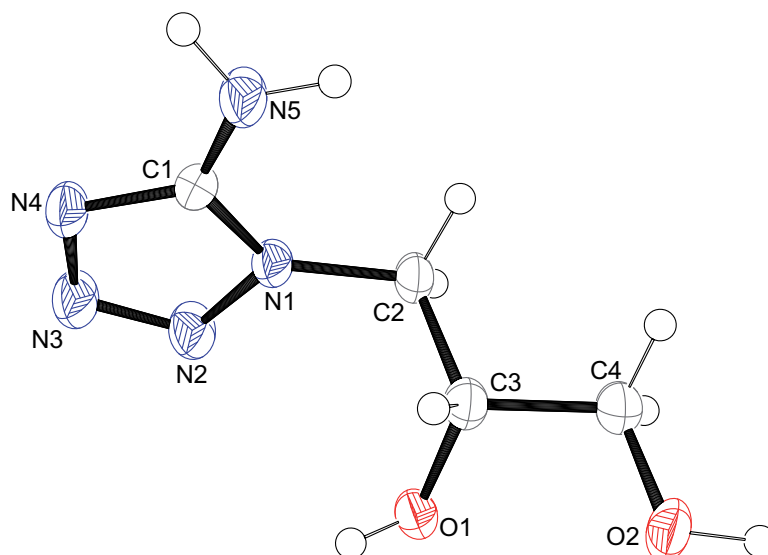


Figure 6.11 Molecular unit of **6a**. Hydrogen atoms are shown as spheres of arbitrary radius and thermal displacements are set at 50 % probability. Geometries: distances (Å) N1–N2 1.365(2), N2–N3 1.284(2), N3–N4 1.363(2), N1–C1 1.347(2), N4–C1 1.331(2), C1–N5 1.333(2), N1–C2 1.458(2), C2–C3 1.526(2), C3–C4 1.513(2), O1–C3 1.428(2), O2–C4 1.425(2); angles (°) N1–C1–N4 108.2(1), N1–C1–N5 125.7(2), N5–C1–N4 126.1(2), C1–N4–N3 105.5(1), N1–N2–N3 106.0(1), N2–N3–N4 111.9(1), N1–C2–C3 110.9(1), N2–N1–C2 121.4(1), C1–N1–N2 108.4(1), C1–N1–C2 130.2(1), C4–C3–C2 110.8(1), O1–C3–C2 109.8(1), O1–C3–C4 108.7(1), O2–C4–C3 107.9(1); torsion angles (°) C1–N1–C2–C3 97.2(2), N2–N1–C2–C3 -80.8(2), C1–N4–N3–N2 -0.2(2), N3–N4–C1–N5 -179.6(2), N3–N4–C1–N1 0.3(2), N2–N1–C1–N4 -0.4(2), C2–N1–C1–N4 -178.6(2), N2–N1–C1–N5 179.6(2), C2–N1–C1–N5 1.4(3), N4–N3–N2–N1 -0.1(2), C1–N1–N2–N3 0.3(2), C2–N1–N2–N3 178.7(2), N1–C2–C3–O1 68.7(2), N1–C2–C3–C4 -171.2(1), C2–C3–C4–O2 175.4(1), O1–C3–C4–O2 -63.8(2).

The packing in **6a** is characterized by layers along the *a* axes which are connected *via* hydrogen bonds (O1–H1[⋯]O2^{*i*}: 0.83(3) Å, 1.90(3) Å, 2.705(2) Å, 164(2)°; *i* -x+1, -y+1, -z+1). Four other types of hydrogen bonds connect the molecules within one layer (N5–H5b[⋯]O1^{*ii*}: 0.87(2) Å, 2.15(2) Å, 3.012(3) Å, 173(2)°; O2–H2[⋯]N3^{*iii*}: 0.92(2) Å, 2.69(2) Å,

3.445(3) Å, 140(2)°; O2–H2···N4ⁱⁱⁱ: 0.92(2) Å, 1.87(2) Å, 2.768(2) Å, 167(2)°; N5–H5a···N3^{iv}: 0.87(3) Å, 2.17(3) Å, 3.035(3) Å, 169(2)°; ⁱⁱ) x, y, z+1, ⁱⁱⁱ) x-1, y, z-1, ^{iv}) x-1, y, z).

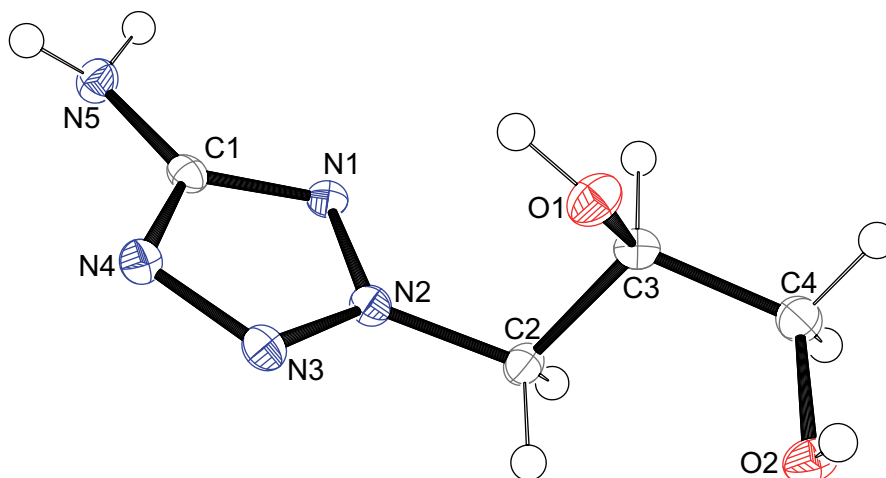


Figure 6.12 Molecular unit of **6b**. Hydrogen atoms are shown as spheres of arbitrary radius and thermal displacements are set at 50 % probability. Geometries: distances (Å) N1–N2 1.343(1), N2–N3 1.309(1), N3–N4 1.332(1), N1–C1 1.339(2), N4–C1 1.351(2), C1–N5 1.359(2), N2–C2 1.457(1), C2–C3 1.534(2), C3–C4 1.517(2), O1–C3 1.419(2), O2–C4 1.430(2); angles (°) N1–C1–N4 112.2(1), N1–C1–N5 124.7(1), N5–C1–N4 123.0(1), C1–N4–N3 106.0(1), N1–N2–N3 114.0(1), N2–N3–N4 106.5(1), N2–C2–C3 110.8(1), N3–N2–C2 122.1(1), C1–N1–N2 101.4(1), N1–N2–C2 123.7(1), C4–C3–C2 110.2(1), O1–C3–C2 111.1(1), O1–C3–C4 107.8(1), O2–C4–C3 112.1(1); torsion angles (°) N2–N3–N4–C1 -0.9(1), N4–N3–N2–N1 0.9(1), N4–N3–N2–C2 174.6(1), C1–N1–N2–N3 -0.5(1), C1–N1–N2–C2 -174.1(1), N2–N1–C1–N4 -0.1(1), N2–N1–C1–N5 -177.4(1), N3–N4–C1–N1 0.6(1), N3–N4–C1–N5 178.0(1), O2–C4–C3–O1 61.3(1), O2–C4–C3–C2 -60.0(1), N3–N2–C2–C3 -100.2(1), N1–N2–C2–C3 72.9(1), O1–C3–C2–N2 54.7(1), C4–C3–C2–N2 174.1(1).

2-(2,3-Dihydroxypropyl)-5-aminotetrazole (**6b**) crystallizes in the orthorhombic space group *Pbca* with eight molecules per unit cell. Its density of 1.518 g/cm³ is slightly lower than the one of the 1-isomer **6a**. Like the hydroxy groups in **6a**, those in **6b** are staggered with a dihedral angle of about 61° (Figure 6.12). Four different hydrogen bonds connect the molecules with each other (N5–H5a···N4ⁱ: 0.88(2) Å, 2.14(2) Å, 3.011(2) Å, 176(2)°, N5–H5b···N3ⁱⁱ: 0.88(2) Å, 2.32(2) Å, 3.167(2) Å, 164(1)°; O1–H1···O2ⁱⁱ: 0.86(2) Å, 1.88(2) Å, 2.731(2) Å, 175(2)°; O2–H2···N1^{iv}: 0.84(2) Å, 2.06(2) Å, 2.883(2) Å, 167(2)°; ⁱ) -x+1/2, y+1/2, z, ⁱⁱ) x-1/2, -y+1/2, -z+1, ⁱⁱⁱ) x-1/2, y, -z+3/2, -x+1, y-1/2, -z+3/2).

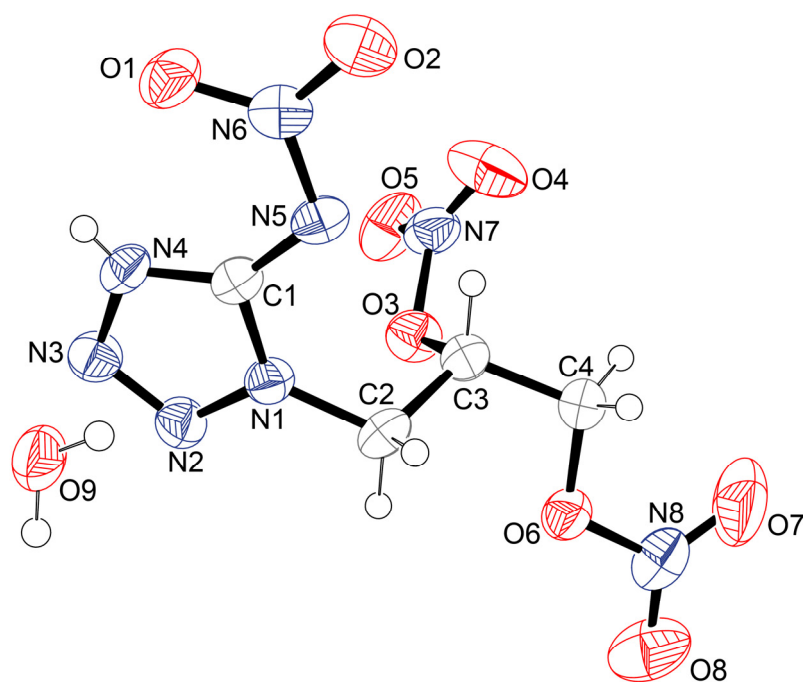


Figure 6.13 Molecular unit of **7**. Hydrogen atoms are shown as spheres of arbitrary radius and thermal displacements are set at 50 % probability. Selected geometries: distances (Å) N1–N2 1.357(4), N2–N3 1.277(4), N3–N4 1.345(4), N1–C1 1.350(4), N4–C1 1.323(4), C1–N5 1.337(4), N5–N6 1.351(4), O1–N6 1.249(3), O2–N6 1.229(4), N1–C2 1.462(4), C2–C3 1.476(5), C3–C4 1.515(5), O3–C3 1.435(4), O3–N7 1.437(4), N7–O4 1.181(5), O5–N7 1.182(4), O6–C4 1.440(5), O6–N8 1.388(4), N8–O7 1.203(5), O8–N8 1.181(5); angles (°) N1–C1–N4 103.1(3), N1–C1–N5 118.3(3), N5–C1–N4 138.6(3), C1–N4–N3 111.1(3), N1–N2–N3 106.8(3), N2–N3–N4 108.4(3), N1–C2–C3 111.5(2), N2–N1–C2 121.7(3), C1–N1–N2 110.5(3), C1–N1–C2 127.6(3), C1–N5–N6 114.7(3), O2–N6–O1 122.6(3), O1–N6–N5 121.4(3), C4–C3–C2 115.4(3), O3–C3–C2 105.8(3), O3–C3–C4 110.2(3), O6–C4–C3 106.9(3), C3–O3–N7 115.3(3), N8–O6–C4 114.5(3), O4–N7–O5 132.4(4), O4–N7–O3 117.7(3), O5–N7–O3 109.9(4), O8–N8–O7 128.6(4), O8–N8–O6 113.9(4), O7–N8–O6 117.4(4); torsion angles (°) N7–O3–C3–C2 144.5(3), O1–N6–N5–C1 2.4(4), C3–O3–N7–O4 1.7(4), C3–O3–N7–O5 179.2(3), C4–O6–N8–O8 173.1(3), C4–O6–N8–O7 -7.3(5), O3–C3–C4–O6 -71.2(4), C2–C3–C4–O6 48.4(4).

The nitration product of **6a**, 1-(2,3-dinitratopropyl)-5-nitriminotetrazole monohydrate (**7**), crystallizes in the monoclinic space group $P2_1/c$ with four molecular units per unit cell. Its density of 1.724 g/cm³ is only slightly smaller than the one of 1-(2-nitrateoethyl)-5-nitriminotetrazole monohydrate (**2**).^[3, 4] Five different hydrogen bonds between the crystal water molecule and the nitriminotetrazole ring can be observed (O9–H9a···N3ⁱ: 0.88(7) Å, 2.13(7) Å, 2.964(5) Å, 158(6)°; O9–H9a···O1ⁱⁱ: 0.81(5) Å, 2.12(5) Å, 2.898(5) Å, 163(4)°; O9–H9a···O2ⁱⁱ: 0.81(5) Å, 2.49(5) Å, 3.159(4) Å, 142(4)°; O9–H9a···N6ⁱⁱ: 0.81(5) Å, 2.62(5) Å, 3.421(5) Å, 169(4)°; N4–H1···O9ⁱⁱⁱ: 0.67(3) Å, 2.00(3) Å, 2.651(4) Å, 168(4)°; ⁱ $x, -y-1/2, z-1/2$, ⁱⁱ $x, -y+1/2, z-1/2$, ⁱⁱⁱ $-x+2, -y, -z$).

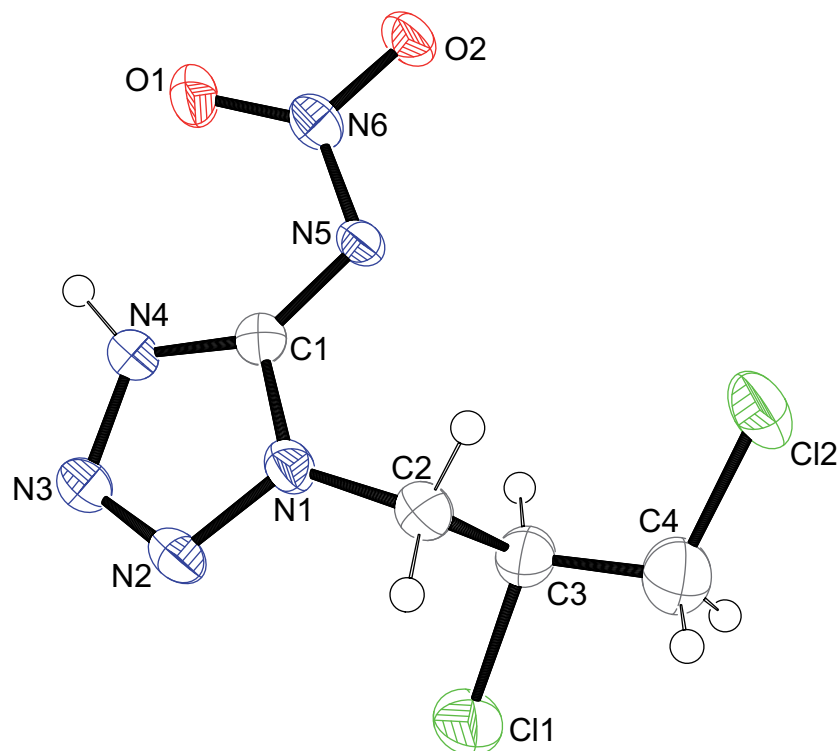


Figure 6.14 Molecular unit of **9**. Hydrogen atoms are shown as spheres of arbitrary radius and thermal displacements are set at 50 % probability. Selected geometries: distances (Å) N1–N2 1.371(3), N2–N3 1.276(4), N3–N4 1.359(4), N1–C1 1.352(4), N4–C1 1.337(4), C1–N5 1.338(4), N5–N6 1.346(3), O1–N6 1.237(3), O2–N6 1.255(3), N1–C2 1.446(4), C2–C3 1.527(5), C3–C4 1.483(5), C11–C3 1.815(4), C12–C4 1.773(4); angles (°) N1–C1–N4 103.3(3), N1–C1–N5 119.2(3), N5–C1–N4 137.2(3), C1–N4–N3 110.9(3), N1–N2–N3 107.5(3), N2–N3–N4 108.1(3), N1–C2–C3 111.0(3), N2–N1–C2 123.3(3), C1–N1–N2 110.2(3), C1–N1–C2 126.5(3), C1–N5–N6 113.9(3), O2–N6–O1 122.4(3), O1–N6–N5 123.2(3), C4–C3–C2 114.9(3), C11–C3–C2 107.8(3), C11–C3–C4 106.3(3), C12–C4–C3 111.8(3); torsion angles (°) O1–N6–N5–C1 8.1(4), N1–C2–C3–C11 –73.9(3), C2–C3–C4–C12 –66.7(4), C11–C3–C4–C12 174.2(2).

1-(2,3-Dichloropropyl)-5-nitriminotetrazole (**9**), the nitration product of **8a**, crystallizes in the monoclinic space group $P2_1/c$ with four molecules per unit cell. Despite the longer propyl substituent its density of 1.759 g/cm³ is higher than the one of 1-(2-chloroethyl)-5-nitriminotetrazole (1.724 g/cm³)^{3, 4}. The packing in **9** is characterized by zig-zag layers formed by the nitriminotetrazole rings along the *b* axes. They are connected by two hydrogen bonds (N4–H4 \cdots O2 i : 0.89(1) Å, 2.00(1) Å, 2.876(4) Å, 169(3)°; N4–H4 \cdots N5 i : 0.89(1) Å, 2.66(3) Å, 3.214(4) Å, 121(2)°; i *x*, –*y*+1/2, *z*+1/2).

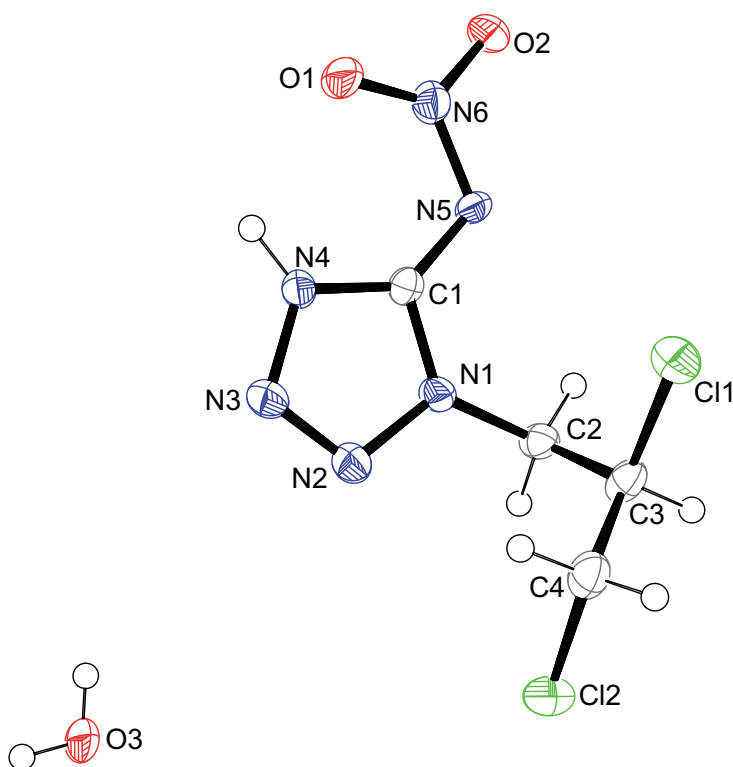


Figure 6.15 Molecular unit of **9_H₂O**. Hydrogen atoms are shown as spheres of arbitrary radius and thermal displacements are set at 50 % probability. Selected geometries: distances (Å) N1–N2 1.370(3), N2–N3 1.276(3), N3–N4 1.360(3), N1–C1 1.343(2), N4–C1 1.348(3), C1–N5 1.341(3), N5–N6 1.364(2), O1–N6 1.229(2), O2–N6 1.244(2), N1–C2 1.457(2), C2–C3 1.511(3), C3–C4 1.499(3), C11–C3 1.806(3), Cl2–C4 1.796(3); angles (°) N1–C1–N4 103.7(1), N1–C1–N5 120.6(1), N5–C1–N4 135.6(1), C1–N4–N3 110.0(1), N1–N2–N3 107.3(2), N2–N3–N4 108.6(2), N1–C2–C3 114.4(2), N2–N1–C2 120.6(2), C1–N1–N2 110.4(2), C1–N1–C2 128.8(2), C1–N5–N6 114.0(1), O2–N6–O1 122.9(2), O1–N6–N5 122.7(1), C4–C3–C2 116.3(2), C11–C3–C2 109.7(2), C11–C3–C4 106.6(2), Cl2–C4–C3 108.8(2); torsion angles (°) O1–N6–N5–C1 6.0(1), N1–C2–C3–C11 -61.5(2), C2–C3–C4–Cl2 61.0(3), C11–C3–C4–Cl2 -176.4(1).

Like **9**, its monohydrate **9_H₂O** crystallizes in the monoclinic space group $P2_1/c$ with four molecular units per unit cell. Its density is 1.745 g/cm³ and is comparable to the one of the water-free **9**. Due to the crystal water molecule three additional hydrogen bonds can be found in **9_H₂O** (O3–H3b··N5 i : 0.95(1) Å, 2.10(2) Å, 3.036(7) Å, 169(4)°; O3–H3b··O2 i : 0.95(1) Å, 2.61(4) Å, 3.166(5) Å, 118(3)°; O3–H3b··N6 i : 0.95(1) Å, 2.75(3) Å, 3.567(6) Å, 145(3)°; i x, y+1, z).

6.1.2.3 Energetic Properties

The energetic properties, such as decomposition temperature (T_{dec}), sensitivity to impact (E_{dr}), friction (F_i) and electric discharge (E_{el}), as well as the combustion energy ($\Delta_c U$) were determined. An overview of the properties of the neutral molecules **6a**, **6b**, **7**, **8a**, **8b**, **9**, and **9_H₂O** is given in Table 6.1.

Table 6.1 Overview of the physico-chemical properties of **6a**, **6b**, **7**, **8a**, **8b**, **9**, and **9_H₂O**.

	6a	6b	7	8a	8b	9	9_H₂O
Formula	C ₄ H ₉ N ₅ O ₂	C ₄ H ₉ N ₅ O ₂	C ₄ H ₈ N ₈ O ₉	C ₄ H ₇ Cl ₂ N ₅	C ₄ H ₇ Cl ₂ N ₅	C ₄ H ₆ Cl ₂ N ₆ O ₂	C ₄ H ₈ Cl ₂ N ₆ O ₃
M [g/mol]	159.15	159.15	312.15	196.04	196.04	241.04	259.05
E_{dr} [J]^a	> 100	> 40	6.0	> 40	> 40	4.0	10
F_r [N]^b	160	216	60	> 360	240	144	144
E_{el} [J]^c	0.10	> 1.5	0.08	1.5	1.5	0.20	0.20
grain size [μm]	250–500	100–250	100–500	100–500	100–500	100–500	500–1000
N [%]^d	44.0	44.0	35.9	35.7	35.7	34.9	32.4
Ω [%]^e	-106 (CO ₂)	-106 (CO ₂)	-15 (CO ₂) +5 (CO)	-86 (CO ₂) -53 (CO)	-86 (CO ₂) -53 (CO)	-53 (CO ₂) -27 (CO)	-49 (CO ₂) -25 (CO)
T_{dec} [°C]^f	251	241	114	219	219	114	129
ρ [g/cm³]^g	1.534	1.518	1.724	1.55* (22 °C)	1.53* (22 °C)	1.759	1.745
Δ_cU [kJ/kg]^h	-15361	-16224	-7406	-13222	-14163	-10999	-10170
Δ_cH^o [kJ/mol]ⁱ	-2442	-2570	-2296	-2588	-2768	-2639	-2622
Δ_fH^o [kJ/mol]^j	-419	-289	-422	110	295	-308	5.4

a) BAM drop hammer ^[6], b) BAM methods ^[6], c) Electric discharge tester, d) Nitrogen content, e) Oxygen balance, f) Decomposition temperature from DSC ($\beta = 5$ K/min), g) determined by X-ray crystallography or pycnometer (*), h) Combustion energy, i) Enthalpy of combustion, j) Molar enthalpy of formation.

The alkylated 5-aminotetrazole derivatives **6a**, **6b**, **8a**, and **8b** are insensitive to impact, but only **8a** is also insensitive to friction. Interestingly, **6a** displays a quite high sensitivity to electric discharge with 0.10 J. As expected, all nitriminotetrazole compounds (**7**, **9**, **9_H₂O**) are sensitive to impact and friction. Compound **7** is even very sensitive to friction with 60 N. Their sensitivities to electric discharge are between 0.08–0.20 J. The aminotetrazole derivatives are thermally about 100 °C more stable (**6a**: 251 °C, **6b**: 241 °C, **8a/b**: 219 °C) than the nitriminotetrazole derivatives (Figure 6.16). Furthermore, all show an endothermic signal caused by melting, before they decompose. The melting points of the N1- (**6a**, **8a**) and N2-isomers (**6b**, **8b**) are similar.

In the DSC thermograms of **7** and **9_H₂O** the loss of crystal water can be observed at 77 °C and 58 °C, respectively (Figure 6.17). Interestingly, **9_H₂O** is about 15 °C thermally more stable than its water-free analogue **9**. Compound **7** decomposes in two steps at 113 °C and 173 °C.

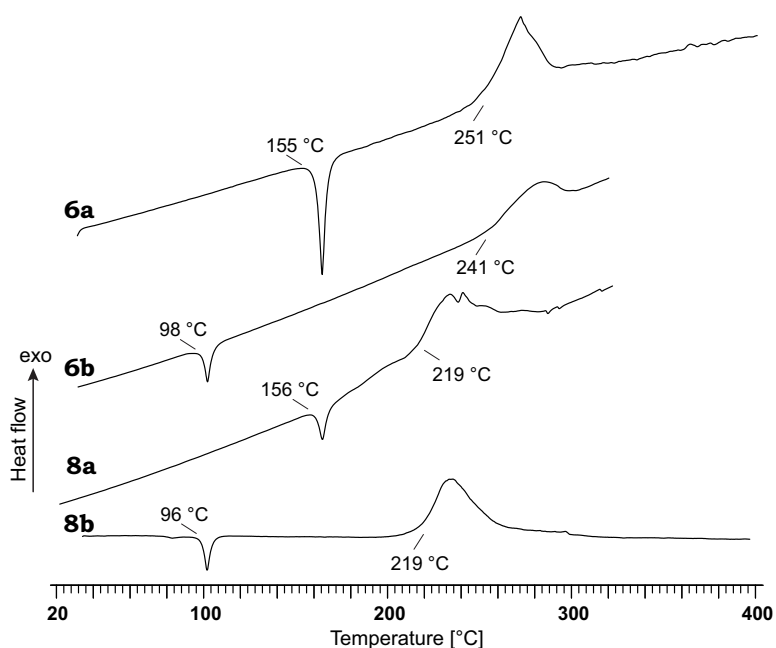


Figure 6.16 DSC thermograms of the 5-aminotetrazole derivatives **6a**, **6b**, **8a**, and **8b** in the temperature range of 25–300 °C and 25–400 °C. Decomposition points are given as onset temperatures.

All compounds **6–9** have a negative oxygen balance, no matter if the formation of CO or CO₂ is considered. An exception is **7**, which has a positive oxygen balance of +5 % considering the formation of CO.

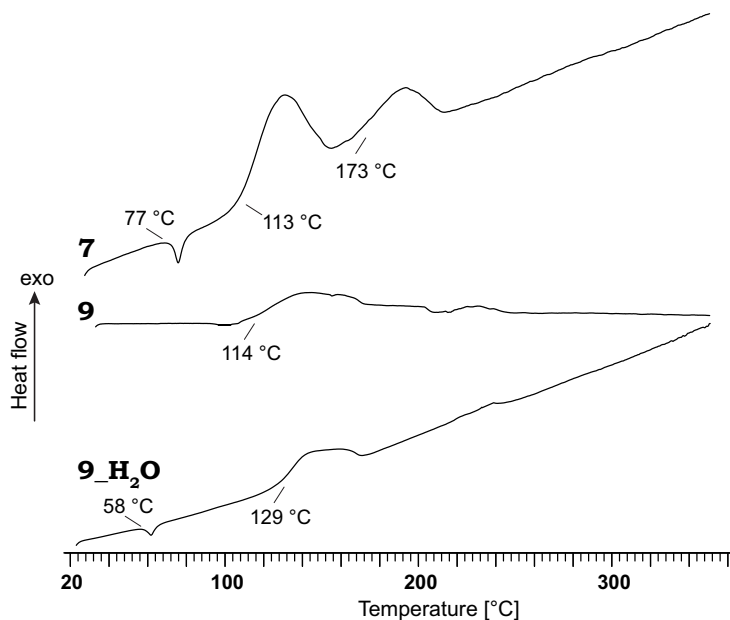


Figure 6.17 DSC thermograms of the 5-nitriminetetrazole derivatives **7**, **9**, and **9_H₂O** in the temperature range of 25 °C–350 °C. Decomposition points are given as onset temperatures.

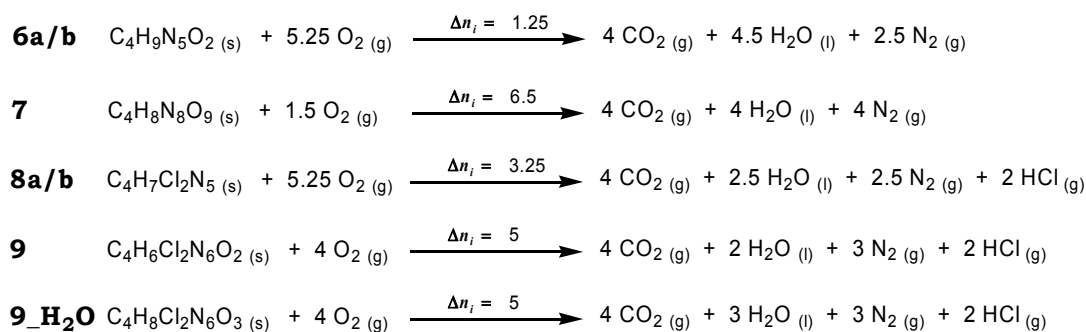
The reported values of the combustion energy ($\Delta_c U$) are the average of three single bomb calorimetry measurements. The standard molar enthalpy of combustion ($\Delta_c H^\circ$) was derived from equation 6.1.

$$\Delta_c H^\circ = \Delta_c U + \Delta n RT \quad (6.1)$$

$$\Delta n = \sum n_i (\text{gaseous products}) - \sum n_i (\text{gaseous educts})$$

n_i = molar amount of gas i .

The enthalpies of formation ($\Delta_f H^\circ$) for **6–9** were calculated at 298.15 K using the HESS thermochemical cycle and the combustion reactions in Scheme 6.8.



Scheme 6.8 Combustion equations of **6a**, **6b**, **7**, **8a**, **8b**, **9**, and **9_H₂O**.

The compounds **6a**, **6b**, **7**, and **9** were calculated to be formed exothermically. Interestingly, the enthalpies of formation of **6a** and **6b** differ more than 100 kJ/mol from each other. This is true for the isomers **8a** and **8b** with $\Delta_f H^\circ = 110$ kJ/mol and $\Delta_f H^\circ = 295$ kJ/mol. The enthalpy of formation of **9_H₂O** is almost zero.

6.1.3 Analytical Data of the Salts of **7** and **9**

6.1.3.1 Molecular Structures

After recrystallization from H₂O, single crystals of the salts **7_K**, **9_Cs**, and **9_Ba** suitable for X-ray diffraction could be obtained. All relevant data and parameters of the X-ray measurements and structure refinements are given in Appendix VI.

In the case of **7_K** one nitrate ester group is strongly disordered, which is responsible for the high wR_2 (< 40%) and GooF (1.396). Also no hydrogen atoms were calculated at that product. However, relevant data like the density of 1.833 g/cm³ could be obtained.

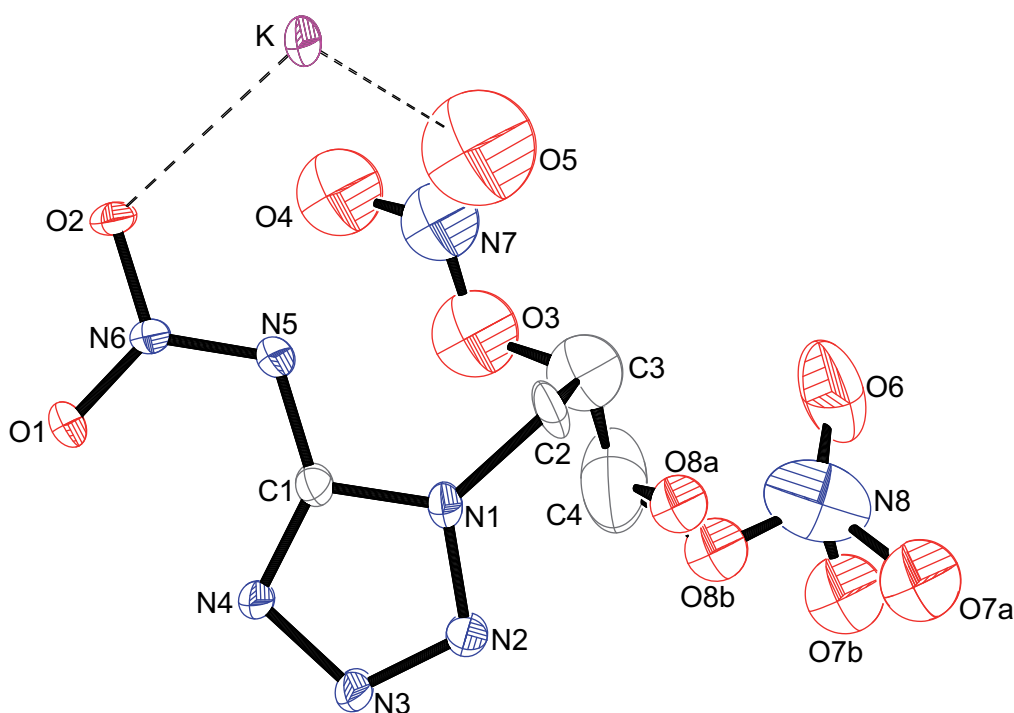


Figure 6.18 Molecular unit of **7_K**. No hydrogen atoms are depicted. Selected geometries: distances (Å) N1–N2 1.356(10), N2–N3 1.299(10), N3–N4 1.374(9), N1–C1 1.366(10), N4–C1 1.325(10), C1–N5 1.377(10), N5–N6 1.312(9), O1–N6 1.267(8), N6–O2 1.246(9), N1–C2 1.468(10), C3–C4 1.56(2), O3–C3 1.480(18), O4–N7 1.310(16), O3–N7 1.328(16), N7–O5 1.115(19), O8a–C4 1.30(2), O8b–C4 1.44(2), N8–O7a 1.05(3), N8–O8b 1.213(18), N8–O6 1.264(16), N8–O7b 1.36(3), N8–O8a 1.64(3), K–O2*i* 2.660(6), K–O1 2.702(6), K–N4*i* 2.786(7), K–O1*ii* 2.824(7), K–O5 2.864(18), K–N2*iii* 2.955(7); angles (°) N1–C1–N4 108.1(7), N1–C1–N5 115.6(7), O1–N6–N5 116.1(6), O1–N6–O2 119.8(6), C1–C3–C2 107.2(3), C4–C3–C1 111.1(3), O3–C3–C2 110.7(11), N7–O3–C3 111.6(13), O5–N7–O4 115.3(15), O5–N7–O3 131.9(17), O4–N7–O3 112.7(14), O8a–C4–O8b 32.3(9), C4–O8a–N8 95.5(14), C4–O8b–N8 110.9(15), O7a–N8–O8b 84(2), O7a–N8–O6 140(2), O8b–N8–O6 126.1(17), O7a–N8–O7b 41.7(19), O8b–N8–O7b 112.7(15), O6–N8–O7b 121.1(17), O7a–N8–O8a 109(2), O8b–N8–O8a 26.5(9), O6–N8–O8a 107.3(14), O7b–N8–O8a 126.3(13), O1–K–O5 94.9(4), O2*i*–K–O1 125.72(18), O2*i*–K–N4*i* 58.36(18), O1–K–N4*i* 173.6(2), O2*i*–K–O5 63.3(4), O1–K–O5 94.9(4), N4*i*–K–O5 82.7(4); torsion angles (°) O1–N6–N5–C1 –179.8(7), N1–C2–C3–O3 53.9(13), N7–O3–C3–C2 74.2(14), C3–O3–N7–O5 3(2), C3–O3–N7–O4 –173.5(12), O7a–N8–O8b–C4 133(2), O6–N8–O8b–C4 –18(3), O7b–N8–O8b–C4 164.5(16), O8a–N8–O8b–C4 –69(2); *i*) $x, -y-1/2, z-1/2$, *ii*) $-x, -y-1, -z+2$, *iii*) $x, y-1, z$.

The molecular unit of **7_K** is depicted in Figure 6.18. It crystallizes in the monoclinic space group $P2_1/c$ with four molecular units per unit cell. Its density is comparable to the one of other potassium salts (**1_K**: 1.873 g/cm³, **2_K**: 1.918 g/cm³, **3_K**: 1.868 g/cm³, **5_K**: 1.863 g/cm³). The potassium cations are sixfold coordinated by the atoms O2*i*, O1, N4*i*, O1*ii*, O5, and N2*iii* (*i*) $x, -y-1/2, z-1/2$, *ii*) $-x, -y-1, -z+2$, *iii*) $x, y-1, z$) forming a distorted octahedron. Due to the disorder of one nitrate ester group, the atoms O7 and O8 needed to be split into O7a and O7b as well as O8a and O8b.

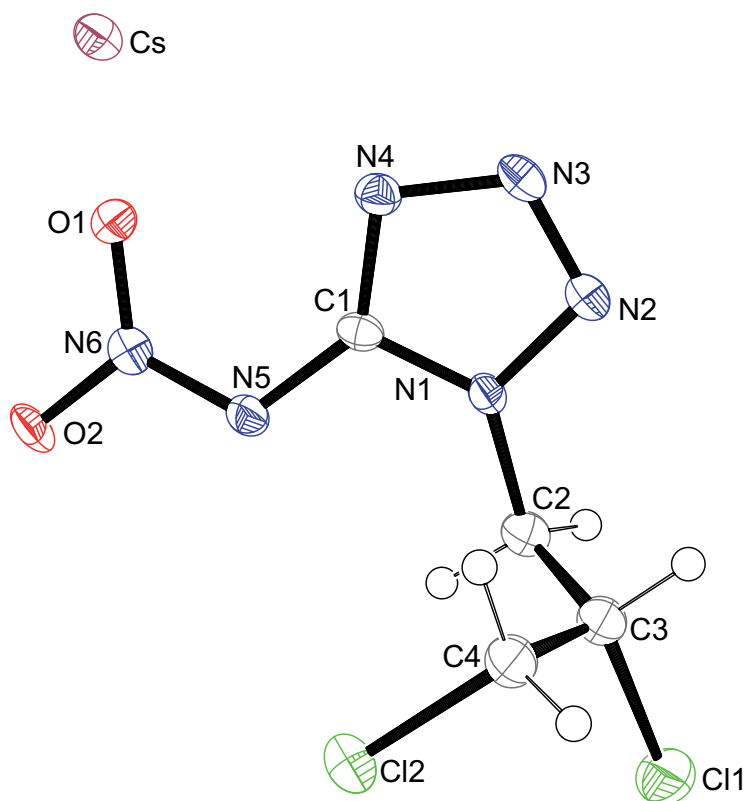


Figure 6.19 Molecular unit of **9-Cs**. Hydrogen atoms are shown as spheres of arbitrary radius and thermal displacements are set at 50 % probability. Selected geometries: distances (Å) N1–N2 1.349(5), N2–N3 1.281(5), N3–N4 1.367(5), N1–C1 1.345(6), N4–C1 1.337(5), C1–N5 1.378(5), N5–N6 1.322(5), O1–N6 1.255(5), N6–O2 1.263(4), N1–C2 1.455(6), C11–C3 1.806(5), Cl2–C4 1.791(4), Cs–O1*i* 3.100(3), Cs–O1*ii* 3.123(3), Cs–O2*iii* 3.128(3), Cs–O1 3.167(3), Cs–N4*ii* 3.217(4), Cs–N3*iv* 3.229(4), Cs–O2*i* 3.350(3), Cs–N4 3.417(4), Cs–O2*v* 3.418(3); angles (°) N1–C1–N4 107.5(4), N1–C1–N5 117.2(4), O1–N6–N5 124.1(3), O1–N6–O2 120.7(4), C11–C3–C2 107.2(3), C4–C3–C11 111.1(3), C3–C4–Cl2 112.5(3), O1–Cs–N4 47.69(8); torsion angles (°) O1–N6–N5–C1 –2.0(6), N1–C2–C3–C11 –171.2(3), Cl2–C4–C3–C2 59.4(5), Cl2–C4–C3–C11 –62.5(4); *i* $x-1, y, z$, *ii* $-x+2, -y, -z+2$, *iii* $-x+3, -y+1, -z+2$, *iv* $-x+1, -y, -z+2$, *v* $-x+2, -y+1, -z+2$.

The molecular unit of cesium 1-(2,3-dichloropropyl)-5-nitriminotetrazolate (**9-Cs**) is depicted in Figure 6.19. It crystallizes in the triclinic space group $P\bar{1}$ with two molecular units per unit cell. Its density of 2.382 g/cm³ is slightly smaller than that of other cesium salts of alkylated 5-nitriminotetrazoles like **1-Cs** and **3-Cs** (see chapter 2 and 4).

Considering distances up to 3.5 Å, the cesium atoms are fivefold coordinated by the atoms N4*ii*, N3*iv*, O2*i*, N4, and O2*v* (*i* $x-1, y, z$, *ii* $-x+2, -y, -z+2$, *iv* $-x+1, -y, -z+2$, *v* $-x+2, -y+1, -z+2$). No hydrogen bonds can be observed.

6.1.3.2 Energetic Properties

The energetic properties, such as decomposition temperature (T_{dec}), sensitivity to impact (E_{dr}), friction (F_r) and electric discharge (E_{el}), as well as the combustion energy ($\Delta_c U$) were determined. Furthermore, the solubility in H₂O at ambient temperature of each salt was investigated. The properties of the salts of **7** are given in Table 6.2. In Table 6.3 and

Table 6.4 an overview of the properties of the alkali metal and alkaline earth metal salts of **9** as well as its copper(II) complexes is given.

Table 6.2 Overview of the physico-chemical properties of the compounds of **7**.

	7_K	7_Sr	7_Ba	7_Cu
Formula	C ₄ H ₅ KN ₆ O ₈	Sr(C ₄ H ₅ N ₆ O ₈) ₂ · H ₂ O	Ba(C ₄ H ₅ N ₆ O ₈) ₂ · H ₂ O	Cu(C ₄ H ₅ N ₆ O ₈) ₂ (H ₂ O) ₂
M [g/mol]	332.25	691.90	741.61	685.84
E_{dr} [J]^a	< 1.0	< 1.0	4.0	< 1.0
F_r [N]^b	20	64	60	40
E_{el} [J]^c	0.10	0.05	0.10	0.10
grain size [µm]	100–500	500–1000	100–250	100–500
N [%]^d	33.7	32.1	30.2	32.7
Ω [%]^e	-22	-21	-13	-14
T_{dec} [°C]^f	154	179	191	128
ρ [g/cm³]^g	1.833	2.05* (23 °C)	2.01* (23 °C)	1.91* (23 °C)
H₂O sol. [wt%]^h	11 (22 °C)	6.9 (22 °C)	< 1.0 (23 °C)	< 0.1 (22 °C)

a) BAM drop hammer ^[6], b) BAM methods ^[6], c) Electric discharge tester, d) Nitrogen content, e) Oxygen balance, f) Decomposition temperature from DSC ($\beta = 5$ K/min), g) determined by X-ray crystallography or pycnometer (*), h) Solubility in H₂O (H₂O temperature).

In analogy to the salts of 1-(2-nitratoethyl)-5-nitriminotetrazole (**2**, chapter 3), the investigated compounds of **7** are very sensitive towards outer stimuli. **7_Ba** displays the lowest sensitivity to impact with 4.0 J. **7_Sr** is the less sensitive salt to friction with 64 N and the most sensitive one to electric discharge with 0.05 J. **Therefore, during the preparation and work up of 7 and its salts corresponding safety precautions must be taken.** Furthermore, the salts investigated decompose at temperatures below 200 °C, **7_Cu** even at 128 °C after its loss of H₂O at 120 °C. The H₂O solubilities of **7_K**, **7_Sr**, **7_Ba**, and **7_Cu** at ambient temperature are given in weight percent (wt%) and were determined according to equation 5.2. Each compound was added to 1 mL of H₂O with definite temperature until the solution became saturated.

$$\text{H}_2\text{O-sol.} = \frac{m_{\text{dissolved Compound}}}{m_{\text{dissolved Compound}} + m_{\text{Solvent}}} \cdot 100 \quad (5.2)$$

All compounds of **7** are lower soluble in H₂O than the corresponding salts of **2** (chapter 3) with solubilities of less than 12 wt%. Particularly, **7_Ba** and **7_Cu** are almost insoluble under these conditions.

Table 6.3 Overview of the physico-chemical properties of the alkali metal salts of **9**.

	9_Li	9_Na	9_K	9_Rb	9_Cs
Formula	C ₄ H ₅ Cl ₂ LiN ₆ O ₂ · 2H ₂ O	C ₄ H ₅ Cl ₂ NaN ₆ O ₂ · 1.5H ₂ O	C ₄ H ₅ Cl ₂ KN ₆ O ₂	C ₄ H ₅ Cl ₂ RbN ₆ O ₂	C ₄ H ₅ Cl ₂ CsN ₆ O ₂
M [g/mol]	283.00	290.04	279.13	325.50	372.95
E_{dr} [J]^a	10	10	8.0	7.0	7.0
F_r [N]^b	288	288	240	240	240
E_{el} [J]^c	0.35	0.30	0.20	0.30	0.30
grain size [μm]	< 100	100–500	< 100	100–500	100–500
N [%]^d	29.70	29.0	30.1	25.8	22.5
Ω [%]^e	-45	-47	-54	-47	-40
T_{dec} [°C]^f	163	154	171	154	163
ρ [g/cm³]^g	1.78* (23 °C)	1.83* (23 °C)	1.91* (23 °C)	2.22* (22 °C)	2.382
Δ_cU [kJ/kg]^h	n.d.**	n.d.**	-9204	-8534	-7206
Δ_cH^o [kJ/mol]ⁱ	-	-	-2559	-2766	-2706
Δ_fH^o [kJ/mol]^j	-	-	-198	152	115
H₂O sol. [wt%]^k	49 (22 °C)	38 (22 °C)	12 (22 °C)	13 (22 °C)	10 (22 °C)

a) BAM drop hammer ^[6], b) BAM methods ^[6], c) Electric discharge tester, d) Nitrogen content, e) Oxygen balance, f) Decomposition temperature from DSC ($\beta = 5$ K/min), g) determined by X-ray crystallography or pycnometer (*), h) Combustion energy, i) Enthalpy of combustion, j) Molar enthalpy of formation, k) Solubility in H₂O (H₂O temperature), ** n.d. = not determined.

The sensitivities to impact of **9_Li**, **9_Na**, **9_K**, **9_Rb**, **9_Cs**, **9_Sr**, **9_Ba**, **9_Cu_H₂O**, and **9_Cu_NH₃** are comparable to those of the corresponding salts of 1-(2-chloroethyl)-5-nitriminotetrazole (**3**, chapter 4).^[3, 4, 7, 8] However, all investigated salts of **9** are sensitive to friction with values between 240 N and 360 N, except **9_Sr** and **9_Cu_NH₃**. The sensitivities to electric discharge were determined between 0.20 J and 0.40 J.

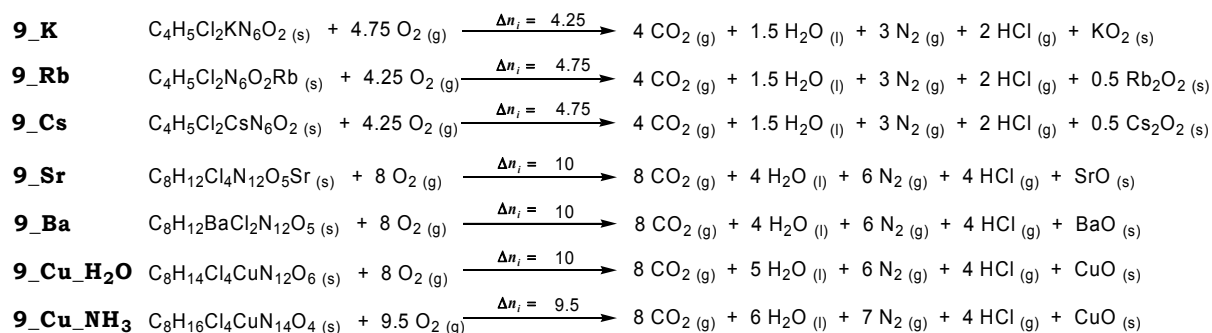
Table 6.4 Overview of the physico-chemical properties of the alkali metal salts of **9**, **9_Cu_H₂O**, and **9_Cu_NH₃**.

	9_Sr	9_Ba	9_Cu_H₂O	9_Cu_NH₃
Formula	Sr(C ₄ H ₅ Cl ₂ N ₆ O ₂) ₂ · H ₂ O	Ba(C ₄ H ₅ Cl ₂ N ₆ O ₂) ₂ · H ₂ O	Cu(C ₄ H ₅ Cl ₂ N ₆ O ₂) ₂ (H ₂ O) ₂	Cu(C ₄ H ₅ Cl ₂ N ₆ O ₂) ₂ (NH ₃) ₂
M [g/mol]	585.69	635.40	579.63	577.66
E_{dr} [J]^a	5.0	5.0	6.0	4.0
F_r [N]^b	> 360	288	360	> 360
E_{el} [J]^c	0.20	0.20	0.20	0.40
grain size [μm]	100–500	100–500	100–500	500–1000
N [%]^d	28.7	26.5	29.0	34.0
Ω [%]^e	-44	-40	-44	-53
T_{dec} [°C]^f	189	184	199	189
ρ [g/cm³]^g	1.83* (22 °C)	2.15* (22 °C)	1.72* (22 °C)	1.79* (22 °C)
Δ_cU [kJ/kg]^h	-8847	-8319	-9360	-10147
Δ_cH^o [kJ/mol]ⁱ	-5156	-5261	-5401	-5844
Δ_fH^o [kJ/mol]^j	-690	-497	139	11
H₂O sol. [wt%]^k	8.7 (22 °C)	1.7 (22 °C)	0.7 (22 °C)	0.8 (22 °C)

a) BAM drop hammer ^[6], b) BAM methods ^[6], c) Electric discharge tester, d) Nitrogen content, e) Oxygen balance, f) Decomposition temperature from DSC ($\beta = 5$ K/min), g) determined by X-ray crystallography or pycnometer (*), h) Combustion energy, i) Enthalpy of combustion, j) Molar enthalpy of formation, k) Solubility in H₂O (H₂O temperature).

Like the salts of **7**, the compounds of **9** decompose at temperatures below 200 °C and are thermally less stable than the corresponding salts of **3** (see chapter 4).^[3, 4, 7, 8] In the DSC thermograms of **9_Li** and **9_Cu_H₂O** one endothermic signal at 98 °C and 87 °C, respectively, can be observed. This is caused by the loss of crystal water molecules. Thus, the water-free copper(II) complex of **9** might be prepared by storing **9_Cu_H₂O** in a dry oven or under high vacuum. This was not tried in this work.

The enthalpy of formation ($\Delta_f H^\circ$) for **9_K**, **9_Rb**, **9-Cs**, **9_Sr**, **9_Ba**, **9_Cu_H₂O**, and **9_Cu_NH₃** was calculated at 298.15 K using the HESS thermochemical cycle and the combustion reactions in Scheme 6.9.



Scheme 6.9 Combustion equations of **9_K**, **9_Rb**, **9-Cs**, **9_Sr**, **9_Ba**, **9_Cu_H₂O**, and **9_Cu_NH₃**.

The salts **9_K**, **9_Sr**, and **9_Ba** were calculated to be formed exothermically. **9_Sr** displays the highest negative value ($\Delta_f H^\circ = -690$ kJ/mol). The highest positive value was calculated for **9_Rb** ($\Delta_f H^\circ = 152$ kJ/mol).

The heats of formation of the combustion products H₂O (l) (-286 kJ/mol), CO₂ (g) (-393 kJ/mol), HCl (g) (-92.3 kJ/mol), KO₂ (s) (-284.5 kJ/mol), Rb₂O₂ (s) (-426 kJ/mol), Cs₂O₂ (s) (-403 kJ/mol), SrO (s) (-592 kJ/mol), BaO (s) (-548 kJ/mol), and CuO (s) (-157 kJ/mol) were taken from literature.^[9, 10]

The solubilities in H₂O at ambient temperature of the investigated compounds of **9** were determined according to equation 5.2. All solubilities are in the range of 0.7–49 wt%. The solubilities of **9_Ba**, **9_Cu_H₂O**, and **9_Cu_NH₃** are the lowest and comparable to those of **3_Ba**, **3_Cu_H₂O**, and **3_Cu_NH₃** (see chapter 4).^[3, 4, 7, 8] The solubility of **9_Sr** (8.7 wt%) is significantly lower than the one of **3_Sr** (see chapter 4).^[3, 4, 7, 8] Therefore, the salts of **9** are suitable as possible colorant agents in pyrotechnic compositions.

6.1.3.3 Flame Color and Combustion Behavior

The compounds **7_Sr**, **7_Ba**, **7_Cu**, **9_Li**, **9_Sr**, **9_Ba**, **9_Cu_H₂O**, and **9_Cu_NH₃** were tested with regard to their color emission during combustion in the flame of a BUNSEN burner. For the tests a few milligrams of each compound on a spatula were put into the flame of a BUNSEN burner.

All salts **7** deflagrate very fast in the flame making a displosive sound. The strontium salt produces an intense red light emission (Figure 6.21). No smoke production or solid

residues were observed. The barium salt **7_Ba** detonated so quickly that no picture of the colored flame could be obtained. The emitted light was more white than green according to the subjective impression. No residues were observed.

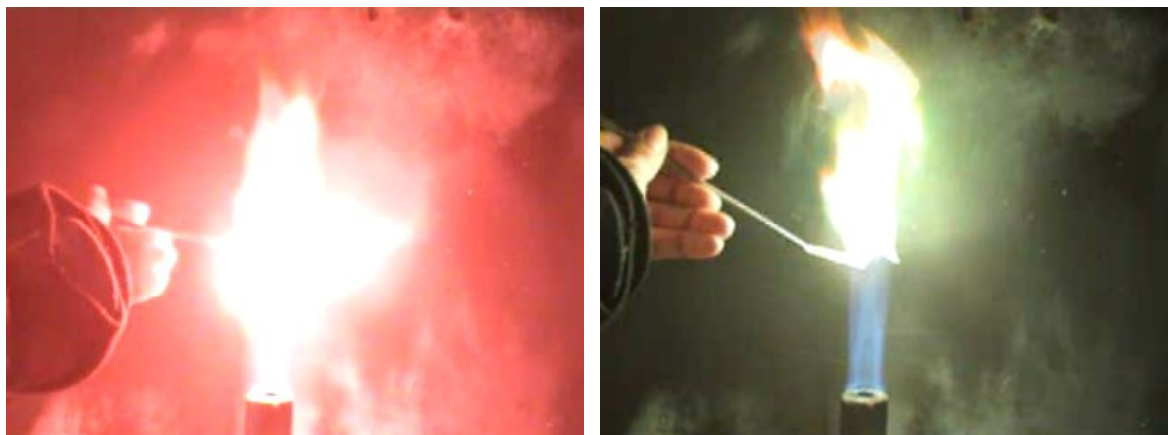


Figure 6.20 Flame color of **7_Sr** (left) and **7_Cu** (right) in the flame of a BUNSEN burner.

The copper(II) compound **7_Cu** deflagrates less vigorous than **7_Sr**. However, the light emission is less intense green than that of other copper(II) compounds mentioned in this work. There is an increased amount of yellow and red light (Figure 6.20). Again, no smoke or solid residues were observed. Due to the vigorous combustion behavior the salts of **7** are not usable as colorants in pyrotechnic compositions, apart from their inappropriate physico-chemical properties.

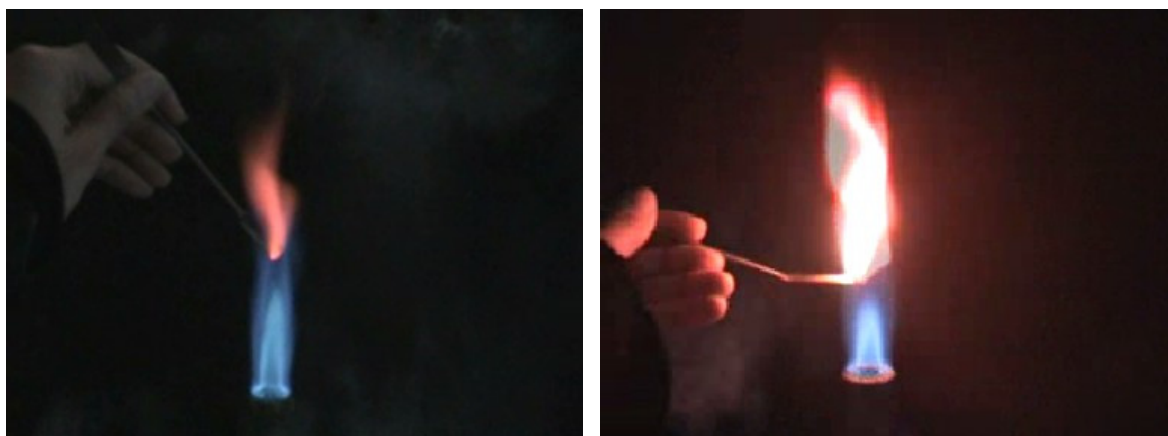


Figure 6.21 Red light emission of **9_Li** (left) and **9_Sr** (right) in the flame of a BUNSEN burner.

In contrast to the above mentioned salts, the salts of **9** do not deflagrate, but combust with a high velocity and without a sound. The lithium salt **9_Li** and strontium salt **9_Sr** emit red light, as expected (Figure 6.21). The flame of **9_Li** is much smaller and less intense than that of **9_Sr**. However, it combusts smoke-free and almost completely. **9_Sr** displays an analogous combustion behavior.



Figure 6.22 Flame color of **4_Ba** in the flame of a BUNSEN burner.

Barium 1-(2,3-dichloropropyl)-nitriminotetrazole monohydrate (**9_Ba**) emits even without an additional chlorine donor, like PVC, a greenish flame (Figure 6.22), because of its chlorine containing substituent. However, the green light emission is less intense than the one of barium 1-(2-chloroethyl)-nitriminotetrazole monohydrate (**3_Ba**, chapter 4). Again, no smoke or solid residues could be observed.



Figure 6.23 Flame color of **9_Cu_H₂O** (left) and **9_Cu_NH₃** (right) in the flame of a BUNSEN burner.

Both copper(II) complexes, **9_Cu_H₂O** and **9_Cu_NH₃** combust without smoke production and residue free. **9_Cu_H₂O** produces a bluish white flame, whereas **9_Cu_NH₃** emits very intense blue light. Therefore, it is more suitable than **9_Cu_H₂O**.

6.2 Experimental Part

*CAUTION! Some of the prepared compounds are sensitive to impact, friction, and electric discharge. Therefore, proper protective measures (safety glasses, face shield, leather coat, earthed equipment and shoes, Kevlar® gloves, and ear plugs) should be used, especially during work on the precursor molecule 1-(2,3-dinitratopropyl)-5-nitriminotetrazole monohydrate (**7**) and its salts as well as 1-(2,3-dichloropropyl)-5-nitriminotetrazole (**9**).*

6.2.1 Preparation of the Neutral Precursor Molecules

6.2.1.1 1-(2,3-Dihydroxypropyl)-5-aminotetrazole (6a) and 2-(2,3-Dihydroxypropyl)-5-aminotetrazole (6b)

A solution of 85.1 g (1.0 mol) 5-aminotetrazole and 40.0 g (1.0 mol) sodium hydroxide in 200 mL H₂O was refluxed at 100 °C, then 84 mL (1.0 mL) 3-chloro-1,2-propanediol were added drop wise within one hour. After refluxing over night, the solvent was evaporated and the yellow residue was extracted several times with a hot solution of 100 mL acetone and 70 mL ethanol. The extracts were combined and the organic solvents were removed by evaporation. After storing for a few days at ambient temperature, a colorless solid precipitated. After filtering off and recrystallization from ethanol, 1-(2,3-dihydroxypropyl)-5-aminotetrazole (**6a**) was obtained as colorless crystals. From the residual solution 2-(2,3-dihydroxypropyl)-5-aminotetrazole (**6b**) was obtained after storing for several days at ambient temperature and recrystallization from ethanol.

1-(2,3-Dihydroxypropyl)-5-aminotetrazole (6a):

Yield: 56 %.

M.p. 156 °C, 251 °C (dec., DSC-measurement, 5 K/min).

Raman (300 mW, 25 °C, cm⁻¹): 3183 (18), 2998 (35), 2957 (53), 2918 (43), 2872 (20), 1650 (21), 1593 (26), 1488 (38), 1378 (26), 1333 (37), 1293 (48), 1235 (11), 1129 (33), 1099 (35), 1050 (32), 988 (10), 914 (14), 872 (50), 798 (100), 717 (21), 480 (29), 366 (28), 307 (27).

IR (Diamond-ATR, cm⁻¹): 3322 (m), 3253 (m), 3176 (s), 1653 (vs), 1593 (s), 1478 (m), 1442 (w), 1363 (w), 1336 (s), 1263 (w), 1129 (m), 1103 (m), 1088 (s), 1034 (s), 989 (w), 905 (w), 873 (m), 797 (m), 720 (s).

¹H NMR (DMSO-*d*₆): 6.47 (s, 2H, NH₂), 5.14 (dd, ³J = 5 Hz, 1H, CHOH), 4.83 (t, ³J = 5 Hz, 1H, CH₂OH), 4.13 (dd, ³J = 4 Hz, ³J = 14 Hz, 1H, CHHOH), 3.96 (dd, ³J = 8 Hz, ³J = 14 Hz, 1H, CHHOH), 3.81–3.78 (m, 1H, CH), 3.36–3.29 (m, 2H, CH₂).

¹³C NMR (DMSO-*d*₆): 156.2 (CNH₂), 70.0 (CHOH), 63.2 (CH₂OH) 48.0 (CH₂).

Elemental analysis C₄H₉N₅O₂ (159.15 g/mol) calc.: C, 30.19; H, 5.70; N, 44.01; found: C, 30.34; H, 5.72; N, 43.83.

m/z (DEI+): 159 (16, M⁺).

E_{dr} > 100 J (250–500 μm).

F_r = 160 N (250–500 μm).

E_{el} = 0.10 J (250–500 μm).

Δ_cU = -3669 cal/g.

2-(2,3-Dihydroxypropyl)-5-aminotetrazole (6b):

Yield: 30 %.

M.p. 98 °C, 241 °C (dec., DSC-measurement, 5 K/min).**IR** (Diamond-ATR, cm^{-1}): 3397 (s), 3354 (m), 3305 (s), 3221 (m), 3173 (m), 2961 (w), 2941 (w), 2884 (w), 1737 (w), 1639 (s), 1553 (s), 1509 (vw), 1445 (m), 1393 (w), 1375 (m), 1313 (m), 1264 (w), 1235 (w), 1208 (m), 1181 (m), 1109 (m), 1079 (m), 1044 (s), 1024 (m), 928 (m), 905 (m), 845 (vw), 826 (m), 755 (m), 734 (w), 611 (m). **^1H NMR** (DMSO- d_6): 5.91 (s, 2H, NH_2), 5.05 (d, $^3J = 6$ Hz, 1H, CHOH), 4.81 (t, $^3J = 5$ Hz, 1H, CH_2OH), 4.39 (dd, $^3J = 4$ Hz, $^3J = 14$ Hz, 1H, CHHOH), 4.36 (dd, $^3J = 4$ Hz, $^3J = 14$ Hz, 1H, CHHOH), 4.23 (m, 1H, CH), 3.88 (m, 2H, CH_2). **^{13}C NMR** (DMSO- d_6): 166.9 (CNH_2), 69.8 (CHOH), 63.3 (CH_2OH), 55.5 (CH_2).**Elemental analysis** $\text{C}_4\text{H}_9\text{N}_5\text{O}_2$ (159.15 g/mol) calc.: C, 30.19; H, 5.70; N, 44.01; found: C, 30.02; H, 5.86; N, 43.93.**m/z** (DCI+): 160 (90, $[\text{M}+\text{H}]^+$). $E_{\text{dr}} > 40$ J (100–250 μm). $F_{\text{r}} = 216$ N (100–250 μm). $E_{\text{el}} > 1.50$ J (100–250 μm). $\Delta_c U = -3875$ cal/g.**6.2.1.2 1-(2,3-Dinitratopropyl)-5-nitriminotetrazole Monohydrate (7)**5.0 g (31 mmol) 1-(2,3-dihydroxypropyl)-5-aminotetrazole (**6a**) was slowly added to 50 mL nitric acid (100 %) at 0 °C. After stirring for 16 hours at ambient temperature the colorless solution was poured onto ice. The crystals formed were filtered off and dried on air. Yield: 88 %.**M.p.** 77 °C (loss of H_2O), 114 °C (dec.), 173 °C (dec., DSC-measurement, 5 K/min).**Raman** (300 mW, 25 °C, cm^{-1}): 3021 (31), 2993 (38), 2971 (100), 2895 (8), 1658 (22), 1625 (19), 1578 (56), 1492 (16), 1454 (29), 1429 (60), 1417 (46), 1371 (27), 1319 (19), 1305 (25), 1288 (80), 1273 (55), 1251 (58), 1184 (10), 1112 (14), 1080 (35), 1041 (31), 978 (30), 945 (16), 924 (13), 877 (44), 841 (25), 784 (13), 760 (42), 719 (29), 697 (14), 609 (15), 560 (32), 541 (35), 506 (23), 459 (25), 328 (17), 302 (24), 253 (46).**IR** (Diamond-ATR, cm^{-1}): 3354 (m), 3021 (w), 1739 (s), 1652 (s), 1624 (s), 1570 (m), 1543 (m), 1483 (w), 1450 (w), 1416 (m), 1366 (s), 1306 (w), 1273 (m), 1231 (s), 1181 (w), 1123 (w), 1062 (w), 1036 (m), 985 (w), 941 (m), 920 (m), 882 (s), 833 (s), 778 (w), 739 (w), 727 (w), 696 (w), 668 (w). **^1H NMR** (DMSO- d_6): 5.78 (m, 1H, CHONO_2), 5.04 (m, 1H, CHHONO_2), 4.88 (m, 1H, CHHONO_2), 4.65 (m, 2H, CH_2). **^{13}C NMR** (DMSO- d_6): 152.0 (CNNO_2), 76.8 (CHONO_2), 70.5 (CH_2ONO_2), 45.3 (CH_2). **^{14}N NMR** (DMSO- d_6): -19 (N6), -47 (N7/8).

¹⁵N NMR (DMSO-*d*₆): -19.4 (N3), -26.9 (N2), -29.5 (N6), -45.6 (N7/8), -48.3 (N7/8), -156.1 (N5), -156.3 (N4), -178.1 (N1).

Elemental analysis C₄H₈N₈O₉ (312.15 g/mol) calc.: C, 15.39; H, 2.58; N, 35.90; found: C, 15.32; H, 2.59; N, 35.17.

m/z (DCI+): 295 (85, [M⁺+H]-H₂O).

***E*_{dr}** = 6.0 J (100–500 μm).

***F*_r** = 60 N (100–500 μm).

***E*_{el}** = 0.08 J (100–500 μm).

Δ_c*U* = -1769 cal/g.

6.2.1.3 Potassium 1-(2,3-Dinitratopropyl)-5-nitriminotetrazolate (7_K)

0.52 g (1.67 mmol) 1-(2,3-Dinitratopropyl)-5-nitriminotetrazole monohydrate (**7**) and 0.09 g (1.67 mmol) potassium hydroxide were dissolved in 20 mL H₂O. After several days storing at ambient temperature colorless single crystals, suitable for X-ray diffraction, were formed. Yield: 89 %.

M.p. 154 °C (dec., DSC-measurement, 5 K/min).

IR (Diamond-ATR, cm⁻¹): 3020 (vw), 1635 (s), 1498 (m), 1452 (m), 1419 (w), 1380 (w), 1338 (m), 1318 (m), 1304 (s), 1279 (s), 1270 (s), 1164 (w), 1100 (w), 1030 (vw), 999 (w), 980 (vw), 927 (vw), 833 (m), 779 (w), 745 (w), 700 (vw), 681 (vw).

¹H NMR (DMSO-*d*₆): 5.82 (*m*, 1H, CH), 5.04–5.01 (*m*, 1H, CH), 4.85–4.81 (*m*, 1H, CH), 4.64–4.54 (*m*, 2H, CH₂).

¹³C NMR (DMSO-*d*₆): 158.0 (CN₄), 77.0 (CHONO₂), 70.5 (CH₂ONO₂), 44.9 (CH₂).

Elemental analysis C₄H₅KN₈O₈ (332.23 g/mol): calc.: C, 14.46; H, 1.52; N, 33.73; found: C, 14.45; H, 1.41; N, 33.61.

***E*_{dr}** < 1.0 J (100–500 μm).

***F*_r** = 20 N (100–500 μm).

***E*_{el}** = 0.10 J (100–500 μm).

H₂O-sol. 11 wt% (22 °C).

6.2.1.4 Strontium 1-(2,3-Dinitratopropyl)-5-nitriminotetrazolate Monohydrate (7_Sr)

0.52 g (1.67 mmol) 1-(2,3-Dinitratopropyl)-5-nitriminotetrazole monohydrate (**7**) and 0.22 g (0.84 mmol) strontium hydroxide octahydrate were dissolved in 20 mL H₂O. After several days storing at ambient temperature a colorless powder was obtained. Yield: 82 %.

M.p. 179 °C (dec., DSC-measurement, 5 K/min).

Raman (400 mW, 25 °C, cm⁻¹): 3231 (9), 3192 (8), 2978 (12), 2726 (11), 2285 (8), 1540 (9), 1510 (100), 1358 (20), 1341 (16), 1288 (21), 1115 (11), 1025 (47), 762 (23), 469 (9), 243 (9).

IR (Diamond-ATR, cm^{-1}): 3626 (vw), 3556 (vw), 3015 (vw), 2975 (vw), 2914 (vw), 1649 (s), 1634 (m), 1511 (m), 1462 (m), 1428 (w), 1392 (m), 1371 (m), 1360 (m), 1337 (m), 1316 (m), 1307 (m), 1288 (m), 1267 (s), 1240 (m), 1164 (vw), 1114 (w), 1062 (vw), 1047 (vw), 1022 (m), 992 (vw), 946 (vw), 926 (w), 851 (m), 828 (m), 770 (vw), 760 (w), 737 (vw), 715 (m), 684 (vw).

^1H NMR (DMSO- d_6): 5.87–5.80 (*m*, 1H, *CH*), 5.04–5.00 (*m*, 1H, *CH*), 4.82–4.75 (*m*, 1H, *CH*), 4.60–4.45 (*m*, 2H, *CH*₂).

^{13}C NMR (DMSO- d_6): 158.0 (CN₄), 77.4 (CH₂ONO₂), 70.7 (CH₂ONO₂), 44.4 (CH).

Elemental analysis C₈H₁₈N₁₆O₁₇Sr (691.90 g/mol): calc.: C, 13.89; H, 1.75; N, 32.39; found: C, 13.80; H, 1.71; N, 32.08.

E_{dr} < 1.0 J (500–1000 μm).

F_{r} = 64 N (500–1000 μm).

E_{el} = 0.05 J (500–1000 μm).

H₂O-sol. 6.9 wt% (22 °C).

6.2.1.5 Barium 1-(2,3-Dinitratopropyl)-5-nitriminotetrazolate Monohydrate (7_Ba)

0.52 g (1.67 mmol) 1-(2,3-Dinitratopropyl)-5-nitriminotetrazole monohydrate (**7**) and 0.26 g (0.84 mmol) barium hydroxide octahydrate were dissolved in 20 mL H₂O. After several days storing at ambient temperature a colorless powder was obtained. Recrystallization from H₂O yielded thin colorless needles. Yield: 88 %.

M.p. 191 °C (dec., DSC-measurement, 5 K/min).

Raman (400 mW, 25 °C, cm^{-1}): 3016 (8), 2972 (14), 1508 (100), 1491 (6), 1459 (8), 1358 (21), 1345 (14), 1287 (21), 1117 (10), 1022 (37), 866 (9), 831 (5), 759 (13), 534 (5), 497 (6), 241 (7).

IR (Diamond-ATR, cm^{-1}): 3536 (vw), 1652 (s), 1508 (m), 1458 (m), 1428 (w), 1393 (m), 1372 (m), 1357 (m), 1338 (m), 1313 (m), 1289 (m), 1270 (s), 1237 (m), 1114 (w), 1061 (vw), 1046 (vw), 1020 (m), 992 (vw), 945 (vw), 926 (w), 855 (m), 827 (m), 769 (vw), 755 (w), 715 (w), 680 (vw).

^1H NMR (DMSO- d_6): 5.88–5.80 (*m*, 1H, *CH*), 5.02–4.99 (*m*, 1H, *CH*), 4.81–4.76 (*m*, 1H, *CH*), 4.58–4.46 (*m*, 2H, *CH*₂).

^{13}C NMR (DMSO- d_6): 158.1 (CN₄), 77.4 (CHONO₂), 70.7 (CH₂ONO₂), 44.4 (CH₂).

Elemental analysis C₈H₁₂BaN₁₆O₁₇ (741.61 g/mol): calc.: C, 12.96; H, 1.63; N, 30.22; found: C, 12.93; H, 1.74; N, 30.10.

E_{dr} = 4.0 J (100–250 μm).

F_{r} = 60 N (100–250 μm).

E_{el} = 0.10 J (100–250 μm).

H₂O-sol. < 1.0 wt% (23 °C).

6.2.1.6 Diaqua 1-(2,3-Dinitratopropyl)-5-nitriminotetrazolato Copper(II) (7_Cu)

A solution of 0.233 g (1.0 mmol) copper(II) nitrate pentahemihydrate in 2 mL H₂O was combined with a solution of 0.624 g (2.0 mmol) 1-(2,3-dinitratopropyl)-5-nitriminotetrazole monohydrate (**7**) in 35 mL H₂O. After storing the green solution at ambient temperature for several days green crystals were obtained. Yield: 54 %.

M.p. 122 °C (loss of H₂O), 128 °C (dec., DSC-measurement, 5 K/min).

IR (Diamond-ATR, cm⁻¹): 3432 (m), 3276 (w), 3023 (vw), 2972 (vw), 1649 (s), 1616 (s), 1520 (m), 1473 (m), 1460 (w), 1401 (m), 1380 (m), 1361 (m), 1346 (m), 1286 (s), 1270 (s), 1251 (s), 1176 (vw), 1123 (vw), 1104 (vw), 1060 (vw), 1042 (vw), 1030 (w), 1013 (vw), 940 (w), 925 (vw), 894 (m), 876 (m), 843 (m), 795 (vw), 765 (vw), 750 (vw), 736 (vw), 723 (vw), 703 (w), 615 (vw).

Elemental analysis C₈H₁₄CuN₁₆O₁₈ (685.84 g/mol): calc.: C, 14.01; H, 2.06; N, 32.68; found: C, 13.92; H, 2.11; N, 32.42.

E_{dr} < 1.0 J (100–500 μm).

F_r = 40 N (100–500 μm).

E_{el} = 0.10 J (100–500 μm).

H₂O-sol. < 0.1 wt% (22 °C).

6.2.1.7 1-(2,3-Dichloropropyl)-5-aminotetrazole (8a)

At 0 °C 10 mL (0.12 mol) of pyridine were added dropwise to 80 mL (0.86 mol) of phosphorus oxychloride. At the same temperature 1-(2,3-dichloropropyl)-5-aminotetrazole (**6a**) was slowly added and the mixture was refluxed at 120 °C for 5 hours. After cooling to ambient temperature, the yellow solution was poured onto ice and neutralized with potassium or sodium hydroxide. The yellow precipitate was filtered off and recrystallized from ethanol. Yield: 70 %.

M.p. 156 °C, 219 °C (dec., DSC-measurement, 5 K/min).

IR (Diamond-ATR, cm⁻¹): 3313 (s), 3138 (s), 2954 (w), 2752 (w), 2360 (w), 1735 (vw), 1656 (s), 1588 (s), 1517 (w), 1485 (m), 1433 (m), 1378 (w), 1342 (m), 1314 (m), 1301 (w), 1285 (m), 1232 (w), 1182 (vw), 1133 (m), 1104 (m), 1053 (w), 1036 (w), 1004 (m), 956 (vw), 936 (w), 870 (w), 808 (w), 742 (w), 671 (m) 636 (w).

¹H NMR (DMSO-*d*₆): 6.83 (s, 2H, NH₂), 4.72–4.67 (*m*, 1H, CH), 4.53 (*dd*, ³*J* = 4 Hz, ³*J* = 15 Hz, 1H, NCHH), 4.45 (*dd*, ³*J* = 8 Hz, ³*J* = 15 Hz, 1H, NCHH), 3.99 (*dd*, ³*J* = 4 Hz, ³*J* = 12 Hz, 1H, ClCHH). 3.94 (*dd*, ³*J* = 5 Hz, ³*J* = 12 Hz, 1H, ClCHH).

¹³C NMR (DMSO-*d*₆): 156.0 (CNH₂), 58.7 (CH), 47.8 (NCH₂) 46.8 (CH₂).

Elemental analysis C₄H₇Cl₂N₅ (196.04 g/mol): calc.: C, 24.51; H, 3.60; N, 35.72; found: C, 24.50; H, 3.82; N, 35.47.

m/z (DEI+): 195 (7, M⁺), 160 (100, [M-Cl]).

E_{dr} > 40 J (100–500 μm).

$$F_r > 360 \text{ N} \quad (100\text{--}500 \mu\text{m}).$$

$$E_{el} = 1.50 \text{ J} \quad (100\text{--}500 \mu\text{m}).$$

$$\Delta_c U = -3158 \text{ cal/g.}$$

6.2.1.8 2-(2,3-Dichloropropyl)-5-aminotetrazole (8b)

Preparation analog to 1-(2,3-dichloropropyl)-5-aminotetrazole (**8a**), starting with 2-(2,3-dihydroxypropyl)-5-aminotetrazole (**6b**). Yield: 66 %.

M.p. 96 °C, 219 °C (dec., DSC-measurement, 5 K/min).

IR (Diamond-ATR, cm^{-1}): 3311 (s), 3221 (m), 3139 (s), 3010 (m), 2754 (w), 2360 (w), 2340 (w), 1746 (vw), 1641 (s), 1587 (s), 1558 (s), 1518 (w), 1486 (m), 1456 (w), 1433 (m), 1380 (m), 1344 (w), 1315 (m), 1287 (w), 1240 (m), 1185 (w), 1147 (w), 1133 (m), 1103 (m), 1032 (w), 1016 (m), 959 (w), 939 (w), 870 (m), 815 (m), 761 (m), 738 (m), 714 (w), 675 (m).

^1H NMR (DMSO- d_6): 6.84 (s, 2H, NH_2), 4.74–4.71 (m, 1H, CH), 4.55–4.49 (m, 2H, CH_2), 4.02–3.98 (m, 2H, CH_2).

^{13}C NMR (DMSO- d_6): 156.5 (CNH_2), 59.2 (CH), 48.3 (CH_2), 47.6 (CH_2).

Elemental analysis $\text{C}_4\text{H}_7\text{Cl}_2\text{N}_5$ (196.04 g/mol): calc.: C, 24.51; H, 3.60; N, 35.72; found: C, 24.19; H, 3.52; N, 35.38.

$$E_{dr} > 40 \text{ J} \quad (100\text{--}500 \mu\text{m}).$$

$$F_r = 240 \text{ N} \quad (100\text{--}500 \mu\text{m}).$$

$$E_{el} = 1.5 \text{ J} \quad (100\text{--}500 \mu\text{m}).$$

$$\Delta_c U = -3383 \text{ cal/g.}$$

6.2.1.9 1-(2,3-Dichloropropyl)-5-nitriminotetrazole (9)

5.0 g (26 mmol) 1-(2,3-Dichloropropyl)-5-aminotetrazole (**8a**) was slowly added to 50 mL nitric acid (100 %) at 0 °C. After stirring for 16 hours at ambient temperature, the colorless solution was poured onto ice. The formed colorless crystals were filtered off and dried on air. Yield: 95 %.

M.p. 114 °C (dec., DSC-measurement, 5 K/min).

IR (Diamond-ATR, cm^{-1}): 3178 (w), 3054 (m), 3001 (m), 2974 (m), 2957 (m), 1584 (s), 1486 (m), 1449 (m), 1436 (m), 1424 (w), 1403 (w), 1379 (vw), 1323 (s), 1310 (s), 1278 (m), 1254 (s), 1236 (s), 1223 (s), 1183 (m), 1130 (vw), 1045 (m), 1032 (m), 995 (m), 986 (m), 936 (w), 900 (vw), 884 (vw), 866 (vw), 777 (w), 763 (vw), 750 (w), 719 (m), 666 (m).

^1H NMR (DMSO- d_6): 4.83–4.77 (m, 1H, CHCl), 4.69–4.64 (m, 1H, CHHCl), 4.56–4.50 (m, 1H, CHHCl), 4.13–4.04 (m, 2H, CH_2Cl).

^{13}C NMR (DMSO- d_6): 151.5 (CN_4), 57.8 (CH_2), 50.2 (CH), 47.0 (CH_2).

Elemental analysis $\text{C}_4\text{H}_6\text{Cl}_2\text{N}_6\text{O}_2$ (241.04 g/mol): calc.: C, 19.93; H, 2.51; N, 34.87; found: C, 19.86; H, 2.56; N, 34.72.

m/z (DEI+): 240 (0.4, M^+), 205 (36, $[\text{M}-\text{Cl}]$).

$$E_{dr} = 4.0 \text{ J} \quad (100\text{--}500 \mu\text{m}).$$

$F_r = 144 \text{ N}$ (100–500 μm).

$E_{el} = 0.20 \text{ J}$ (< 100 μm).

$\Delta_c U = -2627 \text{ cal/g}$.

6.2.1.10 1-(2,3-Dichloropropyl)-5-nitriminotetrazole Monohydrate (**9_H₂O**)

1-(2,3-Dichloropropyl)-5-nitriminotetrazole monohydrate (**9_H₂O**) was obtained after recrystallization of 1-(2,3-dichloropropyl)-5-nitriminotetrazole (**9**) from H₂O. Yield: 99 %.

M.p. 58 °C (loss of H₂O), 129 °C (dec., DSC-measurement, 5 K/min).

IR (Diamond-ATR, cm⁻¹): 3559 (m), 3483 (m), 3014 (w), 2972 (w), 2822 (vw), 2713 (vw), 2638 (w), 2553 (vw), 1780 (vw), 1622 (w), 1573 (s), 1490 (s), 1453 (w), 1442 (w), 1416 (m), 1378 (vw), 1345 (m), 1313 (m), 1283 (w), 1240 (s), 1225 (s), 1211 (m), 1187 (m), 1129 (w), 1058 (m), 1027 (w), 1001 (m), 967 (w), 922 (w), 863 (vw), 779 (w), 763 (vw), 732 (w), 711 (m), 680 (vw), 661 (w).

Elemental analysis C₄H₈Cl₂N₆O₃ (259.05 g/mol): calc.: C, 18.55; H, 3.15; N, 32.44; Cl, 27.37; found: C, 18.55; H, 3.11; N, 32.54; Cl, 27.17.

$E_{dr} = 10 \text{ J}$ (500–1000 μm).

$F_r = 144 \text{ N}$ (500–1000 μm).

$E_{el} = 0.20 \text{ J}$ (500–1000 μm).

$\Delta_c U = -2429 \text{ cal/g}$.

6.2.2 Salts of 1-(2,3-Dichloropropyl)-5-nitriminotetrazole (**9**)

General procedure:

1.2 g (5.0 mmol) of 1-(2,3-dichloropropyl)-5-nitriminotetrazole (**5**) were dissolved in 25 mL H₂O. After adding the corresponding hydroxides (alkali metal: 5.0 mmol, alkaline earth metal: 2.5 mmol), the solution was heated until it became clear.

6.2.2.1 Lithium 1-(2,3-Dichloropropyl)-5-nitriminotetrazolate Dihydrate (**9_Li**)

After recrystallization from H₂O, a colorless solid was obtained. Yield: 65 %.

M.p. 98 °C (loss of H₂O), 163 °C (dec., DSC-measurement, 5 K/min).

IR (Diamond-ATR, cm⁻¹): 3356 (vs, br), 3020 (m), 2941 (w), 2361 (vw), 2331 (vw), 1631 (m), 1512 (m), 1459 (m), 1430 (m), 1374 (m), 1339 (s), 1290 (m), 1239 (m), 1139 (vw), 1117 (w), 1034 (w), 999 (vw), 890 (vw), 773 (vw), 739 (w), 668 (w).

¹H NMR (DMSO-*d*₆): 4.78–4.72 (*m*, 1H, CH), 4.55–4.50 (*m*, 1H, CH), 4.41–4.35 (*m*, 1H, CH), 4.09–3.98 (*m*, 2H, CH₂).

¹³C NMR (DMSO-*d*₆): 158.0 (CN₄), 58.7 (NCH₂), 49.3 (CH₂Cl), 47.3 (CHCl).

Elemental analysis C₄H₉Cl₂LiN₆O₄ (283.00 g/mol): calc.: C, 16.98; H, 3.21; N, 29.70; found: C, 16.51; H, 3.24; N, 28.43.

$E_{dr} = 10 \text{ J}$ ($< 100 \text{ }\mu\text{m}$).

$F_r = 288 \text{ N}$ ($< 100 \text{ }\mu\text{m}$).

$E_{el} = 0.35 \text{ J}$ ($< 100 \text{ }\mu\text{m}$).

H₂O-sol. 49 wt% (22 °C).

6.2.2.2 Sodium 1-(2,3-Dichloropropyl)-5-nitriminotetrazolate Trihemihydrate (9_Na)

After recrystallization from H₂O, a colorless solid was obtained. Yield: 72 %.

M.p. 154 °C (dec., DSC-measurement, 5 K/min).

IR (Diamond-ATR, cm⁻¹): 3427 (w, br), 3009 (vw), 2961 (vw), 2359 (vw), 1980 (vw), 1777 (vw), 1728 (vw), 1641 (vw), 1581 (vw), 1552 (vw), 1496 (m), 1453 (m), 1435 (w), 1388 (m), 1330 (s), 1319 (s), 1284 (m), 1261 (m), 1241 (m), 1220 (m), 1190 (w), 1141 (w), 1104 (m), 1036 (m), 999 (vw), 986 (vw), 951 (vw), 892 (vw), 869 (vw), 777 (w), 757 (vw), 737 (w), 699 (vw), 666 (w).

¹H NMR (DMSO-*d*₆): 4.76–4.70 (*m*, 1H, CH), 4.53–4.48 (*m*, 1H, CH), 4.40–4.34 (*m*, 1H, CH), 4.06–3.96 (*m*, 2H, CH₂).

¹³C NMR (DMSO-*d*₆): 157.7 (CN₄), 58.6 (NCH₂), 49.1 (CH₂Cl), 47.2 (CHCl).

Elemental analysis C₄H₈Cl₂N₆NaO_{3.5} (290.04 g/mol): calc.: C, 16.56; H, 2.78; N, 28.98; found: C, 16.68; H, 2.65; N, 28.92.

$E_{dr} = 10 \text{ J}$ (100–500 μm).

$F_r = 288 \text{ N}$ (100–500 μm).

$E_{el} = 0.30 \text{ J}$ (100–500 μm).

H₂O-sol. 38 wt% (22 °C).

6.2.2.3 Potassium 1-(2,3-Dichloropropyl)-5-nitriminotetrazolate (9_K)

After recrystallization from H₂O, a colorless powder was obtained. Yield: 91 %.

M.p. 171 °C (dec., DSC-measurement, 5 K/min).

IR (Diamond-ATR, cm⁻¹): 3492 (m), 2363 (vw), 2338 (vw), 1649 (vw), 1592 (vw), 1495 (m), 1451 (m), 1428 (m), 1382 (m), 1327 (s), 1305 (s), 1268 (m), 1246 (m), 1234 (m), 1220 (w), 1182 (vw), 1132 (vw), 1103 (w), 1051 (vw), 1030 (w), 1013 (vw), 986 (vw), 938 (vw), 888 (vw), 871 (vw), 805 (vw), 783 (w), 766 (vw), 755 (vw), 737 (w), 700 (vw), 674 (w).

¹H NMR (DMSO-*d*₆): 4.80–4.71 (*m*, 1H, CH), 4.57–4.50 (*m*, 1H, CH), 4.43–4.35 (*m*, 1H, CH), 4.11–3.98 (*m*, 2H, CH₂).

¹³C NMR (DMSO-*d*₆): 158.0 (CN₄), 58.7 (NCH₂), 49.3 (CH₂Cl), 47.3 (CHCl).

Elemental analysis C₄H₅Cl₂KN₆O₂ (279.13 g/mol): calc.: C, 17.21; H, 1.81; N, 30.11; found: C, 17.12; H, 1.81; N, 30.04.

$E_{dr} = 8.0 \text{ J}$ ($< 100 \text{ }\mu\text{m}$).

$F_r = 240 \text{ N}$ ($< 100 \text{ }\mu\text{m}$).

$E_{el} = 0.20 \text{ J}$ ($< 100 \text{ }\mu\text{m}$).

H₂O-sol. 12 wt% (22 °C).

6.2.2.4 Rubidium 1-(2,3-Dichloropropyl)-5-nitriminotetrazolate (9_Rb)

After recrystallization from H₂O, colorless crystals were obtained. Yield: 90 %.

M.p. 154 °C (dec., DSC-measurement, 5 K/min).

IR (Diamond-ATR, cm⁻¹): 2358 (m), 2331 (m), 1581 (w), 1490 (s), 1451 (m), 1427 (m), 1381 (m), 1327 (s), 1305 (s), 1284 (s), 1264 (s), 1244 (m), 1219 (m), 1179 (w), 1133 (vw), 1099 (w), 1028 (w), 979 (vw), 942 (vw), 919 (vw), 877 (w), 777 (w), 734 (w), 734 (w), 666 (w), 617 (w).

¹H NMR (DMSO-*d*₆): 4.80–4.71 (*m*, 1H, CH), 4.59–4.52 (*m*, 1H, CH), 4.45–4.37 (*m*, 1H, CH), 4.11–3.98 (*m*, 2H, CH₂).

¹³C NMR (DMSO-*d*₆): 157.3 (CN₄), 58.6 (NCH₂), 49.4 (CH₂Cl), 47.3 (CHCl).

Elemental analysis C₄H₅Cl₂N₆O₂Rb (325.50 g/mol): calc.: C, 14.76; H, 1.55; N, 25.82; found: C, 14.96; H, 1.57; N, 26.12.

E_{dr} = 4.0 J (100–500 μm).

F_r = 144 N (100–500 μm).

E_{el} = 0.20 J (< 100 μm).

Δ_cU = -2038 cal/g.

H₂O-sol. 13 wt% (22 °C).

6.2.2.5 Cesium 1-(2,3-Dichloropropyl)-5-nitriminotetrazolate (9_Cs)

After recrystallization from H₂O, colorless crystals suitable for X-ray diffraction were obtained. Yield: 92 %.

M.p. 163 °C (dec., DSC-measurement, 5 K/min).

IR (Diamond-ATR, cm⁻¹): 3000 (w), 2949 (vw), 2746 (vw), 1555 (vw), 1490 (s), 1451 (s), 1429 (m), 1384 (m), 1365 (w), 1324 (s), 1310 (s), 1249 (m), 1232 (m), 1221 (s), 1199 (m), 1130 (vw), 1104 (w), 1084 (w), 1028 (w), 975 (vw), 915 (vw), 879 (w), 799 (vw), 778 (w), 736 (vw), 719 (w), 696 (vw), 667 (w).

¹H NMR (DMSO-*d*₆): 4.75–4.69 (*m*, 1H, CH), 4.52–4.48 (*m*, 1H, CH), 4.39–4.33 (*m*, 1H, CH), 4.06–3.96 (*m*, 2H, CH₂).

¹³C NMR (DMSO-*d*₆): 158.0 (CN₄), 58.7 (NCH₂), 49.2 (CH₂Cl), 47.3 (CHCl).

Elemental analysis C₄H₅Cl₂CsN₆O₂ (372.95 g/mol): calc.: C, 12.88; H, 1.35; N, 22.53; Cl, 19.01; found: C, 12.75; H, 1.23; N, 22.56; Cl, 18.93.

E_{dr} = 7.0 J (100–500 μm).

F_r = 240 N (100–500 μm).

E_{el} = 0.30 J (100–500 μm).

Δ_cU = -1741 cal/g.

H₂O-sol. 10 wt% (22 °C).

6.2.2.6 Strontium 1-(2,3-Dichloropropyl)-5-nitriminotetrazolate Monohydrate (9_Sr)

After recrystallization from H₂O, a colorless powder was obtained. Yield: 93 %.

M.p. 189 °C (dec., DSC-measurement, 5 K/min).

IR (Diamond-ATR, cm⁻¹): 3530 (m), 3461 (m), 3015 (vw), 2953 (vw), 2919 (vw), 2846 (vw), 1623 (w), 1511 (m), 1463 (m), 1429 (m), 1387 (s), 1344 (s), 1307 (s), 1240 (m), 1134 (vw), 1110 (w), 1020 (m), 932 (vw), 884 (w), 771 (w), 753 (vw), 735 (w), 707 (w), 671 (w).

¹H NMR (DMSO-*d*₆): 4.75–4.70 (*m*, 1H, CH), 4.53–4.48 (*m*, 1H, CH), 4.39–4.34 (*m*, 1H, CH), 4.06–3.96 (*m*, 2H, CH₂).

¹³C NMR (DMSO-*d*₆): 157.9 (CN₄), 58.7 (NCH₂), 49.2 (CH₂Cl), 47.3 (CHCl).

Elemental analysis C₈H₁₂Cl₄N₁₂O₅Sr (585.69 g/mol): calc.: C, 16.41; H, 2.07; N, 28.70; Cl, 24.21; found: C, 16.29; H, 2.15; N, 28.66; Cl, 23.75.

E_{dr} = 5.0 J (100–500 μm).

F_r > 360 N (100–500 μm).

E_{el} = 0.20 J (100–500 μm).

Δ_cU = -2113 cal/g.

H₂O-sol. 8.7 wt% (22 °C).

6.2.2.7 Barium 1-(2,3-Dichloropropyl)-5-nitriminotetrazolate Monohydrate (9_Ba)

After recrystallization from H₂O, colorless crystals suitable for X-ray diffraction were obtained. Yield: 93 %.

M.p. 184 °C (dec., DSC-measurement, 5 K/min).

IR (Diamond-ATR, cm⁻¹): 3523 (w), 1625 (w), 1507 (m), 1461 (m), 1427 (m), 1382 (s), 1337 (s), 1308 (s), 1281 (m), 1266 (m), 1238 (m), 1188 (w), 1126 (vw), 1107 (m), 1019 (m), 989 (vw), 884 (vw), 871 (vw), 804 (vw), 769 (w), 754 (vw), 733 (ww), 705 (m), 698 (m), 669 (w).

¹H NMR (DMSO-*d*₆): 4.81–4.72 (*m*, 1H, CH), 4.58–4.51 (*m*, 1H, CH), 4.44–4.36 (*m*, 1H, CH), 4.11–3.98 (*m*, 2H, CH₂).

¹³C NMR (DMSO-*d*₆): 157.9 (CN₄), 58.8 (NCH₂), 49.3 (CH₂Cl), 47.3 (CHCl).

Elemental analysis C₈H₁₂BaCl₄N₁₂O₅ (635.40 g/mol): calc.: C, 15.12; H, 1.90; N, 26.45; found: C, 15.05; H, 2.11; N, 26.31.

E_{dr} = 5.0 J (100–250 μm).

F_r = 288 N (100–250 μm).

E_{el} = 0.20 J (100–250 μm).

H₂O-sol. 1.7 wt% (22 °C).

**6.2.2.8 Diaqua 1-(2,3-Dichloropropyl)-5-nitriminotetrazolato Copper(II)
(9_Cu_H₂O)**

A solution of 1.2 g (5.0 mmol) 1-(2,3-dichloropropyl)-5-nitriminotetrazole (**5**) in 20 mL H₂O was combined with 0.58 g (2.5 mmol) copper(II) nitrate pentahemihydrate in 5 mL H₂O. The green solution was stored at ambient temperature until a green solid was formed. It was filtered off and dried on air. Yield: 72 %.

M.p. 87 °C (loss of H₂O), 199 °C (dec., DSC-measurement, 5 K/min).

IR (Diamond-ATR, cm⁻¹): 3462 (m), 3001 (vw), 2957 (vw), 1625 (w), 1519 (m), 1463 (m), 1427 (m), 1395 (s), 1354 (m), 1291 (s), 1238 (s), 1143 (vw), 1113 (w), 1023 (m), 950 (vw), 915 (vw), 884 (w), 871 (w), 785 (vw), 766 (vw), 735 (w), 716 (w), 694 (vw), 672 (w).

Elemental analysis C₈H₁₄Cl₄CuN₁₂O₆ (579.63 g/mol): calc.: C, 16.58; H, 2.43; N, 29.00; found: C, 16.56; H, 2.41; N, 29.10.

E_{dr} = 6.0 J (100–500 μm).

F_r = 360 N (100–500 μm).

E_{el} = 0.20 J (100–500 μm).

Δ_cU = -2336 cal/g.

H₂O-sol. 0.7 wt% (22 °C).

**6.2.2.9 Diammine 1-(2,3-Dichloropropyl)-5-nitriminotetrazolato Copper(II)
(9_Cu_NH₃)**

A solution of 1.2 g (5.0 mmol) 1-(2,3-dichloropropyl)-5-nitriminotetrazole (**5**) in 20 mL H₂O was combined with 0.58 g (2.5 mmol) copper(II) nitrate pentahemihydrate in 5 mL H₂O and 1 mL aqueous ammonia solution (25 %). The dark blue solution was stored at ambient temperature until dark blue crystals were formed. They were filtered off, washed with H₂O and dried on air. Yield: 78 %.

M.p. 189 °C (dec., DSC-measurement, 5 K/min).

IR (Diamond-ATR, cm⁻¹): 3457 (w), 3353 (s), 3323 (m), 3264 (m), 3218 (m), 3172 (m), 2998 (w), 2959 (w), 1624 (vw), 1603 (vw), 1511 (s), 1458 (s), 1395 (s), 1342 (s), 1285 (vs), 1240 (vs), 1142 (vw), 1108 (w), 1030 (w), 1002 (vw), 974 (vw), 949 (vw), 871 (w), 801 (vw), 773 (w), 757 (vw), 734 (w), 712 (w), 690 (w), 670 (vw).

Elemental analysis C₈H₁₆Cl₄CuN₁₄O₄ (577.66 g/mol): calc.: C, 16.63; H, 2.79; N, 33.95; Cl, 24.55; found: C, 16.41; H, 2.82; N, 33.66; Cl, 24.10.

E_{dr} = 4.0 J (500–1000 μm).

F_r > 360 N (500–1000 μm).

E_{el} = 0.40 J (500–1000 μm).

Δ_cU = -2426 cal/g.

H₂O-sol. 0.8 wt% (22 °C).

6.3 Conclusion

The alkylation products of 5-aminotetrazole (**5-At**) with 3-chloro-1,2-propanediol, 1-(2,3-dihydroxypropyl)-5-aminotetrazole (**6a**) and 2-(2,3-dihydroxypropyl)-5-aminotetrazole (**6b**) were prepared and fully characterized. In analogy to **1-OH**, **6a** was nitrated to obtain 1-(2,3-dinitratopropyl)-5-nitriminotetrazolate monohydrate (**7**), which was extensively investigated and the molecular structure was discussed in detail. Its salts potassium 1-(2,3-dinitratopropyl)-5-nitriminotetrazolate (**7_K**), strontium 1-(2,3-dinitratopropyl)-5-nitriminotetrazolate monohydrate (**7_Sr**), barium 1-(2,3-dinitratopropyl)-5-nitriminotetrazolate monohydrate (**7_Ba**), and diaqua 1-(2,3-dinitratopropyl)-5-nitriminotetrazolato copper(II) (**7_Cu**) were prepared and fully characterized. Due to their very high sensitivity to impact, friction, and electric discharge, low decomposition temperatures (< 200 °C), and very vigorous combustion behavior in the flame of a BUNSEN burner, those salts are useless for an application as coloring agents in pyrotechnic compositions. However, the water-free salt **7_K** could be a promising primary explosive. A full characterization of the chlorine containing 5-aminotetrazoles 1-(2,3-dichloropropyl)-5-aminotetrazole (**8a**) and 2-(2,3-dichloropropyl)-5-aminotetrazole (**8b**) is given. The nitration product of **8a**, 1-(2,3-dichloropropyl)-5-nitriminotetrazole (**9**) as well as 1-(2,3-dichloropropyl)-5-nitriminotetrazole monohydrate (**9_H₂O**) were obtained and investigated extensively. The alkali and alkaline earth metal salts lithium 1-(2,3-dichloropropyl)-5-nitriminotetrazolate dihydrate (**9_Li**), sodium 1-(2,3-dichloropropyl)-5-nitriminotetrazolate trihemihydrate (**9_Na**), potassium 1-(2,3-dichloropropyl)-5-nitriminotetrazolate (**9_K**), rubidium 1-(2,3-dichloropropyl)-5-nitriminotetrazolate (**9_Rb**), cesium 1-(2,3-dichloropropyl)-5-nitriminotetrazolate (**9-Cs**), strontium 1-(2,3-dichloropropyl)-5-nitriminotetrazolate monohydrate (**9_Sr**), and barium 1-(2,3-dichloropropyl)-5-nitriminotetrazolate (**9_Ba**), as well as the copper(II) complexes diaqua 1-(2,3-dichloropropyl)-5-nitriminotetrazolato copper(II) (**9_Cu_H₂O**) and diammine 1-(2,3-dichloropropyl)-5-nitriminotetrazolato copper(II) (**9_Cu_NH₃**) were prepared and characterized using vibrational and multinuclear magnetic resonance spectroscopy, elemental analysis, and differential scanning calorimetry (DSC). The crystal structures of **7_K** and **9-Cs** were determined and discussed. Furthermore, their sensitivities to impact, friction and electric discharge were determined. The heats of formation of **9_K**, **9_Rb**, **9-Cs**, **9_Sr**, **9_Ba**, **9_Cu_H₂O**, and **9_Cu_NH₃** were calculated from bomb calorimetric measurements. The solubility in H₂O at ambient temperature, color performance and combustion properties of the pyrotechnically relevant salts **9_Li**, **9_Sr**, **9_Ba**, **9_Cu_H₂O**, and **9_Cu_NH₃** were analyzed with regard to their use as potential coloring agents in pyrotechnic compositions. All show good coloring properties, however the colors are slightly less intense than those of the corresponding salts of **3** (see chapter 4). Furthermore, they are less thermally stable, whereas their sensitivities are comparable and the solubility of **9_Sr** is significantly lower than the one of **3_Sr** (see chapter 4).

Altogether the pyrotechnic relevant salts of **9** are promising candidates as colorants in pyrotechnic compositions. In particular they are suitable as additives for enhancing the color purity and intensity in red, green, or blue light emitting perchlorate-free compositions.

6.4 References

- [1] B. T. Sturman: On the emitter of blue light in copper-containing pyrotechnic flames, *Propellants Explos. Pyrotech.* **2006**, *31*, 70–74.
- [2] J. A. Conkling: *Chemistry of Pyrotechnics: Basic Principles and Theory*. M. Dekker, Inc., New York, **1985**.
- [3] T. M. Klapötke, J. Stierstorfer, K. R. Tarantik: New Energetic Materials: Functionalized 1-Ethyl-5-aminotetrazoles and 1-Ethyl-5-nitriminotetrazoles, *Chem. Eur. J.* **2009**, *15*, 5775–5792.
- [4] J. Stierstorfer: Advanced Energetic Materials based on 5-Aminotetrazole, *PhD Thesis*, **2009**, Ludwig-Maximilian University, Munich.
- [5] M. Hesse, H. Meier, B. Zeeh, *Spektroskopische Methoden in der organischen Chemie*, 7. Ed., Thieme Verlag, Stuttgart, **2005**.
- [6] a) <http://www.bam.de> b) E_{dr} : insensitive > 40 J, less sensitive ≥ 35 J, sensitive ≥ 4 , very sensitive ≤ 3 J; F_r : insensitive > 360 N, less sensitive = 360 N, sensitive < 360 N > 80 N, very sensitive ≤ 80 N, extreme sensitive ≤ 10 N. According to the UN Recommendations on the Transport of Dangerous Goods.
- [7] T. M. Klapötke, J. Stierstorfer, K. R. Tarantik: Salts of 1-(2-chloroethyl)-5-nitriminotetrazole - new candidates for coloring agents in pyrotechnic compositions. *New Trends in Research of Energetic Materials*, Proceedings of the Seminar, 12th, Pardubice, Czech Republic, 1.–3. Apr. **2009**, Pt. 2, 647–665.
- [8] T. M. Klapötke, J. Stierstorfer, K. R. Tarantik: Pyrotechnically Relevant Salts of 1-(2-Chloroethyl)-5-nitriminotetrazole – Synthesis and Coloring Properties, *J. Pyrotech.* **2009**, *28*, 61–77.
- [9] <http://webbook.nist.gov/>
- [10] N. Wiberg, E. Wiberg, A. F. Holleman: *Lehrbuch der Anorganischen Chemie*, deGruyter, Berlin, 102. Ed., **2007**.

7 Salts of 1,2,4-Triazole Derivatives

1,2,4-Triazole derivatives were chosen as anions or ligands of potential pyrotechnically colorants, because of their high nitrogen content and the ability to be deprotonated or act as ligands in copper(II) complexes and they are or can be synthesized low cost starting materials. Furthermore, a higher thermal stability, lower solubility in H₂O as well as a lower sensitivity to impact, friction, and electric discharge of their compounds is expected compared to the corresponding tetrazoles.

The name triazole was first given to the aromatic heterocyclic ring system consisting of two carbon and three nitrogen atoms by BLADIN, who described derivatives of it in 1885.^[1] Several 1,2,4-triazole derivatives and their salts are described and characterized in literature (Figure 7.1).^[2, 3, 4] Most of them have potential to find application as pharmaceuticals, because of their antibacterial, antitumor or antiviral effects.^[5] 1,2,4-Triazoles can be prepared via the EINHORN-BRUNNER reaction using an imide and alkyl hydrazine or the PELLIZZARI reaction using an amide and a hydrazine.^[2, 6, 7] Synthesis of its isomer 1,2,3-triazole is usually carried out via a 1,3-dipolar (HUISGEN) cyclo addition of alkyl azides and acetylene derivatives.^[8]

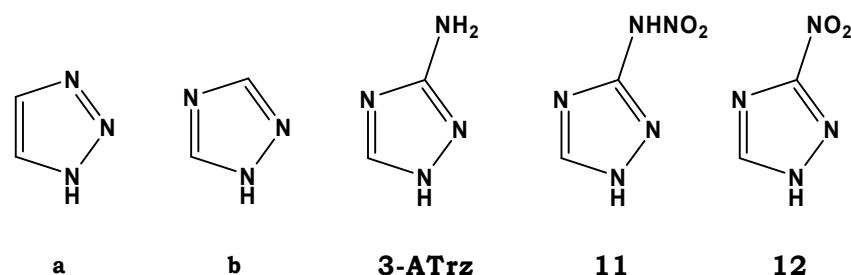


Figure 7.1 Chemical structure of 1H-1,2,3-triazole (**a**), 1H-1,2,4-triazole (**b**), 3-amino-1,2,4-triazole (**3ATrz**), 3-nitramino-1,2,4-triazole (**11**), and 3-nitro-1,2,4-triazole (**12**).

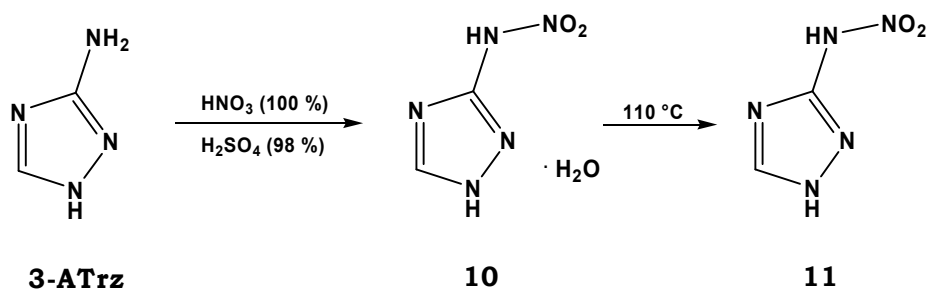
In this work the analogue of 5-aminotetrazole (**5-At**), 3-amino-1,2,4-triazole (**3ATrz**) was chosen as starting material, due of its expected similar reaction behavior. The literature known 1,2,4-triazoles, 3-nitramino-1,2,4-triazole monohydrate (**10**), 3-nitramino-1,2,4-triazole (**11**), and 3-nitro-1,2,4-triazole (**12**) were prepared and fully characterized. Furthermore, the alkylation product of **3ATrz**, 2-carboxymethyl-3-amino-1,2,4-triazole (**13**) and its nitration product 2-carboxymethyl-3-nitrimino-1,2,4-triazole monohydrate (**14**) were investigated.

Several alkali metal and alkaline earth metal salts and copper(II) complexes of the above mentioned 1,2,4-triazole derivatives were investigated also regarding their possible application as colorants in pyrotechnic compositions and compared to their corresponding tetrazole derivatives.

7.1 Results and Discussion

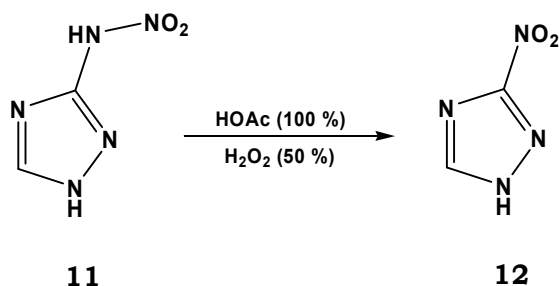
7.1.1 Syntheses

Starting from 3-amino-1,2,4-triazole (**3-ATrz**), the triazole analogue of 5-amino-tetrazole (**5-At**), the compounds 3-nitramino-1,2,4-triazole monohydrate (**10**) and 2-carboxymethyl-3-amino-1,2,4-triazole (**12**) were prepared. For the synthesis of **10**, **3-ATrz** was reacted with nitric acid (100 %) in concentrated sulfuric acid (Scheme 7.1) according to the literature.^[3a, 4] If **10** was stored at 110 °C for three days, the water-free compound 3-nitramino-1,2,4-triazole (**11**) was obtained in quantitative yields.^[3a, 4]



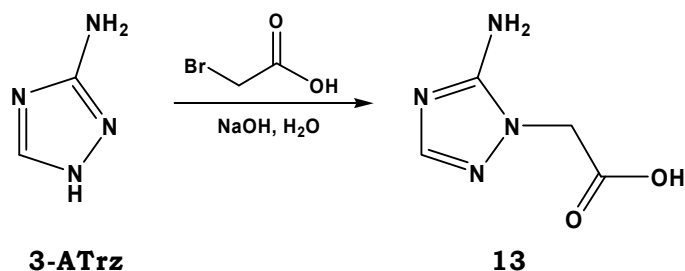
Scheme 7.1 Preparation of **10** and **11**.

The water-free compound **11** is required for the preparation of 3-nitro-1,2,4-triazole (**12**). Thereby, **11** is reacted with 50 % hydrogen peroxide in acetic acid (100 %) at 70 °C (Scheme 7.2). **12** is obtained as colorless precipitate, if the solvent is reduced under high vacuum.^[3a, 4]



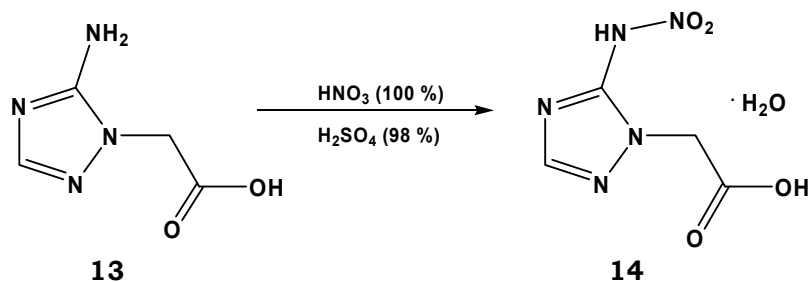
Scheme 7.2 Preparation of 3-nitro-1,2,4-triazole (**12**).

The preparation of 2-carboxymethyl-3-amino-1,2,4-triazole (**13**) was attempted analog to the alkylation of **5-At** with chloroacetic acid.^[9] However, the alkylation of **3-ATrz** was not successful. Therefore, the reaction was performed using the more reactive bromoacetic acid (Scheme 7.3). **13** could be obtained in yields above 50 % applying this method. The work up was analog to the one of 1-carboxymethyl-5-aminotetrazole using concentrated hydrochloric acid (**4**, chapter 5).^[9]



Scheme 7.3 Alkylation of **3-ATrz** with bromoacetic acid.

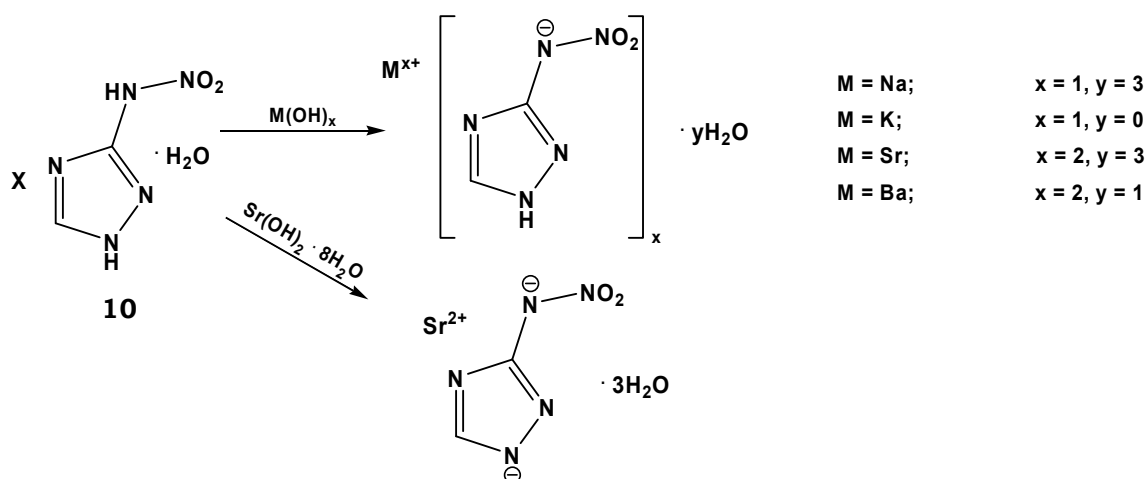
However, if the amount of concentrated hydrochloric acid was too large and the pH-value became less than 1, the salt 2-carboxymethyl-3-amino-1,2,4-triazolium chloride (**13_HCl**) was obtained.



Scheme 7.4 Nitration of **13** with nitric acid (100 %) and sulfuric acid (98 %).

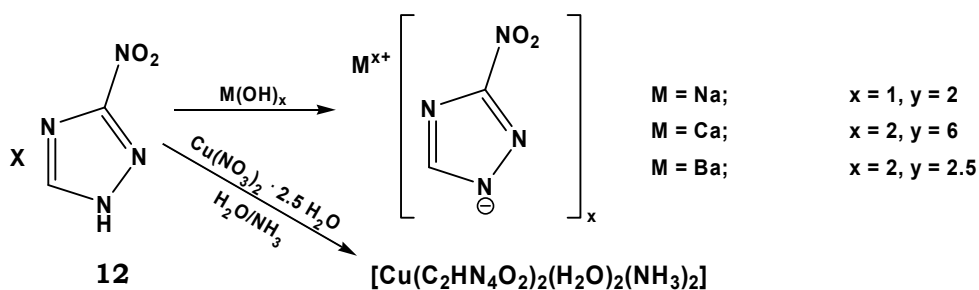
The nitration of **13** was performed analog to the synthesis of **10** using nitric and sulfuric acid (Scheme 7.4). After recrystallization from H₂O, 2-carboxymethyl-3-nitrimino-1,2,4-triazole monohydrate (**14**) was obtained as colorless crystals in lower yields than **10**. Removing the crystal water molecule of **14** should be possible in the analog way to **10**, but was not performed in this work.

The compounds **10**, **12**, **13**, and **14** were reacted with the hydroxides of lithium, sodium, potassium, rubidium, cesium, magnesium, calcium, strontium, and barium in H₂O. However, the deprotonation of the triazole derivatives was more challenging than in the case of the corresponding tetrazoles. In several cases the conversion was incomplete and the separation of educt and product was not possible. Furthermore, the alkali metal or alkaline earth metal carbonates were formed.



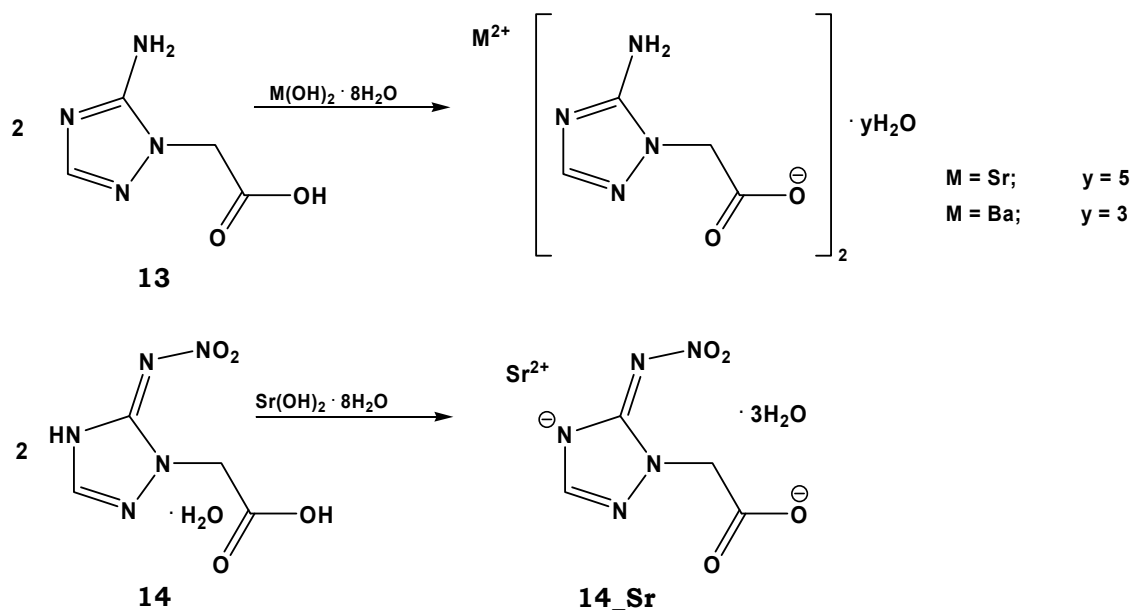
Scheme 7.5 Prepared salts of **10**.

The following salts of **10** could be obtained (Scheme 7.5): sodium 3-nitramino-1,2,4-triazolate trihydrate (**10_Na**), potassium 3-nitramino-1,2,4-triazolate (**10_K**), strontium bis(3-nitramino-1,2,4-triazolate) trihydrate (**10_Sr1**), strontium 3-nitramino-1,2,4-triazolate trihydrate (**10_Sr2**), and barium bis(3-nitramino-1,2,4-triazolate) monohydrate (**10_Ba**).



Scheme 7.6 Prepared compounds of **12**.

The salts sodium 3-nitro-1,2,4-triazolate dihydrate (**12_Na**), calcium bis(3-nitro-1,2,4-triazolate) hexahydrate (**12_Ca**), and barium bis(3-nitro-1,2,4-triazolate) pentahydrate (**12_Ba**) as well as the copper(II) compound *trans*-bis(diammine diaqua 3-nitro-1,2,4-triazolato-*N*1) copper(II) (**12_Cu**) were yielded from **12** (Scheme 7.6). **12_Cu** is described in the literature and characterized only marginally.^[3d]



Scheme 7.7 Prepared alkaline earth metal salts of **13** and **14**.

Furthermore, the alkaline earth metal salts strontium bis[2-(3-amino-1,2,4-triazol-2-yl)-acetate] pentahydrate (**13_Sr**), barium bis[2-(3-amino-1,2,4-triazol-2-yl)-acetate] trihydrate (**13_Ba**), and strontium 2-(3-nitrimino-1,2,4-triazolate)-acetate trihydrate (**14_Sr**) were obtained (Scheme 7.7).

7.1.2 Analytical Data of the Precursor Molecules

7.1.2.1 Spectroscopy

For determining the conversion and purity of the compounds **10–14** NMR spectroscopy, in particular ^1H and ^{13}C NMR spectra, were measured. DMSO- d_6 was used as solvent. Furthermore, IR and Raman spectroscopy were performed.

Two signals can be observed in the ^1H NMR spectra of 3-nitramino-1,2,4-triazole monohydrate (**10**) and 3-nitramino-1,2,4-triazole (**11**). At 14.17 ppm a broad singlet caused by the hydrogen atom at N1 and at 8.49 ppm a sharp singlet caused by the hydrogen atom at C2. The signals are shifted to lower field compared to the ones of 3-amino-1,2,4-triazole (**3ATrz**) at 12.21 ppm and 7.48 ppm. The shifts are comparable to the ones of 5-nitrimino-tetrazoles and can be explained by orbital effects.^[10, 11, 12] Signals for the hydrogen atom of the nitramino group could not be observed, presumably because it is too broad. As expected, two signals can be observed in the ^{13}C NMR spectra at 152.1 ppm (CNHNO₂, C1) and 138.9 ppm (CH, C2). Both signals are shifted to higher fields compared to the ones of **3ATrz** (157.9 ppm and 147.5 ppm). Only two signals were observed in the ^{14}N NMR spectrum of **10**, caused by the nitrogen atom of the nitro group (NO₂: -17 ppm) and a nitrogen atom of the ring (NH: -6 ppm).

The ^1H NMR spectrum of 3-nitro-1,2,4-triazole (**12**) shows as expected two signals.

The singlet of the hydrogen atom at N1 at 15.26 ppm and the one of the hydrogen atom at C2 at 8.87 ppm. Compared to **10** or **11** the signals are shifted to lower field, because of the nitro group. The ^{13}C NMR spectrum of **12** shows two signals (C1: 163.0 ppm, C2: 146.2 ppm). Especially the signal of C1 is much more shifted to lower field than in **10**. The characteristic vibrations of N–H can be observed 3483 cm^{-1} and 3447 cm^{-1} (valence vibrations) as well as at 1585 cm^{-1} and 1536 cm^{-1} (bending vibration) are also observable in the IR spectrum of **10** and **11**. The intensive signal at 1297 cm^{-1} is caused by the vibration of the nitro group.^[13]

The ^1H NMR spectrum of 2-carboxymethyl-3-amino-1,2,4-triazole (**13**) shows three singlets at 7.31 ppm (CH), 6.23 ppm (NH_2), and 4.65 ppm (CH_2). The signal of the hydrogen atom of the carboxy group could not be found, because of its strong shift to lower field. All signals of the four carbon atoms can be found in the ^{13}C NMR spectrum at 169.1 ppm (COOH , C4), 155.8 ppm (CNH_2 , C1), 148.4 ppm (CH, C2), and 47.5 ppm (CH_2 , C3). The signals of the triazole ring carbon atoms and the hydrogen atoms are comparable to the ones of **3ATrz**. The signals of the carboxymethyl residues are analog to the ones of 1-carboxymethyl-5-aminotetrazole (**4**). In the IR spectrum of **13** at 3152 cm^{-1} the valence vibration and at 1559 cm^{-1} the bending vibration of N–H can be observed as well as the C–H valence vibration at 2985 cm^{-1} and the C–H bending vibration of the CH_2 group at 1390 cm^{-1} .^[13]

In the IR spectrum of 3-carboxymethyl-1,2,4-triazolium chloride (**13 HCl**) the O–H stretching vibration of the carboxy group is observed at 3157 cm^{-1} , as well as at 3115 cm^{-1} the N–H stretching vibration of the protonated triazole ring.^[13]

Analog to **13**, in the ^1H NMR spectrum of 2-carboxymethyl-3-nitrimino-1,2,4-triazole monohydrate (**14**) the signal of the hydrogen atom at the carboxymethyl residue can not be observed as well as the signal of the crystal water. Therefore, only two singlets at 8.52 ppm (CH) and 4.79 ppm (CH_2) are observable. The ^{13}C NMR spectrum shows all four carbon signals (C4: 167.7 ppm, C1: 150.3 ppm, C2: 138.4 ppm). They are shifted to higher fields compared to the ones of **13**, except the one of C3 (48.7 ppm). In the IR spectrum of **14** the analog vibrations of N–H and C–H are observable. Additionally, at 1271 cm^{-1} a very strong signal of the symmetric valence vibration of the nitrimino group appears.^[13]

7.1.2.2 Molecular Structures

After recrystallization from H_2O , single crystals of **13**, **13 HCl**, and **14**, suitable for X-ray diffraction could be obtained. All relevant data and parameters of the X-ray measurements and refinements are given in Appendix VII. The molecular structure of **12** in the solid state is discussed in reference ^[3b].

2-Carboxymethyl-3-amino-1,2,4-triazole (**13**) crystallizes in the orthorhombic space group $Pca2_1$ with eight molecules per unit cell. Its density of 1.609 g/cm^3 is significantly lower than the one of its tetrazole derivative 1-carboxymethyl-5-aminotetrazole (**4**, 1.660 g/cm^3).

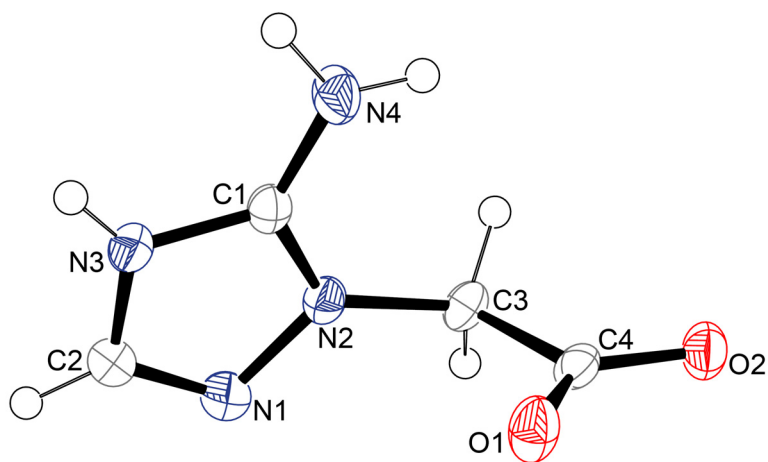


Figure 7.2 Molecular unit of **13**. Hydrogen atoms are shown as spheres of arbitrary radius and thermal displacements are set at 50 % probability. Geometries: distances (Å) N1–N2 1.388(4), N1–C2 1.294(4), N3–C1 1.339(3), N3–C2 1.371(4), N2–C1 1.332(3), N4–C1 1.322(4), N2–C3 1.440(4), C3–C4 1.534(4), O1–C4 1.248(3), O2–C4 1.253(3); angles (°) C1–N2–N1 110.7(2), C1–N2–C3 127.4(2), N1–N2–C3 121.8(2), O1–C4–O2 127.1(2), O1–C4–C3 118.1(2), O2–C4–C3 114.8(2), C1–N3–C2 106.6(2), N2–C3–C4 113.8(2), N1–C2–N3 111.9(3); torsion angles (°) C1–N2–C3–C4 72.6(4), N1–N2–C3–C4 –103.4(3), O1–C4–C3–N2 11.7(4), O2–C4–C3–N2 –168.9(2), N1–N2–C1–N4 –179.5(3), C3–N2–C1–N4 4.1(5), N1–N2–C1–N3 0.0(3), C3–N2–C1–N3 –176.4(3), C2–N3–C1–N4 178.8(3), C2–N3–C1–N2 –0.8(3), C1–N2–N1–C2 0.8(3), C3–N2–N1–C2 177.5(3), N2–N1–C2–N3 –1.3(3), C1–N3–C2–N1 1.4(3).

Interestingly, **13** has a zwitterionic structure (Figure 7.2). The carboxy group is deprotonated and has a negative charge and N3 of the triazole ring is protonated and has a positive charge. The N–N and C–N bond lengths in the triazole ring are smaller than the corresponding single bond lengths (N–N: 1.48 Å, C–N: 1.47 Å)^[14]. This is consistent with the aromaticity of the triazole ring. The bond length of C1–N4 lies in between a C–N single bond and C–N double bond (1.22 Å)^[14] with 1.322(4) Å. The packing in **13** is characterized by layers along the *b* axis. Two of them are connected via hydrogen bonds. In each case a nitrogen atom of the amine group is the donor and an oxygen atom of the carboxy group acts as acceptor (N4–H4a···O4*i*: 0.83(3) Å, 2.01(3) Å, 2.819(3) Å, 164(3)°, N4–H4b···O2*ii*: 0.96(3) Å, 1.84(3) Å, 2.797(2) Å, 175(3)°, N3–H3···O1*ii*: 0.84(2) Å, 1.91(2) Å, 2.737(2) Å, 168(2)°; *i*) –*x*+3/2, *y*, *z*–1/2, *ii*) *x*+1/2, –*y*+1, *z*).

The ratio of data to parameters is quite low (5.9), due to the refinement of the FLACK parameter^[15] led to an inconclusive value^[16] of –10(10). This is generally the case with light atom Mo–K α data, where μ is nearly zero. Therefore, the FRIEDEL equivalents were merged before the final refinement with a MERG 4 command.

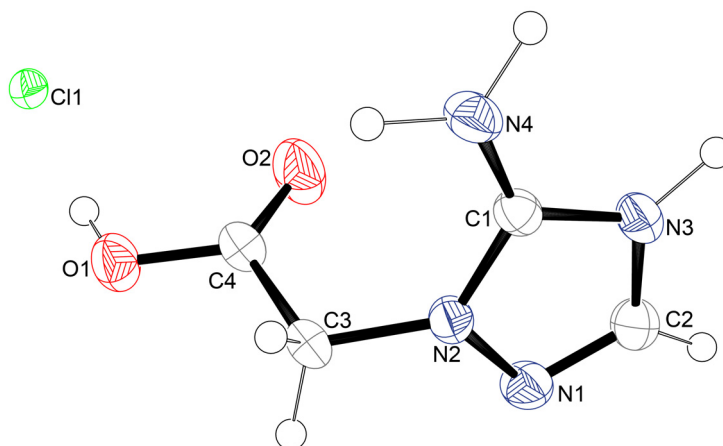


Figure 7.3 Molecular unit of **13_HCl**. Hydrogen atoms are shown as spheres of arbitrary radius and thermal displacements are set at 50 % probability. Geometries: distances (Å) N1–N2 1.382(4), N1–C2 1.291(4), N3–C1 1.345(4), N3–C2 1.363(5), N2–C1 1.335(4), N4–C1 1.323(4), N2–C3 1.439(4), C3–C4 1.518(5), O1–C4 1.322(4), O2–C4 1.198(4); angles (°) C1–N2–N1 111.2(3), C1–N2–C3 126.1(3), N1–N2–C3 121.0(3), O1–C4–O2 125.0(3), O1–C4–C3 111.7(3), O2–C4–C3 123.3(3), C1–N3–C2 106.7(3), N2–C3–C4 110.1(2), N1–C2–N3 112.3(3), C2–N1–N2 103.8(3), N4–C1–N2 126.8(3), N4–C1–N3 127.1(3), N2–C1–N3 106.0(3); torsion angles (°) C1–N2–C3–C4 69.5(4), N1–N2–C3–C4 -94.4(3), O1–C4–C3–N2 -178.1(3), O2–C4–C3–N2 2.2(5), N1–N2–C1–N4 -178.3(3), C3–N2–C1–N4 16.4(5), N1–N2–C1–N3 -2.1(3), C3–N2–C1–N3 -167.4(3), C2–N3–C1–N4 177.4(3), C2–N3–C1–N2 1.3(3), C1–N2–N1–C2 2.1(4), C3–N2–N1–C2 168.2(3), N2–N1–C2–N3 -1.2(4), C1–N3–C2–N1 -0.1(4).

The molecular unit of the chloride salt of **13**, 2-carboxymethyl-3-amino-1,2,4-triazolium chloride (**13_H₂O**) is depicted in Figure 7.3. It crystallizes in the triclinic space group *P*-1 with two molecular units per unit cell and a density of 1.586 g/cm³. In the case of **13_HCl** the carboxy group as well as N3 is protonated and the chloride anion serves as counterion. The packing in **13_HCl** is characterized by layers along the *a* axis. Within these layers the molecules are connected via a hydrogen bond (N4–H4b···N1*i*: 0.98(5) Å, 2.21(5) Å, 3.050(4) Å, 143(4)°; *i*) *x*+1, *y*, *z*). One hydrogen bond can be found between two layers (N4–H4b···O2*ii*: 0.98(5) Å, 2.32(5) Å, 2.911(4) Å, 118(3)°, *ii*) *-x*+2, *-y*+1, *-z*). The chloride anion is acceptor in three further hydrogen bonds (N4–H4a···Cl*iii*: 1.01(5) Å, 2.27(5) Å, 3.253(4) Å, 165(4)°, N3–H3···Cl*ii*: 1.00(4) Å, 2.24(5) Å, 3.236(3) Å, 175(4)°, O1–H1···Cl: 0.80(5) Å, 2.27(5) Å, 3.061(3) Å, 169(5)°; *iii*) *-x*+2, *-y*+2, *-z*). The bond lengths and angles of the triazolium ion are comparable to the ones in **13**.

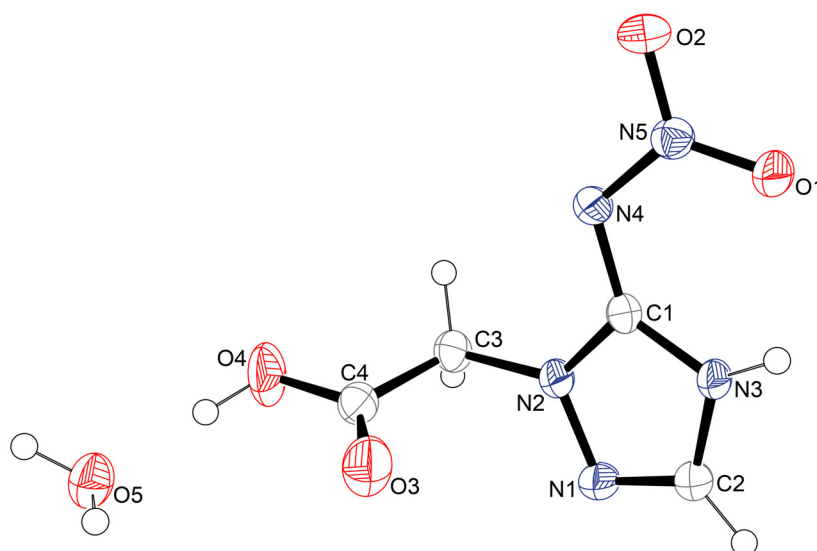


Figure 7.4 Molecular unit of **14**. Hydrogen atoms are shown as spheres of arbitrary radius and thermal displacements are set at 50 % probability. Geometries: distances (Å) N1–N2 1.376(2), N1–C2 1.296(2), N3–C1 1.347(2), N3–C2 1.362(2), N2–C1 1.340(2), N4–C1 1.347(2), N4–N5 1.336(2), O1–N5 1.241(2), O2–N5 1.250(1), N2–C3 1.444(2), C3–C4 1.507(2), O3–C4 1.195(2), O2–C4 1.300(2); angles (°) C2–N1–N2 104.2(1), N1–C2–N3 111.6(1), C1–N2–N1 111.5(1), C1–N2–C3 127.7(1), N1–N2–C3 120.8(1), N5–N4–C1 114.9(1), O1–N5–O2 120.5(1), O1–N5–N4 122.9(1), O2–N5–N4 116.6(1), N2–C1–N4 119.2(1), N2–C1–N3 105.3(1), N4–C1–N3 135.5(1), C1–N3–C2 107.5(1), O3–C4–O4 125.5(2), O3–C4–C3 123.1(2), O4–C4–C3 111.5(2), N2–C3–C4 111.4(1); torsion angles (°) N2–N1–C2–N3 0.2(2), C2–N1–N2–C1 -0.4(2), C2–N1–N2–C3 -177.1(1), C1–N4–N5–O1 3.4(2), C1–N4–N5–O2 -176.5(1), N1–N2–C1–N4 -17.0(1), C3–N2–C1–N4 -2.5(2), N1–N2–C1–N3 0.3(2), C3–N2–C1–N3 176.8(1), N5–N4–C1–N2 -175.6(1), N5–N4–C1–N3 5.4(2), N2–C1–N3–C2 -0.2(2), N4–C1–N3–C2 178.9(2), N1–C2–N3–C1 -0.1(2), C1–N2–C3–C4 -103.6(2), N1–N2–C3–C4 72.6(2), O3–C4–C3–N2 -2.3(2), O4–C4–C3–N2 177.3(1).

The nitrimino derivative of **13**, 2-carboxymethyl-3-nitrimino-1,2,4-triazole monohydrate (**14**), crystallizes in the monoclinic space group $P2_1/c$ with four molecules per unit cell (Figure 7.4). Its density of 1.655 g/cm³ is slightly higher than the one of **13**, but significantly lower than the one of its 5-nitriminotetrazole derivative (**5**, 1.725 g/cm³). In contrast to **13**, **14** is not zwitterionic. Besides that, it is a nitrimino- and not a nitramino-triazole. The nitrogen atom N3 carries a proton instead of N4. Furthermore, the bond length of N4–N5 lies in between a N–N single (1.48 Å) and double bond (1.25 Å) with 1.336(2) Å.^[14] This is also true for the bond length of C1 and N4. As expected the N–O bond lengths are between a N–O single (1.45 Å) and double bond (1.17 Å). Further bond lengths are comparable to the ones in **13**. The oxygen atom of the crystal water molecule acts in two hydrogen bonds as donor atom (O5–H5b···N1*i*: 0.88(2) Å, 2.06(2) Å, 2.925(2) Å, 171(2)°, O5–H5a···O3*ii*: 0.78(2) Å, 1.98(2) Å, 2.762(2) Å, 178(2)°; *i*) $-x+2, y-1/2, -z+1/2$, *ii*) $-x+2, -y+2, -z+1$) and in one as acceptor atom (O4–H4···O5: 0.95(2) Å, 1.63(2) Å, 2.575(2) Å, 175(2)°). In three further hydrogen bonds N3 is the donor atom and each atom of the nitro group acts as donor (N3–H3···O2*iii*: 0.86(2) Å, 2.20(2) Å, 3.051(2) Å, 172(1)°, N3–H3···O1*iii*: 0.86(2) Å, 2.49(2) Å, 2.981(2) Å, 118(1)°, N3–H3···N5*iii*: 0.86(2) Å, 2.69(2) Å, 3.431(2) Å, 145(1)°; *iii*) $-x+1, y+1/2, -z+1/2$).

7.1.2.3 Energetic Properties

The energetic properties, such as decomposition temperature (T_{dec}), sensitivity to impact (E_{dr}), friction (F_{r}) and electric discharge (E_{el}), as well as combustion energy ($\Delta_{\text{c}}U$) were determined. An overview of the energetic properties of the compounds **10**, **11**, **12**, **13**, **13_HCl**, and **14** is given in Table 7.1.

Table 7.1 Overview of the physico-chemical properties of **10**, **11**, **12**, **13**, **13_HCl**, and **14**.

	10	11	12	13	13_HCl	14
Formula	$\text{C}_2\text{H}_5\text{N}_5\text{O}_3$	$\text{C}_2\text{H}_3\text{N}_5\text{O}_2$	$\text{C}_2\text{H}_2\text{N}_4\text{O}_2$	$\text{C}_4\text{H}_6\text{N}_4\text{O}_2$	$\text{C}_4\text{H}_7\text{ClN}_4\text{O}_2$	$\text{C}_4\text{H}_7\text{N}_5\text{O}_5$
M [g/mol]	147.09	129.08	114.06	142.12	178.58	205.13
E_{dr} [J]^a	> 100	3.0	3.4	> 100	> 100	6.0
F_{r} [N]^b	216	192	235	> 360	> 360	324
E_{el} [J]^c	1.0	0.15	0.40	1.5	2.0	0.30
grain size [μm]	500–1000	100–250	100–500	250–500	500–1000	250–500
N [%]^d	47.6	54.3	49.1	39.4	31.4	34.1
Ω [%]^e	-38 (CO ₂) -16 (CO)	-43 (CO ₂) -19 (CO)	-42 (CO ₂) -14 (CO)	-101 (CO ₂) -55 (CO)	-81 (CO ₂) -45 (CO)	-51 (CO ₂) -19 (CO)
T_{dec} [°C]^f	215	218	294	291	> 400	207
ρ [g/cm³]^g	1.83* (23 °C)	2.52* (23 °C)	1.75* (23 °C)	1.61	1.59	1.66
$\Delta_{\text{c}}U$ [kJ/kg]^h	-8654	-10740	-9998	-14725	-10933	-10362
$\Delta_{\text{c}}H^{\circ}$ [kJ/mol]ⁱ	-1266	-1379	-1134	-2089	-1946	-2118
$\Delta_{\text{f}}H^{\circ}$ [kJ/mol]^j	-236	163	61	-343	-578	-457

a) BAM drop hammer [17], b) BAM methods [17], c) Electric discharge tester, d) Nitrogen content, e) Oxygen balance, f) Decomposition temperature from DSC ($\beta = 5$ K/min), g) determined by X-ray crystallography or pycnometer (*), h) Combustion energy, i) Enthalpy of combustion, j) Molar enthalpy of formation.

The compounds **10**, **13**, and **13_HCl** are insensitive to impact, whereas **12** and **14** are sensitive ($E_{\text{dr}} = 3.4$ J and 6.0 J) and **11** is even very sensitive to impact ($E_{\text{dr}} = 3.0$ J). **13** and its chloride salt are also insensitive to friction. All others are sensitive to friction. The compounds **11**, **12**, and **14** also offer a higher sensitivity to electric discharge than **13** and **13_HCl**.

Compound **10** has the best oxygen balance regarding the formation of CO₂ (-38 %). If the formation of CO is considered, **12** has the largest negative value (-14 %).

The decomposition temperatures of **10–14** are above 200 °C (Figure 7.5). In the DSC thermograms of **10** and **14** the loss of crystal water can be observed at 94 °C and 91 °C, respectively. **12** and **13** melt before they decompose. In the case of **12** the phase transitions are significantly separated ($T_{\text{m}} = 215$ °C, $T_{\text{dec}} = 294$ °C), whereas **13** decomposes directly after melting. **13_HCl** shows two endothermic signals at 224 °C and 263 °C, but no exothermic one below 400 °C.

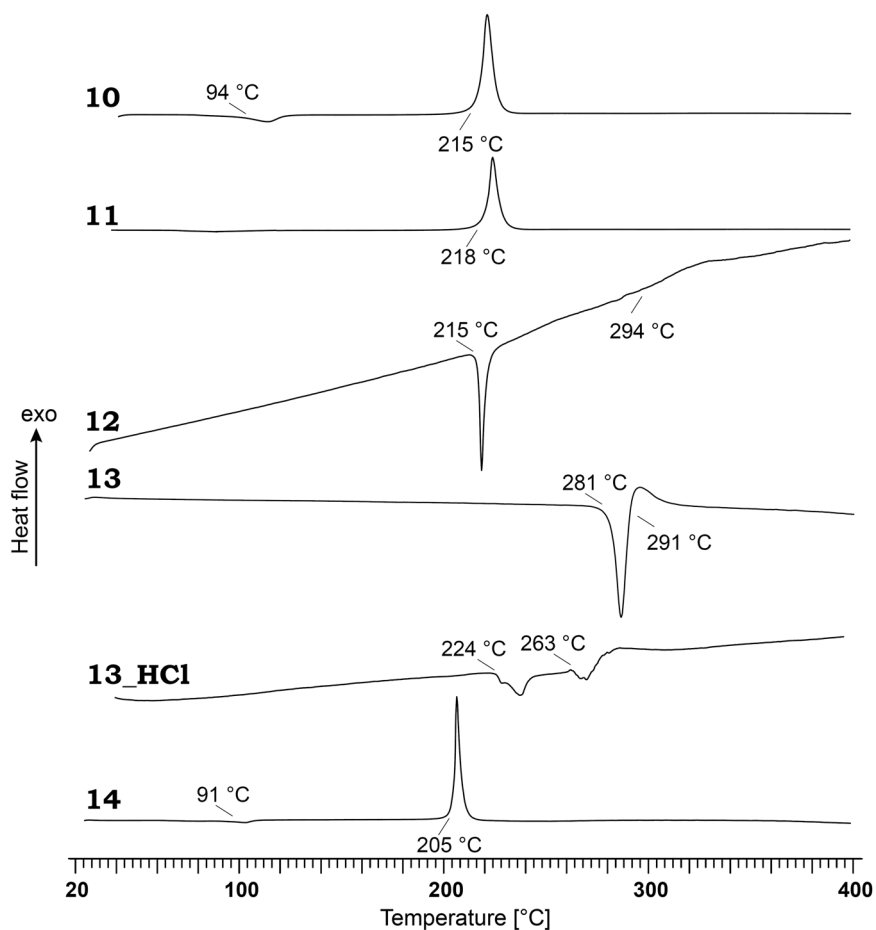


Figure 7.5 DSC thermograms of **10–14** and **13_HCl** in a temperature range of 20 °C–400 °C. Decomposition points are given as onset temperatures.

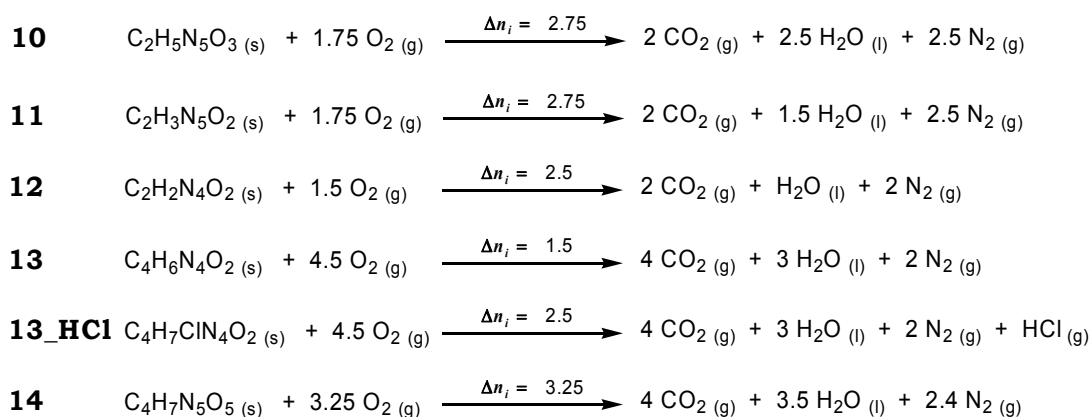
The reported values of the combustion energy ($\Delta_c U$) are the average of three single bomb calorimetry measurements. The standard molar enthalpy of combustion ($\Delta_c H^\circ$) was derived from equation 7.1.

$$\Delta_c H^\circ = \Delta_c U + \Delta n RT \quad (7.1)$$

$$\Delta n = \sum n_i (\text{gaseous products}) - \sum n_i (\text{gaseous educts})$$

n_i = molar amount of gas i .

The enthalpies of formation ($\Delta_f H^\circ$) for the compounds **10–14** were calculated at 298.15 K using the HESS thermochemical cycle and the following combustion reactions (Scheme 7.8).



Scheme 7.8 Combustion equations of the compounds **10–14**.

Except of **11** and **12** ($\Delta_f H^\circ = 163$ kJ/mol and 61 kJ/mol), the compounds are calculated to be formed exothermically. These values are between -578 kJ/mol and -236 kJ/mol.

The heats of formation of the combustion products $\text{H}_2\text{O} (\text{l})$ (-286 kJ/mol), $\text{CO}_2 (\text{g})$ (-393 kJ/mol), and $\text{HCl} (\text{g})$ (-92.3 kJ/mol) were adopted from literature.^[18]

7.1.3 Analytical Data of the Salts

7.1.3.1 Molecular Structures

After recrystallization from H_2O , single crystals of the salts **10_Na**, **10_K**, **10_Sr1**, **12_Na**, **12_Ca**, **12_Cu**, **13_Sr**, **13_Ba**, and **14_Sr** suitable for X-ray diffraction could be obtained. All relevant data and parameters of the X-ray measurements and refinements are given in Appendix VII.

The sodium salt of **10**, sodium 3-nitramino-1,2,4-triazolate trihydrate (**10_Na**), crystallizes in the monoclinic space group $P2_1/c$ with four molecular units per unit cell and a density of 1.651 g/cm³. Its molecular unit is depicted in Figure 7.6.

The sodium atoms are coordinated sixfold by the atoms O3, O4, O1*i*, O2*ii*, O3*iii*, and N1 (*i*) $x, -y+3/2, z+1/2$, *ii*) $x, y, z+1$, *iii*) $-x+1, -y+1, -z+2$) forming a distorted octahedron. Layers of connected dimers along the *b* axis are formed. Thereby, two nearby sodium atoms are bridged by one crystal water molecule (O3). The shortest observed distance between two sodium ions is $3.625(1)$ Å. The ionic radius of sixfold coordinated sodium atoms is 1.16 Å.^[14]

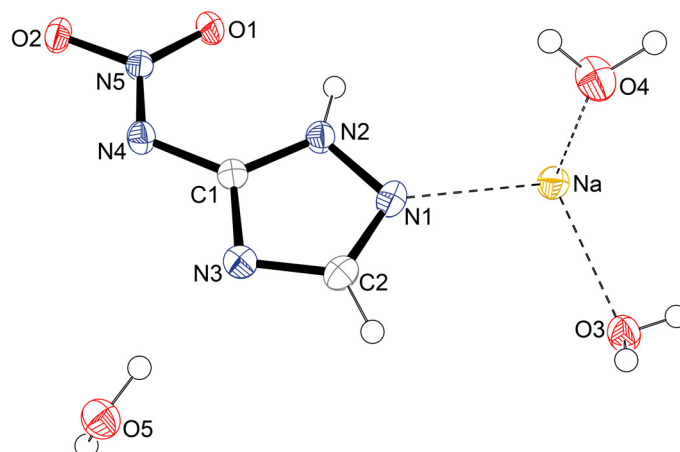


Figure 7.6 Molecular unit of **10_Na**. Hydrogen atoms are shown as spheres of arbitrary radius and thermal displacements are set at 50 % probability. Selected geometries: distances (Å) C1–N4 1.390(2), N4–N5 1.301(2), N5–O1 1.252(2), N5–O2 1.283(1), Na–O3 2.343(1), Na–O4 2.392(1), Na–O1*i* 2.394(1), Na–O2*ii* 2.417(1), Na–O3*iii* 2.436(1), Na–N1 2.460(1); angles (°) N2–C1–N4 130.5(1), C1–N4–N5 117.0(1), N4–N5–O1 124.5(1), N4–N5–O2 116.4(1), O1–N5–O2 119.1(1), O3–Na–O4 104.4(1), O3–Na–O1*i* 157.9(1), O4–Na–O1*i* 83.1(0), O3–Na–O2*ii* 87.6(0), O4–Na–O2*ii* 89.5(0), O3–Na–N1 101.2(1), O4–Na–N1 84.8(0), O1*i*–Na–N1 100.1(0), O2*ii*–Na–N1 170.4(1); torsion angles (°) N2–C1–N4–N5 11.9(2), C1–N4–N5–O1 -0.1(2), C1–N4–N5–O2 178.3(1), O3–Na–N1–C2 -6.7(1), O4–Na–N1–C2 -110.4(1), O3–Na–N1–N2 -163.5(1), O4–Na–N1–N2 92.8(1); *i*) $x, -y+3/2, z+1/2$, *ii*) $x, y, z+1$, *iii*) $-x+1, -y+1, -z+2$.

The crystal water molecule (O5), which is not coordinated to the sodium atom is located between the layers, but is connected via hydrogen bonds (O4–H4a···O5*iv*: 0.90(2) Å, 1.93(2) Å, 2.826(2) Å, 173(2)°, O5–H5b···O2*v*: 0.85(2) Å, 2.12(2) Å, 2.955(2) Å, 171(2)°, O5–H5a···N3: 0.85(2) Å, 1.99(2) Å, 2.840(2) Å, 173(2)°, O4–H4b···O5*vi*: 0.82(1) Å, 2.06(1) Å, 2.850(2) Å, 161(2); *iv*) $-x, y+1/2, -z+3/2$, *v*) $-x+1, y-1/2, -z+1/2$, *vi*) $-x, -y+1, -z+1$). Three further hydrogen bonds are between the anions and the crystal water molecules (N2–H1···O2*i*: 0.86(2) Å, 2.11(2) Å, 2.960(2) Å, 168(1)°, O3–H3b···N4*ii*: 0.77(2) Å, 2.11(2) Å, 2.863(2) Å, 168(2)°, O3–H3a···O4*vi*: 0.83(2) Å, 2.02(2) Å, 2.834(2) Å, 168(2)°; *vii*) $-x, -y+1, -z+2$).

Potassium 3-nitramino-1,2,4-triazolate (**10_K**) crystallizes in the monoclinic space group $P2_1$ with two molecules per unit cell. The molecular unit of **10_K** is depicted in Figure 7.7. Its density of 1.988 g/cm³ is significantly higher than the one of **10_Na**. One reason for this might be the absence of crystal water in **10_K**. The potassium atoms are coordinated eightfold regarding distances up to 3.2 Å. Coordinating atoms are O2*i*, O2*ii*, N1*iii*, N4*ii*, O1*i*, N3, N4, and O1*iv* (*i*) $-x, y+1/2, -z+2$, *ii*) $x+1, y, z$, *iii*) $-x+1, y+1/2, -z+1$, *iv*) $-x+1, y+1/2, -z+2$). One intramolecular hydrogen bond between N2 and O1 can be observed (N2–H1···O1: 0.77 Å, 2.25 Å, 2.626 Å, 110.5°) and one intermolecular hydrogen bond (N2–H1···N3*v*: 0.77 Å, 2.22 Å, 2.937 Å, 155.5°; *v*) $-x, y-1/2, -z+1$).

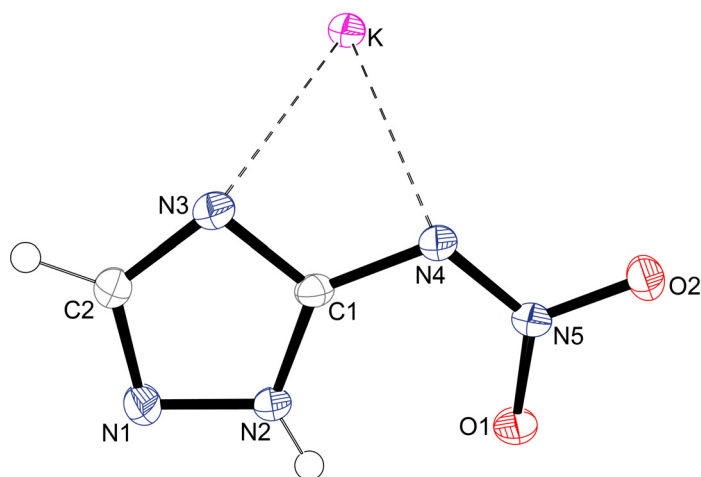


Figure 7.7 Molecular unit of **10_K**. Hydrogen atoms are shown as spheres of arbitrary radius and thermal displacements are set at 50 % probability. Selected geometries: distances (Å) C1–N4 1.382(2), N4–N5 1.307(2), N5–O1 1.262(2), N5–O2 1.265(2), K–O2*i* 2.720(1), K–O2*ii* 2.797(1), K–N1*iii* 2.807(1), K–N4*ii* 2.860(1), K–O1*i* 2.871(1), K–N3 3.051(1), K–N4 3.077(1), K–O1*iv* 3.147(1); angles (°) N2–C1–N4 131.9(1), C1–N4–N5 117.6(1), N4–N5–O1 124.4(1), N4–N5–O2 115.8(1), O1–N5–O2 119.8(1), N3–K–N4 44.84(4), O2*i*–K–O2*ii* 138.14(1); torsion angles (°) N1–N2–C1–N4 178.2(2), N2–C1–N4–N5 2.5(3), C1–N4–N5–O1 6.1(2), C1–N4–N5–O2 –174.1(1), O2*i*–K–N4–N5 41.7(1); *i*) $-x, y+1/2, -z+2$, *ii*) $x+1, y, z$, *iii*) $-x+1, y+1/2, -z+1$, *iv*) $-x+1, y+1/2, -z+2$.

The molecular unit of strontium bis(3-nitramino-1,2,4-triazolate) trihydrate (**10_Sr1**) is depicted in Figure 7.8. It crystallizes in the orthorhombic space group *Pbca* with eight molecular units per unit cell and a density of 2.109 g/cm³. This value is slightly lower than the one of its 5-nitriminotetrazole analog strontium bis(5-nitrimino-1*H*-tetrazolate) tetrahydrate (**Sr1HAtNO2**, chapter 9).^[12, 19] The strontium atoms are coordinated by the oxygen atoms of the three crystal water molecules (O5, O6, O7) as well as the oxygen atoms O2, O3, and O4 and the nitrogen atoms N1 and N4 of the anions. Interestingly, the triazole ring proton is on the one hand bound at the N2 position of one anion and on the other hand on the N1 position of the other anion.

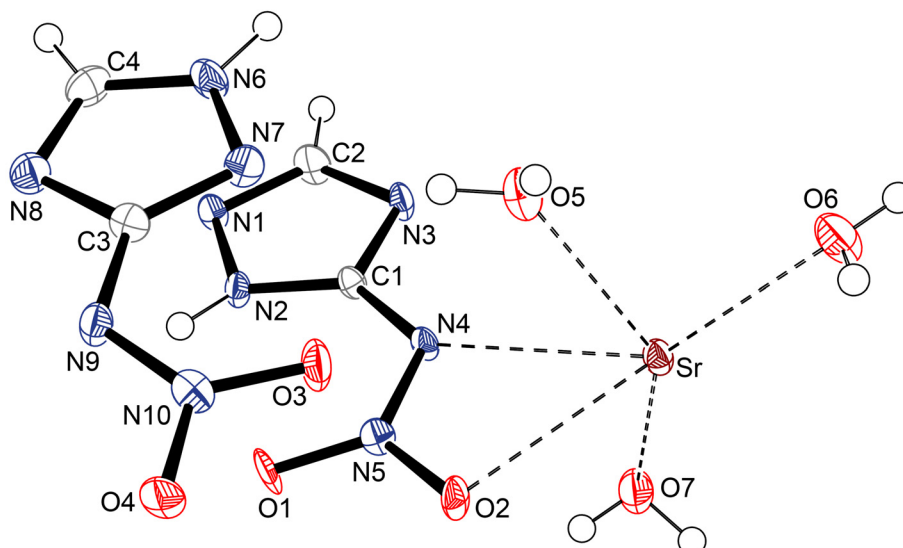


Figure 7.8 Molecular unit of **10_Sr1**. Hydrogen atoms are shown as spheres of arbitrary radius and thermal displacements are set at 50 % probability. Selected geometries: distances (Å) C1–N4 1.376(3), N4–N5 1.306(3), N5–O1 1.252(3), N5–O2 1.284(3), N9–C3 1.382(4), N9–N10 1.288(3), O3–N10 1.259(3), O4–N10 1.291(3), Sr–O7 2.578(3), Sr–O5 2.586(3), Sr–O3 i 2.604(2), Sr–O6 2.619(3), Sr–O2 2.626(2), Sr–N1 ii 2.682(2), Sr–O2 i 2.692(2), Sr–N4 2.737(2), Sr–O4 i 2.852(2); angles (°) N2–C1–N4 132.3(3), C1–N4–N5 118.2(2), N4–N5–O1 124.8(3), N4–N5–O2 114.9(2), O1–N5–O2 120.3(2), N7–C3–N9 130.1(3), O3–N10–N9 124.3(3), N9–N10–O4 118.5(3), O3–N10–O4 117.2(3), O2–Sr–N4 48.0(1), O5–Sr–N4 70.7(1), O6–Sr–N4 145.1(1), O7–Sr–N4 69.8(1), O5–Sr–O2 80.9(1), O6–Sr–O2 136.4(1), O7–Sr–O2 73.9(1), O5–Sr–O6 76.1(1), O7–Sr–O5 140.5(1), O7–Sr–O6 141.9(1); torsion angles (°) N1–N2–C1–N4 179.3(4), N2–C1–N4–N5 6.4(6), C1–N4–N5–O1 -0.7(5), C1–N4–N5–O2 178.1(3), N10–N9–C3–N7 -10.6(5), C3–N9–N10–O3 0.9(5), C3–N9–N10–O4 -177.9(3), O5–Sr–O2–N5 69.3(2), O6–Sr–O2–N5 128.0(2), O7–Sr–O2–N5 -80.1(2); i $-x-1, -y+1, -z+2$, ii $x-1/2, y, -z+3/2$.

The packing in **10_Sr1** is characterized by waved layers along the c axis. The molecules within these layer are connected via one hydrogen bond with nitrogen atoms as donors and acceptors (N2–H2 \cdots N3 iii : 0.85 Å, 2.05 Å, 2.867 Å, 162.7°, N6–H6 \cdots N8 ii : 0.90 Å, 2.07 Å, 2.949 Å, 168.0°; ii) $x-1/2, y, -z+3/2$, iii) $x+1/2, y, -z+3/2$). Further hydrogen bonds connect the layers with each other, whereas all oxygen atoms of the crystal water molecules act as donors (O5–H5a \cdots O4 iv : 0.71 Å, 2.25 Å, 2.946 Å, 168.4°, O5–H5b \cdots N7: 0.84 Å, 2.09 Å, 2.923 Å, 175.7°, O5–H5b \cdots O3: 0.84 Å, 2.42 Å, 2.865 Å, 114.2°, O6–H6b \cdots O1 i : 0.73 Å, 2.21 Å, 2.899 Å, 157.7°, O6–H6b \cdots O2 i : 0.73 Å, 2.57 Å, 2.945 Å, 113.7°, O6–H6a \cdots O4 v : 0.73 Å, 2.08 Å, 2.795 Å, 165.0°, O7–H7a \cdots O6 vi : 0.84 Å, 2.23 Å, 2.946 Å, 144.6°, O7–H7b \cdots N9 vii : 0.76 Å, 2.11 Å, 2.862 Å, 173.8°; i) $-x-1, -y+1, -z+2$ iv) $x-1/2, -y+1/2, -z+2$, v) $x-1, y, z$, vi) $-x-3/2, y+1/2, z$, vii) $-x-1/2, y+1/2, z$).

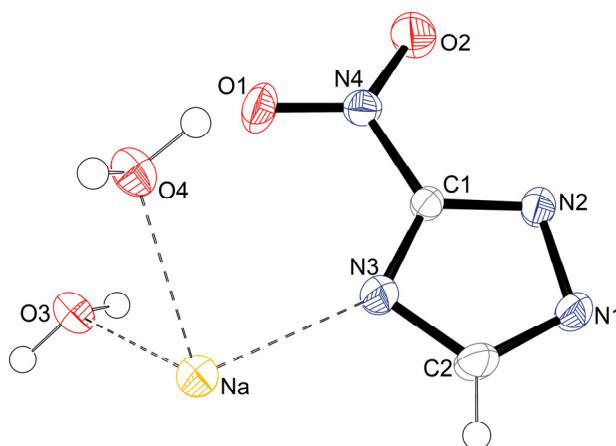


Figure 7.9 Molecular unit of **12_Na**. Hydrogen atoms are shown as spheres of arbitrary radius and thermal displacements are set at 50 % probability. Selected geometries: distances (Å) C1–N4 1.447(3), N4–O1 1.225(3), N4–O2 1.216(3), Na–O4 2.389(2), Na–O3 2.401(2), Na–O4*i* 2.412(2), Na–N3 2.426(2), Na–O3*i* 2.430(2), Na–O1*i* 2.565(2); angles (°) N2–C1–N4 120.3(2), C1–N4–O1 118.3(2), C1–N4–O2 117.3(2), O1–N4–O2 124.5(2), O4–Na–O3 82.1(1), O4–Na–N3 93.4(1), O3–Na–N3 96.4(1), O3–Na–O3*i* 168.1(1), O4–Na–O4*i* 168.0(1); torsion angles (°) N1–N2–C1–N4 179.9(2), O1–N4–C1–N2 178.7(2), O2–N4–C1–N2 -1.1(4), O4–Na–N3–C1 -27.4(3), O3–Na–N3–C1 55.0(3); *i* $-x+1/2, y-1/2, -z+1/2$.

Sodium 3-nitro-1,2,4-triazolate dihydrate (**12_Na**) crystallizes analog to **10_Na** in the monoclinic space group $P2_1/c$ with four molecules per unit cell (Figure 7.9). Its density of 1.751 g/cm³ is significantly higher than the one of **10_Na**, but comparable to its tetrazole derivative sodium 5-nitrotetrazolate dihydrate (1.731 g/cm³)^[20]. The sodium ions are coordinated sixfold by the oxygen atoms of the crystal water molecules (O3, O4) as well as the atoms N3 and O1 of the nitrotriazole anion forming a distorted octahedron. The distance of two sodium atoms is 3.617(1) Å. Two sodium atoms are linked by the oxygen atoms of the crystal water molecules and the atoms N3 and O1 of the anions along the *b* axis. Hydrogen bonds can only be observed between the crystal water molecules and the triazole rings (O4–H4b··N2*ii*: 0.82(4) Å, 2.12(4) Å, 2.929(3) Å, 170(3)°, O4–H4a··N1*iii*: 0.84(4) Å, 2.17(4) Å, 2.982(3) Å, 162(3)°, O3–H3a··N1*iv*: 0.81(3) Å, 2.12(4) Å, 2.912(3) Å, 163(3)°, O3–H3b··N2*v*: 0.77(3) Å, 2.28(4) Å, 3.027(3) Å, 163(3)°; *ii*) $-x, -y+1, -z+1$, *iii*) $x-1/2, -y+1/2, z-1/2$, *iv*) $x+1/2, -y+1/2, z-1/2$, *v*) $-x+1, -y+1, -z+1$).

Calcium bis(3-nitro-1,2,4-triazolate) hexahydrate (**12_Ca**) crystallizes in the triclinic space group $P-1$ with two molecular units per unit cell. Its density of 1.728 g/cm³ is comparable to its nitrotetrazole analog calcium bis(5-nitrotetrazolate) hexahydrate (1.783 g/cm³)^[20]. Each calcium atom is coordinated eightfold by four crystal water molecules and the nitrogen atoms N3 and N7 as well as the oxygen atoms O1 and O3 of the nitrotriazole anions (Figure 7.10). Thereby, the coordination distances of Ca–O5 and Ca–O8 are almost similar with a difference of less than 0.009 Å. In contrast, the distance Ca–O6 (2.417(2) Å) is significantly longer than the one of Ca–O7 (2.350(2) Å), which is the shortest. The distances of the coordinating atoms of the anions are longer than the ones of the water molecules. The distances between the nitrogen atoms and the calcium ion are also almost

similar, whereas the ones of the oxygen atoms differ significantly from each other. The two further crystal water molecules do not interact with the calcium atoms. In all observed hydrogen bonds the oxygen atoms of the crystal water molecules act as donor atoms (Table 7.2).

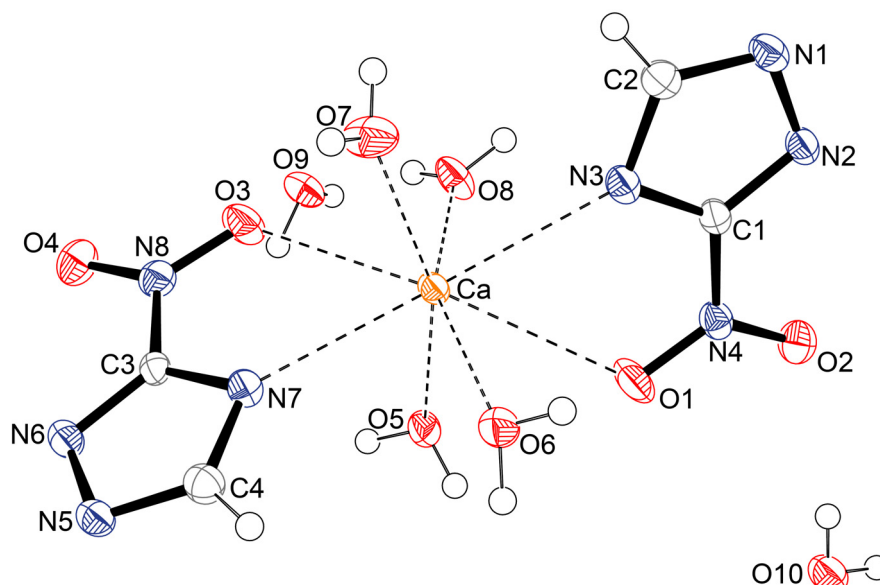


Figure 7.10 Molecular unit of **12_Ca**. Hydrogen atoms are shown as spheres of arbitrary radius and thermal displacements are set at 50 % probability. Selected geometries: distances (Å) C1–N4 1.430(2), N4–O1 1.231(1), N4–O2 1.231(2), Ca–O7 2.350(2), Ca–O8 2.387(2), Ca–O5 2.395(2), Ca–O6 2.417(2), Ca–N3 2.551(1), Ca–N7 2.563(1), Ca–O3 2.674(2), Ca–O1 2.800(2); angles (°) N2–C1–N4 121.9(1), C1–N4–O1 117.5(1), C1–N4–O2 118.9(1), O1–N4–O2 123.7(1), O7–Ca–O8 97.2(1), O7–Ca–O5 159.5(0), O8–Ca–O5 82.1(1), O7–Ca–O6 96.4(1), O8–Ca–O6 155.1(0), O5–Ca–O6 92.2(1), O7–Ca–N3 78.4(0), O8–Ca–N3 78.0(0), O5–Ca–N3 121.1(0), O6–Ca–N3 84.4(0), O7–Ca–N7 83.2(1), O8–Ca–N7 126.3(0), O5–Ca–N7 80.9(1), O6–Ca–N7 76.0(0), N3–Ca–N7 151.4(0), O7–Ca–O3 77.8(0), O8–Ca–O3 66.1(5), O5–Ca–O3 83.3(0), O6–Ca–O3 137.6(0), N3–Ca–O3 133.4(0), N7–Ca–O3 61.6(0), O7–Ca–O1 137.7(0), O8–Ca–O1 83.3(1), O5–Ca–O1 62.8(1), O6–Ca–O1 72.7(1), N3–Ca–O1 60.2(0), N7–Ca–O1 130.1(0), O3–Ca–O1 137.3(0); torsion angles (°) N1–N2–C1–N4 -179.7(1), O1–N4–C1–N2 178.6(1), O2–N4–C1–N2 -1.4(2), O7–Ca–O1–N4 -28.1(1), O8–Ca–O1–N4 65.2(1), O5–Ca–O1–N4 149.8(1), O6–Ca–O1–N4 -108.4(1), N3–Ca–O1–N4 -14.8(1), N7–Ca–O1–N4 -162.0(1), O3–Ca–O1–N4 108.4(1), O7–Ca–O3–N8 -100.1(1), O8–Ca–O3–N8 156.2(1), O5–Ca–O3–N8 71.9(1), O6–Ca–O3–N8 -14.0(1), N3–Ca–O3–N8 -160.9(1), N7–Ca–O3–N8 -11.3(1).

Table 7.2 Hydrogen bonds in **12_Ca** (*i*) $x, y+1, z$, *ii*) $-x+2, -y+1, -z$, *iii*) $x-1, y, z$, *iv*) $-x+1, -y, -z$, *v*) $-x+1, -y, -z+1$, *vi*) $x-1, y-1, z$, *vii*) $x+1, y-1, z$.

D–H···A	D–H [Å]	H···A [Å]	D···A [Å]	<(DHA) [°]
O6–H6b···O3 <i>i</i>	0.84(2)	2.17(2)	2.972(2)	158(2)
O10–H10a···N2 <i>ii</i>	0.84(2)	1.97(2)	2.807(2)	169(2)
O6–H6a···O10 <i>iii</i>	0.81(2)	1.90(2)	2.703(2)	169(2)
O10–H10b···O2	0.79(2)	2.27(2)	3.053(2)	168(2)
O8–H8a···N1 <i>iv</i>	0.80(2)	2.02(2)	2.805(2)	170(2)
O8–H8a···N2 <i>iv</i>	0.80(2)	2.68(2)	3.334(2)	141(2)
O9–H9b···N5 <i>v</i>	0.82(2)	2.03(2)	2.850(2)	177(2)
O5–H5b···N6 <i>v</i>	0.84(2)	1.95(2)	2.784(2)	172(2)
O8–H8b···O9	0.83(2)	2.12(2)	2.943(2)	168(2)
O7–H7b···O10 <i>vi</i>	0.76(2)	2.12(2)	2.852(2)	160(2)
N9–H9a···O6 <i>vii</i>	0.77(2)	2.25(2)	3.021(2)	177(2)
O5–H5a···O9 <i>i</i>	0.81(2)	2.05(2)	2.848(3)	169(2)
O7–H7a···O5 <i>iii</i>	0.79(2)	2.16(2)	2.935(2)	165(2)

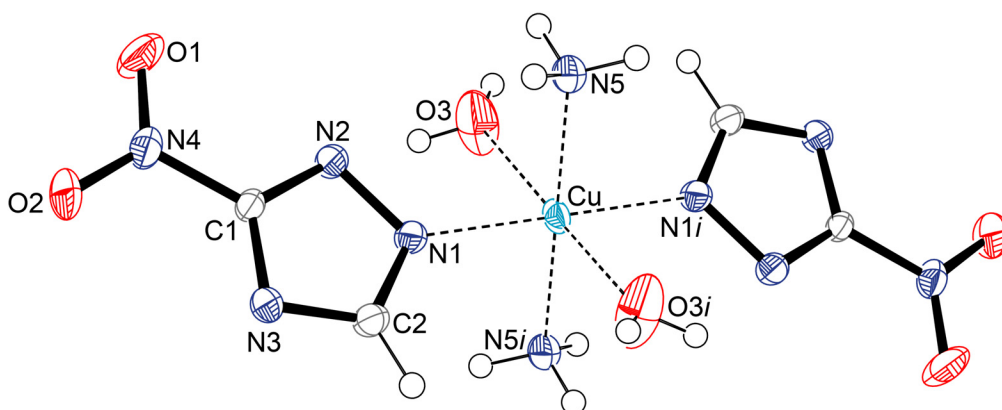


Figure 7.11 Molecular unit of **12_Cu**. Hydrogen atoms are shown as spheres of arbitrary radius and thermal displacements are set at 50 % probability. Selected geometries: distances (Å) C1–N4 1.443(3), N4–O1 1.231(3), N4–O2 1.223(3), Cu–O3 2.519(3), Cu–N1 2.013(2), Cu–N5 1.999(2); angles (°) N2–C1–N4 120.3(2), C1–N4–O1 118.2(2), C1–N4–O2 118.4(2), O1–N4–O2 123.4(2), O3–Cu–N1 90.3(1), N5–Cu–O3 88.0(1), N5–Cu–N1 89.3(1); torsion angles (°) N1–N2–C1–N4 180.0(2), O1–N4–C1–N2 –4.1(3), O2–N4–C1–N2 176.1(2), O3–Cu–N1–N2 –37.2(2); *i*) –*x*, –*y*, –*z*.

trans-Bis(diammine diaqua 3-nitro-1,2,4-triazolato-*N*1) copper(II) (**12_Cu**) crystallizes analog to **12_Na** in the monoclinic space group $P2_1/c$ with two molecular units per unit cell and a density of 1.865 g/cm³. The copper(II) atoms are coordinated sixfold by two ammine and two aqua ligands as well as the N1 atoms of the nitrotriazole ligands (Figure 7.11). The formed coordination octahedron is elongated. The coordination distances between the copper(II) atoms and the nitrogen atoms are almost similar (Cu–N1 2.013(2) Å, Cu–N5 1.999(2) Å). The distance Cu–O3 is significantly longer with 2.519(2) Å. Hence, this X-ray diffraction could clarify that in **12_Cu** the copper(II) ions are coordinated octahedrally and the nitrotriazole anions are monodentate ligands. This conclusion could not be drawn in reference [3d], by investigation of its infrared spectrum. The corresponding coordination angles are close to 90°. The observed hydrogen bonds are formed between the ammine and aqua ligands and the anions (N5–H5a··O2*ii*: 0.87 Å, 2.52 Å, 3.349 Å, 160.7°; N5–H5b··N3*iii*: 0.87 Å, 2.40 Å, 3.266 Å, 170.6°; N5–H5c··N3*iv*: 0.87 Å, 2.39 Å, 3.257 Å, 176.8°; O3–H3a··O1*v*: 0.83 Å, 2.33 Å, 3.068 Å, 148.9°; O3–H3a··N2*v*: 0.83 Å, 2.43 Å, 3.124 Å, 142.2°; O3–H3b··O2*vi*: 0.83 Å, 2.21 Å, 2.999 Å, 159.1°; *ii*) –*x*–1, *y*–1/2, –*z*–1/2, *iii*) –*x*, *y*–1/2, –*z*–1/2, *iv*) *x*, –*y*+1/2, *z*–1/2, *v*) –*x*–1, –*y*, –*z*, *vi*) *x*, –*y*+1/2, *z*+1/2.

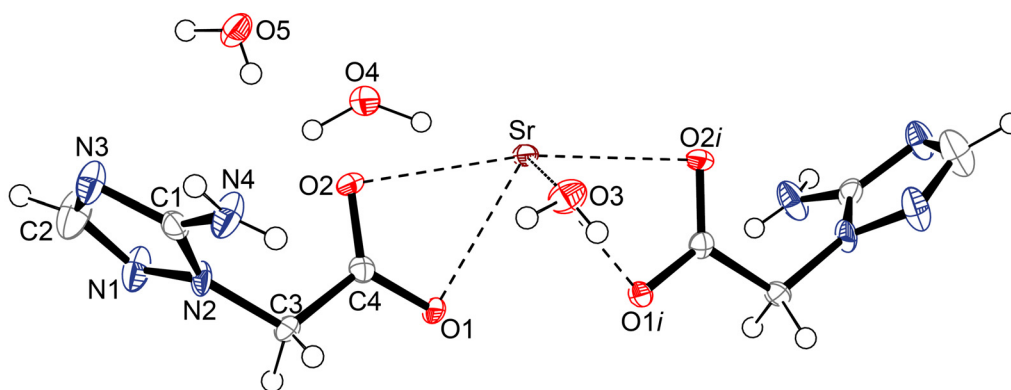


Figure 7.12 Molecular unit of **13_Sr**. Hydrogen atoms are shown as spheres of arbitrary radius and thermal displacements are set at 50 % probability. Selected geometries: distances (Å) N1–N2 1.376(3), C1–N4 1.336(5), C4–O1 1.259(3), O2–C4 1.248(3), O2–Sr 2.646(2), Sr–O1 2.493(2), Sr–O1*i* 2.493(2), Sr–O3*i* 2.600(3), Sr–O3 2.600(3), Sr–O2*i* 2.646(2), Sr–O1*ii* 2.644(2), Sr–O1*iii* 2.644(2); angles (°) N2–C1–N4 124.5(3), O1–C4–C3 116.4(2), O2–C4–C3 120.5(3), O2–C4–O1 123.2(3), O1–Sr–O2 76.0(1), O3–Sr–O2 88.2(1); torsion angles (°) N1–N2–C1–N4 177.0(3), N1–N2–C3–C4 –85.0(3), O1–C4–C3–N2 176.6(3), O2–C4–C3–N2 –4.5(4), O3–Sr–O1–C4 64.2(5), C4–O2–Sr–O3 67.1(2), Sr–O2–C4–C3 –163.8(2); *i*) $-x+3/2, -y+1, z$, *ii*) $-x+3/2, y, z+1/2$, *iii*) $x, -y+1, z+1/2$.

The strontium salt of **13**, strontium bis(2-(3-amino-1,2,4-triazol-2-yl)-acetate) pentahydrate (**13_Sr**) crystallizes in the orthorhombic space group *Pcca* with four molecular units per unit cell (Figure 7.12). Its density of 1.746 g/cm³ is comparable to its tetrazole analog strontium 2-(5-aminotetrazol-1-yl)-acetate pentahydrate (**4_Sr**, chapter 5). The strontium atoms are coordinated eightfold by the oxygen atoms of the carboxy group (O1, O2) and the crystal water molecule (O3). The two further crystal water molecules do not coordinate to the cation, but are connected via hydrogen bonds to the coordinating water molecule and the anions (N4–H4b···O5: 0.73(3) Å, 2.27(3) Å, 2.994(4) Å, 171(4)°; O3–H3c···O5: 0.85(4) Å, 1.87(4) Å, 2.705(4) Å, 167(4)°, O3–H3d···O4: 0.65(3) Å, 2.15(3) Å, 2.793(4) Å, 170(4)°). The packing of **13_Sr** is characterized by waved layers along the *a* axis. Thereby, the strontium ions are linked by the O1 atom of the anions. The anions are connected within these layers by one hydrogen bond (N4–H4a···N3*iv*: 0.94(3) Å, 2.28(3) Å, 3.200(4) Å, 165(3)°; *iv*) $-x+1, -y+1, -z$). The four further hydrogen bonds connect the layers with each other.

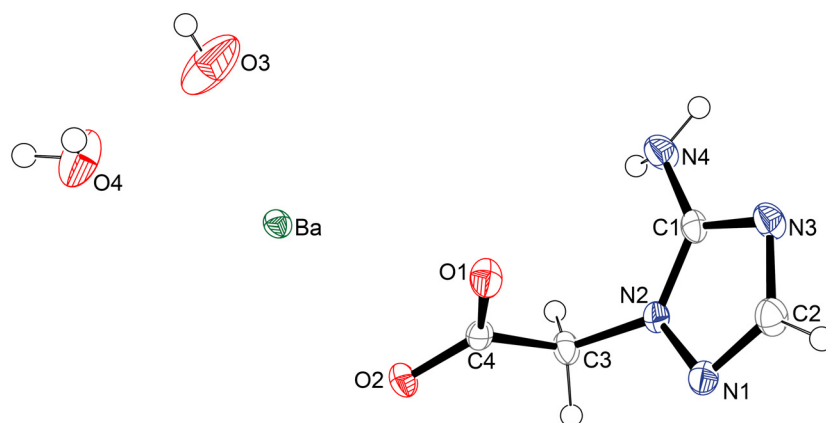


Figure 7.13 Asymmetric unit of **13_Ba**. Hydrogen atoms are shown as spheres of arbitrary radius and thermal displacements are set at 50 % probability. Selected geometries: distances (Å) N1–N2 1.385(2), C1–N4 1.350(3), C4–O1 1.241(2), O2–C4 1.264(2), Ba–O3 2.673(3), Ba–O2*i* 2.689(2), Ba–O2*ii* 2.689(2), Ba–O2*iii* 2.847(2), Ba–O2 2.847(2), Ba–O4*iii* 2.852(2), Ba–O4 2.852(2), Ba–O1 2.894(2), Ba–O1*iii* 2.894(2); angles (°) N2–C1–N4 125.2(2), O1–C4–C3 119.5(2), O2–C4–C3 115.9(2), O2–C4–O1 124.6(2), O4–Ba–O1 145.3(1), O2–Ba–O1 45.5(0), O2*i*–Ba–O2 89.9(1), O3–Ba–O1 128.7(0), O3–Ba–O2 135.1(0), O2–Ba–O4 148.0(1), O3–Ba–O4 68.3(0); torsion angles (°) N1–N2–C1–N4 –174.7(2), N1–N2–C3–C4 75.5(2), O1–C4–C3–N2 17.6(2), O2–C4–C3–N2 –164.3(2), O2–Ba–O1–C4 15.6(1), O3–Ba–O1–C4 –103.3(1), O4–Ba–O1–C4 147.7(1), O1–Ba–O2–C4 –15.3(1), O3–Ba–O2–C4 89.5(1), O4–Ba–O2–C4 –142.4(1); *i*) $x, -y, z-1/2$, *ii*) $-x, -y, -z+1$, *iii*) $-x, y, -z+1/2$.

The asymmetric unit of barium bis(2-(3-amino-1,2,4-triazol-2-yl)-acetate) trihydrate (**13_Ba**) is depicted in Figure 7.13. It crystallizes in the monoclinic space group $P2_1/c$ with two molecular units per unit cell. Its density of 1.991 g/cm³ is significantly higher than the one of **13_Sr**, but smaller than the one of its tetrazole analog barium 2-(5-aminotetrazol-1-yl)-acetate trihydrate (**4_Ba**, chapter 5). The barium ions are coordinated ninefold by the atoms O3, O2*i*, O2*ii*, O2*iii*, O2, O4*iii*, O4, O1, and O1*iii* (*i*) $x, -y, z-1/2$, *ii*) $-x, -y, -z+1$, *iii*) $-x, y, -z+1/2$). Two barium ions are linked by the oxygen atom O2 of the anions. The packing of **13_Ba** consists of waved layers along the *a* axis. Five different hydrogen bonds can be observed (N4–H4a···N3*iv*: 0.83(3) Å, 2.28(3) Å, 3.109(3)Å, 177(2)°, N4–H4b···N3*v*: 0.71(3) Å, 2.64(3) Å, 3.271(3) Å, 150(3)° O4–H4d···O1*vi*: 0.74(3) Å, 2.10(3) Å, 2.817(3) Å, 163(3)°, O4–H4c···N1*vii*: 0.77(3) Å, 2.31(3) Å, 3.074(3) Å, 170(3)°, O3–H3···O2*viii*: 0.80(4) Å, 2.26(5) Å, 2.927(3) Å, 140(5)°; *iv*) $-x-1, -y, -z$, *v*) $x, -y, z+1/2$, *vi*) $-x, -y, -z$, *vii*) $-x, y+1, -z+1/2$, *viii*) $x, y+1, z$).

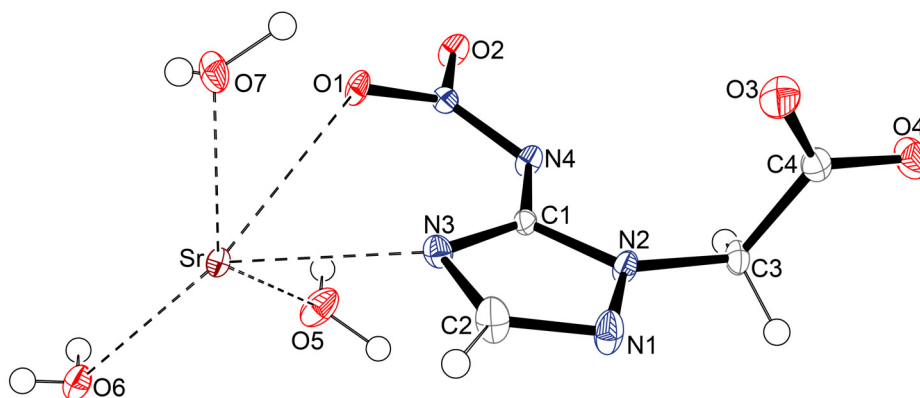


Figure 7.14 Molecular unit of **14_Sr**. Hydrogen atoms are shown as spheres of arbitrary radius and thermal displacements are set at 50 % probability. Selected geometries: distances (Å) N1–N2 1.364(4), C1–N4 1.383(4), N4–N5 1.315(4), O2–N5 1.259(3), O1–N5 1.271(3), O3–C4 1.262(4), O4–C4 1.254(4), Sr–O3*i* 2.526(2), Sr–O7 2.549(3), Sr–O5 2.559(3), Sr–N3 2.656(3), Sr–O6 2.673(3), Sr–O1*ii* 2.681(2), Sr–O6*iii* 2.725(3), Sr–O2*ii* 2.735(3), Sr–O1 2.781(3); angles (°) N2–C1–N4 117.4(3), O3–C4–C3 118.4(3), O4–C4–C3 115.1(3), O4–C4–O3 126.5(3), O3*i*–Sr–O1 127.31(8), O7–Sr–O1 62.2(1), O5–Sr–O1 69.3(1), N3–Sr–O1 59.2(1), O6–Sr–O1 130.4(1), O3*i*–Sr–O7 82.4(1), O3*i*–Sr–O5 133.2(1), O7–Sr–O5 131.4(1), O3*i*–Sr–N3 77.2(1), O7–Sr–N3 78.3(1), O5–Sr–N3 79.8(1), O3*i*–Sr–O6 102.1(1), O7–Sr–O6 137.9(1), O5–Sr–O6 74.8(1), N3–Sr–O6 143.7(1); torsion angles (°) N1–N2–C1–N4 –179.6(3), C1–N4–N5–O1 1.0(5), C1–N4–N5–O2 179.2(3), O3–C4–C3–N2 –2.2(5), O4–C4–C3–N2 179.3(3), O3*i*–Sr–O1–N5 97.5(2), O7–Sr–O1–N5 151.3(3), O5–Sr–O1–N5 –31.7(2), N3–Sr–O1–N5 58.6(2), O6–Sr–O1–N5 –77.9(3); *i*) –*x*, *y*+1/2, –*z*+1/2, *ii*) –*x*, –*y*, –*z*+1, *iii*) –*x*, –*y*+1, –*z*+1.

The molecular unit of strontium 2-(3-nitrimino-1,2,4-triazolate-2-yl)-acetate trihydrate (**14_Sr**) is depicted in Figure 7.14. It crystallizes analog to **14** and its tetrazole analogue strontium 2-(5-nitriminotetrazolate)-acetate trihydrate (**5_Sr2**, chapter 5) in the monoclinic space group $P2_1/c$ with four molecular units per unit cell. Its density of 2.117 g/cm³ is comparable to the one of **5_Sr2** (see chapter 5). Each strontium ion is coordinated ninefold by the atoms O3*i*, O7, O5, N3, O6, O1*ii*, O6*iii*, O2*ii*, and O1 regarding distances up to 2.8 Å (*i*) –*x*, *y*+1/2, –*z*+1/2, *ii*) –*x*, –*y*, –*z*+1, *iii*) –*x*, –*y*+1, –*z*+1). Two strontium atoms are linked by the crystal water molecule (O6) and the oxygen atom O1 of the anions. All crystal water molecules are involved in hydrogen bonds (O5–H5a···O4*iv*: 0.91(4) Å, 1.87(4) Å, 2.725(4) Å, 155(4)°, O7–H7b···N1*v*: 0.92(6) Å, 1.93(6) Å, 2.853(4) Å, 174(5)°, O5–H5b···O7*ii*: 0.75(5) Å, 2.26(6) Å, 2.924(5) Å 148(6)°, O5–H5b···O2*vii*: 0.75(5) Å, 2.52(5) Å, 3.046(4) Å, 129(5)°, O7–H7a···N4*viii*: 0.64(5) Å, 2.24(5) Å, 2.845(5) Å, 159(6)°, O6–H6a···O4*ix*: 0.67(4) Å, 2.10(4) Å, 2.724(5) Å, 157(5)°, O6–H6b···N1*x*: 0.92(5) Å, 2.50(5) Å, 3.420(4) Å, 174(4)°; *iv*) –*x*+1, *y*+1/2, –*z*+1/2, *v*) –*x*, *y*–1/2, –*z*+1/2, *vi*) –*x*+1, –*y*, –*z*+1, *vii*) –*x*–1, *y*, *z*, *viii*) *x*–1, –*y*+1/2, *z*+1/2, *ix*) *x*, –*y*+1/2, *z*+1/2, *x*) –*x*+1, *y*+1/2, –*z*+1/2.)

7.1.3.2 Energetic Properties

The energetic properties, such as decomposition temperature (T_{dec}) and sensitivity to impact (E_{dr}), friction (F_{r}), and electric discharge (E_{el}), as well as combustion energy ($\Delta_c U$) were determined. An overview of the energetic properties of the salts of **10**, is given in Table 7.3

and of the compounds of **12** in Table 7.4. In Table 7.5 the properties of **13_Sr**, **13_Ba**, and **14_Sr** are given.

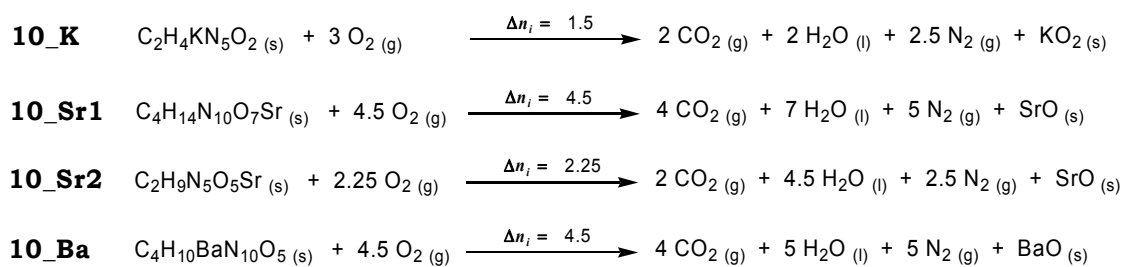
Table 7.3 Overview of the physico-chemical properties of the prepared salts of **10**.

	10_Na	10_K	10_Sr1	10_Sr2	10_Ba
Formula	NaC ₂ H ₄ N ₅ O ₂ · 3H ₂ O	KC ₂ H ₄ N ₅ O ₂	Sr(C ₂ H ₄ N ₅ O ₂) ₂ · 3H ₂ O	Sr(C ₂ H ₃ N ₅ O ₂) · 3H ₂ O	Ba(C ₂ H ₄ N ₅ O ₂) ₂ · H ₂ O
M [g/mol]	205.11	167.17	397.81	268.73	411.48
E_{dr} [J]^a	> 100	5.0	> 90	> 100	10
F_r [N]^b	324	240	288	> 360	> 360
E_{el} [J]^c	0.75	0.40	0.30	0.30	0.50
grain size [μm]	100–250	100–500	250–500	80–160	> 1000
N [%]^d	34.15	41.89	35.21	26.06	34.04
Ω [%]^e	-39	-57	-36	-28	-35
T_{dec} [°C]^f	255	253	231	348	294
ρ [g/cm³]^g	1.64	1.99	2.11	2.26* (23 °C)	2.25* (23 °C)
Δ_cU [kJ/kg]^h	n.d.**	-6485	-4371	-3986	-6263
Δ_cH^o [kJ/mol]ⁱ	-	-1080	-1728	-1066	-2566
Δ_fH^o [kJ/mol]^j	-	-848	-3032	-2192	-1534
H₂O sol. [wt%]^k	n.d.**	n.d.**	6.5 (22 °C)	< 0.1 (23 °C)	5.2 (22 °C)

a) BAM drop hammer [17], b) BAM methods [17], c) Electric discharge tester, d) Nitrogen content, e) Oxygen balance, f) Decomposition temperature from DSC ($\beta = 5$ K/min), g) determined by X-ray crystallography or pycnometer (*), h) Combustion energy, i) Enthalpy of combustion, j) Molar enthalpy of formation, k) Solubility in H₂O (H₂O temperature), ** n.d. = not determined.

Both strontium salts of **10** and **10_Na** are insensitive to impact, whereas **10_K** and **10_Ba** are sensitive with 5.0 J and 10 J, respectively. Except **10_Sr2** and **10_Ba**, all prepared salts of **10** are sensitive to friction. The determined sensitivities to electric discharge are between 0.30 J and 0.75 J. All salts of **10** decompose at temperatures above 230 °C and are slightly thermally more stable than the corresponding salts of 5-nitrimino-tetrazole (**H₂AtNO₂**).^[12, 19, 21] Especially **10_Sr2**, with the twice deprotonated anion is thermally very stable ($T_{dec} = 348$ °C). In the DSC thermograms of **10_Na** and the alkaline earth metal salts of **10** the loss of crystal water can be observed (**10_Na**: 113 °C, **10_Sr1**: 151 °C, **10_Sr2**: 115 °C, 169 °C, **10_Ba**: 201 °C).

The reported values of the combustion energy ($\Delta_c U$) are the average of three single bomb calorimetry measurements. The standard molar enthalpy of combustion ($\Delta_c H^o$) was derived from equation 7.1. The enthalpies of formation ($\Delta_f H^o$) for the salts of **10** were calculated at 298.15 K using the HESS thermochemical cycle and the combustion reactions in Scheme 7.9.



Scheme 7.9 Combustion equations of **10_K**, **10_Sr1**, **10_Sr2**, and **10_Ba**.

According to the combustion equations **10_K**, **10_Sr1**, **10_Sr2**, and **10_Ba** were determined to be formed exothermically. **10_Sr1** offers the highest negative value with -3032 kJ/mol and **10_K** the lowest negative one with -848 kJ/mol .

The heats of formation of the combustion products $\text{H}_2\text{O} (\text{l})$ (-286 kJ/mol), $\text{CO}_2 (\text{g})$ (-393 kJ/mol), $\text{Na}_2\text{O}_2 (\text{s})$ (-513 kJ/mol), $\text{KO}_2 (\text{s})$ (-284.5 kJ/mol), $\text{CaO} (\text{s})$ (-635 kJ/mol), $\text{SrO} (\text{s})$ (-592 kJ/mol), and $\text{BaO} (\text{s})$ (-548 kJ/mol) were adopted from literature.^[18]

The solubilities of the alkaline earth metal salts **10_Sr1**, **10_Sr2**, and **10_Ba** were determined and are given in percent by weight (wt%). They were calculated according to equation 7.2.

$$\text{H}_2\text{O-sol.} = \frac{m_{\text{dissolved Compound}}}{m_{\text{dissolved Compound}} + m_{\text{Solvent}}} \cdot 100 \quad (7.2)$$

All investigated salts are very low soluble in H_2O at ambient temperature with solubilities of less than 7 wt%. **10_Sr2** is almost insoluble with less than 0.1 wt%.

Table 7.4 Overview of the physico-chemical properties of the prepared compounds of **12**.

	12_Na	12_Ca	12_Ba	12_Cu
Formula	$\text{NaC}_2\text{HN}_4\text{O}_2 \cdot 2\text{H}_2\text{O}$	$\text{Ca}(\text{C}_2\text{HN}_4\text{O}_2)_2 \cdot 6\text{H}_2\text{O}$	$\text{Ba}(\text{C}_2\text{HN}_4\text{O}_2)_2 \cdot 2.5\text{H}_2\text{O}$	$[\text{Cu}(\text{C}_2\text{HN}_4\text{O}_2)_2 (\text{H}_2\text{O})_2(\text{NH}_3)_2]$
M [g/mol]	172.08	365.27	408.48	359.78
E_{dr} [J]^a	> 40	25	20	20
F_r [N]^b	214	> 360	> 360	> 360
E_{el} [J]^c	0.20	0.30	0.20	2.5
grain size [μm]	100–500	> 1000	100–250	250–500
N [%]^d	32.56	29.94	27.43	38.93
Ω [%]^e	-32	-26	-24	-44
T_{dec} [°C]^f	255	377	342	340
ρ [g/cm³]^g	1.75	1.73	2.01 (23 °C)*	1.87
H₂O sol. [wt%]^h	n.d.**	n.d.**	n.d.**	< 0.3 (23 °C)

^a) BAM drop hammer ^[17], ^b) BAM methods ^[17], ^c) Electric discharge tester, ^d) Nitrogen content, ^e) Oxygen balance, ^f) Decomposition temperature from DSC ($\beta = 5 \text{ K/min}$), ^g) determined by X-ray crystallography or pycnometer (*), ^h) Solubility in H_2O (H_2O temperature), **) n.d. = not determined.

Although **12** is much more sensitive to outer stimuli than **10**, the prepared alkaline earth metal salts of **12** and also **12_Cu** are insensitive to friction. However, they are sensitive to impact with 20 J or 25 J. **12_Na** is insensitive to impact, but friction with 214 N.

It also offers a quite low decomposition temperature of 255 °C compared to **12_Ca**, **12_Ba**, and **12_Cu**, which decompose at temperatures above 340 °C. They are thermally much more stable than the corresponding compounds of 5-nitrotetrazole.^[20] In the case of **12_Ca** and **12_Ba** the loss of crystal water can be observed at 150 °C and 152 °C, respectively. **12_Cu** shows two endothermic signals at 130 °C and 203 °C due to the loss of aqua or ammonia ligands.

12_Cu is almost insoluble in H₂O at ambient temperature with less than 0.3 wt%. The solubilities of **12_Na**, **12_Ca**, and **12_Ba** were not determined, because of a too small amount of the neat compounds.

Table 7.5 Overview of the physico-chemical properties of **13_Sr**, **13_Ba**, and **14_Sr**.

	13_Sr	13_Ba	14_Sr
Formula	Sr(C ₄ H ₅ N ₄ O ₂) ₂ · 5H ₂ O	Ba(C ₄ H ₅ N ₄ O ₂) ₂ · 3H ₂ O	Sr(C ₄ H ₃ N ₅ O ₄) · 3H ₂ O
M [g/mol]	459.91	473.59	326.76
E_{dr} [J]^a	> 40	> 100	5.0
F_r [N]^b	324	> 360	> 360
E_{el} [J]^c	0.30	1.5	0.20
grain size [μm]	100–500	500–1000	100–500
N [%]^d	24.36	23.66	21.43
Ω [%]^e	-63	-61	-32
T_{dec} [°C]^f	377	348	357
ρ [g/cm³]^g	1.75	1.99	2.12

a) BAM drop hammer ^[17], b) BAM methods ^[17], c) Electric discharge tester, d) Nitrogen content, e) Oxygen balance, f) Decomposition temperature from DSC (β = 5 K/min), g) determined by X-ray crystallography or pycnometer (*).

13_Sr as well as **13_Ba** are insensitive to impact and **13_Ba** and **14_Sr** are insensitive to friction. **13_Sr** is sensitive to friction with 324 N and **14_Sr** is sensitive to impact with 5.0 J. Only the strontium salts of **13** and **14** are sensitive to electric discharge with 0.30 J and 0.20 J, respectively. The sensitivities are comparable to the ones of their corresponding tetrazole derivatives (see chapter 5). **13_Sr**, **13_Ba** as well as **14_Sr** offer very high decomposition temperatures above 345 °C. The triazole derivatives show higher decomposition temperatures than the corresponding tetrazole derivatives (see chapter 5). They are approximately 50 °C thermally more stable. In each DSC thermogram the loss of crystal water can be observed as endothermic signal at 61 °C, 118 °C, and 180 °C, respectively.

The solubilities in H₂O of **13_Sr**, **13_Ba**, and **14_Sr** at ambient temperature could not be determined, because of a too small amount of the neat compounds.

7.1.3.3 Flame Color and Combustion Behavior

The compounds **10_Sr1**, **10_Sr2**, **10_Ba**, **12_Ba**, **12_Cu**, **13_Sr**, **13_Ba**, and **14_Sr** were tested with regard to their emitting color during combustion in the flame of a BUNSEN burner. Therefore, a few milligrams of each compound on a spatula were put into the flame of a BUNSEN burner.



Figure 7.15 Flame color of **10_Sr1** (left) and **10_Sr2** (right) in the flame of a BUNSEN burner.

Both strontium salts of **10** produce a red light emission, whereas the flame of **10_Sr1** is bigger and shows a more intense red flame color (Figure 7.15). They combust slowly but smoke-free with a very small amount of black residues.



Figure 7.16 Flame color of **10_Ba** (left) and a mixture of **10_Ba** and PVC (right).

The barium salt **10_Ba** shows a white light emission in the flame of a Bunsen burner (Figure 7.16). In combination with PVC in a ratio of 50 wt%:50 wt%, the flame shows a green seam. In both cases the combustion occurs smoke-free and slowly. More solid residues were obtained with PVC.

This is also true for the barium salt of **12**, which combusts faster than **10_Ba**. Furthermore, **12_Ba** shows in combination with PVC (50 wt%:50 wt%) a more intense green light emission (Figure 7.17) and overall less residues.



Figure 7.17 Flame color of **12_Ba** (top, left), a mixture of **12_Ba** and PVC (top, right) and **12_Cu** (down).

As expected, the copper(II) compound **12_Cu** produces a very intense dark green flame during the whole combustion (Figure 7.17).

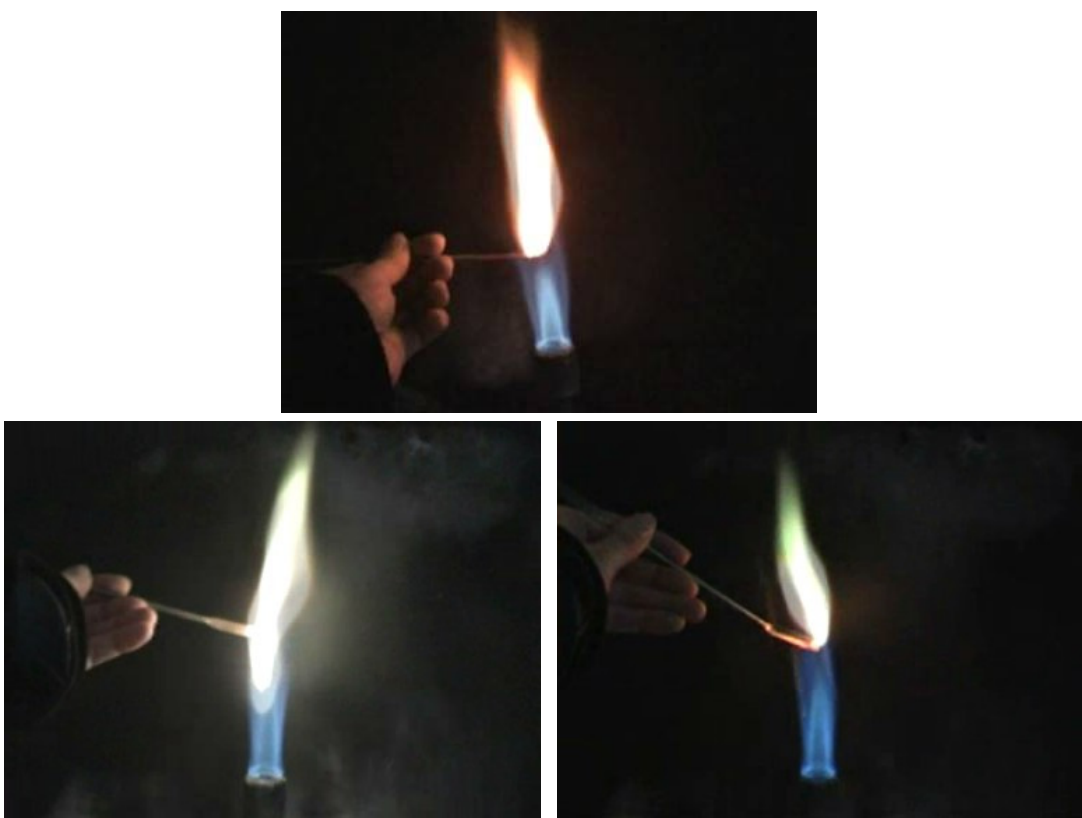


Figure 7.18 Flame color of **13_Sr** (top), **13_Ba** (down, left) and a mixture of **13_Ba** and PVC (down, right).

Again, no smoke and a very small amount of residues were observed.

The strontium and barium salt of **13** combust with a tall flame and without any smoke production (Figure 7.18). The light emission of **13_Sr** is less intense than the one of **10_Sr1** or **10_Sr2**. However, its combustion occurs faster without any residues. This is true for **13_Ba**. If PVC is added in a ratio of 50 wt%:50 wt%, the flame changes into pale green, especially its seam.



Figure 7.19 Flame color of **14_Sr** in the flame of a BUNSEN burner.

The strontium salt **14_Sr** offers a small but very intense red flame (Figure 7.19). Its combustion is quite fast but without sound, smoke production or residues.

Compared to the analog tetrazole salts, the color performance of the neat 1,2,4-triazole salts is only slightly worse.

7.2 Experimental Part

*CAUTION! Some of the prepared compounds are sensitive to impact, friction, and electric discharge. Therefore, proper protective measures (safety glasses, face shield, leather coat, earthed equipment and shoes, Kevlar® gloves, and ear plugs) should be used, especially during work on the precursor molecules 3-nitramino-1,2,4-triazole (**11**), 3-nitro-1,2,4-triazole (**12**), and 2-carboxymethyl-3-nitrimino-1,2,4-triazole monohydrate (**14**).*

7.2.1 Preparation of the Neutral Precursor Molecules

7.2.1.1 3-Nitramino-1,2,4-triazole Monohydrate (**10**)

Preparation according to literature.^[3a, 4] At 0 °C 8.4 g (0.1 mol) 3-amino-1,2,4-triazole (**3-ATrz**) were slowly dissolved in 50 mL sulfuric acid (98 %) and then 8.0 mL (0.2 mol) nitric acid (100 %) were added dropwise. The yellow solution was refluxed at 50 °C for five hours and after cooling to ambient temperature poured onto ice. The yellow precipitate was recrystallized from H₂O to yield a pale yellow powder. Yield: 83 %.

M.p. 92 °C (loss of H₂O), 215 °C (dec., DSC-measurement, 5 K/min).

Raman (200 mW, 25 °C, cm^{-1}): 3171 (1), 1585 (33), 1533 (100), 1430 (24), 1400 (18), 1317 (4), 1286 (4), 1253 (9), 1147 (2), 1083 (6), 1005 (43), 954 (7), 844 (9), 753 (21), 725 (3), 642 (2), 491 (8), 419 (12), 352 (7), 241 (9).

IR (Diamond-ATR, cm^{-1}): 3483 (m), 3447 (m), 3170 (w), 3058 (m), 2800 (m), 2112 (w), 1585 (s), 1536 (s), 1441 (m), 1387 (w), 1279 (vs), 1249 (vs), 1069 (m), 952 (m), 880 (m), 841 (m), 768 (m), 752 (m), 723 (m), 643 (m).

^1H NMR (DMSO- d_6): 14.17 (s, 1H, NH), 8.49 (s, 1H, CH)

^{13}C NMR (DMSO- d_6): 152.1 (CNHNO₂), 138.9 (CH).

^{14}N NMR (DMSO- d_6): -6 (NHNO₂), -17 (NO₂).

Elemental analysis C₂H₅N₅O₃ (147.09 g/mol) calc.: C, 16.33; H, 3.43; N, 47.61. found: C, 16.31; H, 3.53; N, 49.60.

$E_{\text{dr}} > 100 \text{ J}$ (500–1000 μm).

$F_{\text{r}} = 216 \text{ N}$ (500–1000 μm).

$E_{\text{el}} = 1.00 \text{ J}$ (500–1000 μm).

$\Delta_c U = -2067 \text{ cal/g}$.

7.2.1.2 3-Nitramino-1,2,4-triazole (11)

Preparation according to literature.^[3a, 4] 3.0 g (0.02 mol) 3-nitramino-1,2,4-triazole monohydrate (**10**) was stored at 110 °C for three days. The water free product was obtained as a pale yellow solid. Yield: 100 %.

M.p. 218 °C (dec., DSC-measurement, 5 K/min).

Raman (200 mW, 25 °C, cm^{-1}): 3181 (2), 1584 (33), 1536 (100), 1431 (20), 1400 (16), 1317 (4), 1253 (8), 1084 (5), 1005 (40), 844 (8), 753 (19), 727 (2), 647 (1), 491 (7), 418 (8), 352 (4), 239 (7).

IR (Diamond-ATR, cm^{-1}): 3483 (m), 3447 (m), 3170 (w), 3058 (m), 2800 (m), 2112 (w), 1585 (s), 1536 (s), 1441 (m), 1387 (w), 1279 (vs), 1249 (vs), 1069 (m), 952 (m), 880 (m), 841 (m), 768 (m), 752 (m), 723 (m), 643 (m).

^1H NMR (DMSO- d_6): 14.19 (s, 1H, NH), 8.48 (s, 1H, CH).

^{13}C NMR (DMSO- d_6): 152.8 (CNHNO₂), 139.5 (CH).

Elemental analysis C₂H₃N₅O₂ (129.08 g/mol) calc.: C, 18.61; H, 2.34; N, 54.26. found: C, 18.89; H, 2.39; N, 54.69.

$E_{\text{dr}} = 3.0 \text{ J}$ (100–250 μm).

$F_{\text{r}} = 192 \text{ N}$ (100–250 μm).

$E_{\text{el}} = 0.15 \text{ J}$ (100–250 μm).

$\Delta_c U = -2565 \text{ cal/g}$.

7.2.1.3 3-Nitro-1,2,4-triazole (12)

To a solution of 6.52 g (50.5 mmol) of 3-nitramino-1,2,4-triazole (**11**) in 75 mL acetic acid (100%) were added 29 mL (500 mmol) H₂O₂ (50%) and then refluxed at 70 °C for six hours. After removing most of the solvent in vacuum, a colorless solid precipitated and was filtered off. Yield: 56 %.

M.p. 215 °C, 294 °C (dec., DSC-measurement, 5 K/min).

Raman (200 mW, 25 °C, cm⁻¹): 3162 (8), 2852 (2), 1576 (6), 1521 (2), 1481 (18), 1425 (100), 1382 (63), 1312 (16), 1270 (13), 1177 (25), 1108 (13), 1019 (16), 982 (5), 835 (9), 774 (7), 535 (3), 449 (12), 278 (4), 258 (6), 245 (17).

IR (Diamond-ATR, cm⁻¹): 3163 (m), 3099 (w), 3059 (w), 3026 (w), 2962 (w), 2851 (s), 2818 (m), 2775 (s), 2723 (m), 2702 (m), 2650 (m), 2605 (m), 2538 (w), 2493 (w), 2440 (w), 2353 (vw), 1778 (vw), 1562 (m), 1520 (s), 1481 (s), 1424 (s), 1380 (s), 1309 (s), 1269 (m), 1181 (w), 1107 (w), 1018 (w), 980 (m), 918 (vw), 878 (w), 838 (m), 770 (vw).

¹H NMR (DMSO-*d*₆): 15.26 (s, 1H, NH), 8.87 (s, 1H, CH).

¹³C NMR (DMSO-*d*₆): 163.0 (CNO₂), 146.2 (CH).

Elemental analysis C₂H₂N₄O₂ (114.06 g/mol) calc.: C, 21.06; H, 1.77; N, 49.12. found: C, 20.93; H, 1.88; N, 48.54.

$$E_{dr} = 3.4 \text{ J} \quad (100\text{--}500 \text{ }\mu\text{m}).$$

$$F_r = 235 \text{ N} \quad (100\text{--}500 \text{ }\mu\text{m}).$$

$$E_{el} = 0.40 \text{ J} \quad (100\text{--}500 \text{ }\mu\text{m}).$$

$$\Delta_c U = -2388 \text{ cal/g}.$$

7.2.1.4 2-Carboxymethyl-3-amino-1,2,4-triazole (13)

To a solution of 9.4 g (11 mmol) 3-amino-1,2,4-triazole monohydrate (**10**) and 9.4 g (235 mmol) sodium hydroxide in 500 mL methanol was added slowly 15.56 g (112 mmol) bromoacetic acid at 80 °C. After refluxing the solution for 16 hours the solvent was removed in vacuum. The white residue was dissolved in H₂O and the pH of the solution was reduced to 2 with concentrated hydrochloric acid (37 %). After recrystallization from H₂O colorless single crystals, suitable for X-ray diffraction, were obtained. Yield: 55 %.

M.p. 281 °C, 291 °C (dec., DSC-measurement, 5 K/min).

Raman (400 mW, 25 °C, cm⁻¹): 3152 (19), 2985 (76), 2946 (100), 1706 (13), 1678 (16), 1650 (7), 1559 (28), 1493 (13), 1440 (31), 1390 (64), 1314 (80), 1281 (28), 1235 (13), 1140 (5), 1070 (14), 958 (29), 919 (40), 824 (38), 747 (56), 719 (10), 677 (10), 625 (8), 585 (11), 490 (26), 414 (16), 320 (27), 277 (11).

IR (Diamond-ATR, cm⁻¹): 3149 (m), 2985 (s), 2942 (m), 2764 (w), 2689 (w), 1704 (w), 1681 (s), 1648 (w), 1594 (vs), 1492 (w), 1431 (m), 1386 (vs), 1332 (w), 1312 (s), 1279 (w), 1232 (w), 1173 (w), 1132 (m), 1067 (w), 955 (m), 921 (m), 879 (m), 843 (m), 824 (m), 735 (m), 713 (w), 677 (m).

¹H NMR (DMSO-*d*₆): 7.31 (s, 1H, CH), 6.23 (s, 2H, NH₂), 4.65 (s, 2H, CH₂).

¹³C NMR (DMSO-*d*₆): 169.1 (COO), 155.8 (CNH₂), 148.4 (CH), 47.5 (CH₂).

Elemental analysis C₄H₆N₄O₂ (142.12 g/mol) calc.: C, 33.81; H, 4.26; N, 39.42. found: C, 33.62; H, 4.25; N, 39.34.

m/z (DEI+): 142 (80, M⁺).

E_{dr} > 100 J (250–500 μm).

F_r > 360 N (250–500 μm).

E_{el} = 1.5 J (250–500 μm).

Δ_cU = -3517 cal/g.

7.2.1.5 2-Carboxymethyl-3-amino-1,2,4-triazolium Chloride (13_HCl)

Preparation analog to **13**. However, the pH of the solution was reduced to less than 1 with concentrated hydrochloric acid (37 %). After recrystallization from H₂O, colorless single crystals suitable for X-ray diffraction were obtained. Yield: 20 %.

M.p. 224 °C, 263 °C, > 400 °C (dec., DSC-measurement, 5 K/min).

Raman (400 mW, 25 °C, cm⁻¹): 3157 (50), 3115 (33), 2971 (100), 2942 (77), 1766 (16), 1745 (12), 1676 (32), 1575 (74), 1498 (21), 1432 (17), 1413 (27), 1395 (21), 1328 (28), 1291 (85), 1246 (20), 1211 (18), 1134 (18), 1107 (8), 1062 (10), 962 (38), 879 (21), 824 (85), 741 (59), 716 (11), 645 (14), 548 (8), 478 (11), 408 (10), 346 (17), 264 (9).

IR (Diamond-ATR, cm⁻¹): 3334 (m), 3140 (w), 3111 (w), 2970 (w), 2796 (w), 2593 (w), 2524 (w), 2358 (w), 1738 (m), 1682 (vs), 1572 (m), 1429 (m), 1395 (m), 1330 (w), 1290 (m), 1242 (w), 1201 (s), 1134 (w), 1101 (w), 1058 (w), 978 (w), 960 (m), 872 (m), 818 (w), 798 (w), 749 (w), 735 (m), 710 (w).

¹H NMR (DMSO-*d*₆): 8.42 (s, 1H, NH), 8.27 (s, 1H, CH), 6.43 (s, 2H, NH₂), 4.89 (s, 2H, CH₂).

¹³C NMR (DMSO-*d*₆): 168.3 (COOH), 151.0 (CNH₂), 140.0 (CH), 49.0 (CH₂).

Elemental analysis C₄H₇ClN₄O₂ (178.58 g/mol) calc.: C, 26.90; H, 3.95; N, 31.37. found: C, 26.27; H, 3.91; N, 30.54.

E_{dr} > 100 J (500–1000 μm).

F_r > 360 N (500–1000 μm).

E_{el} = 2.0 J (500–1000 μm).

Δ_cU = -2611 cal/g.

7.2.1.6 2-Carboxymethyl-3-nitrimino-1,2,4-Triazole Monohydrate (14)

At 0 °C 6.0 g (42 mmol) 2-carboxymethyl-3-amino-1,2,4-triazole (**13**) were slowly dissolved in 21 mL sulfuric acid (98 %) and then 3.5 mL (84 mmol) nitric acid (100 %) were added dropwise. The yellow solution was refluxed at 50 °C for five hours and after cooling to ambient temperature poured onto ice. The orange precipitate was recrystallized from H₂O to yield colorless single crystals, suitable for X-ray diffraction. Yield: 26 %.

M.p. 91 °C (loss of H₂O), 207 °C (dec., DSC-measurement, 5 K/min).

Raman (400 mW, 25 °C, cm⁻¹): 3168 (5), 2985 (6), 2965 (11), 1739 (8), 1524 (100), 1544 (85), 1482 (33), 1438 (12), 1399 (11), 1338 (21), 1308 (16), 1257 (11), 1093 (13), 1018 (51), 967 (18), 889 (17), 786 (9), 756 (22), 716 (4), 646 (5), 485 (13), 396 (3), 360 (10), 304 (22), 281 (17), 215 (4).

IR (Diamond-ATR, cm⁻¹): 3490 (m), 3437 (w), 3156 (m), 3004 (w), 2957 (w), 2849 (w), 2751 (w), 2640 (w), 2544 (w), 2116 (w), 1775 (w), 1728 (s), 1618 (w), 1564 (s), 1548 (m), 1480 (s), 1414 (s), 1359 (w), 1341 (w), 1314 (w), 1301 (w), 1271 (vs), 1239 (vs), 1212 (w), 1126 (m), 1096 (m), 1018 (m), 954 (m), 904 (w), 890 (w), 789 (s), 758 (m), 719 (m), 664 (m).

¹H NMR (DMSO-*d*₆): 8.52 (s, 1H, CH), 4.79 (s, 2H, CH₂).

¹³C NMR (DMSO-*d*₆): 167.7 (COOH), 150.3 (CNHNO₂), 138.4 (CH), 48.7 (CH₂).

Elemental analysis C₄H₇N₅O₅ (205.13 g/mol) calc.: C, 23.42; H, 3.44; N, 34.14. found: C, 23.15; H, 3.57; N, 33.86.

E_{dr} = 6.0 J (250-500 μm).

F_r = 324 N (250-500 μm).

E_{el} = 0.30 J (250-500 μm).

Δ_cU = -2475 cal/g.

7.2.2 Preparation of the Salts of the Triazole Derivatives

7.2.2.1 Salts of 3-Nitramino-1,2,4-triazole Monohydrate (10)

General procedure:

To 3.0 g (20 mmol) 3-Nitramino-1,2,4-triazole monohydrate (**10**) in 50 mL H₂O the corresponding hydroxides were added (**10_Na**, **10_K**, **10_Sr2**: 20 mmol; **10_Sr1**, **10_Ba**: 10 mmol). The solution was heated until it became clear and then stored at ambient temperature.

Sodium 3-Nitramino-1,2,4-triazolate Trihydrate (10_Na):

After recrystallization from H₂O, colorless single crystals suitable for X-ray diffraction were obtained. Yield: 63 %.

M.p. 113 °C (loss of H₂O), 255 °C (dec., DSC-measurement, 5 K/min).

IR (Diamond-ATR, cm⁻¹): 3468 (w), 3348 (m), 3254 (m), 3100 (w), 2780 (m), 2403 (w), 2359 (w), 2181 (w), 1819 (w), 1773 (w), 1677 (m), 1533 (s), 1486 (s), 1439 (w), 1407 (w), 1384 (m), 1333 (vs), 1281 (s), 1246 (vs), 1208 (w), 1106 (s), 1066 (vs), 1016 (s), 975 (s), 890 (m), 864 (s), 766 (m), 744 (m), 723 (s), 682 (w), 628 (w), 618 (w).

¹H NMR (DMSO-*d*₆): 12.77 (s, 1H, NH), 7.50 (s, 1H, CH).

¹³C NMR (DMSO-*d*₆): 157.1 (CNNO₂), 148.9 (CH).

Elemental analysis C₂H₈N₅NaO₅ (205.11 g/mol) calc.: C, 11.71; H, 3.93; N, 34.15. found: C, 12.54; H, 2.97; N, 35.60.

$E_{dr} > 100$ J (100-250 μm).

$F_r = 324$ N (100-250 μm).

$E_{el} = 0.75$ J (100-250 μm).

Potassium 3-Nitramino-1,2,4-triazolate (10_K):

After recrystallization from H_2O , yellow single crystals suitable for X-ray diffraction were obtained. Yield: 86 %.

M.p. 253 °C (dec., DSC-measurement, 5 K/min).

Raman (200 mW, 25 °C, cm^{-1}): 3139 (12), 1533 (72), 1493 (37), 1384 (18), 1363 (11), 1335 (23), 1275 (20), 1210 (6), 1010 (100), 977 (5), 968 (9), 858 (6), 744 (26), 487 (6), 431 (10), 415 (13), 376 (11), 240 (6).

IR (Diamond-ATR, cm^{-1}): 3093 (m), 2361 (m), 1780 (w), 1516 (m), 1487 (m), 1372 (s), 1356 (s), 1333 (vs), 1256 (vs), 1204 (s), 1093 (m), 1059 (m), 1008 (m), 992 (w), 964 (m), 891 (m), 855 (m), 794 (m), 786 (m), 723 (m), 651 (w).

^1H NMR (DMSO- d_6): 12.77 (s, 1H, NH), 7.49 (s, 1H, CH).

^{13}C NMR (DMSO- d_6): 157.0 (CNNO₂), 148.4 (CH).

Elemental analysis $\text{C}_2\text{H}_2\text{KN}_5\text{O}_2$ (167.17 g/mol) calc.: C, 14.37; H, 1.21; N, 41.89. found: C, 14.24; H, 1.39; N, 42.51.

$E_{dr} = 5.0$ J (100-500 μm).

$F_r = 240$ N (100-500 μm).

$E_{el} = 0.40$ J (100-500 μm).

$\Delta_c U = -1549$ cal/g.

Strontium bis(3-Nitramino-1,2,4-triazolate) Trihydrate (10_Sr1):

After recrystallization from H_2O , yellow single crystals suitable for X-ray diffraction were obtained. Yield: 66 %.

M.p. 151 °C (loss of H_2O), 231 °C (dec., DSC-measurement, 5 K/min).

Raman (200 mW, 25 °C, cm^{-1}): 3139 (4), 1543 (32), 1486 (100), 1458 (55), 1423 (9), 1382 (35), 1362 (18), 1303 (4), 1283 (12), 1223 (3), 1200 (6), 1078 (7), 1057 (7), 1021 (37), 1013 (21), 970 (10), 876 (4), 744 (7), 440 (5), 420 (8), 395 (9), 383 (6), 242 (6), 212 (5).

IR (Diamond-ATR, cm^{-1}): 3737 (w), 3439 (m), 2364 (m), 1631 (m), 1477 (s), 1439 (s), 1396 (vs), 1268 (vs), 1197 (s), 1073 (s), 1036 (m), 1013 (m), 863 (m), 747 (m).

^1H NMR (DMSO- d_6): 12.76 (s, 1H, NH), 7.48 (s, 1H, CH).

^{13}C NMR (DMSO- d_6): 156.9 (CNNO₂), 148.7 (CH).

Elemental analysis $\text{C}_4\text{H}_{10}\text{N}_{10}\text{O}_7\text{Sr}$ (397.81 g/mol) calc.: C, 12.08; H, 2.53; N, 35.21. found: C, 11.94; H, 2.73; N, 35.17.

$E_{dr} > 90$ J (250-500 μm).

$F_r = 288$ N (250-500 μm).

$E_{el} = 0.30$ J (250-500 μm).

$$\Delta_c U = -1044 \text{ cal/g.}$$

H₂O-sol. 6.5 wt% (22 °C).

Strontium 3-Nitramino-1,2,4-triazolate Trihydrate (10_Sr2):

A bright yellow powder was obtained after storing the solution at ambient temperature for a few hours. Yield: 68 %.

M.p. 115 °C (loss of H₂O), 169 °C (loss of H₂O), 348 °C (dec., DSC-measurement, 5 K/min).

Raman (200 mW, 25 °C, cm⁻¹): 3120 (3), 1477 (26), 1443 (100), 1357 (16), 1317 (3), 1271 (3), 1199 (3), 1076 (2), 1040 (5), 1019 (27), 996 (6), 868 (2), 758 (2), 740 (2), 431 (4), 389 (3), 250 (2).

IR (Diamond-ATR, cm⁻¹): 3490 (m, br), 1632 (m), 1479 (s), 1441 (s), 1398 (s), 1357 (m), 1305 (s), 1269 (s), 1198 (s), 1150 (w), 1075 (s), 1037 (w), 1015 (m), 993 (w), 894 (vw), 856 (m), 747 (w), 734(w), 703 (vw), 680 (w), 641 (w), 626 (w), 610 (w).

¹H NMR (DMSO-*d*₆): 7.57 (s, 1H, CH).

¹³C NMR (DMSO-*d*₆): 156.3 (CNNO₂), 148.3 (CH).

Elemental analysis C₂H₇N₅O₅Sr (268.73 g/mol) calc.: C, 8.94; H, 2.63; N, 26.06. found: C, 8.99; H, 2.80; N, 26.25.

$$E_{dr} > 100 \text{ J} \quad (80\text{-}160 \text{ }\mu\text{m}).$$

$$F_r > 360 \text{ N} \quad (80\text{-}160 \text{ }\mu\text{m}).$$

$$E_{el} = 0.30 \text{ J} \quad (80\text{-}160 \text{ }\mu\text{m}).$$

$$\Delta_c U = -952 \text{ cal/g.}$$

H₂O-sol. < 1.0 wt% (23 °C).

Barium bis(3-Nitramino-1,2,4-triazolate) Monohydrate (10_Ba):

After recrystallization from H₂O, a yellow powder was obtained. Yield: 71 %.

M.p. 201 °C (loss of H₂O), 394 °C (dec., DSC-measurement, 5 K/min).

Raman (200 mW, 25 °C, cm⁻¹): 3135 (8), 1538 (38), 1476 (100), 1377 (71), 1355 (16), 1282 (10), 1222 (5), 1112 (4), 1072 (7), 1013 (32), 971 (11), 860 (5), 752 (4), 739 (5), 665 (2), 486 (4), 413 (7), 385 (11), 239 (4).

IR (Diamond-ATR, cm⁻¹): 3737 (m), 3324 (m), 2937 (m), 1635 (vw), 1526 (w), 1474 (m), 1402 (s), 1373 (s), 1285 (s), 1270 (s), 1219 (m), 1108 (m), 1069 (s), 1014 (vw), 996 (vw), 982 (w), 966 (w), 915 (w), 888 (vw), 859 (w), 824 (w), 792 (vw), 759 (vw), 751 (vw), 730 (w), 663 (vw).

¹H NMR (DMSO-*d*₆): 12.74 (s, 1H, NH), 7.59 (s, 1H, CH).

¹³C NMR (DMSO-*d*₆): 156.8 (CNNO₂), 148.4 (CH).

Elemental analysis C₄H₇N₅O₅ (411.48 g/mol) calc.: C, 11.68; H, 1.47; N, 34.04. found: C, 11.55; H, 1.76; N, 33.77.

$$E_{dr} = 10 \text{ J} \quad (> 1000 \text{ }\mu\text{m}).$$

$$F_r > 360 \text{ N} \quad (> 1000 \text{ }\mu\text{m}).$$

$E_{el} = 0.50 \text{ J}$ ($> 1000 \mu\text{m}$).

$\Delta_c U = -1496 \text{ cal/g}$.

H₂O-sol. 5.2 wt% (22 °C).

7.2.2.2 Salts of 3-Nitro-1,2,4-triazole (**12**)

General procedure:

To a solution of 0.57 g (5.0 mmol) 3-nitro-1,2,4-triazole (**12**) in 50 mL H₂O the corresponding hydroxides were added (**12_Na**: 5.0 mmol; **12_Ca**, **12_Ba**: 2.5 mmol). The solution was heated until it became clear and then stored at ambient temperature.

Sodium 3-Nitro-1,2,4-triazole Dihydrate (12_Na):

After recrystallization from H₂O yellow crystals suitable for X-ray diffraction were obtained. Yield: 96 %.

M.p. 255 °C (dec., DSC-measurement, 5 K/min).

Raman (200 mW, 25 °C, cm⁻¹): 3135 (10), 1540 (26), 1496 (14), 1477 (8), 1398 (65), 1358 (100), 1296 (5), 1267 (10), 1174 (40), 1074 (45), 1033 (5), 999 (8), 967 (2), 832 (2), 766 (1), 544 (2), 449 (1), 424 (2), 371 (3), 239 (6).

IR (Diamond-ATR, cm⁻¹): 3367 (w), 3275 (w), 3133 (w), 2695 (w), 2660 (w), 2571 (w), 2537 (w), 2472 (w), 2431 (w), 2372 (w), 2250 (w), 2136 (w), 1843 (w), 1798 (w), 1641 (m), 1534 (m), 1492 (w), 1393 (w), 1361 (vs), 1301 (m), 1267 (m), 1177 (w), 1101 (w), 1074 (s), 1034 (w), 990 (w), 890 (w), 835 (m), 767 (w), 726 (w), 657 (w), 685 (w).

¹H NMR (DMSO-*d*₆): 7.71 (s, 1H, CH).

¹³C NMR (DMSO-*d*₆): 163.2 (CNO₂), 152.2 (CH).

Elemental analysis C₂H₅N₄NaO₄ (172.08 g/mol) calc.: C, 13.96; H, 2.93; N, 32.56. found: C, 13.90; H, 2.89; N, 32.55.

$E_{dr} > 40 \text{ J}$ (100–500 μm).

$F_r = 210 \text{ N}$ (100–500 μm).

$E_{el} = 0.20 \text{ J}$ (100–500 μm).

Calcium bis(3-Nitro-1,2,4-triazole) Hexahydrate (12_Ca):

After recrystallization from H₂O colorless crystals suitable for X-ray diffraction were obtained. Yield: 89 %.

M.p. 150 °C (loss of H₂O), 377 °C (dec., DSC-measurement, 5 K/min).

IR (Diamond-ATR, cm⁻¹): 3544 (w), 3344 (w), 3254 (m), 3102 (w), 1670 (m), 1536 (s), 1487 (s), 1420 (s), 1396 (w), 1361 (s), 1301 (m), 1282 (w), 1269 (w), 1246 (w), 1204 (w), 1159 (m), 1106 (m), 1067 (s), 1016 (m), 996 (w), 975 (m), 887 (w), 864 (m), 842 (m), 766 (w), 742 (w), 681 (m), 654 (m).

¹H NMR (DMSO-*d*₆): 7.70 (s, 1H, CH).

^{13}C NMR (DMSO- d_6): 163.1 (CNO₂), 152.1 (CH).

Elemental analysis C₄H₁₄CaN₈O₁₀ (365.27 g/mol) calc.: C, 12.84; H, 3.77; N, 29.94. found: C, 13.25; H, 3.31; N, 29.94.

$E_{\text{dr}} = 25 \text{ J}$ (> 1000 μm).

$F_{\text{r}} > 360 \text{ N}$ (> 1000 μm).

$E_{\text{el}} = 0.30 \text{ J}$ (> 1000 μm).

Barium bis(3-Nitro-1,2,4-triazole) Pentahemihydrate (12_Ba):

After recrystallization from H₂O yellow crystals were obtained. Yield: 78 %.

M.p. 152 °C (loss of H₂O), 342 °C (dec., DSC-measurement, 5 K/min).

IR (Diamond-ATR, cm⁻¹): 3586 (w), 3161 (m), 2956 (w), 2770 (w), 2362 (vw), 2233 (vw), 1633 (w), 1535 (m), 1484 (s), 1459 (m), 1403 (s), 1355 (vs), 1299 (s), 1276 (m), 1247 (m), 1160 (w), 1103 (w), 1063 (m), 1000 (w), 979 (m), 868 (w), 840 (m), 748 (w), 728 (vw), 681 (w), 654 (m).

^1H NMR (DMSO- d_6): 7.70 (s, 1H, CH).

^{13}C NMR (DMSO- d_6): 163.1 (CNO₂), 152.2 (CH).

Elemental analysis C₄H₇BaN₈O_{6.5} (408.48 g/mol) calc.: C, 11.76; H, 1.73; N, 27.43. found: C, 11.79; H, 1.65; N, 27.72.

$E_{\text{dr}} = 20 \text{ J}$ (100–500 μm).

$F_{\text{r}} > 360 \text{ N}$ (100–500 μm).

$E_{\text{el}} = 0.20 \text{ J}$ (100–500 μm).

trans Bis(diammine diaqua 3-nitro-1,2,4-triazolato-N1) Copper(II) (12_Cu):

A solution of 0.46 g (4.0 mmol) 3-nitro-1,2,4-triazole (**12**) in 100 mL aqueous ammonia solution (12 %) was combined with a solution of 0.47 g (2.0 mmol) copper(II) nitrate pentahemihydrate in 10 mL H₂O. The solution turned into dark blue and after a few hours storing at ambient temperature dark blue crystals suitable for X-ray diffraction formed. Yield: 80 %.

M.p. 130 °C (loss of H₂O or NH₃), 203 °C (loss of H₂O or NH₃), 340 °C (dec., DSC-measurement, 5 K/min).

IR (Diamond-ATR, cm⁻¹): 3615 (m), 3519 (w), 3352 (w), 3334 (m), 3256 (w), 3185 (m), 3139 (m), 1631 (m), 1618 (w), 1552 (w), 1522 (m), 1504 (w), 1484 (vs), 1403 (s), 1375 (s), 1299 (s), 1247 (s), 1171 (m), 1106 (s), 1022 (w), 1004 (m), 885 (m), 837 (s), 741 (m), 657 (m).

Elemental analysis C₄H₁₂CuN₁₀O₆ (359.75 g/mol) calc.: C, 13.35; H, 3.36; N, 38.93. found: C, 13.21; H, 3.32; N, 38.47.

$E_{\text{dr}} = 20 \text{ J}$ (250–500 μm).

$F_{\text{r}} > 360 \text{ N}$ (250–500 μm).

$E_{\text{el}} = 2.5 \text{ J}$ (250–500 μm).

H₂O-sol. < 0.3 wt% (23 °C).

7.2.2.3 Salts of 2-Carboxymethyl-3-amino-1,2,4-triazole (13) and 2-Carboxymethyl-3-nitrimino-1,2,4-triazole Monohydrate (14)

Strontium bis(2-(3-amino-1,2,4-triazol-2-yl)-acetate) Pentahydrate (13_Sr):

A solution of 2.8 g (20 mmol) 2-carboxymethyl-3-amino-1,2,4-triazole (**13**) and 2.7 g (10 mmol) strontium hydroxide octahydrate in 75 mL H₂O was heated until it became clear. A colorless precipitate formed after storing the solution at ambient temperature for a few days. After recrystallization from H₂O colorless crystals suitable for X-ray diffraction were obtained. Yield: 13 %.

M.p. 61 °C (loss of H₂O), 372 °C (dec., DSC-measurement, 5 K/min).

IR (Diamond-ATR, cm⁻¹): 3544 (w), 3436 (w), 3383 (w), 3294 (w), 3236 (w), 3007 (w), 2978 (w), 2790 (w), 2729 (w), 2319 (w), 1766 (w), 1727 (m), 1666 (m), 1576 (vs), 1532 (s), 1496 (w), 1437 (s), 1396 (s), 1367 (w), 1318 (s), 1303 (w), 1260 (w), 1212 (m), 1148 (m), 1127 (w), 1074 (m), 1029 (w), 984 (m), 953 (w), 933 (w), 887 (w), 855 (w), 825 (m), 744 (m), 698 (m), 682 (w).

¹H NMR (DMSO-*d*₆): 7.21 (s, 1H, CH), 5.92 (s, 2H, NH₂), 4.21 (s, 2H, CH₂).

¹³C NMR (DMSO-*d*₆): 170.2 (CO₂), 155.5 (CNH₂), 147.1 (CH), 51.6 (CH₂).

Elemental analysis C₈H₂₀N₈O₉Sr (459.91 g/mol) calc.: C, 20.89; H, 4.38; N, 24.36. found: C, 20.18; H, 4.79; N, 23.52.

E_{dr} > 40 J (100–500 μm).

F_r = 324 N (100–500 μm).

E_{el} = 0.30 J (100–500 μm).

Barium bis(2-(3-amino-1,2,4-triazol-2-yl)-acetate) Trihydrate (13_Ba):

A solution of 2.8 g (20 mmol) 2-carboxymethyl-3-amino-1,2,4-triazole (**13**) and 3.6 g (10 mmol) barium hydroxide octahydrate in 75 mL H₂O was heated until it became clear. A colorless precipitate was formed after storing the solution at ambient temperature for few days. After recrystallization from H₂O colorless crystals suitable for X-ray diffraction were obtained. Yield: 12 %.

M.p. 118 °C (loss of H₂O), 348 °C (dec., DSC-measurement, 5 K/min).

IR (Diamond-ATR, cm⁻¹): 3137 (83), 3108 (54), 2989 (53), 2956 (67), 1654 (27), 1576 (55), 1440 (65), 1404 (72), 1340 (100), 1284 (38), 1259 (41), 1206 (31), 1140 (21), 1087 (22), 975 (19), 930 (58), 824 (74), 741 (37), 482 (29), 416 (33), 305 (32).

¹H NMR (DMSO-*d*₆): 7.18 (s, 1H, CH), 5.90 (s, 2H, NH₂), 4.16 (s, 2H, CH₂).

¹³C NMR (DMSO-*d*₆): 169.9 (CO₂), 155.4 (CNH₂), 147.0 (CH), 51.4 (CH₂).

Elemental analysis C₈H₁₆BaN₈O₇ (473.59 g/mol) calc.: C, 20.29; H, 3.41; N, 23.66. found: C, 20.34; H, 3.33; N, 23.62.

E_{dr} > 100 J (500–1000 μm).

F_r > 360 N (500–1000 μm).

$$E_{el} = 1.5 \text{ J} \quad (500\text{--}1000 \mu\text{m}).$$

Strontium 2-(3-nitrimino-1,2,4-triazolate)-acetate Trihydrate (14_Sr):

A solution of 2.0 g (10 mmol) 2-carboxymethyl-3-nitrimino-1,2,4-triazole (**14**) and 2.7 g (10 mmol) strontium hydroxide octahydrate in 50 mL H₂O was heated until it became clear. A colorless precipitate formed after storing the solution at ambient temperature for a few days. After recrystallization from H₂O colorless crystals suitable for X-ray diffraction were obtained. Yield: 34 %.

M.p. 180 °C (loss of H₂O), 357 °C (dec., DSC-measurement, 5 K/min).

IR (Diamond-ATR, cm⁻¹): 3543 (w) 3369 (w), 3266 (w), 3137 (w), 2992 (w), 2951 (w), 2362 (w), 1772 (w), 1651 (m), 1600 (m), 1511 (m), 1493 (m), 1432 (m), 1420 (w), 1372 (s), 1343 (vs), 1304 (s), 1277 (m), 1230 (w), 1198 (w), 1122 (w), 1027 (s), 995 (w), 960 (w), 922 (w), 898 (w), 800 (w), 773 (w), 760 (m), 728 (w), 686 (w), 656 (w).

¹H NMR (DMSO-*d*₆): 7.52 (s, 1H, CH), 4.30 (s, 2H, CH₂).

Elemental analysis C₄H₉N₅O₇Sr (326.76 g/mol) calc.: C, 14.70; H, 2.78; N, 21.43. found: C, 14.51; H, 2.84; N, 21.32.

$$E_{dr} = 5.0 \text{ J} \quad (100\text{--}500 \mu\text{m}).$$

$$F_r > 360 \text{ N} \quad (100\text{--}500 \mu\text{m}).$$

$$E_{el} = 0.20 \text{ J} \quad (100\text{--}500 \mu\text{m}).$$

7.3 Conclusion

Starting from 3-amino-1,2,4-triazole (**3ATrz**), the in literature partly characterized compounds 3-nitramino-1,2,4-triazole monohydrate (**10**), 3-nitramino-1,2,4-triazole (**11**), and 3-nitro-1,2,4-triazole (**12**) were characterized via Raman-, IR-, NMR spectroscopy and elemental analysis, their decomposition temperatures, heats of formation and sensitivities to impact, friction and electric discharge were determined. Furthermore, the alkylated derivatives 2-carboxymethyl-3-amino-1,2,4-triazole (**13**), its chloride salt (**13_HCl**) and 2-carboxymethyl-3-nitrimino-1,2,4-triazole monohydrate (**14**) were investigated including the discussion of their crystal structures. All prepared triazole derivatives were compared to their tetrazole analogues.

Via deprotonation of **10** the following alkali metal and alkaline earth metal salts were prepared and fully characterized: sodium 3-nitramino-1,2,4-triazolate trihydrate (**10_Na**), potassium 3-nitramino-1,2,4-triazolate (**10_K**), strontium bis(3-nitramino-1,2,4-triazolate) trihydrate (**10_Sr1**), strontium 3-nitramino-1,2,4-triazolate trihydrate (**10_Sr2**), and barium bis(3-nitramino-1,2,4-triazolate) monohydrate (**10_Ba**). Besides their molecular structures the decomposition temperatures and sensitivities to outer stimuli were determined. The H₂O solubility at ambient temperature and color performance of **10_Sr1**, **10_Sr2**, and **10_Ba** was investigated.

Sodium 3-nitro-1,2,4-triazolate dihydrate (**12_Na**), calcium bis(3-nitro-1,2,4-triazolate) hexahydrate (**12_Ca**), and barium bis(3-nitro-1,2,4-triazolate pentahemihydrate) (**12_Ba**) were yielded from **12**. Besides spectroscopic methods of analysis, their energetic properties were investigated. The until now rarely described copper(II) compound *trans*-bis(diammine diaqua 3-nitro-1,2,4-triazolato-N1) copper(II) (**12_Cu**) was also investigated and its molecular structure discussed and compared to the assumption in reference [3d].

The molecular structures of the alkaline earth metal salts strontium bis(2-(3-amino-1,2,4-triazol-2-yl)-acetate) pentahydrate (**13_Sr**), barium bis(2-(3-amino-1,2,4-triazol-2-yl)-acetate) trihydrate (**13_Ba**), and strontium 2-(3-nitrimino-1,2,4-triazolate)-acetate trihydrate (**14_Sr**) were determined and discussed. Furthermore, their decomposition temperatures, sensitivities as well as color performance and combustion behavior in the flame of a BUNSEN burner were investigated.

In comparison to the salts of the corresponding tetrazole derivatives, the color performance and combustion behavior of the investigated salts is worse. Nevertheless, they offer a higher thermal stability, lower solubility in H₂O and are less sensitive to impact, friction, and electric discharge.

For a completion of the 1,2,4-triazole derivatives and their compounds the missing salts should be prepared. Besides that, the synthesis of 2-hydroxyethyl-3-amino-1,2,4-triazole and its nitration as well as chlorination could be investigated. In doing so, its corresponding salts can be compared to salts of 1-(2-hydroxyethyl)-5-nitriminotetrazole (**1**, chapter 2) and 1-(2-chloroethyl)-5-nitriminotetrazole (**3**, chapter 4). Depending of the color performance, combustion behavior, and physico-chemical properties of pyrotechnic relevant salts, pyrotechnic compositions based on these salts could be investigated. Especially, the strontium salts **10_Sr1**, **10_Sr2**, and **13_Sr** are promising candidates as colorant agents.

7.4 References

- [1] a) J. A. Bladin, Ber. **1885**, 18, 1544. b) J. A. Bladin, Ber. **1886**, 19, 2598.
- [2] K. T. Potts: The Chemistry of 1,2,4-Triazoles. *Chem. Rev.* **1961** 61, 87–127.
- [3] a) L. I. Bagal, M. S. Pevzer, A. N. Fralov, N. I. Sheludyakova, *Khim. Geterosiki. Soed.* **1970**, 259. b) G. Evrard, F. Durant, A. Michel, J. G. Fripiat, J. L. Closset, A. Copin: Crystal structure of 3-nitro-1,2,4-triazole, *Bull. Soc. Chim. Belg.* **1984**, 93, 233–234. c) S.-S. Yun, J.-K. Kim, C.-H. Kim: Lanthanide complexes of some high energetic compounds, crystal structures and thermal properties of 3-nitro-1,2,4-triazole-5-one (NTO) complexes, *J. Alloys Compd.* **2006**, 408, 945–951. d) J. G. Vos, W. L. Driessen, J. Van der Waal, W. L. Groeneveld: Pyrazolato and related anions. Part VII. Salts of 3-nitro-1,2,4-triazole, *Inorg. Nucl. Chem. Letters* **1978**, 14, 479–483.

- [4] T. P. Kofman, G. Kartseva, M. B. Shcherbinin: 5-Amino-3-nitro-1,2,4-triazole and Its Derivatives, *Russ. J. Org. Chem.* **2002**, 38, 1343–1350.
- [5] a) C. Ainsworth, N. R. Easton, M. Livezey, D. E. Morrison, W. R. Gibson: The anticonvulsant activity of 1,2,4-triazoles, *J. Med. Chem.* **1962**, 5, 383–389. b) B. Blank, D. M. Nichols, P. D. Vaidya: Synthesis of 1,2,4-triazoles as potential hypoglycemic agents, *J. Med. Chem.* **1972**, 15, 694–696. c) S. Jantova, G. Greif, R. Pavlovicova, L. Cipak: Antibacterial effects of some 1-substituted 1,2,4-triazoles, *Folia microbiologica* **1998**, 43, 75–78.
- [6] A. Einhorn, E. Bischkopff, B. Szelinski, G. Schupp, E. Spröngerts, C. Ladisch, T. Mauermayer: Ueber die N-Methylolverbindungen der Säureamide, *Justus Liebig's Annalen der Chemie* **1905**, 343, 207–305. b) K. Brunner: Eine neue Darstellungsweise von sekundären Säureamiden, *Chem. Ber.* **1914**, 47, 2671–2680. c) K. Brunner: Eine neue Darstellungsweise von Triazolen, *Monatsheft für Chemie* **1915**, 36, 509–534. d) M. R. Atkinson, J. B. Polya: Triazoles. Part II. N-substitution of some 1,2,4-triazoles, *J. Chem. Soc.*, **1954**, 29, 141–145.
- [7] G. Pellizzari, *Gazz. Chim. Ital.* **1911**, 41, 20.
- [8] a) R. H. Wiley, K. F. Hussung, J. Moffat: The preparation of 1,2,3-triazole, *J. Org. Chem.* **1956**, 21, 190–192; b) R. Huisgen, G. Szeimies, L. Moebius: 1,3-Dipolar cycloadditions. XXIV. Triazolines from organic azides and α,β -unsaturated carbonyl compounds or nitriles., *Chem. Ber.* **1966**, 99, 475–490; c) K. Banert: Reactions of unsaturated azides. 5. Cycloaddition reactions of 2,3-diazido-1,3-butadienes, *Chem. Ber.* **1989**, 122, 123–128.
- [9] F. Einberg: Alkylation of 5-Substituted Tetrazoles with α -Chlorocarbonyl Compounds, *J. Org. Chem.* **1970**, 35, 3978–3980.
- [10] H. R. Meier, H. Heimgartner: *Methoden der organischen Chemie*, Vol. E 8d, 4. Ed., (Ed.: E. Schaumann), Thieme Verlag, Stuttgart, **1994**, 664.
- [11] T. M. Klapötke, J. Stierstorfer, K. R. Tarantik: New Energetic Materials: Functionalized 1-Ethyl-5-aminotetrazoles and 1-Ethyl-5-nitriminotetrazoles, *Chem. Eur. J.* **2009**, 15, 5775–5792.
- [12] J. Stierstorfer: Advanced Energetic Materials based on 5-Aminotetrazole, *PhD Thesis*, **2009**, Ludwig-Maximilian University, Munich.
- [13] M. Hesse, H. Meier, B. Zeeh, *Spektroskopische Methoden in der organischen Chemie*, 7. Ed., Thieme Verlag, Stuttgart, **2005**.
- [14] N. Wiberg, E. Wiberg, A. F. Holleman: *Lehrbuch der Anorganischen Chemie*, deGruyter, Berlin, 102.Ed., **2007**.
- [15] H. D. Flack: On enantiomorph-polarity estimation, *Acta Crystallogr.* **1983**, A39, 876–881.

- [16] H. D. Flack, G. Bernardinelli: Reporting and evaluating absolute-structure and absolute-configuration diffractions, *J. Appl. Crystallogr.* **2000**, 33, 1143–1148.
- [17] a) <http://www.bam.de> b) E_{dr} : insensitive > 40 J, less sensitive \geq 35 J, sensitive \geq 4, very sensitive \leq 3 J; F_r : insensitive > 360 N, less sensitive = 360 N, sensitive < 360 N > 80 N, very sensitive \leq 80 N, extreme sensitive \leq 10 N. According to the UN Recommendations on the Transport of Dangerous Goods.
- [18] <http://webbook.nist.gov/>
- [19] T. M. Klapötke, J. Stierstorfer, K. R. Tarantik, I. D. Thoma: Strontium Nitriminotetrazolates - Suitable Colorants in Smokeless Pyrotechnic Compositions, *Z. Anorg. Allg. Chem.* **2008**, 634, 2777–2784.
- [20] a) T. M. Klapötke, C. M. Sabaté: Primary explosives: metal salts of 5-nitrotetrazole, *New Trends in Research of Energetic Materials*, Proceedings of the Seminar, 10th, Pardubice, Czech Republic, 25.–27. Apr. **2007**, Pt. 1, 230–239. b) T. M. Klapötke, C. M. Sabaté, J. M. Welch: Alkaline earth metal salts of 5-nitro-2H-tetrazole: prospective candidates for environmentally friendly energetic applications, *Eur. J. Inorg. Chem.* **2009**, 6, 769–776. c) T. M. Klapötke, C. M. Sabaté, J. M. Welch: Alkali metal 5-nitrotetrazolate salts : prospective replacements for service lead(II) azide in explosive initiators, *Dalton Trans.* **2008**, 45, 6372–6380. d) C. M. Sabaté: Azole-based energetic materials: Advances in Nitrogen-Rich chemistry, *PhD Thesis*, **2008**, Ludwig-Maximilian University, Munich.
- [21] B. C. Tappan, C. D. Incarvito, A. L. Rheingold, T. B. Brill: Thermal decomposition of energetic materials. 79. Thermal, vibrational, and X-ray structural characterization of metal salts of mono- and di-anionic 5-nitraminotetrazole, *Thermochim. Acta* **2002**, 384, 113–120.

8 Barium Salts of Tetrazole Derivatives – Suitable Colorants?

In this chapter, six barium salts of the nitrogen-rich compounds 1*H*-tetrazole (**1H-Tz**), 5-aminotetrazole (**5At**), 5-nitrimino-1,4*H*-tetrazole (**H₂AtNO₂**), 1-methyl-5-nitrimino-tetrazole (**H1MeAtNO₂**), and 2-methyl-5-nitraminotetrazole (**H2MeAtNO₂**) were investigated. The salts, barium tetrazolate (**BaTz**), barium 5-aminotetrazolate tetrahydrate (**BaAt**), and barium 5-nitriminotetrazolate dihydrate (**BaAtNO₂**) are described in literature. [1, 2, 3] **BaAt** is mentioned, as well as its corresponding strontium salt **SrAt**, as coloring agent in a patent about pyrotechnics and fireworks compositions.^[4]

Barium salts, mostly barium nitrate, are widely used in pyrotechnic composition to achieve an intense white or green flame color. A white-light emission is created by the formation of barium oxide (BaO) at temperatures above 2000 °C. For this reason the metals magnesium, aluminum or titanium are added. The green-light emitter (505–535 nm) barium monochloride (BaCl) is unstable above 2000 °C. Therefore, in green flame color mixtures the amount of metal must be held to a minimum and a chlorine donor, like PVC (poly vinyl chloride), is necessary.^[5]

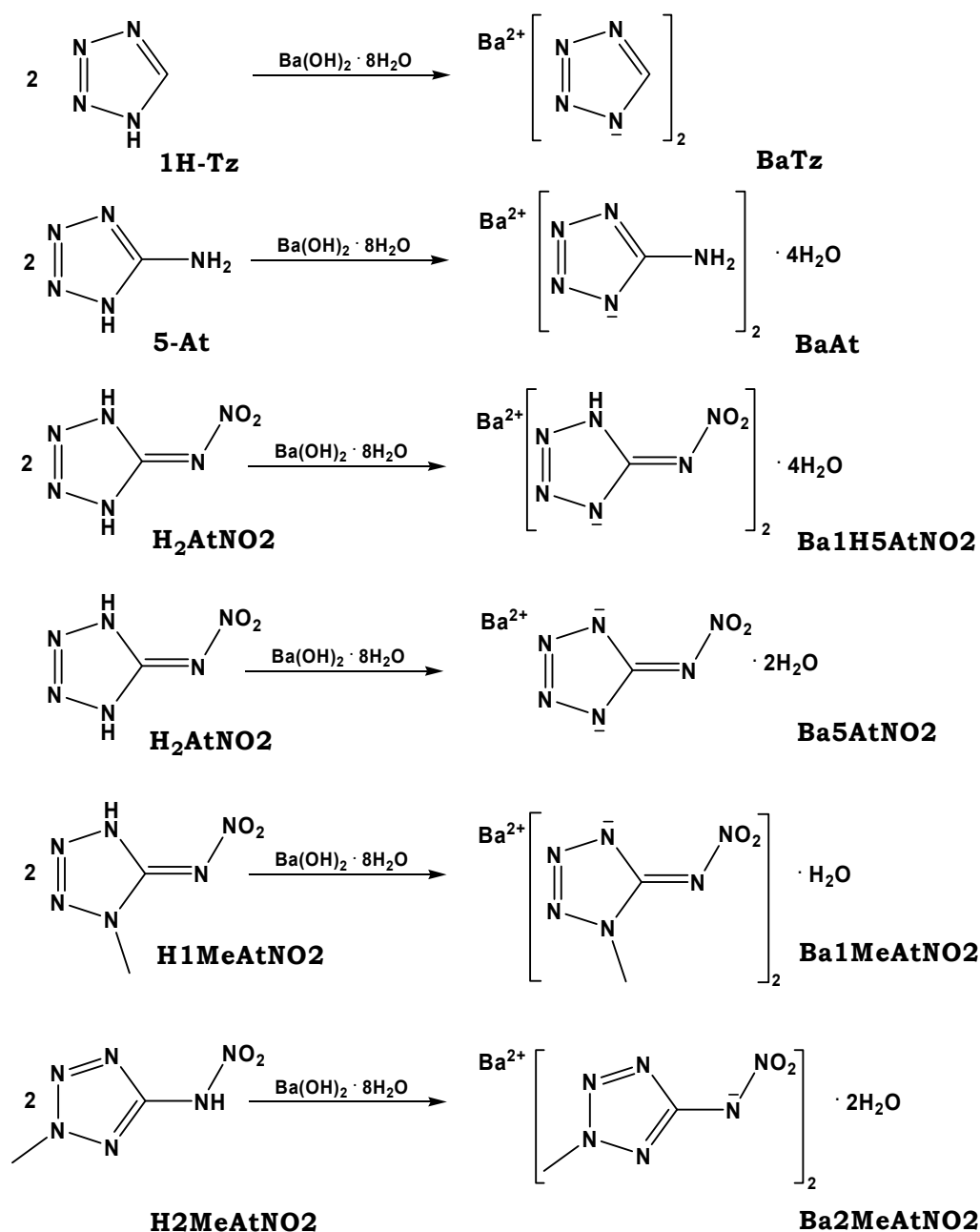
In addition to the syntheses of barium tetrazolate (**BaTz**), barium 5-aminotetrazolate tetrahydrate (**BaAt**), barium bis(5-nitrimino-1*H*-tetrazolate) tetrahydrate (**Ba1HAtNO₂**), barium 5-nitriminotetrazolate dihydrate (**BaAtNO₂**), barium 1-methyl-5-nitriminotetrazolate monohydrate (**Ba1MeAtNO₂**), and barium 2-methyl-5-nitriminotetrazolate dihydrate (**Ba2MeAtNO₂**), a comprehensive characterization as well as the energetic properties are given. Their solubilities in H₂O at ambient temperature also were determined. Furthermore, the combustion behavior and color performance in the flame of a BUNSEN burner of the neat barium compounds and in combination with PVC was investigated.

From these results an evaluation of the prepared barium salts as suitable colorants in white- or green-light emitting pyrotechnic compositions is given.

8.1 Results and Discussion

8.1.1 Syntheses

The syntheses of the barium salts, barium tetrazolate (**BaTz**), barium 5-aminotetrazolate tetrahydrate (**BaAt**), barium bis(5-nitrimino-1*H*-tetrazolate) tetrahydrate (**Ba1HAtNO₂**), barium 5-nitriminotetrazolate dihydrate (**BaAtNO₂**), barium 1-methyl-5-nitriminotetrazolate monohydrate (**Ba1MeAtNO₂**), and barium 2-methyl-5-nitriminotetrazolate dihydrate (**Ba2MeAtNO₂**) were performed using barium hydroxide octahydrate as reagent and H₂O as solvent (Scheme 8.1).



Scheme 8.1 Preparation of the barium salts **BaTz**, **BaAt**, **Ba1HAtNO₂**, **BaAtNO₂**, **Ba1MeAtNO₂**, and **Ba2MeAtNO₂**.

As starting materials the corresponding tetrazoles were used: 1*H*-tetrazole (**1H-Tz**), 5-amino-1*H*-tetrazole (**5-At**), 5-nitrimino-1,4*H*-tetrazole (**H₂AtNO₂**), 1-methyl-5-nitrimino-tetrazole (**H1MeAtNO₂**) and 2-methyl-5-nitraminotetrazole (**H2MeAtNO₂**). The nitrimino-tetrazoles were obtained by nitration of the corresponding 5-aminotetrazoles according to a procedure described in literature.^[6] After recrystallization from H₂O all barium salts could be obtained in good yields above 90 %.

8.1.2 Molecular Structures

Suitable single crystals of **BaAt**, **Ba1HAtNO₂**, **Ba1MeAtNO₂**, and **Ba2MeAtNO₂** for X-ray diffraction measurements could be obtained *via* recrystallization from H₂O. Also single crystals of **BaTz** have been obtained from a water/ethanol mixture. However, its structure solution could only be refined insufficiently due to strongly disordered tetrazole moieties and is therefore not further discussed. All relevant data and parameters of the X-ray measurements and refinements are given in Appendix VIII. The molecular structures of **BaAt** and **BaAtNO₂** are extensively described in the literature.^[2, 3]

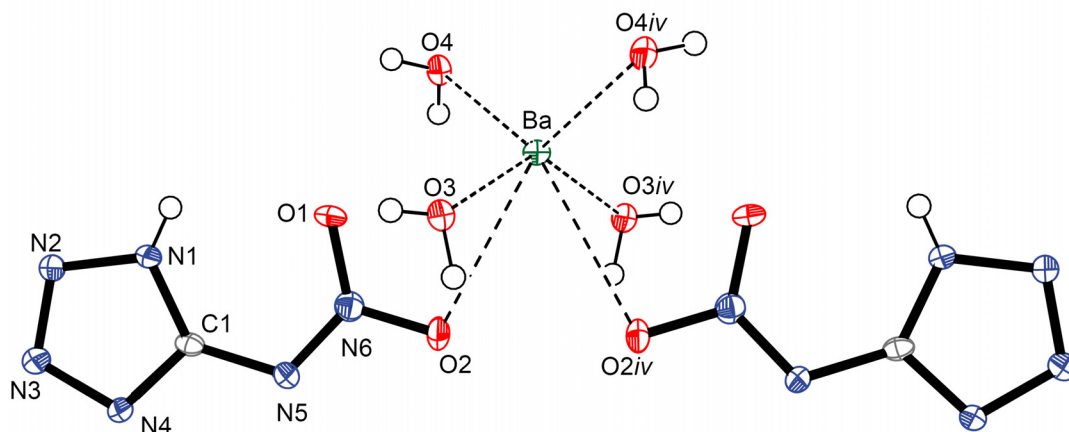


Figure 8.1 Molecular unit of **Ba1HAtNO₂**. Hydrogen atoms are shown as spheres of arbitrary radius and thermal displacements are set at 50 % probability. Selected coordination distances (Å): O1–Ba 2.996(2), O2–Ba 2.867(2), O3–Ba 2.785(3), O4–Ba 2.874(3); *iv*) 1–x, y, 0.5–z.

Barium bis(5-nitrimino-1*H*-tetrazolate) tetrahydrate (**Ba1HAtNO₂**) crystallizes in the orthorhombic space group *Pbcn* with four molecular units per unit cell (Figure 8.1). The density of 2.326 g/cm³ is significantly lower than the density observed for barium 5-nitriminotetrazolate dihydrate (**BaAtNO₂**) of 2.911 g/cm³.^[2, 3] All crystal water molecules are coordinated to the barium centers, whereby half of them are μ^2 coordinated forming towels along the *c* axis. Including also the longer Ba–O1 coordination distances (2.996(2) Å), the barium atoms are tenfold coordinated. Analog to its corresponding strontium salt, the packing of **Ba1HAtNO₂** is characterized by the formation of stacks along the *c* axis. The stacks are built by bridging H₂O molecules in the centers. Both 5-nitriminotetrazole anions coordinated to one barium atom are located at the same side.

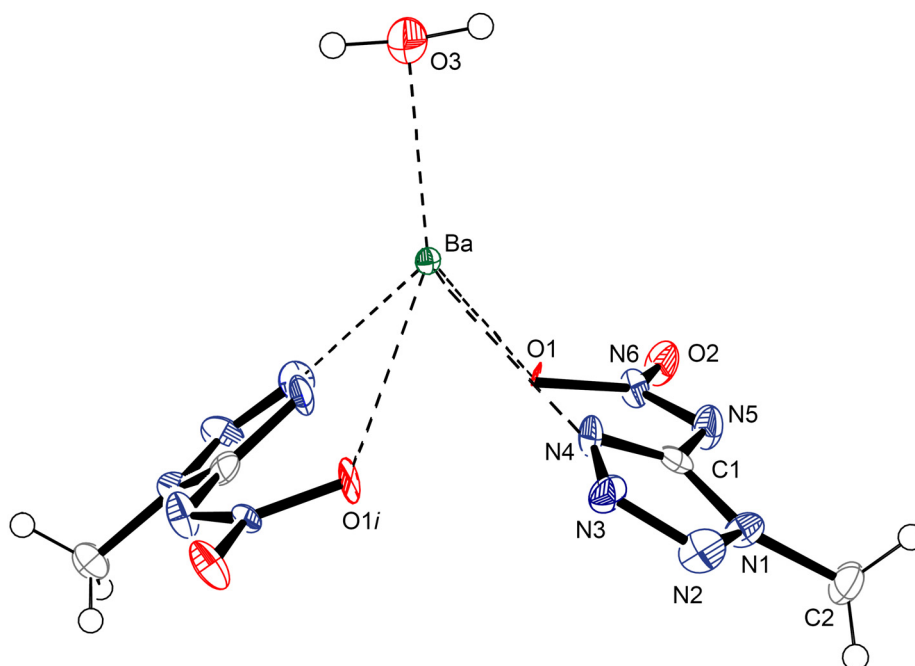


Figure 8.2 Molecular unit of **Ba1MeAtNO2**. Hydrogen atoms are shown as spheres of arbitrary radius and thermal displacements are set at 50 % probability. Selected coordination distances (Å): O1–Ba 2.89(1), N4–Ba 2.92(1), Ba–O3 2.79(2); i $-x, y, 0.5-z$.

Barium 1-methyl-5-nitriminotetrazolate monohydrate (**Ba1MeAtNO2**), shown in Figure 8.2, crystallizes in the monoclinic space group $C2/c$ with a density of 2.303 g/cm³. The barium as well as the oxygen atom of the H₂O molecule are located on the special position 0, y , 1/4. Taking into account coordination distances up to 3.03 Å, the barium centers are surrounded by eleven neighbors. The structure of the 1-methyl-5-nitriminotetrazolate anion is in the range of these observed for its strontium,^[2, 7] as well as potassium salt.^[2, 8] The N6–O1(2) bonds are twisted $\sim 20^\circ$ out of the tetrazolate ring plane.

The packing of **Ba1MeAtNO2** is again strongly influenced by the formation of stacks along the c axis. Analog to its corresponding strontium salt **Sr1MeAtNO2**,^[2, 7] the connection within the stacks are generated by the tridentate coordination modes of the atoms N4, O1 and O2 within one anion. The crystal water affects no bridging and the water molecules are coordinated alternating up and down.

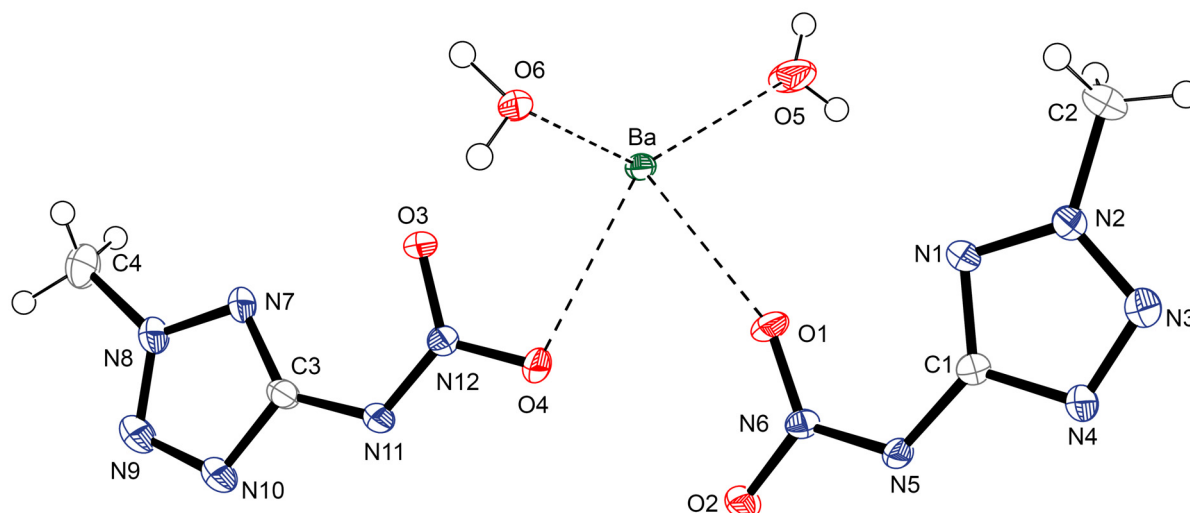


Figure 8.3 A view on the asymmetric unit of **Ba2MeAtNO2**. Hydrogen atoms are shown as spheres of arbitrary radius and thermal displacements are set at 50 % probability. Selected coordination distances (Å): Ba–O1 2.859(2), Ba–O3 2.990(2), Ba–O2*i* 2.870(2), Ba–O5 2.669(2), Ba–O4 2.824(2), Ba–O6 2.850(2), Ba–N5*i* 2.936(2), Ba–N12 3.341(2); *i* –1+x, y, z.

The solid state structure of barium 2-methyl-5-nitriminotetrazolate dihydrate (**Ba2MeAtNO2**) is considerably different to its 1-methyl analog. **Ba2MeAtNO2** crystallizes in the triclinic space group *P*-1 with two molecular moieties (one shown in Figure 8.3) per unit cell. Its density of 2.154 g/cm³ is comparable to the density of barium 5-aminotetrazolate tetrahydrate **BaAt** (2.128 g/cm³ [2, 3]). The barium cations are again tenfold coordinated. The molecular moieties are arranged in layers which are connected by the μ^2 -bridging oxygen atom O6 along the *b* axis. The structural geometry of the anions is comparable to this observed for the corresponding strontium salt.[2, 7] In contrast to **Ba1MeAtNO2**, the nitro groups are almost located in the tetrazole ring plane.

Bond lengths of the tetrazole anions are listed in Table 8.1. For a better comparison the literature adopted bond lengths of **BaAt** and **BaAtNO2** were added.[2, 3]

Table 8.1 Bond lengths (Å) for selected anions in the solid state structures of **BaAt**, **Ba1H5AtNO2**, **BaAtNO2**, **Ba1MeAtNO2**, and **Ba2MeAtNO2** with estimated standard deviations in parentheses.

	BaAt	Ba1HAtNO2	BaAtNO2	Ba1MeAtNO2	Ba2MeAtNO2
N1–N2	1.350(8)	1.348(4)	1.356(3)	1.32(2)	1.329(3)
N2–N3	1.302(9)	1.301(3)	1.316(3)	1.29(2)	1.316(3)
N3–N4	1.359(9)	1.351(3)	1.347(3)	1.32(2)	1.321(3)
N4–C1	1.330(9)	1.330(4)	1.348(4)	1.37(2)	1.356(3)
N1–C1	1.344(9)	1.340(4)	1.335(3)	1.37(2)	1.339(3)
C1–N5	1.374(9)	1.379(4)	1.389(4)	1.36(2)	1.380(3)
N5–N6		1.298(3)	1.293(3)	1.30(2)	1.301(3)
O1–N6		1.257(3)	1.277(3)	1.30(1)	1.252(2)
O2–N6		1.274(3)	1.275(3)	1.21(1)	1.279(2)
N1(2)–C2				1.47(2)	1.466(3)

8.1.3 Energetic Properties

The energetic properties such as the decomposition temperature (T_{dec}), sensitivities to impact (E_{dr}), friction (F_r) and electric discharge (E_{el}), as well as the combustion energy ($\Delta_c U$) were determined or adopted from literature to yield a complete overview.^[2, 3] Furthermore, the solubility in H₂O at ambient temperature of each compound was defined. An overview of the energetic properties is given in Table 8.2.

Table 8.2 Energetic properties of **BaTz**, **BaAt**, **Ba1HAtNO2**, **BaAtNO2**, **Ba1MeAtNO2**, and **Ba2MeAtNO2**.

Salt	BaTz	BaAt	Ba1HAtNO2	BaAtNO2	Ba1MeAtNO2	Ba2MeAtNO2
Formula	Ba(C ₂ H ₁₀ N ₈) ₂	Ba(CH ₂ N ₅) ₂ · 4H ₂ O	Ba(CHN ₆ O ₂) ₂ · 4H ₂ O	Ba(CN ₆ O ₂) · 2H ₂ O	Ba(C ₂ H ₃ N ₆ O ₂) ₂ · H ₂ O	Ba(C ₂ H ₃ N ₆ O ₂) ₂ · 2H ₂ O
M [g/mol]	275.42	377.51	467.50	301.41	441.51	459.53
E_{dr} [J]^a	35	> 100	7.0	30	15	7.0
F_r [N]^b	> 360	244	252	240	> 360	> 360
E_{el} [J]^c	0.80	1.25	0.60	0.60	0.65	0.50
grain size [μm]	250–500	> 1000	160–250	160–250	250–500	250–500
N [%]^d	40.68	37.10	35.95	27.88	38.07	36.58
Ω [%]^e	-34.86	-29.67	-6.84	-5.31	-43.49	-41.78
T_{dec} [°C]^f	323	360	236	376	349	257
ρ [g/cm³]^g	2.28* (25 °C)	2.13	2.33	2.91	2.30	2.15
Δ_cU [cal/g]^h	-5905	-5657	-4270	-2860	-6050	-7071
Δ_cH^o [kJ/mol]	-1618	-2125	-1977	-853	-2654	-3235
Δ_fH^o [kJ/mol]	-3	-925	-797	-660	-612	-317
H₂O sol. [wt%]ⁱ	31 (22°C)	(22°C)	(22°C)	(22°C)	(21°C)	11 (22°C)

a) BAM drop hammer^[9], b) BAM methods^[9], c) Electric discharge tester, d) Nitrogen content; e) Oxygen balance; f) Decomposition temperature from DSC ($\beta = 5$ K/min); g) determined by X-ray crystallography or pycnometer (*); h) Combustion energy, i) Solubility in H₂O (H₂O temperature).

The thermal behavior of ~1.5 mg of the barium salts in the temperature range from 30–400 °C is illustrated as DSC thermograms in Figure 8.4. The endothermic signals have been checked using a *Büchi* melting point apparatus to differ melting points from loss of crystal water. No melting of all compounds was observed in the investigated temperature range. All salts show decomposition at temperatures above 230 °C. Compound **Ba1HAtNO2** offers the lowest decomposition point at 236 °C. It loses crystal water at 128 °C. The salts **BaAt** and **BaAtNO2** also lose their crystal water (at 76 °C, 137 °C and 174 °C, respectively), before they decompose (**BaAt**: $T_{\text{dec}} = 360$ °C, **BaAtNO2**: $T_{\text{dec}} = 376$ °C). The compounds **BaTz**, **Ba1MeAtNO2** and **Ba2MeAtNO2** decompose at 323 °C, 349 °C and 257 °C, respectively, without prior endothermic reactions. With these results the thermal behavior of **BaTz**, **BaAt**, **Ba1HAtNO2**, **BaAtNO2**, **Ba1MeAtNO2**, and **Ba2MeAtNO2** is comparable to the corresponding strontium salts strontium tetrazolate pentahydrate (**SrTz**), strontium 5-aminotetrazolate tetrahydrate (**SrAt**), strontium bis(5-nitrimino-1*H*-tetrazolate) tetrahydrate (**Sr1HAtNO2**), strontium 5-nitriminotetrazolate monohydrate (**SrAtNO2**),

strontium 1-methyl-5-nitriminotetrazolate monohydrate (**Sr1MeAtNO2**), and strontium 2-methyl-5-nitriminotetrazolate dihydrate (**Sr2MeAtNO2**) (see chapter 9).^[2, 7] Regarding the application in pyrotechnics of the prepared salts, as nitrogen-rich fuels or colorants, the opportunity of removing the crystal water of the compounds **BaAt**, **Ba1HAtNO2**, and **BaAtNO2** by drying at temperatures above 140 °C, 130 °C, and 175 °C, respectively, exists. Besides that, the compounds can be dried under high vacuum.

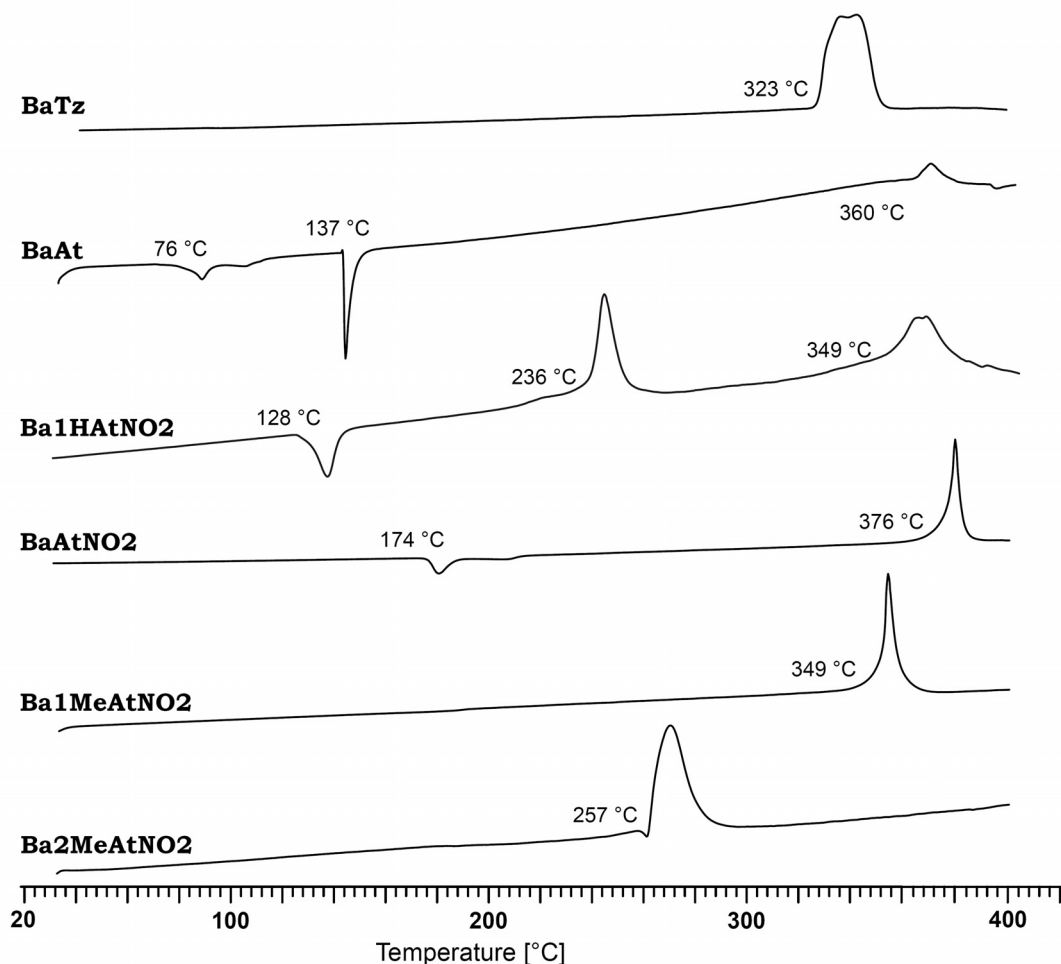


Figure 8.4 DSC thermograms (exo up) of **BaTz**, **BaAt**, **Ba1HAtNO2**, **BaAtNO2**, **Ba1MeAtNO2**, and **Ba2MeAtNO2** in the temperature range of 30–400 °C.

All sensitivities of the barium salts were determined with the following grain sizes: 160–250 μm (**Ba1HAtNO2**, **BaAtNO2**), 250–500 μm (**BaTz**, **Ba1MeAtNO2**, and **Ba2MeAtNO2**), and >1 mm (**BaAt**). Except for **BaAt** ($E_{\text{dr}} > 100$ J), which has shown to have potential in initiation systems,^[10] all compounds show sensitivity to impact (**Ba1HAtNO2**, **Ba2MeAtNO2**: 7.0 J, **BaAtNO2**: 30 J, **Ba1MeAtNO2**: 15 J) according to literature.^[9] **BaTz** is less sensitive to impact with 35 J, but as well as the salts **Ba1MeAtNO2** and **Ba2MeAtNO2** insensitive to friction. All other barium salts are sensitive to friction (**BaAt**: 244 N, **Ba1HAtNO2**: 252 N, **BaAtNO2**: 240 N).

All determined values for the electrostatic sensitivity are in the range of 0.50–1.25 J (**Ba2MeAtNO2**: 0.50 J; **Ba1HAtNO2**, **BaAtNO2**: 0.60 J; **Ba1MeAtNO2**: 0.65 J, **BaTz**: 0.80 J; **BaAt**: 1.25 J).

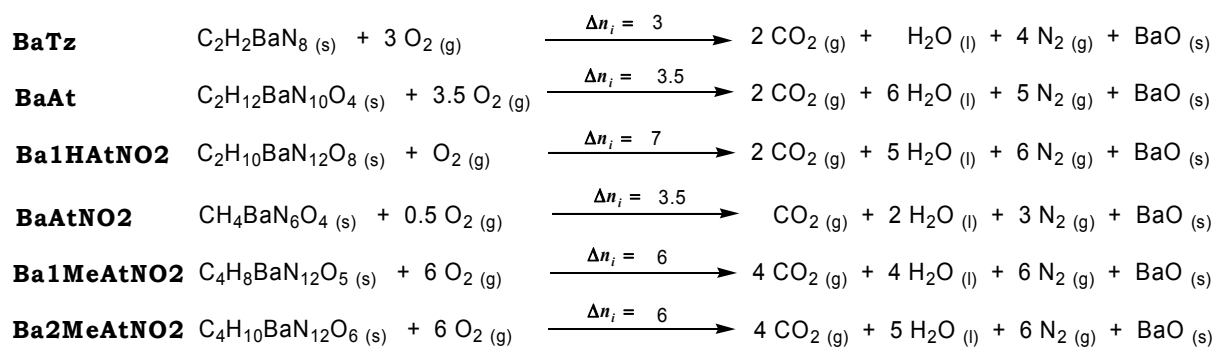
The reported values of the combustion energies ($\Delta_c U$) are the average of three single bomb calorimetry measurements. The standard molar enthalpy of combustion ($\Delta_c H^\circ$) was derived from equation 8.1.

$$\Delta_c H^\circ = \Delta_c U + \Delta nRT \quad (8.1)$$

$$\Delta n = \sum n_i (\text{gaseous products}) - \sum n_i (\text{gaseous educts})$$

n_i = molar amount of gas i .

The enthalpies of formation ($\Delta_f H^\circ$) for **BaTz**, **BaAt**, **Ba1HAtNO2**, **BaAtNO2**, **Ba1MeAtNO2**, and **Ba2MeAtNO2** were calculated at 298.15 K using the HESS thermochemical cycle and the following combustion reactions (Scheme 8.2). The heats of formation of the combustion products $\text{H}_2\text{O}_{(l)}$ (-286 kJ/mol), $\text{CO}_2_{(g)}$ (-393 kJ/mol), and $\text{BaO}_{(s)}$ (-548 kJ/mol) were adopted from literature.^[11]



Scheme 8.2 Combustion equations of **BaTz**, **BaAt**, **Ba1HAtNO2**, **BaAtNO2**, **Ba1MeAtNO2**, and **Ba2MeAtNO2**.

All barium salts were calculated to be formed exothermically, whereas **BaTz** offers the lowest value. **BaAt** shows the highest exothermic heat of formation with -925 kJ/mol. Certainly the higher heat of formation of **BaTz** results from the combustion of its water-free status.

All barium salts were tested, with respect to their solubility, in pure water at ambient temperature. Therefore, each salt was added to 1 mL H_2O with before noted temperature until the solution was saturated. The solubilities of **BaTz**, **BaAt**, **Ba1HAtNO2**, **BaAtNO2**, **Ba1MeAtNO2**, and **Ba2MeAtNO2** are given in percent by weight (wt%) and were calculated according to equation 8.2.

$$\text{H}_2\text{O-sol.} = \frac{m_{\text{dissolved Compound}}}{m_{\text{dissolved Compound}} + m_{\text{Solvent}}} \cdot 100 \quad (8.2)$$

The H_2O temperature was 22 °C, except in the case of **Ba1MeAtNO2**, which was dissolved at 21 °C. **BaTz** offers the highest solubility with 31 wt%. This might be caused by the fact that it does not contain any chemically bound water molecules. The salts **BaAt** and

Ba2MeAtNO2 are almost comparable as both are soluble in H₂O with 10 wt% and 11 wt%, respectively. Both salts of **H₂AtNO2** show a low solubility (**Ba1HATNO2**: 2.5 wt%, **BaAtNO2**: 0.9 wt%). The solubility of **Ba1MeAtNO2** was determined with 1.8 wt%. For comparison, barium nitrate obeys a solubility of 9.7 wt% at 21 °C in H₂O. The solubilities of all barium salts increase by increasing the temperature of the solvent.

8.1.4 Flame Color and Combustion Behavior

For determining the color performance of the pure compounds, a few milligrams of each barium salt were put on a spatula into an oxygen rich flame of a BUNSEN burner. The produced flames are depicted in Figure 8.5.

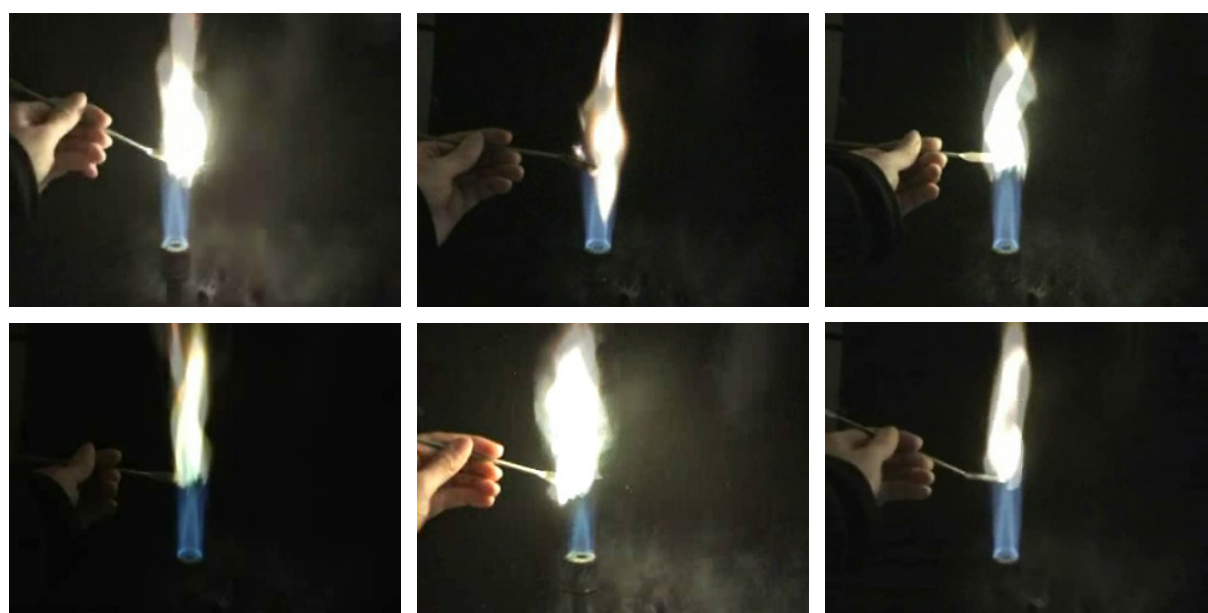


Figure 8.5 Color performance of the barium salts **BaTz** (top, left), **BaAt** (top, center), **Ba1HAtNO2** (top, right), **BaAtNO2** (down, left), **Ba1MeAtNO2** (down, center), and **Ba2MeAtNO2** (down, right) in the flame of a BUNSEN burner.

All barium salts combust without any remarkable smoke production and only a very small amount of solid residues. Compound **Ba1MeAtNO2** shows the best color performance with the most greenish flame. The barium salts **BaTz**, **BaAt**, and **Ba2MeAtNO2** offer a bright colorless flame. The salts **Ba1HAtNO2** and **BaAtNO2** combust with a partly greenish flame and while sizzling analog to the strontium salts **Sr1HAtNO2** and **SrAtNO2** (see chapter 9).

Furthermore, the combustion behavior of the barium salt **Ba1MeAtNO2** was qualitatively characterized with a simple smoke test method. Therefore, approx. 1 g of the compound was placed in a heated crucible with a gas torch for observation of color, smoke, burn ability (propagation), and level of residue. It verified the observed white-green flame color in the BUNSEN burner. Neither smoke nor residues were observed.



Figure 8.6 Color performance of the barium chloride dihydrate (left), barium nitrate (center), and a mixture of barium chloride dihydrate and barium nitrate (right) in the flame of a BUNSEN burner.

For comparison the color performance in the flame of a BUNSEN burner, barium chloride dihydrate and barium nitrate as well as a mixture of both salts (50 wt%:50 wt%) was determined (Figure 8.6).

The flame of barium chloride dihydrate is intense white with a reddish seam. The same result could be observed with the mixture. Only barium nitrate offers a partly yellow-green flame.

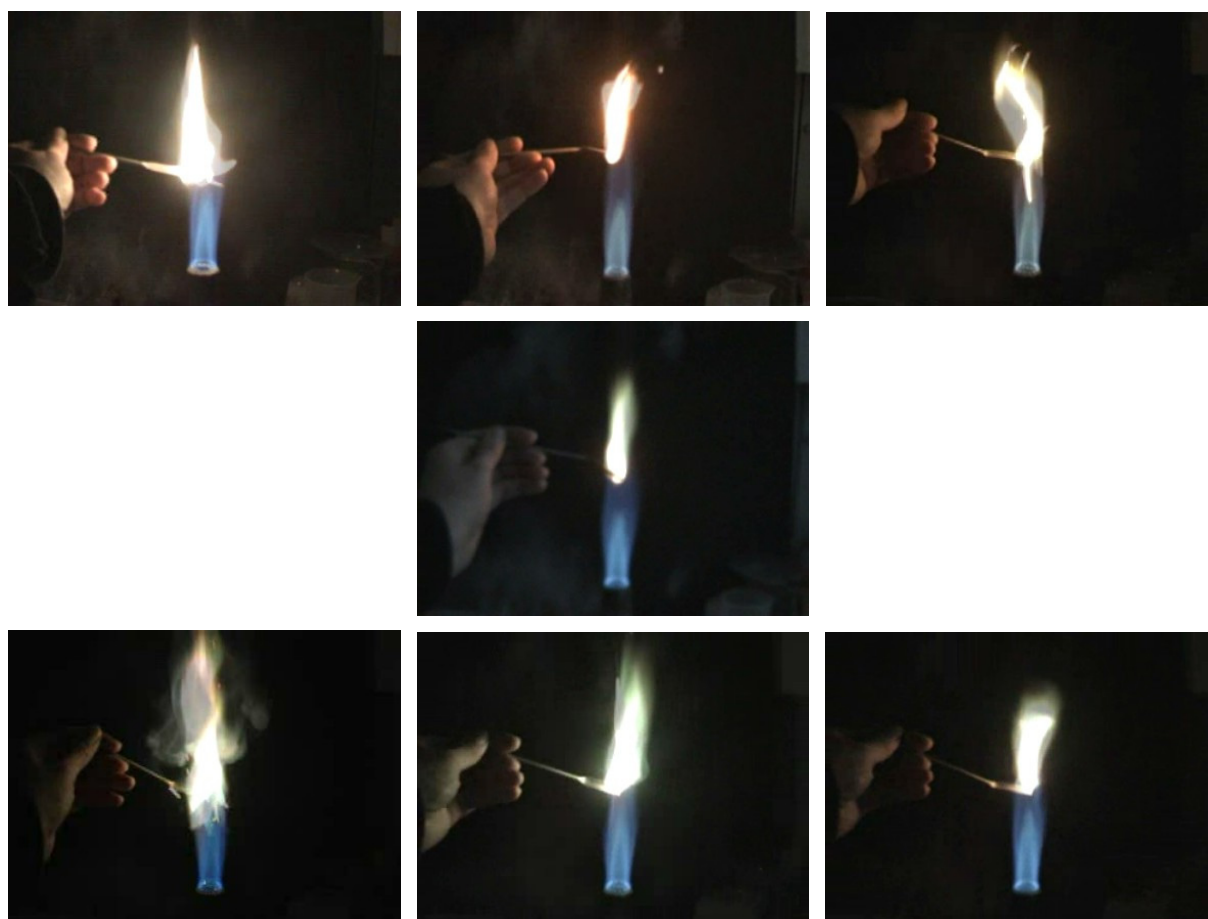


Figure 8.7 Color performance of the mixtures of PVC and the barium salts **BaTz** (top, left), **BaAt** (top, center), **Ba1HAtNO2** (top, right), $\text{Ba}(\text{NO}_3)_2$ (center), **BaAtNO2** (down, left), **Ba1MeAtNO2** (down, center), and **Ba2MeAtNO2** (down, right) in the flame of a BUNSEN burner.

Pyrotechnic compositions containing barium nitrate and some chlorine donor offer a very intense green light. This might be true for the prepared nitrogen-rich barium salts. To

get a first impression, the salts were mixed with PVC (poly vinyl chloride) at the ratio of 50 wt%:50 wt% and then put into the flame of a BUNSEN burner (Figure 8.7). Except **BaTz** and **BaAt**, all barium salts show a pale yellow-green flame color. **Ba1MeAtNO2** offers the best performance with an intense green flame. For comparison, barium nitrate was mixed with PVC. The mixture is more intense green than neat barium nitrate (Figure 8.7, middle), however less green than the mixture with **Ba1MeAtNO2**.

Due to these results it can be concluded, the neat prepared barium compounds **BaTz**, **BaAt**, **Ba1HAtNO2**, **BaAtNO2**, **Ba1MeAtNO2**, and **Ba2MeAtNO2** are suitable for the substitution of barium nitrate in white-light emitting composition, which does not contain any chlorine donors. However, if chlorine is present, the barium salts of the 5-nitriminotetrazole derivatives offer a very convincing color performance.

8.2 Experimental Part

*CAUTION! Some barium salts are sensitive to impact, friction and electric discharge. Therefore, proper protective measures (safety glasses, face shield, leather coat, earthed equipment and shoes, Kevlar® gloves, and ear plugs) should be used, especially during work on the precursor molecules 5-nitriminotetrazole (**H2AtNO2**), 1-methyl-5-nitriminotetrazole (**H1MeAtNO2**), and 2-methyl-5-nitriminotetrazole (**H2MeAtNO2**).*

8.2.1 Barium Tetrazolate (**BaTz**)

Preparation according to THIELE [1]. A solution of 1.00 g (14.3 mmol) 1H-tetrazole (**1H-Tz**) and 2.26 g (7.15 mmol) barium hydroxide octahydrate in 20 mL H₂O was refluxed for 15 minutes. The solvent was evaporated to obtain a colorless powder. Yield: 87 %.

M.p. 323 °C (dec., DSC-measurement, 5 K/min).

Raman (200 mW, 25 °C, cm⁻¹): 3152 (19), 1478 (1), 1445 (2), 1428 (15), 1400 (1), 1285 (29), 1193 (100), 1151 (1), 1137 (9), 1093 (11), 1019 (5), 1007 (3), 895 (1), 736 (1), 701 (4), 208 (5).

IR (Diamond-ATR, cm⁻¹): 3151 (w), 1792 (vw), 1444 (w), 1427 (m), 1286 (m), 1192 (s), 1158 (s), 1151 (m), 1135 (m), 1094 (w), 1017 (s), 1004 (s), 896 (s), 699 (s).

¹H NMR (DMSO-*d*₆): 8.06.

¹³C NMR (DMSO-*d*₆): 149.2.

Elemental analysis C₂H₂BaN₈ (275.42 g/mol): calc.: C, 8.72; H, 0.73; N, 40.68; found: C, 8.68; H, 0.77; N, 40.72.

E_{dr} = 35 J (250–500 μm).

F_r > 360 N (250–500 μm).

E_{el} = 0.80 J (250–500 μm).

Δ_cU = -1410 cal/g.

H₂O-sol. 31 wt% (22 °C).

8.2.2 Barium 5-Aminotetrazolate Tetrahydrate (BaAt)

Preparation according to the literature.^[2, 3] A solution of 3.71 g (11.8 mmol) barium hydroxide octahydrate and 2.00 g (23.5 mmol) 5-amino-1*H*-tetrazole (**5-At**) in 60 mL H₂O was refluxed for 20 minutes. After evaporation of the solvent and recrystallization from H₂O a colorless powder could be obtained. Yield: 95 %.

M.p. 76 °C (loss of H₂O), 137 °C (loss of H₂O), 360 °C (dec., DSC-measurement, 5 K/min).

Raman (300 mW, 25 °C, cm⁻¹): 3232 (12), 1628 (12), 1539(39), 1508 (8), 1439 (15), 1236 (27), 1220 (27), 1128 (50), 1070 (100), 1013 (18), 748 (37), 421 (15), 212 (13).

IR (Diamond-ATR, cm⁻¹): 3408 (s), 3320 (s), 3210 (s), 1621 (m), 1520 (s), 1440 (m), 1355 (w), 1262 (vw), 1234 (w), 1214 (w), 1156 (w), 1127 (w), 1097 (w), 1064 (vw), 1012 (vw), 850 (vw), 749 (w).

¹H NMR (DMSO-*d*₆): 6.46 (s, NH₂), 3.33 (s, H₂O).

¹³C NMR (DMSO-*d*₆): 164.5.

Elemental analysis C₂H₁₂BaN₁₀O₄ (377.51 g/mol): calc.: C, 6.36; H, 3.20; N, 37.10; found: C, 6.26; H, 3.08; N, 35.80.

E_{dr} > 100 J (> 1000 μm).

F_r = 244 N (> 1000 μm).

E_{el} = 1.25 J (> 1000 μm).

Δ_cU = -1350 cal/g.

H₂O-sol. 10 wt% (22 °C).

8.2.3 Barium bis(5-Nitrimino-1*H*-tetrazolate) Tetrahydrate (Ba1HAtNO2)

A solution of 3.15 g (10.0 mmol) barium hydroxide octahydrate and 2.60 g (20.0 mmol) 5-nitriminotetrazole (**H₂AtNO₂**) in 100 mL H₂O was refluxed for 25 minutes. The solvent was evaporated to obtain a colorless powder. Recrystallization from H₂O yielded 4.29 g of colorless needles suitable for X-ray diffraction after storing the solution at ambient temperature for several days. Yield: 92 %.

M.p. 128 °C (loss of H₂O), 236 °C (dec., DSC-measurement, 5 K/min).

Raman (200 mW, 25 °C, cm⁻¹): 3294 (2), 1659 (1), 1543 (100), 1382 (9), 1366 (6), 1331 (35), 1170 (3), 1161 (8), 1122 (4), 1112 (5), 1062 (7), 1038 (36), 994 (16), 869 (5), 756 (9), 739 (1), 701 (1), 498 (3), 466 (2), 436 (5), 418 (9), 371 (6), 251 (2), 223 (8).

IR (Diamond-ATR, cm⁻¹): 3387 (s), 3278 (s), 2922 (m, br), 2689 (m, br), 2365 (w), 1793 (vw), 1668 (w), 1527 (m), 1414 (s), 1363 (s), 1325 (s), 1248 (s), 1156 (vw), 1110 (w), 1062 (s), 1035 (m), 989 (m), 926 (w), 900 (w), 867 (w), 728 (s), 699 (s).

¹H NMR (DMSO-*d*₆): 14.88 (s, NH), 3.33 (s, H₂O).

¹³C NMR (DMSO-*d*₆): 158.4.

Elemental analysis $C_2H_{10}BaN_{12}O_8$ (467.50 g/mol): calc.: C, 5.14; H, 2.16; N, 35.95; found: C, 5.15; H, 2.13; N, 35.55.

$$E_{dr} = 7.0 \text{ J} \quad (160\text{--}250 \mu\text{m}).$$

$$F_r = 252 \text{ N} \quad (160\text{--}250 \mu\text{m}).$$

$$E_{el} = 0.60 \text{ J} \quad (160\text{--}250 \mu\text{m}).$$

$$\Delta_c U = -1019 \text{ cal/g.}$$

H₂O-sol. 2.5 wt% (22 °C).

8.2.4 Barium 5-Nitriminotetrazolate Dihydrate (BaAtNO₂)

Preparation according to the literature.^[2, 3] A solution of 6.30 g (20.0 mmol) barium hydroxide octahydrate and 2.60 g (20.0 mmol) 5-nitriminotetrazole (**H₂AtNO₂**) in 200 mL H₂O was refluxed for 25 minutes. After filtration, the crude product was recrystallized from hot water obtaining colorless crystals. Yield: 92 %.

M.p. 174 °C (loss of H₂O), 376 °C (dec., DSC-measurement, 5 K/min).

Raman (200 mW, 25 °C, cm⁻¹): 3215 (4), 2537 (2), 1450 (100), 1383 (7), 1215 (10), 1142 (7), 1082 (3), 1039 (4), 1015 (24), 881 (1), 767 (1), 705 (1), 492 (2), 428 (5), 400 (6), 259 (1), 152 (3).

IR (Diamond-ATR, cm⁻¹): 3433 (m), 3196 (m, br), 3018 (m), 2967 (m), 1648 (w), 1580 (m), 1502 (s), 1454 (s), 1391 (s), 1348 (vs), 1307 (s), 1257 (s), 1137 (w), 1105 (w), 1077 (w), 1037 (w), 1018 (m), 910 (vw), 878 (w), 855 (w), 775 (w), 751 (w), 726 (vw), 696 (w), 678 (w).

¹H NMR (DMSO-*d*₆): 3.35 (s, H₂O).

¹³C NMR (DMSO-*d*₆): 164.8.

Elemental analysis $CH_4BaN_6O_4$ (301.41 g/mol): calc.: C, 3.98; H, 1.34; N, 27.88; found: C, 4.15; H, 1.39; N, 27.96.

$$E_{dr} = 30 \text{ J} \quad (160\text{--}250 \mu\text{m}).$$

$$F_r = 240 \text{ N} \quad (160\text{--}250 \mu\text{m}).$$

$$E_{el} = 0.60 \text{ J} \quad (160\text{--}250 \mu\text{m}).$$

$$\Delta_c U = -683 \text{ cal/g.}$$

H₂O-sol. 0.9 wt% (22 °C).

8.2.5 Barium 1-Methyl-5-nitriminotetrazolate Monohydrate (Ba1MeAtNO₂)

A solution of 6.31 g (20.0 mmol) barium hydroxide octahydrate and 5.76 g (40.0 mmol) 1-methyl-5-nitriminotetrazole (**H1MeAtNO₂**) in 250 mL H₂O was refluxed for 15 minutes. The solvent was removed *in vacuo* to obtain a light yellow powder. Recrystallization from H₂O yielded very light yellow needles suitable for X-ray diffraction, after storing the reaction solution at ambient temperature for several days. Yield: 96 %.

M.p. 349 °C (dec., DSC-measurement, 5 K/min).

Raman (200 mW, 25 °C, cm^{-1}): 3015 (3), 2963 (15), 1539 (9), 1509 (100), 1466 (38), 1417 (10), 1373 (20), 1342 (32), 1298 (24), 1235 (7), 1116 (17), 1060 (4), 1025 (52), 991 (6), 879 (8), 757 (14), 737 (3), 704 (3), 689 (13), 501 (11), 459 (6), 382 (9), 297 (13), 243 (7), 213 (9).

IR (Diamond-ATR, cm^{-1}): 3534 (vw), 1621 (vw), 1510 (w), 1464 (m), 1418 (w), 1369 (m), 1322 (s), 1291 (m), 1234 (m), 1113 (w), 1055 (vw), 1022 (m), 989 (w), 876 (w), 769 (w), 756 (w), 735 (w), 704 (vw), 689 (w).

^1H NMR (DMSO- d_6): 3.63 (s, 6H, CH_3), 3.37 (s, 2H, H_2O).

^{13}C NMR (DMSO- d_6): 157.6 (CN_4), 33.1 (CH_3).

Elemental analysis $\text{C}_4\text{H}_8\text{BaN}_{12}\text{O}_5$ (441.51 g/mol): calc.: C, 10.88; H, 1.83; N, 38.07; found: C, 10.83; H, 1.71; N, 37.85.

$E_{\text{dr}} = 15 \text{ J}$ (250–500 μm).

$F_{\text{r}} > 360 \text{ N}$ (250–500 μm).

$E_{\text{el}} = 0.65 \text{ J}$ (250–500 μm).

$\Delta_c U = -1444 \text{ cal/g}$.

H_2O -sol. 1.8 wt% (21 °C).

8.2.6 Barium 2-Methyl-5-nitriminotetrazolate Dihydrate ($\text{Ba}_2\text{MeAtNO}_2$)

A solution of 2.88 g (20 mmol) 2-methyl-5-nitraminotetrazole (**$\text{H}_2\text{MeAtNO}_2$**) and 3.15 g (10 mmol) barium hydroxide octahydrate was refluxed for 10 minutes. The orange solution was cooled down and stored for several days at ambient temperature to obtain colorless crystals suitable for X-ray diffraction. Yield: 91 %.

M.p. 257 °C (dec., DSC-measurement, 5 K/min).

Raman (200 mW, 25 °C, cm^{-1}): 3030 (2), 2956 (9), 1494 (100), 1486 (35), 1458 (7), 1414 (6), 1402 (6), 1352 (3), 1218 (2), 1204 (2), 1096 (1), 1041 (10), 1018 (25), 901 (1), 751 (2), 735 (2), 706 (7), 450 (4), 399 (2), 341 (5), 210 (2).

IR (Diamond-ATR, cm^{-1}): 3463 (m), 3358 (m), 1641 (vw), 1594 (vw), 1494 (m), 1483 (s), 1411 (m), 1393 (s), 1349 (m), 1333 (s), 1271 (m), 1215 (m), 1199 (m), 1104 (w), 1094 (w), 1034 (m), 900 (w), 887 (w), 756 (w), 703 (m).

^1H NMR (DMSO- d_6): 4.20 (s, 6H, CH_3), 3.37 (s, 4H, H_2O).

^{13}C NMR (DMSO- d_6): 168.3 (CN_4), 39.7 (CH_3).

Elemental analysis $\text{C}_4\text{H}_{10}\text{BaN}_{12}\text{O}_6$ (459.53 g/mol): calc.: C, 10.45; H, 2.19; N, 36.58; found: C, 10.50; H, 2.37; N, 37.05.

$E_{\text{dr}} = 7.0 \text{ J}$ (250–500 μm).

$F_{\text{r}} > 360 \text{ N}$ (250–500 μm).

$E_{\text{el}} = 0.50 \text{ J}$ (250–500 μm).

$\Delta_c U = -1689$ cal/g.

H₂O-sol. 11 wt% (22 °C).

8.3 Conclusion

The barium salts barium tetrazolate (**BaTz**), barium 5-aminotetrazolate tetrahydrate (**BaAt**), barium bis(5-nitrimino-1*H*-tetrazolate) tetrahydrate (**Ba1HatNO₂**), barium 5-nitriminotetrazolate dihydrate (**BaAtNO₂**), barium 1-methyl-5-nitriminotetrazolate monohydrate (**Ba1MeAtNO₂**), and barium 2-methyl-5-nitriminotetrazolate dihydrate (**Ba2MeAtNO₂**) were synthesized, characterized and their energetic properties such as the decomposition temperature, combustion energy and sensitivities to impact, friction, and electric discharge were determined. The molecular structures of **Ba1HatNO₂**, **Ba1MeAtNO₂**, and **Ba2MeAtNO₂** have been determined by X-ray diffraction and a short discussion is given. The solubility in H₂O at ambient temperature of all prepared barium salts was determined. In comparison to barium nitrate, **Ba1HatNO₂**, **BaAtNO₂**, and **Ba1MeAtNO₂** are much worse soluble, while the solubilities of **BaAt** and **Ba2MeAtNO₂** are comparable, whereas **BaTz**'s solubility is about three times greater. With regard to their possible usage as coloring agents in pyrotechnic compositions the color performance of each barium salt with and without a chlorine donor were investigated in the flame of a BUNSEN burner. For comparison the color performance of neat barium chloride dihydrate and barium nitrate, a mixture of both salts, and a mixture of PVC and barium nitrate was determined.

Concluding can be stated, the investigated barium salts, especially with anions containing a nitrimino group (**Ba1HatNO₂**, **BaAtNO₂**, **Ba1MeAtNO₂**, and **Ba2MeAtNO₂**), might be a “greener” alternative in replacing barium nitrate in white or green light emitting pyrotechnic compositions. All offer a comparable or lower solubility than barium nitrate in H₂O at ambient temperature and show without chlorine a very intense white flame. If a chlorine donor is present, especially **Ba1MeAtNO₂** offers a very intense green flame. Besides their good coloring properties, **Ba1MeAtNO₂** and **Ba2MeAtNO₂** are insensitive to friction. Furthermore, all presented barium salts can be prepared easily and from cheap starting materials.

The barium salts **Ba1HatNO₂** and **BaAtNO₂** could find further application, if sizzling sound effects are desired.

8.4 References

- [1] J. Thiele: Über einige Derivate des Tetrazols, *J. Lieb. Ann.* **1895**, 287, 233–265.
- [2] J. Stierstorfer: Advanced Energetic Materials based on 5-Aminotetrazole, *PhD Thesis*, **2009**, Ludwig-Maximilian University, Munich.

- [3] R. Damavarapu, T. M. Klapötke, J. Stierstorfer, K. R. Tarantik: Barium Salts of Tetrazole Derivatives – Synthesis and Characterization, *Propellants, Explos. Pyrotech.* **2010**, *in press*.
- [4] J. F. Zevenbergen, R. Webb, M. P. Van Rooijen: Pyrotechnic and fireworks compositions with metal salts of 5-aminotetrazole for colored flames. Eur. Patent Application, EP 1982969 A1, **2008**, Netherlands.
- [5] J. A. Conkling: *Chemistry of Pyrotechnics: Basic Principles and Theory*. M. Dekker, Inc., New York, **1985**.
- [6] T. M. Klapötke, J. Stierstorfer: Nitration products of 5-amino-1H-tetrazole and methyl-5-amino-1H-tetrazoles - structures and properties of promising energetic materials., *Helv. Chim. Acta*, **2007**, *90*, 2132–2150.
- [7] T. M. Klapötke, J. Stierstorfer, K. R. Tarantik, I. D. Thoma: Strontium Nitriminotetrazolates - Suitable Colorants in Smokeless Pyrotechnic Compositions, *Z. Anorg. Allg. Chem.* **2008**, *634*, 2777–2784.
- [8] T. M. Klapötke, H. Radies, J. Stierstorfer,: Alkali salts of 1-methyl-5-nitrimino-tetrazole - structures and properties, *Z. Naturforsch. B* **2007**, *62*, 1344–1352.
- [9] a) <http://www.bam.de> b) E_{dr} : insensitive > 40 J, less sensitive \geq 35 J, sensitive \geq 4, very sensitive \leq 3 J; F_r : insensitive > 360 N, less sensitive = 360 N, sensitive < 360 N > 80 N, very sensitive \leq 80 N, extreme sensitive \leq 10 N. According to the UN Recommendations on the Transport of Dangerous Goods.
- [10] L. R. Bates, *Symposium on Explosives and Pyrotechnics*, Proceedings, 13th, Hilton Head Island, USA, 2.–4. Dec. **1986**, III1–III10.
- [11] <http://webbook.nist.gov/>

9 Pyrotechnic Compositions Containing Nitrogen-rich Strontium Salts

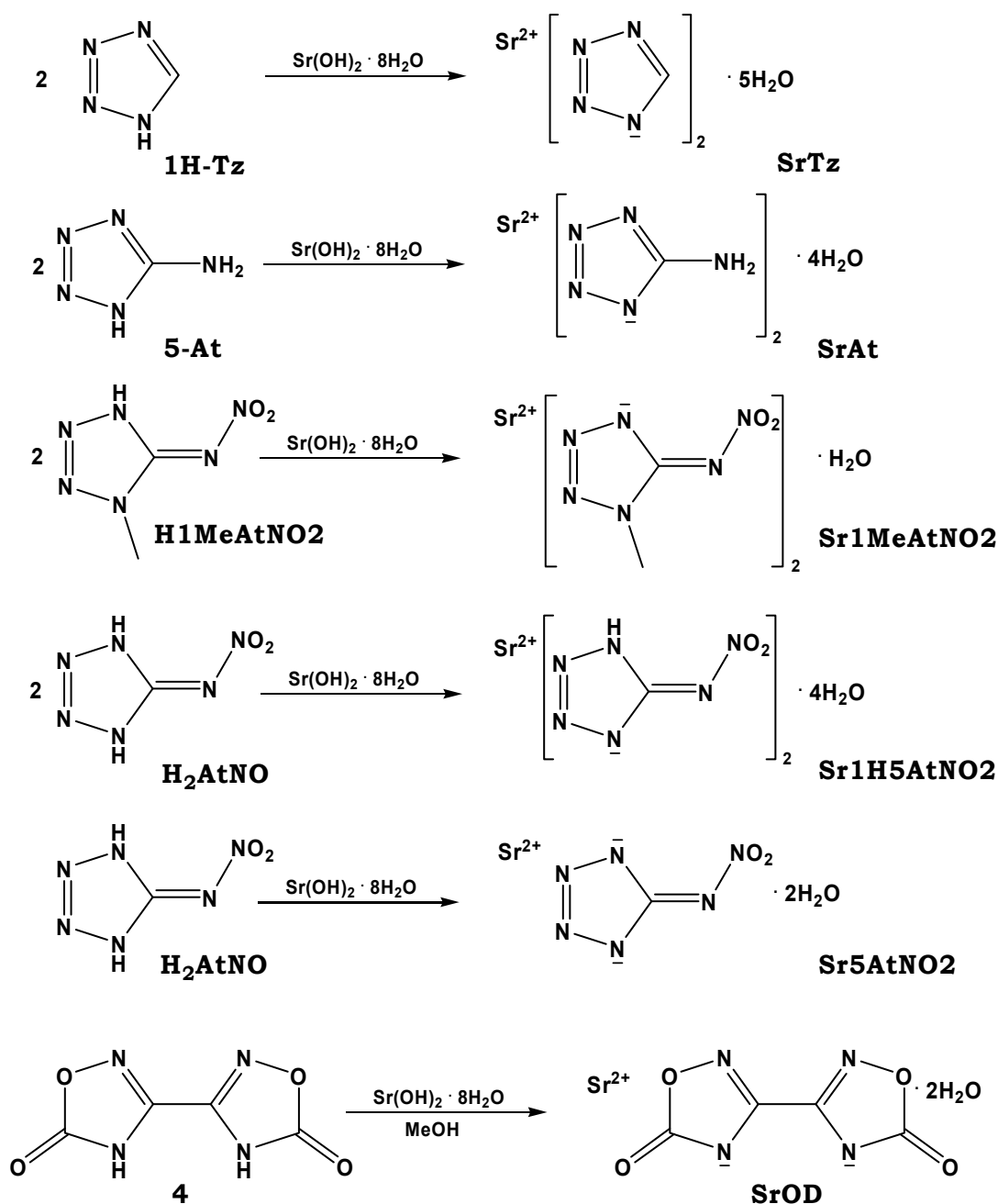
In this chapter, red pyrotechnic compositions with reduced smoke production and renunciation of potassium perchlorate were investigated with the usage of the nitrogen-rich strontium salts strontium tetrazolate pentahydrate (**SrTz**), strontium 5-aminotetrazolate tetrahydrate (**SrAt**), strontium 1-methyl-5-nitriminotetrazolate monohydrate (**Sr1MeAtNO2**), strontium bis(5-nitrimino-1*H*-tetrazolate) tetrahydrate (**Sr1HAtNO2**), strontium 5-nitriminotetrazolate monohydrate (**SrAtNO2**), and strontium 3,3'-bis(1,2,4-oxadiazol-5-onate) dihydrate (**SrOD**).

The strontium salts, **SrTz**, **SrAt**, **Sr1MeAtNO2**, **Sr1HAtNO2**, **SrAtNO2**, and **SrOD**, were investigated as possible colorants in pyrotechnic compositions yielding a red flame. These were selected because of their high nitrogen content (> 33 %, except **SrOD**). Furthermore, they are less sensitive or insensitive to impact and/or friction and decompose at temperatures above 220 °C. Besides that, they are easy to synthesize from cheap starting materials like 5-aminotetrazole (**5-At**). All salts are stable in water and not hygroscopic. Of course, all neat compounds show an intense red flame color during combustion. Among all above mentioned compounds, **SrTz** is suggested in literature as promising nitrogen-rich colorant.^[1] **SrAt** is mentioned in a recently published patent about pyrotechnics and fireworks compositions,^[2] therefore its behavior in compositions is of special interest. The patent is about chlorine containing pyrotechnic compositions. No chlorine donor, like PVC, was added in the investigated compositions, thus interference with requirements of the patent was avoided.

9.1 Results and Discussion

9.1.1 Syntheses

All prepared strontium salts are known and characterized in literature.^[3,4,5,6] The syntheses of strontium tetrazolate pentahydrate (**SrTz**), strontium 5-aminotetrazolate tetrahydrate (**SrAt**), strontium 1-methyl-5-nitriminotetrazolate monohydrate (**Sr1MeAtNO2**), strontium bis(5-nitrimino-1*H*-tetrazolate) tetrahydrate (**Sr1HAtNO2**), and strontium 5-nitriminotetrazolate monohydrate (**SrAtNO2**), were performed in water, except strontium 3,3'-bis(1,2,4-oxadiazol-5-onate) dihydrate (**SrOD**), using strontium hydroxide octahydrate and the corresponding nitrogen-rich neutral molecules, 1*H*-tetrazole (**1H-Tz**), 5-amino-tetrazole (**5-At**), 1-methyl-5-nitriminotetrazole (**H1MeAtNO2**), 1,4*H*-5-nitriminotetrazole (**H2AtNO2**), and 3,3'-bis(1,2,4-oxadiazol-5-one) (**H2OD**), respectively (Scheme 9.1). Methanol was used during preparation and recrystallization of **SrOD**. All other salts were recrystallized from H₂O.



Scheme 9.1 Preparation of the strontium salts **SrTz**, **SrAt**, **Sr1MeAtNO2**, **Sr1HAtNO2**, **SrAtNO2**, and **SrOD**.

The starting materials, 1-methyl-5-nitriminotetrazole (**H1MeAtNO2**) and 5-nitriminotetrazole (**H₂AtNO2**), were obtained by nitration of the corresponding 5-aminotetrazoles using nitric acid (100 %) according to literature procedures.^[5, 7] 3,3'-Bis(1,2,4-oxadiazol-5-one) (**H₂OD**) was prepared according to reference [6].

9.1.2 Energetic Properties and Solubility in H₂O

The energetic properties such as the decomposition temperature (T_{dec}), sensitivities to impact (E_{dr}), friction (F_r) and electric discharge (E_{el}), and the combustion energy ($\Delta_c U$) were

determined or adopted from the literature.^[4, 5, 6] Furthermore, the solubility in H₂O at ambient temperature of each compound was measured. An overview of the energetic properties is given in Table 9.1.

All strontium salts offer very high decomposition temperatures above 330 °C, except **Sr1HAtNO2** with a decomposition temperature of 227 °C. **Sr1HAtNO2** is the most sensitive one to impact (20 J) as well as **SrAtNO2**, which shows a sensitivity to impact (30 J). Furthermore, **Sr1HAtNO2** is sensitive to friction with 288 N. All other prepared salts are insensitive with impact sensitivities above 40 J.

Table 9.1 Energetic properties of **SrTz**, **SrAt**, **Sr1MeAtNO2**, **Sr1HAtNO2**, **SrAtNO2**, and **SrOD**.

Salt	SrTz	SrAt	Sr1MeAtNO2	Sr1HAtNO2	SrAtNO2	SrOD
Formula	Sr(C ₂ H ₁₀ N ₈) ₂ · 5H ₂ O	Sr(CH ₂ N ₅) ₂ · 4H ₂ O	Sr(C ₂ H ₃ N ₆ O ₂) ₂ · H ₂ O	Sr(C ₂ HN ₆ O ₂) ₂ · 4H ₂ O	Sr(CN ₆ O ₂) ₂ · 2H ₂ O	Sr(C ₄ N ₄ O ₄) · 2H ₂ O
M [g/mol]	315.79	327.80	391.80	417.80	251.70	291.72
E_{dr} [J]^a	> 100	> 40	> 40	20	30	> 100
F_r [N]^b	> 360	> 360	> 360	288	> 360	> 360
E_{el} [J]^c	1.0	1.5	0.90	0.40	1.0	0.30
grain size [µm]	250–500	250–500	100–500	100–250	100–250	< 160
N [%]^d	35.48	42.73	42.90	40.23	33.39	19.21
Ω [%]^e	-30	-34	-33	-7.7	-6.4	-27
T_{dec} [°C]^f	335	355	350	227	351	315
ρ [g/cm³]^g	1.88	2.02* (23 °C)	2.19	2.20	2.42	2.39* (22 °C)
Δ_cU [cal/g]^h	-1308	-1252	-1770	-997	-673	-1181
H₂O sol. [wt%]ⁱ	24 (22 °C)	11 (21 °C)	10 (22 °C)	2.6 (22 °C)	2.3 (22 °C)	3.8 (22 °C)

a) BAM drop hammer ^[8], b) BAM methods ^[8], c) Electric discharge tester, d) Nitrogen content; e) Oxygen balance; f) Decomposition temperature from DSC ($\beta = 5$ K/min); g) determined by X-ray crystallography or pycnometer (*); h) Combustion energy, i) Solubility in H₂O (H₂O temperature).

For the solubility determination each compound was added to 1 mL H₂O at constant and before noted temperature until the solution was saturated. The solubilities are given in percent by weight (wt%) and were calculated according to equation 9.1.

$$\text{H}_2\text{O-sol.} = \frac{m_{\text{dissolved Compound}}}{m_{\text{dissolved Compound}} + m_{\text{Solvent}}} \cdot 100 \quad (9.1)$$

The determined solubilities are between 2.3 and 24 wt% at 21–22 °C. Strontium salt **SrTz** is the most soluble compound, while **SrAtNO2** is the worst soluble one in H₂O. **Sr1HAtNO2** and **SrOD** also are very low soluble (2.6 wt% and 3.8 wt%). The values of compounds **SrAt** and **Sr1MeAtNO2** are in the same range of about 10 wt%.

All compounds are not sensitive to moisture and are stable in H₂O.

9.1.3 Color Performance and Combustion Behavior

All strontium salts were tested regarding to their flame color in the flame of a BUNSEN burner. They all show the expected red flame color and combust without any visible smoke production. The strontium salts **Sr1HAtNO2** and **SrAtNO2** deflagrate subsonically making a sizzling sound. The flames of all strontium salts are shown in Figure 9.1.



Figure 9.1 Flame color of **SrTz** (top, left), **SrAt** (top, middle), **Sr1MeAtNO2** (top, right), **Sr1HAtNO2** (down, left), **SrAtNO2** (down, middle), **SrOD** (down, right).

Furthermore, the combustion behavior of the strontium salts **SrTz**, **Sr1MeAtNO2** and **SrOD** was qualitatively characterized with a simple smoke test method. Therefore, approx. 1 g of each sample was placed in a heated crucible with a gas torch for observation of color, smoke, burn ability (propagation) and level of residue. All of them verified the already in the BUNSEN burner observed red flame color, but needed a constant torch. Smoke and residues were only observed in the case of **Sr1MeAtNO2**.

9.1.4 Pyrotechnic Compositions

Only the most promising formulations with the prepared strontium salts are mentioned in this chapter. As oxidizers potassium nitrate, potassium permanganate, ammonium nitrate, ammonium dinitramide, strontium nitrate, manganese dioxide, and potassium perchlorate were used. Magnesium, magnalium (MgAl), aluminum, **5-At**, sulfur, and charcoal were added as fuel. All prepared compositions can be found in chapters 9.2.2.1–9.2.2.6. The performance of each composition has been evaluated with respect to the following categories:

- color emission (subjective impression)
- smoke generation
- morphology and amount of solid residues
- thermal stability
- moisture sensitivity

The three points mentioned first were evaluated with the aid of video recording. For thermal stability the decomposition points of the compositions were determined by DSC-measurements ($\beta = 5$ K/min). Sensitivity to moisture could be investigated by storing the composition in an open vessel for several weeks.

All mentioned compositions were prepared by hand. Details can be found in chapter 9.2.2.

The US Army red flare composition # M126 A1 (red parachute), consisting of 39 % strontium nitrate, 30 % magnesium, 13 % potassium perchlorate, and 8 % VAAR, was a measure of the red light compositions' performance (Figure 9.2). Its decomposition point was determined to 360 °C with a DSC-measurement ($\beta = 5$ K/ min). M126 A1 is sensitive to impact with 10 J, to friction with 144 N, and to electric discharge with 0.75 J.



Figure 9.2 Burn down of the US Army composition # M126 A1.

SrTz was combined with the oxidizers potassium permanganate, ammonium nitrate, potassium nitrate, and strontium nitrate. Magnesium powder was used as fuel. The mixtures containing potassium and ammonium nitrate showed no convincing results regarding color performance compared to M126 A1. The composition **SrTz**_1 with the strontium salt **SrTz** (19 wt%) also contains 47 wt% potassium permanganate, 19 wt% magnesium and 15 wt% VAAR (Table 9.3). It combusts with very high velocity, comparable with US Army red flare composition # M126 A1. Its color performance is very good. A tall intense red flame was observed with little smoke production (Figure 9.3). After burn down only a very small amount of a white powder (presumably MgO) could be observed.



Figure 9.3 Burn down of the compositions **SrTz_1** (left) and **SrTz_3.2** (right).

The decomposition temperature is high ($T_{\text{dec}} = 260\text{ }^{\circ}\text{C}$) (Figure 9.4) and it is stable to moisture. But it is sensitive to impact (5 J) and very sensitive to friction (24 N). Its sensitivity to electric discharge is moderate with 1.0 J. Another promising composition **SrTz_3.2** contains **SrTz** (20 wt%), strontium nitrate (58 wt%), magnesium (10 wt%), and VAAR (12 wt%) (Table 9.6). The observed flame is smaller than the one of **SrTz_1** but is also very intense red (Figure 9.3). The combustion velocity is comparable. Smoke could be observed during burn down and a very small amount of solid residues. The composition offers a very high decomposition temperature ($T_{\text{dec}} = 372\text{ }^{\circ}\text{C}$) (Figure 9.4). Furthermore, it is not sensitive to friction (> 360 N) but sensitive to impact with 8.0 J. Its sensitivity to electric discharge is low with 1.5 J. No sensitivity to moisture could be observed.

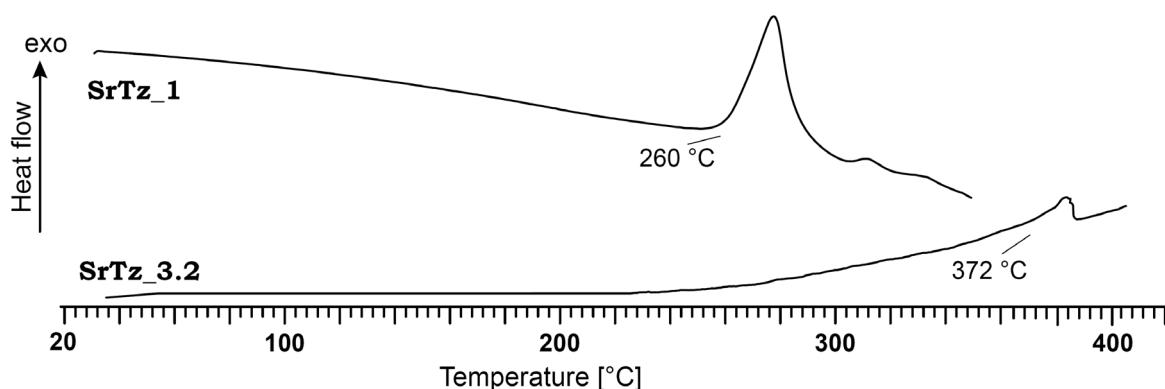


Figure 9.4 DSC thermograms of the pyrotechnic compositions **SrTz_1** and **SrTz_3.2** in a temperature range of 20–350 °C and 400 °C. Decomposition points are given as onset temperatures.

Besides the mixtures containing **SrTz** as pentahydrate salt, one composition with water free strontium tetrazolate (**SrTz_H₂Ofree**) was tested (Table 9.4). Surprisingly, the color performance was worse. Therefore, no further investigation with water free strontium tetrazolate as colorant in pyrotechnic compositions was undertaken.

SrAt was combined with the fuels magnesium, magnalium or **5-At**. The oxidizers potassium permanganate, ADN, ammonium nitrate, and potassium nitrate were added. Potassium permanganate, ammonium nitrate and potassium nitrate did not convince as

oxidizer. These compositions burned slowly and with a small red or violet flame. The composition, containing **SrAt**, with the best color performance is **SrAt_4.2** and consists of 13 wt% **SrAt**, 51 wt% ADN, 13 wt% **5-At**, 13 wt% magnesium, and 10 wt% VAAR (Table 9.11). Its flame is very intense red and has a moderate height (Figure 9.5). The burn down occurs very fast with less smoke production and some magnesium sparks. The combustion is complete with no solid residues. Unfortunately, there are two decomposition points (98 °C and 174 °C) at temperatures below 200 °C (Figure 9.6). The decomposition at 98 °C might occur due to the combination of fuel and oxidizer, which makes the compositions less stable than its neat components. The exothermic signal at 174 °C is caused by the decomposition of the oxidizer ADN. The composition **SrAt_4.2** is sensitive to impact (5 J) and to friction (96 N). The sensitivity to electric discharge is with 1.0 J in the range of the before mentioned ones. Although the composition contains ADN no sensitivity to moisture could be observed.



Figure 9.5 Burn down of the compositions **SrAt_4.2** (left) and **SrAt_6.7** (right).

Composition **SrAt_6.7** was prepared of 27 wt% **SrAt**, 36 wt% ADN, 14 wt% potassium nitrate, 12 wt% **5-At** and 11 wt% VAAR (Table 9.13). The emitted light is intense red but less than the one of **SrAt_4.2** (Figure 9.5). The combustion occurs very fast with little smoke and almost no solid residues. The composition is sensitive to impact with 5.0 J and to friction with 192 N. Its sensitivity to electric discharge is very low with 1.5 J. The mixture decomposes at temperatures above 160 °C (Figure 9.6), but it is stable to moisture.

The strontium salt **Sr1MeAtNO2** was mixed with the fuel magnesium and the oxidizers potassium permanganate, potassium nitrate, manganese oxide or ammonium nitrate. If manganese oxide or potassium nitrate were added, the corresponding compositions were difficult to ignite and the observed flame color was yellow or violet. Only potassium permanganate and ammonium nitrate were convincing oxidizers.

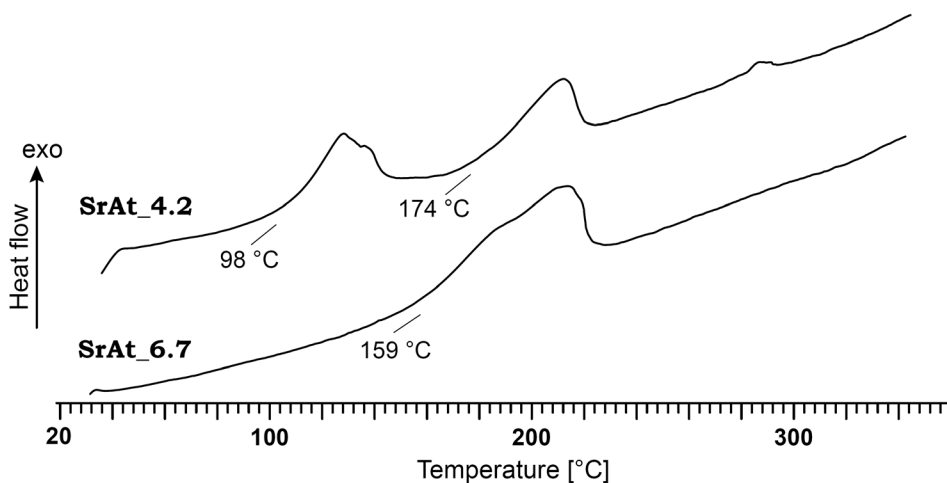


Figure 9.6 DSC thermograms of the pyrotechnic compositions **SrAt_4.2** and **SrAt_6.7** in a temperature range of 20–350 °C. Decomposition points are given as onset temperatures.

Composition **Sr1MeAtNO2_1** contains, analog to **SrTz_1**, potassium permanganate (44 wt%) as oxidizer, magnesium (22 wt%) as fuel, VAAR (12 wt%), and 22 wt% **Sr1MeAtNO2** (Table 9.14). The combustion occurs very fast with smoke and some magnesium sparks. The flame is intense red and tall (Figure 9.7). Only a small amount of white solid residues could be observed, presumably MgO. The composition decomposes at temperatures above 238 °C (Figure 9.8). It is sensitive to impact (10 J) and very sensitive to friction (20 N). Also its sensitivity to electric discharge is very high (0.12 J).

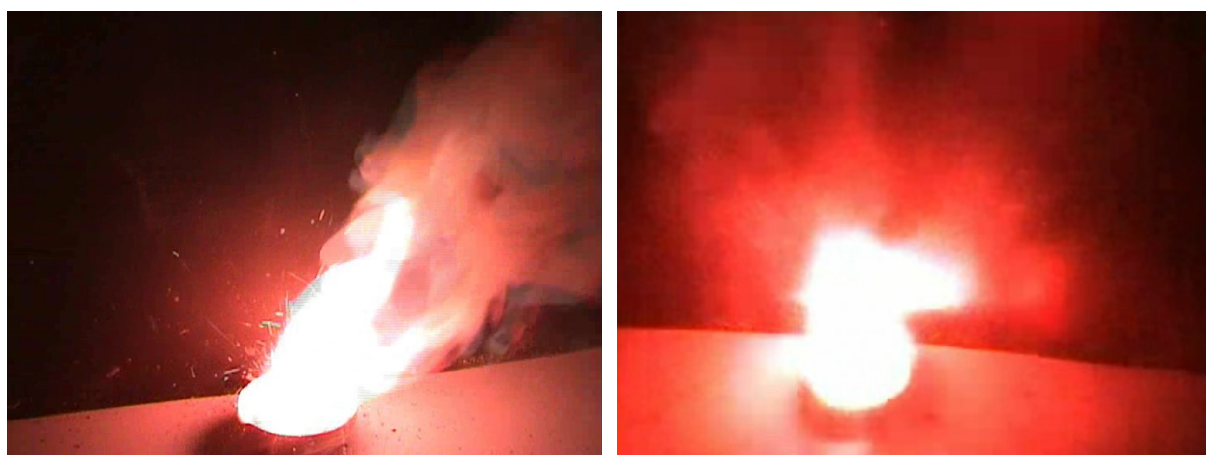


Figure 9.7 Burn down of the compositions **Sr1MeAtNO2_1** (left) and **Sr1MeAtNO2_5.4** (right).

Sr1MeAtNO2_5.4 contains 13 wt% **Sr1MeAtNO2**, 61 wt% ammonium nitrate, 15 wt% magnesium, and 11 wt% VAAR (Table 9.18). The observed flame is very intense red (Figure 9.7). The residue-free combustion occurs with a moderate velocity, some smoke and a few magnesium sparks were observed. The composition starts to decompose at 181 °C (Figure 9.8). The sensitivity to impact of **Sr1MeAtNO2_5.4** was determined with 10 J and the one to friction with 216 N. The sensitivity to electric discharge is quite high with 0.3 J. Both, **Sr1MeAtNO2_1** and **Sr1MeAtNO2_5.4**, are stable to moisture.

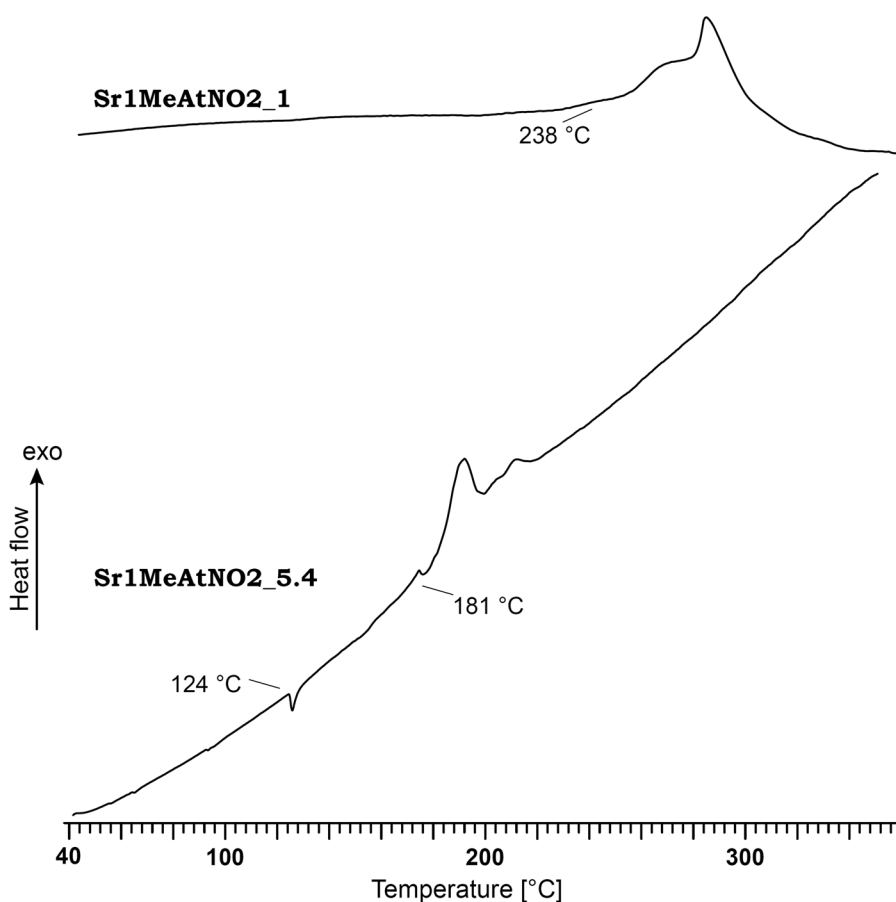


Figure 9.8 DSC thermograms of the pyrotechnic compositions **Sr1MeAtNO2_1** and **Sr1MeAtNO2_5.4** in a temperature range of 40–350 °C. Decomposition points are given as onset temperatures.

Using **Sr1HAtNO2** as colorant, only one composition, **Sr1HAtNO2_7**, with good color and burning performance could be found. It consists of 11 wt% **Sr1HAtNO2**, 66 wt% ADN, 11 wt% **5-At**, and 12 wt% VAAR (Table 9.25). The combustion occurs very fast with an intense red and tall flame (Figure 9.9). No significant smoke production but a small amount of solid glowing residues could be observed. Similar to the neat compound, composition **Sr1HAtNO2_7** makes a sizzling sound during burn down. The decomposition temperature of 157 °C is quite low due to using ADN as oxidizer (Figure 9.10). **Sr1HAtNO2_7** is sensitive to impact (7.5 J) and friction (160 N). The sensitivity to electric discharge is very low with 0.1 J. No sensitivity to moisture could be observed.

Due to the unsatisfactory properties as colorants, a test composition using potassium perchlorate as oxidizer was investigated (Table 9.21). The composition **Sr1HAtNO2_3**, containing 13 wt% **Sr1HAtNO2**, 65 wt% potassium perchlorate, 12 wt% magnesium and 10 wt% VAAR, was hard to ignite and no continuous burning was achieved. The short-lasting flames had an intense red flame color, but they were rather a product of deflagration than combustion.

Analog to **Sr1HAtNO2**, one composition based on **SrAtNO2** with a convincing performance was investigated. The mixture **SrAtNO2_7.4** was prepared of 15 wt% **SrAtNO2**, 47 wt% ADN, 27 wt% **5-At**, and 11 wt% VAAR (Table 9.33).

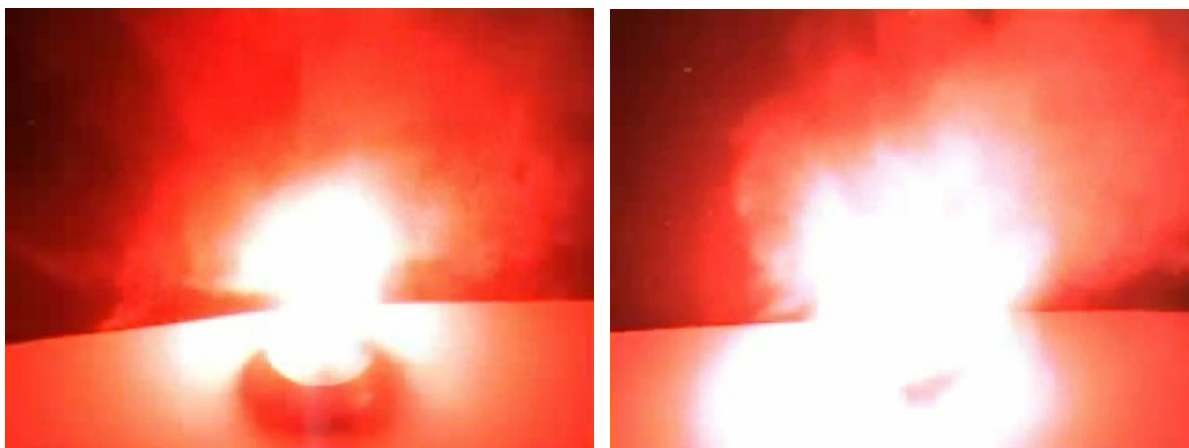


Figure 9.9 Burn down of the compositions **Sr1HAtNO2_7** (left) and **SrAtNO2_7.4** (right).

The combustion occurs with a very high velocity and more vigorously than **Sr1HAtNO2_7**. Also an intense red, tall flame and less smoke could be observed (Figure 9.9). In contrast to **Sr1HAtNO2_7** the combustion proceeds completely. Also **SrAtNO2_7.4** is very sensitive to impact (3.0 J), sensitive to friction (192 N) and electric discharge (0.15 J). The decomposition occurs at temperatures above 155 °C due to using ADN as oxidizer (Figure 9.10).

A test composition **SrAtNO2_3** with 8 wt% **SrAtNO2**, 75 wt% potassium perchlorate, 7 wt% magnesium and 10 wt% VAAR, was prepared to proof the coloring properties of **SrAtNO2** (Table 9.29). It was not possible to ignite this composition. No further investigation using these additives was done.

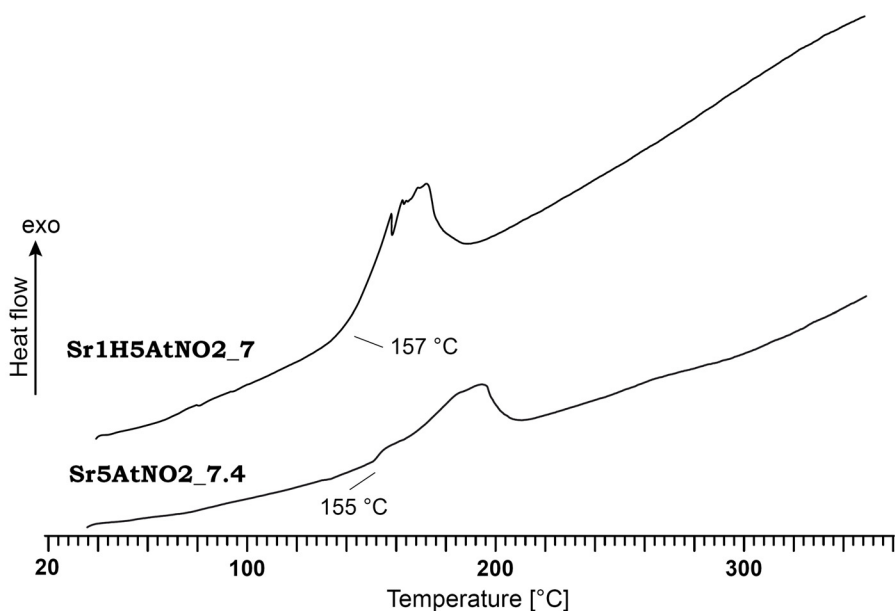


Figure 9.10 DSC thermograms of the pyrotechnic compositions **Sr1HAtNO2_7** and **SrAtNO2_7.4** in a temperature range of 20–350 °C. Decomposition points are given as onset temperatures.

SrOD was combined with the fuels magnesium, magnalium, aluminum or **5-At** and the oxidizers potassium permanganate, ammonium nitrate, ammonium dinitramide and potassium nitrate. All compositions containing potassium permanganate or ammonium

nitrate show bad color and/or combustion properties. If aluminum powder and not grit is used, the burning velocity increases. This is a result of the larger surface and therefore higher reactivity of powder compared to grit. Composition **SrOD_6.3** consists of 13 wt% **SrOD**, 52 wt% ADN, 26 wt% **5-At** and 9 wt% VAAR (Table 9.39). The combustion occurs very fast and with almost no smoke production. The observed flame is very intense red compared to the red parachute standard (Figure 9.11). A small amount of solid glowing residues could not be avoided by increasing the oxidizer amount. When ADN was increased to 57 wt% the reaction was too violently (and the composition flies through the fume hood) (**SrOD_6.4**). **SrOD_6.3** is sensitive to impact (5.0 J), and friction (144 N). The sensitivity to electric discharge was determined to 0.10 J.



Figure 9.11 Burn down of the compositions **SrOD_6.3** (left) and **SrOD_7.1** (right).

SrOD_6.3 shows a comparatively low decomposition temperature of 166 °C (Figure 9.12). This is true for composition **SrOD_7.1** which decomposes at temperatures above 169 °C. **SrOD_7.1** consists of 10 wt% **SrOD**, 48 wt% ADN, 7 wt% potassium nitrate, 26 wt% **5-At** and 9 wt% VAAR (Table 9.40). Potassium nitrate was added to reduce the amount of ADN. The observed combustion behavior is similar to **SrOD_6.3**, whereas less smoke is produced and the amount of solid glowing residues is smaller (Figure 9.11).

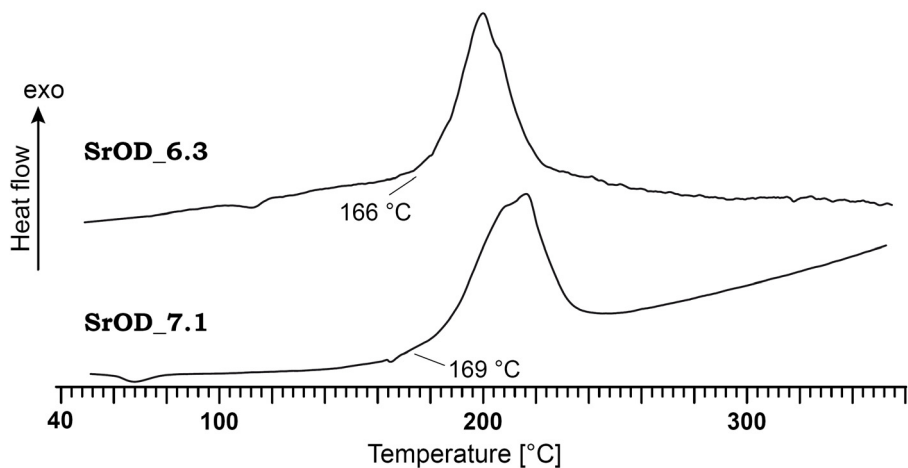


Figure 9.12 DSC thermograms of the pyrotechnic compositions **SrOD_6.3** and **SrOD_7.1** in a temperature range of 40–350 °C. Decomposition points are given as onset temperatures.

SrOD_7.1 is sensitive to impact (10 J) and very sensitive to friction (60 N). The sensitivity to electric discharge (1.0 J) is similar to the one mentioned before. A slight sensitivity to moisture was observed after storing the composition in an open vessel over several months, whereas ignition was still possible.

Besides the mentioned compositions, each of the strontium salts **SrTz**, **Sr1MeAtNO2**, and **SrOD** was formulated with magnesium powder, polyvinyl chloride, and polyester/styrene binder, leaving the ratio unchanged.^[9] The dry ingredients were sieved through a 10-mesh screen and dried prior to mixing in a ceramic bowl. The final dry mixes were pressed to 1.27 cm pellets, each with approx. 6 g. The pellets were consolidated in a die with two increments at a loading pressure of 6000 psi (41.3 MPa). The currently used M126 A1 igniter slurry (aluminum, silicon, charcoal, potassium nitrate, iron oxide, and nitrocellulose) was applied on top of the pellets as initiator.

Static burn test on the experimental pellets was conducted in a blackened light tunnel. The samples were placed 50 ft (15.24 m) from the measurement equipment and initiated with an electric match. Color was measured with an *Ocean Optics* HR2000 spectrometer after calibration. Color measurements were based on the 1931 CIE (*Commission Internationale d'Eclairage*) international standard and calculated using the *Ocean Optics* Spectra-suite software. The CIE chart displays all the chromaticities average human eyes can observe. The three values calculated based on the CIE color matching functions are referred to X, Y and Z. The dominant wavelength (DW) and excitation purity (%) for a test sample were numerically determined with respect to the coordinates of Illuminant C, an established light source. The luminous intensity was measured using an *International Light SEL033* silicon detector coupled to a photopic filter and lens hood.

Static burn test results for **SrTz**, and **Sr1MeAtNO2** formulated pellets as well as the perchlorate-based control pellets^[10] are shown in Table 9.2. **SrOD** formulated pellets did not burn.

Table 9.2 Experimental pellets performance data.

Compound	SrTz	Sr1MeAtNO2	Control
burn time [s]	10	8.3	11.8
average intensity [cd]	2779	3876	1570
integrated intensity [cd·s]	25235	31592	19749
dominant wavelength [nm]	611	611	610
spectral purity [%]	94	94	85

The representative still images captured from the static burn test are illustrated below (Figure 9.13).

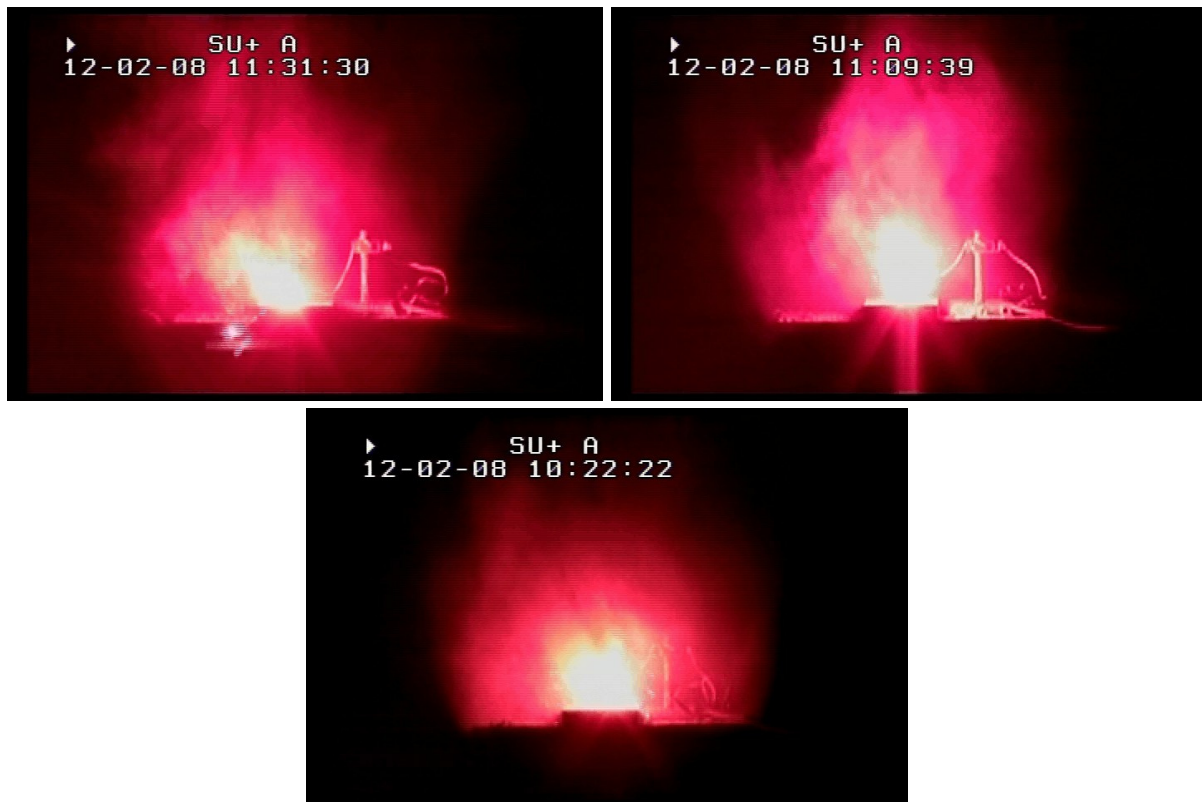


Figure 9.13 Static burn test of **SrTz** (top, left), **Sr1MeAtNO2** (top, right), and Control (down).

The results suggest there is no significant difference among the three sample groups in flame size based on visual observation. It was also found, all pellet groups burned bright, with an intense red flame and their respective color purity exceeded the control value. **SrTz** yielded some broken pellets, suggesting a higher consolidation force is required. **Sr1MeAtNO2** yielded the best pellet integrity and burning consistency. The deficiency in burn times can be elongated by increasing the amount of binder and/or high loading density. Variation of magnesium content in formulation and particle size/distribution can also be considered to adjust burn time.

9.2 Experimental Part

9.2.1 Synthesis of the Strontium Salts

*CAUTION! The strontium salts or their pyrotechnic compositions are sensitive to impact, friction, and electric discharge. Therefore, proper protective measures (safety glasses, face shield, leather coat, earthed equipment and shoes, Kevlar® gloves, and ear plugs) should be used, especially during work on the precursor molecules 1-methyl-5-nitriminotetrazole (**H1MeAtNO2**) and 5-nitriminotetrazole (**H2AtNO2**).*

Strontium tetrazolate pentahydrate (SrTz): Preparation according to literature.^[3, 5] Yield: 97 %.

M.p. 110–130 °C (loss of H₂O), 335 °C (dec., DSC-measurement, 5 K/min).

Raman (200 mW, 25 °C, cm⁻¹): 3320 (8), 3131 (66), 1686 (3), 1434 (24), 1294 (67), 1197 (100), 1187 (83), 1155 (15), 1134 (24), 1085 (21), 1024 (16), 1006 (12), 883 (3), 704 (10), 594 (3), 442 (6), 386 (5), 273 (7), 216 (8).

IR (Diamond-ATR, cm⁻¹): 3433 (s), 3250 (m), 3168 (m), 2158 (vw), 1797 (vw), 1755 (vw), 1663 (w), 1627 (m), 1446 (w), 1430 (s), 1290 (m), 1200 (s), 1180 (w), 1163 (s), 1141 (s), 1101 (w), 1080 (vw), 1018 (s), 1007 (s), 905 (s), 877 (w), 702 (s).

¹H NMR (DMSO-*d*₆): 8.55 (s, CH), 4.74 (s, H₂O).

¹³C NMR (DMSO-*d*₆): 150.2.

Elemental analysis C₂H₁₂N₈O₅Sr (315.79 g/mol): calc.: C, 7.61; H, 3.83; N, 35.48; found: C, 7.72; H, 3.77; N, 35.44.

E_{dr} = 40 J (250–500 μm).

F_r > 360 N (250–500 μm).

E_{el} = 1.0 J (> 1000 μm).

H₂O-sol. 24 wt% (22 °C).

Strontium 5-aminotetrazolate tetrahydrate (SrAt): Preparation according to literature.^[5] Yield: 93 %.

M.p. 141 °C (loss of H₂O), 165 °C (loss of H₂O), 198 °C (loss of H₂O), 355 °C (dec., DSC-measurement, 5 K/min).

Raman (200 mW, 25 °C, cm⁻¹): 3343 (4), 3267 (9), 3200 (15), 1636 (17), 1560 (28), 1519 (14), 1454 (15), 1415 (13), 1299 (10), 1228 (63), 1138 (31), 1126 (40), 1076 (100), 1063 (96), 1007 (15), 759 (33), 746 (36), 434 (26), 336 (13), 225 (13).

IR (Diamond-ATR, cm⁻¹): 3423 (s), 3347 (s), 3296 (s), 3185 (s), 1643 (m), 1611 (m), 1535 (m), 1520 (s), 1452 (m), 1411 (w), 1225 (m), 1173 (w), 1158 (w), 1126 (w), 1072 (w), 1024 (vw), 1004 (vw), 758 (w).

¹H NMR (DMSO-*d*₆): 6.44 (s).

¹³C NMR (DMSO-*d*₆): 157.2.

Elemental analysis C₂H₁₂N₁₀O₄Sr (327.80 g/mol): calc.: C, 7.33; H, 3.69; N, 42.73; found: C, 7.42; H, 3.67; N, 42.34.

E_{dr} = 40 J (250–500 μm).

F_r > 360 N (250–500 μm).

E_{el} = 1.5 J (250–500 μm).

H₂O-sol. 11 wt% (21 °C).

Strontium 1-methyl-5-nitriminotetrazolate monohydrate (Sr1MeATNO2): Preparation according to literature.^[4,5] Yield: 93 %.

M.p. 350 °C (dec., DSC-measurement, 5 K/min).

Raman (200 mW, 25 °C, cm⁻¹): 2965 (11), 1514 (100), 1470 (34), 1419 (9), 1376 (16), 1346 (30), 1299 (23), 1239 (5), 1117 (14), 1055 (5), 1027 (59), 992 (6), 882 (10), 788 (4), 762 (13), 739 (2), 691 (12), 505 (11), 464 (4), 388 (6), 303 (12), 249 (6), 217 (7), 187 (10).

IR (Diamond-ATR, cm⁻¹): 3609 (vw), 3544 (w), 3319 (vw), 3140 (vw), 2401 (vw), 2354 (vw), 2311 (vw), 1668 (vw), 1616 (w), 1515 (m), 1468 (s), 1421 (m), 1374 (s), 1324 (vs), 1293 (s), 1240 (s), 1114 (m), 1056 (w), 1024 (s), 990 (m), 878 (m), 771 (m), 760 (m), 738 (m), 705 (w), 694 (m).

¹H NMR (DMSO-*d*₆): 3.68 (s, 6H, CH₃), 3.37 (s, 2H, H₂O).

¹³C NMR (DMSO-*d*₆): 157.6 (CN₄), 33.1 (CH₃).

Elemental analysis C₄H₈N₁₂O₅Sr (391.80 g/mol): calc.: C, 12.26; H, 2.06; N, 42.90; found: C, 12.41; H, 2.25; N, 43.18.

E_{dr} = 40 J (100–500 μm).

F_r > 360 N (100–500 μm).

E_{el} = 0.90 J (100–500 μm).

H₂O-sol. 10 wt% (22 °C).

Strontium bis(5-nitrimino-1H-tetrazolate) tetrahydrate (Sr1HAtNO2): Preparation according to literature.^[4,5] Yield: 92 %.

M.p. 163 °C (loss of H₂O), 227 °C (dec., DSC-measurement, 5 K/min).

Raman (400 mW, 25 °C, cm⁻¹): 3354 (2), 1660 (2), 1544 (100), 1448 (2), 1386 (9), 1333 (34), 1175 (3), 1165 (9), 1130 (6), 1069 (7), 1040 (49), 987 (14), 915 (2), 870 (9), 760 (14), 741 (3), 705 (2), 506 (7), 445 (7), 418 (10), 372 (9), 227 (13), 184 (22), 157 (7).

IR (Diamond-ATR, cm⁻¹): 3377 (s), 3251 (s), 2913 (m), 2797 (m), 2675 (m), 2544 (m), 2359 (m), 1910 (vw), 1823 (vw), 1659 (w), 1526 (m), 1416 (m), 1357 (m), 1323 (s), 1254 (m), 1175 (w), 1159 (w), 1117 (w), 1068 (m), 1036 (m), 983 (m), 934 (m), 866 (w), 771 (w), 740 (m), 717 (m), 699 (m), 595 (w).

¹H NMR (DMSO-*d*₆): 3.26 (s).

^{13}C NMR (DMSO- d_6): 158.4.

Elemental analysis $\text{C}_2\text{H}_{10}\text{N}_{12}\text{O}_8\text{Sr}$ (417.80 g/mol): calc.: C, 5.75; H, 2.41; N, 40.23; found: C, 5.62; H, 2.38; N, 39.69.

$E_{\text{dr}} = 20 \text{ J}$ (100–250 μm).

$F_{\text{r}} = 288 \text{ N}$ (100–250 μm).

$E_{\text{el}} = 0.40 \text{ J}$ (100–250 μm).

$\Delta_c U = -997 \text{ cal/g}$.

H₂O-sol. 2.6 wt% (22 °C).

Strontium 5-nitriminotetrazolate dihydrate (SrAtNO₂): Preparation according to literature.^[4,5] Yield: 89 %.

M.p. 351 °C (dec., DSC-measurement, 5 K/min).

Raman (200 mW, 25 °C, cm^{-1}): 1956 (1), 1462 (100), 1314 (1), 1214 (3), 1164 (4), 1142 (4), 1085 (3), 1035 (4), 1025 (22), 881 (1), 752 (1), 494 (1), 422 (8), 406 (2), 262 (2), 164 (2), 136 (1).

IR (Diamond-ATR, cm^{-1}): 3454 (s), 3335 (s), 2484 (w), 2435 (w), 2342 (w), 1957 (w), 1648 (m), 1465 (s), 1418 (s), 1396 (s), 1313 (m), 1257 (m), 1160 (m), 1138 (w), 1082 (m), 1016 (m), 869 (m), 829 (w), 753 (m), 726 (w), 593 (m).

^1H NMR (DMSO- d_6): 3.39 (s).

^{13}C NMR (DMSO- d_6): 164.8.

Elemental analysis $\text{CH}_4\text{N}_6\text{O}_4\text{Sr}$ (251.70 g/mol): calc.: C, 4.77; H, 1.60; N, 33.39; found: C, 4.73; H, 1.96; N, 32.35.

$E_{\text{dr}} = 30 \text{ J}$ (100–250 μm).

$F_{\text{r}} > 360 \text{ N}$ (100–250 μm).

$E_{\text{el}} = 1.0 \text{ J}$ (100–250 μm).

$\Delta_c U = -673 \text{ cal/g}$.

H₂O-sol. 2.3 wt% (22 °C).

Strontium 3,3'-bis(1,2,4-oxadiazol-5-one) dihydrate (SrOD): Preparation according to literature.^[6] Yield: 73 %.

M.p. 143 °C (loss of H_2O), 315 °C (dec., DSC-measurement, 5 K/min).

IR (Diamond-ATR, cm^{-1}): 3653 (w), 3608 (w), 3592 (w), 3379 (w), 2364 (vw), 1663 (s), 1584 (m), 1485 (s), 1452 (m), 1399 (w), 1286 (s), 1232 (s), 1025 (w), 988 (vw), 952 (m), 896 (m), 786 (s).

^{13}C NMR (DMSO- d_6): 172.7 (CO), 162.0 (CN).

Elemental analysis $\text{C}_4\text{H}_4\text{N}_4\text{O}_6\text{Sr}$ (291.72 g/mol): calc.: C, 16.47; H, 1.38; N, 19.21; found: C, 16.23; H, 1.32; N, 18.95.

$E_{\text{dr}} > 100 \text{ J}$ (< 160 μm).

$F_r > 360 \text{ N}$ ($< 160 \mu\text{m}$).

$E_{el} = 0.30 \text{ J}$ ($< 160 \mu\text{m}$).

H₂O-sol. 3.8 wt% (22 °C).

9.2.2 Pyrotechnic Compositions

For the preparation of the pyrotechnic compositions all substances, except the binder, were carefully mixed in a mortar. Then the binder, dissolved in a few milliliters of ethyl acetate, was added. The mixture was formed by hand and dried under high vacuum for several hours.

The controlled burn down was recorded using a digital video camera recorder (SONY, DCR-HC37E).

A solution of 25 % vinyl alcohol acetate resin (VAAR) was used as binder. All compounds are given in percent by weight (wt%).

9.2.2.1 Pyrotechnic Compositions based on Strontium Tetrazolate Pentahydrate (SrTz)

In Table 9.3–Table 9.7 the different pyrotechnic compositions based on **SrTz** are summarized. The oxidizers potassium permanganate, potassium nitrate, strontium nitrate, and ammonium nitrate were used. Magnesium was added as fuel.

Table 9.3 Pyrotechnic formulation containing **SrTz** and potassium permanganate.

	SrTz [wt%]	KMnO₄ [wt%]	Mg [wt%]	VAAR [wt%]	observed behavior
SrTz_1	19	47	19	15	intense red, easy to ignite, high velocity, less smoke, almost no solid residues

Table 9.4 Pyrotechnic formulation containing **SrTz_H₂Ofree** and potassium permanganate.

	SrTz_H₂Ofree [wt%]	KMnO₄ [wt%]	Mg [wt%]	VAAR [wt%]	observed behavior
SrTz_1.2	25	38	25	12	violet-red flame, easy to ignite, high velocity, moderate smoke production, almost no solid residues

Table 9.5 Pyrotechnic formulation containing **SrTz** and potassium nitrate.

	SrTz [wt%]	KNO₃ [wt%]	Mg [wt%]	VAAR [wt%]	observed behavior
SrTz_2	10	63	10	16	violet flame, hard to ignite, moderate velocity, much smoke, almost no solid residues

Table 9.6 Pyrotechnic formulations containing **SrTz** and strontium nitrate.

	SrTz	Sr(NO₃)₂	Mg	VAAR	observed behavior
	[wt%]	[wt%]	[wt%]	[wt%]	
SrTz_3.1	14	55	14	17	red flame, easy to ignite, moderate velocity, much smoke, almost no solid residues
SrTz_3.2	20	58	10	12	intense red, easy to ignite, high velocity, smoke, almost no solid residues

Table 9.7 Pyrotechnic formulations containing **SrTz** and ammonium nitrate.

	SrTz	NH₄NO₃	Mg	VAAR	observed behavior
	[wt%]	[wt%]	[wt%]	[wt%]	
SrTz_4.1	19	47	19	15	very intense red, easy to ignite, moderate velocity, blinking, less smoke, Mg sparks, solid residues
SrTz_4.2	20	59	15	6	intense red, easy to ignite, low velocity, blinking, smoke, Mg sparks, almost no solid residues
SrTz_4.3	18	62	14	6	intense red, easy to ignite, moderate velocity, blinking, smoke, Mg sparks, no solid residues
SrTz_4.4	11	74	8	7	violet-red flame, burning unsteadily, less smoke, many Mg sparks, almost no solid residues
SrTz_4.5	18	75	0	7	yellow-red flame, hard to ignite, burning unsteadily, small flame
SrTz_4.6	12	57	25	6	very intense red, easy to ignite, low velocity, blinking, less smoke, many Mg sparks, almost no solid residues

9.2.2.2 Pyrotechnic Compositions based on Strontium 5-Aminotetrazolate Tetrahydrate (SrAt)

In Table 9.8–Table 9.13 the different pyrotechnic compositions based on **SrAt** are summarized. The oxidizers potassium permanganate, potassium nitrate, and ammonium dinitramide were used. The fuels magnesium, magnalium (MgAl) or **5-At** were added.

Table 9.8 Pyrotechnic formulations containing **SrAt** and potassium permanganate.

	SrAt	KMnO₄	Mg	VAAR	observed behavior
	[wt%]	[wt%]	[wt%]	[wt%]	
SrAt_1.1	15	60	15	10	red flame, easy to ignite, moderate velocity, smoke, small amount of solid glowing residues
SrAt_1.2	26	52	13	9	violet flame, easy to ignite, moderate velocity, much smoke, almost no solid residues

Table 9.9 Pyrotechnic formulation containing **SrAt** and potassium permanganate and ammonium nitrate.

	SrAt [wt%]	KMnO₄ [wt%]	NH₄NO₃ [wt%]	VAAR [wt%]	observed behavior
SrAt_2	13	52	26	9	small yellow-red flame, hard to ignite, low velocity, smoke, no proper burning

Table 9.10 Pyrotechnic formulations containing **SrAt** and ammonium dinitramide (ADN).

	SrAt [wt%]	ADN [wt%]	5-At [wt%]	VAAR [wt%]	observed behavior
SrAt_3.1	21	42	21	16	very intense red, easy to ignite, low velocity, unsteady burning, less smoke, solid glowing residues
SrAt_3.2	24	48	16	12	very intense red, easy to ignite, moderate velocity, much smoke, solid glowing residues

Table 9.11 Pyrotechnic formulations containing **SrAt**, ADN and magnesium.

	SrAt [wt%]	ADN [wt%]	5-At [wt%]	Mg [wt%]	VAAR [wt%]	observed behavior
SrAt_4.1	16	47	16	8	13	very intense red, easy to ignite, high velocity, less smoke, few Mg sparks, very small amount of solid glowing residues
SrAt_4.2	13	51	13	13	10	very intense red, easy to ignite, high velocity, less smoke, few Mg sparks, no solid residues
SrAt_4.3	13	53	14	9	11	very intense red, easy to ignite, high velocity, less smoke, few Mg sparks, almost no solid residues

Table 9.12 Pyrotechnic formulations containing **SrAt**, ADN, and potassium nitrate.

	SrAt [wt%]	ADN [wt%]	KNO₃ [wt%]	5-At [wt%]	Mg [wt%]	VAAR [wt%]	observed behavior
SrAt_5.1	15	38	15	13	7	12	violet-red flame, easy to ignite, high velocity, less smoke, Mg sparks, no solid residues
SrAt_5.2	17	39	16	16	0	12	violet-red flame, easy to ignite, moderate velocity, smoke, few Mg sparks, small amount of solid residues
SrAt_5.3	16	38	15	15	4	12	red flame, easy to ignite, high velocity, less smoke, almost no solid residues

Table 9.13 Pyrotechnic formulations containing **SrAt**, **ADN**, and **5-At**.

	SrAt	ADN	KNO₃	5-At	MgAl	VAAR	observed behavior
	[wt%]	[wt%]	[wt%]	[wt%]	[wt%]	[wt%]	
SrAt_6.1	18	39	15	15	3	10	violet-red flame, easy to ignite, moderate velocity, smoke, small amount of solid residues
SrAt_6.2	17	38	17	12	5	11	red flame, easy to ignite, low velocity, less smoke, almost no solid residues
SrAt_6.3	24	40	16	8	0	12	violet flame, easy to ignite, low velocity, blinking, smoke, almost no solid residues
SrAt_6.4	24	36	14	14	0	12	red flame, easy to ignite, moderate velocity, less smoke, small amount of solid residues
SrAt_6.5	25	37	15	13	0	10	bright red flame, easy to ignite, high velocity, less smoke, small amount of solid residues
SrAt_6.6	26	36	15	13	0	10	violet-red flame, easy to ignite, moderate velocity, smoke, almost no solid residues
SrAt_6.7	27	36	14	12	0	11	intense red, easy to ignite, high velocity, smoke, almost no solid residues

9.2.2.3 Pyrotechnic Compositions based on Strontium 1-Methyl-5-nitrimino-tetrazolate Monohydrate (Sr1MeAtNO₂)

In Table 9.14–Table 9.18 the different pyrotechnic compositions based on **Sr1MeAtNO₂** are shown. The oxidizers potassium permanganate, potassium nitrate, manganese oxide, and ammonium nitrate were used. The fuel magnesium was added.

Table 9.14 Pyrotechnic formulation containing **Sr1MeAtNO₂** and potassium permanganate.

	Sr1MeAtNO₂	KMnO₄	Mg	VAAR	observed behavior
	[wt%]	[wt%]	[wt%]	[wt%]	
Sr1MeAtNO₂_1	22	44	22	12	intense red, easy to ignite, high velocity, smoke, almost no solid residues

Table 9.15 Pyrotechnic formulation containing **Sr1MeAtNO2** and potassium nitrate.

	Sr1MeAtNO2 [wt%]	KNO₃ [wt%]	Mg [wt%]	VAAR [wt%]	observed behavior
Sr1MeAtNO2_2	11	64	11	14	violet flame, hard to ignite, low velocity, smoke, almost no solid residues

Table 9.16 Pyrotechnic formulations containing **Sr1MeAtNO2**, potassium permanganate, and potassium nitrate.

	Sr1MeAtNO2 [wt%]	KMnO₄ [wt%]	KNO₃ [wt%]	Mg [wt%]	VAAR [wt%]	observed behavior
Sr1MeAtNO2_3.1	12	24	36	12	16	red flame, easy to ignite, high velocity, smoke, small amount of solid glowing residues
Sr1MeAtNO2_3.2	21	21	32	11	15	violet-red flame, easy to ignite, high velocity, smoke, almost no solid residues

Table 9.17 Pyrotechnic formulation containing **Sr1MeAtNO2** and manganese oxide.

	Sr1MeAtNO2 [wt%]	MnO₂ [wt%]	Mg [wt%]	VAAR [wt%]	observed behavior
Sr1MeAtNO2_4	21	63	21	15	yellow-red flame, very hard to ignite, high velocity, smoke, Mg sparks, almost no solid residues

Table 9.18 Pyrotechnic formulations containing **Sr1MeAtNO2** and ammonium nitrate.

	Sr1MeAtNO2 [wt%]	NH₄NO₃ [wt%]	Mg [wt%]	VAAR [wt%]	observed behavior
Sr1MeAtNO2_5.1	25	50	15	15	intense red, easy to ignite, low velocity, blinking, smoke, Mg sparks, almost no solid residues
Sr1MeAtNO2_5.2	17	53	17	13	very intense red, easy to ignite, moderate velocity, blinking, less smoke, Mg sparks, no solid residues
Sr1MeAtNO2_5.3	13	62	13	12	intense red, easy to ignite, low velocity, blinking, smoke, Mg sparks, almost no solid residues
Sr1MeAtNO2_5.4	13	61	15	11	very intense red, easy to ignite, moderate velocity, smoke, few Mg sparks, no solid residues

Sr1MeAtNO2_5.5	8	74	11	7	bright red flame, easy to ignite, unsteady burning, low velocity, blinking, smoke, Mg sparks, no solid residues
-----------------------	---	----	----	---	---

9.2.2.4 Pyrotechnic Compositions based on Strontium bis(5-Nitrimino-1H-tetrazolate) Tetrahydrate (Sr1HAtNO2)

In Table 9.19–Table 9.26 the different pyrotechnic compositions based on **Sr1HAtNO2** are summarized. The oxidizers potassium permanganate, potassium perchlorate, potassium nitrate, ammonium nitrate, and ammonium dinitramide were used. The fuels magnesium, sulfur, charcoal or **5-At** were added.

Table 9.19 Pyrotechnic formulations containing **Sr1HAtNO2** and potassium permanganate.

	Sr1HAtNO2 [wt%]	KMnO4 [wt%]	Mg [wt%]	VAAR [wt%]	observed behavior
Sr1HAtNO2_1.1	25	43	24	8	cannot be ignited, in flame of BUNSEN burner intense red, Mg sparks, smoke, sizzling noise
Sr1HAtNO2_1.2	17	60	17	6	cannot be ignited, in flame of BUNSEN burner intense red, Mg sparks, smoke, sizzling noise
Sr1HAtNO2_1.3	11	70	11	8	cannot be ignited, in flame of lighter intense red, Mg sparks, less smoke, sizzling noise

Table 9.20 Pyrotechnic formulations containing **Sr1HAtNO2** and ammonium nitrate.

	Sr1HAtNO2 [wt%]	NH4NO3 [wt%]	Mg [wt%]	VAAR [wt%]	observed behavior
Sr1HAtNO2_2.1	11	79	0	10	did not burn
Sr1HAtNO2_2.2	8	78	7	7	white-reddish flame, easy to ignite, low velocity, blinking, less smoke, many Mg sparks, sizzling noise, solid residues

Table 9.21 Test formulation containing **Sr1HAtNO2** and potassium perchlorate.

	Sr1HAtNO2 [wt%]	KClO4 [wt%]	Mg [wt%]	VAAR [wt%]	observed behavior
Sr1HAtNO2_3	13	65	12	10	violet-red flame, very hard to ignite, no burning, deflagration, less smoke, Mg sparks

Table 9.22 Pyrotechnic formulation containing **Sr1HAtNO2** and sulfur.

	Sr1HAtNO2	NH₄NO₃	S	VAAR	observed behavior
	[wt%]	[wt%]	[wt%]	[wt%]	
Sr1HAtNO2_4	8	75	7	10	cannot be ignited

Table 9.23 Pyrotechnic formulation containing **Sr1HAtNO2** and charcoal.

	Sr1HAtNO2	KMnO₄	C	VAAR	observed behavior
	[wt%]	[wt%]	[wt%]	[wt%]	
Sr1HAtNO2_5	11	66	11	12	cannot be ignited, carbon sparks

Table 9.24 Pyrotechnic formulations containing **Sr1HAtNO2** and **5-At**.

	Sr1HAtNO2	KMnO₄	5-At	VAAR	observed behavior
	[wt%]	[wt%]	[wt%]	[wt%]	
Sr1HAtNO2_6.1	9	69	9	13	violet flame, moderate to ignite, low velocity, Mg sparks, sizzling noise, solid glowing residues
Sr1HAtNO2_6.2	6	65	19	10	violet flame, easy to ignite, low velocity, smoke, Mg sparks, sizzling noise, solid glowing residues
Sr1HAtNO2_6.3	13	63	15	9	violet-red flame, easy to ignite, low velocity, smoke, Mg sparks, sizzling noise, small amount of solid residues
Sr1HAtNO2_6.4	17	61	9	13	cannot be ignited, did not burn
Sr1HAtNO2_6.5	15	59	15	11	violet flame, unsteady burning

Table 9.25 Pyrotechnic formulation containing **Sr1HAtNO2** and ammonium dinitramide.

	Sr1HAtNO2	ADN	5-At	VAAR	observed behavior
	[wt%]	[wt%]	[wt%]	[wt%]	
Sr1HAtNO2_7	11	66	11	12	very intense red, easy to ignite, high velocity, no smoke, almost no solid residues

Table 9.26 Pyrotechnic formulations containing **Sr1HAtNO2**, ADN and potassium nitrate.

	Sr1HAtNO2	ADN	KNO₃	5-At	VAAR	observed behavior
	[wt%]	[wt%]	[wt%]	[wt%]	[wt%]	
Sr1HAtNO2_8.1	19	30	19	19	13	reacts too violently, flies away
Sr1HAtNO2_8.2	19	10	39	19	13	violet flame, easy to ignite, no proper burning, smoke, few Mg sparks, sizzling noise, almost no solid residues

Sr1HAtNO2_8.3	22	22	22	22	12	violet-red flame, easy to ignite, moderate velocity, smoke, sizzling noise, almost no solid residues
Sr1HAtNO2_8.4	21	24	21	22	12	violet-red flame, easy to ignite, low velocity, blinking, smoke, sizzling noise, almost no solid residues

9.2.2.5 Pyrotechnic Compositions based on Strontium 5-Nitriminoetrazolate Dihydrate (SrAtNO2)

In Table 9.27–Table 9.33 the different pyrotechnic compositions based on **SrAtNO2** are given. The oxidizers potassium permanganate, potassium perchlorate, ammonium nitrate, and ammonium dinitramide were used. The fuels magnesium, sulfur, charcoal or **5-At** were added.

Table 9.27 Pyrotechnic formulations containing **SrAtNO2** and potassium permanganate.

	SrAtNO2 [wt%]	KMnO₄ [wt%]	Mg [wt%]	VAAR [wt%]	observed behavior
SrAtNO2_1.1	27	39	27	7	red flame, hard to ignite, no proper burning, no smoke, Mg sparks, cracking, solid residues
SrAtNO2_1.2	19	56	19	6	cannot be ignited
SrAtNO2_1.3	11	74	11	4	hard to ignite, Mg sparks, cracking

Table 9.28 Pyrotechnic formulations containing **SrAtNO2** and ammonium nitrate.

	SrAtNO2 [wt%]	NH₄NO₃ [wt%]	Mg [wt%]	VAAR [wt%]	observed behavior
SrAtNO2_2.1	11	75	5	9	hard to ignite, Mg sparks, no proper burning, cracking
SrAtNO2_2.2	8	79	6	7	bright red flame, moderate to ignite, Mg sparks, no proper burning, cracking

Table 9.29 Test formulation containing **SrAtNO2** and potassium perchlorate.

	SrAtNO2 [wt%]	KClO₄ [wt%]	Mg [wt%]	VAAR [wt%]	observed behavior
SrAtNO2_3	8	75	7	10	cannot be ignited, cracking

Table 9.30 Pyrotechnic formulation containing **SrAtNO2** and sulfur.

	SrAtNO2 [wt%]	NH₄NO₃ [wt%]	S [wt%]	VAAR [wt%]	observed behavior
SrAtNO2_4	8	75	7	10	cannot be ignited

Table 9.31 Pyrotechnic formulation containing **SrAtNO2** and charcoal.

	SrAtNO2 [wt%]	NH₄NO₃ [wt%]	C [wt%]	VAAR [wt%]	observed behavior
SrAtNO2_5	13	66	13	8	white flame, hard to ignite, moderate velocity, carbon sparks, cracking

Table 9.32 Pyrotechnic formulations containing **SrAtNO2** and **5-At**.

	SrAtNO2 [wt%]	KMnO₄ [wt%]	5-At [wt%]	VAAR [wt%]	observed behavior
SrAtNO2_6.1	10	72	10	8	cannot be ignited
SrAtNO2_6.2	8	72	14	6	violet flame, very hard to ignite, cracking, no proper burning, Mg sparks

Table 9.33 Pyrotechnic formulations containing **SrAtNO2** and ADN.

	SrAtNO2 [wt%]	ADN [wt%]	5-At [wt%]	VAAR [wt%]	observed behavior
SrAtNO2_7.1	22	45	22	11	reacts too violently, flies away
SrAtNO2_7.2	29	29	29	13	intense red, easy to ignite, no proper burning, cracking
SrAtNO2_7.3	17	47	26	10	intense red, easy to ignite, less smoke, unsteady burning, small amount of solid residues
SrAtNO2_7.4	15	47	27	11	intense red, easy to ignite, less smoke, high velocity, small amount of solid residues

9.2.2.6 Pyrotechnic Compositions based on Strontium 3,3'-Bis(1,2,4-oxadiazol-5-one) Dihydrate (SrOD)

In Table 9.34–Table 9.41 the different pyrotechnic compositions based on **SrOD** are given. The oxidizers potassium permanganate, potassium nitrate, ammonium nitrate, and ammonium dinitramide were used. The fuels magnesium, aluminum, magalium or **5-At** were added.

Table 9.34 Pyrotechnic formulations containing **SrOD** and potassium permanganate.

	SrOD [wt%]	KMnO₄ [wt%]	Mg [wt%]	VAAR [wt%]	observed behavior
SrOD_1.1	13	64	13	10	violet flame, easy to ignite, high velocity, much smoke, solid glowing residues
SrOD_1.2	14	69	7	10	violet flame, easy to ignite, moderate velocity, much smoke, solid glowing residues
SrOD_1.3	11	75	4	10	yellow-violet flame, easy to ignite, moderate velocity, much smoke, huge amount of solid glowing residues
SrOD_1.3 + 3 wt% LiCl	11	72	4	10	yellow flame, easy to ignite, moderate velocity, much smoke, huge amount of solid glowing residues

Table 9.35 Pyrotechnic formulations containing **SrOD** and aluminum.

	SrOD [wt%]	KMnO₄ [wt%]	Al [wt%]	VAAR [wt%]	observed behavior
SrOD_2.1	13	64	13 (grit)	10	small yellow flame, easy to ignite, low velocity, smoke, huge amount of solid glowing residues
SrOD_2.2	23	57	11 (powder)	9	orange flame, moderate to ignite, moderate velocity, smoke, solid residues
SrOD_2.3	14	69	7 (powder)	10	easy to ignite, no flame, only glowing, huge amount of solid residues

Table 9.36 Pyrotechnic formulation containing **SrOD** and ammonium nitrate.

	SrOD [wt%]	NH₄NO₃ [wt%]	Al (powder) [wt%]	VAAR [wt%]	observed behavior
SrOD_3	9	69	9	13	cannot be ignited

Table 9.37 Pyrotechnic formulation containing **SrOD** and potassium nitrate.

	SrOD [wt%]	NH₄NO₃ [wt%]	5-At [wt%]	VAAR [wt%]	observed behavior
SrOD_4	13	67	13	7	small white flame, hard to ignite, no proper burning, smoke

Table 9.38 Pyrotechnic formulation containing **SrOD** and magnalium.

	SrOD [wt%]	KMnO₄ [wt%]	MgAl [wt%]	VAAR [wt%]	observed behavior
SrOD_5	13	66	13	8	violet flame, easy to ignite, moderate velocity, smoke, solid glowing residues

Table 9.39 Pyrotechnic formulations containing **SrOD** and **ADN**.

	SrOD [wt%]	ADN [wt%]	5-At [wt%]	VAAR [wt%]	observed behavior
SrOD_6.1	18	55	18	9	very intense red, easy to ignite, high velocity, less smoke, small amount of solid glowing residues
SrOD_6.2	12	57	23	8	very intense red, reacts too violently, lifts off
SrOD_6.3	13	52	26	9	very intense red, easy to ignite, high velocity, less smoke, almost no solid glowing residues
SrOD_6.4	10	54	26	10	very intense red, reacts too violently, lifts off
SrOD_6.5	11	51	28	10	very intense red, easy to ignite, high velocity, less smoke, small amount of solid glowing residues

Table 9.40 Pyrotechnic formulations containing **SrOD** and **5-At**.

	SrOD [wt%]	ADN [wt%]	KNO₃ [wt%]	5-At [wt%]	VAAR [wt%]	observed behavior
SrOD_7.1	10	48	7	26	9	very intense red, easy to ignite, high velocity, small amount of solid glowing residues
SrOD_7.2	10	45	10	26	9	intense red, easy to ignite, moderate velocity, smoke, almost no solid glowing residues

Table 9.41 Pyrotechnic formulations containing **SrOD**, **ADN** and magnesium.

	SrOD [wt%]	ADN [wt%]	KNO₃ [wt%]	Mg [wt%]	5-At [wt%]	VAAR [wt%]	observed behavior
SrOD_8.1	10	43	10	3	24	10	very intense red, reacts too violently, lifts off
SrOD_8.2	10	39	16	2	23	10	intense red, easy to ignite, high velocity, less smoke, Mg sparks, almost no solid glowing residues

9.3 Conclusion

It was possible to achieve at least one red burning pyrotechnic composition with convincing properties of each investigated strontium salt, strontium tetrazolate pentahydrate (**SrTz**), strontium 5-aminotetrazolate tetrahydrate (**SrAt**), strontium 1-methyl-5-nitriminotetrazolate monohydrate (**Sr1MeAtNO2**), strontium bis(5-nitrimino-1*H*-tetrazolate) tetrahydrate (**Sr1HAtNO2**), strontium 5-nitriminotetrazolate monohydrate (**SrAtNO2**), and strontium 3,3'-bis(1,2,4-oxadiazol-5-onate) dihydrate (**SrOD**). Especially the compositions **SrTz_1** and **Sr1MeAtNO2_1** show besides their good coloring and combustion properties high decomposition temperatures. Their determined sensitivities to impact, friction and electric discharge are comparable to M126 A1 and other commercially available pyrotechnic compositions.^[1] The compositions **SrTz_1** and **Sr1MeAtNO2_1** are also presented in Klapötke *et al.*^[2]

Comparing **SrTz** and **Sr1MeAtNO2** with a control composition, containing strontium nitrate, one has to recognize that both offer higher spectral purity and average intensity, but a shorter burn time. **Sr1MeAtNO2** possesses the best properties with regard to high decomposition temperature, sensitivity to impact and friction, its behavior in the tested pyrotechnic compositions, and a low solubility in H₂O. Although **SrAt** is mentioned in a patent as ingredient in “pyrotechnic and fireworks compositions [...] for colored flames”,^[2] it could not convince as colorant agent as neat compound in the flame of a BUNSEN burner nor in the investigated compositions. This may change, if a chlorine donor, as supposed in the patent, is added.

The strontium salts **Sr1HAtNO2** and **SrAtNO2** could find application, if sizzling sound effects are desired.

Further investigations of varying the ingredients or using other additives might result in even better formulations. Whereas, it could be shown that the substitution of potassium perchlorate with nitrogen-rich strontium salts is possible.

9.4 References

- [1] a) T. M. Klapötke, G. Steinhauser: 'Green' Pyrotechnics: A Chemists' Challenge, *Angew. Chem. Int. Ed.* **2008**, *47*, 3330–3347. b) T. M. Klapötke, G. Steinhauser: Pyrotechnik mit dem "Ökosiegel": eine chemische Herausforderung, *Angew. Chem.* **2008**, *120*, 3376–3394.
- [2] J. F. Zevenbergen, R. Webb, M. P. Van Rooijen: Pyrotechnic and fireworks compositions with metal salts of 5-aminotetrazole for colored flames. Eur. Patent Application, EP 1982969 A1, **2008**, Netherlands.

- [3] T. M. Klapötke, M. Stein, J. Stierstorfer: Salts of 1H-tetrazole – synthesis, characterization and properties, *Z. Anorg. Allg. Chem.* **2008**, *643*, 1711–1723.
- [4] T. M. Klapötke, J. Stierstorfer, K. R. Tarantik, I. D. Thoma: Strontium Nitriminotetrazolates - Suitable Colorants in Smokeless Pyrotechnic Compositions, *Z. Anorg. Allg. Chem.* **2008**, *634*, 2777–2784.
- [5] J. Stierstorfer: Advanced Energetic Materials based on 5-Aminotetrazole, *PhD Thesis*, **2009**, Ludwig-Maximilian University, Munich.
- [6] T. M. Klapötke, N. T. Mayr, S. Seel: Smokeless pyrotechnical colorants based on 3,3'-bis-(1,2,4-oxadiazol)-5-one salts., *New Trends in Research of Energetic Materials*, Proceedings of the Seminar, *12th*, Pardubice, Czech Republic, 9.–11. Apr. **2009**, Pt. 2, 596–607.
- [7] T. M. Klapötke, J. Stierstorfer: Nitration products of 5-amino-1H-tetrazole and methyl-5-amino-1H-tetrazoles - structures and properties of promising energetic materials., *Helv. Chim. Acta*, **2007**, *90*, 2132–2150.
- [8] a) <http://www.bam.de> b) E_{dr} : insensitive > 40 J, less sensitive \geq 35 J, sensitive \geq 4, very sensitive \leq 3 J; F_r : insensitive > 360 N, less sensitive = 360 N, sensitive < 360 N > 80 N, very sensitive \leq 80 N, extreme sensitive \leq 10 N. According to the UN Recommendations on the Transport of Dangerous Goods.
- [9] G. R. Lakshminarayanan, G. Chen, R. Ames, W. T. Lee, J. Wejsa, K. Meiser, *Laminac Binder Replacement Program*, Aug. **2006**.
- [10] G. Chen, *Application of High Nitrogen Energetics in Pyrotechnic*, Program Review Presentation to US Army RDECOM, 20. Jan. **2009**.
- [11] U. Krone, H. Treumann: Pyrotechnic flash compositions, *Propellants, Explos. Pyrotech.* **1990**, *15*, 115–120.
- [12] T. M. Klapötke, K. Tarantik: Green Pyrotechnic Compositions, *New Trends in Research of Energetic Materials*, Proceedings of the Seminar, *11th*, Pardubice, Czech Republic, 9.–11. Apr. **2008**, Pt. 2, 586–597.

10 Pyrotechnic Compositions Containing Nitrogen-rich Copper(II) Compounds

In this chapter, the literature known copper(II) compounds, diammine bis(tetrazol-5-yl)-aminato- $\kappa^2N1,N6$ copper(II) ($[\text{Cu}(\text{bta})(\text{NH}_3)_2]$), bis{bis(tetrazol-5-yl)-amine- $\kappa^2N1,N6$ } copper(II) nitrate hemihydrate ($[\text{Cu}(\text{H}_2\text{bta})_2](\text{NO}_3)_2$), diaqua bis(1-methyl-5-aminotetrazole- $N4$) copper(II) nitrate ($[\text{Cu}(\text{1MeAt})_2(\text{H}_2\text{O})_2](\text{NO}_3)_2$), diaqua tetrakis(1-methyl-5-aminotetrazole- $N4$) copper(II) nitrate ($[\text{Cu}(\text{1MeAt})_4(\text{H}_2\text{O})_2](\text{NO}_3)_2$), diammine bis(1-methyl-5-nitrimino-tetrazolato- $\kappa^2N4,O1$) copper(II) ($[\text{Cu}(\text{1MeAtNO}_2)_2(\text{NH}_3)_2]$), bis((triammine) μ_2 -(5-nitrimino-tetrazolato- $N1,O1$) copper(II)) ($[\text{Cu}(\text{AtNO}_2)(\text{NH}_3)_3]_2$), basic copper(II) nitrate ($\text{Cu}_2(\text{OH})_3(\text{NO}_3)$), and tetrammine copper(II) dinitramide ($[\text{Cu}(\text{NH}_3)_4][\text{N}(\text{NO}_2)_2]_2$) were investigated as possible colorants in pyrotechnic compositions yielding a green flame.^[1-10]

Copper compounds, such as metallic copper, copper(I) chloride, basic copper(II) carbonate, copper(I) and copper(II) oxide, and copper(II) sulfide, are widely used in pyrotechnic compositions, usually for emitting in presence of chlorine a blue light by forming the emitting species $\text{Cu}(\text{I})\text{Cl}$ in the gas phase.^[11] In the absence of chlorine, copper is able to emit both green and red light, depending on the combustion temperature and amount of oxygen. At temperatures above 1200 °C $\text{Cu}(\text{I})\text{Cl}$ is unstable and $\text{Cu}(\text{I})\text{OH}$ – the emitter of green light (525–555 nm) – and CuO , which emits in the red region – are formed.^[12] Therefore, in the absence of chlorine, copper(II) compounds are suitable to be used as green light emitting colorants and an environmentally more benign alternative to barium salts.

$[\text{Cu}(\text{bta})(\text{NH}_3)_2]$ was chosen, since it is insensitive to impact and friction, thermally very stable, and easy to prepare in larger scales.^[1, 2] The similar copper(II) compound $[\text{Cu}(\text{H}_2\text{bta})_2](\text{NO}_3)_2$ is more sensitive and thermally less stable.^[2, 3] However, it offers a less negative oxygen balance.

$[\text{Cu}(\text{1MeAt})_2(\text{H}_2\text{O})_2](\text{NO}_3)_2$ and $[\text{Cu}(\text{1MeAt})_4(\text{H}_2\text{O})_2](\text{NO}_3)_2$ also contain the oxygen-rich anion nitrate. The nitrogen-rich ligand 1-methyl-5-aminotetrazole should guarantee a smoke reduced combustion.

The copper(II) complexes $[\text{Cu}(\text{1MeAtNO}_2)_2(\text{NH}_3)_2]$ and $[\text{Cu}(\text{AtNO}_2)(\text{NH}_3)_3]_2$ were selected because of their nitriminotetrazole anions. Due to their ammine ligands they are less sensitive to impact and friction than their ammine free derivatives.^[6, 7]

$\text{Cu}_2(\text{OH})_3(\text{NO}_3)$ is known as the rare mineral gerhardtite. The natural mineral crystallizes in the orthorhombic crystal system, whereas the synthetic compound crystallizes mostly in the monoclinic system.^[13] It offers high thermal stability and low hygroscopicity and can be prepared from low cost materials. Furthermore, it is an oxidizer ($\Omega = +17\%$), that contains both copper and hydroxide, which makes it interesting as a potential coloring agent for pyrotechnic applications. Furthermore, it is known as an additive for gas generating compositions with metal complexes of nitrogen-rich ligands.^[14]

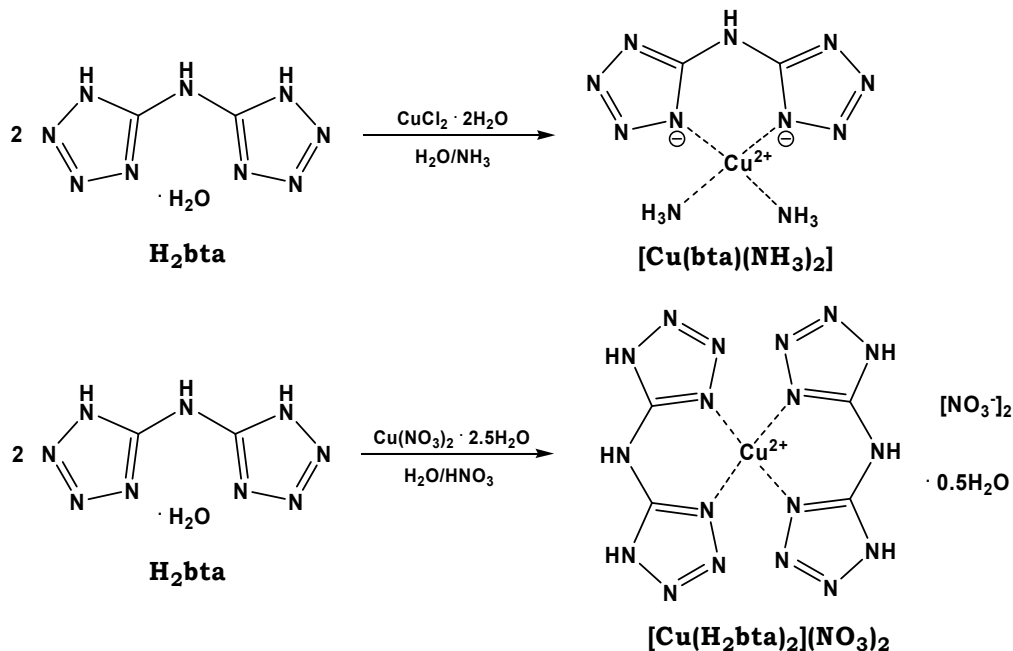
$[\text{Cu}(\text{NH}_3)_4\text{N}(\text{NO}_2)_2]$ is another copper(II) compound offering a positive oxygen balance despite its ammine ligands.

Several pyrotechnic compositions containing these copper(II) compounds were prepared and the ones with the best performance regarding emitting green light and burning properties were further investigated.

10.1 Results and Discussion

10.1.1 Syntheses

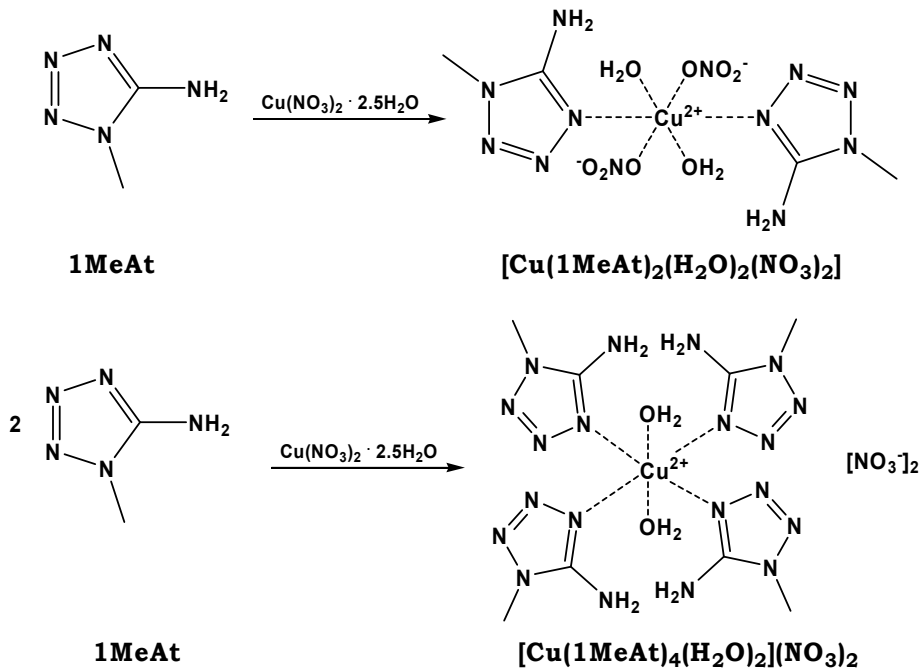
All prepared copper(II) compounds are known and characterized in the literature.^[1-10] Diammine bis(tetrazol-5-yl)-aminato- $\kappa^2\text{N}1, \text{N}6$ copper(II) ($[\text{Cu}(\text{bta})(\text{NH}_3)_2]$) and bis{bis(tetrazol-5-yl)-amine- $\kappa^2\text{N}1, \text{N}6$ } copper(II) nitrate hemihydrate ($[\text{Cu}(\text{H}_2\text{bta})_2](\text{NO}_3)_2$) were prepared starting from *N,N*-bis(1*H*-tetrazol-5-yl)-amine monohydrate (H_2bta) (Scheme 10.1). $[\text{Cu}(\text{bta})(\text{NH}_3)_2]$ can be yielded by the reaction of H_2bta with copper(II) chloride dihydrate in aqueous ammonia solution.^[1, 2] The reaction can be easily done with 0.1 mol starting material to obtain $[\text{Cu}(\text{bta})(\text{NH}_3)_2]$ as a dark blue powdered participate in very high yields. If dissolved H_2bta is combined with copper(II) nitrate pentahydrate in diluted nitric acid, blue crystals of $[\text{Cu}(\text{H}_2\text{bta})_2](\text{NO}_3)_2$ can be yielded.^[2, 3] In this case H_2bta acts as neutral bidentate ligand in contrast to an anion in $[\text{Cu}(\text{bta})(\text{NH}_3)_2]$.



Scheme 10.1 Preparation of $[\text{Cu}(\text{bta})(\text{NH}_3)_2]$ and $[\text{Cu}(\text{H}_2\text{bta})_2](\text{NO}_3)_2$.

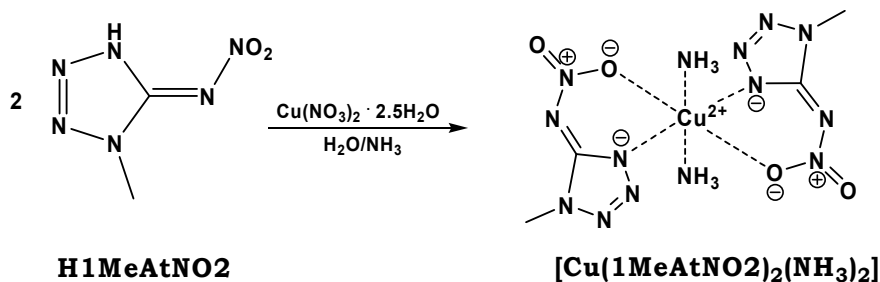
Starting material for diaqua bis(1-methyl-5-aminotetrazole-*N*4) copper(II) nitrate ($[\text{Cu}(\text{1MeAt})_2(\text{H}_2\text{O})_2(\text{NO}_3)_2]$) and diaqua tetrakis(1-methyl-5-aminotetrazole-*N*4) copper(II) nitrate ($[\text{Cu}(\text{1MeAt})_4(\text{H}_2\text{O})_2](\text{NO}_3)_2$) is 1-methyl-5-aminotetrazole (**1MeAt**). It was prepared according to HENRY *et al.*^[15]. Depending on the molar ratio of **1MeAt** to copper(II) nitrate pentahydrate $[\text{Cu}(\text{1MeAt})_2(\text{H}_2\text{O})_2(\text{NO}_3)_2]$ (1:1) or $[\text{Cu}(\text{1MeAt})_4(\text{H}_2\text{O})_2](\text{NO}_3)_2$ (2:1) could

be obtained (Scheme 10.2).^[4] H₂O was used as solvent in both syntheses. Crystals of **[Cu(1MeAt)₂(H₂O)₂(NO₃)₂]** are darker blue and are more grown together than the blocks of **[Cu(1MeAt)₄(H₂O)₂](NO₃)₂**. After storing the filtered mother liquor of **[Cu(1MeAt)₄(H₂O)₂](NO₃)₂** at ambient temperature crystals of **[Cu(1MeAt)₂(H₂O)₂(NO₃)₂]** could be obtained.



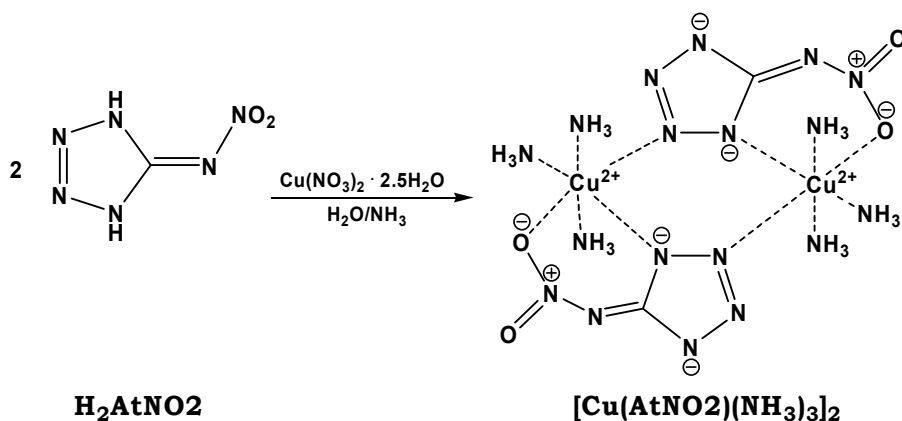
Scheme 10.2 Preparation of **[Cu(1MeAt)₂(H₂O)₂(NO₃)₂]** and **[Cu(1MeAt)₄(H₂O)₂](NO₃)₂**.

1-Methyl-5-nitriminotetrazole (**H1MeAtNO2**) is the nitration product of **1MeAt** and starting material of the preparation of diammine bis(1-methyl-5-nitriminotetrazolato- $\kappa^2\text{N}_4, \text{O}_1$) copper(II) (**[Cu(1MeAtNO2)₂(NH₃)₂]**) (Scheme 10.3). Copper(II) chloride or nitrate can be reacted with **H1MeAtNO2**, dissolved in aqueous ammonia solution. Both ways yielded **[Cu(1MeAtNO2)₂(NH₃)₂]**. Another synthesis route starts from ammonium 1-methyl-5-nitriminotetrazolate, which is less sensitive to impact and friction than **H1MeAtNO2**.^[7, 16] Thereby, diammine bis(1-methyl-5-nitriminotetrazolato- $\kappa^2\text{N}_4, \text{O}_1$) copper(II) monohydrate (**[Cu(1MeAtNO2)₂(NH₃)₂·H₂O]**) was obtained as first deep violet precipitate. The thin needles changed during drying on air to unclear bright violet. Elemental analysis verified the monohydrate. Furthermore, the IR-spectrum shows a broad vibration signal at 3553 cm⁻¹, which derives from crystal water and lacks in the IR-spectrum of **[Cu(1MeAtNO2)₂(NH₃)₂]**. Different copper(II) complexes of **H1MeAtNO2** are described in literature.^[7, 17] Due to their higher sensitivities to impact and friction, no further investigations regarding their application possibilities as coloring agent in pyrotechnic compositions were done.



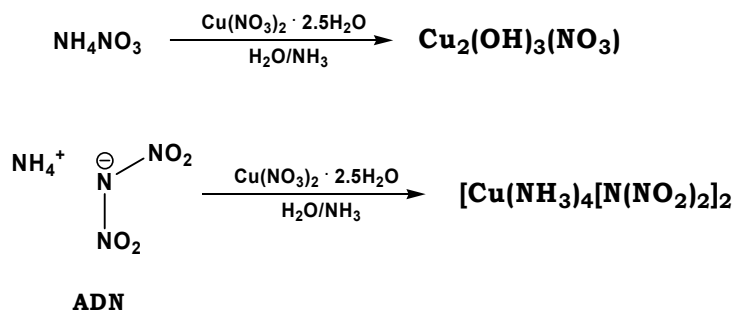
Scheme 10.3 Preparation of **[Cu(1MeAtNO2)₂(NH₃)₂]**.

Another nitration product, 5-nitriminotetrazole (**H₂AtNO₂**) obtained *via* nitration of 5-aminotetrazole (**5-At**) with 100 % HNO₃,^[7, 18] is reactant in the synthesis of bis[(triammine) μ_2 -(5-nitriminotetrazolato-*N*1,*O*1) copper(II)] (**[Cu(AtNO₂)(NH₃)₃]₂**) (Scheme 10.4).^[6, 7]



Scheme 10.4 Preparation of **[Cu(AtNO₂)(NH₃)₃]₂**.

Basic copper(II) nitrate (**Cu₂(OH)₃(NO₃)**) also known as the rare mineral gerhardtite, can be prepared easily from the low cost starting materials ammonium nitrate, copper(II) nitrate pentahydrate, and aqueous ammonia solution (Scheme 10.5).^[9] After two days stirring at 65 °C a light turquoise powder of **Cu₂(OH)₃(NO₃)** was obtained in yields above 60 %.



Scheme 10.5 Preparation of **Cu₂(OH)₃(NO₃)** and **[Cu(NH₃)₄][N(NO₂)₂]₂**.

Tetrammine copper(II) dinitramide (**[Cu(NH₃)₄][N(NO₂)₂]₂**) is prepared from ammonium dinitramide (ADN) dissolved in H₂O and copper(II) sulfate pentahydrate dissolved in aqueous ammonia solution (25 %) (Scheme 10.5).^[9, 10] Deep violet crystals of

$[\text{Cu}(\text{NH}_3)_4][\text{N}(\text{NO}_2)_2]_2$ were filtered off and dried on air to avoid the removal of ammine ligands and not dried under vacuum according to the literature^[10].

10.1.2 Energetic Properties and Solubility in H₂O

The energetic properties such as the decomposition temperature (T_{dec}), sensitivity to impact (E_{dr}), friction (F_r) and electric discharge (E_{el}) were determined or adopted from literature.^[1–10] Furthermore, the solubility in H₂O at ambient temperature of each compound was defined. An overview of the energetic properties is given in Table 10.1 and Table 10.2.

Table 10.1 Energetic properties of $[\text{Cu}(\text{bta})(\text{NH}_3)_2]$, $[\text{Cu}(\text{H}_2\text{bta})_2](\text{NO}_3)_2$, $[\text{Cu}(\text{1MeAt})_2(\text{H}_2\text{O})_2(\text{NO}_3)_2]$, and $[\text{Cu}(\text{1MeAt})_4(\text{H}_2\text{O})_2](\text{NO}_3)_2$.

	$[\text{Cu}(\text{bta})(\text{NH}_3)_2]$	$[\text{Cu}(\text{H}_2\text{bta})_2](\text{NO}_3)_2$	$[\text{Cu}(\text{1MeAt})_2(\text{H}_2\text{O})_2(\text{NO}_3)_2]$	$[\text{Cu}(\text{1MeAt})_4(\text{H}_2\text{O})_2](\text{NO}_3)_2$
Formula	$\text{C}_2\text{H}_7\text{CuN}_{11}$	$\text{C}_4\text{H}_7\text{CuN}_{20}\text{O}_{6.5}$	$\text{C}_4\text{H}_{14}\text{CuN}_{12}\text{O}_8$	$\text{C}_8\text{H}_{24}\text{CuN}_{22}\text{O}_8$
<i>M</i> [g/mol]	248.70	502.78	421.78	619.97
<i>E</i>_{dr} [J]^a	> 100	3.9	> 30	> 30
<i>F</i>_r [N]^b	> 360	196	196	120
<i>E</i>_{el} [J]^c	0.70	0.10	2.0	2.0
grain size [μm]	< 100	> 1000	500–1000	500–1000
<i>N</i> [%]^d	61.95	55.72	39.85	49.70
<i>Ω</i> [%]^e	–55	–19	–30	–54
<i>T</i>_{dec} [°C]^f	281	156	142	168
<i>ρ</i> [g/cm³]^g	1.99	2.14	1.95	1.71
H₂O sol. [wt%]^h	1.5 (22 °C)	< 0.4 (21 °C)	13 (22 °C)	8.8 (22 °C)

a) BAM drop hammer ^[19], *b)* BAM methods ^[19], *c)* Electric discharge tester, *d)* Nitrogen content, *e)* Oxygen balance, *f)* Decomposition temperature from DSC ($\beta = 5$ K/min), *g)* determined by X-ray crystallography or pycnometer (*), *h)* Solubility in H₂O (H₂O temperature).

Table 10.2 Energetic properties of $[\text{Cu}(\text{1MeAtNO}_2)_2(\text{NH}_3)_2]$, $[\text{Cu}(\text{AtNO}_2)(\text{NH}_3)_3]_2$, $\text{Cu}_2(\text{OH})_3(\text{NO}_3)$, and $[\text{Cu}(\text{NH}_3)_4][\text{N}(\text{NO}_2)_2]_2$.

	$[\text{Cu}(\text{1MeAtNO}_2)_2(\text{NH}_3)_2]$	$[\text{Cu}(\text{AtNO}_2)(\text{NH}_3)_3]_2$	$\text{Cu}_2(\text{OH})_3(\text{NO}_3)$	$[\text{Cu}(\text{NH}_3)_4][\text{N}(\text{NO}_2)_2]_2$
Formula	$\text{C}_4\text{H}_{12}\text{CuN}_{14}\text{O}_4$	$\text{C}_2\text{H}_{18}\text{Cu}_2\text{N}_{18}\text{O}_4$	$\text{Cu}_2\text{H}_3\text{NO}_6$	$\text{H}_{12}\text{CuN}_{10}\text{O}_8$
<i>M</i> [g/mol]	383.78	485.38	240.12	343.70
<i>E</i>_{dr} [J]^a	7.0	5.0	> 40	2.5
<i>F</i>_r [N]^b	288	288	> 360	48
<i>E</i>_{el} [J]^c	0.75	0.20	0.10	0.47
grain size [μm]	500–1000	500–1000	< 100	> 1000
<i>N</i> [%]^d	51.10	51.94	5.83	40.57
<i>Ω</i> [%]^e	–50	–30	+17	+5
<i>T</i>_{dec} [°C]^f	242	250	271	183
<i>ρ</i> [g/cm³]^g	1.85	2.01	3.38* (22 °C)	1.98
H₂O sol. [wt%]^h	1.5 (23 °C)	< 0.5 (21 °C)	< 0.4 (21 °C)	2.7 (22 °C)

a) BAM drop hammer ^[19], *b)* BAM methods ^[19], *c)* Electric discharge tester, *d)* Nitrogen content, *e)* Oxygen balance, *f)* Decomposition temperature from DSC ($\beta = 5$ K/min), *g)* determined by X-ray crystallography or pycnometer (*), *h)* Solubility in H₂O (H₂O temperature).

The moiety of the copper(II) compounds starts to decompose at temperatures above 240 °C ($[\text{Cu}(\text{1MeAtNO}_2)_2(\text{NH}_3)_2]$: $T_{\text{dec}} = 241$ °C, $[\text{Cu}(\text{AtNO}_2)(\text{NH}_3)_3]_2$: $T_{\text{dec}} = 250$ °C, $\text{Cu}_2(\text{OH})_3(\text{NO}_3)$: $T_{\text{dec}} = 271$ °C, and $[\text{Cu}(\text{H}_2\text{bta})_2](\text{NO}_3)_2$: $T_{\text{dec}} = 281$ °C). Lower decomposition

points offer **[Cu(1MeAt)₂(H₂O)₂(NO₃)₂]**, **[Cu(1MeAt)₄(H₂O)₂(NO₃)₂]**, **[Cu(H₂bta)₂(NO₃)₂]**, and **[Cu(NH₃)₄][N(NO₂)₂]₂** with 142 °C, 168 °C, 156 °C and 183 °C, respectively.

All sensitivities to impact, friction, and electric discharge were determined with the following grain sizes: < 100 μm (**[Cu(bta)(NH₃)₂]**, **Cu₂(OH)₃(NO₃)**), 500–1000 μm (**[Cu(1MeAt)₂(H₂O)₂(NO₃)₂]**, **[Cu(1MeAt)₄(H₂O)₂(NO₃)₂]**, **[Cu(1MeAtNO₂)₂(NH₃)₂]**, and **[Cu(AtNO₂)(NH₃)₃]₂**), and > 1000 μm (**[Cu(H₂bta)₂(NO₃)₂]**, **[Cu(NH₃)₄][N(NO₂)₂]₂**). **[Cu(bta)(NH₃)₂]** as well as **Cu₂(OH)₃(NO₃)** are insensitive to impact and friction. All other copper(II) compounds are sensitive to friction, **[Cu(NH₃)₄][N(NO₂)₂]₂** is even very sensitive to friction with 48 N as well as to impact (2.5 J). Sensitive to impact are **[Cu(H₂bta)₂(NO₃)₂]** (3.5 J), **[Cu(1MeAtNO₂)₂(NH₃)₂]** (7.0 J), and **[Cu(AtNO₂)(NH₃)₃]₂** (5.0 J). The sensitivities to electric discharge are in the range of 0.10–2.0 J.

For the solubility determination, each compound was added to 1 mL H₂O with before noted temperature until the solution was saturated. The solubilities are given in percent by weight (wt%) and were calculated according to equation 10.1.

$$\text{H}_2\text{O-sol.} = \frac{m_{\text{dissolved Compound}}}{m_{\text{dissolved Compound}} + m_{\text{Solvent}}} \cdot 100 \quad (10.1)$$

All prepared copper compounds offer a very low solubility in H₂O. **[Cu(1MeAt)₂(H₂O)₂(NO₃)₂]** and **[Cu(1MeAt)₄(H₂O)₂(NO₃)₂]** are the best soluble ones with 13 wt% and 8.8 wt%, respectively. **[Cu(NH₃)₄][N(NO₂)₂]₂**, **[Cu(bta)(NH₃)₂]**, and **[Cu(1MeAtNO₂)₂(NH₃)₂]** are between 1.5 and 2.7 wt% soluble in H₂O. The solubilities of the others are lower than 1.0 wt%. All compounds are stable in H₂O.

10.1.3 Color Performance and Combustion Behavior

The formation of the green light emitting species CuOH in the gas phase is very dependent on flame temperature. Therefore, it makes a difference, if the copper(II) compound is held into the oxidizing or reducing flame of a BUNSEN burner (Figure 10.1). In the hotter and more oxygen-rich oxidizing flame, the flame color changes from green to yellow with a red seam caused by the formation of CuO.^[12] An intense green flame can be observed in the reducing flame. All copper(II) compounds were tested regarding to their flame color in the flame of a BUNSEN burner. Due to the absence of chlorine, all offer the expected green flame color and combust without any visible smoke production.

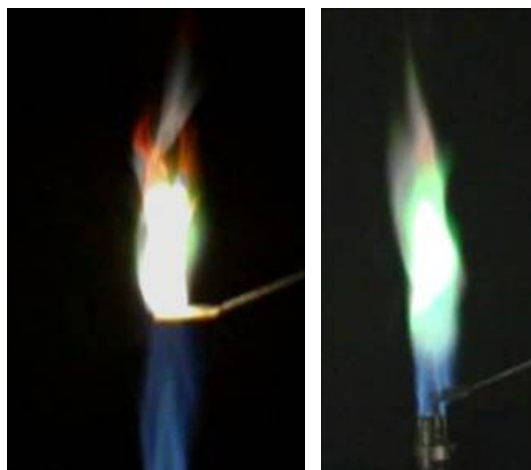


Figure 10.1 Copper(II) nitrate in the oxidizing flame (left) and reducing flame (right) of a BUNSEN burner.

In Figure 10.2 the colored flames are shown. $[\text{Cu}(\text{1MeAt})_4(\text{H}_2\text{O})_2](\text{NO}_3)_2$, $[\text{Cu}(\text{1MeAtNO}_2)_2(\text{NH}_3)_2]$, $[\text{Cu}(\text{1MeAtNO}_2)_2(\text{NH}_3)_2] \cdot \text{H}_2\text{O}$, and $[\text{Cu}(\text{AtNO}_2)(\text{NH}_3)_3]_2$ make a sizzling sound during combustion.

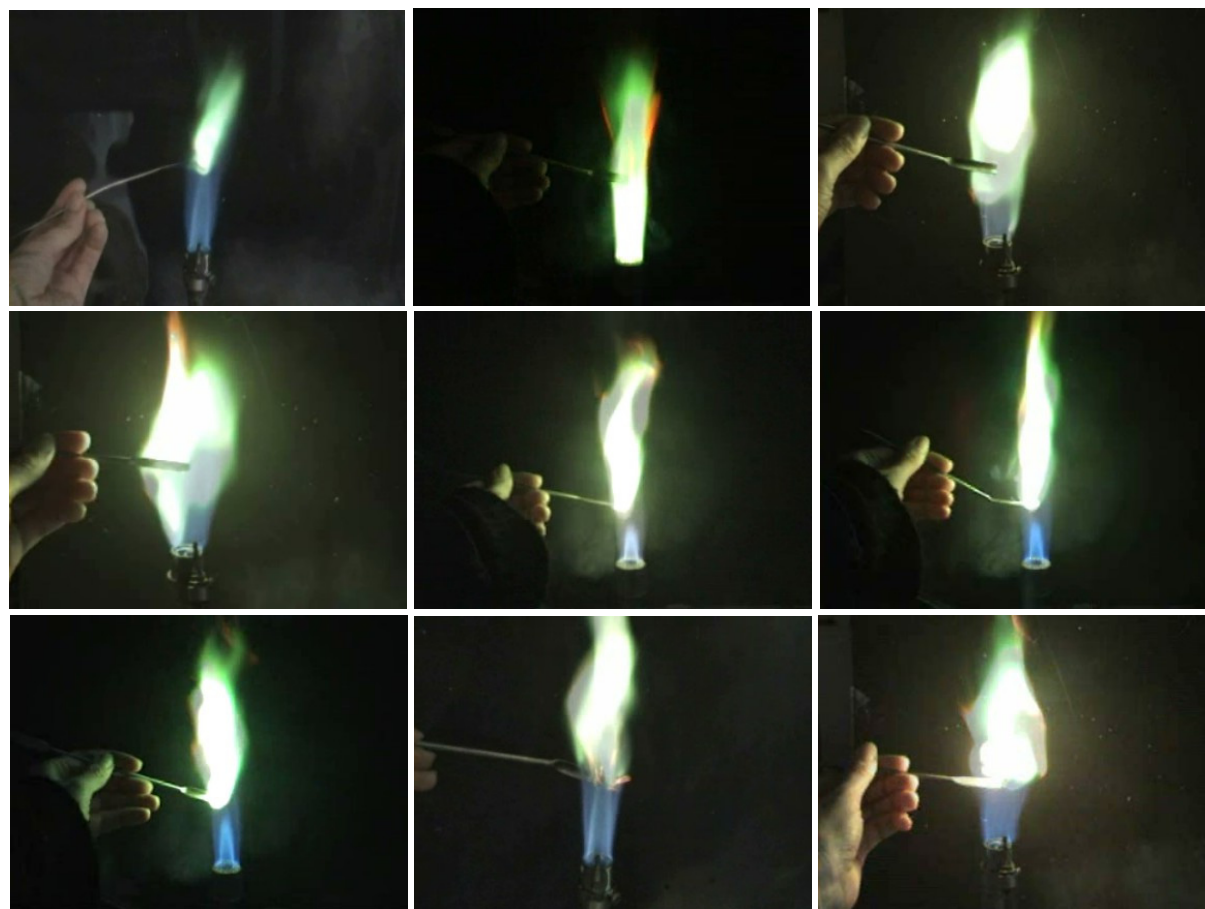


Figure 10.2 Flame color of $[\text{Cu}(\text{bta})(\text{NH}_3)_2]$, $[\text{Cu}(\text{H}_2\text{bta})_2](\text{NO}_3)_2$, $[\text{Cu}(\text{1MeAt})_2(\text{H}_2\text{O})_2](\text{NO}_3)_2$, $[\text{Cu}(\text{1MeAt})_4(\text{H}_2\text{O})_2](\text{NO}_3)_2$, $[\text{Cu}(\text{1MeAtNO}_2)_2(\text{NH}_3)_2]$, $[\text{Cu}(\text{1MeAtNO}_2)_2(\text{NH}_3)_2] \cdot \text{H}_2\text{O}$, $[\text{Cu}(\text{AtNO}_2)(\text{NH}_3)_3]_2$, $\text{Cu}_2(\text{OH})_3(\text{NO}_3)$, and $[\text{Cu}(\text{NH}_3)_4][\text{N}(\text{NO}_2)_2]_2$ (from left up to right down) in the flame of a BUNSEN burner.

Furthermore, the combustion behavior of the copper(II) compounds **[Cu(bta)(NH₃)₂]**, **[Cu(1MeAt)₂(H₂O)₂(NO₃)₂]**, **[Cu(1MeAt)₄(H₂O)₂(NO₃)₂]**, **[Cu(1MeAtNO₂)₂(NH₃)₂]**, **[Cu(1MeAtNO₂)₂(NH₃)₂·H₂O]**, and **[Cu(NH₃)₄][N(NO₂)₂]₂** were qualitatively characterized with a simple smoke test method. Therefore, approx. 1 g sample of each compound was placed in a heated crucible with a gas torch for observation of color, smoke, burn ability (propagation) and level of residue.

[Cu(1MeAt)₂(H₂O)₂(NO₃)₂] and **[Cu(1MeAt)₄(H₂O)₂(NO₃)₂]** show a green flame color, whereas **[Cu(1MeAt)₂(H₂O)₂(NO₃)₂]** is less intense than **[Cu(1MeAt)₄(H₂O)₂(NO₃)₂]**. **[Cu(bta)(NH₃)₂]**, **[Cu(1MeAtNO₂)₂(NH₃)₂]**, and **[Cu(1MeAtNO₂)₂(NH₃)₂·H₂O]** combust with a mostly white flame, which changes at the end into light yellow or orange. Except **[Cu(1MeAtNO₂)₂(NH₃)₂]** and **[Cu(1MeAtNO₂)₂(NH₃)₂·H₂O]** all investigated copper(II) compounds combust with smoke production and needed a constant torch. After the combustion **[Cu(1MeAt)₂(H₂O)₂(NO₃)₂]**, **[Cu(1MeAt)₄(H₂O)₂(NO₃)₂]**, and **[Cu(1MeAtNO₂)₂(NH₃)₂]** left no solid residues.

10.1.4 Pyrotechnic Compositions

Only the most promising formulations with the prepared copper(II) compounds are mentioned in this chapter. As oxidizers potassium nitrate, potassium permanganate, ammonium nitrate, ammonium dinitramide, and manganese dioxide were used. Magnesium (MgAl), titanium, silicon, sulfur, boron, boric acid, 5-aminotetrazole (**5-At**), and 5-amino-tetrazole monohydrate (**5-At·H₂O**), were added as fuel. Although it is known, that the Cu²⁺ ion is incompatible with magnesium, zinc and aluminum, especially in a moist environment, they are components of some compositions.^[20] The copper compounds, copper(I) oxide, copper(I) iodide, copper(II) sulfate pentahydrate, basic copper(II) carbonate, copper(II) nitrate pentahemihydrate, and tetraqua 3,3'-bis(1,2,4-oxadiazol-5-onate) copper(II) (**[Cu(H₂O)₄(OD)]**) were added. To obtain a better thermal stability or more stability towards moisture, urea and potassium aluminum sulfate dodecahydrate were added in very small amounts. All prepared compositions can be found in chapters 10.2.2.1–10.2.2.8. The performance of each composition has been evaluated with respect to the following categories:

- color emission (subjective impression)
- smoke generation
- morphology and amount of solid residues
- thermal stability
- moisture sensitivity

The three points mentioned first were evaluated with the aid of video recording. For thermal stability the decomposition points of the compositions were determined by DSC-

measurements ($\beta = 5$ K/min). Sensitivity to moisture could be investigated by storing the composition in an open vessel for several weeks.

The performance of the compositions were compared to the barium nitrate-based US Army composition # M125 A1 (green parachute): 50 wt% $\text{Ba}(\text{NO}_3)_2$, 30 wt% Mg, 15 wt% PVC, 5 wt% VAAR (Figure 10.3). Its determined decomposition point is 244 °C (DSC-measurement, $\beta = 5$ K/min). It is sensitive to impact (9.0 J), friction (288 N), and electric discharge (1.2 J).



Figure 10.3 Burn down of the US Army composition # M125 A1.

All mentioned compositions were prepared by hand. Details can be found in chapter 10.2.2.

In order to get a first impression, how copper(II) compounds might act as colorants for green flames, some pyrotechnic compositions based on copper(II) nitrate pentahemihydrate were investigated. Therefore, copper(II) nitrate was combined with 5-aminotetrazole (**5-At**). **5-At** was chosen as fuel due to its high nitrogen content, high thermal stability, and its tetrazole ring is the skeleton structure of all used ligands. First of all, both compounds were carefully mixed in a mortar and the homogeneous powder was ignited. The resulted flame was intense green, but the combustion velocity was quite low. Some pellets containing copper(II) nitrate pentahemihydrate and **5-At** were prepared. Alternatively, aluminum grit or magnalium was added. The pellet prepared of copper(II) nitrate pentahemihydrate (50 wt%) and **5-At** (50 wt%) burned self-consistent with a green flame. The add-on of aluminum grit improved the combustion properties regarding flame color and velocity. The combination with magnalium was easier to ignite. However, some sparks were observed. Further attempts were performed using the binder VAAR. Unfortunately, this combination is extremely thermally unstable. The pyrotechnic composition made of 43 wt% copper(II) nitrate pentahemihydrate, 43 wt% **5-At**, 1 wt% urea and 13 wt% VAAR, combusts without smoke and only a very small amount of solid residues and a very intense green flame (Figure 10.4). However, its decomposition occurs at temperatures above 130 °C and after storing it at 80 °C for some hours its performance became worse. The thermal instability of copper(II) nitrate pentahemihydrate might be a

reason for this result. Therefore, the usage of thermally more stable copper(II) compounds should lead to thermally more stable compositions.



Figure 10.4 Burn down of a pyrotechnic composition based on copper(II) nitrate pentahemihydrate and **5-At**.

Diammine {bis(tetrazol-5-yl)-aminato- $\kappa^2N1,N6$ } copper(II) (**[Cu(bta)(NH₃)₂]**) was combined with the oxidizers potassium permanganate, potassium nitrate, manganese dioxide, basic copper(II) carbonate, copper(II) nitrate pentahydrate, ADN, and ammonium nitrate. Magnesium, silicon, sulfur, and boron were added as fuel. The additives boric acid, potassium aluminum sulfate dodecahydrate, copper(I) oxide or copper(II) sulfate pentahydrate were used. Only ADN could convince as oxidizer. With all other used oxidizers the compositions could not be ignited or did not show a green flame. In the following, four pyrotechnic compositions based on **[Cu(bta)(NH₃)₂]** and ADN are presented. The pyrotechnic composition **[Cu(bta)(NH₃)₂]_{15.1}** consists of 27 wt% **[Cu(bta)(NH₃)₂]**, 64 wt% ADN, and 9 wt% VAAR (Table 10.18). The combustion occurs extremely fast with a pale green flame (Figure 10.5). No smoke or solid residues were observed. The composition decomposes at 175 °C. At 84 °C an endothermic signal can be observed in the DSC thermogram (Figure 10.6). This is a result of the melting of ADN.^[21] **[Cu(bta)(NH₃)₂]_{15.1}** is very sensitive to impact (3.0 J) and friction (60 N), and sensitive to electric discharge (0.30 J).

To composition **[Cu(bta)(NH₃)₂]_{16.1}**, which consists of 33 wt% **[Cu(bta)(NH₃)₂]**, 49 wt% ADN, and 9 wt% VAAR, copper(II) sulfate pentahydrate (9 wt%) was added to intensify the green flame (Table 10.19). This was successful; the flame is more intense green. Furthermore, the combustion velocity is less than the one of **[Cu(bta)(NH₃)₂]_{15.1}**. However, some smoke and solid glowing residues were observed. Its sensitivities were determined to impact with 4.0 J, to friction with 60 N, and to electric discharge with 0.30 J. **[Cu(bta)(NH₃)₂]_{16.1}** starts to decompose at temperatures above 138 °C (Figure 10.6). Analog to composition **[Cu(bta)(NH₃)₂]_{15.1}** at 86 °C an endothermic reaction occurs. At temperatures above 274 °C a further exothermic signal is shown due to the decomposition of **[Cu(bta)(NH₃)₂]**.

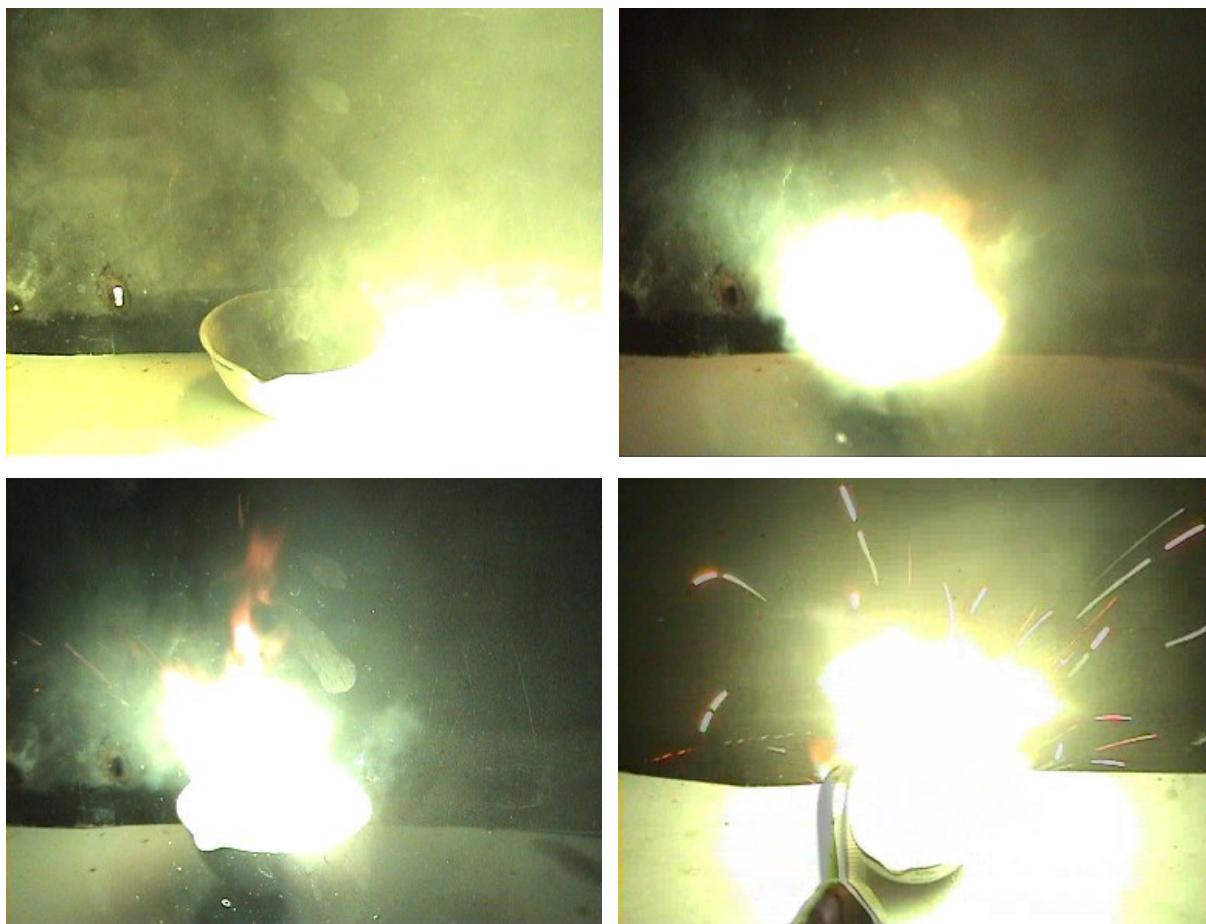


Figure 10.5 Burn down of the pyrotechnic compositions **[Cu(bta)(NH₃)₂]_{15.1}** (up, left), **[Cu(bta)(NH₃)₂]_{16.1}** (up, right), **[Cu(bta)(NH₃)₂]₁₈** (down, left), and **[Cu(bta)(NH₃)₂]_{31.4}** (down, right).

Composition **[Cu(bta)(NH₃)₂]₁₈** consists of 36 wt% of **[Cu(bta)(NH₃)₂]**, 54 wt% ADN, 1 wt% potassium aluminum sulfate dodecahydrate, and 9 wt% VAAR (Table 10.21). Potassium aluminum sulfate dodecahydrate was added to avoid a potential sensitivity to moisture. **[Cu(bta)(NH₃)₂]₁₈** combusts with an intense green flame (Figure 10.5) and slower than the two compositions mentioned above. Again, neither smoke nor solid residues were observed. Furthermore, **[Cu(bta)(NH₃)₂]₁₈** is less sensitive to impact (5.0 J) and friction (80 N). The determined value of the sensitivity to electric discharge is equal (0.3 J). **[Cu(bta)(NH₃)₂]₁₈** decomposes at temperatures above 173 °C (Figure 10.6). Further decomposition takes place at 273 °C, caused by the decomposition of **[Cu(bta)(NH₃)₂]**. Due to the melting of ADN, an endothermal signal at 90 °C can be observed.

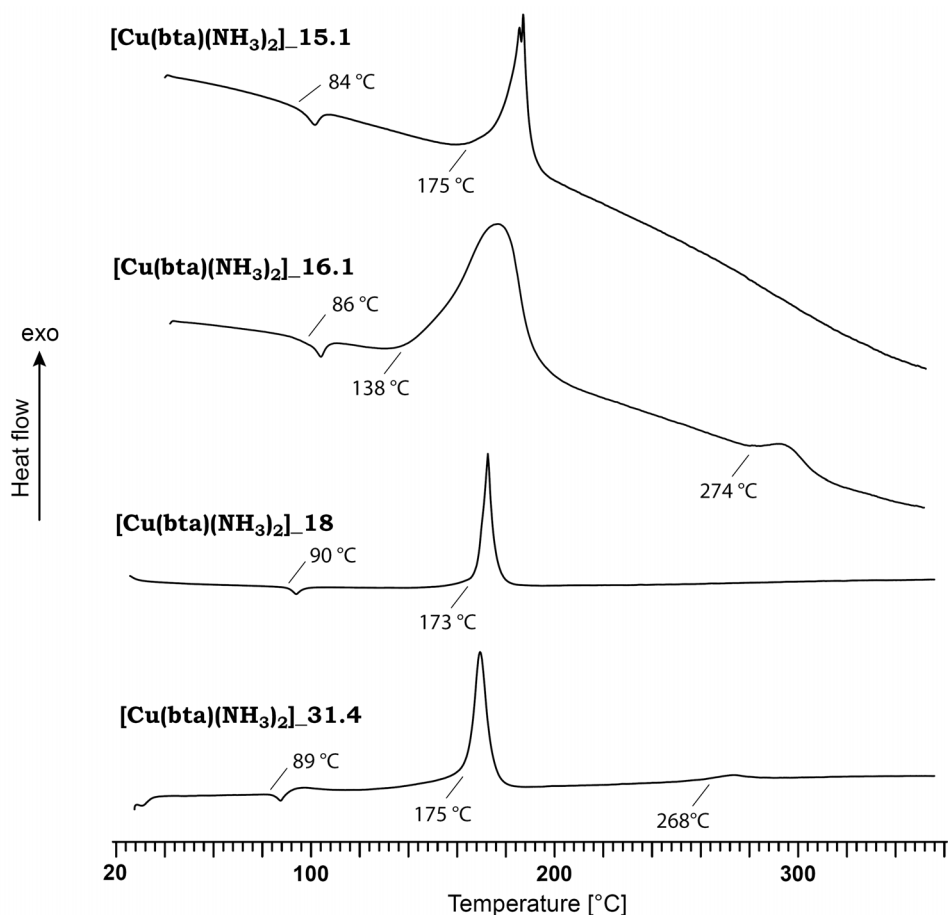


Figure 10.6 DSC thermograms of the pyrotechnic compositions **[Cu(bta)(NH₃)₂]_{15.1}**, **[Cu(bta)(NH₃)₂]_{16.1}**, **[Cu(bta)(NH₃)₂]₁₈**, and **[Cu(bta)(NH₃)₂]_{31.4}** in a temperature range of 20–350 °C. Decomposition points are given as onset temperatures.

Pyrotechnic composition **[Cu(bta)(NH₃)₂]_{31.4}** is made of 40 wt% **[Cu(bta)(NH₃)₂]**, 41 wt% ADN, 5 wt% boron, 5 wt% zinc, and 9 wt% VAAR (Table 10.34). It combusts with a pale green flame, analog to **[Cu(bta)(NH₃)₂]_{15.2}** and **[Cu(bta)(NH₃)₂]_{16.1}** (Figure 10.5). However, some sparks and glowing residues were observed. The combustion velocity is comparable to the one of **[Cu(bta)(NH₃)₂]₁₈**. **[Cu(bta)(NH₃)₂]_{31.4}** decomposes at 175 °C (Figure 10.6). Analog to the before mentioned compositions containing **[Cu(bta)(NH₃)₂]**, at 89 °C an endothermic signal and at 268 °C another exothermic signal can be observed. The sensitivities to impact, friction, and electric discharge were determined to 1.0 J, 96 N, and 0.2 J, respectively. All presented compositions of **[Cu(bta)(NH₃)₂]** are not sensitive to moisture, the addition of potassium aluminum sulfate dodecahydrate did not draw a distinction.

Although the oxygen balance of **[Cu(H₂bta)₂](NO₃)₂** is negative ($\Omega = -19\%$), it was only combined with the fuels boron and 5-aminotetrazole (**5-At**) and/or copper compounds **[Cu(bta)(NH₃)₂]** and copper(I) iodide. Nevertheless, some compositions reacted too heavily and lifted off or combust with a white- or yellow-green flame. The best performing composition is **[Cu(H₂bta)₂](NO₃)₂ 2.11**. It consists of 25 wt% **[Cu(H₂bta)₂](NO₃)₂**, 50 wt% **[Cu(bta)(NH₃)₂]**, 8 wt% boron, and 17 wt% VAAR (Table 10.44). **[Cu(H₂bta)₂](NO₃)₂ 2.11** is

easy to ignite and combusts fast with a very intense dark green flame (Figure 10.7). A small amount of smoke and long glowing residues were observed.



Figure 10.7 Burn down of the pyrotechnic composition $[\text{Cu}(\text{H}_2\text{bta})_2](\text{NO}_3)_2_{2.11}$.

$[\text{Cu}(\text{H}_2\text{bta})_2](\text{NO}_3)_2_{2.11}$ is very sensitive to impact (3.0 J), sensitive to friction (240 N), and electric discharge (0.40 J). The decomposition of $[\text{Cu}(\text{H}_2\text{bta})_2](\text{NO}_3)_2_{2.11}$ starts at 154 °C (Figure 10.8), further decomposition takes place at 278 °C. This is consistent with the decomposition temperatures of $[\text{Cu}(\text{H}_2\text{bta})_2](\text{NO}_3)_2$ and $[\text{Cu}(\text{bta})(\text{NH}_3)_2]$. The composition is stable to moisture.

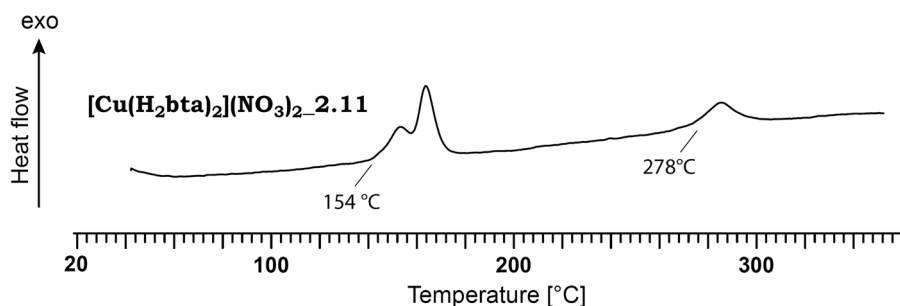


Figure 10.8 DSC thermogram of the pyrotechnic composition $[\text{Cu}(\text{H}_2\text{bta})_2](\text{NO}_3)_2_{2.11}$ in a temperature range of 40–350 °C. Decomposition points are given as onset temperatures.

The copper(II) complex $[\text{Cu}(\text{1MeAt})_2(\text{H}_2\text{O})_2(\text{NO}_3)_2]$ was combined with the oxidizers potassium nitrate and potassium permanganate, whose compositions either offered no green flame or were hard to ignite. Therefore, all other tested compositions contain no oxidizer despite the negative oxygen balance of $[\text{Cu}(\text{1MeAt})_2(\text{H}_2\text{O})_2(\text{NO}_3)_2]$ ($\Omega = -30\%$). Other additives were **5-At**, sulfur, boron, zinc, magnesium, magnalium, copper(I) oxide, $[\text{Cu}(\text{bta})(\text{NH}_3)_2]$, and $[\text{Cu}(\text{1MeAt})_4(\text{H}_2\text{O})_2(\text{NO}_3)_2]$. The composition with the best performance is $[\text{Cu}(\text{1MeAt})_2(\text{H}_2\text{O})_2(\text{NO}_3)_2]_{6.1}$, which is made of 72 wt% $[\text{Cu}(\text{1MeAt})_2(\text{H}_2\text{O})_2(\text{NO}_3)_2]$, 9 wt% boron, and 19 wt% VAAR (Table 10.52). It combusts fast with a pale green flame (Figure 10.9). No smoke, but some sparks and glowing residues were observed.



Figure 10.9 Burn down of the pyrotechnic composition $[\text{Cu}(\text{1MeAt})_2(\text{H}_2\text{O})_2(\text{NO}_3)_2]_{6.1}$.

$[\text{Cu}(\text{1MeAt})_2(\text{H}_2\text{O})_2(\text{NO}_3)_2]_{6.1}$ is very sensitive to impact (1.5 J), although neat $[\text{Cu}(\text{1MeAt})_2(\text{H}_2\text{O})_2(\text{NO}_3)_2]$ is insensitive to impact. The sensitivity to friction was determined to 108 N and electric discharge to 1.1 J. Unfortunately, $[\text{Cu}(\text{1MeAt})_2(\text{H}_2\text{O})_2(\text{NO}_3)_2]_{6.1}$ decomposes at temperatures above 119 °C (Figure 10.10). At 218 °C further decomposition takes place. No sensitivity to moisture was observed.

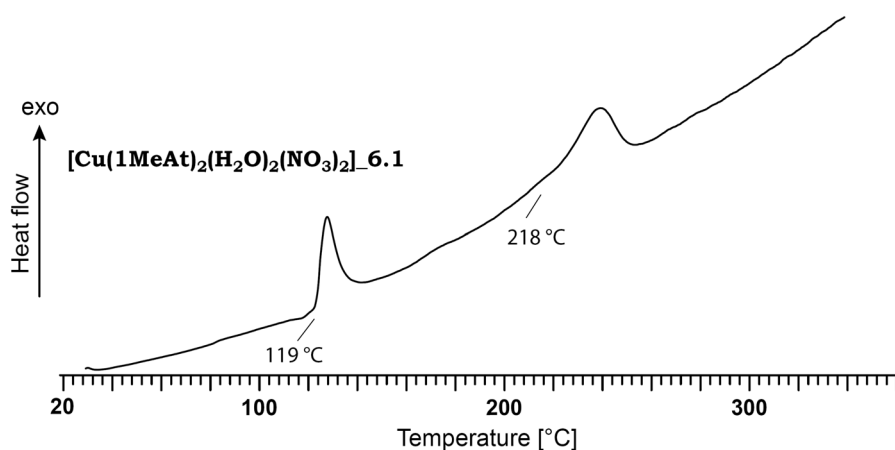


Figure 10.10 DSC thermogram of the pyrotechnic composition $[\text{Cu}(\text{1MeAt})_2(\text{H}_2\text{O})_2(\text{NO}_3)_2]_{6.1}$ in a temperature range of 30–350 °C. Decomposition points are given as onset temperatures.

A comparable composition was prepared with $[\text{Cu}(\text{1MeAt})_4(\text{H}_2\text{O})_2](\text{NO}_3)_2$, consisting of 86 wt% $[\text{Cu}(\text{1MeAt})_4(\text{H}_2\text{O})_2](\text{NO}_3)_2$, 5 wt% boron, and 9 wt% VAAR (Table 10.59). The composition $[\text{Cu}(\text{1MeAt})_4(\text{H}_2\text{O})_2](\text{NO}_3)_2_{1.6}$ combusts with a dark green flame, which changes in the end into yellow (Figure 10.11). The combustion velocity is lower than the one of $[\text{Cu}(\text{1MeAt})_2(\text{H}_2\text{O})_2(\text{NO}_3)_2]_{6.1}$. No smoke and only a small amount of black solid residues were observed.



Figure 10.11 Burn down of the pyrotechnic composition $[\text{Cu}(\text{1MeAt})_2(\text{H}_2\text{O})_2](\text{NO}_3)_2_{1.6}$.

$[\text{Cu}(\text{1MeAt})_4(\text{H}_2\text{O})_2](\text{NO}_3)_2_{1.6}$ is sensitive to impact (6.0 J) and electric discharge (1.1 J), but insensitive to friction (> 360 N). Compared to $[\text{Cu}(\text{1MeAt})_2(\text{H}_2\text{O})_2](\text{NO}_3)_2_{6.1}$ it is less sensitive. Again, decomposition occurs at very low temperatures ($T_{\text{dec}} = 109\text{ }^\circ\text{C}$). Two further decompositions can be observed at $163\text{ }^\circ\text{C}$ and $225\text{ }^\circ\text{C}$ (Figure 10.12). $[\text{Cu}(\text{1MeAt})_4(\text{H}_2\text{O})_2](\text{NO}_3)_2_{1.6}$ is stable to moisture.

$[\text{Cu}(\text{1MeAt})_4(\text{H}_2\text{O})_2](\text{NO}_3)_2$ was, besides boron, mixed with the compounds sulfur, copper(I) iodide, $[\text{Cu}(\text{bta})(\text{NH}_3)_2]$ and $[\text{Cu}(\text{1MeAt})_2(\text{H}_2\text{O})_2](\text{NO}_3)_2$. With these combinations the flame color was rather white or yellow than green. Despite its negative oxygen balance ($\Omega = -54\%$), no additionally use of oxidizers was necessary. All prepared compositions could be ignited.

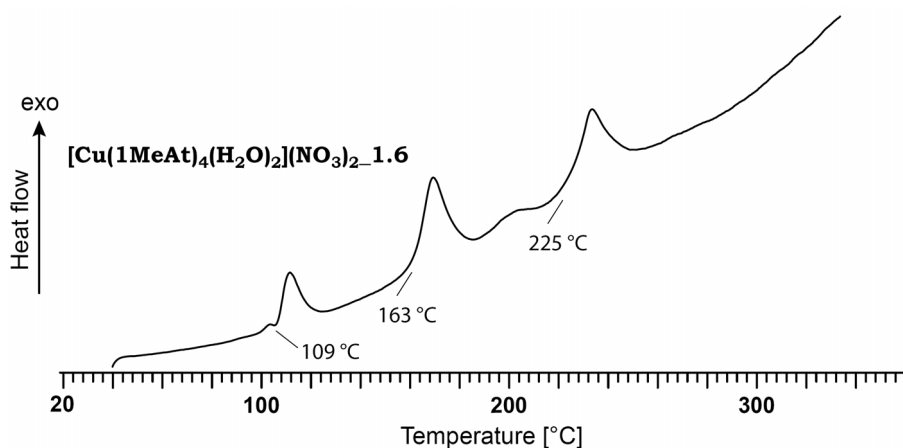


Figure 10.12 DSC thermogram of the pyrotechnic composition $[\text{Cu}(\text{1MeAt})_4(\text{H}_2\text{O})_2](\text{NO}_3)_2_{1.6}$ in a temperature range of 40–350 °C. Decomposition points are given as onset temperatures.

The copper(II) ammine complex $[\text{Cu}(\text{1MeAtNO}_2)_2(\text{NH}_3)_2]$ was combined with fuels boron, **5-At**, 5-aminotetrazole monohydrate (**5-At**·H₂O) and the copper compounds copper(I) iodide, $[\text{Cu}(\text{bta})(\text{NH}_3)_2]$ and tetraaqua 3,3'-bis(1,2,4-oxadiazol-5-onate) copper(II) ($[\text{Cu}(\text{H}_2\text{O})_4(\text{OD})]$). The best performing composition $[\text{Cu}(\text{1MeAtNO}_2)_2(\text{NH}_3)_2]_{1.3}$ consists of 60 wt% $[\text{Cu}(\text{1MeAtNO}_2)_2(\text{NH}_3)_2]$, 30 wt% **5-At**, and 10 wt% VAAR (Table 10.64). It combusts

with a small green, partly yellow, flame with red seam (Figure 10.13). The combustion velocity is slow, but no smoke and a very small amount of solid residues were observed.

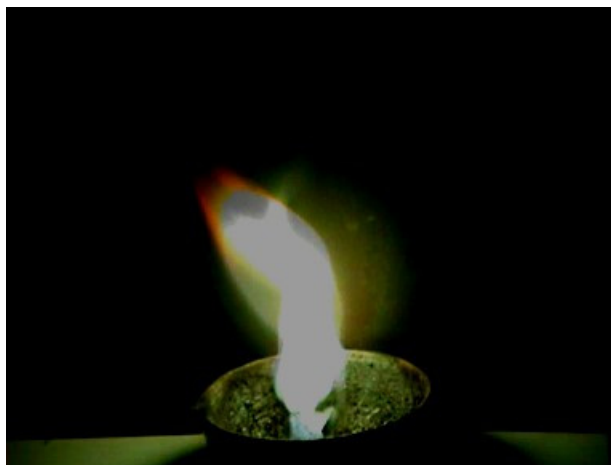


Figure 10.13 Burn down of the pyrotechnic composition $[\text{Cu}(\text{1MeAtNO}_2)_2(\text{NH}_3)_2]_{1.3}$.

The composition is sensitive to impact (10 J), friction (120 N), and electric discharge (0.3 J). Its decomposition temperature of 196 °C is quite high (Figure 10.14). No sensitivity to moisture could be observed.

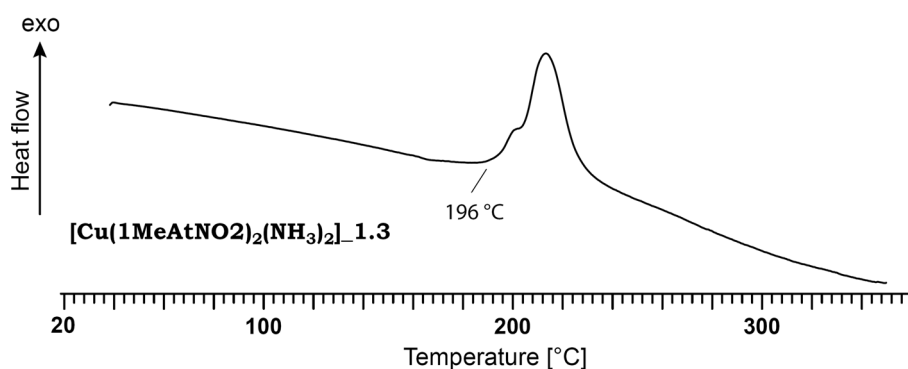


Figure 10.14 DSC thermogram of the pyrotechnic composition $[\text{Cu}(\text{1MeAtNO}_2)_2(\text{NH}_3)_2]_{1.3}$ in a temperature range of 30–350 °C. Decomposition points are given as onset temperatures.

The copper(II) ammine complex of 5-nitriminotetrazole (H_2AtNO_2), $[\text{Cu}(\text{AtNO}_2)(\text{NH}_3)_3]_2$, was mixed with **5-At**, boron, and magnesium. Analog to the strontium salts of H_2AtNO_2 (see chapter 9), it was hard to find a composition, which could be ignited. The best performing composition, $[\text{Cu}(\text{AtNO}_2)(\text{NH}_3)_3]_2_{1.1}$ (52 wt% $[\text{Cu}(\text{AtNO}_2)(\text{NH}_3)_3]_2$, 39 wt% **5-At**, 9 wt% VAAR, Table 10.70), combusts with a white-green flame (Figure 10.15). However, the burning is not continuous, several ignitions with a lighter are necessary. Furthermore, some smoke and glowing residues were observed.



Figure 10.15 Burn down of the pyrotechnic composition $[\text{Cu}(\text{AtNO}_2)(\text{NH}_3)_3]_2_{1.1}$.

$[\text{Cu}(\text{AtNO}_2)(\text{NH}_3)_3]_2_{1.1}$ is sensitive to impact (5.0 J), less sensitive to friction (360 N), and electric discharge (0.5 J). The composition is stable to moisture. Decomposition of $[\text{Cu}(\text{AtNO}_2)(\text{NH}_3)_3]_2_{1.1}$ occurs at temperatures above 204 °C (Figure 10.16). At 249 °C another exothermic signal can be observed, this is in accord with the decomposition temperature of neat $[\text{Cu}(\text{AtNO}_2)(\text{NH}_3)_3]_2$.

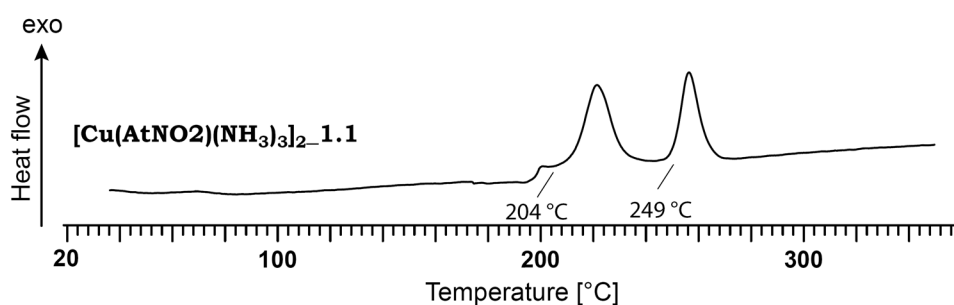


Figure 10.16 DSC thermogram of the pyrotechnic composition $[\text{Cu}(\text{AtNO}_2)(\text{NH}_3)_3]_2_{1.1}$ in a temperature range of 30–350 °C. Decomposition points are given as onset temperatures.

Due to the fact, that basic copper(II) nitrate $\text{Cu}_2(\text{OH})_3(\text{NO}_3)$ produces in combination with nitrogen-rich molecules much smoke,^[14] it was mixed with the fuels magnesium, magnalium, sulfur, aluminum, boron, titanium, and silicon. To verify the smoke production with nitrogen-rich molecules, test compositions with **5-At** were prepared. All offered no flame, however glowed generating much smoke (Table 10.73). Most of the investigated compositions could not be ignited or offered yellow or white flames. The best fuel was magnesium. The pyrotechnic composition $\text{Cu}_2(\text{OH})_3(\text{NO}_3)_{2.1}$ consists of 77 wt% $\text{Cu}_2(\text{OH})_3(\text{NO}_3)$, 8 wt% Mg, and 15 wt% VAAR (Table 10.74). Although the composition is hard to ignite, it combusts with a green flame (Figure 10.17). No smoke, but some sparks and glowing residues were observed. The combustion velocity is quite low. $\text{Cu}_2(\text{OH})_3(\text{NO}_3)_{2.1}$ is stable to moisture.



Figure 10.17 Burn down of the pyrotechnic composition $\text{Cu}_2(\text{OH})_3(\text{NO}_3)_2$.

The sensitivities of $\text{Cu}_2(\text{OH})_3(\text{NO}_3)_2$ to impact, friction, and electric discharge were determined with 10 J, 360 N, and 0.3 J, respectively. The DSC thermogram shows a very broad decomposition, starting at 201 °C (Figure 10.18).

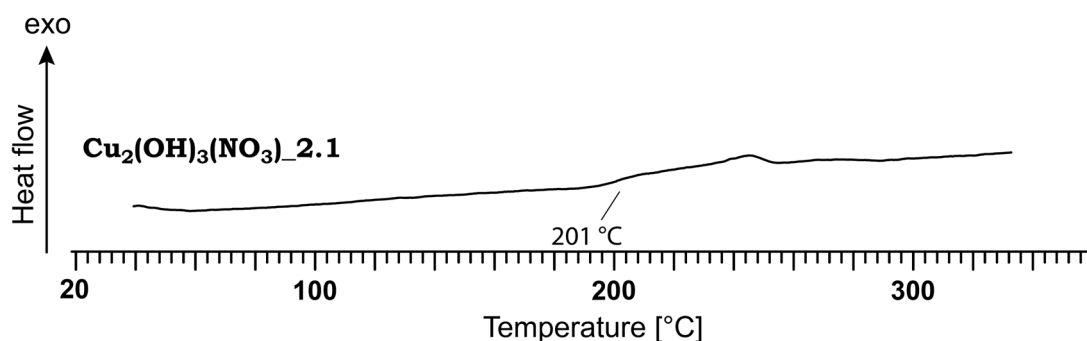


Figure 10.18 DSC thermogram of the pyrotechnic composition $\text{Cu}_2(\text{OH})_3(\text{NO}_3)_2$ in a temperature range of 40–350 °C. Decomposition points are given as onset temperatures.

Tetrammine copper(II) dinitramide ($[\text{Cu}(\text{NH}_3)_4][\text{N}(\text{NO}_2)_2]_2$) was combined with the fuels **5-At**, **5-At_H₂O**, boron, magnesium, and sulfur. The copper(II) compounds copper(II) sulfate pentahydrate, basic copper(II) nitrate, $[\text{Cu}(\text{bta})(\text{NH}_3)_2]$, and $[\text{Cu}(\text{1MeAt})_2(\text{H}_2\text{O})_2(\text{NO}_3)_2]$ were added. Due to its positive oxygen balance ($\Omega = +5\%$), the use of oxidizers was not necessary. The pyrotechnic composition $[\text{Cu}(\text{NH}_3)_4][\text{N}(\text{NO}_2)_2]_2$ 9.3 consists of 77 wt% $[\text{Cu}(\text{NH}_3)_4][\text{N}(\text{NO}_2)_2]_2$, 13 wt% boron, 1 wt% urea, and 9 wt% VAAR (Table 10.89). Urea was added to increase the thermal stability. The composition is very easy to ignite and combusts with a green flame (Figure 10.19). Some red-glowing sparks, but almost no smoke could be observed. A disadvantage is the black solid residue, which moreover glows for a few seconds. $[\text{Cu}(\text{NH}_3)_4][\text{N}(\text{NO}_2)_2]_2$ 9.3 is very sensitive to impact (2.0 J), and sensitive to friction (109 N) and electric discharge (1.0 J). Despite adding of urea the compositions decomposes at 191 °C (Figure 10.20).

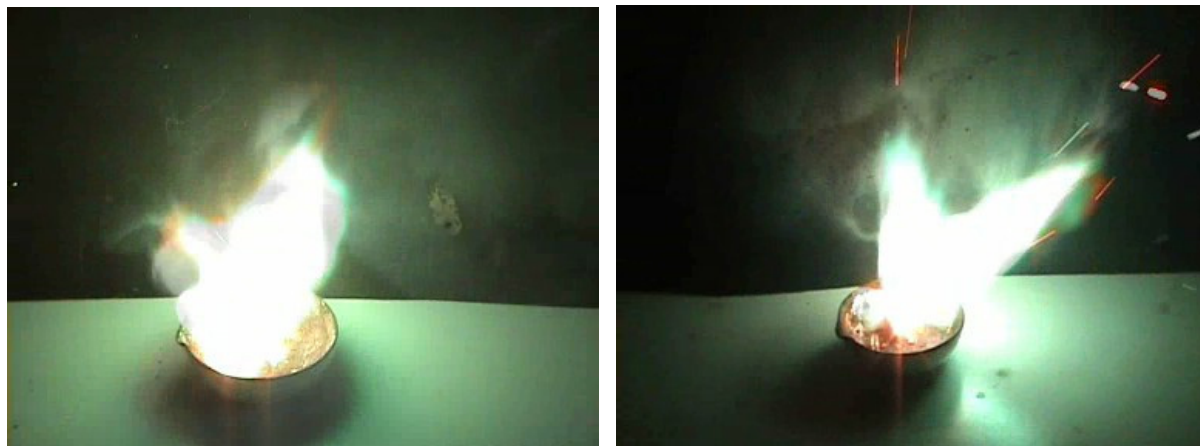


Figure 10.19 Burn down of the compositions $[\text{Cu}(\text{NH}_3)_4][\text{N}(\text{NO}_2)_2]_2$ _9.3 (left) and $[\text{Cu}(\text{NH}_3)_4][\text{N}(\text{NO}_2)_2]_2$ _9.9 (right).

For comparison, an analogue composition ($[\text{Cu}(\text{NH}_3)_4][\text{N}(\text{NO}_2)_2]_2$ _9.9) without urea was prepared: 77 wt% $[\text{Cu}(\text{NH}_3)_4][\text{N}(\text{NO}_2)_2]_2$, 13 wt% boron, and 10 wt% VAAR (Figure 10.19). The combustion behavior is identical, whereas the combustion velocity of $[\text{Cu}(\text{NH}_3)_4][\text{N}(\text{NO}_2)_2]_2$ _9.9 is slightly higher. Its decomposition point of 191 °C leads to the assumption, that adding 1 wt% urea has no effect on the thermal stability (Figure 10.20). However, it decreases the sensitivities. $[\text{Cu}(\text{NH}_3)_4][\text{N}(\text{NO}_2)_2]_2$ _9.9 is very sensitive to impact (1.0 J) and friction (56 N), whereas the sensitivity of $[\text{Cu}(\text{NH}_3)_4][\text{N}(\text{NO}_2)_2]_2$ _9.3 to electric discharge is lower (2.5 J). Both, $[\text{Cu}(\text{NH}_3)_4][\text{N}(\text{NO}_2)_2]_2$ _9.3 and $[\text{Cu}(\text{NH}_3)_4][\text{N}(\text{NO}_2)_2]_2$ _9.9, are stable to moisture.

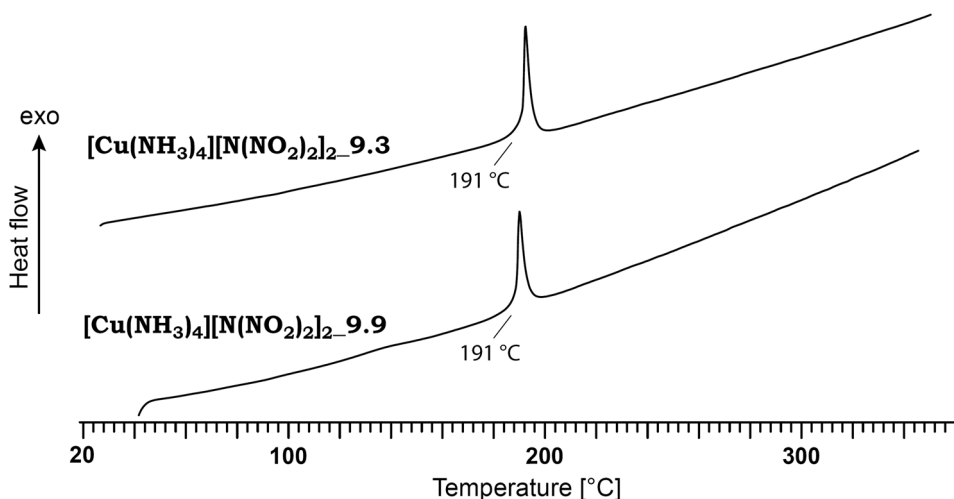


Figure 10.20 DSC thermograms of the pyrotechnic compositions $[\text{Cu}(\text{NH}_3)_4][\text{N}(\text{NO}_2)_2]_2$ _9.3 and $[\text{Cu}(\text{NH}_3)_4][\text{N}(\text{NO}_2)_2]_2$ _9.9 in a temperature range of 30–350 °C. Decomposition points are given as onset temperatures.

$[\text{Cu}(\text{NH}_3)_4][\text{N}(\text{NO}_2)_2]_2$ was also combined with the copper(II) compound $[\text{Cu}(\text{bta})(\text{NH}_3)_2]$ and boron. Composition $[\text{Cu}(\text{NH}_3)_4][\text{N}(\text{NO}_2)_2]_2$ _16.4 consists of 64 wt% $[\text{Cu}(\text{NH}_3)_4][\text{N}(\text{NO}_2)_2]_2$, 18 wt% $[\text{Cu}(\text{bta})(\text{NH}_3)_2]$, 9 wt% boron, and 9 wt% VAAR (Table 10.96). It combusts very fast

with an intense green flame and without any smoke (Figure 10.21). Again glowing residues were observed.



Figure 10.21 Burn down of the composition $[\text{Cu}(\text{NH}_3)_4][\text{N}(\text{NO}_2)_2]_2_{16.4}$.

The decomposition temperature of 192 °C is comparable to the compositions $[\text{Cu}(\text{NH}_3)_4][\text{N}(\text{NO}_2)_2]_2_{9.3}$ and $[\text{Cu}(\text{NH}_3)_4][\text{N}(\text{NO}_2)_2]_2_{9.9}$ and can be explained by the decomposition temperature of $[\text{Cu}(\text{NH}_3)_4][\text{N}(\text{NO}_2)_2]_2$ ($T_{\text{dec}} = 183$ °C). At temperatures above 255 °C further decomposition takes place (Figure 10.22), presumably due to a starting decomposition of $[\text{Cu}(\text{bta})(\text{NH}_3)_2]$ ($T_{\text{dec}} = 281$ °C). This can occur in pyrotechnic compositions, which are mixtures of several components. $[\text{Cu}(\text{NH}_3)_4][\text{N}(\text{NO}_2)_2]_2_{16.4}$ is very sensitive to impact (1.0 J), sensitive to friction (120 N), and electric discharge (0.60 J).

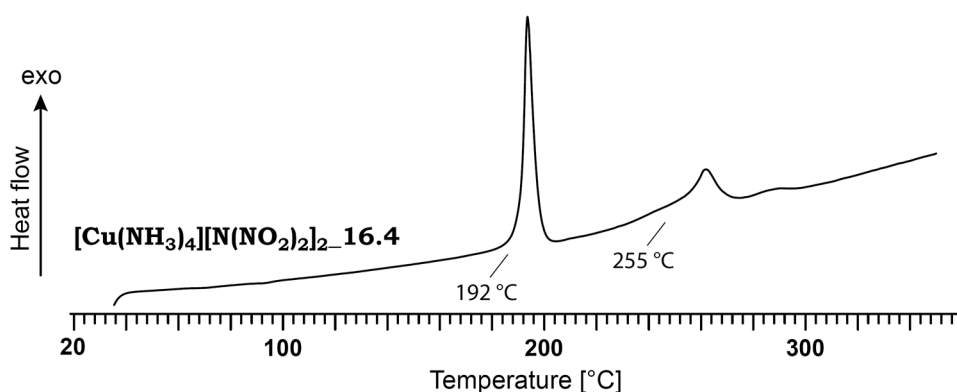


Figure 10.22 DSC thermogram of the pyrotechnic composition $[\text{Cu}(\text{NH}_3)_4][\text{N}(\text{NO}_2)_2]_2_{16.4}$ in a temperature range of 30–350 °C. Decomposition points are given as onset temperatures.

Copper(I) iodide was added to some pyrotechnic compositions (see Table 10.45, Table 10.53, Table 10.60, and Table 10.67) to intensify the emitted green light. It was selected, because of its high melting point (588 °C), high density (5.62 g/cm³ at 20 °C), and extremely low solubility in H₂O (< 8·10⁻³ wt% at 18 °C).^[22] Furthermore, it emits green light in the flame of a BUNSEN burner (Figure 10.23). Besides that, the copper(I) ion can both be oxidized and reduced.



Figure 10.23 Flame color of CuI in the flame of a BUNSEN burner.

The pyrotechnic composition **CuI_1**, containing CuI (10 wt%) as coloring agent, ammonium nitrate (58 wt%) as oxidizer, boron (25 wt%) as fuel, and VAAR (7 wt%), is easy to ignite and combusts slowly with a blue-green flame (Figure 10.24). Some smoke and a huge amount of black solid residues were observed.



Figure 10.24 Burn down of the pyrotechnic composition **CuI_1**.

CuI_1 is sensitive to impact (5.0 J) and electric discharge (0.5 J). No sensitivity to friction could be observed. In the DSC thermogram, two endothermic signals at 127 °C and 168 °C can be observed, before the composition starts to decompose at 232 °C (Figure 10.25). This is consistent with the phase transitions of ammonium nitrate.^[23]

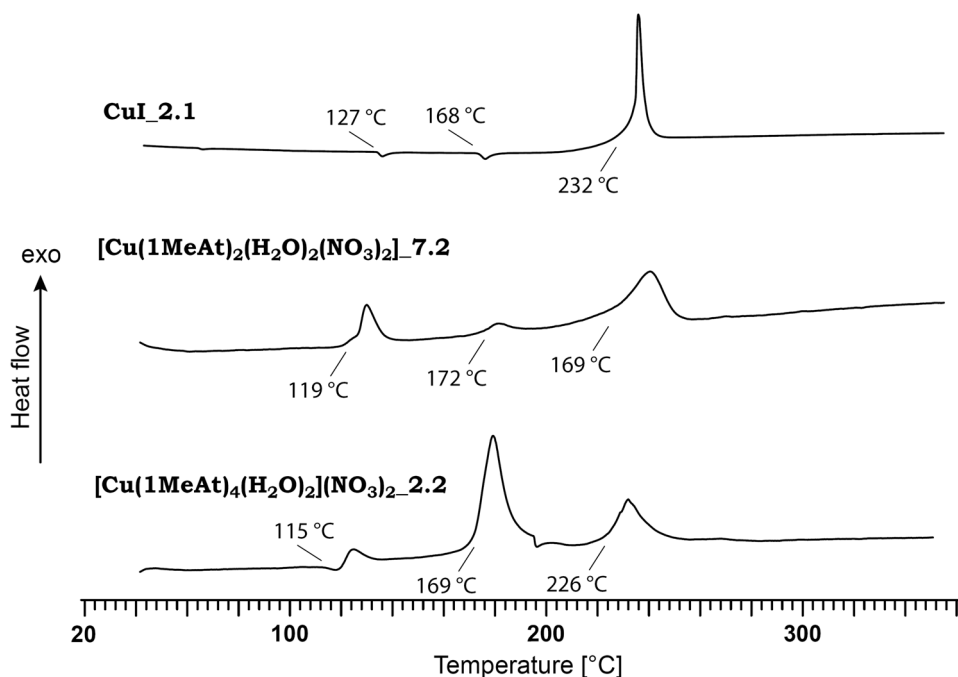


Figure 10.25 DSC thermogram of the pyrotechnic compositions **CuI_1**, **[Cu(1MeAt)₂(H₂O)₂(NO₃)₂]_{7.2}**, and **[Cu(1MeAt)₄(H₂O)₂](NO₃)₂_{2.2}** in a temperature range of 40–350 °C. Decomposition points are given as onset temperatures.

To two pyrotechnic compositions, containing the same components as **[Cu(1MeAt)₂(H₂O)₂(NO₃)₂]_{6.1}**, some copper(I) iodide was added to improve the green flame color (Table 10.53). The composition containing 5 wt% copper(I) iodide offers a green-blue flame. However, the composition **[Cu(1MeAt)₂(H₂O)₂(NO₃)₂]_{7.2}**, made of 68 wt% **[Cu(1MeAt)₂(H₂O)₂(NO₃)₂]**, 10 wt% boron, 6 wt% copper(I) iodide, and 16 wt% VAAR, combusts with a pale green flame (Figure 10.26). Compared to **[Cu(1MeAt)₂(H₂O)₂(NO₃)₂]_{6.1}**, the color performance is worse (Figure 10.9). Furthermore, during the combustion of **[Cu(1MeAt)₂(H₂O)₂(NO₃)₂]_{7.2}** some smoke and glowing residues were observed. The additional copper(I) iodide has no effect on the decomposition temperature of 119 °C (Figure 10.25). However, the sensitivity to impact and friction is decreased ($E_{\text{dr}} = 3.0 \text{ J}$, $F_{\text{r}} > 360 \text{ N}$). **[Cu(1MeAt)₂(H₂O)₂(NO₃)₂]_{7.2}** is more sensitive to electric discharge with 0.50 J.



Figure 10.26 Burn down of the pyrotechnic compositions $[\text{Cu}(\text{1MeAt})_2(\text{H}_2\text{O})_2(\text{NO}_3)_2]_{7.2}$ (left) and $[\text{Cu}(\text{1MeAt})_2(\text{H}_2\text{O})_2(\text{NO}_3)_2]_{2.2}$ (right).

In contrast to these results, the color performance of an analog composition of $[\text{Cu}(\text{1MeAt})_4(\text{H}_2\text{O})_2(\text{NO}_3)_2]_{1.6}$ could be improved by adding copper(I) iodide (Figure 10.11). The resulted flame offers more blue character, whereas the emitted light is more intense (Figure 10.26). $[\text{Cu}(\text{1MeAt})_4(\text{H}_2\text{O})_2(\text{NO}_3)_2]_{2.2}$ consists of 81 wt% $[\text{Cu}(\text{1MeAt})_4(\text{H}_2\text{O})_2(\text{NO}_3)_2$, 5 wt% boron, 4 wt% copper(I) iodide, and 10 wt% VAAR (Table 10.60). The decomposition temperature is slightly higher with 115 °C (Figure 10.25). The sensitivities to impact (5.0 J), friction (240 N) and electric discharge (0.30 J) are comparable to the ones of $[\text{Cu}(\text{1MeAt})_4(\text{H}_2\text{O})_2(\text{NO}_3)_2]_{1.6}$.

Concluding can be said, the adding of copper(I) iodide can improve the color performance, whereas the amount must be very low (≤ 5 wt%) to avoid a white or blue flame.

Analog to the strontium salts (see chapter 9), a static burn test with $[\text{Cu}(\text{bta})(\text{NH}_3)_2]$, $[\text{Cu}(\text{1MeAt})_2(\text{H}_2\text{O})_2(\text{NO}_3)_2]$, and $[\text{Cu}(\text{1MeAt})_4(\text{H}_2\text{O})_2(\text{NO}_3)_2]$ was performed. Therefore, the copper(II) compounds were formulated with magnesium powder and polyester/styrene binder, leaving the ratio unchanged.^[24] The dry ingredients were sieved through a 10-mesh screen and dried prior to mixing in a ceramic bowl. The final dry mixes were pressed to 1.27 cm pellets, each with approx. 6 g. The pellets were consolidated in a die with two increments at a loading pressure of 6000 psi (41.3 MPa). The US Army pyrotechnic composition # M195 (46 wt% barium nitrate, 27 wt% magnesium, 10 wt% potassium perchlorate, and 4.5 wt% binder) was used as control. The current M125 A1 igniter slurry (aluminum, silicon, charcoal, potassium nitrate, iron oxide, and nitrocellulose) was applied on top of the pellets.

Static burn test on the experimental pellets was conducted in a blackened light tunnel. The samples were placed 50 ft (15.24 m) from the measurement equipment and initiated with an electric match. Color was measured with an *Ocean Optics* HR2000 spectrometer after calibration. Color measurements were based on the 1931 CIE (*Commission Internationale d'Eclairage*) international standard and calculated using the *Ocean Optics* Spectra-suite software. The CIE chart displays all the chromaticities average

human eyes can observe. The three values calculated based on the CIE color matching functions are referred to X, Y and Z. The dominant wavelength (DW) and excitation purity (%) for a test sample were numerically determined with respect to the coordinates of Illuminant C, an established light source. The luminous intensity was measured using an *International Light SEL033* silicon detector coupled to a photopic filter and lens hood. At least seven pellets of each compound were investigated.

Results of the static burn test for **[Cu(bta)(NH₃)₂]**, **[Cu(1MeAt)₂(H₂O)₂(NO₃)₂]**, and **[Cu(1MeAt)₄(H₂O)₂](NO₃)₂** formulated pellets as well as the perchlorate-based control pellets^[25] are shown in Table 10.3.

Table 10.3 Experimental pellets performance data.

Compound	[Cu(bta)(NH₃)₂]	[Cu(1MeAt)₂(H₂O)₂(NO₃)₂]	[Cu(1MeAt)₄(H₂O)₂](NO₃)₂	Control
burn time [s]	36.4	31.1	34.3	43.3
average intensity [cd]	114.5	136.1	110.9	170.8
integrated intensity [cd·s]	4062	3922.2	3709.3	6536.7
peak intensity [cd]	954.7	838.1	869.5	1568.5
dominant wavelength [nm]	551	555–561	556–560	548–564
spectral purity [%]	65.7	56–68	37–64	63.2

[Cu(1MeAt)₂(H₂O)₂(NO₃)₂] offers the shortest burn time, whereas all tested compounds combust faster than the control. The burn time average intensity of all tested copper(II) compounds is lower than the control's one. This is true for the integrated intensity. The peak intensity of the control is nearly twice than the other ones. The measured dominant wavelengths are all in the same range. The spectral purity of the **[Cu(bta)(NH₃)₂]** based pellets is comparable to the control, whereas it varied over a huge range.

The representative still images captured from the static burn tests are depicted in Figure 10.27.

The images suggest no significant difference among the sample groups in flame size. However, the compounds **[Cu(1MeAt)₂(H₂O)₂(NO₃)₂]** and **[Cu(1MeAt)₄(H₂O)₂](NO₃)₂** offer a different green compared to the control and **[Cu(bta)(NH₃)₂]**.

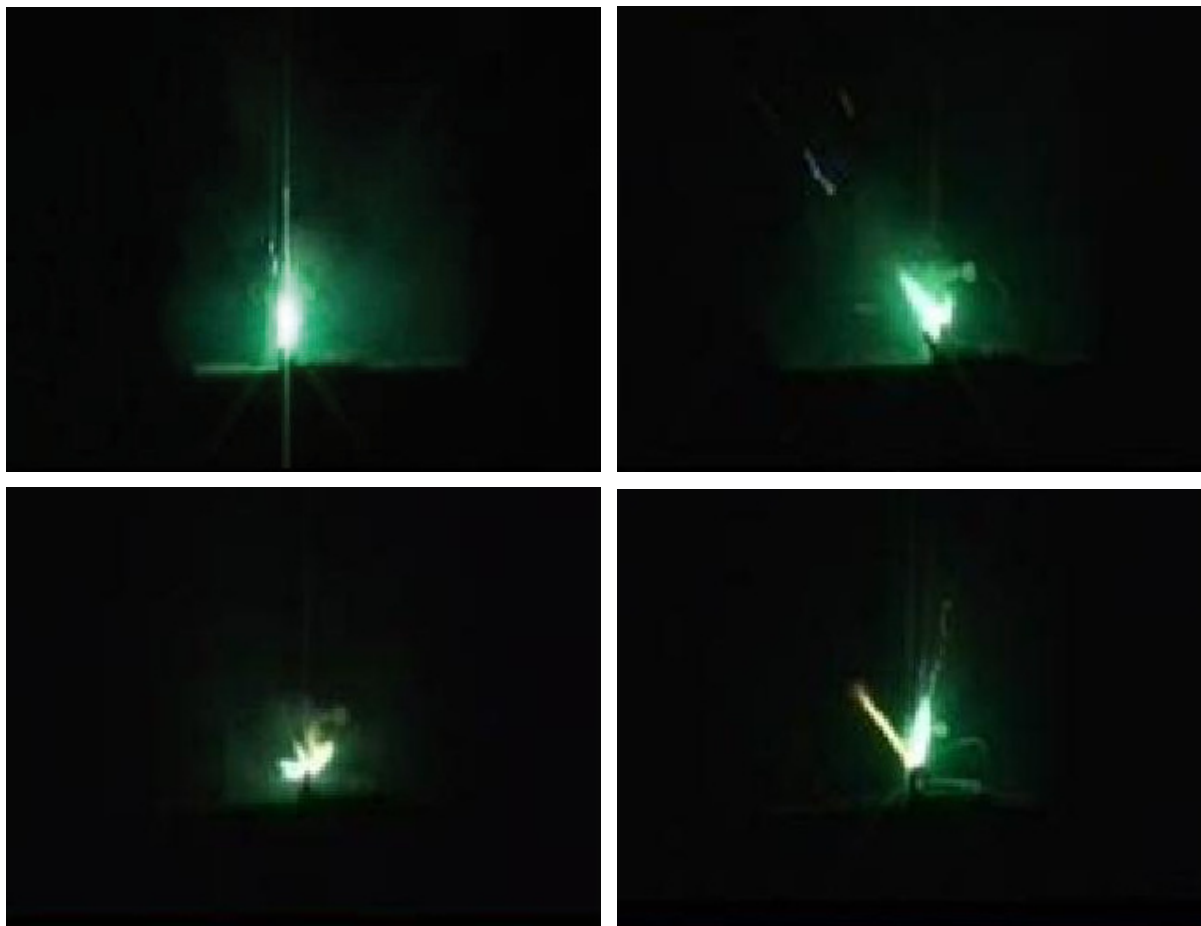


Figure 10.27 Static burn test of M195 A1 (top, left), $[\text{Cu}(\text{bta})(\text{NH}_3)_2]$ (top, right), $[\text{Cu}(\text{1MeAt})_2(\text{H}_2\text{O})_2(\text{NO}_3)_2]$ (down, left), and $[\text{Cu}(\text{1MeAt})_4(\text{H}_2\text{O})_2](\text{NO}_3)_2$ (down, right).

10.2 Experimental Part

10.2.1 Preparation of the Copper Compounds

*CAUTION! The copper compounds as well as their pyrotechnic compositions are sensitive to impact, friction, and electric discharge. Therefore, proper protective measures (safety glasses, face shield, leather coat, earthed equipment and shoes, Kevlar[®] gloves, and ear plugs) should be used, especially during work on the precursor molecules ADN, 1-methyl-5-nitriminotetrazole (**H1MeAtNO2**), ammonium 1-methyl-5-nitriminotetrazolate, and 5-nitriminotetrazole (**H2AtNO2**).*

Diammine bis(tetrazol-5-yl)-aminato- $\kappa^2\text{N1,N6}$ copper(II) ($[\text{Cu}(\text{bta})(\text{NH}_3)_2]$): Preparation according to the literature.^[1, 2] Yield: 95 %.

M.p. 281 °C (dec., DSC-measurement, 5 K/min).

IR (Diamond-ATR, cm^{-1}): 3373 (w), 3321 (s), 3254 (m), 3127 (m), 3053 (m), 2915 (m), 2826 (w), 2656 (vw), 1612 (vs), 1545 (s), 1497 (vs), 1463 (w), 1445 (m), 1327 (w), 1232 (s),

1161 (vw), 1141 (vw), 1123 (w), 1116 (vw), 1017 (vw), 853 (vw), 806 (vw), 746 (m), 723 (m), 675 (w), 620 (vw).

Elemental analysis C₂H₇CuN₁₁ (248.70 g/mol): calc.: C, 9.66; H, 2.84; N, 61.95; found: C, 9.79; H, 3.00; N, 61.40.

E_{dr} > 100 J (< 100 μm).

F_r > 360 N (< 100 μm).

E_{el} = 0.70 J (< 100 μm).

H₂O-sol. 1.5 wt% (22 °C).

Bis[bis(tetrazol-5-yl)-amine-κ²N1,N6} copper(II) nitrate hemihydrate ([Cu(H₂bta)₂](NO₃)₂):

Preparation according to the literature.^[2, 3] Yield: 52 %.

M.p. 156 °C (dec., DSC-measurement, 5 K/min).

IR (Diamond-ATR, cm⁻¹): 3446 (vw), 3251 (w), 3151 (w), 3029 (w), 2781 (w), 2671 (w), 2449 (w), 1647 (s), 1614 (s), 1553 (s), 1506 (m), 1466 (s), 1396 (m), 1306 (s), 1269 (s), 1161 (m), 1133 (m), 1054 (s), 1040 (s), 1034 (s), 1018 (s), 993 (m), 825 (m), 815 (s), 711 (s), 703 (s), 666 (s), 634 (s).

Elemental analysis C₄H₇CuN₂₀O_{6.5} (502.78 g/mol): calc.: C, 9.56; H, 1.40; N, 55.75; found: C, 9.39; H, 1.12; N, 54.88.

E_{dr} = 3.5 J (> 1000 μm).

F_r = 196 N (> 1000 μm).

E_{el} = 0.10 J (> 1000 μm).

H₂O-sol. < 0.4 wt% (21 °C).

Diaqua bis(1-methyl-5-aminotetrazole-N4) copper(II) nitrate ([Cu(1MeAt)₂(H₂O)₂](NO₃)₂):

Preparation according to the literature.^[4, 5] Yield: 61 %.

M.p. 142 °C (dec., DSC-measurement, 5 K/min).

IR (Diamond-ATR, cm⁻¹): 3456 (w), 3398 (s), 3314 (m), 3261 (m), 3203 (m), 3166 (s), 2443 (vw), 1760 (vw), 1647 (m), 1597 (w), 1497 (w), 1420 (m), 1326 (s), 1236 (w), 1139 (w), 1079 (w), 1050 (w), 983 (vw), 817 (w), 784 (w), 739 (vw), 718 (vw), 688 (w).

Elemental analysis C₄H₁₄CuN₁₂O₈ (421.78 g/mol): calc.: C, 11.39; H, 3.35; N, 39.85; found: C, 11.24; H, 3.29; N, 39.25.

E_{dr} > 30 J (500–1000 μm).

F_r = 196 N (500–1000 μm).

E_{el} > 2.0 J (500–1000 μm).

H₂O-sol. 13 wt% (22 °C).

Diaqua tetrakis(1-methyl-5-aminotetrazole-N4) copper(II) nitrate

[(Cu(1MeAt)₄(H₂O)₂](NO₃)₂]: Preparation according to the literature.^[4, 5] Yield: 56 %.

M.p. 168 °C (dec., DSC-measurement, 5 K/min).

IR (Diamond-ATR, cm⁻¹): 3484 (m), 3402 (s), 3308 (m), 3256 (m), 3194 (s), 3152 (s), 1641 (s), 1597 (w), 1497 (m), 1461 (w), 1399 (m), 1348 (m), 1316 (s), 1132 (w), 1071 (w), 1053 (w), 1040 (w), 982 (vw), 828 (vw), 787 (w), 733 (vw), 678 (vw).

Elemental analysis C₈H₂₄CuN₂₂O₈ (619.97 g/mol): calc.: C, 15.50; H, 3.90; N, 49.70; found: C, 15.42; H, 3.82; N, 49.57.

E_{dr} > 30 J (500–1000 μm).

F_r = 120 N (500–1000 μm).

E_{el} > 2.0 J (500–1000 μm).

H₂O-sol. 8.8 wt% (22 °C).

Diammine bis(1-methyl-5-nitriminotetrazolato-κ²N4,O1) copper(II)

[(Cu(1MeAtNO₂)₂(NH₃)₂)]:

Preparation analog to the literature.^[6, 7] A solution of 3.22 g (20 mmol) ammonium 1-methyl-5-nitriminotetrazolate in 40 mL 12 % aqueous ammonia solution and a solution of 2.33 g (10 mmol) copper(II) nitrate pentahemihydrate in 10 mL H₂O were combined at 80 °C. The deep blue mixture was cooled down to ambient temperature and stored until deep blue crystal blocks were formed. They were filtered off and dried on air. Yield: 56 %.

M.p. 242 °C (dec., DSC-measurement, 5 K/min).

Raman (200 mW, 25 °C, cm⁻¹): 3270 (12), 3192 (15), 3012 (9), 2965 (27), 1516 (90), 1475 (30), 1415 (17), 1327 (47), 1245 (10), 1122 (21), 1030 (49), 879 (14), 758 (19), 687 (14), 499 (22), 409 (15), 293 (14), 185 (16).

IR (Diamond-ATR, cm⁻¹): 3327 (s), 3311 (s), 3240 (m), 3186 (s), 3039 (w), 2506 (vw), 2393 (vw), 2283 (vw), 1783 (vw), 1631 (w), 1519 (m), 1468 (s), 1442 (w), 1408 (s), 1375 (s), 1322 (s), 1283 (s), 1233 (vs), 1123 (m), 1056 (vw), 1030 (w), 1001 (w), 877 (w), 771 (w), 756 (w), 734 (m), 703 (w), 689 (w).

Elemental analysis C₄H₁₂CuN₁₄O₄ (383.78 g/mol): calc.: C, 12.52; H, 3.15; N, 51.10; found: C, 12.52; H, 3.24; N, 51.01.

E_{dr} = 7.0 J (500–1000 μm).

F_r = 288 N (500–1000 μm).

E_{el} = 0.75 J (500–1000 μm).

H₂O-sol. 1.5 wt% (23 °C).

Diammine bis(1-methyl-5-nitriminotetrazolato-κ²N4,O1) copper(II) monohydrate

[(Cu(1MeAtNO₂)₂(NH₃)₂)]_H₂O: Byproduct during the synthesis of ***[(Cu(1MeAtNO₂)₂(NH₃)₂)]***.

The deep blue mixture was cooled to ambient temperature and stored until deep violet

crystal needles were formed. They were filtered off and dried on air, and then turned diffuse bright violet. After a few days of storing the residual solution at ambient temperature deep blue crystal of **[Cu(1MeAtNO₂)₂(NH₃)₂]** could be obtained Yield: 44 %.

M.p. 60 °C (loss of H₂O), 242 °C (dec., DSC-measurement, 5 K/min).

IR (Diamond-ATR, cm⁻¹): 3553 (w), 3329 (s), 3264 (m), 3188 (m), 1620 (w), 1515 (m), 1463 (m), 1410 (m), 1370 (m), 1325 (s), 1274 (s), 1234 (vs), 1117 (m), 1030 (m), 1001 (w), 880 (w), 774 (w), 759 (w), 737 (m), 701 (m), 688 (m).

Elemental analysis C₄H₁₄CuN₁₄O₅ (401.79 g/mol): calc.: C, 11.96; H, 3.51; N, 48.80; found: C, 11.76; H, 3.51; N, 48.61.

E_{dr} = 7.0 J (250–500 μm).

F_r = 324 N (250–500 μm).

E_{el} = 0.75 J (250–500 μm).

H₂O-sol. 1.0 wt% (23 °C).

Bis[(triammine) μ₂-(5-nitriminotetrazolato-N1,O1) copper(II)] **[[Cu(AtNO₂)(NH₃)₃]₂]:**

Preparation according to the literature.^[6, 7] Yield: 72 %.

M.p. 250 °C (dec., DSC-measurement, 5 K/min).

IR (Diamond-ATR, cm⁻¹): 3329 (m), 3297 (m), 3236 (m), 3166 (m), 3028 (w), 2388 (vw), 2160 (vw), 1760 (vw), 1625 (w), 1506 (vw), 1454 (s), 1396 (s), 1365 (s), 1298 (s), 1234 (s), 1212 (s), 1153 (m), 1135 (w), 1094 (m), 1025 (m), 865 (w), 751 (m), 737 (w), 719 (w), 696 (w).

Elemental analysis C₂H₁₈Cu₂N₁₈O₄ (485.38 g/mol): calc.: C, 4.95; H, 3.74; N, 51.94; found: C, 5.05; H, 3.80; N, 51.57.

E_{dr} = 5.0 J (500–1000 μm).

F_r = 288 N (500–1000 μm).

E_{el} = 0.20 J (500–1000 μm).

H₂O-sol. < 0.5 wt% (21 °C).

Basic copper(II) nitrate (Cu₂(OH)₃(NO₃)): Preparation according to the literature.^[5, 8] Yield: 66 %.

M.p. 271 °C (dec., DSC-measurement, 5 K/min).

IR (Diamond-ATR, cm⁻¹): 3540 (s), 3411 (s), 2837 (w), 2739 (w), 2465 (w), 2343 (w), 1762 (w), 1415 (vs), 1349 (s), 1321 (s), 1046 (m), 871 (m), 807 (m), 775 (m), 717 (m), 669 (m).

Elemental analysis Cu₂H₃NO₆ (240.12 g/mol): calc.: H, 1.26; N, 5.83; found: H, 1.63; N, 5.88%.

E_{dr} > 30 J (< 100 μm).

F_r > 360 N (< 100 μm).

E_{el} = 0.10 J (< 100 μm).

H₂O-sol. < 0.4 wt% (21 °C).

Tetrammine copper(II) dinitramide ($[\text{Cu}(\text{NH}_3)_4][\text{N}(\text{NO}_2)_2]_2$): Preparation according to the literature.^[9, 10]. Yield: 66 %.

M.p. 65 °C (loss of NH_3), 183 °C (dec., DSC-measurement, 5 K/min).

IR (Diamond-ATR, cm^{-1}): 3566 (vw), 3336 (vs), 3272 (s), 3194 (m), 2832 (vw), 2589 (vw), 2475 (vw), 1956 (vw), 1612 (w), 1500 (s), 1425 (s), 1323 (m), 1272 (m), 1254 (m), 1169 (s), 1010 (m), 962 (m), 820 (m), 776 (w), 760 (m), 688 (m).

Elemental analysis $\text{H}_{12}\text{CuN}_{10}\text{O}_8$ (343.70 g/mol): calc.: H, 3.52; N, 40.57; found: H, 3.50; N, 40.35.

E_{dr} = 2.5 J (> 1000 μm).

F_{r} = 48 N (> 1000 μm).

E_{el} = 0.47 J (> 1000 μm).

$\text{H}_2\text{O-sol.}$ 2.7 wt% (22 °C).

10.2.2 Pyrotechnic Compositions

For the preparation of the pyrotechnic compositions, all substances except the binder were carefully mixed in a mortar. Then the binder, dissolved in a few milliliters of ethyl acetate, was added. The mixture was formed by hand and dried under high vacuum for several hours.

The controlled burn down was filmed with a digital video camera recorder (SONY, DCR-HC37E).

A solution of 25 % vinyl alcohol acetate resin (VAAR) was used as binder. All compound ratios are given in percent by weight (wt%).

10.2.2.1 Pyrotechnic Compositions based on Diammine bis(Tetrazol-5-yl)-aminato- $\kappa^2\text{N1,N6}$ Copper(II) ($[\text{Cu}(\text{bta})(\text{NH}_3)_2]$)

In Table 10.4–Table 10.42 the different pyrotechnic compositions based on $[\text{Cu}(\text{bta})(\text{NH}_3)_2]$ are given. The oxidizers potassium permanganate, potassium nitrate, manganese oxide, basic copper(II) carbonate, copper(II) nitrate pentahydrate, ADN, and ammonium nitrate were used. Magnesium, silicon, sulfur, copper(I) oxide, zinc, and boron were added as fuel. As further additives boric acid, potassium aluminum sulfate dodecahydrate, or copper(II) sulfate pentahydrate were used.

Table 10.4 Pyrotechnic formulation containing $[\text{Cu}(\text{bta})(\text{NH}_3)_2]$, manganese dioxide, and silicon.

	$[\text{Cu}(\text{bta})(\text{NH}_3)_2]$	MnO_2	Si	VAAR	observed behavior
	[wt%]	[wt%]	[wt%]	[wt%]	
$[\text{Cu}(\text{bta})(\text{NH}_3)_2]_1$	5	51	37	8	cannot be ignited

Table 10.5 Pyrotechnic formulations containing $[\text{Cu}(\text{bta})(\text{NH}_3)_2]$, manganese dioxide, and magnesium.

	$[\text{Cu}(\text{bta})(\text{NH}_3)_2]$ [wt%]	MnO_2 [wt%]	Mg [wt%]	VAAR [wt%]	observed behavior
$[\text{Cu}(\text{bta})(\text{NH}_3)_2]$ _2.1	4	66	22	8	white flame, hard to ignite, sparks, solid residues
$[\text{Cu}(\text{bta})(\text{NH}_3)_2]$ _2.2	24	65	2	9	no flame, hard to ignite, sparks, solid residues
$[\text{Cu}(\text{bta})(\text{NH}_3)_2]$ _2.3	19	71	2	8	no flame, hard to ignite, sparks, solid residues

Table 10.6 Pyrotechnic formulations containing $[\text{Cu}(\text{bta})(\text{NH}_3)_2]$, potassium nitrate, and sulfur.

	$[\text{Cu}(\text{bta})(\text{NH}_3)_2]$ [wt%]	KNO_3 [wt%]	S [wt%]	VAAR [wt%]	observed behavior
$[\text{Cu}(\text{bta})(\text{NH}_3)_2]$ _3.1	12	68	12	8	green-violet flame, hard to ignite, low velocity, much smoke, solid residues
$[\text{Cu}(\text{bta})(\text{NH}_3)_2]$ _3.2	18	69	5	8	cannot be ignited

Table 10.7 Pyrotechnic formulation containing $[\text{Cu}(\text{bta})(\text{NH}_3)_2]$, potassium nitrate, boric acid, and sulfur.

	$[\text{Cu}(\text{bta})(\text{NH}_3)_2]$ [wt%]	KNO_3 [wt%]	S [wt%]	$\text{B}(\text{OH})_3$ [wt%]	VAAR [wt%]	observed behavior
$[\text{Cu}(\text{bta})(\text{NH}_3)_2]$ _4	9	65	7	11	8	cannot be ignited

Table 10.8 Pyrotechnic formulation containing $[\text{Cu}(\text{bta})(\text{NH}_3)_2]$ and potassium permanganate.

	$[\text{Cu}(\text{bta})(\text{NH}_3)_2]$ [wt%]	KMnO_4 [wt%]	VAAR [wt%]	observed behavior
$[\text{Cu}(\text{bta})(\text{NH}_3)_2]$ _5	27	63	10	white-violet flame, easy to ignite, solid residues

Table 10.9 Pyrotechnic formulation containing $[\text{Cu}(\text{bta})(\text{NH}_3)_2]$, potassium permanganate, and manganese dioxide.

	$[\text{Cu}(\text{bta})(\text{NH}_3)_2]$ [wt%]	KMnO_4 [wt%]	MnO_2 [wt%]	VAAR [wt%]	observed behavior
$[\text{Cu}(\text{bta})(\text{NH}_3)_2]$ _6	27	18	45	10	red golden sparks, solid residues

Table 10.10 Pyrotechnic formulation containing $[\text{Cu}(\text{bta})(\text{NH}_3)_2]$, potassium permanganate, and potassium nitrate.

	$[\text{Cu}(\text{bta})(\text{NH}_3)_2]$ [wt%]	KMnO_4 [wt%]	KNO_3 [wt%]	VAAR [wt%]	observed behavior
$[\text{Cu}(\text{bta})(\text{NH}_3)_2]$ _7	27	18	45	10	red golden sparks

Table 10.11 Pyrotechnic formulations containing $[\text{Cu}(\text{bta})(\text{NH}_3)_2]$, potassium permanganate, potassium nitrate, and boric acid.

	$[\text{Cu}(\text{bta})(\text{NH}_3)_2]$ [wt%]	KMnO_4 [wt%]	KNO_3 [wt%]	$\text{B}(\text{OH})_3$ [wt%]	VAAR [wt%]	observed behavior
$[\text{Cu}(\text{bta})(\text{NH}_3)_2]$ _8.1	18	12	43	18	9	cannot be ignited
$[\text{Cu}(\text{bta})(\text{NH}_3)_2]$ _8.2	22	37	15	15	11	just glows

Table 10.12 Pyrotechnic formulations containing $[\text{Cu}(\text{bta})(\text{NH}_3)_2]$, potassium permanganate, potassium nitrate, and potassium aluminum sulfate dodecahydrate.

	$[\text{Cu}(\text{bta})(\text{NH}_3)_2]$ [wt%]	KMnO_4 [wt%]	KNO_3 [wt%]	$\text{KAl}(\text{SO}_4)_2 \cdot 12\text{H}_2\text{O}$ [wt%]	VAAR [wt%]	observed behavior
$[\text{Cu}(\text{bta})(\text{NH}_3)_2]$ _9.1	18	12	43	18	9	hard to ignite, glowing
$[\text{Cu}(\text{bta})(\text{NH}_3)_2]$ _9.2	27	36	18	9	9	hard to ignite, glowing

Table 10.13 Pyrotechnic formulation containing $[\text{Cu}(\text{bta})(\text{NH}_3)_2]$, potassium permanganate, potassium nitrate, and copper(II) sulfate pentahydrate.

	$[\text{Cu}(\text{bta})(\text{NH}_3)_2]$ [wt%]	KMnO_4 [wt%]	KNO_3 [wt%]	$\text{CuSO}_4 \cdot 5\text{H}_2\text{O}$ [wt%]	VAAR [wt%]	observed behavior
$[\text{Cu}(\text{bta})(\text{NH}_3)_2]$ _10	14	36	27	14	9	hard to ignite, glowing

Table 10.14 Pyrotechnic formulation containing $[\text{Cu}(\text{bta})(\text{NH}_3)_2]$, potassium permanganate, magnesium, and copper(II) sulfate pentahydrate

	$[\text{Cu}(\text{bta})(\text{NH}_3)_2]$ [wt%]	KMnO_4 [wt%]	Mg [wt%]	$\text{CuSO}_4 \cdot 5\text{H}_2\text{O}$ [wt%]	VAAR [wt%]	observed behavior
$[\text{Cu}(\text{bta})(\text{NH}_3)_2]$ _11	14	54	9	14	9	violet flame, moderate to ignite, many solid residues

Table 10.15 Pyrotechnic formulation containing $[\text{Cu}(\text{bta})(\text{NH}_3)_2]$, potassium permanganate, magnesium, and basic copper(II) carbonate.

	$[\text{Cu}(\text{bta})(\text{NH}_3)_2]$ [wt%]	KMnO_4 [wt%]	Mg [wt%]	$\text{CuCO}_3 \cdot \text{Cu}(\text{OH})_2$ [wt%]	VAAR [wt%]	observed behavior
$[\text{Cu}(\text{bta})(\text{NH}_3)_2]$ _12	12	49	9	12	10	violet flame, moderate to ignite, many solid residues

Table 10.16 Pyrotechnic formulation containing $[\text{Cu}(\text{bta})(\text{NH}_3)_2]$ and copper(II) nitrate pentahydrate.

	$[\text{Cu}(\text{bta})(\text{NH}_3)_2]$ [wt%]	$\text{Cu}(\text{NO}_3)_2 \cdot 2.5\text{H}_2\text{O}$ [wt%]	VAAR [wt%]	observed behavior
$[\text{Cu}(\text{bta})(\text{NH}_3)_2]_{13}$	27	64	9	short-lasting green flame, glowing, many solid residues

Table 10.17 Pyrotechnic formulation containing $[\text{Cu}(\text{bta})(\text{NH}_3)_2]$, potassium permanganate, sulfur, and basic copper(II) carbonate.

	$[\text{Cu}(\text{bta})(\text{NH}_3)_2]$ [wt%]	KMnO_4 [wt%]	$\text{CuCO}_3 \cdot \text{Cu}(\text{OH})_2$ [wt%]	S [wt%]	VAAR [wt%]	observed behavior
$[\text{Cu}(\text{bta})(\text{NH}_3)_2]_{14}$	13	48	17	13	9	violet flame, moderate to ignite, huge amount of solid residues

Table 10.18 Pyrotechnic formulations containing $[\text{Cu}(\text{bta})(\text{NH}_3)_2]$ and ADN.

	$[\text{Cu}(\text{bta})(\text{NH}_3)_2]$ [wt%]	ADN [wt%]	VAAR [wt%]	observed behavior
$[\text{Cu}(\text{bta})(\text{NH}_3)_2]_{15.1}$	27	64	9	pale green flame, easy to ignite, very high velocity, no residues
$[\text{Cu}(\text{bta})(\text{NH}_3)_2]_{15.2}$	36	55	9	green-white flame, easy to ignite, high velocity, no residues
$[\text{Cu}(\text{bta})(\text{NH}_3)_2]_{15.3}$	55	36	9	no flame, glowing

Table 10.19 Pyrotechnic formulations containing $[\text{Cu}(\text{bta})(\text{NH}_3)_2]$, copper(II) sulfate pentahydrate, and ADN.

	$[\text{Cu}(\text{bta})(\text{NH}_3)_2]$ [wt%]	ADN [wt%]	$\text{CuSO}_4 \cdot 5\text{H}_2\text{O}$ [wt%]	VAAR [wt%]	observed behavior
$[\text{Cu}(\text{bta})(\text{NH}_3)_2]_{16.1}$	33	49	9	9	pale green flame, easy to ignite, very high velocity, small amount of solid residues
$[\text{Cu}(\text{bta})(\text{NH}_3)_2]_{16.2}$	30	46	15	9	no flame, glowing, lifts off

Table 10.20 Pyrotechnic formulations containing $[\text{Cu}(\text{bta})(\text{NH}_3)_2]$, copper(I) oxide, and ADN.

	$[\text{Cu}(\text{bta})(\text{NH}_3)_2]$ [wt%]	ADN [wt%]	Cu_2O [wt%]	VAAR [wt%]	observed behavior
$[\text{Cu}(\text{bta})(\text{NH}_3)_2]_{17.1}$	35	53	2	10	yellow-green flame, easy to ignite, high velocity, almost no solid residues
$[\text{Cu}(\text{bta})(\text{NH}_3)_2]_{17.2}$	30	46	15	9	pale green flame, few residues

Table 10.21 Pyrotechnic formulation containing $[\text{Cu}(\text{bta})(\text{NH}_3)_2]$, ADN, and potassium aluminum sulfate dodecahydrate.

	$[\text{Cu}(\text{bta})(\text{NH}_3)_2]$ [wt%]	ADN [wt%]	$\text{KAl}(\text{SO}_4)_2 \cdot 12\text{H}_2\text{O}$ [wt%]	VAAR [wt%]	observed behavior
$[\text{Cu}(\text{bta})(\text{NH}_3)_2]_{18}$	36	54	1	9	green flame, high velocity, no smoke, no solid residues

Table 10.22 Pyrotechnic formulations containing $[\text{Cu}(\text{bta})(\text{NH}_3)_2]$, ADN, and basic copper(II) carbonate.

	$[\text{Cu}(\text{bta})(\text{NH}_3)_2]$ [wt%]	ADN [wt%]	$\text{CuCO}_3 \cdot \text{Cu}(\text{OH})_2$ [wt%]	VAAR [wt%]	observed behavior
$[\text{Cu}(\text{bta})(\text{NH}_3)_2]_{19.1}$	30	46	15	9	yellow-green flame, easy to ignite, high velocity, almost no solid residues
$[\text{Cu}(\text{bta})(\text{NH}_3)_2]_{19.2}$	33	50	8	9	yellow-green flame, lifts off, glowing

Table 10.23 Pyrotechnic formulations containing $[\text{Cu}(\text{bta})(\text{NH}_3)_2]$, ADN, basic copper(II) carbonate, and urea.

	$[\text{Cu}(\text{bta})(\text{NH}_3)_2]$ [wt%]	ADN [wt%]	$\text{CuCO}_3 \cdot \text{Cu}(\text{OH})_2$ [wt%]	Urea [wt%]	VAAR [wt%]	observed behavior
$[\text{Cu}(\text{bta})(\text{NH}_3)_2]_{20.1}$	28	41	21	1	9	glowing, lifts off
$[\text{Cu}(\text{bta})(\text{NH}_3)_2]_{20.2}$	30	45	15	1	9	glowing, lifts off

Table 10.24 Pyrotechnic formulation containing $[\text{Cu}(\text{bta})(\text{NH}_3)_2]$, copper(I) oxide, urea, and ADN.

	$[\text{Cu}(\text{bta})(\text{NH}_3)_2]$ [wt%]	ADN [wt%]	Cu_2O [wt%]	Urea [wt%]	VAAR [wt%]	observed behavior
$[\text{Cu}(\text{bta})(\text{NH}_3)_2]_{21}$	27	41	14	10	9	yellow-green flame, high velo- city, glowing residues

Table 10.25 Pyrotechnic formulations containing $[\text{Cu}(\text{bta})(\text{NH}_3)_2]$, ADN, and basic copper(II) nitrate.

	$[\text{Cu}(\text{bta})(\text{NH}_3)_2]$ [wt%]	ADN [wt%]	$\text{Cu}_2(\text{OH})_3(\text{NO}_3)$ [wt%]	VAAR [wt%]	observed behavior
$[\text{Cu}(\text{bta})(\text{NH}_3)_2]_{22.1}$	33	50	8	9	yellow-green flame, high velo- city, glowing, smoke
$[\text{Cu}(\text{bta})(\text{NH}_3)_2]_{22.2}$	30	46	15	9	alternating green-yellow flame and glowing, smoke

Table 10.26 Pyrotechnic formulations containing $[\text{Cu}(\text{bta})(\text{NH}_3)_2]$ and copper(II) nitrate pentahemihydrate.

	$[\text{Cu}(\text{bta})(\text{NH}_3)_2]$ [wt%]	$\text{Cu}(\text{NO}_3)_2 \cdot 2.5\text{H}_2\text{O}$ [wt%]	VAAR [wt%]	observed behavior
$[\text{Cu}(\text{bta})(\text{NH}_3)_2]$ _23.1	25	65	10	glowing
$[\text{Cu}(\text{bta})(\text{NH}_3)_2]$ _23.2	18	72	10	glowing, sizzling noise

Table 10.27 Pyrotechnic formulation containing $[\text{Cu}(\text{bta})(\text{NH}_3)_2]$, ADN, and copper(II) nitrate pentahemihydrate.

	$[\text{Cu}(\text{bta})(\text{NH}_3)_2]$ [wt%]	ADN [wt%]	$\text{Cu}(\text{NO}_3)_2 \cdot 2.5\text{H}_2\text{O}$ [wt%]	VAAR [wt%]	observed behavior
$[\text{Cu}(\text{bta})(\text{NH}_3)_2]$ _24	28	35	28	9	yellow-green flame, less smoke, no solid residues

Table 10.28 Pyrotechnic formulation containing $[\text{Cu}(\text{bta})(\text{NH}_3)_2]$, ADN, copper(II) nitrate pentahemihydrate, copper(II) sulfate pentahydrate, and urea.

	$[\text{Cu}(\text{bta})(\text{NH}_3)_2]$ [wt%]	ADN [wt%]	$\text{Cu}(\text{NO}_3)_2 \cdot 2.5\text{H}_2\text{O}$ [wt%]	$\text{CuSO}_4 \cdot 5\text{H}_2\text{O}$ [wt%]	Urea [wt%]	VAAR [wt%]	observed behavior
$[\text{Cu}(\text{bta})(\text{NH}_3)_2]$ _25	28	34	21	7	1	9	yellow-green flame, lifts off

Table 10.29 Pyrotechnic formulation containing $[\text{Cu}(\text{bta})(\text{NH}_3)_2]$, ADN, copper(II) nitrate pentahemihydrate, basic copper(II) carbonate, and urea.

	$[\text{Cu}(\text{bta})(\text{NH}_3)_2]$ [wt%]	ADN [wt%]	$\text{Cu}(\text{NO}_3)_2 \cdot 2.5\text{H}_2\text{O}$ [wt%]	$\text{CuCO}_3 \cdot \text{Cu}(\text{OH})_2$ [wt%]	Urea [wt%]	VAAR [wt%]	observed behavior
$[\text{Cu}(\text{bta})(\text{NH}_3)_2]$ _26	28	34	21	7	1	9	yellow-green flame, lifts off

Table 10.30 Pyrotechnic formulations containing $[\text{Cu}(\text{bta})(\text{NH}_3)_2]$, ADN, ammonium nitrate, and urea.

	$[\text{Cu}(\text{bta})(\text{NH}_3)_2]$ [wt%]	ADN [wt%]	NH_4NO_3 [wt%]	Urea [wt%]	VAAR [wt%]	observed behavior
$[\text{Cu}(\text{bta})(\text{NH}_3)_2]$ _27.1	35	19	35	1	10	no flame, glowing
$[\text{Cu}(\text{bta})(\text{NH}_3)_2]$ _27.2	31	22	37	1	9	green-yellow-red flame, easy to ignite, moderate velocity, less smoke, solid residues
$[\text{Cu}(\text{bta})(\text{NH}_3)_2]$ _27.3	30	30	30	1	9	green-yellow-red flame, easy to ignite, moderate velocity, less smoke, no residues

Pyrotechnic Compositions Containing Nitrogen-rich Copper(II) Compounds

[Cu(bta)(NH₃)₂]_{27.4}	25	19	45	1	10	green-yellow-red flame, easy to ignite, low velocity, less smoke, almost no solid residues
[Cu(bta)(NH₃)₂]_{27.5}	21	16	53	1	9	yellow-red flame, hard to ignite, low velocity, smoke, almost no solid residues

Table 10.31 Pyrotechnic formulations containing [Cu(bta)(NH₃)₂], ADN, ammonium nitrate, copper(II) sulfate pentahydrate, and urea.

	[Cu(bta)(NH₃)₂] [wt%]	ADN [wt%]	NH₄NO₃ [wt%]	CuSO₄ · 5H₂O [wt%]	Urea [wt%]	VAAR [wt%]	observed behavior
[Cu(bta)(NH₃)₂]_{28.1}	28	28	28	6	1	9	no flame, glowing green-yellow-red flame, moderate velocity, almost no solid residues
[Cu(bta)(NH₃)₂]_{28.2}	29	29	29	3	1	9	

Table 10.32 Pyrotechnic formulations containing [Cu(bta)(NH₃)₂], ADN, ammonium nitrate, basic copper(II) carbonate, and urea.

	[Cu(bta)(NH₃)₂] [wt%]	ADN [wt%]	NH₄NO₃ [wt%]	CuCO₃ · Cu(OH)₂ [wt%]	Urea [wt%]	VAAR [wt%]	observed behavior
[Cu(bta)(NH₃)₂]_{29.1}	29	29	29	3	1	9	green-yellow-red flame, moderate velocity, almost no solid residues
[Cu(bta)(NH₃)₂]_{29.2}	28	29	29	4	1	9	green-yellow-red flame, easy to ignite, almost no solid residues
[Cu(bta)(NH₃)₂]_{29.3}	29	28	28	5	1	9	green-yellow-red flame, less smoke, almost no solid residues
[Cu(bta)(NH₃)₂]_{29.4}	28	28	28	6	1	9	green-yellow-red flame, almost no solid residues

Table 10.33 Pyrotechnic formulations containing **[Cu(bta)(NH₃)₂]**, ADN, and boron.

	[Cu(bta)(NH₃)₂] [wt%]	ADN [wt%]	B [wt%]	VAAR [wt%]	observed behavior
[Cu(bta)(NH₃)₂] _30.1	40	40	10	10	yellow flame, easy to ignite, moderate velocity, no smoke, glowing residue
[Cu(bta)(NH₃)₂] _30.2	36	45	9	10	no flame, sparks, lifts off
[Cu(bta)(NH₃)₂] _30.3	38	43	10	9	green in the beginning yellow flame, easy to ignite, high velocity, sparks, glowing residues
[Cu(bta)(NH₃)₂] _30.4	40	41	10	9	yellow flame, easy to ignite, sparks, no smoke, glowing residue
[Cu(bta)(NH₃)₂] _30.5	38	42	10	10	yellow-green flame, sparks, lifts off
[Cu(bta)(NH₃)₂] _30.6	38	40	12	10	yellow-green flame, sparks, lifts off
[Cu(bta)(NH₃)₂] _30.7	35	37	18	10	yellow flame, easy to ignite, sparks, no smoke, glowing residue

Table 10.34 Pyrotechnic formulations containing **[Cu(bta)(NH₃)₂]**, ADN, boron, and zinc.

	[Cu(bta)(NH₃)₂] [wt%]	ADN [wt%]	B [wt%]	Zn [wt%]	VAAR [wt%]	observed behavior
[Cu(bta)(NH₃)₂] _31.1	26	51	7	7	9	yellow-green flame, easy to ignite, sparks, no smoke, lifts off, glowing residue
[Cu(bta)(NH₃)₂] _31.2	33	45	6	6	10	yellow-green flame, sparks, no smoke, lifts off, glowing residue
[Cu(bta)(NH₃)₂] _31.3	37	43	5	5	10	yellow flame, no smoke, glowing residue
[Cu(bta)(NH₃)₂] _31.4	40	41	5	5	9	green flame, easy to ignite, high velocity, sparks, no smoke, glowing residues
[Cu(bta)(NH₃)₂] _31.5	40	40	5	5	10	yellow flame, sparks, lifts off
[Cu(bta)(NH₃)₂] _31.6	42	39	5	5	9	yellow flame, sparks, lifts off
[Cu(bta)(NH₃)₂] _31.7	40	40	6	5	9	yellow flame, sparks, lifts off
[Cu(bta)(NH₃)₂] _31.8	36	36	9	10	9	yellow-green flame, easy to ignite, moderate velocity, sparks, glowing residue
[Cu(bta)(NH₃)₂] _31.9	36	36	11	8	9	yellow-green flame, easy to ignite, moderate velocity, sparks, glowing residue

Table 10.35 Pyrotechnic formulations containing [Cu(bta)(NH₃)₂], ADN, boron, and magnesium.

	[Cu(bta)(NH ₃) ₂] [wt%]	ADN [wt%]	B [wt%]	Mg [wt%]	VAAR [wt%]	observed behavior
[Cu(bta)(NH ₃) ₂] _{32.1}	40	40	5	5	10	yellow flame, some sparks, no smoke, glowing residue
[Cu(bta)(NH ₃) ₂] _{32.2}	39	41	5	5	10	yellow-green flame, sparks, lifts off
[Cu(bta)(NH ₃) ₂] _{32.3}	40	41	5	5	9	yellow-green flame, sparks, no smoke, glowing residue
[Cu(bta)(NH ₃) ₂] _{32.4}	43	38	5	5	9	yellow flame, sparks, lifts off

Table 10.36 Pyrotechnic formulations containing [Cu(bta)(NH₃)₂], ADN, boron, and copper(II) sulfate pentahydrate.

	[Cu(bta)(NH ₃) ₂] [wt%]	ADN [wt%]	B [wt%]	CuSO ₄ · 5H ₂ O [wt%]	VAAR [wt%]	observed behavior
[Cu(bta)(NH ₃) ₂] _{33.1}	37	40	9	5	9	yellow-green flame, sparks, too violently, no smoke, glowing residue
[Cu(bta)(NH ₃) ₂] _{33.2}	36	39	11	5	9	sparks, yellow flame, no smoke, glowing residue
[Cu(bta)(NH ₃) ₂] _{33.3}	35	37	13	5	10	yellow flame, sparks, lifts off
[Cu(bta)(NH ₃) ₂] _{33.4}	36	34	13	8	9	sparks, lifts off

Table 10.37 Pyrotechnic formulations containing [Cu(bta)(NH₃)₂], ADN and ammonium nitrate.

	[Cu(bta)(NH ₃) ₂] [wt%]	ADN [wt%]	NH ₄ NO ₃ [wt%]	VAAR [wt%]	observed behavior
[Cu(bta)(NH ₃) ₂] _{34.1}	17	8	66	9	small green flame with red frame, hard to ignite, unsteady burning, low velocity, no residues
[Cu(bta)(NH ₃) ₂] _{34.2}	15	11	65	9	cannot be ignited
[Cu(bta)(NH ₃) ₂] _{34.3}	8	11	72	9	small white-green flame, hard to ignite, low velocity, no smoke, glowing residue
[Cu(bta)(NH ₃) ₂] _{34.4}	10	10	70	10	small green flame, low velocity, less smoke, no residues
[Cu(bta)(NH ₃) ₂] _{34.5}	6	10	75	9	very small white flame with red frame, unsteady burning

Table 10.38 Pyrotechnic formulations containing [Cu(bta)(NH₃)₂], ADN, ammonium nitrate, and boron.

	[Cu(bta)(NH ₃) ₂] [wt%]	ADN [wt%]	NH ₄ NO ₃ [wt%]	B [wt%]	VAAR [wt%]	observed behavior
[Cu(bta)(NH ₃) ₂] _{35.1}	13	8	67	3	9	small pale green flame, easy to ignite, no smoke, low velocity, solid residue
[Cu(bta)(NH ₃) ₂] _{35.2}	13	6	69	3	9	small pale green flame, easy to ignite, no smoke, few sparks, low velocity, solid residue
[Cu(bta)(NH ₃) ₂] _{35.3}	12	7	69	3	9	white-green flame, moderate to ignite, less smoke, low velocity, solid residue
[Cu(bta)(NH ₃) ₂] _{35.4}	11	6	69	5	9	white-green flame, easy to ignite, no smoke, low velocity, solid residue
[Cu(bta)(NH ₃) ₂] _{35.4}	6	7	75	3	9	yellow-white flame, easy to ignite, no smoke, low velocity, solid residue

Table 10.39 Pyrotechnic formulations containing [Cu(bta)(NH₃)₂], ADN, ammonium nitrate, and sulfur.

	[Cu(bta)(NH ₃) ₂] [wt%]	ADN [wt%]	NH ₄ NO ₃ [wt%]	S [wt%]	VAAR [wt%]	observed behavior
[Cu(bta)(NH ₃) ₂] _{36.1}	10	10	66	5	9	small pale green flame with red frame, moderate to ignite, less smoke, glowing residue
[Cu(bta)(NH ₃) ₂] _{36.2}	9	7	70	5	9	small white flame with red frame, smoke, unsteady burning
[Cu(bta)(NH ₃) ₂] _{36.3}	9	9	68	5	9	small white flame with red frame, smoke, unsteady burning

Table 10.40 Pyrotechnic formulations containing [Cu(bta)(NH₃)₂], ADN, ammonium nitrate, boron, and sulfur.

	[Cu(bta)(NH ₃) ₂] [wt%]	ADN [wt%]	NH ₄ NO ₃ [wt%]	B [wt%]	S [wt%]	VAAR [wt%]	observed behavior
[Cu(bta)(NH ₃) ₂] _{37.1}	14	9	64	2	2	9	blue-green flame, easy to ignite, low velocity, no smoke, solid residue
[Cu(bta)(NH ₃) ₂] _{37.2}	14	8	64	2	3	9	blue-green flame, easy to ignite, low velocity, no smoke, solid residue
[Cu(bta)(NH ₃) ₂] _{37.3}	13	7	65	2	3	10	small green flame, easy to ignite, low velocity, no smoke, solid residue

Table 10.41 Pyrotechnic formulations containing [Cu(bta)(NH₃)₂], ADN, ammonium nitrate, boron, sulfur, and copper(I) oxide.

	[Cu(bta)(NH ₃) ₂] [wt%]	ADN [wt%]	NH ₄ NO ₃ [wt%]	B [wt%]	S [wt%]	Cu ₂ O [wt%]	VAAR [wt%]	observed behavior
[Cu(bta)(NH ₃) ₂] _{37.1}	9	9	64	3	2	4	9	small green flame, easy to ignite, low velocity, no smoke, solid residue
[Cu(bta)(NH ₃) ₂] _{37.2}	9	17	58	2	3	2	9	pale yellow flame, easy to ignite, low velocity, no smoke, solid residue

Table 10.42 Pyrotechnic formulations containing $[\text{Cu}(\text{bta})(\text{NH}_3)_2]$, ADN, ammonium nitrate, boron, and magnesium.

	$[\text{Cu}(\text{bta})(\text{NH}_3)_2]$ [wt%]	ADN [wt%]	NH_4NO_3 [wt%]	B [wt%]	Mg [wt%]	VAAR [wt%]	observed behavior
$[\text{Cu}(\text{bta})(\text{NH}_3)_2]$ _37.1	10	10	67	2	2	9	pale yellow flame, easy to ignite, low velocity, no smoke, few sparks, solid residue
$[\text{Cu}(\text{bta})(\text{NH}_3)_2]$ _37.2	9	9	68	4	2	8	yellow flame, easy to ignite, sparks, almost no residues

10.2.2.2 Pyrotechnic Compositions based on Bis{bis(tetrazol-5-yl-ate)-amine- $\kappa^2\text{N1,N6}$ } Copper(II) Nitrate Hemihydrate ($[\text{Cu}(\text{H}_2\text{bta})_2](\text{NO}_3)_2$)

In Table 10.43–Table 10.46 the different pyrotechnic compositions based on $[\text{Cu}(\text{H}_2\text{bta})_2](\text{NO}_3)_2$ are given. The fuels boron, $[\text{Cu}(\text{bta})(\text{NH}_3)_2]$, 5-aminotetrazole (**5-At**) and copper(I) iodide were used. No oxidizers were added.

Table 10.43 Pyrotechnic formulations containing $[\text{Cu}(\text{H}_2\text{bta})_2](\text{NO}_3)_2$ and boron.

	$[\text{Cu}(\text{H}_2\text{bta})_2](\text{NO}_3)_2$ [wt%]	B [wt%]	VAAR [wt%]	observed behavior
$[\text{Cu}(\text{H}_2\text{bta})_2](\text{NO}_3)_2$ _1.1	68	8	24	greenish flame, easy to ignite, combusts too violently, less smoke, sparks, solid black residues
$[\text{Cu}(\text{H}_2\text{bta})_2](\text{NO}_3)_2$ _1.2	65	16	19	greenish flame, easy to ignite, lifts off, no smoke, sparks, solid black residues
$[\text{Cu}(\text{H}_2\text{bta})_2](\text{NO}_3)_2$ _1.3	37	37	26	yellow flame, easy to ignite, solid long glowing residue
$[\text{Cu}(\text{H}_2\text{bta})_2](\text{NO}_3)_2$ _1.4	49	33	18	greenish flame, easy to ignite, lifts off, no smoke, sparks, solid black residues

Table 10.44 Pyrotechnic formulations containing $[\text{Cu}(\text{H}_2\text{bta})_2](\text{NO}_3)_2$ and $[\text{Cu}(\text{bta})(\text{NH}_3)_2]$.

	$[\text{Cu}(\text{H}_2\text{bta})_2](\text{NO}_3)_2$ [wt%]	$[\text{Cu}(\text{bta})(\text{NH}_3)_2]$ [wt%]	B [wt%]	VAAR [wt%]	observed behavior
$[\text{Cu}(\text{H}_2\text{bta})_2](\text{NO}_3)_2$ 2.1	63	13	6	18	green flame, easy to ignite, combusts too violently, no smoke, sparks, solid glowing residues
$[\text{Cu}(\text{H}_2\text{bta})_2](\text{NO}_3)_2$ 2.2	58	15	7	20	green flame, easy to ignite, combusts too violently, no smoke, sparks, solid glowing residues
$[\text{Cu}(\text{H}_2\text{bta})_2](\text{NO}_3)_2$ 2.3	34	34	12	20	yellow partly green flame, easy to ignite, moderate velocity, solid glowing residue
$[\text{Cu}(\text{H}_2\text{bta})_2](\text{NO}_3)_2$ 2.4	50	25	8	17	green flame, easy to ignite, lifts off
$[\text{Cu}(\text{H}_2\text{bta})_2](\text{NO}_3)_2$ 2.5	44	29	7	20	easy to ignite, lifts off
$[\text{Cu}(\text{H}_2\text{bta})_2](\text{NO}_3)_2$ 2.6	40	31	8	21	easy to ignite, lifts off
$[\text{Cu}(\text{H}_2\text{bta})_2](\text{NO}_3)_2$ 2.7	28	56	0	16	green-yellow flame, easy to ignite, lifts off
$[\text{Cu}(\text{H}_2\text{bta})_2](\text{NO}_3)_2$ 2.8	9	72	0	19	green flame, hard to ignite, no burning, smoke
$[\text{Cu}(\text{H}_2\text{bta})_2](\text{NO}_3)_2$ 2.9	16	66	0	18	hard to ignite, no burning, smoke
$[\text{Cu}(\text{H}_2\text{bta})_2](\text{NO}_3)_2$ 2.10	18	55	9	18	green-yellow flame, easy to ignite, high velocity, unsteady flame, glowing residue
$[\text{Cu}(\text{H}_2\text{bta})_2](\text{NO}_3)_2$ 2.11	25	50	8	17	green flame, easy to ignite, high velocity, glowing residue

[Cu(H₂bta)₂](NO₃)₂_2.12	26	44	12	18	green flame, easy to ignite, moderate velocity, unsteady flame, glowing residue
[Cu(H₂bta)₂](NO₃)₂_2.13	28	48	9	15	no flame, smoke
[Cu(H₂bta)₂](NO₃)₂_2.14	29	43	14	14	did not burn
[Cu(H₂bta)₂](NO₃)₂_2.15	27	40	19	15	yellow-white flame, easy to ignite, less smoke, moderate velocity, glowing residue

Table 10.45 Pyrotechnic formulation containing **[Cu(H₂bta)₂](NO₃)₂** and copper(I) iodide.

	[Cu(H₂bta)₂](NO₃)₂	[Cu(bta)(NH₃)₂]	CuI	VAAR	observed behavior
	[wt%]	[wt%]	[wt%]	[wt%]	
[Cu(H₂bta)₂](NO₃)₂_3	44	35	11	10	easy to ignite, lifts off

Table 10.46 Pyrotechnic formulations containing **[Cu(H₂bta)₂](NO₃)₂** and **5-At**.

	[Cu(H₂bta)₂](NO₃)₂	5-At	VAAR	observed behavior
	[wt%]	[wt%]	[wt%]	
[Cu(H₂bta)₂](NO₃)₂_4.1	17	66	17	white-green flame, moderate to ignite, low velocity, less smoke, solid glowing residue
[Cu(H₂bta)₂](NO₃)₂_4.2	21	62	17	white-green flame, moderate to ignite, low velocity, less smoke, solid glowing residue
[Cu(H₂bta)₂](NO₃)₂_4.3	28	57	15	yellow-green flame, moderate to ignite, low velocity, less smoke, solid glowing residue

10.2.2.3 Pyrotechnic Compositions based on Diaqua bis(1-Methyl-5-amino-tetrazole-N₄) Copper(II) Nitrate ([Cu(1MeAt)₂(H₂O)₂(NO₃)₂])

In Table 10.47–Table 10.58 the different pyrotechnic compositions based on **[Cu(1MeAt)₂(H₂O)₂(NO₃)₂]** are given. The oxidizers potassium nitrate and potassium permanganate were used. The fuels **5-At**, sulfur, boron, zinc, magnesium, magnalium, copper(I) oxide, **[Cu(bta)(NH₃)₂]** and **[Cu(1MeAt)₄(H₂O)₂](NO₃)₂** were added.

Table 10.47 Pyrotechnic formulation containing $[\text{Cu}(\text{1MeAt})_2(\text{H}_2\text{O})_2(\text{NO}_3)_2]$ and potassium nitrate.

	$[\text{Cu}(\text{1MeAt})_2(\text{H}_2\text{O})_2(\text{NO}_3)_2]$ [wt%]	KNO_3 [wt%]	S [wt%]	VAAR [wt%]	observed behavior
$[\text{Cu}(\text{1MeAt})_2(\text{H}_2\text{O})_2(\text{NO}_3)_2]$ _1	11	69	11	9	orange flame, easy to ignite, less smoke, small amount of residues

Table 10.48 Pyrotechnic formulations containing $[\text{Cu}(\text{1MeAt})_2(\text{H}_2\text{O})_2(\text{NO}_3)_2]$ and potassium permanganate.

	$[\text{Cu}(\text{1MeAt})_2(\text{H}_2\text{O})_2(\text{NO}_3)_2]$ [wt%]	KMnO_4 [wt%]	S [wt%]	VAAR [wt%]	observed behavior
$[\text{Cu}(\text{1MeAt})_2(\text{H}_2\text{O})_2(\text{NO}_3)_2]$ _2.1	17	52	17	14	violet flame, easy to ignite, less smoke, small amount of residues
$[\text{Cu}(\text{1MeAt})_2(\text{H}_2\text{O})_2(\text{NO}_3)_2]$ _2.2	26	43	17	14	hard to ignite, no flame, glowing residue

Table 10.49 Pyrotechnic formulations containing $[\text{Cu}(\text{1MeAt})_2(\text{H}_2\text{O})_2(\text{NO}_3)_2]$ and magnalium.

	$[\text{Cu}(\text{1MeAt})_2(\text{H}_2\text{O})_2(\text{NO}_3)_2]$ [wt%]	MgAl [wt%]	VAAR [wt%]	observed behavior
$[\text{Cu}(\text{1MeAt})_2(\text{H}_2\text{O})_2(\text{NO}_3)_2]$ _3.1	81	2	17	yellow-green flame, easy to ignite, less smoke, glowing
$[\text{Cu}(\text{1MeAt})_2(\text{H}_2\text{O})_2(\text{NO}_3)_2]$ _3.2	67	17	16	green flame, less smoke, low velocity, glowing residue

Table 10.50 Pyrotechnic formulation containing $[\text{Cu}(\text{1MeAt})_2(\text{H}_2\text{O})_2(\text{NO}_3)_2]$ and sulfur.

	$[\text{Cu}(\text{1MeAt})_2(\text{H}_2\text{O})_2(\text{NO}_3)_2]$ [wt%]	S [wt%]	VAAR [wt%]	observed behavior
$[\text{Cu}(\text{1MeAt})_2(\text{H}_2\text{O})_2(\text{NO}_3)_2]$ _4	54	27	19	blue-green flame, no proper burning, much smoke, many residues

Table 10.51 Pyrotechnic formulation containing $[\text{Cu}(\text{1MeAt})_2(\text{H}_2\text{O})_2(\text{NO}_3)_2]$ and 5-At.

	$[\text{Cu}(\text{1MeAt})_2(\text{H}_2\text{O})_2(\text{NO}_3)_2]$ [wt%]	5-At [wt%]	VAAR [wt%]	observed behavior
$[\text{Cu}(\text{1MeAt})_2(\text{H}_2\text{O})_2(\text{NO}_3)_2]$ _5	63	21	16	green-yellow flame, easy to ignite, moderate velocity, no smoke, glowing residue

Table 10.52 Pyrotechnic formulations containing $[\text{Cu}(\text{1MeAt})_2(\text{H}_2\text{O})_2(\text{NO}_3)_2]$ and boron.

	$[\text{Cu}(\text{1MeAt})_2(\text{H}_2\text{O})_2(\text{NO}_3)_2]$ [wt%]	B [wt%]	VAAR [wt%]	observed behavior
$[\text{Cu}(\text{1MeAt})_2(\text{H}_2\text{O})_2(\text{NO}_3)_2]$ _6.1	72	9	19	green flame, easy to ignite, high velocity, sparks, no smoke, glowing residue
$[\text{Cu}(\text{1MeAt})_2(\text{H}_2\text{O})_2(\text{NO}_3)_2]$ _6.2	75	8	17	yellow flame, easy to ignite, high velocity, sparks, no smoke, glowing residue
$[\text{Cu}(\text{1MeAt})_2(\text{H}_2\text{O})_2(\text{NO}_3)_2]$ _6.3	73	10	17	yellow flame, easy to ignite, high velocity, sparks, no smoke, glowing residue

Table 10.53 Pyrotechnic formulations containing $[\text{Cu}(\text{1MeAt})_2(\text{H}_2\text{O})_2(\text{NO}_3)_2]$ and copper(I) iodide.

	$[\text{Cu}(\text{1MeAt})_2(\text{H}_2\text{O})_2(\text{NO}_3)_2]$ [wt%]	B [wt%]	CuI [wt%]	VAAR [wt%]	observed behavior
$[\text{Cu}(\text{1MeAt})_2(\text{H}_2\text{O})_2(\text{NO}_3)_2]$ _7.1	69	9	5	17	pale green-blue flame, easy to ignite, high velocity, less smoke, glowing residue
$[\text{Cu}(\text{1MeAt})_2(\text{H}_2\text{O})_2(\text{NO}_3)_2]$ _7.2	68	10	6	16	pale green flame, smoke, easy to ignite, high velocity, glowing residue

Table 10.54 Pyrotechnic formulations containing $[\text{Cu}(\text{1MeAt})_2(\text{H}_2\text{O})_2(\text{NO}_3)_2]$, magnesium, and boron.

	$[\text{Cu}(\text{1MeAt})_2(\text{H}_2\text{O})_2(\text{NO}_3)_2]$ [wt%]	B [wt%]	Mg [wt%]	VAAR [wt%]	observed behavior
$[\text{Cu}(\text{1MeAt})_2(\text{H}_2\text{O})_2(\text{NO}_3)_2]$ _8.1	68	9	9	14	pale green flame, easy to ignite, high velocity, sparks, small amount of solid residues white-green flame, easy to ignite, combusts violently, sparks, glowing residues
$[\text{Cu}(\text{1MeAt})_2(\text{H}_2\text{O})_2(\text{NO}_3)_2]$ _8.2	71	9	5	14	yellow flame, low velocity, less smoke, glowing residue
$[\text{Cu}(\text{1MeAt})_2(\text{H}_2\text{O})_2(\text{NO}_3)_2]$ _8.3	66	10	10	14	yellow flame, easy to ignite, moderate velocity, less smoke, glowing residue
$[\text{Cu}(\text{1MeAt})_2(\text{H}_2\text{O})_2(\text{NO}_3)_2]$ _8.4	68	10	8	14	yellow flame, easy to ignite, moderate velocity, less smoke, glowing residue

Table 10.55 Pyrotechnic formulations containing $[\text{Cu}(\text{1MeAt})_2(\text{H}_2\text{O})_2(\text{NO}_3)_2]$, boron, and zinc.

	$[\text{Cu}(\text{1MeAt})_2(\text{H}_2\text{O})_2(\text{NO}_3)_2]$ [wt%]	B [wt%]	Zn [wt%]	VAAR [wt%]	observed behavior
$[\text{Cu}(\text{1MeAt})_2(\text{H}_2\text{O})_2(\text{NO}_3)_2]$ _9.1	68	9	9	14	yellow flame, easy to ignite, moderate velocity, less smoke, glowing residue
$[\text{Cu}(\text{1MeAt})_2(\text{H}_2\text{O})_2(\text{NO}_3)_2]$ _9.2	69	8	8	15	yellow flame, easy to ignite, low velocity, less smoke, glowing residue
$[\text{Cu}(\text{1MeAt})_2(\text{H}_2\text{O})_2(\text{NO}_3)_2]$ _9.3	66	10	10	14	yellow flame, moderate velocity, less smoke, glowing residue

Table 10.56 Pyrotechnic formulations containing $[\text{Cu}(\text{1MeAt})_2(\text{H}_2\text{O})_2(\text{NO}_3)_2]$, $[\text{Cu}(\text{bta})(\text{NH}_3)_2]$, and boron

	$[\text{Cu}(\text{1MeAt})_2(\text{H}_2\text{O})_2(\text{NO}_3)_2]$ [wt%]	B [wt%]	$[\text{Cu}(\text{bta})(\text{NH}_3)_2]$ [wt%]	VAAR [wt%]	observed behavior
$[\text{Cu}(\text{1MeAt})_2(\text{H}_2\text{O})_2(\text{NO}_3)_2]$ _10.1	68	9	9	14	yellow-red flame, easy to ignite, moderate velocity, no smoke, glowing residue
$[\text{Cu}(\text{1MeAt})_2(\text{H}_2\text{O})_2(\text{NO}_3)_2]$ _10.2	70	8	8	14	yellow-white flame, easy to ignite, moderate velocity, no smoke, glowing residue

Table 10.57 Pyrotechnic formulations containing $[\text{Cu}(\text{1MeAt})_2(\text{H}_2\text{O})_2(\text{NO}_3)_2]$, boron, and $[\text{Cu}(\text{1MeAt})_4(\text{H}_2\text{O})_2(\text{NO}_3)_2]$.

	$[\text{Cu}(\text{1MeAt})_2(\text{H}_2\text{O})_2(\text{NO}_3)_2]$ [wt%]	B [wt%]	$[\text{Cu}(\text{1MeAt})_4(\text{H}_2\text{O})_2(\text{NO}_3)_2]$ [wt%]	VAAR [wt%]	observed behavior
$[\text{Cu}(\text{1MeAt})_2(\text{H}_2\text{O})_2(\text{NO}_3)_2]$ _11.1	66	10	10	14	yellow flame, easy to ignite, moderate velocity, glowing residue
$[\text{Cu}(\text{1MeAt})_2(\text{H}_2\text{O})_2(\text{NO}_3)_2]$ _11.2	61	14	9	16	yellow flame, low velocity, glowing residue
$[\text{Cu}(\text{1MeAt})_2(\text{H}_2\text{O})_2(\text{NO}_3)_2]$ _11.3	68	9	9	14	green-yellow flame, low velocity, glowing residue

[Cu(1MeAt)₂(H₂O)₂(NO₃)₂] _11.4	60	7	18	15	yellow flame, easy to ignite, moderate velocity, glowing residue
--	----	---	----	----	---

Table 10.58 Pyrotechnic formulation containing **[Cu(1MeAt)₂(H₂O)₂(NO₃)₂]**, boron, and sulfur.

	[Cu(1MeAt)₂(H₂O)₂(NO₃)₂] [wt%]	B [wt%]	S [wt%]	VAAR [wt%]	observed behavior
[Cu(1MeAt)₂(H₂O)₂(NO₃)₂] _12	68	9	9	14	yellow-red flame, easy to ignite, smoke, moderate velocity, glowing residue

10.2.2.4 Pyrotechnic Compositions based on Diaqua tetrakis(1-Methyl-5-amino-tetrazole-*N*4) Copper(II) Nitrate ([Cu(1MeAt)₄(H₂O)₂](NO₃)₂)

In Table 10.59–Table 10.63 the different pyrotechnic compositions based on **[Cu(1MeAt)₄(H₂O)₂](NO₃)₂** are given. The fuels sulfur, boron, copper(I) iodide, **[Cu(bta)(NH₃)₂]**, and **[Cu(1MeAt)₂(H₂O)₂(NO₃)₂]** were used. No oxidizers were added.

Table 10.59 Pyrotechnic formulations containing **[Cu(1MeAt)₄(H₂O)₂](NO₃)₂** and boron.

	[Cu(1MeAt)₄(H₂O)₂](NO₃)₂ [wt%]	B [wt%]	VAAR [wt%]	observed behavior
[Cu(1MeAt)₄(H₂O)₂](NO₃)₂] _1.1	77	10	13	yellow flame, easy to ignite, no smoke, low velocity, glowing residue
[Cu(1MeAt)₄(H₂O)₂](NO₃)₂] _1.2	83	5	11	green-white flame, easy to ignite, no smoke, low velocity, glowing residue
[Cu(1MeAt)₄(H₂O)₂](NO₃)₂] _1.3	85	4	9	green flame, combusts violently, no smoke, glowing residue
[Cu(1MeAt)₄(H₂O)₂](NO₃)₂] _1.4	85	5	10	pale green flame, easy to ignite, less smoke, mo- derate velocity, glowing resi- due

[Cu(1MeAt)₄(H₂O)₂](NO₃)₂_1.5	85	6	9	green-white flame, easy to ignite, less smoke, low velocity, glowing residue
[Cu(1MeAt)₄(H₂O)₂](NO₃)₂_1.6	86	5	9	green flame, easy to ignite, less smoke, moderate velocity, glowing residue

Table 10.60 Pyrotechnic formulations containing [Cu(1MeAt)₄(H₂O)₂](NO₃)₂ and copper(I) iodide.

	[Cu(1MeAt)₄(H₂O)₂](NO₃)₂ [wt%]	B [wt%]	CuI [wt%]	VAAR [wt%]	observed behavior
[Cu(1MeAt)₄(H₂O)₂](NO₃)₂_2.1	82	5	4	9	blue-green flame, easy to ignite, less smoke, moderate velocity, glowing residue
[Cu(1MeAt)₄(H₂O)₂](NO₃)₂_2.2	81	5	4	10	green-white flame, easy to ignite, less smoke, low velocity, glowing residue

Table 10.61 Pyrotechnic formulations containing [Cu(1MeAt)₄(H₂O)₂](NO₃)₂ and [Cu(bta)(NH₃)₂].

	[Cu(1MeAt)₄(H₂O)₂](NO₃)₂ [wt%]	[Cu(bta)NH₃]₂ [wt%]	VAAR [wt%]	observed behavior
[Cu(1MeAt)₄(H₂O)₂](NO₃)₂_3	77	10	13	green-white flame, moderate to ignite, no smoke, low velocity, glowing residue

Table 10.62 Pyrotechnic formulations containing $[\text{Cu}(\text{1MeAt})_4(\text{H}_2\text{O})_2](\text{NO}_3)_2$, $[\text{Cu}(\text{bta})(\text{NH}_3)_2]$, and boron.

	$[\text{Cu}(\text{1MeAt})_4(\text{H}_2\text{O})_2](\text{NO}_3)_2$ [wt%]	B [wt%]	$\text{Cu}(\text{bta})(\text{NH}_3)_2$ [wt%]	VAAR [wt%]	observed behavior
$[\text{Cu}(\text{1MeAt})_4(\text{H}_2\text{O})_2](\text{NO}_3)_2$ _4.1	68	10	8	14	green-yellow flame, easy to ignite, no smoke, low velocity, glowing residue
$[\text{Cu}(\text{1MeAt})_4(\text{H}_2\text{O})_2](\text{NO}_3)_2$ _4.2	62	16	8	14	green-white flame, easy to ignite, less smoke, low velocity, glowing residue

Table 10.63 Pyrotechnic formulations containing $[\text{Cu}(\text{1MeAt})_4(\text{H}_2\text{O})_2](\text{NO}_3)_2$, boron, and sulfur.

	$[\text{Cu}(\text{1MeAt})_4(\text{H}_2\text{O})_2](\text{NO}_3)_2$ [wt%]	B [wt%]	S [wt%]	VAAR [wt%]	observed behavior
$[\text{Cu}(\text{1MeAt})_4(\text{H}_2\text{O})_2](\text{NO}_3)_2$ _5.1	67	8	8	17	yellow-green flame, easy to ignite, less smoke, moderate velocity, glowing residue
$[\text{Cu}(\text{1MeAt})_4(\text{H}_2\text{O})_2](\text{NO}_3)_2$ _5.2	71	11	4	14	white flame, easy to ignite, less smoke, low velocity, glowing residue
$[\text{Cu}(\text{1MeAt})_4(\text{H}_2\text{O})_2](\text{NO}_3)_2$ _5.3	72	4	9	15	yellow-green flame, easy to ignite, smoke, low velocity, glowing residue

10.2.2.5 Pyrotechnic Compositions based on Diammine bis(1-Methyl-5-nitrimino-tetrazolato- $\kappa^2N4, O1$) Copper(II) ($[\text{Cu}(\text{1MeAtNO}_2)_2(\text{NH}_3)_2]$)

In Table 10.64–Table 10.69, the different pyrotechnic compositions based on $[\text{Cu}(\text{1MeAtNO}_2)_2(\text{NH}_3)_2]$ are given. The fuels **5-At**, **5-At_H₂O**, boron, copper(I) iodide, $[\text{Cu}(\text{bta})(\text{NH}_3)_2]$, and tetraaqua 3,3'-bis(1,2,4-oxadiazol-5-onate) copper(II) ($[\text{Cu}(\text{H}_2\text{O})_4(\text{OD})]$) were used. ($[\text{Cu}(\text{H}_2\text{O})_4(\text{OD})]$ was prepared by N. MAYR.) No oxidizers were added.

Table 10.64 Pyrotechnic formulations containing $[\text{Cu}(\text{1MeAtNO}_2)_2(\text{NH}_3)_2]$ and **5-At**.

	$[\text{Cu}(\text{1MeAtNO}_2)_2(\text{NH}_3)_2]$ [wt%]	5-At [wt%]	VAAR [wt%]	observed behavior
$[\text{Cu}(\text{1MeAtNO}_2)_2(\text{NH}_3)_2]$ _1.1	44	44	12	yellow-green flame, easy to ignite, moderate velocity, small amount of solid residues
$[\text{Cu}(\text{1MeAtNO}_2)_2(\text{NH}_3)_2]$ _1.2	54	36	10	yellow-green flame, easy to ignite, moderate velocity, almost no solid residues
$[\text{Cu}(\text{1MeAtNO}_2)_2(\text{NH}_3)_2]$ _1.3	60	30	10	green, partly yellow flame, easy to ignite, moderate velocity, no smoke, almost no solid residues
$[\text{Cu}(\text{1MeAtNO}_2)_2(\text{NH}_3)_2]$ _1.4	65	25	10	yellow-green flame, easy to ignite, moderate velocity, almost no solid residues

Table 10.65 Pyrotechnic formulation containing $[\text{Cu}(\text{1MeAtNO}_2)_2(\text{NH}_3)_2]$ and **5-At_H₂O**.

	$[\text{Cu}(\text{1MeAtNO}_2)_2(\text{NH}_3)_2]$ [wt%]	5-At_H₂O [wt%]	VAAR [wt%]	observed behavior
$[\text{Cu}(\text{1MeAtNO}_2)_2(\text{NH}_3)_2]$ _2	60	30	10	yellow-green flame, easy to ignite, moderate velocity, almost no solid residues

Table 10.66 Pyrotechnic formulations containing $[\text{Cu}(\text{1MeAtNO}_2)_2(\text{NH}_3)_2]$ and boron.

	$[\text{Cu}(\text{1MeAtNO}_2)_2(\text{NH}_3)_2]$ [wt%]	B [wt%]	VAAR [wt%]	observed behavior
$[\text{Cu}(\text{1MeAtNO}_2)_2(\text{NH}_3)_2]$ _3.1	86	3	11	yellow flame, easy to ignite, moderate velocity, less smoke, glowing residues
$[\text{Cu}(\text{1MeAtNO}_2)_2(\text{NH}_3)_2]$ _3.2	83	4	13	yellow flame, easy to ignite, moderate velocity, smoke, glowing residues
$[\text{Cu}(\text{1MeAtNO}_2)_2(\text{NH}_3)_2]$ _3.3	83	5	12	yellow-green flame, easy to ignite, burns too violently, less smoke, glowing residues
$[\text{Cu}(\text{1MeAtNO}_2)_2(\text{NH}_3)_2]$ _3.4	80	7	13	yellow-green flame, easy to ignite, moderate velocity, smoke, glowing residues

Table 10.67 Pyrotechnic formulations containing $[\text{Cu}(\text{1MeAtNO}_2)_2(\text{NH}_3)_2]$, boron, and copper(I) iodide.

	$[\text{Cu}(\text{1MeAtNO}_2)_2(\text{NH}_3)_2]$ [wt%]	B [wt%]	CuI [wt%]	VAAR [wt%]	observed behavior
$[\text{Cu}(\text{1MeAtNO}_2)_2(\text{NH}_3)_2]$ _4.1	71	12	5	12	yellow flame, easy to ignite, low velocity, smoke, glowing residues
$[\text{Cu}(\text{1MeAtNO}_2)_2(\text{NH}_3)_2]$ _4.2	72	7	7	14	yellow flame, easy to ignite, moderate velocity, glowing residues, smoke
$[\text{Cu}(\text{1MeAtNO}_2)_2(\text{NH}_3)_2]$ _4.3	77	5	5	13	yellow flame, moderate to ignite, moderate velocity, smoke, glowing residues
$[\text{Cu}(\text{1MeAtNO}_2)_2(\text{NH}_3)_2]$ _4.4	80	4	4	12	white-green flame, easy to ignite, moderate velocity, smoke, glowing residues

Table 10.68 Pyrotechnic formulations containing $[\text{Cu}(\text{1MeAtNO}_2)_2(\text{NH}_3)_2]$ and $[\text{Cu}(\text{bta})(\text{NH}_3)_2]$.

	$[\text{Cu}(\text{1MeAtNO}_2)_2(\text{NH}_3)_2]$ [wt%]	B [wt%]	$[\text{Cu}(\text{bta})(\text{NH}_3)_2]$ [wt%]	VAAR [wt%]	observed behavior
$[\text{Cu}(\text{1MeAtNO}_2)_2(\text{NH}_3)_2]$ _5.1	58	3	29	10	white flame, easy to ignite, moderate velocity, glowing residues, smoke
$[\text{Cu}(\text{1MeAtNO}_2)_2(\text{NH}_3)_2]$ _5.2	63	3	23	11	white flame, easy to ignite, moderate velocity, less smoke, glowing residues
$[\text{Cu}(\text{1MeAtNO}_2)_2(\text{NH}_3)_2]$ _5.3	62	3	25	10	green-yellow flame, easy to ignite, moderate velocity, smoke, glowing residues

[Cu(1MeAtNO₂)₂(NH₃)₂] _5.4	60	0	30	10	yellow flame, unsteady burning, glowing residues
---	----	---	----	----	--

Table 10.69 Pyrotechnic formulations containing **[Cu(1MeAtNO₂)₂(NH₃)₂]**, **5-At**, and **[Cu(H₂O)₄OD]**.

	[Cu(1MeAtNO₂)₂(NH₃)₂] [wt%]	[Cu(H₂O)₄OD] [wt%]	5-At [wt%]	VAAR [wt%]	observed behavior
[Cu(1MeAtNO₂)₂(NH₃)₂] _6.1	47	38	5	10	yellow flame, hard to ignite, less smoke, low velocity, large residue
[Cu(1MeAtNO₂)₂(NH₃)₂] _6.2	60	30	0	10	cannot be ignited

10.2.2.6 Pyrotechnic Compositions based on Bis(triammine) μ_2 -(5-Nitrimino-tetrazolato) Dicopper(II) (**[Cu(AtNO₂)(NH₃)₃]₂**)

In Table 10.70–Table 10.72 the different pyrotechnic compositions based on **[Cu(AtNO₂)(NH₃)₃]₂** are given. The fuels **5-At**, boron, and magnesium were used. No oxidizers were added.

Table 10.70 Pyrotechnic formulations containing **[Cu(AtNO₂)(NH₃)₃]₂** and **5-At**.

	[Cu(AtNO₂)(NH₃)₃]₂ [wt%]	5-At [wt%]	VAAR [wt%]	observed behavior
[Cu(AtNO₂)(NH₃)₃]₂ _1.1	52	39	9	short-lasting green flame, hard to ignite, low velocity, glowing residue
[Cu(AtNO₂)(NH₃)₃]₂ _1.2	68	23	9	yellow flame, hard to ignite, smoke, low velocity, glowing residue

Table 10.71 Pyrotechnic formulations containing **[Cu(AtNO₂)(NH₃)₃]₂** and boron.

	[Cu(AtNO₂)(NH₃)₃]₂ [wt%]	B [wt%]	VAAR [wt%]	observed behavior
[Cu(AtNO₂)(NH₃)₃]₂ _2.1	77	13	10	small yellow flame, hard to ignite, less smoke, low velocity, glowing residue
[Cu(AtNO₂)(NH₃)₃]₂ _2.2	87	3	10	no flame, glowing with much smoke
[Cu(AtNO₂)(NH₃)₃]₂ _2.3	82	8	10	short-lasting yellow flame, hard to ignite, less smoke, low velocity, glowing residue

Table 10.72 Pyrotechnic formulation containing $[\text{Cu}(\text{AtNO}_2)(\text{NH}_3)_3]_2$ and magnesium.

	$[\text{Cu}(\text{AtNO}_2)(\text{NH}_3)_3]_2$ [wt%]	B [wt%]	Mg [wt%]	VAAR [wt%]	observed behavior
$[\text{Cu}(\text{AtNO}_2)(\text{NH}_3)_3]_2_3$	84	3	3	10	yellow flame, hard to ignite, less smoke, low velocity, glowing residue

10.2.2.7 Pyrotechnic Compositions based on Basic Copper(II) Nitrate ($\text{Cu}_2(\text{OH})_3(\text{NO}_3)$)

In Table 10.73–Table 10.80 the different pyrotechnic compositions based on $\text{Cu}_2(\text{OH})_3(\text{NO}_3)$ are given. The fuels **5-At**, magnesium, magnalium, sulfur, aluminum, boron, titanium, and silicon were used. No oxidizers were added.

Table 10.73 Pyrotechnic formulations containing $\text{Cu}_2(\text{OH})_3(\text{NO}_3)$ and **5-At**.

	$\text{Cu}_2(\text{OH})_3(\text{NO}_3)$ [wt%]	5-At [wt%]	VAAR [wt%]	observed behavior
$\text{Cu}_2(\text{OH})_3(\text{NO}_3)_1.1$	35	52	13	no flame, easy to ignite, slowly glowing, much smoke
$\text{Cu}_2(\text{OH})_3(\text{NO}_3)_1.2$	42	42	16	no flame, easy to ignite, slowly glowing, much smoke

Table 10.74 Pyrotechnic formulations containing $\text{Cu}_2(\text{OH})_3(\text{NO}_3)$ and magnesium.

	$\text{Cu}_2(\text{OH})_3(\text{NO}_3)$ [wt%]	Mg [wt%]	VAAR [wt%]	observed behavior
$\text{Cu}_2(\text{OH})_3(\text{NO}_3)_2.1$	77	8	15	green-yellow flame, hard to ignite, no smoke, Mg sparks, small amount of glowing residues
$\text{Cu}_2(\text{OH})_3(\text{NO}_3)_2.2$	54	28	18	very hard to ignite, white flame after deceleration
$\text{Cu}_2(\text{OH})_3(\text{NO}_3)_2.3$	42	42	16	white-green flame, hard to ignite, moderate velocity, no smoke, almost no residues
$\text{Cu}_2(\text{OH})_3(\text{NO}_3)_2.4$	71	15	14	white-green flame, Mg sparks, less smoke, small amount of solid residues

Table 10.75 Pyrotechnic formulation containing $\text{Cu}_2(\text{OH})_3(\text{NO}_3)$ and magnalium.

	$\text{Cu}_2(\text{OH})_3(\text{NO}_3)$ [wt%]	MgAl [wt%]	VAAR [wt%]	observed behavior
$\text{Cu}_2(\text{OH})_3(\text{NO}_3)_3$	53	27	20	white flame, hard to ignite, less smoke, moderate velocity, small amount of solid residues

Table 10.76 Pyrotechnic formulations containing $\text{Cu}_2(\text{OH})_3(\text{NO}_3)$ and sulfur.

	$\text{Cu}_2(\text{OH})_3(\text{NO}_3)$ [wt%]	S [wt%]	VAAR [wt%]	observed behavior
$\text{Cu}_2(\text{OH})_3(\text{NO}_3)$ _4.1	77	8	15	cannot be ignited
$\text{Cu}_2(\text{OH})_3(\text{NO}_3)$ _4.2	42	42	16	cannot be ignited

Table 10.77 Pyrotechnic formulations containing $\text{Cu}_2(\text{OH})_3(\text{NO}_3)$ and aluminum.

	$\text{Cu}_2(\text{OH})_3(\text{NO}_3)$ [wt%]	Al [wt%]	VAAR [wt%]	observed behavior
$\text{Cu}_2(\text{OH})_3(\text{NO}_3)$ _5.1	77	8 (grid)	15	green-white flame, much smoke, no self-consistent burning, glowing residue
$\text{Cu}_2(\text{OH})_3(\text{NO}_3)$ _5.2	55	28 (powder)	17	green-white flame, much smoke, no self-consistent burning, glowing residue

Table 10.78 Pyrotechnic formulations containing $\text{Cu}_2(\text{OH})_3(\text{NO}_3)$ and boron.

	$\text{Cu}_2(\text{OH})_3(\text{NO}_3)$ [wt%]	B [wt%]	VAAR [wt%]	observed behavior
$\text{Cu}_2(\text{OH})_3(\text{NO}_3)$ _6.1	77	8	15	green-yellow flame, less smoke, no self-consistent burning, glowing residue
$\text{Cu}_2(\text{OH})_3(\text{NO}_3)$ _6.2	56	29	15	yellow flame, less smoke, moderate velocity, glowing residue
$\text{Cu}_2(\text{OH})_3(\text{NO}_3)$ _6.3	69	17	14	yellow-red flame, less smoke, low velocity, glowing residue

Table 10.79 Pyrotechnic formulation containing $\text{Cu}_2(\text{OH})_3(\text{NO}_3)$ and titanium.

	$\text{Cu}_2(\text{OH})_3(\text{NO}_3)$ [wt%]	Ti [wt%]	VAAR [wt%]	observed behavior
$\text{Cu}_2(\text{OH})_3(\text{NO}_3)$ _7	57	29	14	colors lighter flame green, hard to ignite, no self-consistent burning, smoke, glowing residue

Table 10.80 Pyrotechnic formulation containing $\text{Cu}_2(\text{OH})_3(\text{NO}_3)$ and silicon.

	$\text{Cu}_2(\text{OH})_3(\text{NO}_3)$ [wt%]	Si [wt%]	VAAR [wt%]	observed behavior
$\text{Cu}_2(\text{OH})_3(\text{NO}_3)$ _8	57	28	15	hard to ignite, no self-consistent burning, smoke, glowing residue

10.2.2.8 Pyrotechnic Compositions based on Tetrammine Copper(II) Dinitramide ([Cu(NH₃)₄][N(NO₂)₂]₂)

In Table 10.81–Table 10.97 the different pyrotechnic compositions based on [Cu(NH₃)₄][N(NO₂)₂]₂ are given. The fuels **5-At**, **5-At_H₂O**, boron, magnesium, sulfur, copper(II) sulfate pentahydrate, basic copper(II) nitrate, [Cu(bta)(NH₃)₂], and [Cu(1MeAt)₂(H₂O)₂(NO₃)₂] were used. No oxidizers were added. The addition of urea should achieve more thermal stable compositions.

Table 10.81 Pyrotechnic formulation containing [Cu(NH₃)₄][N(NO₂)₂]₂ and **5-At**.

	[Cu(NH ₃) ₄][N(NO ₂) ₂] ₂ [wt%]	5-At [wt%]	VAAR [wt%]	observed behavior
[Cu(NH ₃) ₄][N(NO ₂) ₂] _{2_1}	54	36	10	green-yellow flame, easy to ignite, less smoke, small amount of solid residues

Table 10.82 Pyrotechnic formulations containing [Cu(NH₃)₄][N(NO₂)₂]₂, **5-At**, and urea.

	[Cu(NH ₃) ₄][N(NO ₂) ₂] ₂ [wt%]	5-At [wt%]	Urea [wt%]	VAAR [wt%]	observed behavior
[Cu(NH ₃) ₄][N(NO ₂) ₂] _{2_2.1}	59	30	1	10	green-yellow flame, red frame, easy to ignite, less smoke, small amount of solid residues
[Cu(NH ₃) ₄][N(NO ₂) ₂] _{2_2.2}	64	26	1	9	green-yellow flame, red frame, easy to ignite, less smoke, small amount of glowing residues
[Cu(NH ₃) ₄][N(NO ₂) ₂] _{2_2.3}	67	22	1	9	green flame, red frame, easy to ignite, less smoke, almost no glowing residues
[Cu(NH ₃) ₄][N(NO ₂) ₂] _{2_2.4}	70	20	1	9	green flame, red frame, easy to ignite, less smoke, small amount of glowing residues

Table 10.83 Pyrotechnic formulation containing [Cu(NH₃)₄][N(NO₂)₂]₂, **5-At_H₂O**, and urea.

	[Cu(NH ₃) ₄][N(NO ₂) ₂] ₂ [wt%]	5-At_H₂O [wt%]	Urea [wt%]	VAAR [wt%]	observed behavior
[Cu(NH ₃) ₄][N(NO ₂) ₂] _{2_3}	66	24	1	9	green-yellow-red flame, easy to ignite, less smoke, glowing residues

Table 10.84 Pyrotechnic formulations containing $[\text{Cu}(\text{NH}_3)_4][\text{N}(\text{NO}_2)_2]_2$ and $[\text{Cu}(\text{1MeAt})_2(\text{H}_2\text{O})_2(\text{NO}_3)_2]$.

	$[\text{Cu}(\text{NH}_3)_4][\text{N}(\text{NO}_2)_2]_2$ [wt%]	$[\text{Cu}(\text{1MeAt})_2(\text{H}_2\text{O})_2(\text{NO}_3)_2]$ [wt%]	VAAR [wt%]	observed behavior
$[\text{Cu}(\text{NH}_3)_4][\text{N}(\text{NO}_2)_2]_2$ _4.1	61	30	9	yellow-green flame, easy to ignite, less smoke, no residues
$[\text{Cu}(\text{NH}_3)_4][\text{N}(\text{NO}_2)_2]_2$ _4.2	55	36	9	yellow-green flame, easy to ignite, smoke, glowing residue
$[\text{Cu}(\text{NH}_3)_4][\text{N}(\text{NO}_2)_2]_2$ _4.3	68	22	10	yellow-green-red flame, easy to ignite, less smoke, glowing residue

Table 10.85 Pyrotechnic formulations containing $[\text{Cu}(\text{NH}_3)_4][\text{N}(\text{NO}_2)_2]_2$, $[\text{Cu}(\text{1MeAt})_2(\text{H}_2\text{O})_2(\text{NO}_3)_2]$, urea, and 5-At.

	$[\text{Cu}(\text{NH}_3)_4][\text{N}(\text{NO}_2)_2]_2$ [wt%]	$[\text{Cu}(\text{1MeAt})_2(\text{H}_2\text{O})_2(\text{NO}_3)_2]$ [wt%]	5-At [wt%]	Urea [wt%]	VAAR [wt%]	observed behavior
$[\text{Cu}(\text{NH}_3)_4][\text{N}(\text{NO}_2)_2]_2$ _5.1	53	18	18	1	10	green flame, less smoke, almost no glowing residue
$[\text{Cu}(\text{NH}_3)_4][\text{N}(\text{NO}_2)_2]_2$ _5.2	57	16	16	1	10	yellow-green flame, glowing residue
$[\text{Cu}(\text{NH}_3)_4][\text{N}(\text{NO}_2)_2]_2$ _5.3	60	15	15	1	9	yellow-green flame, glowing residue

Table 10.86 Pyrotechnic formulations containing $[\text{Cu}(\text{NH}_3)_4][\text{N}(\text{NO}_2)_2]_2$ and $[\text{Cu}(\text{bta})(\text{NH}_3)_2]$.

	$[\text{Cu}(\text{NH}_3)_4][\text{N}(\text{NO}_2)_2]_2$ [wt%]	$[\text{Cu}(\text{bta})(\text{NH}_3)_2]$ [wt%]	Urea [wt%]	VAAR [wt%]	observed behavior
$[\text{Cu}(\text{NH}_3)_4][\text{N}(\text{NO}_2)_2]_2$ _6.1	68	22	1	9	green-yellow flame, red frame, easy to ignite, less smoke, small amount of glowing residues
$[\text{Cu}(\text{NH}_3)_4][\text{N}(\text{NO}_2)_2]_2$ _6.2	64	26	1	9	green-yellow flame, red frame, moderate to ignite, smoke, small amount of glowing residues

Table 10.87 Pyrotechnic formulations containing $[\text{Cu}(\text{NH}_3)_4][\text{N}(\text{NO}_2)_2]_2$, $[\text{Cu}(\text{bta})(\text{NH}_3)_2]$, and $[\text{Cu}(\text{1MeAt})_2(\text{H}_2\text{O})_2(\text{NO}_3)_2]$.

	$[\text{Cu}(\text{NH}_3)_4][\text{N}(\text{NO}_2)_2]_2$ [wt%]	$[\text{Cu}(\text{bta})(\text{NH}_3)_2]$ [wt%]	$[\text{Cu}(\text{1MeAt})_2(\text{H}_2\text{O})_2(\text{NO}_3)_2]$ [wt%]	VAAR [wt%]	observed behavior
$[\text{Cu}(\text{NH}_3)_4][\text{N}(\text{NO}_2)_2]_2$ _7.1	61	10	20	9	white flame, red frame, no residue
$[\text{Cu}(\text{NH}_3)_4][\text{N}(\text{NO}_2)_2]_2$ _7.2	45	23	23	9	green-yellow flame, red frame, glowing residue

Table 10.88 Pyrotechnic formulations containing $[\text{Cu}(\text{NH}_3)_4][\text{N}(\text{NO}_2)_2]_2$, $[\text{Cu}(\text{bta})(\text{NH}_3)_2]$, $[\text{Cu}(\text{1MeAt})_2(\text{H}_2\text{O})_2(\text{NO}_3)_2]$, and boron.

	$[\text{Cu}(\text{NH}_3)_4][\text{N}(\text{NO}_2)_2]_2$ [wt%]	$[\text{Cu}(\text{bta})(\text{NH}_3)_2]$ [wt%]	$[\text{Cu}(\text{1MeAt})_2(\text{H}_2\text{O})_2(\text{NO}_3)_2]$ [wt%]	B [wt%]	VAAR [wt%]	observed behavior
$[\text{Cu}(\text{NH}_3)_4][\text{N}(\text{NO}_2)_2]_2$ _8.1	26	26	26	13	9	green-yellow-red flame, sparks, glowing residue
$[\text{Cu}(\text{NH}_3)_4][\text{N}(\text{NO}_2)_2]_2$ _8.2	43	21	21	5	10	green flame, too vigorous, glowing residue
$[\text{Cu}(\text{NH}_3)_4][\text{N}(\text{NO}_2)_2]_2$ _8.3	14	24	48	6	8	green-red flame, glowing residue
$[\text{Cu}(\text{NH}_3)_4][\text{N}(\text{NO}_2)_2]_2$ _8.4	16	27	41	6	10	white-red flame, glowing residue
$[\text{Cu}(\text{NH}_3)_4][\text{N}(\text{NO}_2)_2]_2$ _8.5	12	24	49	6	9	yellow flame, glowing residue

Table 10.89 Pyrotechnic formulations containing $[\text{Cu}(\text{NH}_3)_4][\text{N}(\text{NO}_2)_2]_2$ and boron.

	$[\text{Cu}(\text{NH}_3)_4][\text{N}(\text{NO}_2)_2]_2$ [wt%]	B [wt%]	Urea [wt%]	VAAR [wt%]	observed behavior
$[\text{Cu}(\text{NH}_3)_4][\text{N}(\text{NO}_2)_2]_2$ _9.1	73	18	0	9	white-green flame, red frame, easy to ignite, high velocity, less smoke, glowing residue
$[\text{Cu}(\text{NH}_3)_4][\text{N}(\text{NO}_2)_2]_2$ _9.2	60	30	1	9	yellow flame, easy to ignite, moderate velocity, less smoke, glowing residue
$[\text{Cu}(\text{NH}_3)_4][\text{N}(\text{NO}_2)_2]_2$ _9.3	77	13	1	9	green flame, easy to ignite, high velocity, less smoke, some sparks, glowing residue

[Cu(NH₃)₄][N(NO₂)₂]₂_9.4	80	11	0	9	green flame, sparks, lifts off
[Cu(NH₃)₄][N(NO₂)₂]₂_9.5	78	12	0	10	green flame, easy to ignite, high velocity, less smoke, some sparks, glowing residue
[Cu(NH₃)₄][N(NO₂)₂]₂_9.6	79	13	0	8	green flame, red frame, lifts off, glowing residues
[Cu(NH₃)₄][N(NO₂)₂]₂_9.7	76	14	0	9	green flame, easy to ignite, sparks, too violently
[Cu(NH₃)₄][N(NO₂)₂]₂_9.8	75	15	0	10	green flame, red frame, easy to ignite, sparks, too violently
[Cu(NH₃)₄][N(NO₂)₂]₂_9.9	77	13	0	10	green flame, red frame, easy to ignite, high velocity, less smoke, sparks, glowing residue
[Cu(NH₃)₄][N(NO₂)₂]₂_9.10	74	16	0	10	yellow-green flame, easy to ignite, moderate velocity, less smoke, sparks, glowing residue

Table 10.90 Pyrotechnic formulations containing **[Cu(NH₃)₄][N(NO₂)₂]₂**, magnesium, and boron.

	[Cu(NH₃)₄][N(NO₂)₂]₂ [wt%]	B [wt%]	Mg [wt%]	VAAR [wt%]	observed behavior
[Cu(NH₃)₄][N(NO₂)₂]₂_10.1	77	7	7	9	easy to ignite, sparks, lifts off
[Cu(NH₃)₄][N(NO₂)₂]₂_10.2	73	9	9	9	easy to ignite, sparks, lifts off, glowing residues
[Cu(NH₃)₄][N(NO₂)₂]₂_10.3	60	15	15	10	green flame, easy to ignite, sparks, high velocity, less smoke, glowing residues
[Cu(NH₃)₄][N(NO₂)₂]₂_10.4	58	17	15	10	yellow flame, easy to ignite, sparks, moderate velocity, less smoke, glowing residues
[Cu(NH₃)₄][N(NO₂)₂]₂_10.5	58	16	16	10	yellow flame, easy to ignite, sparks, moderate velocity, less smoke, glowing residues
[Cu(NH₃)₄][N(NO₂)₂]₂_10.6	59	16	16	9	green-yellow flame, easy to ignite, sparks, moderate velocity, less smoke, glowing residues

Pyrotechnic Compositions Containing Nitrogen-rich Copper(II) Compounds

[Cu(NH₃)₄][N(NO₂)₂]₂ 10.7	61	16	13	10	green-yellow flame, easy to ignite, sparks, moderate velocity, less smoke, glowing residues
---	----	----	----	----	---

Table 10.91 Pyrotechnic formulations containing [Cu(NH₃)₄][N(NO₂)₂]₂, [Cu(bta)(NH₃)₂], magnesium, and boron.

	[Cu(NH₃)₄][N(NO₂)₂]₂ [wt%]	[Cu(bta)(NH₃)₂] [wt%]	B [wt%]	Mg [wt%]	VAAR [wt%]	observed behavior
[Cu(NH₃)₄][N(NO₂)₂]₂ 11.1	51	13	13	13	10	green flame, easy to ignite, high velocity, less smoke, sparks, small amount of glowing residues
[Cu(NH₃)₄][N(NO₂)₂]₂ 11.2	46	23	11	11	9	green-yellow flame, easy to ignite, high velocity, less smoke, sparks, small amount of glowing residues
[Cu(NH₃)₄][N(NO₂)₂]₂ 11.3	49	15	13	13	10	green flame, easy to ignite, high velocity, less smoke, sparks, small amount of glowing residues

Table 10.92 Pyrotechnic formulations containing [Cu(NH₃)₄][N(NO₂)₂]₂, copper(II) sulfate pentahydrate, magnesium, and boron.

	[Cu(NH₃)₄][N(NO₂)₂]₂ [wt%]	CuSO₄ · 5H₂O [wt%]	B [wt%]	Mg [wt%]	VAAR [wt%]	observed behavior
[Cu(NH₃)₄][N(NO₂)₂]₂ 12.1	51	13	13	13	10	green-yellow flame, easy to ignite, high velocity, smoke, sparks, glowing residues

[Cu(NH₃)₄][N(NO₂)₂]₂_12.2	57	6	14	14	9	green flame, easy to ignite, high velocity, smoke, sparks, almost no glowing residues
[Cu(NH₃)₄][N(NO₂)₂]₂_12.3	55	8	14	14	19	green-yellow flame, easy to ignite, smoke, sparks, glowing residues

Table 10.93 Pyrotechnic formulations containing **[Cu(NH₃)₄][N(NO₂)₂]₂**, basic copper(II) carbonate, magnesium, and boron

	[Cu(NH₃)₄][N(NO₂)₂]₂ [wt%]	CuCO₃ · Cu(OH)₂ [wt%]	B [wt%]	Mg [wt%]	VAAR [wt%]	observed behavior
[Cu(NH₃)₄][N(NO₂)₂]₂_13.1	57	6	14	14	9	green-yellow flame, sparks, less smoke, glowing residues
[Cu(NH₃)₄][N(NO₂)₂]₂_13.2	55	6	15	15	9	white flame, less smoke, sparks, almost no glowing residues
[Cu(NH₃)₄][N(NO₂)₂]₂_13.3	52	6	16	16	10	yellow flame, moderate velocity, glowing residues
[Cu(NH₃)₄][N(NO₂)₂]₂_13.4	52	9	15	15	9	green-yellow flame, sparks, less smoke, glowing residues

Table 10.94 Pyrotechnic formulations containing **[Cu(NH₃)₄][N(NO₂)₂]₂**, boron, and **[Cu(1MeAt)₂(H₂O)₂(NO₃)₂]**.

	[Cu(NH₃)₄][N(NO₂)₂]₂ [wt%]	[Cu(1MeAt)₂(H₂O)₂(NO₃)₂] [wt%]	B [wt%]	VAAR [wt%]	observed behavior
[Cu(NH₃)₄][N(NO₂)₂]₂_14.1	56	19	17	9	yellow flame, moderate velocity, glowing residues
[Cu(NH₃)₄][N(NO₂)₂]₂_14.2	48	16	26	10	yellow-green flame, glowing residues

Pyrotechnic Compositions Containing Nitrogen-rich Copper(II) Compounds

[Cu(NH₃)₄][N(NO₂)₂]₂_14.3	45	15	30	10	white-green flame, smoke, glowing residues
[Cu(NH₃)₄][N(NO₂)₂]₂_14.4	42	16	32	10	white-green flame, smoke, glowing residues
[Cu(NH₃)₄][N(NO₂)₂]₂_14.5	22	22	45	11	yellow flame, low velocity, glowing residue
[Cu(NH₃)₄][N(NO₂)₂]₂_14.6	47	32	12	9	white-green flame, too violently, small amount of glowing residues
[Cu(NH₃)₄][N(NO₂)₂]₂_14.7	32	43	16	9	green-yellow-red flame, high velocity, less smoke, small amount of glowing residues, sparks
[Cu(NH₃)₄][N(NO₂)₂]₂_14.8	36	36	18	10	green flame, lifts off
[Cu(NH₃)₄][N(NO₂)₂]₂_14.9	35	35	20	10	green-yellow flame, less smoke, glowing residues, sparks
[Cu(NH₃)₄][N(NO₂)₂]₂_14.10	34	34	22	10	green flame, less smoke, high, velocity, glowing residues, sparks

Table 10.95 Pyrotechnic formulations containing [Cu(NH₃)₄][N(NO₂)₂]₂, boron, and zinc.

	[Cu(NH₃)₄][N(NO₂)₂]₂ [wt%]	B [wt%]	Zn [wt%]	VAAR [wt%]	observed behavior
[Cu(NH₃)₄][N(NO₂)₂]₂_15.1	60	15	15	10	green flame, too violently, sparks, glowing residues
[Cu(NH₃)₄][N(NO₂)₂]₂_15.2	58	16	16	10	yellow-red flame, easy to ignite, smoke, glowing residue

Table 10.96 Pyrotechnic formulations containing [Cu(NH₃)₄][N(NO₂)₂]₂, [Cu(bta)(NH₃)₂], and boron.

	[Cu(NH₃)₄][N(NO₂)₂]₂ [wt%]	[Cu(bta)(NH₃)₂] [wt%]	B [wt%]	VAAR [wt%]	observed behavior
[Cu(NH₃)₄][N(NO₂)₂]₂_16.1	57	17	17	9	yellow-green flame, easy to ignite, less smoke, sparks, glowing residue
[Cu(NH₃)₄][N(NO₂)₂]₂_16.2	58	16	16	10	yellow flame, easy to ignite, less smoke, glowing residue

[Cu(NH₃)₄][N(NO₂)₂]₂_16.3	66	16	8	10	green-white flame, easy to ignite, high velocity, no smoke, sparks, small amount of glowing residues
[Cu(NH₃)₄][N(NO₂)₂]₂_16.4	64	18	9	9	green flame, easy to ignite, high velocity, no smoke, small amount of glowing residues
[Cu(NH₃)₄][N(NO₂)₂]₂_16.5	63	19	9	9	green flame, easy to ignite, too violently, no smoke, small amount of glowing residues
[Cu(NH₃)₄][N(NO₂)₂]₂_16.6	61	19	10	10	green-yellow flame, easy to ignite, no smoke, some sparks, glowing residues
[Cu(NH₃)₄][N(NO₂)₂]₂_16.7	58	24	8	10	green-white flame, too violently, no smoke, sparks, small amount of glowing residues
[Cu(NH₃)₄][N(NO₂)₂]₂_16.8	54	30	7	9	green-white flame, too violently, less smoke, small amount of glowing residues
[Cu(NH₃)₄][N(NO₂)₂]₂_16.9	55	28	8	9	green-yellow flame, too violently, less smoke, small amount of glowing residues
[Cu(NH₃)₄][N(NO₂)₂]₂_16.10	56	28	6	10	green-yellow flame, less smoke, small amount of glowing residues

Table 10.97 Pyrotechnic formulations containing [Cu(NH₃)₄][N(NO₂)₂]₂ and sulfur.

	[Cu(NH₃)₄][N(NO₂)₂]₂ [wt%]	S [wt%]	VAAR [wt%]	observed behavior
[Cu(NH₃)₄][N(NO₂)₂]₂_17.1	78	12	10	green flame, red frame, smoke, high velocity, solid residue
[Cu(NH₃)₄][N(NO₂)₂]₂_17.2	75	15	10	yellow-green flame, much smoke, moderate velocity, glowing residue

10.3 Conclusion

The literature known copper(II) compounds, diammine bis(tetrazol-5-yl)-aminato- $\kappa^2N1,N6$ copper(II) ($[\text{Cu}(\text{bta})(\text{NH}_3)_2]$), bis{bis(tetrazol-5-yl)-amine- $\kappa^2N1,N6$ } copper(II) nitrate hemihydrate ($[\text{Cu}(\text{H}_2\text{bta})_2](\text{NO}_3)_2$), diaqua bis(1-methyl-5-aminotetrazole-*N4*) copper(II) nitrate ($[\text{Cu}(\text{1MeAt})_2(\text{H}_2\text{O})_2](\text{NO}_3)_2$), diaqua tetrakis(1-methyl-5-aminotetrazole-*N4*) copper(II) nitrate ($[\text{Cu}(\text{1MeAt})_4(\text{H}_2\text{O})_2](\text{NO}_3)_2$), diammine bis(1-methyl-5-nitriminotetrazolato- $\kappa^2N4,O1$) copper(II) ($[\text{Cu}(\text{1MeAtNO}_2)_2(\text{NH}_3)_2]$), bis((triammine) μ_2 -(5-nitriminotetrazolato) copper(II)) ($[\text{Cu}(\text{AtNO}_2)(\text{NH}_3)_3]_2$), basic copper(II) nitrate ($\text{Cu}_2(\text{OH})_3(\text{NO}_3)$), and tetrammine copper(II) dinitramide ($[\text{Cu}(\text{NH}_3)_4][\text{N}(\text{NO}_2)_2]_2$) were prepared and investigated regarding their properties as coloring agents in pyrotechnic compositions. Therefore, their solubilities in H_2O at ambient temperature as well as their coloring properties and combustion behavior as neat compounds in the flame of a BUNSEN burner were investigated. The determined solubilities are very low (< 13 wt%). All copper(II) compounds offered a green flame without any visible smoke production in the flame of a BUNSEN burner. $[\text{Cu}(\text{AtNO}_2)(\text{NH}_3)_3]_2$, $[\text{Cu}(\text{1MeAt})_4(\text{H}_2\text{O})_2](\text{NO}_3)_2$, $[\text{Cu}(\text{1MeAtNO}_2)_2(\text{NH}_3)_2]$, and $[\text{Cu}(\text{1MeAtNO}_2)_2(\text{NH}_3)_2] \cdot \text{H}_2\text{O}$ make a sizzling sound during combustion. Furthermore, the combustion behavior of the copper(II) compounds $[\text{Cu}(\text{bta})(\text{NH}_3)_2]$, $[\text{Cu}(\text{1MeAt})_2(\text{H}_2\text{O})_2](\text{NO}_3)_2$, $[\text{Cu}(\text{1MeAt})_4(\text{H}_2\text{O})_2](\text{NO}_3)_2$, $[\text{Cu}(\text{1MeAtNO}_2)_2(\text{NH}_3)_2]$, $[\text{Cu}(\text{1MeAtNO}_2)_2(\text{NH}_3)_2] \cdot \text{H}_2\text{O}$, and $[\text{Cu}(\text{NH}_3)_4][\text{N}(\text{NO}_2)_2]_2$ were qualitatively characterized with a simple smoke test method. $[\text{Cu}(\text{1MeAt})_2(\text{H}_2\text{O})_2](\text{NO}_3)_2$ and $[\text{Cu}(\text{1MeAt})_4(\text{H}_2\text{O})_2](\text{NO}_3)_2$ show a green flame color, whereas $[\text{Cu}(\text{1MeAt})_4(\text{H}_2\text{O})_2](\text{NO}_3)_2$, $[\text{Cu}(\text{bta})(\text{NH}_3)_2]$, $[\text{Cu}(\text{1MeAtNO}_2)_2(\text{NH}_3)_2]$, and $[\text{Cu}(\text{1MeAtNO}_2)_2(\text{NH}_3)_2] \cdot \text{H}_2\text{O}$ combust with a mostly white flame, which changes at the end into light yellow or orange. $[\text{Cu}(\text{1MeAtNO}_2)_2(\text{NH}_3)_2]$ and $[\text{Cu}(\text{1MeAtNO}_2)_2(\text{NH}_3)_2] \cdot \text{H}_2\text{O}$ combust without any smoke production and did not need a constant torch. After the combustion $[\text{Cu}(\text{1MeAt})_2(\text{H}_2\text{O})_2](\text{NO}_3)_2$, $[\text{Cu}(\text{1MeAt})_4(\text{H}_2\text{O})_2](\text{NO}_3)_2$ and $[\text{Cu}(\text{1MeAtNO}_2)_2(\text{NH}_3)_2]$ left no solid residues.

Some preliminary tests were performed using 5-aminotetrazole (**5-At**) and copper(II) nitrate pentahemihydrate as coloring agent. The results suggested that achieving a green flame color using copper compounds is possible, whereas these pretest compositions are thermally very unstable.

Therefore, various pyrotechnic compositions containing the copper(II) compounds $[\text{Cu}(\text{bta})(\text{NH}_3)_2]$, $[\text{Cu}(\text{H}_2\text{bta})_2](\text{NO}_3)_2$, $[\text{Cu}(\text{1MeAt})_2(\text{H}_2\text{O})_2](\text{NO}_3)_2$, $[\text{Cu}(\text{1MeAt})_4(\text{H}_2\text{O})_2](\text{NO}_3)_2$, $[\text{Cu}(\text{1MeAtNO}_2)_2(\text{NH}_3)_2]$, $[\text{Cu}(\text{AtNO}_2)(\text{NH}_3)_3]_2$, $\text{Cu}_2(\text{OH})_3(\text{NO}_3)$, and $[\text{Cu}(\text{NH}_3)_4][\text{N}(\text{NO}_2)_2]_2$ were prepared and investigated. In combination with boron as fuel, $[\text{Cu}(\text{NH}_3)_4][\text{N}(\text{NO}_2)_2]_2$ offered the best results regarding green color and smoke production. A point of concern might be the high sensitivity to impact and friction of the neat copper(II) compound and its compositions. However, the investigated compositions $[\text{Cu}(\text{NH}_3)_4][\text{N}(\text{NO}_2)_2]_2$ _9.3, $[\text{Cu}(\text{NH}_3)_4][\text{N}(\text{NO}_2)_2]_2$ _9.9, and $[\text{Cu}(\text{NH}_3)_4][\text{N}(\text{NO}_2)_2]_2$ _16.4 offer quite high decomposition temperatures. Worst color performance showed the copper(II) compounds

[Cu(1MeAtNO₂)₂(NH₃)₂] and **[Cu(AtNO₂)(NH₃)₃]₂**. Also **Cu₂(OH)₃(NO₃)** could not convince as coloring agent. The adding of copper(I) iodide can improve the green light emission.

A static burn test with **[Cu(bta)(NH₃)₂]**, **[Cu(1MeAt)₂(H₂O)₂(NO₃)₂]**, and **[Cu(1MeAt)₄(H₂O)₂(NO₃)₂]** was performed. All tested compounds combusted faster than the control. However, all showed a green flame. The burn time average intensity of all tested copper(II) compounds is lower than the control's one. This is true for the integrated intensity. The peak intensity of the control is nearly twice than the other ones.

Concluding can be said, that nitrogen-rich copper(II) compounds can be used as green colorants in pyrotechnic compositions. However, the combination with oxidizers and fuels is much more challenging compared to barium salts. Points of concern are the very low decomposition points of some investigated compositions as well as their high sensitivity to impact and friction. If these problems can get under control, nitrogen-rich copper(II) compounds are an environmentally more benign alternative to barium salts.

10.4 References

- [1] M. Friedrich, J. C. Gálvez-Ruiz, T. M. Klapötke, P. Mayer, B. Weber, J. J. Weigand: BTA Copper Complexes, *Inorg. Chem.* **2005**, *44*, 8044–8052.
- [2] J. J. Weigand: High Energy Density Materials Based on Tetrazole and Nitramine Compounds - Synthesis, Scale-Up and Testing, *PhD Thesis*, **2005**, Ludwig-Maximilian University, Munich.
- [3] a) J. Stierstorfer: "Chemistry of H₂bta" – Synthese, Salze und Komplexe von Bis(tetrazolyl)aminen, *Diploma Thesis*, **2005**, Ludwig-Maximilian University, Munich. b) T. M. Klapötke, P. Mayer, K. Polborn, J. Stierstorfer, J. J. Weigand: 5,5'-Bis-(1H-tetrazolyl)amine (H₂bta) and 5,5'-bis-(2-methyl-tetrazolyl)amine (Me₂bta): promising ligands in new copper based priming charges (PC). *International Annual Conference of ICT 2006*, *37th* (Energetic Materials), Karlsruhe, Germany, 134/1–134/14. c) T. M. Klapötke, P. Mayer, K. Polborn, J. Stierstorfer, J. J. Weigand: 5,5'-Bis-(1H-tetrazolyl)amine (H₂BTA): a promising ligand in novel copper based priming charges (PC). *New Trends in Research of Energetic Materials*, Proceedings of the Seminar, *9th*, Pardubice, Czech Republic, 19.–21. Apr. **2006**, *Pt. 2*, 641–651.
- [4] H. Radies: Synthese und Charakterisierung von energetischen Übergangsmetall-Tetrazolat-Komplexen, *Diploma thesis*, **2006**, Ludwig-Maximilian University, Munich.
- [5] a) G. Steinhauser, K. Tarantik, T. M. Klapötke: Copper in Pyrotechnics, *J. Pyrotech.* **2008**, *27*, 3–13. b) T. M. Klapötke, K. Tarantik: Green Pyrotechnic Compositions, *New Trends in Research of Energetic Materials*, Proceedings of the Seminar, *11th*, Pardubice, Czech Republic, 9.–11. Apr. **2008**, *Pt. 2*, 586–597.

- [6] J. Stierstorfer: Advanced Energetic Materials based on 5-Aminotetrazole, *PhD Thesis*, **2009**, Ludwig-Maximilian University, Munich.
- [7] T. M. Klapötke, J. Stierstorfer, B. Weber: New Energetic Materials: Synthesis and Characterization of Copper 5-Nitriminotetrazolates, *Inorg. Chim. Acta* **2009**, *362*, 2311–2320.
- [8] L. Ilcheva, J. Bjerrum: Metal ammine formation in solution. XVII. Stability constants of copper(II) methylamine and diethylamine complexes obtained from solubility measurements with gerhardtite, (Cu(OH)_{1.5}(NO₃)_{0.5}), *Acta Chem. Scand.* **1976**, *A 30*, 343–350.
- [9] O. A. Luk'yanov, O. V. Anikin, V. P. Gorelik, V. A. Tartakovskiy: Dinitramide and its salts, *Russ. Chem. Bull.* **1994**, *43*, 1457–1461.
- [10] H.-G. Ang, W. Fraenk, K. Karaghiosoff, T. M. Klapötke, P. Mayer, H. Nöth, J. Sprott, M. Warchold: Synthesis, Characterization, and Crystal Structures of Cu, Ag, and Pd Dinitramide Salts, *Z. Anorg. Allg. Chem.* **2002**, *628*, 2894–2900.
- [11] B. T. Sturman: On the Emitter of Blue Light in Copper-Containing Pyrotechnic Flames, *Propellants, Explos., Pyrotech.* **2006**, *31*, 70–74.
- [12] J. A. Conkling: *Chemistry of Pyrotechnics: Basic Principles and Theory*. M. Dekker, Inc., New York, **1985**.
- [13] H.R. Oswald: Über natürlichen und künstlichen Gerhardtit, *Z. Kristallogr.* **1961**, *116*, 210–219.
- [14] a) R. D. Taylor, I. V. Mendenhall: Airbag propellants with enhanced burn rate containing basic copper nitrate reaction products as oxidants. PCT Int. Appl., WO 2006047085 A2, **2006**, b) I. V. Mendenhall, R. D. Taylor: Gas-generating compositions containing non-azide nitrogen fuel and reaction products of basic transition metal nitrates with organic nitrogen compounds. U.S. Pat. Appl. Publ., US 2006054257 A1, **2006**. c) D. L. Hordos, S. P. Burns: Autoignitable gas-generating propellant containing DL-tartaric acid for use in inflation of vehicle airbags. U.S. Pat. Appl. Publ., US 2007246138 A1, **2007**. d) G. K. Lund: Metal complexes for use as gas generants for inflation of airbags. PCT Int. Appl., WO 9806486 A2, **1998**.
- [15] R. A. Henry, W. G. Finnegan: Mono-alkylation of Sodium 5-Aminotetrazole in Aqueous Medium, *J. Am. Chem. Soc.* **1954**, *76*, 923–926.
- [16] T. M. Klapötke, H. A. Laub, J. Stierstorfer: Synthesis and characterization of a new class of energetic compounds - ammonium nitriminotetrazolates, *Propellants, Explos., Pyrotech.* **2008**, *33*, 421–430.
- [17] G. Geisberger, T. M. Klapötke, J. Stierstorfer: Copper Bis(1-methyl-5-nitriminotetrazolate): A Promising New Primary Explosive, *Eur. J. Inorg. Chem.* **2007**, *30*, 4743–4750.

- [18] T. M. Klapötke, J. Stierstorfer: Nitration products of 5-amino-1H-tetrazole and methyl-5-amino-1H-tetrazoles - structures and properties of promising energetic materials., *Helv. Chim. Acta*, **2007**, *90(11)*, 2132–2150.
- [19] a) <http://www.bam.de> b) E_{dr} : insensitive > 40 J, less sensitive ≥ 35 J, sensitive ≥ 4 , very sensitive ≤ 3 J; F_r : insensitive > 360 N, less sensitive = 360 N, sensitive < 360 N > 80 N, very sensitive ≤ 80 N, extreme sensitive ≤ 10 N. According to the UN Recommendations on the Transport of Dangerous Goods.
- [20] C. Jennings-White, K. Kosanke: Hazardous Chemical Combinations, *J. Pyrotech.* **1995**, *2*, 22-35.
- [21] Albert S. Tompa: Thermal analysis of ammonium dinitramide (ADN), *Thermochim. Acta* **2000**, *357–358*, 177–193.
- [22] GESTIS-Stoffdatenbank, Gefahrstoffinformationssystem der Deutschen Gesetzlichen Unfallversicherung: www.dguv.de/ifa/stoffdatenbank/
- [23] G. Rasulic, S. Jovanovic and Lj. Milanovic: Ammonium Nitrate Changes During Thermal Analysis, *J. Thermal Anal.* **1985**, *30*, 65–72.
- [24] G. R. Lakshminarayanan, G. Chen, R. Ames, W. T. Lee, J. Wejsa, K. Meiser, *Laminac Binder Replacement Program*, Aug. **2006**.
- [25] G. Chen, *Application of High Nitrogen Energetics in Pyrotechnic*, Program Review Presentation to US Army RDECOM, 20. Jan. **2009**.

11 Résumé

This thesis is focused on the investigation of new green and red light emitting pyrotechnic compositions. They should provide, besides a comparable or better color and combustion performance than the pyrotechnic formulations used, less smoke production as well as lower toxicity of the components and their combustion products. This should be achieved by the usage of nitrogen-rich molecules and their salts to avoid the usage of barium nitrate and potassium perchlorate.

Thus, several derivatives of 5-aminotetrazole (**5-At**) that are partly described in literature, were prepared, including: 1-(2-hydroxyethyl)-5-nitriminotetrazole (**1**), 1-(2-nitrate-ethyl)-5-nitriminotetrazole monohydrate (**2**), 1-(2-chloroethyl)-5-nitriminotetrazole (**3**), 1-carboxymethyl-5-aminotetrazole (**4**), 1-carboxymethyl-5-nitriminotetrazole monohydrate (**5**), 1- and 2-(2,3-dihydroxypropyl)-5-aminotetrazole (**6a/b**), 1-(2,3-dinitratopropyl)-5-nitriminotetrazolate monohydrate (**7**), 1- and 2-(2,3-dichloropropyl)-5-aminotetrazole (**8a/b**), and 1-(2,3-dichloropropyl)-5-nitriminotetrazole (**9**) (Figure 11.1).

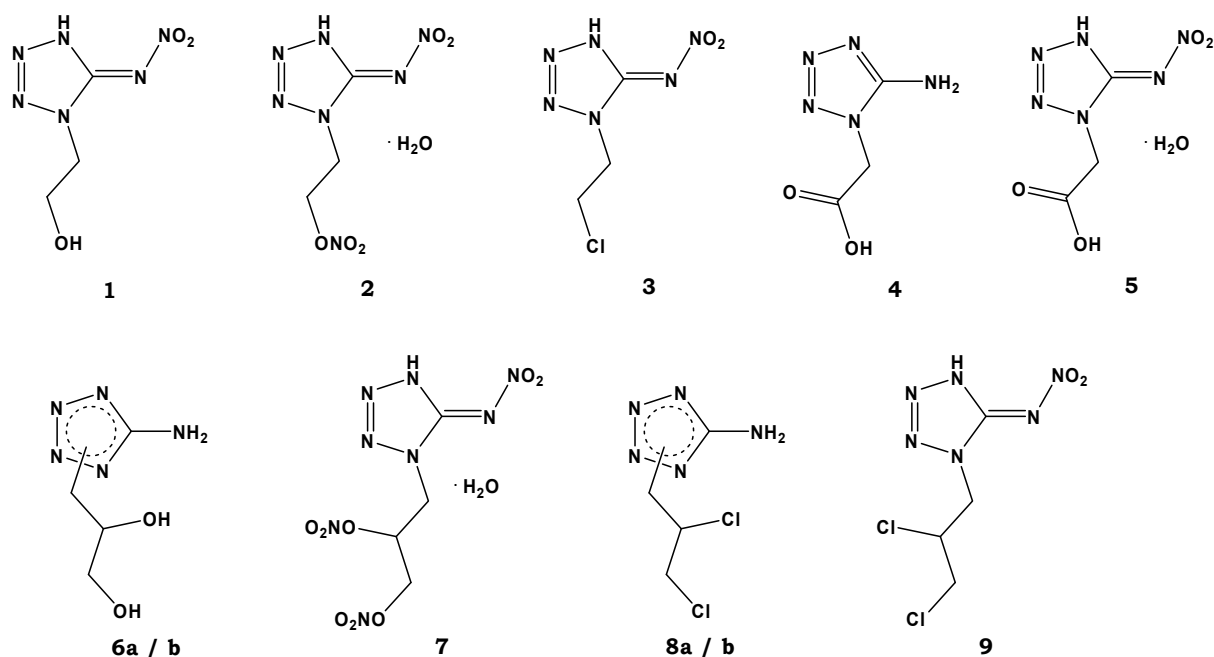


Figure 11.1 Chemical structures of compounds **1-9**.

The alkali and alkaline earth metal salts of **1-5**, **7** and **9** were prepared and in addition to conventional characterization their sensitivities to mechanical and electric stimuli, thermal stability, and solubility in H₂O at ambient temperature were determined. This is also true for several copper(II) complexes with these tetrazole derivatives as ligands.

The lithium, calcium, strontium, barium, and copper(II) salts were additionally investigated with respect to their color performance and combustion properties in the flame of a BUNSEN burner. The best performance as neat compound had strontium 1-(2-chloroethyl)-5-nitriminotetrazolate monohydrate (**3_Sr**) and barium 1-(2-chloroethyl)-5-nitrimino-

tetrazolate monohydrate (**3_Ba**). In Figure 11.2 their colored flames are depicted. The pyrotechnically relevant salts of **9** are also promising candidates as colorants in pyrotechnic compositions. In particular they are suitable as additives for enhancing the color purity and intensity in red, green, or blue light emitting perchlorate-free compositions

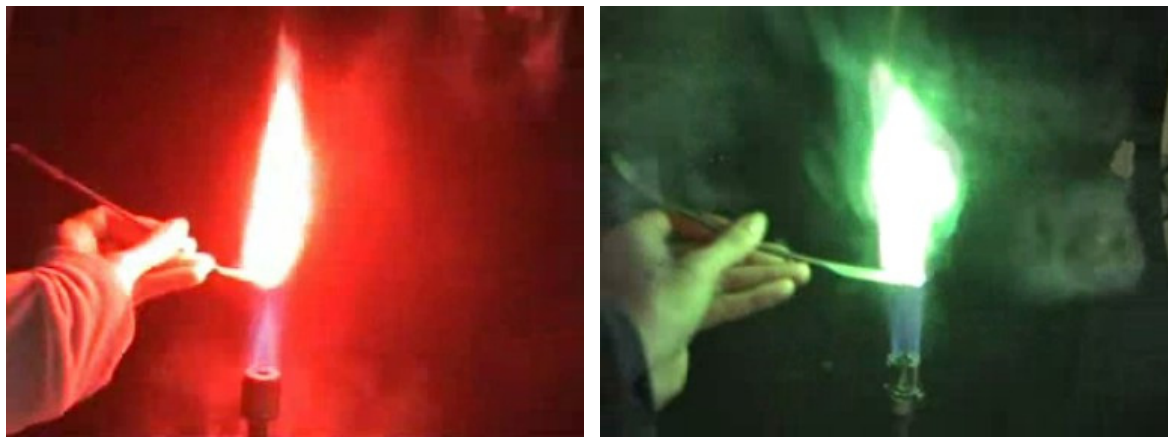


Figure 11.2 Flame color of **3_Sr** (left) and **3_Ba** (right) in the flame of a BUNSEN burner.

The barium salts of **1**, **2**, **4**, **5**, and **7** needed an additional chlorine source (PVC) to produce a green flame. All salts tested had a good combustion behavior with low smoke production and a small amount of residues. However, the salts of **2** and **7** combust too vigorously to find application as colorants, whereas an application as primary explosives might be possible. This accounts in particular for the water-free salts alkali metal salts **2_Na**, **2_K**, **2_Rb**, and **2-Cs** as well as **7_K**.

Furthermore, the salts with the best properties were investigated as coloring agent in several pyrotechnic compositions. No potassium perchlorate and barium nitrate were used. The performances of these compositions were compared to known formulations. The best performing two or three compositions were further investigated with respect to their sensitivity.

Most promising are the formulations **3_Sr_8.3** and **3_Ba_4.2**, containing ADN as oxidizer, with respect to color performance, reduced smoke production and high combustion velocity. The best formulation containing **3_Cu_H₂O** shows heavy smoke production due to the use of starch as fuel. Unfortunately, all further investigated mixtures show decomposition temperatures below 180 °C. This probably can be improved, if a different oxidizer offering an equal performance or a stabilizing additive is used. The controlled combustion of **3_Sr_8.3** and **3_Ba_4.2** is depicted in Figure 11.3. The salts **3_Sr**, **3_Ba**, and **3_Cu_H₂O** represent a step forward towards the preparation of more environmentally benign pyrotechnic compositions without potassium perchlorate.



Figure 11.3 Controlled burn down of the compositions **3_Sr_8.3** (left) and **3_Ba_4.2** (right).

The mixtures **4_Ba_4.2** and **4_Ba_14.2** displayed a green flame, whereas composition **4_Ba_11.3** produced an intense white flame. Therefore, **4_Ba** might also find application as additive in white flame pyrotechnic compositions. Good results were achieved using **4_Sr**. The best performing compositions **4_Sr_2.7** and **4_Sr_7.2** have, in addition to a tall very intense red flame, quite high decomposition temperatures of above 280 °C. Furthermore, they are less sensitive towards outer stimuli. Due to the insensitivity to impact, friction, and electric discharge, to its easy preparation from low cost materials and the low solubility in H₂O, **4_Sr** is a very promising coloring agent, which might find application in environmentally more benign pyrotechnic compositions without potassium perchlorate.

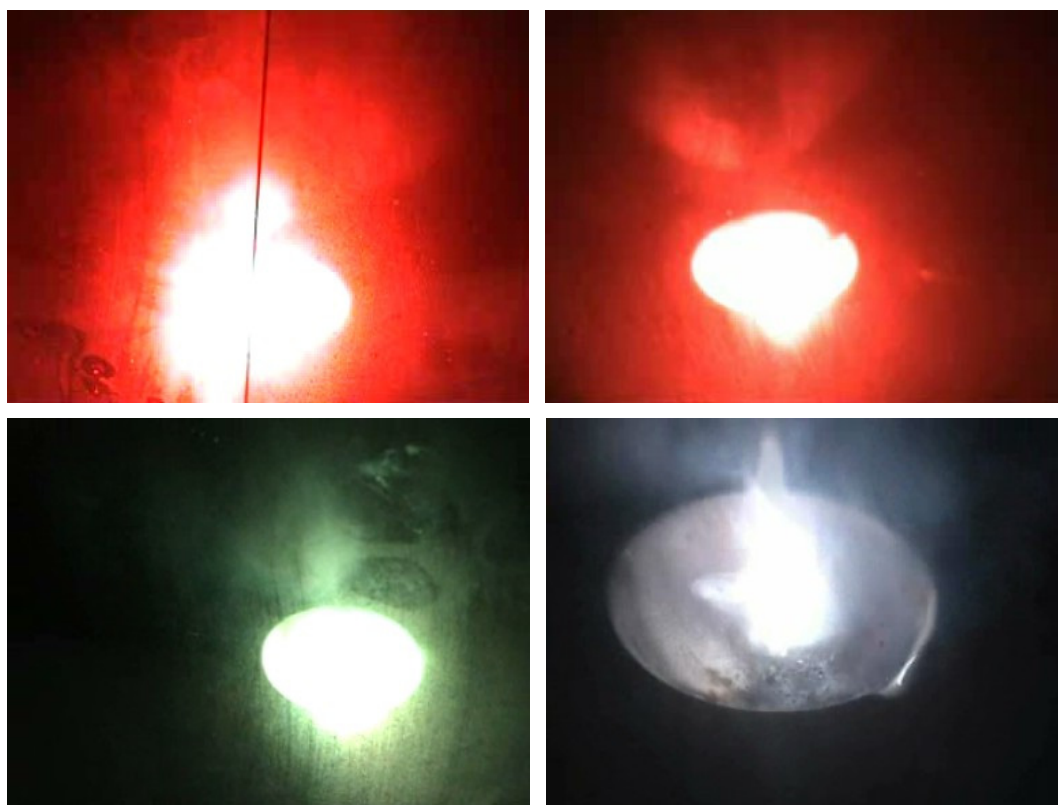


Figure 11.4 Controlled burn down of the compositions **4_Sr_2.7** (top, left), **4_Sr_7.2** (top, right) and **4_Ba_4.2** (down, left), **4_Ba_11.3** (down, right).

The strontium and barium salts of **5**, especially **5_Sr2**, and **5_Ba2**, are suitable as coloring agents in more environmentally benign pyrotechnic compositions without potassium perchlorate due to their properties. The combustion of their best performing composition is depicted in Figure 11.5.

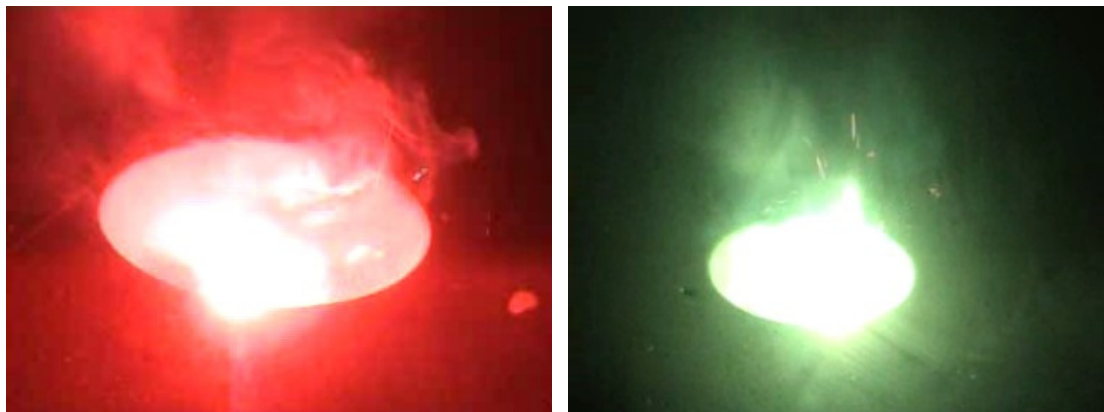


Figure 11.5 Controlled burn down of the compositions **5_Sr2_4.1** (left) and **5_Ba2_3.2** (right).

Like **4_Ba**, the barium salts of **5** might also find application in white light emitting pyrotechnic compositions.

The nitrogen-rich barium salts barium tetrazolate (**BaTz**), barium 5-aminotetrazolate tetrahydrate (**BaAt**), barium bis(5-nitrimino-1*H*-tetrazolate) tetrahydrate (**Ba1HatNO2**), barium 5-nitriminotetrazolate dihydrate (**BaAtNO2**), barium 1-methyl-5-nitriminotetrazolate monohydrate (**Ba1MeAtNO2**), and barium 2-methyl-5-nitriminotetrazolate dihydrate (**Ba2MeAtNO2**), partly described in literature, were prepared and their energetic properties such as the decomposition temperature, combustion energy and sensitivities to impact, friction, and electric discharge were determined. With regard to their possible usage as coloring agents in pyrotechnic compositions the color performance of each barium salt with and without a chlorine donor were investigated in the flame of a BUNSEN burner. For comparison the color performance of neat barium chloride dihydrate and barium nitrate, a mixture of both salts, and a mixture of PVC and barium nitrate was determined. Concluding it can be stated, that the barium salts investigated, especially with anions containing a nitrimino group (**Ba1HAtNO2**, **BaAtNO2**, **Ba1MeAtNO2**, and **Ba2MeAtNO2**), might be a “greener” alternative in replacing barium nitrate in white or green light emitting pyrotechnic compositions. All offer a comparable or lower solubility than barium nitrate in H₂O at ambient temperature and show without chlorine a very intense white flame (Figure 11.6). The barium salts **Ba1HAtNO2** and **BaAtNO2** could find further application, if sizzling sound effects are desired.

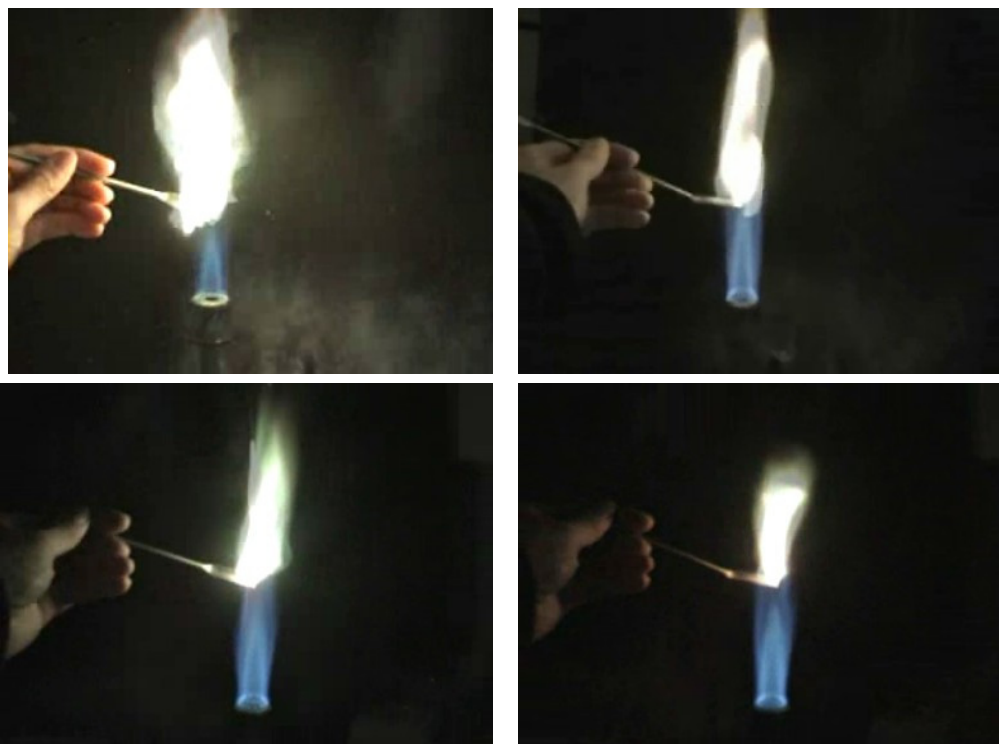


Figure 11.6 Color performance of the barium salts **Ba1MeAtNO2** (top, left), **Ba2MeAtNO2** (top, right), **Ba1MeAtNO2** and **pvc** (down, left), and **Ba2MeAtNO2** and **pvc** (down, right) in the flame of a BUNSEN burner.

Furthermore, some nitrogen-rich strontium salts were investigated with respect to their coloring properties. It was possible to achieve at least one red burning pyrotechnic composition with convincing properties of each investigated strontium salt: strontium tetrazolate pentahydrate (**SrTz**), strontium 5-aminotetrazolate tetrahydrate (**SrAt**), strontium 1-methyl-5-nitriminotetrazolate monohydrate (**Sr1MeAtNO2**), strontium bis(5-nitrimino-1H-tetrazolate) tetrahydrate (**Sr1HAtNO2**), strontium 5-nitriminotetrazolate monohydrate (**SrAtNO2**), and strontium 3,3'-bis(1,2,4-oxadiazol-5-onate) dihydrate (**SrOD**). Especially the compositions **SrTz_1** and **Sr1MeAtNO2_1** show in addition to their good coloring and combustion properties also high decomposition temperatures. If ADN was used as oxidizer, the smoke production was very low and the emitted red light very intense, however the decomposition temperature of the compositions was below 190 °C (Figure 11.7).

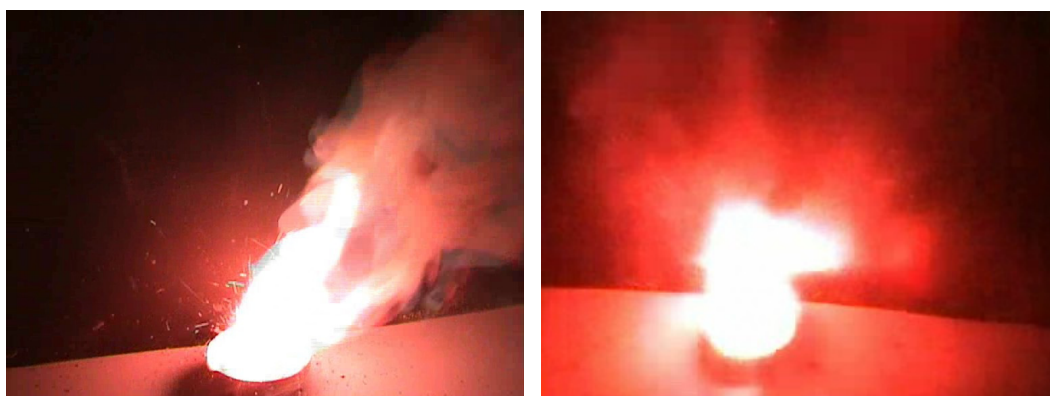


Figure 11.7 Burn down of the compositions **Sr1MeAtNO2_1** (left, no ADN) and **Sr1MeAtNO2_5.4** (right, with ADN).

The copper(II) complexes, diammine bis(tetrazol-5-yl)-aminato- $\kappa^2N1,N6$ copper(II) ($[\text{Cu}(\text{bta})(\text{NH}_3)_2]$), bis{bis(tetrazol-5-yl)-amine- $\kappa^2N1,N6$ } copper(II) nitrate hemihydrate ($[\text{Cu}(\text{H}_2\text{bta})_2](\text{NO}_3)_2$), diaqua bis(1-methyl-5-aminotetrazole- $N4$) copper(II) nitrate ($[\text{Cu}(\text{1MeAt})_2(\text{H}_2\text{O})_2](\text{NO}_3)_2$), diaqua tetrakis(1-methyl-5-aminotetrazole- $N4$) copper(II) nitrate ($[\text{Cu}(\text{1MeAt})_4(\text{H}_2\text{O})_2](\text{NO}_3)_2$), diammine bis(1-methyl-5-nitriminotetrazolato- $\kappa^2N4,O1$) copper(II) ($[\text{Cu}(\text{1MeAtNO}_2)_2(\text{NH}_3)_2]$), bis((triammine) μ_2 -(5-nitriminotetrazolato) copper(II)) ($[\text{Cu}(\text{AtNO}_2)(\text{NH}_3)_3]_2$), basic copper(II) nitrate ($\text{Cu}_2(\text{OH})_3(\text{NO}_3)$), and tetrammine copper(II) dinitramide ($[\text{Cu}(\text{NH}_3)_4][\text{N}(\text{NO}_2)_2]_2$) were prepared and investigated regarding their properties as coloring agents in pyrotechnic compositions. All copper(II) complexes produced a green flame without any visible smoke production in the flame of a BUNSEN burner. Therefore, various pyrotechnic compositions containing the copper(II) compounds $[\text{Cu}(\text{bta})(\text{NH}_3)_2]$, $[\text{Cu}(\text{H}_2\text{bta})_2](\text{NO}_3)_2$, $[\text{Cu}(\text{1MeAt})_2(\text{H}_2\text{O})_2](\text{NO}_3)_2$, $[\text{Cu}(\text{1MeAt})_4(\text{H}_2\text{O})_2](\text{NO}_3)_2$, $[\text{Cu}(\text{1MeAtNO}_2)_2(\text{NH}_3)_2]$, $[\text{Cu}(\text{AtNO}_2)(\text{NH}_3)_3]_2$, $\text{Cu}_2(\text{OH})_3(\text{NO}_3)$, and $[\text{Cu}(\text{NH}_3)_4][\text{N}(\text{NO}_2)_2]_2$ were prepared and investigated. In combination with boron as fuel, $[\text{Cu}(\text{NH}_3)_4][\text{N}(\text{NO}_2)_2]_2$ showed the best results regarding green color and smoke production (Figure 11.8).



Figure 11.8 Burn down of the composition $[\text{Cu}(\text{NH}_3)_4][\text{N}(\text{NO}_2)_2]_2$ 16.4.

Concluding it can be said, that nitrogen-rich copper(II) complexes can be used as green colorants in pyrotechnic compositions. However, the combination with oxidizers and fuels is much more challenging compared to barium salts. Points of concern are the very low decomposition points of some investigated compositions as well as their high sensitivity to impact and friction. If these problems can be solved, nitrogen-rich copper(II) complexes are an environmentally more benign alternative to barium salts.

The 1,2,4-triazoles 3-nitramino-1,2,4-triazole monohydrate (**10**), 3-nitro-1,2,4-triazole (**12**), 2-carboxymethyl-3-amino-1,2,4-triazole (**13**), and 2-carboxymethyl-3-nitrimino-1,2,4-triazole monohydrate (**14**) were prepared as well as some of their alkali metal, alkaline earth metal salts and copper(II) complexes (Figure 11.9).

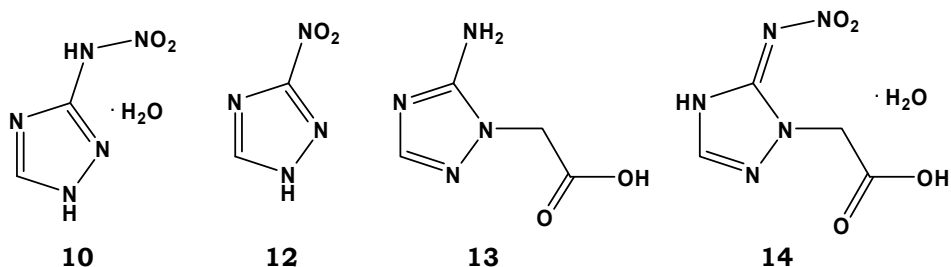


Figure 11.9 Chemical structures of compounds **10**, **12–14**.

In comparison to the salts of the corresponding tetrazole derivatives, the color performance and combustion behavior of the investigated triazole salts is worse. Nevertheless, they display a higher thermal stability, lower solubility in H₂O and are less sensitive to impact, friction, and electric discharge. Depending of the color performance, combustion behavior, and physico-chemical properties of pyrotechnic relevant salts, pyrotechnic compositions based on these triazole salts might be investigated. Especially the strontium salts **10_Sr1**, **10_Sr2**, and **13_Sr** are promising candidates as colorant agents.

Further investigations of the best performing compounds, which are considered as coloring agents in pyrotechnic compositions, might be the determination of their toxicity, regarding human beings as well as the biota, their biodegradation and the toxicity of their combustion and degradation products.

Appendix

I. Crystallographic Data of 2-OH and Salts of 1

	2-OH	1_Li	1_Na	1_K
Formula	C ₃ H ₇ N ₅ O	C ₃ H ₇ LiN ₆ O ₄	C ₃ H ₅ N ₆ NaO ₃	C ₃ H ₅ KN ₆ O ₃
<i>M</i> [g/mol]	129.12	198.09	196.12	212.23
Crystal System	monoclinic	triclinic	triclinic	monoclinic
Space Group	<i>P</i> 2 ₁ / <i>c</i> (14)	<i>P</i> -1 (2)	<i>P</i> -1 (2)	<i>P</i> 2 ₁ / <i>c</i> (14)
Color / Habit	colorless blocks	colorless blocks	colorless blocks	colorless rods
Size [mm]	0.30×0.20×0.20	0.25×0.20×0.15	0.35×0.25×0.15	0.40×0.15×0.10
<i>a</i> [Å]	4.6244(3)	7.4261(4)	8.938(6)	10.9540(9)
<i>b</i> [Å]	12.5193(7)	11.9065(6)	9.560(5)	5.0298(3)
<i>c</i> [Å]	10.4014(6)	19.2485(10)	10.469(5)	14.3549(11)
<i>α</i> [°]	90	99.830(4)	64.881(5)	90
<i>β</i> [°]	99.237(5)	99.803(5)	68.335(5)	107.880(8)
<i>γ</i> [°]	90	100.008(4)	65.902(6)	90
<i>V</i> [Å ³]	594.37(6)	1615.99(15)	718.3(7)	752.70(10)
<i>Z</i>	4	8	4	4
ρ_{calc} [g/cm ³]	1.443	1.628	1.814	1.873
μ [mm ⁻¹]	0.114	0.143	0.205	0.692
<i>F</i> (000)	272	816	400	432
<i>T</i> [K]	200	200	100	200
θ min–max [°]	3.8, 26.0	4.17, 26.00	3.77, 25.99	3.91, 28.62
Dataset [h; k; l]	-23:26, -11:12, -5:7	-9:8, -14:14, -16:23	-11:11, -11:11, -12:12	-14:13, -6:4, -18:12
Reflections Collected	5901	11221	10811	2117
Independent Reflections	1167	6190	2816	1928
<i>R</i> _{int}	0.0189	0.0284	0.0232	0.0226
Observed Reflections	924	3581	2300	775
No. Parameters	90	553	243	122
Restraints	2	0	0	0
<i>R</i> ₁ (obs)	0.0316	0.0387	0.0272	0.0261
w <i>R</i> ₂ (all data)	0.0915	0.0737	0.0769	0.0504
Goof	1.107	0.815	1.052	0.879
Resd. Dens. [e/Å ³]	-0.271, 0.269	-0.425, 0.719	-0.327, 0.267	-0.212, 0.180
Solution	SIR-92	SIR-92	SIR-97	SHELXS-97
Refinement	SHELXL-97	SHELXL-97	SHELXL-97	SHELXL-97
CCDC	-	-	-	-

	1_Rb	1_Cs	1_Mg	1_Ca
Formula	C ₃ H ₅ N ₆ O ₃ Rb	C ₃ H ₅ CsN ₆ O ₃	C ₆ H ₂₆ MgN ₁₂ O ₁₄	C ₆ H ₁₄ CaN ₁₂ O ₈
<i>M</i> [g/mol]	258.60	306.04	514.70	422.37
Crystal System	monoclinic	monoclinic	monoclinic	triclinic
Space Group	<i>P</i> 2 ₁ / <i>c</i> (14)	<i>P</i> 2 ₁ (4)	<i>C</i> 2 ₁ / <i>c</i> (15)	<i>P</i> -1 (2)
Color / Habit	colorless rods	colorless blocks	colorless blocks	colorless rods
Size [mm]	0.25×0.15×0.02	0.25×0.20×0.10	0.35×0.25×0.15	0.35×0.25×0.10
<i>a</i> [Å]	11.0017(7)	7.740(5)	15.907(4)	9.056(6)
<i>b</i> [Å]	5.1619(2)	5.411(5)	7.8380(19)	9.634(4)
<i>c</i> [Å]	14.7224(8)	10.599(5)	18.040(5)	10.007(5)
<i>α</i> [°]	90	90	90	96.087(4)
<i>β</i> [°]	109.124(7)	109.620(5)	106.736(3)	116.158(5)
<i>γ</i> [°]	90	90	90	90.822(4)
<i>V</i> [Å ³]	789.94(7)	418.1(5)	2153.9(10)	777.4(7)
<i>Z</i>	4	2	4	2
$\rho_{\text{calc.}}$ [g/cm ³]	2.174	2.431	1.587	1.804
μ [mm ⁻¹]	6.255	4.416	0.175	0.479
<i>F</i> (000)	504	288	1080	436
<i>T</i> [K]	200	200	200	100
θ min–max [°]	4.21, 26.00	4.08, 30.00	4.28, 26.50	4.12, 26.00
Dataset [h; k; l]	-12:13, -6:6, -18:9	-9:9, -6:6, -13:13	-19:19, -9:9, -22:22	-11:11, -11:11, -12:12
Reflections Collected	3266	6255	10922	11129
Independent Reflections	1539	953	2220	3048
<i>R</i> _{int}	0.0340	0.0369	0.0281	0.0304
Observed Reflections	1010	874	1782	2365
No. Parameters	122	122	187	268
Restraints	0	3	0	0
<i>R</i> ₁ (obs)	0.0240	0.0230	0.0254	0.0236
w <i>R</i> ₂ (all data)	0.0449	0.0663	0.0672	0.0500
Goof	0.814	1.092	0.976	0.909
Resd. Dens. [e/Å ³]	-0.440, 0.479	-0.693, 0.982	-0.253, 0.203	-0.236, 0.219
Solution	SIR-92	SIR-97	SIR-92	SIR-92
Refinement	SHELXL-97	SHELXL-97	SHELXL-97	SHELXL-97
CCDC	–	–	–	–

	1_Sr	1_Cu_NH₃
Formula	C ₆ H ₁₄ N ₁₂ O ₈ Sr	C ₆ H ₂₂ CuN ₁₆ O ₆
<i>M</i> [g/mol]	469.91	477.94
Crystal System	triclinic	monoclinic
Space Group	<i>P</i> -1 (2)	<i>P</i> 2 ₁ / <i>n</i> (14)
Color / Habit	colorless blocks	blue blocks
Size [mm]	0.20×0.20×0.15	0.25×0.15×0.10
<i>a</i> [Å]	9.2918(7)	16.5901(9)
<i>b</i> [Å]	9.6446(6)	6.8826(3)
<i>c</i> [Å]	10.1604(6)	17.1702(9)
<i>α</i> [°]	96.174(5)	90
<i>β</i> [°]	115.945(7)	110.091(6)
<i>γ</i> [°]	91.697(6)	90
<i>V</i> [Å ³]	811.01(9)	1841.24(18)
<i>Z</i>	2	4
$\rho_{\text{calc.}}$ [g/cm ³]	1.924	1.724
μ [mm ⁻¹]	3.396	1.254
<i>F</i> (000)	472	988
<i>T</i> [K]	200	200
θ min–max [°]	3.99, 26.00	3.86, 26.50
Dataset [h; k; l]	–11:11, –10:11, –12:9	–19:20, –7:8, –18:21
Reflections Collected	5564	7446
Independent Reflections	3177	3815
<i>R</i> _{int}	0.0262	0.0287
Observed Reflections	2550	2667
No. Parameters	268	318
Restraints	0	0
<i>R</i> ₁ (obs)	0.0264	0.0308
w <i>R</i> ₂ (all data)	0.0417	0.0679
Goof	0.875	0.896
Resd. Dens. [e/Å ³]	–0.345, 0.282	–0.496, 0.318
Solution	SIR–92	SIR–92
Refinement	SHELXL–97	SHELXL–97
CCDC	–	–

II. Crystallographic Data of 2, 2a, and Salts of 2

	2a	2_Na	2_K	2_Rb
Formula	C ₃ H ₇ N ₇ O ₆	C ₃ H ₄ N ₇ NaO ₅	C ₃ H ₄ KN ₇ O ₅	C ₃ H ₄ N ₇ O ₅ Rb
<i>M</i> [g/mol]	237.16	241.12	257.23	303.60
Crystal System	monoclinic	triclinic	orthorhombic	orthorhombic
Space Group	<i>P</i> 2 ₁ / <i>c</i>	<i>P</i> -1 (2)	<i>P</i> 2 ₁ 2 ₁ 2 ₁ (19)	<i>P</i> 2 ₁ 2 ₁ 2 ₁ (19)
Color / Habit	colorless blocks	colorless blocks	colorless blocks	colorless rods
Size [mm]	0.35×0.25×0.20	0.25×0.20×0.10	0.25×0.25×0.01	0.35×0.10×0.02
<i>a</i> [Å]	23.499(2)	8.6279(3)	5.2908(3)	5.30710(10)
<i>b</i> [Å]	5.5543(5)	10.1435(4)	7.0741(4)	7.3415(2)
<i>c</i> [Å]	14.3477(13)	10.8626(4)	23.7969(13)	23.9203(6)
<i>α</i> [°]	90	109.748(4)	90	90
<i>β</i> [°]	102.769(9)	90.345(3)	90	90
<i>γ</i> [°]	90	104.265(3)	90	90
<i>V</i> [Å ³]	1826.3(3)	863.00(6)	890.66(9)	931.98(4)
<i>Z</i>	8	4	4	4
$\rho_{\text{calc.}}$ [g/cm ³]	1.725	1.856	1.918	2.164
μ [mm ⁻¹]	0.163	0.210	0.623	5.338
<i>F</i> (000)	976	488	520	592
<i>T</i> [K]	200	200	200	200
θ min–max [°]	3.77, 28.82	3.83, 30.00	3.84, 28.67	4.19, 32.34
Dataset [h; k; l]	-22:28, -6:6, -17:13	-10:10, -12:12, -13:13	-6:5, -8:7, -29:16	-6:6, -9:9, -29:29
Reflections Collected	7383	13492	2257	13637
Independent Reflections	3561	3578	1536	1821
<i>R</i> _{int}	0.0258	0.0232	0.0229	0.0338
Observed Reflections	2270	2861	1272	1703
No. Parameters	313	289	145	145
Restraints	0	0	0	0
<i>R</i> ₁ (obs)	0.0345	0.0279	0.0342	0.0148
w <i>R</i> ₂ (all data)	0.0745	0.0814	0.0694	0.0317
GooF	0.881	1.068	0.932	0.996
Resd. Dens. [e/Å ³]	-0.206, 0.211	-0.246, 0.262	-0.280, 0.273	-0.171, 0.214
Solution	SIR-92	SIR-92	SIR-92	SIR-92
Refinement	SHELXL-97	SHELXL-97	SHELXL-97	SHELXL-97
CCDC	766629	–	–	–

	2_Mg	2_Ca	2_Cu_H2O	2_Cu_NH3
Formula	C ₆ H ₂₀ MgN ₁₄ O ₁₆	C ₆ H ₁₄ CaN ₁₄ O ₁₃	C ₆ H ₁₂ CuN ₁₄ O ₁₂	C ₆ H ₁₄ CuN ₁₆ O ₁₀
<i>M</i> [g/mol]	568.67	530.39	535.84	533.87
Crystal System	triclinic	triclinic	monoclinic	monoclinic
Space Group	<i>P</i> -1 (2)	<i>P</i> -1 (2)	<i>P</i> 2 ₁ / <i>c</i> (14)	<i>P</i> 2 ₁ / <i>c</i> (14)
Color / Habit	colorless blocks	colorless blocks	blue plates	blue rods
Size [mm]	0.25×0.20×0.15	0.23×0.15×0.03	0.20×0.10×0.02	0.30×0.10×0.10
<i>a</i> [Å]	9.353(5)	7.1625(4)	15.9220(9)	15.8515(7)
<i>b</i> [Å]	11.055(5)	9.4420(6)	5.2603(3)	5.5039(3)
<i>c</i> [Å]	11.520(5)	14.6187(11)	10.9728(7)	10.9286(6)
<i>α</i> [°]	112.084(5)	80.774(5)	90	90
<i>β</i> [°]	92.353(5)	81.889(5)	100.817(6)	99.257(4)
<i>γ</i> [°]	93.744(5)	87.868(5)	90	90
<i>V</i> [Å ³]	1098.6(9)	965.98(11)	902.69(9)	941.05(8)
<i>Z</i>	2	2	2	2
ρ_{calc} [g/cm ³]	1.719	1.824	1.971	1.884
μ [mm ⁻¹]	0.189	0.427	1.312	1.253
<i>F</i> (000)	588	544	542	542
<i>T</i> [K]	100	100	200	200
θ min–max [°]	3.82, 28.76	4.12, 26.50	3.91, 26.00	3.90, 28.68
Dataset [h; k; l]	-11:9; -13:9; -12:14	-7:7; -8:11; -17:18	-19:13; -6:4; -9:13	-19:19; -5:6; -12:13
Reflections Collected	7615	6660	3285	3746
Independent Reflections	4315	3711	1768	1848
<i>R</i> _{int}	0.0202	0.0420	0.0274	0.0264
Observed Reflections	3013	1913	1244	1329
No. Parameters	385	331	159	163
Restraints	0	0	0	2
<i>R</i> ₁ (obs)	0.0336	0.0360	0.0333	0.0313
w <i>R</i> ₂ (all data)	0.0782	0.0475	0.0732	0.0672
Goof	0.920	0.717	0.888	0.896
Resd. Dens. [e/Å ³]	-0.289, 0.203	-0.390, 0.266	-0.423, 0.416	-0.347, 0.286
Solution	SIR-92	SIR-92	SIR-92	SIR-92
Refinement	SHELXL-97	SHELXL-97	SHELXL-97	SHELXL-97
CCDC	–	–	–	–

III. Crystallographic Data of Salts of 3

	3_K	3_Rb	3_Cs	3_Mg
Formula	C ₃ H ₄ ClKN ₆ O ₂	C ₃ H ₄ ClN ₆ O ₂ Rb	C ₃ H ₄ ClCsN ₆ O ₂	C ₆ H ₂₀ Cl ₂ MgN ₁₂ O ₁₀
<i>M</i> [g/mol]	230.65	277.04	324.48	515.51
Crystal System	monoclinic	monoclinic	monoclinic	triclinic
Space Group	<i>P</i> 2 ₁ / <i>c</i> (14)	<i>P</i> 2 ₁ / <i>c</i> (14)	<i>P</i> 2 ₁ / <i>c</i> (14)	<i>P</i> -1 (2)
Color / Habit	colorless rods	colorless blocks	colorless blocks	colorless blocks
Size [mm]	0.15×0.12×0.09	0.35×0.25×0.20	0.30×0.25×0.20	0.18×0.11×0.08
<i>a</i> [Å]	10.1160(5)	10.0705(6)	10.0233(4)	7.2277(5)
<i>b</i> [Å]	9.9464(4)	10.0801(4)	10.2991(3)	9.0036(6)
<i>c</i> [Å]	8.6448(4)	8.7758(4)	8.8589(3)	9.1905(5)
<i>α</i> [°]	90	90	90	114.010(6)
<i>β</i> [°]	109.461(5)	108.925(6)	106.812(4)	105.004(5)
<i>γ</i> [°]	90	90	90	98.821(5)
<i>V</i> [Å ³]	820.13(7)	842.69(7)	875.43(5)	504.51(6)
<i>Z</i>	4	4	4	1
$\rho_{\text{calc.}}$ [g/cm ³]	1.868	2.184	2.462	1.697
μ [mm ⁻¹]	0.950	6.170	4.513	0.429
<i>F</i> (000)	464	536	608	266
<i>T</i> [K]	200	200	200	200
θ min–max [°]	4.27, 25.5	4.25, 26.46	4.14, 25.00	4.18, 26.50
Dataset [h; k; l]	-12:11; -12:9; -8:10	-7:12, -11:12, -10:11	-6:11, -12:12, -10:10	-9:9, -11:11, -11:11
Reflections Collected	3986	3185	5985	7935
Independent Reflections	1517	1717	1536	4146
<i>R</i> _{int}	0.0244	0.0335	0.0292	0.0276
Observed Reflections	1198	1262	1343	2087
No. Parameters	118	118	118	166
Restraints	0	0	0	0
<i>R</i> ₁ (obs)	0.0248	0.0320	0.0166	0.0263
w <i>R</i> ₂ (all data)	0.0651	0.0604	0.0375	0.0681
GooF	1.112	0.925	1.029	1.067
Resd. Dens. [e/Å ³]	-0.318, 0.242	-0.675, 0.585	-0.347, 0.653	-0.270, 0.207
Solution	SIR-92	SIR-92	SIR-92	SIR-92
Refinement	SHELXL-97	SHELXL-97	SHELXL-97	SHELXL-97
CCDC	718892	–	–	–

	3_Sr	3_Ba	3_Cu	3_Cu_NH₃
Formula	C ₆ H ₁₀ Cl ₂ N ₁₂ O ₅ Sr	C ₆ H ₁₀ BaCl ₂ N ₁₂ O ₅	C ₆ H ₈ Cl ₂ CuN ₁₂ O ₄	C ₆ H ₁₄ Cl ₂ CuN ₁₄ O ₄
<i>M</i> [g/mol]	488.78	538.50	446.68	480.75
Crystal System	orthorhombic	triclinic	monoclinic	monoclinic
Space Group	<i>Pbca</i> (61)	<i>P</i> -1 (2)	<i>P</i> 2 ₁ / <i>c</i> (14)	<i>P</i> 2 ₁ / <i>c</i> (14)
Color / Habit	colorless blocks	colorless plates	green disks	blue pads
Size [mm]	0.12×0.11×0.07	0.10×0.10×0.03	0.32×0.25×0.03	0.40×0.20×0.01
<i>a</i> [Å]	12.9331(4)	8.5674(2)	11.273(6)	14.4769(5)
<i>b</i> [Å]	8.3175(3)	9.0807(3)	6.451(3)	5.5805(2)
<i>c</i> [Å]	29.6896(10)	11.8239(3)	9.685(5)	10.7259(5)
<i>α</i> [°]	90	98.756(3)	90	90
<i>β</i> [°]	90	96.802(2)	90.925(5)	101.154(4)
<i>γ</i> [°]	90	113.050(3)	90	90
<i>V</i> [Å ³]	3193.74(19)	820.38(5)	704.2(7)	850.16(6)
<i>Z</i>	8	2	2	2
ρ_{calc} [g/cm ³]	2.033	2.180	2.107	1.878
μ [mm ⁻¹]	3.765	2.798	1.981	1.651
<i>F</i> (000)	1936	520	446	486
<i>T</i> [K]	200	200	100	200
θ min–max [°]	3.99, 26.0	3.88, 26.0	3.79, 28.7	3.86, 26.0
Dataset [h; k; l]	-10:15, -9:10, -36:36	-10:10, -11:11, -14:14	-13:13, -7:7, -11:11	-17:11; -3:6; -13:11
Reflections Collected	15296	18013	4557	3194
Independent Reflections	3120	3205	1371	1661
<i>R</i> _{int}	0.0756	0.0327	0.0345	0.0237
Observed Reflections	1862	2849	1138	1284
No. Parameters	243	243	115	136
Restraints	3	0	0	0
<i>R</i> ₁ (obs)	0.0428	0.0265	0.0409	0.0254
w <i>R</i> ₂ (all data)	0.1358	0.0691	0.1285	0.0573
Goof	1.047	1.118	1.142	0.922
Resd. Dens. [e/Å ³]	-1.242, 1.635	-0.734, 1.392	-1.014, 0.710	-0.244, 0.353
Solution	SIR-92	SIR-92	SIR-97	SIR-92
Refinement	SHELXL-97	SHELXL-97	SHELXL-97	SHELXL-97
CCDC	718890	718891	733993	733994

IV. Crystallographic Data of 4 and its Salts

	4	4_Li	4_Na	4_K
Formula	C ₃ H ₅ N ₅ O ₂	C ₃ H ₆ N ₅ O ₃ Li	C ₃ H ₁₀ N ₅ NaO ₅	C ₃ H ₄ KN ₅ O ₂
<i>M</i> [g/mol]	143.10	167.05	219.15	181.21
Crystal System	orthorhombic	monoclinic	triclinic	monoclinic
Space Group	<i>Pbca</i> (61)	<i>P2₁/c</i> (14)	<i>P</i> -1 (2)	<i>P2₁/c</i> (14)
Color / Habit	colorless platelet	colorless block	colorless platelet	colorless platelet
Size [mm]	0.25×0.15×0.15	0.30×0.20×0.05	0.40×0.30×0.25	0.40×0.10×0.05
<i>a</i> [Å]	9.8865(8)	13.234(5)	5.6150(2)	14.810(5)
<i>b</i> [Å]	7.8220(6)	5.027(5)	6.0758(3)	4.068(5)
<i>c</i> [Å]	14.8112(10)	11.287(5)	13.9525(7)	11.538(5)
<i>α</i> [°]	90	90	89.606(4)	90
<i>β</i> [°]	90	113.178(5)	88.152(4)	108.277(5)
<i>γ</i> [°]	90	90	71.762(4)	90
<i>V</i> [Å ³]	1145.38(15)	690.3(8)	451.85(4)	660.1(9)
<i>Z</i>	8	4	2	4
ρ_{calc} [g/cm ³]	1.660	1.608	1.611	1.824
μ [mm ⁻¹]	0.140	0.137	0.185	0.758
<i>F</i> (000)	592	344	228	368
<i>T</i> [K]	200	100	200	200
θ min–max [°]	4.12, 25.99	4.38, 30.00	3.81, 32.29	3.90, 28.61
Dataset [h; k; l]	-12:10, -8:9, -18:17	-16:16, -6:6, -14:13	-6:6, -7:7, -17:17	-17:18, -4:5, -9:14
Reflections Collected	4121	5060	6556	2415
Independent Reflections	1117	1428	1782	1358
<i>R</i> _{int}	0.0405	0.0249	0.0161	0.0239
Observed Reflections	672	1041	1571	1020
No. Parameters	99	125	159	108
Restraints	0	0	0	0
<i>R</i> ₁ (obs)	0.0324	0.0261	0.0240	0.0299
w <i>R</i> ₂ (all data)	0.0586	0.0615	0.0679	0.0628
GooF	0.847	0.888	1.103	0.931
Resd. Dens. [e/Å ³]	-0.175, 0.147	-0.178, 0.160	-0.190, 0.207	-0.261, 0.336
Solution	SIR-92	SIR-92	SIR-92	SIR-92
Refinement	SHELXL-97	SHELXL-97	SHELXL-97	SHELXL-97
CCDC	-	-	-	-

	4_Rb	4_Cs	4_Mg	4_Ca
Formula	C ₃ H ₆ N ₅ O ₃ Rb	C ₃ H ₄ CsN ₅ O ₂	C ₆ H ₁₆ MgN ₁₀ O ₈	C ₆ H ₁₆ CaN ₁₀ O ₈
<i>M</i> [g/mol]	245.60	275.02	380.60	396.37
Crystal System	triclinic	triclinic	triclinic	monoclinic
Space Group	<i>P</i> -1 (2)	<i>P</i> -1 (2)	<i>P</i> -1 (2)	<i>C</i> 2/ <i>c</i> (15)
Color / Habit	colorless platelet	colorless block	colorless block	colorless block
Size [mm]	0.20×0.10×0.11	0.15×0.10×0.05	0.15×0.10×0.06	0.20×0.10×0.03
<i>a</i> [Å]	6.098(5)	4.558(5)	6.1055(5)	38.010(5)
<i>b</i> [Å]	7.596(5)	8.794(5)	6.5625(6)	5.944(5)
<i>c</i> [Å]	9.397(5)	8.928(5)	9.5330(7)	13.763(5)
<i>α</i> [°]	78.774(5)	89.806(5)	78.933(7)	90
<i>β</i> [°]	71.589(5)	89.601(5)	83.101(6)	103.548(5)
<i>γ</i> [°]	68.062(5)	87.386(5)	75.853(7)	90
<i>V</i> [Å ³]	381.6(4)	357.5(5)	362.41(5)	3023(3)
<i>Z</i>	2	2	1	8
$\rho_{\text{calc.}}$ [g/cm ³]	2.137	2.555	1.744	1.742
μ [mm ⁻¹]	6.464	5.136	0.193	0.483
<i>F</i> (000)	240	256	198	1648
<i>T</i> [K]	100	100	200	200
θ min–max [°]	3.83, 28.73	4.48, 26.49	3.94, 26.00	3.81, 26.50
Dataset [h; k; l]	-7:7, -9:9, -11:11	-5:5, -5:11, -9:11	-6:7, -8:7, -11:11	-47:47, -7:7, -15:17
Reflections Collected	2730	1374	2492	11136
Independent Reflections	1576	1118	1417	3132
<i>R</i> _{int}	0.0330	0.0144	0.0238	0.0362
Observed Reflections	1241	1007	995	2147
No. Parameters	125	108	139	290
Restraints	0	0	1	0
<i>R</i> ₁ (obs)	0.0309	0.0259	0.0337	0.0279
w <i>R</i> ₂ (all data)	0.0546	0.0588	0.0725	0.0525
Goof	0.877	0.984	0.923	0.842
Resd. Dens. [e/Å ³]	-0.628, 0.466	-1.089, 0.690	-0.212, 0.222	-0.244, 0.186
Solution	SIR-92	SIR-92	SIR-92	SIR-92
Refinement	SHELXL-97	SHELXL-97	SHELXL-97	SHELXL-97
CCDC	–	–	–	–

	4_Sr	4_Ba
Formula	C ₆ H ₁₈ N ₁₀ O ₉ Sr	C ₆ H ₁₄ BaN ₁₀ O ₇
<i>M</i> [g/mol]	461.92	475.57
Crystal System	triclinic	monoclinic
Space Group	<i>P</i> -1 (2)	<i>P</i> 2 ₁ / <i>m</i> (14)
Color / Habit	colorless platelet	colorless rods
Size [mm]	0.25×0.20×0.02	0.45×0.10×0.06
<i>a</i> [Å]	8.5889(4)	4.464(5)
<i>b</i> [Å]	9.5673(4)	28.756(5)
<i>c</i> [Å]	11.4414(5)	5.933(5)
<i>α</i> [°]	90.088(4)	90
<i>β</i> [°]	106.652(4)	100.186(5)
<i>γ</i> [°]	97.828(4)	90
<i>V</i> [Å ³]	891.53(7)	749.6(11)
<i>Z</i>	2	2
$\rho_{\text{calc.}}$ [g/cm ³]	1.721	2.107
μ [mm ⁻¹]	3.089	2.708
<i>F</i> (000)	468	464
<i>T</i> [K]	200	200
θ min–max [°]	3.72, 26.00	3.77, 26.50
Dataset [h; k; l]	-10:10, -11:11, -14:8	-5:2, -36:18, -7:7
Reflections Collected	6548	3134
Independent Reflections	3460	1588
<i>R</i> _{int}	0.0324	0.0324
Observed Reflections	2856	1368
No. Parameters	291	140
Restraints	0	0
<i>R</i> ₁ (obs)	0.0284	0.0269
w <i>R</i> ₂ (all data)	0.0538	0.0436
Goof	0.965	0.922
Resd. Dens. [e/Å ³]	-0.559, 0.566	-0.581, 0.762
Solution	SIR-92	SIR-92
Refinement	SHELXL-97	SHELXL-97
CCDC	-	-

V. Crystallographic Data of 5 and its Salts

	5	5_K	5_Rb
Formula	C ₃ H ₆ N ₆ O ₅	C ₃ H ₅ KN ₆ O ₅	C ₃ H ₅ N ₆ O ₅ Rb
<i>M</i> [g/mol]	206.14	244.23	290.60
Crystal System	orthorhombic	monoclinic	monoclinic
Space Group	<i>Pbcn</i> (60)	<i>P2₁/c</i> (14)	<i>P2₁/c</i> (14)
Color / Habit	colorless platelet	colorless block	colorless rod
Size [mm]	0.35×0.30×0.10	0.20×0.15×0.10	0.50×0.10×0.08
<i>a</i> [Å]	23.053(5)	12.397(5)	12.687(5)
<i>b</i> [Å]	8.582(5)	5.044(5)	5.116(5)
<i>c</i> [Å]	8.025(5)	13.965(5)	14.196(5)
<i>α</i> [°]	90	90	90
<i>β</i> [°]	90	94.307(5)	93.430(5)
<i>γ</i> [°]	90	90	90
<i>V</i> [Å ³]	1587.7(14)	870.8(10)	919.8(10)
<i>Z</i>	8	4	4
$\rho_{\text{calc.}}$ [g/cm ³]	1.725	1.863	2.099
μ [mm ⁻¹]	0.160	0.628	5.400
<i>F</i> (000)	848	496	568
<i>T</i> [K]	200	200	100
θ min–max [°]	3.90, 28.73	4.24, 26.50	4.19, 26.50
Dataset [h; k; l]	-16:30, -11,10 -5:10	-15:15, -6:3, -17:16	-15:15, -6:6, -11:17
Reflections Collected	5021	3360	4797
Independent Reflections	1816	1798	1902
<i>R</i> _{int}	0.0332	0.0362	0.0358
Observed Reflections	1136	1049	1405
No. Parameters	151	148	148
Restraints	0	0	0
<i>R</i> ₁ (obs)	0.0319	0.0335	0.0294
w <i>R</i> ₂ (all data)	0.0616	0.0481	0.0595
GooF	0.876	0.757	0.893
Resd. Dens. [e/Å ³]	-0.211, 0.181	-0.275, 0.231	-0.618, 0.741
Solution	SIR-92	SIR-92	SIR-92
Refinement	SHELXL-97	SHELXL-97	SHELXL-97
CCDC	–	–	–

	5_Mg1	5_Mg2	5_Ca1	5_Ca2
Formula	C ₆ H ₂₆ MgN ₁₂ O ₁₈	C ₃ H ₁₈ MgN ₆ O ₁₂	C ₆ H ₁₀ CaN ₁₂ O ₁₀	C ₃ H ₈ CaN ₆ O ₇
<i>M</i> [g/mol]	578.70	354.54	450.34	280.23
Crystal System	monoclinic	triclinic	monoclinic	triclinic
Space Group	<i>P</i> 2 ₁ / <i>c</i> (14)	<i>P</i> -1 (2)	<i>C</i> 2/ <i>c</i> (15)	<i>P</i> -1 (2)
Color / Habit	colorless block	colorless block	colorless block	colorless block
Size [mm]	0.35×0.25×0.10	0.25×0.20×0.10	0.30×0.20×0.07	0.10×0.08×0.05
<i>a</i> [Å]	18.5898(9)	6.6103(3)	15.967(5)	7.087(5)
<i>b</i> [Å]	9.0941(4)	9.6261(5)	7.961(5)	8.363(5)
<i>c</i> [Å]	6.8352(4)	11.7477(6)	14.036(5)	9.198(5)
<i>α</i> [°]	90	90.958(4)	90	112.053(5)
<i>β</i> [°]	93.529(5)	96.100(4)	117.973(5)	91.710(5)
<i>γ</i> [°]	90	107.896(4)	90	98.454(5)
<i>V</i> [Å ³]	1153.35(10)	706.36(6)	1575.7(12)	497.6(5)
<i>Z</i>	2	2	4	2
ρ_{calc} [g/cm ³]	1.666	1.667	1.898	1.870
μ [mm ⁻¹]	0.186	0.203	0.489	0.673
<i>F</i> (000)	604	372	920	288
<i>T</i> [K]	200	200	200	100
θ min–max [°]	4.24, 26.50	4.24, 26.50	4.62, 25.98	4.22, 26.50
Dataset [h; k; l]	-21:23, -11,11 -8:8	-8:8, -12:12, -14:14	-18:19, -7:9, -17:7	-8:8, -10:10, -11:11
Reflections Collected	9209	7304	3266	3514
Independent Reflections	2392	2904	1533	2060
<i>R</i> _{int}	0.0233	0.0393	0.0215	0.0295
Observed Reflections	1944	2178	1218	1491
No. Parameters	213	266	144	178
Restraints	0	0	0	0
<i>R</i> ₁ (obs)	0.0236	0.0276	0.0250	0.0341
w <i>R</i> ₂ (all data)	0.0727	0.0611	0.0587	0.0706
GooF	0.796	0.911	0.959	0.897
Resd. Dens. [e/Å ³]	-0.241, 0.273	-0.224, 0.241	-0.272, 0.245	-0.320, 0.319
Solution	SIR-92	SIR-92	SIR-92	SHELXS-97
Refinement	SHELXL-97	SHELXL-97	SHELXL-97	SHELXL-97
CCDC	-	-	-	-

	5_Sr1	5_Sr2	5_Ba1
Formula	C ₆ H ₈ N ₁₂ O ₉ Sr	C ₃ H ₈ N ₆ O ₇ Sr	C ₆ H ₈ BaN ₁₂ O ₉
<i>M</i> [g/mol]	479.86	327.77	529.48
Crystal System	monoclinic	monoclinic	monoclinic
Space Group	<i>C</i> 2/ <i>c</i> (15)	<i>P</i> 2 ₁ / <i>c</i> (14)	<i>C</i> 2/ <i>c</i> (15)
Color / Habit	colorless block	colorless platelet	colorless block
Size [mm]	0.30×0.25×0.05	0.20×0.10×0.05	0.60×0.20×0.05
<i>a</i> [Å]	19.450(5)	7.2228(3)	19.4348(9)
<i>b</i> [Å]	10.337(5)	8.1793(4)	10.5478(4)
<i>c</i> [Å]	8.311(5)	17.2010(7)	8.4639(4)
<i>α</i> [°]	90	90	90
<i>β</i> [°]	100.244(5)	93.151(3)	100.724(4)
<i>γ</i> [°]	90	90	90
<i>V</i> [Å ³]	1644.3(13)	1014.65(8)	1704.75(13)
<i>Z</i>	4	4	4
$\rho_{\text{calc.}}$ [g/cm ³]	1.938	2.146	2.063
μ [mm ⁻¹]	3.357	5.355	2.405
<i>F</i> (000)	952	648	1024
<i>T</i> [K]	100	200	200
θ min–max [°]	3.94, 26.49	3.79, 26.49	3.86, 29.02
Dataset [h; k; l]	–23:24, –12:12 –10:9	–8:9, –10:10, –21:15	–25:25, –13:12, –11:6
Reflections Collected	7655	3689	3712
Independent Reflections	1702	2084	1947
<i>R</i> _{int}	0.0298	0.0279	0.0290
Observed Reflections	1510	1327	1740
No. Parameters	136	178	129
Restraints	0	2	1
<i>R</i> ₁ (obs)	0.0205	0.0283	0.0323
w <i>R</i> ₂ (all data)	0.0464	0.0572	0.0819
GooF	0.980	0.829	1.023
Resd. Dens. [e/Å ³]	–0.241, 0.402	–0.807, 0.454	–1.741, 1.495
Solution	SIR–97	SIR–92	SIR–92
Refinement	SHELXL–97	SHELXL–97	SHELXL–97
CCDC	–	–	–

	5_Cu_H2Oa (green)	5_Cu_H2Ob (blue)	5_Cu_NH3
Formula	C ₆ H ₁₄ CuN ₁₂ O ₁₂	C ₆ H ₁₄ CuN ₁₂ O ₁₂	C ₃ H ₁₁ CuN ₈ O _{5.5}
<i>M</i> [g/mol]	509.83	509.83	310.74
Crystal System	monoclinic	monoclinic	monoclinic
Space Group	<i>P</i> 2 ₁ / <i>c</i> (14)	<i>P</i> 2 ₁ / <i>n</i> (14)	<i>C</i> 2/ <i>c</i> (15)
Color / Habit	green platelet	blue block	blue block
Size [mm]	0.20×0.10×0.02	0.25×0.25×0.15	0.30×0.20×0.10
<i>a</i> [Å]	15.198(5)	5.6499(3)	24.659(5)
<i>b</i> [Å]	10.997(5)	12.8139(6)	4.906(5)
<i>c</i> [Å]	5.134(5)	12.3520(7)	17.874(5)
<i>α</i> [°]	90	90	90
<i>β</i> [°]	93.993(5)	99.047(5)	97.502(5)
<i>γ</i> [°]	90	90	90
<i>V</i> [Å ³]	856.0(10)	883.13(8)	2144(2)
<i>Z</i>	2	2	8
$\rho_{\text{calc.}}$ [g/cm ³]	1.978	1.917	1.925
μ [mm ⁻¹]	1.375	1.332	2.074
<i>F</i> (000)	518	518	1264
<i>T</i> [K]	200	200	100
θ min–max [°]	3.71, 26.50	4.24, 28.70	3.79, 26.50
Dataset [h; k; l]	–19:19, –13,13 –6:6	–15:15, –6:3, –17:16	–30:30, –6:6, –22:22
Reflections Collected	12554	3546	15672
Independent Reflections	1776	1812	2221
<i>R</i> _{int}	0.0504	0.0321	0.0237
Observed Reflections	1531	1245	1991
No. Parameters	162	162	195
Restraints	4	0	0
<i>R</i> ₁ (obs)	0.0384	0.0296	0.0191
w <i>R</i> ₂ (all data)	0.1219	0.0544	0.0561
GooF	1.116	0.885	1.073
Resd. Dens. [e/Å ³]	–0.757, 0.458	–0.434, 0.395	–0.322, 0.325
Solution	SIR–97	SIR–92	SIR–97
Refinement	SHELXL–97	SHELXL–97	SHELXL–97
CCDC	–	–	–

VI. Crystallographic Data of 6a, 6b, 7, 9, 9_H₂O and some Salts

	6a	6b	7	7_K
Formula	C ₄ H ₉ N ₅ O ₂	C ₄ H ₉ N ₅ O ₂	C ₄ H ₈ N ₈ O ₉	C ₄ H ₅ KN ₆ O ₈
<i>M</i> [g/mol]	159.16	159.16	312.18	332.25
Crystal System	triclinic	orthorhombic	monoclinic	monoclinic
Space Group	<i>P</i> -1 (2)	<i>Pbca</i> (61)	<i>P</i> 2 ₁ / <i>c</i> (14)	<i>P</i> 2 ₁ / <i>c</i> (14)
Color / Habit	colorless blocks	colorless needle	colorless platelet	colorless block
Size [mm]	0.30×0.25×0.08	0.25×0.15×0.10	0.20×0.20×0.05	0.20×0.08×0.05
<i>a</i> [Å]	6.052(5)	9.425(5)	18.9487(8)	11.8572(10)
<i>b</i> [Å]	7.682(5)	8.898(5)	9.0510(4)	8.5585(4)
<i>c</i> [Å]	7.709(5)	16.607(5)	7.0500(3)	11.7869(7)
<i>α</i> [°]	94.113(5)	90	90	90
<i>β</i> [°]	97.138(5)	90	95.913(4)	97.538(7)
<i>γ</i> [°]	103.102(5)	90	90	90
<i>V</i> [Å ³]	344.5(4)	1392.7(12)	1202.67(9)	1185.80(13)
<i>Z</i>	2	8	4	4
ρ_{calc} [g/cm ³]	1.534	1.518	1.724	1.833
μ [mm ⁻¹]	0.125	0.123	0.166	0.510
<i>F</i> (000)	168	672	640	652
<i>T</i> [K]	200	200	200	200
θ min-max [°]	3.89, 26.49	4.32, 26.50	3.92, 26.00	4.21, 26.00
Dataset [h; k; l]	-7:7, -9:9, -9:9	-11:11, -7:11, -19:20	-21:23, -11:7, -8:8	-14:8, -9:10, -14:13
Reflections Collected	3531	5826	5301	4645
Independent Reflections	1415	1439	2319	2316
<i>R</i> _{int}	0.0269	0.0278	0.0240	0.0387
Observed Reflections	1017	1078	1321	1288
No. Parameters	116	116	202	166
Restraints	0	0	0	0
<i>R</i> ₁ (obs)	0.0370	0.0282	0.0569	0.1325
w <i>R</i> ₂ (all data)	0.1090	0.0698	0.1718	0.4060
GooF	1.122	0.959	1.066	1.396
Resd. Dens. [e/Å ³]	-0.186, 0.203	-0.189, 0.251	-0.273, 0.906	-0.979, 2.548
Solution	SIR-97	SIR-92	SIR-92	SHELXS-97
Refinement	SHELXL-97	SHELXL-97	SHELXL-97	SHELXL-97
CCDC	-	-	-	-

	9	9_H₂O	9_Cs
Formula	C ₄ H ₆ Cl ₂ N ₆ O ₂	C ₄ H ₈ Cl ₂ N ₆ O ₃	C ₄ H ₅ Cl ₂ CsN ₆ O ₂
<i>M</i> [g/mol]	241.05	259.00	372.95
Crystal System	monoclinic	monoclinic	triclinic
Space Group	<i>P</i> 2 ₁ / <i>c</i> (14)	<i>P</i> 2 ₁ / <i>c</i> (14)	<i>P</i> -1 (2)
Color / Habit	colorless block	colorless block	colorless plate
Size [mm]	0.20×0.08×0.07	0.20×0.07×0.06	0.48×0.21×0.05
<i>a</i> [Å]	13.5103(12)	7.460(5)	5.0150(3)
<i>b</i> [Å]	7.2293(6)	7.264(5)	7.0303(4)
<i>c</i> [Å]	9.9143(9)	18.218(5)	15.5634(11)
<i>α</i> [°]	90	90	102.507(5)
<i>β</i> [°]	109.91(1)	92.836(5)	94.084(5)
<i>γ</i> [°]	90	90	102.066(5)
<i>V</i> [Å ³]	910.45(14)	986.0(10)	519.95(6)
<i>Z</i>	4	4	2
$\rho_{\text{calc.}}$ [g/cm ³]	1.759	1.745	2.382
μ [mm ⁻¹]	0.698	0.658	352
<i>F</i> (000)	488	528	4.065
<i>T</i> [K]	200	200	100
θ min–max [°]	4.21, 25.00	4.38, 26.49	4.19, 26.50
Dataset [h; k; l]	-16:12, -5:8, -8:11	-9:5, -8:9, -22:18	-6:6, -8:8, -19:7
Reflections Collected	3156	3874	3640
Independent Reflections	1603	2031	2150
<i>R</i> _{int}	0.0414	0.0458	0.0298
Observed Reflections	850	1082	1880
No. Parameters	131	136	136
Restraints	1	0	0
<i>R</i> ₁ (obs)	0.0421	0.0420	0.0296
w <i>R</i> ₂ (all data)	0.0761	0.0597	0.0685
GooF	0.792	0.754	0.993
Resd. Dens. [e/Å ³]	-0.269, 0.505	-0.297, 0.310	-0.794, 1.225
Solution	SIR-97	SIR-92	SIR-92
Refinement	SHELXL-97	SHELXL-97	SHELXL-97
CCDC	-	-	-

VII. Crystallographic Data of 13, 13_HCl, 14 and some Salts

	10_Na	10_K	10_Sr1	12_Na
Formula	C ₂ H ₈ N ₅ NaO ₅	C ₂ H ₂ KN ₅ O ₂	C ₄ H ₁₀ N ₁₀ O ₇ Sr	C ₂ H ₅ N ₄ O ₄ Na
<i>M</i> [g/mol]	205.12	167.19	397.84	172.09
Crystal System	monoclinic	monoclinic	orthorhombic	monoclinic
Space Group	<i>P</i> 2 ₁ / <i>c</i> (14)	<i>P</i> 2 ₁ (4)	<i>Pbca</i> (61)	<i>P</i> 2 ₁ / <i>c</i> (14)
Color / Habit	colorless rods	yellow blocks	yellow blocks	yellow blocks
Size [mm]	0.30×0.15×0.03	0.40×0.30×0.20	0.40×0.25×0.05	0.25×0.20×0.15
<i>a</i> [Å]	6.5449(3)	4.0893(3)	9.9619(3)	6.6964(9)
<i>b</i> [Å]	13.5063(6)	10.0136(5)	19.6753(6)	7.1673(10)
<i>c</i> [Å]	9.3514(4)	7.0195(4)	12.7880(5)	13.6349(18)
<i>α</i> [°]	90	90	90	90
<i>β</i> [°]	93.604(4)	103.635(6)	90	93.787(13)
<i>γ</i> [°]	90	90	90	90
<i>V</i> [Å ³]	825.00(6)	279.34(3)	2506.49(15)	652.98(15)
<i>Z</i>	4	2	8	4
ρ_{calc} [g/cm ³]	1.651	1.988	2.109	1.751
μ [mm ⁻¹]	0.196	0.886	4.365	0.215
<i>F</i> (000)	424	168	1584	352
<i>T</i> [K]	200	200	200	200
θ min–max [°]	4.34, 26.50	4.07, 25.98	3.80, 26.00	4.13, 26.50
Dataset [h; k; l]	–8:7, –16:8, –5:11	–5:5, –12:12, –8:8	–10:12, –14:15, –18:24	–8:8, –8:8, –17:16
Reflections Collected	3524	2787	12155	5031
Independent Reflections	1694	1080	2454	0.0560
<i>R</i> _{int}	0.0190	0.0151	0.0653	1348
Observed Reflections	1344	1050	1510	813
No. Parameters	146	95	231	120
Restraints	1	1	1	0
<i>R</i> ₁ (obs)	0.0299	0.0162	0.0273	0.0423
w <i>R</i> ₂ (all data)	0.0809	0.0395	0.0454	0.0980
GooF	1.021	0.757	0.788	0.843
Resd. Dens. [e/Å ³]	–0.200, 0.240	–0.169, 0.158	–0.423 / 0.534	–0.226, 0.576
Solution	SIR–92	SIR–92	SIR–92	SIR–92
Refinement	SHELXL–97	SHELXL–97	SHELXL–97	SHELXL–97
CCDC	–	–	–	–

	12_Ca	12_Cu	13	13_HCl
Formula	C ₄ H ₁₄ CaN ₈ O ₁₀	C ₄ H ₁₂ CuN ₁₀ O ₆	C ₄ H ₆ N ₄ O ₂	C ₄ H ₇ ClN ₄ O ₂
<i>M</i> [g/mol]	374.31	359.78	142.13	178.59
Crystal System	triclinic	monoclinic	orthorhombic	triclinic
Space Group	<i>P</i> -1 (2)	<i>P</i> 2 ₁ / <i>c</i> (14)	<i>Pca</i> 2 ₁ (29)	<i>P</i> -1 (2)
Color / Habit	colorless rods	blue rods	colorless rod	colorless block
Size [mm]	0.20×0.10×0.03	0.25×0.20×0.10	0.28×0.12×0.10	0.35×0.30×0.15
<i>a</i> [Å]	6.397(5)	6.9386(7)	12.2878(4)	6.328(5)
<i>b</i> [Å]	6.917(5)	13.5595(11)	4.8408(2)	7.498(5)
<i>c</i> [Å]	16.338(5)	6.8313(6)	19.7314(7)	7.884(5)
<i>α</i> [°]	87.574(5)	90	90	90.249(5)
<i>β</i> [°]	87.699(5)	94.684(9)	90	90.227(5)
<i>γ</i> [°]	85.440(5)	90	90	91.879(5)
<i>V</i> [Å ³]	719.5(8)	640.57(10)	1173.68(7)	373.9(5)
<i>Z</i>	2	2	8	2
$\rho_{\text{calc.}}$ [g/cm ³]	1.728	1.865	1.609	1.586
μ [mm ⁻¹]	0.508	1.756	0.132	0.466
<i>F</i> (000)	388	366	592	184
<i>T</i> [K]	200	200	200	200
θ min–max [°]	4.18, 26.50	4.21, 26.50	4.13, 26.50	4.12, 26.00
Dataset [h; k; l]	-7:8, -8:7, -20:20	-8:8, -15:17, -8:8	-15:15, -6:6, -24:24	-7:7, -9:9, -9:9
Reflections Collected	5201	2940	11269	5357
Independent Reflections	2970	1326	1245	1471
<i>R</i> _{int}	0.0144	0.0320	0.0324	0.0240
Observed Reflections	2481	926	1056	1313
No. Parameters	256	117	213	116
Restraints	0	2	2	0
<i>R</i> ₁ (obs)	0.0256	0.0301	0.0242	0.0378
w <i>R</i> ₂ (all data)	0.0624	0.0649	0.0625	0.1209
GooF	0.975	0.887	0.981	1.330
Resd. Dens. [e/Å ³]	-0.266, 0.333	-0.295, 0.597	-0.140, 0.136	-0.283, 0.331
Solution	SIR-97	SIR-92	SIR-92	SIR-92
Refinement	SHELXL-97	SHELXL-97	SHELXL-97	SHELXL-97
CCDC	–	–	–	–

	13_Sr	13_Ba	14	14_Sr
Formula	C ₈ H ₂₀ N ₈ O ₉ Sr	C ₈ H ₁₆ BaN ₈ O ₇	C ₄ H ₇ N ₅ O ₅	C ₄ H ₉ N ₅ O ₇ Sr
<i>M</i> [g/mol]	459.94	473.63	205.15	326.78
Crystal System	orthorhombic	monoclinic	monoclinic	monoclinic
Space Group	<i>Pcca</i> (54)	<i>P2/c</i> (13)	<i>P2₁/c</i> (14)	<i>P2₁/c</i> (14)
Color / Habit	colorless rod	colorless platelet	colorless rod	yellow block
Size [mm]	0.20×0.05×0.02	0.30×0.25×0.03	0.20×0.15×0.10	0.25×0.20×0.10
<i>a</i> [Å]	28.854(2)	14.240(5)	14.503(1)	7.228(5)
<i>b</i> [Å]	7.3667(6)	6.816(5)	8.3815(8)	8.079(5)
<i>c</i> [Å]	8.2334(5)	8.272(5)	6.8305(8)	17.566(5)
<i>α</i> [°]	90	90	90	90
<i>β</i> [°]	90	100.191(5)	97.30(1)	92.099(5)
<i>γ</i> [°]	90	90	90	90
<i>V</i> [Å ³]	1750.1(2)	790.2(8)	823.56(15)	1025.1(10)
<i>Z</i>	4	2	4	4
ρ_{calc} [g/cm ³]	1.746	1.991	1.655	2.117
μ [mm ⁻¹]	3.144	2.565	0.151	5.298
<i>F</i> (000)	936	464	424	648
<i>T</i> [K]	200	200	200	200
θ min–max [°]	4.24, 26.50	4.17, 26.49	4.25, 26.50	4.30, 26.50
Dataset [h; k; l]	–29:39, –8:9, –5:10	–17:17, –8:8, –10:10	–18:14, –9:10, –8:6	–8:9, –6:10, –22:18
Reflections Collected	4391	11917	3374	3934
Independent Reflections	1812	1639	1710	2101
<i>R</i> _{int}	0.0521	0.0261	0.0226	0.0382
Observed Reflections	1100	1581	1082	1337
No. Parameters	147	130	143	182
Restraints	0	0	0	0
<i>R</i> ₁ (obs)	0.0300	0.0143	0.0327	0.0300
w <i>R</i> ₂ (all data)	0.0520	0.0371	0.0678	0.0608
GooF	0.780	1.059	0.832	0.834
Resd. Dens. [e/Å ³]	–0.639, 0.345	–0.494, 0.491	–0.213, 0.166	–0.876, 0.832
Solution	SIR–92	SIR–92	SIR–92	SIR–92
Refinement	SHELXL–97	SHELXL–97	SHELXL–97	SHELXL–97
CCDC	–	–	–	–

VIII. Crystallographic Data of Nitrogen-rich Barium Salts

	Ba1H5AtNO2	Ba1MeAtNO2	Ba2MeAtNO2
Formula	C ₂ H ₁₀ BaN ₁₂ O ₈	C ₄ H ₈ BaN ₁₂ O ₅	C ₄ H ₁₀ BaN ₁₂ O ₆
<i>M</i> [g/mol]	467.55	441.51	459.58
Crystal System	orthorhombic	monoclinic	triclinic
Space Group	Pbcn (60)	C2/c (15)	P-1 (2)
Color / Habit	colorless blocks	colorless rods	colorless rods
Size [mm]	0.12×0.12×0.06	0.10×0.04×0.03	0.17×0.12×0.08
<i>a</i> [Å]	2121.45(6)	2070.2(2)	723.77(4)
<i>b</i> [Å]	974.27(3)	727.62(6)	823.11(4)
<i>c</i> [Å]	645.90(2)	851.42(5)	1362.73(7)
<i>α</i> [°]	90	90	88.635(4)
<i>β</i> [°]	90	96.702(6)	76.583(4)
<i>γ</i> [°]	90	90	64.240(5)
<i>V</i> [Å ³]	1334.99(7)	1273.76(16)	708.45(7)
<i>Z</i>	4	4	2
$\rho_{\text{calc.}}$ [g/cm ³]	2.326	2.303	2.154
μ [mm ⁻¹]	3.048	3.171	2.860
<i>F</i> (000)	904	848	444
<i>T</i> [K]	200	200	200
θ min–max [°]	3.8, 26.0	3.8, 25.0	3.9, 28.6
Dataset [h; k; l]	–23:26, –11:12, –5:7	–24:19, –6:8, –10:9	–9:9, –11:10, –18:16
Reflections Collected	6155	2777	5938
Independent Reflections	1304	1112	3188
<i>R</i> _{int}	0.038	0.056	0.022
Observed Reflections	936	996	2804
No. Parameters	125	106	210
Restraints	0	1	0
<i>R</i> ₁ (obs)	0.0206	0.0732	0.0217
w <i>R</i> ₂ (all data)	0.0454	0.1868	0.0424
GooF	0.93	1.08	0.96
Resd. Dens. [e/Å ³]	–0.520, 0.422	–1.336, 7.987	–0.668, 0.697
Solution	SIR–92	SIR–92	SHELXS–97
Refinement	SHELXL–97	SHELXL–97	SHELXL–97
CCDC	732144	732143	732141

IX. List of Abbreviations

abbreviation	meaning
AD	<i>anno Domini</i>
β	heating rate [K/min]
BAM	<i>Bundesanstalt für Materialforschung und -prüfung</i>
calc.	calculated
COSY	correlation spectroscopy (2D NMR method)
δ	chemical shift [ppm]
dec.	decomposition
DMSO- d_6	dimethylsulfoxide- d_6
DSC	differential scanning calorimetry
E_{dr}	impact energy [J]
E_{el}	electric discharge energy [J]
F_r	friction force [N]
GooF	goodness of fit
H ₂ O	demineralized water
H ₂ O-sol.	solubility in water [wt%]
HMBC	heteronuclear multiple bond coherence (2D NMR method)
HMQC	heteronuclear single quantum coherence (2D NMR method)
IR spectroscopy (vs, s, m, w, vw)	infrared spectroscopy (very strong, strong, medium, weak, very weak)
J	coupling constant [Hz]
λ	wavelength [nm]
lat.	Latin
M	molar [mol/L]
M	molecular weight [g/mol]
m.p.	melting point [°C]
MSDS	material safety data sheet
n.d.	not determined
NMR (s, d, t, q, m, dd)	nuclear magnetic resonance (singlet, doublet, triplet, quartet, multiplet, doublet of doublets)
PVC	polyvinyl chloride
ρ	density [g/cm ³]
T_b	boiling temperature
T_{dec}	decomposition temperature [°C]
T_m	melting temperature
u	atomic weight
V	cell volume [Å ³]
ν_b	burning velocity
wt%	percent by weight
Z	number of molecular units per unit cell

Ω

oxygen balance [%],
calculated according to the equation:

$$\Omega = [(aO - 2bC - 1/2(c - d)H - 2eS) \cdot 1600]/M$$

(*a*: number of oxygen atoms, *b*: number of carbon atoms, *c*: number of hydrogen atoms, *d*: number of chlorine atoms, *e*: number of sulfur atoms, *M*: molecular weight) in reference: a) R. Meyer, J. Köhler, A. Homburg: *Explosives*, 6. ed., Wiley-VCH, Weinheim, **2007**, 240–241. b) N. Kubota: Propellant Chemistry, *J. Pyrotech.* **2000**, *11*, 25–45.

All other used abbreviations are explained in the text.

X. Curriculum Vitae

Personal Data

Name: Karina Rosa TARANTIK
Birth Date: 30. September 1982 in Dachau
(Germany)
Nationality: German



Education

1993 – 2002: Secondary School: Louise-Schroeder-Gymnasium,
Munich (Germany)
2002 – 2007: B. Sc. Degree in Chemistry and Biochemistry, Ludwig-
Maximilian-University, Munich, Germany
2007 –2009: M. Sc. Degree in Chemistry, Ludwig-Maximilian-
University, Munich, Germany
1. Oct. 2007: Ph. D. (of Prof. KLAPÖTKE) at the Ludwig-Maximilian-
University, Munich, Germany

Knowledge of Languages

German: native speaker
English: fluent
French: basic knowledge

Work Experience

2000 Temporary employee at Feinkost Fratzl, Munich
2001 Temporary employee at Bayerisches Hauptstaatsarchiv,
Munich
2007 Student assistant at the Ludwig-Maximilian University,
Munich
2007 – present Doctoral research at the Ludwig-Maximilian University,
Munich (supervisor of bachelor and undergraduate research
students, teaching lab instructor for 1st, 3rd and 5th/6th
semester)

Awards

2009: Travel Bursary (Int. Pyrotechnic Seminar and Symposium 2009,
Rotterdam, The Netherlands)

XI. Full List of Publications

Papers

- [1] Georg Steinhauser, Karina Tarantik, Thomas M. Klapötke: Copper in Pyrotechnics, *J. Pyrotech.* **2008**, 27, 3–13.
- [2] Thomas M. Klapötke, Karina R. Tarantik: Green pyrotechnic compositions, *New Trends in Research of Energetic Materials*, 11th, Pardubice, Czech Republic, Apr. 9–11, **2008**, Pt. 2. 586–597.
- [3] Jörg Stierstorfer, Thomas M. Klapötke, Karina R. Tarantik, Ines D. Thoma: Strontium nitriminotetrazolates - suitable colorants in smokeless pyrotechnic compositions, *Z. Allg Anorg. Chem.* **2008**, 634, 2777–2784.
- [4] Jörg Stierstorfer, Thomas M. Klapötke, Karina R. Tarantik: New Energetic Materials: Functionalized 1-Ethyl-5-aminotetrazoles and 1-Ethyl-5-nitriminotetrazoles, *Chem.-Eur. J.* **2009**, 15(23), 5775–5792.
- [5] Jörg Stierstorfer, Thomas M. Klapötke, Karina R. Tarantik: Salts of 1-(2-chloro ethyl)-5-nitriminotetrazole - new candidates for coloring agents in pyrotechnic compositions, *New Trends in Research of Energetic Materials*, 12th, Pardubice, Czech Republic, Apr. 1–3, **2009**, Pt. 2, 647–665.
- [6] Jörg Stierstorfer, Thomas M. Klapötke, Karina R. Tarantik: Pyrotechnically Relevant Salts of 1-(2-Chloroethyl)-5-nitriminotetrazole – Synthesis and Coloring Properties, *J. Pyrotech.* **2009**, 28, 61–77.
- [7] Thomas M. Klapötke, Hendrik Radies, Jörg Stierstorfer, Karina R. Tarantik, Gary Chen, and Amita Nagori: Coloring Properties of Various High-Nitrogen Compounds in Pyrotechnic Compositions, *36th International Pyrotechnics Seminar and Symposium*, Proceedings, Rotterdam, The Netherlands, Aug. 23–28. **2009**, 65–72. c) T. M. Klapötke, H. Radies, J. Stierstorfer, K. R. Tarantik, G. Chen, and Amita Nagori: Coloring Properties of Various High-Nitrogen Compounds in Pyrotechnic Compositions, *Propellants, Explos. Pyrotech.* **2010**, in press.
- [8] Niko Fischer, Thomas M. Klapötke, Jörg Stierstorfer, Karina R. Tarantik: 1-Nitrato ethyl-5-nitriminotetrazole Derivatives – Shaping Future High Explosives, *New Trends in Research of Energetic Materials*, 13th, Pardubice, Czech Republic, Apr. 21–23, **2010**, Pt. 2, 455–467.
- [9] R. Damavarapu, T. M. Klapötke, J. Stierstorfer, K. R. Tarantik, *Propellants, Explos. Pyrotech.* **2010**, in press.

Posters

- [1] Thomas M. Klapötke, Karina R. Tarantik: Green pyrotechnic compositions, *New Trends in Research of Energetic Materials*, 11th, Pardubice, Czech Republic, Apr. 9–11, **2008**.
- [2] Jörg Stierstorfer, Thomas M. Klapötke, Karina R. Tarantik: Salts of 1-(2-chloroethyl)-5-nitriminotetrazole - new candidates for coloring agents in pyrotechnic compositions, *New Trends in Research of Energetic Materials*, 12th, Pardubice, Czech Republic, Apr. 1–3, **2009**.
- [3] Niko Fischer, Thomas M. Klapötke, Jörg Stierstorfer, Karina R. Tarantik: 1-Nitratoethyl-5-nitriminotetrazole Derivatives – Shaping Future High Explosives, *New Trends in Research of Energetic Materials*, 13th, Pardubice, Czech Republic, Apr. 21–23, **2010**.

Oral Presentations

- [1] T. M. Klapötke, K. R. Tarantik: Aluminum and Silicon Hydrides as Energetic Fuels, *Workshop: Contribution of metal hydrides in hybride or solide propulsion*, November 14th **2008**.
- [2] T. M. Klapötke, K. R. Tarantik: Green Pyrotechnic Compositions, *New Trends in Research of Energetic Materials*, 12th, Pardubice, Czech Republic, Apr. 1–3, **2009**
- [3] T. M. Klapöke, J. Stierstorfer, K. R. Tarantik: Salts of 1-(2-Chloroethyl)-5-nitrimino tetrazole – New Pyrotechnic Colorants, *7th Workshop on Pyrotechnic Combustion Mechanisms*, Rotterdam, The Netherlands, Aug. 22nd **2009**.
- [4] T. M. Klapötke, H. Radies, J. Stierstorfer, K. R. Tarantik, G. Chen, and A. Nagori: Coloring Properties of Various High-Nitrogen Compounds in Pyrotechnic Compositions, *36th International Pyrotechnics Seminar and Symposium*, Rotterdam, The Netherlands, Aug. 23–28. **2009**.

Press Releases

- [1] <http://environmentalresearchweb.org>, T. M. Klapötke, J. Stierstorfer, K. R. Tarantik, Green Pyrotechnics.
- [2] GdCh Wochenschau, T, M. Klapötke, J. Stierstorfer, K. R. Tarantik, <http://www.aktuelle-wochenschau.de/2008/woche37/woche37.html>4. GdCh Trendberichte 2008, J. Beckmann, R. Pietschnig, S. Rau, C. Schulzke, Anorganische Chemie 2008.